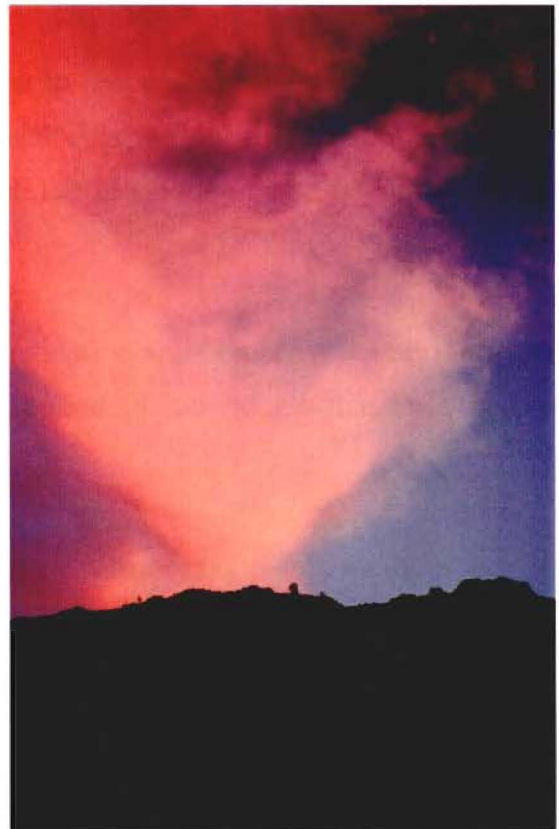
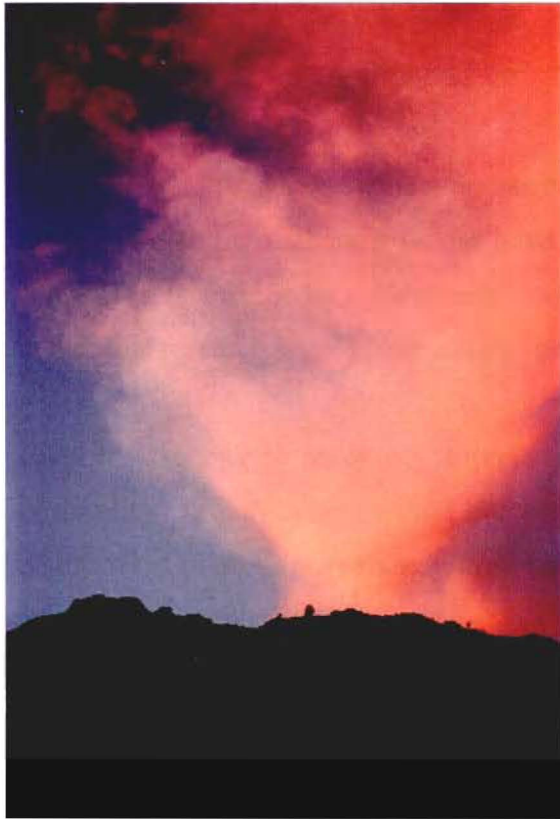


A SEDIMENTOLOGICAL PROFILE OF THE PAHAU TERRANE TYPE LOCALITY

A thesis
submitted in partial fulfilment
of the requirements for the Degree
of
Master of Science in Geology
in the
University of Canterbury
by
R. J. Orlowski

University of Canterbury
2001





FRONTISPIECE
sunset over a sandstone strike ridge

ACKNOWLEDGEMENTS

I would like to thank everyone who has contributed in some way towards this research for without some of them it would have not been possible. Kudos to my supervisor Kari Bassett for the enlightenment and thought provoking conversations, without which this research would have surely met with tragedy.

I would also like to show my appreciation to the staff of Lochiel Station for their hospitality. In particular I would like to thank Alistar Dunbar for the numerous loans of the farm bike. I never knew how much fun dirt biking could be and it certainly saves on the walking.

Thanks Neil and Liz I enjoyed the accommodation and company. To all my friends (especially Tim and Mike) and any other random individuals that have bespoke encouragement, it helps so much, thankyou.

What acknowledgement is complete without a warm fuzzy thanks to mum and dad, who are always there no matter what whenever you need them.

TABLE OF CONTENTS

FONTISPIECE	i
ACKNOWLEDGEMENTS	ii
TABLE OF CONTENTS	iii
TABLE OF FIGURES	x
ABSTRACT	xiii

INTRODUCTION

CHAPTER ONE

1.1 THE GEOLOGICAL FRAMEWORK OF NEW ZEALAND	1
1.1.1 Regional Background	2
1.2 THE TORLESSE SUPERTERRANE	3
1.2.1 Rakaia Terrane	4
1.2.2 Esk Head Terrane	6
1.2.3 Pahau Terrane	6
1.2.4 Provenance Relationships	7
1.3 STUDY AREA	8
1.4 PREVIOUS WORK	11
1.5 OBJECTIVES AND METHODOLOGY	12

LITHOFACIES AND STRATIGRAPHY

CHAPTER TWO

2.1	INTRODUCTION	14
2.2	METHODOLOGY	14
2.2.1	Stratigraphic section logging	15
2.2.2	Field Mapping	18
2.3	LITHOFACIES DESCRIPTIONS	20
2.3.1	Mudstone lithofacies	20
2.3.2	Interbedded mudstone – sandstone lithofacies	22
2.3.3	Sandstone lithofacies	26
2.3.4	Conglomerate lithofacies	28
2.4	STRATIGRAPHIC COLUMNS	31
2.4.1	Mount Saul C section	32
2.4.2	Pahau River A section	33
2.4.3	Pahau River B section	38
2.4.4	Pahau River C section	41
2.4.5	Waiau River section	43
2.4.6	Mount Holmes section	46
2.4.7	Mount Saul A & B sections	49
2.4.8	Shale Peak section	53
2.4.9	Castle Hill section	54
2.5	DISCUSSION	57

PROPOSED NOMENCLATURE

CHAPTER THREE

3.1	INTRODUCTION	59
3.2	DESCRIPTIVE HISTORY	59
3.2.1	The Torlesse Sediments	59
3.2.2	The Pahau Sediments	61
3.3	PROPOSED STRATIGRAPHIC NAMES	63
3.3.1	The Mount Saul Formation	64
3.3.2	The Ship Spur Formation	64
3.3.3	The Pahau River Group	65
3.4	STRATIGRAPHIC CODE AND REQUIREMENTS	65
3.5	DISCUSSION	65

DEPOSITIONAL PROCESSES IN MARGINAL MARINE ENVIRONMENTS

CHAPTER FOUR

4.1	INTRODUCTION	67
4.2	FLUVIAL PROCESSES	70
4.2.1	Current flow bedload transport	71
4.2.2	Current flow suspension	74

4.3	SHORELINE PROCESSES	75
4.3.1	Density interactions	75
4.3.2	Wave reworking and tidal currents	76
4.4	OFFSHORE DEPOSITIONAL PROCESSES	79
4.4.1	Bottom current reworking	79
4.4.2	Hemipelagic – pelagic fallout	79
4.4.3	Fluidised – liquefied flows	80
4.4.4	Debris flows	82
4.4.5	Turbidity currents	84
4.5	INTRACLASTS	89
4.6	DISCUSSION	94

DEPOSITIONAL SETTING

CHAPTER FIVE

5.1	INTRODUCTION	95
5.2	DEPOSITIONAL SETTING	96
5.2.1	The prodelta	96
5.2.2	The delta front – slope	98
5.2.3	The delta plain	102
5.3	FAN DELTA MODEL	103
5.4	ANCIENT AND MODERN ANALOGUES	107

5.4.1 The Coloso and Lombriz Formations, Chile	107
5.4.2 The Kosi Fan, India	108
5.5 DISCUSSION AND CONCLUSIONS	110

PROVENANCE

CHAPTER SIX

6.1 INTRODUCTION	112
6.2 THE HISTORY OF TORLESSE PROVENANCE ANALYSIS	113
6.2.1 Permian – Triassic Terranes – Rakaia and Caples	113
6.2.2 Source and emplacement of the Esk Head Terrane	115
6.2.3 The origins of the Pahau Terrane	116
6.3 PROVENANCE IN THE PAHAU RIVER AREA	118
6.3.1 Age control	119
6.3.2 Palaeoflow indicators	120
6.4 QFL PROVENANCE METHODOLOGY	121
6.4.1 Sample collection	121
6.4.2 Feldspar staining	122
6.4.3 Gazzi – Dickinson Point Counting Technique	123
6.5 QFL PROVENANCE RESULTS	124
6.6 DISCUSSION	126

CONCLUSIONS

CHAPTER SEVEN

7.1 LITHOFACIES SUMMARY	128
7.2 STRATIGRAPHIC NOMENCLATURE	129
7.3 DEPOSITIONAL SETTING	130
7.4 TECTONIC SETTING AND PROVENANCE	132
7.5 IMPLICATIONS	133

REFERENCES	135
-------------------	------------

APPENDIX I	142
-------------------	------------

SECTION LOGS

PAHAU RIVER A	143
PAHAU RIVER B	181
PAHAU RIVER C	198
WAIAU RIVER	222
MOUNT HOLMES	248
MOUNT SAUL A	269
MOUNT SAUL B	274
MOUNT SAUL C	287
SHALE PEAK	290
CASTLE HILL	294

APPENDIX II	300
--------------------	-----

THIN SECTION DATA	
--------------------------	--

RAW DATA	300
-----------------	-----

STATISTICAL ANALYSIS	301
-----------------------------	-----

APPENDIX III	302
---------------------	-----

PALAEOFLOW DATA	
------------------------	--

RAW DATA	302
-----------------	-----

TABLE OF FIGURES

INTRODUCTION

CHAPTER ONE

1.1	The New Zealand Tectonostratigraphic Map	3
1.2	The Pahau River location map	9
1.3	Structural map of the Pahau River study area	11

LITHOFACIES AND STRATIGRAPHY

CHAPTER TWO

2.1	Stratigraphic log deformation levels	17
2.2	Pahau River area lithofacies map	19
2.3	Mudstone lithofacies high deformation	20
2.4	Mudstone lithofacies undeformed	21
2.5	Interbedded mudstone – sandstone lithofacies	23
2.6	Macrofossil within massive sandstone bed	25
2.7	Massive sandstone lithofacies	27
2.8	Macrofossil shell bed in sandstone lithofacies	27
2.9	Bioturbation within sandstone lithofacies	28
2.10	Cross stratification within conglomerate lithofacies	29
2.11	Flame structure within conglomerate lithofacies	31
2.12	Stratigraphic section location map	32
2.13	Mt Saul C stratigraphic section log	34
2.14	Pahau River A stratigraphic section log	35
2.15	Soft sediment deformation in PRA section	36
2.16	Sandstone lenses in PRA section	37
2.17	Rootlets from PRA and MS sections	38

2.18	Pahau River B section log	40
2.19	Pahau River C section log	42
2.20	Waiau River section log	44
2.21	Volcanic dyke crosscutting WR section	45
2.22	Mount Holmes section log	47
2.23	Log imprint in the Mount Holmes section	48
2.24	Mount Saul A & B section logs	50
2.25	Matrix type and clast sorting graph with lithologies	52
2.26	Coal fragment with peripheral sulphur staining	53
2.27	Regular bedding in CH section	54
2.28	Shale Peak section log	55
2.29	Castle Hill section log	56

PROPOSED NOMENCLATURE

CHAPTER THREE

3.1	Provisional Cretaceous timescale 1995	63
-----	---------------------------------------	----

DEPOSITIONAL PROCESSES IN MARGINAL MARINE ENVIRONMENTS

CHAPTER FOUR

4.1	A modified Hjustrom diagram	72
4.2	The morphology and effects of a wave on the beach face	78
4.3	Fluidisation structures	81
4.4	The simplified morphology of a debris flow	83
4.5	Low density turbidity currents	86
4.6	High density turbidity currents	87
4.7	Intraclast breakup	90
4.8	Interpretative chart for the distribution of intraclasts within a bed	93

DEPOSITIONAL SETTING

CHAPTER FIVE

5.1	Fan delta depositional model for the Pahau River deposits	104
5.2	Gilbert-type fan delta model	106
5.3	Slope-type fan delta model	106
5.4	Shelf-type fan delta model	107

PROVENANCE

CHAPTER SIX

6.1	The five fossil zones of the South Island Torlesse Superterrane	114
6.2	Unadjusted and adjusted Pahau River deposit palaeoflow directions	121
6.3	Location map of thin section samples	122
6.4	QFL ternary plot for sandstone provenance	124
6.5	QFL comparison with other known Torlesse QFL values	125
6.6	Abbreviated statistical values of the Pahau River QFL analysis	125

ABSTRACT

The Pahau Terrane as part of the Torlesse Superterrane extends for over 30% of the New Zealand landmass. Although an unofficial type locality around the Pahau River has been proposed, it has never been adequately described or defined. One of the main goals of this research was to describe in detail the deposits of the Pahau River area in order to define the type locality.

In total ~900m of section was logged describing four lithofacies; mudstone, interbedded mudstone – sandstone, sandstone, and conglomerate. Two formation names and a group name are proposed and intended for widespread use. The Mt Saul Formation is proposed for coarse-grained conglomeratic lithofacies whereas the Ship Spur Formation is proposed for the combined fine-grained sedimentary lithofacies. The Pahau River Group encompasses these formations.

Stratigraphic logs clearly show coarsening and thickening upward, progradational sequences, at the tops of which either highly carbonaceous beds or rootlets can be observed. The bedding in the conglomerate lithofacies are dominated by bedload transport structures including large scale cross stratification, imbrication and clast support. Micro and macrofossil collection suggest a nearshore marine sequence yet rootlets suggest subaerial indicating a range from fully marine to terrestrial depositional environments, making them the only known terrestrial deposits in the Pahau Terrane. This suggests a fan-delta depositional setting. Very few bi-directional structures were observed, suggesting that these deposits were not influenced by wave reworking and tidal currents to any great degree but are fluvially dominated.

Thin section analysis of fine to medium sandstones suggests a transitional to mixed arc provenance. Measurable indicators suggest a palaeoflow direction towards the east to northeast. These results are similar to previous studies indicating the suitability of the Pahau River area as a type locality for the Pahau Terrane.

INTRODUCTION

CHAPTER ONE

1.1 - THE GEOLOGICAL FRAMEWORK OF NEW ZEALAND

The rock assemblage in New Zealand can be viewed as a series of tectonostratigraphic terranes. A terrane is an assemblage of rocks bounded by faults outside of which there is no exact correlative. Terranes can however be grouped together into "superterranes", or as "assemblages" which can also include superterranes. This is usually achieved by associating terranes based upon similar geochemical, petrological, or depositional nature.

The tectonostratigraphic framework in New Zealand is subdivided into two distinct provinces, the Eastern and Western Province. The Western Province is composed of two terranes, the Takaha and Buller Terranes suspected to be remnants of a Gondwanaland foreland basin (Cooper, 1989). The Eastern Province, depending on which nomenclature you accept, can contain up to fifteen terranes, two superterranes and three terrane assemblages. The most widely accepted nomenclature includes the Brook Street, Murihiku, Maitai – Dun Mountain, Caples – Waipapa, and Torlesse Terranes. The most recently published papers suggest that what have been known as the Subterrane of the Waipapa and Torlesse be elevated to the terranes based on their unique geochemical or petrological signatures. This elevates the Rakaia, Esk Head, Pahau and Waioeka Subterrane of the Torlesse Terrane and the Omahuta, Bay of Island, and Manaia Hill Subterrane of the Waipapa to Terranes. Thus the Torlesse and Waipapa become Superterranes (Black, 1996; Campbell and Grant-Mackie, 2000; Landis *et al.*, 1999). This elevated Terrane – Superterrane nomenclature has been adopted for this research.

The various superterranes and terranes of the Eastern Province can also be divided into assemblages based on their tectonic setting. The Brook Street, Murihiku and Maitai – Dun Mountain Terranes or Hokonui Assemblage have been widely inferred to represent accreted allochthonous oceanic arc sequence (Campbell and Grant-Mackie,

2000). These are separated from the Alpine Assemblage, which is composed of the Aspiring, Te Akatarawa, Kakahu, Rakaia, Esk Head and Pahau Terranes. The Alpine Assemblage is thought to represent deposits between the forearc and trench on the East Gondwana Margin (Landis *et al.*, 1999).

1.1.1 REGIONAL BACKGROUND

The Torlesse Superterrane is unanimously agreed upon by geologists to represent two juxtaposed continental arc trench deposits (Adams and Graham, 1996; Bradshaw, 1989; Campbell and Grant-Mackie, 2000; Kamp, 1999; Landis *et al.*, 1999; MacKinnon, 1983; Mortimer, 1995) in part due to the level and style of metamorphism as well as the high degree of deformation seen throughout the Torlesse. The Torlesse Superterrane is a fault-bounded sequence of complexly deformed strata composed of four petrographically distinct terranes. The Torlesse Superterrane is segmented into four units known as the Rakaia, Esk Head, Pahau, and Waioeka Terranes (figure 1.1).

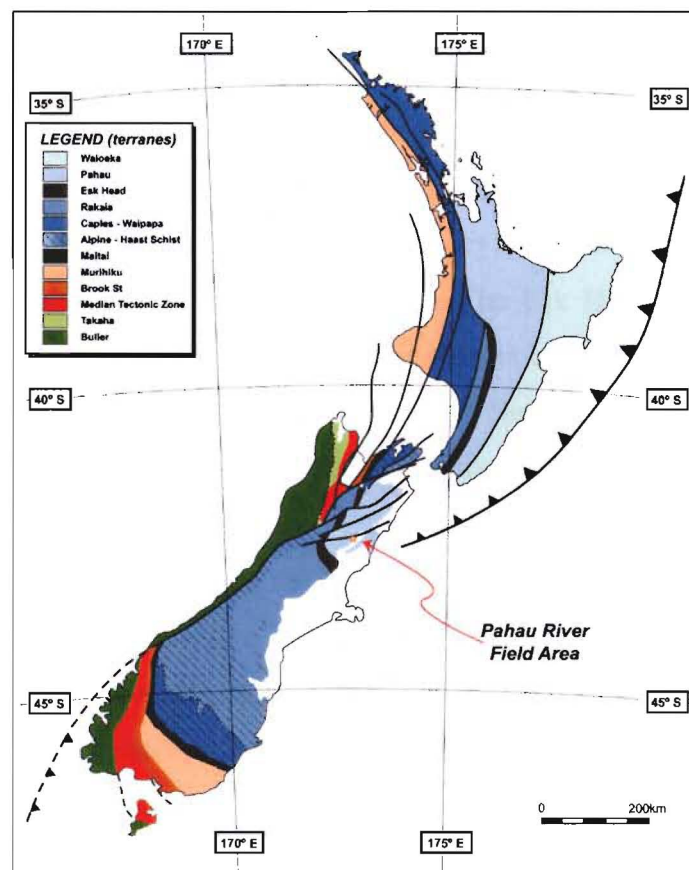


FIGURE 1.1 – The New Zealand Tectonostratigraphic Map. The eastern province includes the Torlesse Superterrane (Waioeka, Pahau, Esk Head, Rakaia Terranes), Waipapa–Caples, Maitai, Murihiku, Brook Street Terranes, the western province includes the Takaha and Buller Terrane. Notice the Median Tectonic Zone dividing the east and west provinces (Wandres, Unpublished).

Peter Andrews mapped the Pahau River area in the late 1970s as a supplement to palynological studies as the area was relatively undeformed and accessible. Since then the Pahau River area has been used as an *unofficial type locality* for the Pahau Terrane. The purpose of this study is to define the depositional setting for the area currently recognised as type locality for the Pahau Terrane.

1.2 THE TORLESSE SUPERTERRANE

The Torlesse Superterrane has been widely inferred by geologists to represent two juxtaposed Permian to Cretaceous accretionary wedges of a continental magmatic arc. The Torlesse is estimated to be at least 25km thick, although it may extend to the base of the continent that is just over 30km (Bradshaw, 1989; Campbell and Grant-Mackie, 2000; Mortimer, 1995). An accretionary wedge tectonic setting is widely accepted due to the pervasive syn- and post-depositional thrust faulting, normal faulting and folding commonly observed in the Torlesse Superterrane.

The Torlesse Superterrane is comprised of four terranes, the Rakaia, Pahau, Waioeka, and the Esk Head (figure 1.1). All of the terranes are present in the South Island except the Waioeka, which is present with the other three terranes in the North Island. The Rakaia and Pahau Terranes are interpreted as having formed in a supra-subduction zone tectonic setting as accretionary wedges (Campbell and Grant-Mackie, 2000; Kamp, 1999; Mortimer, 1995). The Esk Head Terrane represents a thin melange of sediments that separates the Rakaia and the Pahau Terranes along much of their contact. In several places the Esk Head Terrane is absent and large faults mark the boundary between the Pahau and the Rakaia Terranes (John Bradshaw pers. comm. 2001).

The Rakaia, Pahau and Waioeka Terranes are composed of predominantly marine sedimentary strata. The stratigraphies of these terranes contain enormous sequences of alternating mudstone and sandstones frequently interrupted by faults. Fine grained deposits include those formed from pelagic fallout, hemipelagic fallout, turbidity currents and debris flows. Uncommon conglomerate deposits, basic meta-volcanics, limestone and chert are also scattered about the terrane in limited quantities (George, 1992). The Esk Head in contrast is a melange primarily composed of blocks from an

ocean floor assemblage (basic volcanics, limestone, chert etc.) with matrix composed mostly of Pahau Terrane material or detritus (Campbell and Grant-Mackie, 2000; Silberling *et al.*, 1988).

Sedimentological differences between the Rakaia, Pahau and Waioeka Terranes are minor. Many geologists feel that sedimentologically the Pahau Terrane was deposited in a shallower environment than the Rakaia Terrane (Kari Bassett and Anekant Wandres, pers. comm. 2001). The older Rakaia Terrane has a generally higher ratio of sandstone to mudstone compared to the Pahau and Waioeka Terranes. Differences between the terranes are essentially petrological, with the Rakaia and Pahau Terranes representing feldsarenites and the Waioeka Terrane dominated by volcanic litharenites (Mortimer, 1995). The Pahau is distinguished from the Rakaia by having a significantly higher lithic content, this has been attributed to the autocannibalisation of the Rakaia into the Pahau (Bradshaw, 1989; Wandres, Unpubl. PhD Thesis)

The Torlesse Superterrane is believed to be almost completely submarine in origin, however, there are seven published very shallow marine to terrestrial locations scattered throughout the Rakaia Terrane (MacKinnon, 1983; Mortimer, 1995). MacKinnon (1983) estimated the approximate volume of terrestrial sediments within the South Island Torlesse Superterrane to be around 0.5%. There are no known terrestrial outcrops in the North Island Torlesse Superterrane (pers comm. John Bradshaw). Rocks formed by sediment gravity flows, principally turbidity currents with subordinate cohesive and cohesionless debris flows, dominate the Torlesse Terrane.

1.2.1 RAKAIA TERRANE

The oldest of the three terranes, the Rakaia, is bound in the south by the Caples Terrane, to the west by the Haast Schist, to the north by the Esk Head Terrane and to the east by oceanic crust. The Rakaia Terrane has the highest biostratigraphic definition containing the four oldest out of the five faunal zones within the Torlesse (MacKinnon, 1983).

Typically sequences of Rakaia Terrane are dominated by thick to very thick sandstone sediment gravity flow deposits >60cm thick (MacKinnon, 1983). Ratios of sandstone to mudstone tend to be 3:1 or 2:1 for the bulk of the terrane, this is usually represented by very thick sandstone sequences up to several hundred metres thick followed by much thinner mudstone deposits. Gradational sequences involving fining, coarsening, thickening or thinning upwards are also rarely observed (MacKinnon, 1983).

Deposition in the Rakaia Terrane during the Permian to the Late Triassic has been interpreted to represent deep-water marine deposits with localised shallow marine clastic sequences (Landis *et al.*, 1999). These deposits have primarily been produced as a result of oblique subduction along an ocean-continent convergent margin causing the production of an accretionary prism (Landis *et al.*, 1999; MacKinnon, 1983; Mortimer, 1995).

The Rakaia Terrane folded and amalgamated with the Caples Terrane during the beginning of the Jurassic (Bradshaw, 1989). Deformation and metamorphism within the Rakaia Terrane increase toward the south and west, from zeolite through to prehnite-pumpellyite metamorphic facies before eventually grading into the Haast schist (MacKinnon, 1983). The pattern of deformation seen within the Rakaia Terrane has been attributed to a syn-depositional compressional tectonic regime that was influencing this area during the Permian to Late Jurassic. An increased episode of compression just before subduction ceased during the Early Cretaceous caused further deformation in the form of thrusting and folding (Bradshaw, 1989).

The ages of deposition, burial, amalgamation, and metamorphism have been deciphered by numerous methods. These have primarily been discovered by isotope geochemical methods including Ar-K, Ar-Ar, Rb-Sr, and U-Pb dating, heavy mineral rare earth element analysis have also been utilised (Adams and Graham, 1996; Adams and Kelley, 1998; Ireland, 1992; Kamp, 1999; Nemec, 1990; Roser and Cooper, 1990; Smale, 1997). More generalised dating methods include macrofossil studies, the most comprehensive of which was done by MacKinnon (1983). Microfossil and palynological studies provide greater definition of the sediment age, the identification of spores, pollens, dinoflagellates, and foraminifers have all helped pinpoint different

stages and events in the evolution of the Rakaia (MacKinnon, 1983; Raine, 1977; Silberling *et al.*, 1988).

1.2.2 ESK HEAD TERRANE

The Esk Head Terrane (or melange) is a chaotic assemblage of limestone, chert, pillow basalts and fine-grained mudstones typically observable in a 10-20km belt separating the Rakaia from the Pahau (Silberling *et al.*, 1988). The mudstone matrix of the Esk Head is predominantly composed of Pahau Terrane material, although Rakaia sediment may form a portion of the matrix near the contact with the Rakaia Terrane. Blocks of well-indurated sandstone located near the contact with the Rakaia Terrane are thought to be from the Rakaia Terrane (John Bradshaw, pers comm. 2001). The Esk Head is interpreted as being composed of an ocean floor assemblage that was subducted beneath the Gondwana margin on to which the Pahau accretionary wedge was deposited (Bradshaw, 1989). Limestone fragments from the Esk Head return ages of Late Triassic to Late Jurassic (Silberling *et al.*, 1988). It is hypothesised that this material was accreted to the base of the Torlesse then subsequently intruded in the form of elongate diapiric bodies or was faulted into place (Bradshaw, 1989); Mark Rattenbury, pers. comm. 2000). No rock older than Late Triassic has been found in the Esk Head Terrane, this is interesting because the adjacent Rakaia Terrane has been interpreted as Permian to Late Triassic. There are several explanations for the lack of older material; (1) material laid down on the plate older than Late Triassic may have been subducted too far to be accreted, or (2) that no datable material was formed prior to Late Triassic, or (3) simply no datable material from that period has yet been found.

The Esk Head Terrane has yet to be found to the west of the Pahau River (Mark Rattenbury, pers. comm. 2000). The Esk Head Terrane has therefore been extrapolated from known locations to the southwest of the Pahau River study area north towards the Hope Fault. The location of the Esk Head is currently being surveyed as part of the Institute of Geological and Nuclear Sciences (IGNS) QMAP project. It is possible that the Esk Head is represented only by a fault trace in that location.

1.2.3 PAHAU TERRANE

The Pahau Terrane is located to the northeast of the Esk Head and Rakaia Terranes and is the youngest of the three South Island terranes. The age of the Pahau Terrane has been interpreted to be Early Jurassic to Cretaceous (MacKinnon, 1983). It encapsulates the transition from a convergent to an extensional tectonic regime thought to have occurred in the late Cretaceous (c. 105 ± 5 Ma; Bradshaw, 1989). Located further away from the accretionary contact with the Caples Terrane and the Alpine schist, the metamorphic rank is lower only reaching zeolite facies.

The younger Cretaceous sediments of the Pahau Terrane differ only slightly from Rakaia Terrane sediments, with many sequences having sandstone to mudstone ratio around 1:1 (MacKinnon, 1983). Thick sandstone dominated sequences still exist throughout all of the terranes in the Torlesse Superterrane. This may suggest a subtle change of depositional environment, sediment source, or tectonic setting. Age dating techniques for the Pahau Terrane do not differ from those mentioned for the Rakaia Terrane.

Although the Pahau Terrane most likely represents a separate juxtaposed accretionary wedge it is remarkably similar to the Rakaia wedge (Bradshaw, 1989). The Pahau Terrane has a comparative QFL composition with slightly lower feldspar and higher lithic contents (MacKinnon, 1983). The higher lithic content of the Pahau Terrane sedimentary rocks has been ascribed to the partial cannibalisation of Rakaia Terrane (Wandres, Unpubl. PhD Thesis). If the Rakaia Terrane was exposed subaerially and eroded it would explain why there are more lithics in the Pahau Terrane. Relatively low feldspar percentages can be explained by invoking a cannibalistic relationship with the Rakaia Terrane as the availability of lithics would have much higher than that of feldspar.

1.2.4 PROVENANCE RELATIONSHIPS

Irrespective of age and location Torlesse sediments have a relatively similar composition. Five macrofossil faunal zones show a relatively simple pattern of

northeasterly younging crudely defining the age of the Torlesse (MacKinnon, 1983). The general absence of macrofossils throughout the Torlesse has made it difficult to define the age accurately at any point. Macrofossils are not useful in defining the terranes as the fifth fossil zone represents both the Pahau and Waioeka Terranes, but they are useful for provenance studies in the Rakaia (MacKinnon, 1983).

The most discernible difference between the Torlesse Terranes is the petrological composition, this is observed by plotting the varying ratios between volcanic and sedimentary lithics (Bradshaw *et al.*, 1993). The Rakaia Terrane has a relatively high percentage of volcanic lithics whereas the Pahau Terrane has a relatively high percentage of sedimentary lithics. This is one of the reasons why it is thought that the Pahau Terrane may be partly composed of eroded from Rakaia Terrane (Wandres, Unpubl. PhD Thesis).

The provenance of the Torlesse has been somewhat of an enigma over previous years. To date there is no published account that accurately defines the source area though sources including Victoria Land (Roser and Korsch, 2000), Marie Byrd Land (Andrews *et al.*, 1976), New England Fold Belt Northern Queensland (Adams, 1998; Campbell and Grant-Mackie, 2000), Western Province and Median Tectonic Zone (NZ) (Wandres, Unpubl. PhD Thesis), and SE China (Adams, 1998). Ireland (1992) proposed studying the geochemistry of igneous clasts within uncommon Torlesse conglomerates, as it was believed this could provide the solution to this problem. This is part of a current study by Anekant Wandres to decipher the provenance of the Torlesse. Preliminary results tend to suggest that some of the source area was probably in located in the Western Province (Wandres, Unpubl. PhD Thesis).

1.3 STUDY AREA

The study area is situated on Lochiel Station and Medway Station, located on the southern side of the Hanmer Basin, North Canterbury, New Zealand. The perimeter of the study area can traced by a line drawn approximately from the Waiau Ferry Bridge in the northeast to Castle Hill then to Mt Cropp in the southeast, from Mt Cropp westward to Windy Knob, northeast to Pahau Pass then north to the

intersection of Gabriel’s Gully and the Waiau River, finally east back to the Waiau Ferry Bridge (figure 1.2).

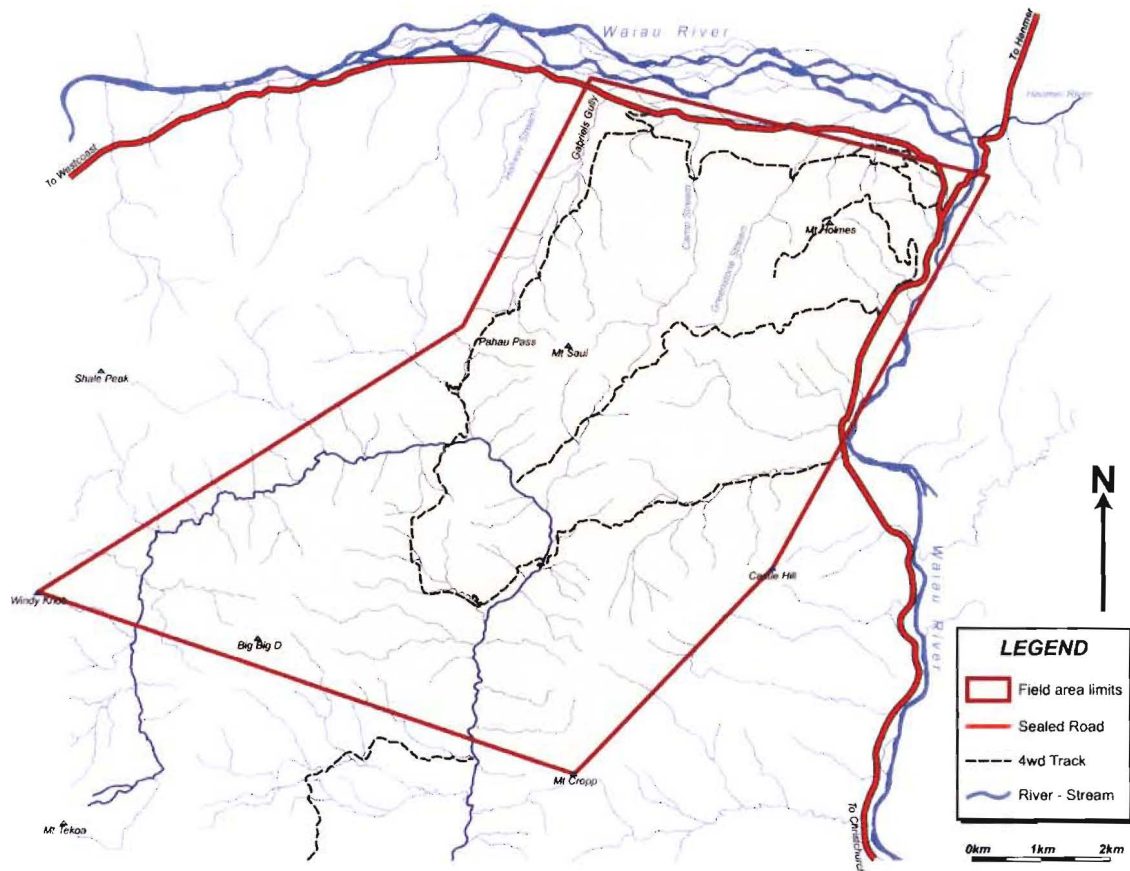


Figure 1.2 – The Pahau River study field area, with access routes.

Numerous major faults segment the study area into several fault blocks predominantly trending NE – SW or E – W. The largest of the northerly trending faults include the Pahau Pass Fault, the Cabbage Tree Fault and two other as yet unnamed faults (figure 1.3). The unnamed faults splay around the Mt Saul conglomerate together forming the Mt Saul fault duplex proposed here. Several smaller northerly trending faults also dissect Mt Holmes, and are possibly related to the Cabbage Tree Fault.

Two major faults run roughly perpendicular to these older faults; the Hope Fault, which is the northern boundary of the field area and a previously unnamed fault that runs through grid reference NZMS 260 -M32 893 385 to 838 396 here known as the Mt Cropp Fault (figure 1.3). The Hope Fault is the farthest south of four major faults that splay off the Alpine Fault to create the Marlborough Fault system (Wood *et al.*, 1994). The fault system stretches for a total of 230km on land from the Alpine Fault west of Arthurs Pass to Kaikoura before disappearing offshore. The Hope Fault

displays dextral strike-slip motion that manifests itself north of the study area in the form of a pull-apart basin (Wood *et al.*, 1994).

The rocks in the study area strike on average ~50° NE ranging between 340° NW and 110° E, dipping on average at ~45° to the SE ranging between 30° and 70°. Overturned bedding exists in the Pahau River between Pahau Pass fault and the Mt Saul Fault duplex, strike and dip relationships are similar although dipping to the northwest. Bedding orientations are most clearly seen in the numerous sandstone strike ridges that dominate the topography. Other topographically significant features of the study area include the several conglomeratic bodies scattered through it. Mt Saul, the largest of these is an unusually large conglomerate body for the Torlesse Superterrane (John Bradshaw, pers. comm. 2001). Other conglomerates in the area worth mentioning include the Mt Holmes conglomerate, a large conglomerate body just to the east of Mt Saul and several smaller lenses scattered throughout the area. Another conglomerate body outcrops just to the southwest of the field area at Mt Tekoa. Mt Tekoa, Mt Holmes and Mt Saul run in a line roughly along strike from each other, and are thought to be correlative to conglomerate bodies observed on the northern side of the Hope Fault 22km to the east (Freund, 1971). As there are faults between each of the major conglomerate bodies it is not possible to ascertain whether or not they were actually deposited laterally from each other. It is possible conglomerate deposition was more or less in the same place.

Bradshaw and Andrews (1980) describe the structure of the area as reflecting a simple upright syncline plunging to the southwest. Stratigraphic sections are situated within at least four fault blocks. Though the faulting is often quite complex, the offsets on faults that dissect the core of the study area do not invalidate an interpretation of the depositional setting. Deformation levels typically increase with decreasing grain size and proximity to major faults. Unfortunately this means that areas dominated by mudstone are often quite deformed and of little use sedimentologically other than to say that energy levels at the time of deposition in this area were probably low.

Although conglomerate deposits are interesting they are particularly uncommon within the Torlesse Superterrane and do not dominate sedimentation in the Pahau

River area. Massive sandstone, massive mudstone or an interbedded mixture of sandstone and mudstone dominate sedimentary facies in the area.

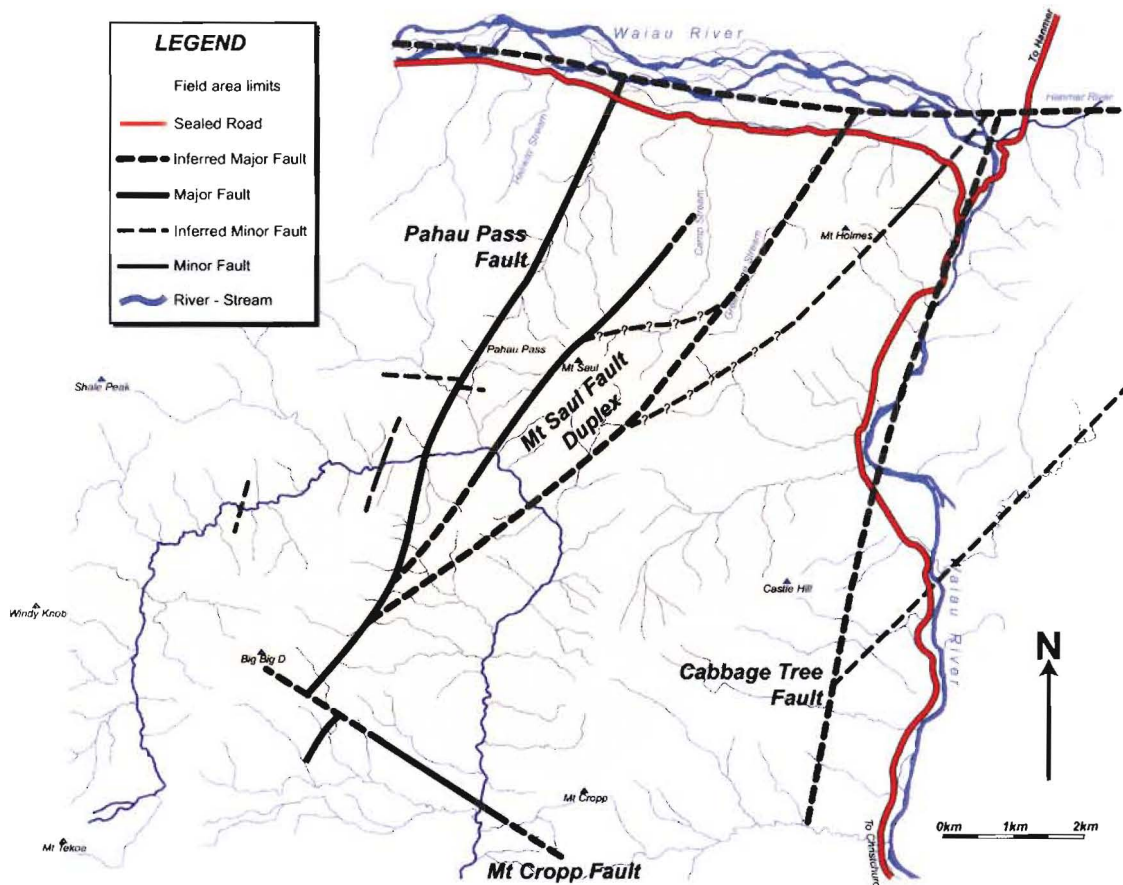


Figure 1.3 - Structural Map for the Pahau River Field Area, notice the fault segmentation around Mount Saul.

1.4 PREVIOUS WORK

The first work on Pahau River deposits was done by various reconnaissance studies in the late 19th and early 20th century (Haast, 1871; McKay, 1885; Fyfe, 1931 & 1935). Detailed sedimentological studies include field mapping and reconnaissance section logging (Bradshaw and Andrews, 1980; Pescini, 1997). These also suggest a palaeoflow direction originating in the northwest taken from crossbedding, imbrication, and uncommon flute casts.

Two depositional environments have been proposed for the Pahau River sediments. An alluvial-deltaic marginal marine facies assemblage was proposed by Bradshaw and Andrews (1980) citing the abundance of plant stems and organic matter in the area as support for their theory. Subsequent sedimentological examination of the area

suggested a deep marine environment dominated by channelised mass-flow deposits, probably within a submarine canyon (Pescini, 1997).

Several provenance studies have focused on the area. Studies include examining igneous clast geochemistry from the Mt Saul conglomerate, QFL analysis of pebble-sized sandstone clasts from conglomerates, and QFL analysis of sandstone beds (Bradshaw and Andrews, 1980; Dean, 1993; Pescini, 1997; Wandres, Unpubl. PhD Thesis).

Geomorphological features in the area relating to changes in grainsize due to weathering rates (e.g. conglomerates verses mudstone) were used to decipher offsets on the Hope Fault (Freund, 1971).

Various palaeontological studies have been undertaken in the Pahau River area producing depositional dates. Siberling *et al.* (1988) examined blocks of crinoidal limestone taken from Mt Saul. IGNS are preparing a current palaeontological study of the area on spores and pollens extracted from the sediments in the Pahau River. Palynological data from IGNS is giving preliminary dates of latest Barremian (?) to early Albian (Ian Raine, in prep.).

1.5 OBJECTIVES AND METHODOLOGY

The main objective of this study is to formally define the formations of the informal type locality for the Pahau Terrane. Secondary objectives include detailed geological mapping of Mt Saul conglomerate and directly adjacent lithological units, reconnaissance mapping of other areas and provenance studies. Several methods were employed to achieve this, including the mapping of lithofacies and tectonic features, sedimentological section logging and thin section analysis. The majority of the fieldwork was undertaken during the summer and autumn months of 2000.

Rock assemblages in the Pahau River area have been separated into four different lithofacies. Three lithofacies have been defined by predominance (>80%) of a certain grainsize range; conglomerate, sandstone, mudstone. The fourth lithofacies, termed the interbedded mudstone – sandstone facies, is defined as having 20% to 80% of

material $> 4\phi$ with the approximate inverse percentage of material from -3ϕ to 4ϕ . All lithofacies, in order to be recognised and mapped, had to show these characteristics over an interval at least 10m thick and with significant lateral continuity.

Stratigraphic section logging coincided with the completion of the initial survey for undeformed sections. Several relatively undeformed sections were immediately identified in and around the Pahau River including several well-exposed sections on Mt Saul. Other sections logged include those at Mt Holmes, Waiau Ferry Bridge, Castle Hill, and a tributary of the Pahau River near Shale Peak. Section logging included the collection of information such as deformation level, outcrop clarity, sedimentological (bedforms, palaeoflow indicators etc.), colour, induration, thickness, contact type, grain size, sorting, rounding, composition and other miscellaneous features (i.e. small cross cutting dykes). Section logging was undertaken at 25cm, 10cm, or 5cm increments depending primarily on deformation level. Thin beds and laminae were either grouped together to form larger units or included as “contact beds” between thicker sedimentary units. In most sections beds were rounded to the nearest 5 or 10cm depending on deformation level and clarity needed.

To test the current theory, that the source of the Pahau River sediments was from an active continental margin, a small provenance study was undertaken. Samples were collected in the fine to medium sandstone size range for thin section analysis. Unfortunately the lack of unweathered fine – medium sandstones in the field area made sample collection difficult. As a result very fine sandstone samples were included, these were analysed and compared with coarser fine and medium sandstones to determine their validity. All of the sections analysed were then compared and contrasted with other locations in the Pahau and Rakaia Terranes.

Other research methods included extensive reviews of published and unpublished literature, as well as contacting other geologists who are and/or have been working on the Pahau Terrane type area.

LITHOFACIES AND STRATIGRAPHY

CHAPTER TWO

2.1 INTRODUCTION

The rock assemblage present within Pahau River area can be divided into four broad lithofacies. Each lithofacies can be found grading into or interfingering with one another typically over a distance of several metres or less.

The following four subdivisions were chosen as most representative –

- Mudstone
- Interbedded Mudstone – Sandstone
- Sandstone
- Conglomerate

Lithofacies mapping of the Pahau River area has been done twice in the past 25 years. In the late 1970s, Peter Andrews mapped the area dividing lithologies into an alluvial deltaic association and a flysch association distinguishing massive sandstone, thickly and thinly bedded flysch and mudstone flysch (Bradshaw *et al.*, 1980) although the map was never published. Pescini (1997) mapped the area differentiating conglomerates, and massive sandstones bodies with the remaining lithologies mapped as undifferentiated sediments. Lithofacies mapping from this study supports that of Bradshaw and Andrews (1980) over Pescini (1997).

2.2 METHODOLOGY

Fieldwork was carried out in several one to three week periods over the year 2000, consisting primarily of logging stratigraphic sections, lithofacies mapping and sample collection for provenance studies. The objective was to define the characteristic lithological assemblages and the depositional setting of the Pahau River area with the

intent of creating a “Pahau River Group” and an official type locality for the Pahau Terrane.

2.2.1 STRATIGRAPHIC SECTION LOGGING

In total ten stratigraphic sections were logged, comprising a total of 877m of non-correlative strata. Varying scales were used to log each section, using a thickness threshold under which beds were lumped together. Scales were predefined depending on deformation levels, location and the usefulness of the section.

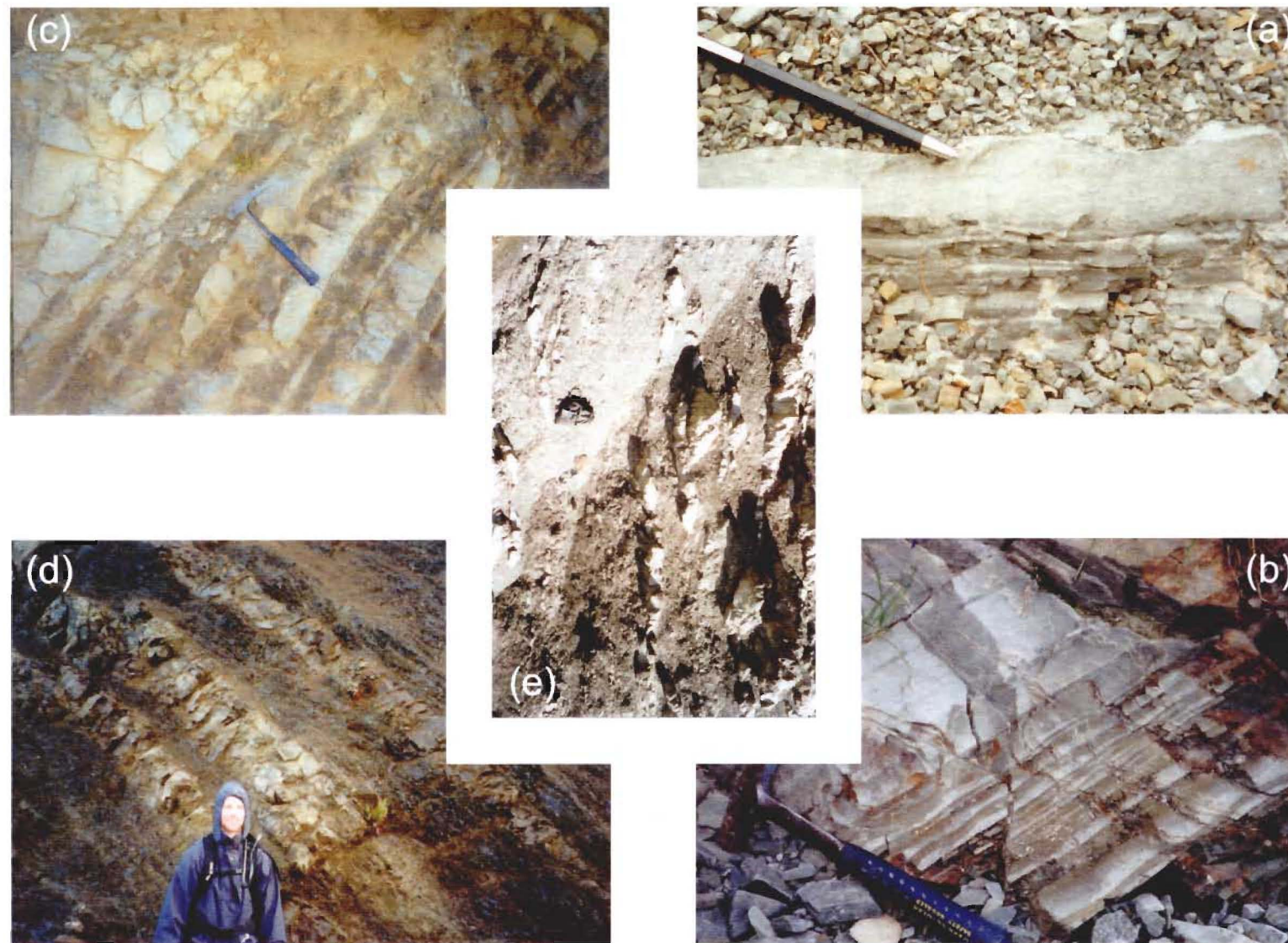
Thickness thresholds were applied by grouping thin beds of similar nature together as a unit large enough to be logged. Where this was not possible (e.g. a single 2cm thick bed located between two 50cm beds) the thin bed was identified as a contact bed. Sections were logged at one of three different scales; ultra high definition 5cm threshold, high definition 10cm threshold or low definition 25cm threshold. To increase logging and data entry efficiency bedding thickness was rounded to 1cm (ultra high), 5cm (high) and 10cm (low).

The bedding structure, texture and composition defined each bed where possible. Key identifying features included grainsize, grading, sorting, rounding, induration, bedding structures, composition and rare features (e.g. fossils, rootlets, etc.). In the case of the conglomerate facies additional features such as matrix percentage/composition and sphericity were also included. Colour was not found to provide useful additional help as weathering in many locations discoloured beds. In general, non-conglomeratic beds were light to dark grey, whereas conglomerates varied in colour relative to their composition.

Deformation varied so markedly over extremely short distances that these were marked in graphically next to each stratigraphic column. Five levels of deformation were identified with gradations between –

-
- Level 1** – No apparent deformation (figure 2.1a)
- Level 2** – Minor deformation (figure 2.1b)
- Poorly developed cleavage and fracturing in mudstone.
 - Minor fracturing in sandstones and conglomerate.
- Level 3** – Moderate deformation (figure 2.1c)
- Well developed cleavage, extensive fracturing with some loss of internal structure in mudstone.
 - Moderate fracturing in sandstones and conglomerate.
- Level 4** – Extensive deformation (figure 2.1d)
- Total loss of internal structure, deformation becomes ductile in mudstone, interbedded sandstone becomes boudinage.
 - Thick to thickly bedded sandstones become highly fractured and lose internal structures.
 - Conglomerates become highly fractured with minor faults up to 2m displacing individual beds.
- Level 5** – Extreme deformation (figure 2.1e)
- Total loss of structure for mudstone and interbedded mudstone and sandstone (i.e. bedding is non-existent), boudinage is non-connective and widespread.
 - Sandstones are extremely fractured and bedding is not identifiable.
 - Conglomerates become highly faulted and no laterally extensive bedding planes are readily recognisable.
-

Figure 2.1 – Five levels of deformation can be identified within the deposits in the Pahau River area, increasing deformation levels can be observed from level 1 (a) to level 5 (e).



Outcrop quality is often something that is overlooked when developing a useful stratigraphic section. How useful is a section based upon a 1m wide strip of weathered river bank as opposed to an unweathered 20m wide slump scarp? Outcrop quality was defined using a three-tiered system that considered outcrop width, vegetation (e.g. lichen, grass etc.) and loose debris.

Level 1 – At least 5m of lateral bedding fully exposed with no vegetation or debris.

Level 2 – At least 1m of lateral bedding and may be partially obscured with lichen, debris etc.

Level 3 – Less than 1m of lateral bedding, almost or completely obscured by vegetation or loose debris, however, structure, texture etc. are readily identifiable.

Outcrop quality is shown next to deformation level in each of the stratigraphic sections (Appendix I), the presence of weathering is shown as white diagonal lines across outcrop quality. Weathering often hides the true nature of bedding. In well-exposed sections along riverbanks bedding can appear to look like massive mudstone but in lower river worn sections they were clearly thickly to finely laminated coarse siltstone laminations. River worn sections were not available at all localities where mudstone and sandstone units were logged.

2.2.2 FIELD MAPPING

Field mapping concentrated on an area bounded by four major faults. These were the Hope Fault, Pahau Pass Fault, Cabbage Tree Fault and the Mt Cropp fault (figure 1.1). Mapping was achieved by sketching lithofacies, tectonic and man-made structures onto a collage of aerial photos covered with mylar plastic. The collage was compiled on a computer where scanned images were pasted together inside of a picture-editing package called Stitch Master Pro. The collages were made from aerial photos 1799(1-10), 1800(1-11), 1801(1-9) and 1802(1-9) from the 1950 national aerial photo archive. After the lithofacies map was drafted in the field it was scanned into the computer and retraced to produce the final map (figure 2.2).

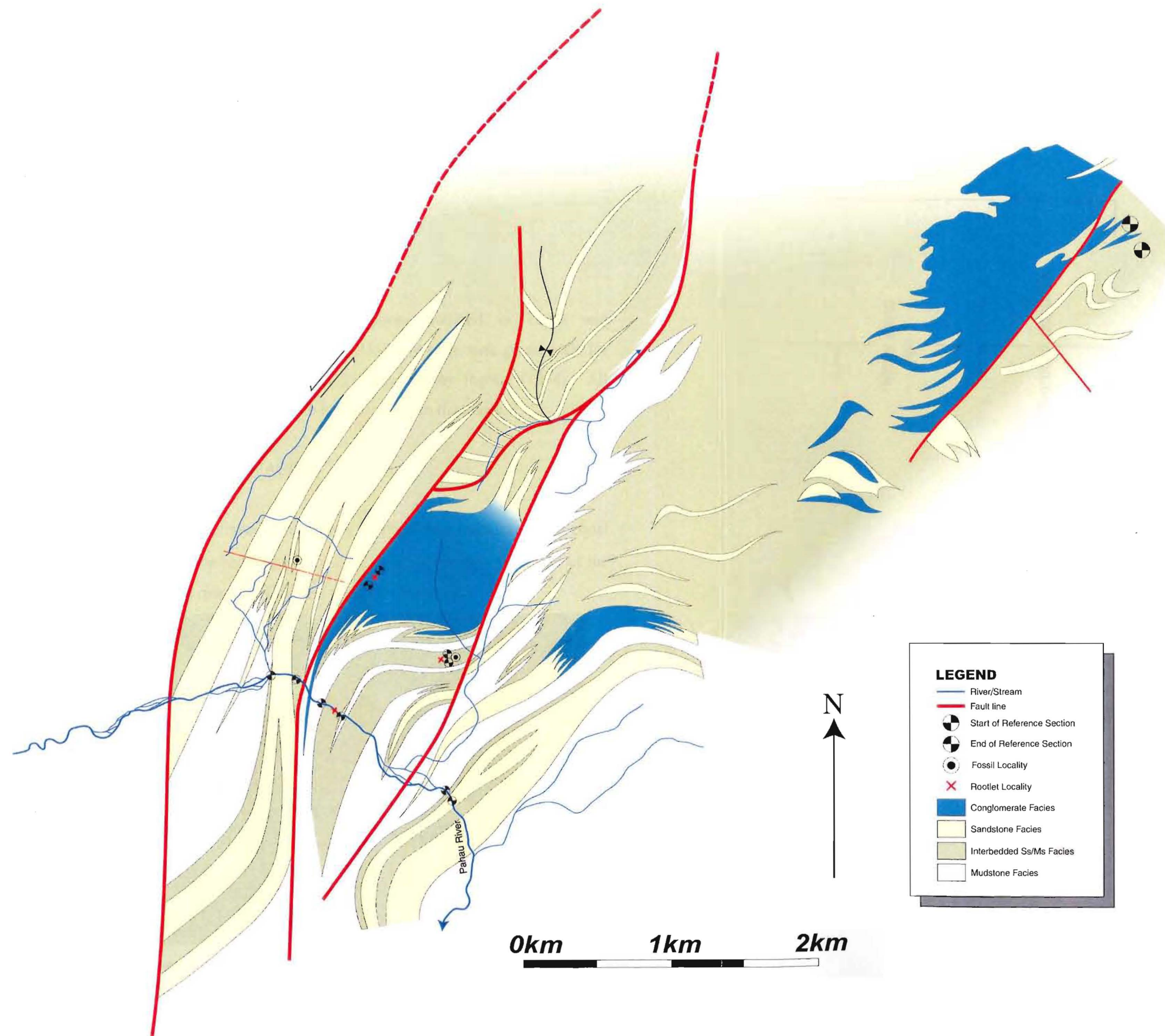


Figure 2.2 – A lithofacies map of the Pahau River area with selected stratigraphic section locations.

Mapping was carried out primarily along vehicle tracks, river cuts and ridgelines as vegetation tends to cover almost everything else. Lithofacies were interpolated between outcrops using aerial photo interpretation, topographic change, though strikes and dips were the most important techniques in data retrieval. Included on the map were depositional setting indicators such as fossil, rootlet and stratigraphic section localities as this is one of the objectives of this thesis. Sample localities for provenance work were chosen for their low weathering, deformation levels and grainsize.

2.3 LITHOFACIES DESCRIPTION

Terminology here follows lithological descriptions outlined in Lewis and McConchie (1994). Grainsizes are given by the Udden-Wentworth grade scale for grainsizes. Bed thicknesses follow terminology described by Ingram (1954). All facies descriptions relate to a set of strata no less than 10m in thickness.

2.3.1 MUDSTONE LITHOFACIES

The mudstone facies was defined by containing >80% of material less than or equal to 4ϕ , dominated by massive bedding (figure 2.3). It outcrops best in the bed of the Pahau River and along the many 4WD access track cuts in the area.



Figure 2.3– Mudstone lithofacies in the Pahau River (lower section Pahau River B – Appendix I), notice the high deformation levels, boudinage sandstone is common within this lithofacies.

The thickness of sub-4 ϕ bedding was often quite difficult to define. Bedding structure and texture were extremely difficult to observe at this grainsize especially grading, sorting and the presence or absence of laminations. Inability to distinguish bedding due to the absence of bedforms and the uniformity of grainsize makes true bed thickness of massive mudstone beds next to impossible to define.

Massive mudstone beds were typically thinly to thickly bedded, though a ~15m thick bed was observed by Pescini (1997). These beds were commonly defined stratigraphically above and below by the presence of thinly bedded, massive or normally graded, very fine sand (figure 2.4). Bedding within this facies appeared sheet-like with the exception of the some clusters of coarser sediments that appeared lensoidal.



Figure 2.4

Typical undeformed mudstone lithofacies sediments, massive mudstone was interrupted at regular intervals by massive or normally graded sandstone, backpack for scale is approximately 25 x 40cm.

Up to 20% of this lithofacies was composed of lithologies other than mudstone including pebbly mudstones, muddy sandstones and sandstones all of which were frequently observed within this lithofacies.

Pebbly mudstones formed in beds up to 10m thick that could often be observed to wedge out laterally from adjacent conglomerate bodies. No internal bedding structures were apparent within these deposits and clasts were evenly distributed within beds. Grains were observed having a bimodal size distribution, clay to silt and granule to very coarse pebble with rare boulders. The average pebble clast size (D50) was typically 30 – 60mm. Pebbles were typically very well rounded though granules

and fine pebbles were commonly sub-rounded. Clasts of igneous (intrusive and extrusive), sandstone, vein quartz and chert were observed. Clasts were polished to varying degrees, sandstones were the least polished, vein quartz and igneous pebbles being the most.

Muddy sandstones were usually found in close proximity to pebbly mudstones. These exhibited similar geometries to pebbly mudstones and also lack internal structures, although bedding tended to be thinner (< 3m). Grainsizes ranged up to granule though 70-90% of clasts were typically mudstone to fine sandstone. Composition was practically indistinguishable from pebbly mudstones, although rounding differed ranging from sub-angular to well-rounded. Due to their poorly sorted, massive nature and location relative to pebbly mudstones it is highly likely that these were sourced, transported and deposited in much the same way.

Sandstones in this lithofacies were typically normally graded though massive beds were present. Bed thicknesses appeared to range from thin laminae through to relatively uncommon thick beds (30-40cm). Internal bedding structures were present in the form of cross-stratification, asymmetrical ripples and rare flute casts. A sandstone dyke was also present at one location observed to intrude through two beds above it.

Mudstone lithofacies lacking deformation can be observed in the Castle Hill and lower Pahau River A sections (Appendix I; figure 2.28; figure 2.13). Muddy sandstones and pebbly mudstones in laterally extensive geometries were absent from all logged sections. These lithologies typically occurred as slightly to moderately deformed horizons within highly deformed inner cores of substantially thick mudstone lithofacies, located between coarsening and thickening upwards sequences.

2.3.2 INTERBEDDED MUDSTONE – SANDSTONE LITHOFACIES

The interbedded mudstone – sandstone lithofacies was defined as having 20% to 80% of material > 4 ϕ with the approximate inverse percentage of material from -3 ϕ to 4 ϕ . The least weathered and deformed example of this lithofacies can be seen in the

Pahau River at grid reference NZMS 260-M32 857 432. This location was logged as mid to upper Pahau River A (figure 2.13).

Figure 2.5

Interbedded
mudstone
sandstone facies
sediments in the
Pahau River,
Hammer (25cm
long) for scale.



The interbedded lithofacies was the most widespread lithofacies and was most easily observed in ridgelines, tracks and river cuts (figure 2.5). When the interbedded lithofacies was stratigraphically above or below the mudstone lithofacies, it exhibited a lensoidal pattern (figure 2.2). Interbedded mudstone – sandstone lithofacies interfingered or graded into or out of the sandstone and mudstone lithofacies. Bedding within this lithofacies typically appeared sheet-like, although clusters of massive and normally graded sandstones commonly appeared lensoidal.

The lithofacies was dominated by alternating thinly to thickly bedded, normally graded, very fine sandstone to mudstone or massive sandstone with thinly bedded massive mudstone beds. Mudstone percentages within normally graded sandstone beds were typically proportional to sandstone thickness. Mudstone generally ranged from <1% to 30% of the total thickness. It was impossible to observe by the naked eye a contact between sandstone that grades normally into mudstone and a massive mudstone unit above it, potentially deposited by a different depositional event. The average percentages of mudstone in normally graded beds around a great thickness of massive mudstone were occasionally used to suggest gradational contacts between massive mudstone beds underlying normally graded beds. One example of this was located in PRAD₀₃ at 11710cm (Appendix I) where a normally graded sandstone bed

graded into massive mudstone. In this instance the massive mudstone above was thicker than the sandstone unit below, it was inferred that the massive mudstone here was likely to be caused by a different event so a gradational contact was suggested in PRAD₀₃ at 11735cm.

Bedding thickness typically varied with proximity to the other facies. Generally ranging from thinly to very thickly bedded, although very thick beds were uncommon unless closely bordering the sandstone lithofacies. Thin to thick, normally graded coarse siltstone laminations were commonly observed near the mudstone lithofacies, but less commonly observed near the sandstone lithofacies.

Sandstone deposits were moderately to well sorted, angular to sub-rounded and very well indurated. Exceptions to this were observed when the average grainsize increased past very fine sandstone. Coarser sandstones were usually poorly to moderately sorted and sub-angular to well rounded.

An extensive array of bedforms can be observed within this lithofacies. Bedforms include flame structures, load structures, convolute bedding, parallel laminations, planar laminations, ripples (asymmetrical, symmetrical, climbing), and crossbedding. Flame structures were uncommon tending to be observed more frequently at the base of thinly bedded units. Flame structures were typically composed of mudstone sized grains and were not usually larger than 30mm high. Load structures were slightly more common and have a widespread distribution. Convolute bedding was particularly rare, observed only twice in the field area, both times in a bedding sequence reminiscent of a classic "bouma sequence". The abundance of structures associated with deformation of softer underlying sediments infers that the deposition was exceptionally rapid.

Parallel laminations were observed in sub-medium grained sandstones manifested as very fine sand laminations, and in mudstones as silt laminations.

Asymmetrical ripples were the most common bedform in this lithofacies. Symmetrical ripples were observed at one location, as were climbing ripples. All observed ripples tended to have wavelengths between 100mm and 300m and

amplitudes generally less than 25mm. Crossbedding was not uncommon within thin to medium beds but was observed rarely in thick and very thick beds.

Numerous palaeoflow indicators were located and measured including flute casts, tool marks, preferred orientation of organic matter, three dimensional flame structures and ripples.

Organic matter content was almost always particularly high in this lithofacies. Carbonaceous material was preserved in the form of flattened plant fragments, carbonaceous grains, laminations, logs, and occasionally as rootlets. Carbonaceous material typically increased with bed thickness and was not commonly observed within thinly bedded units, rarely seen within mudstones.

Partially recrystallised fossils (figure 2.6) and fossil casts were observed at two locations within this facies. The fossils appeared to be bivalves although unfortunately the absence or recrystallisation of shell material prohibited a more refined identification.



Figure 2.6 – Macrofossil within massive sandstone bed at the Mount Saul C section, note the partial recrystallisation of the shell, approx. 5cm long. Also notice the planar lamination.

Two minor lithologies were infrequently present within this lithofacies, conglomerates and pebbly sandstones. Pebbly sandstones at the outcrop scale were observed in narrow trough-like geometries usually less than 200cm wide by 100cm thick. Poorly-sorted mudstone to coarse pebble clasts were well rounded to sub-angular in nature. High concentrations of intraclasts (commonly referred to as ripup clasts) were observed within each channel structure. Channel structures were typically only filled with a single bed that grades normally. Pebble clasts were

concentrated basally and became smaller and disseminated upwards; intraclasts also increased upwards.

Uncommon conglomerate beds were lensoidal in shape and often represented beds interfingering from conglomerate lithofacies. This was most readily observed at Mt Holmes where the interbedded lithofacies graded into the conglomerate lithofacies (c.f. MH figure 2.21). Bedding was thick to very thick, with maximum observed thickness of ~100cm. Conglomerates were clast supported or matrix supported, moderately-sorted to poorly-sorted, sub-rounded to well-rounded and well indurated. Grainsizes varied from granule to coarse pebble, matrix varied between mudstone and sandstone or both. Clasts composed of igneous (intrusive and uncommon extrusive), sandstone, vein quartz and chert were observed in varying degrees.

2.3.3 SANDSTONE LITHOFACIES

The sandstone lithofacies was defined as having >80% of the clasts between 4 ϕ and -3 ϕ . The best examples of this lithofacies can be observed to the west of Mt Saul in the form of three major strike ridges.

This lithofacies often occurred in very large, elongate, lensoidal bodies up to approximately 5km in length and 400m thick (figure 2.7). Very thick sandstone beds dominated the sandstone facies. Beds with significant lateral continuity unchanging in lithology or character were observed up to 26 m thick. It was unlikely that beds of this thickness represented one depositional event but rather were deposited by many through a process called amalgamation (Walker 1979). Amalgamation occurs when a flow erodes down into previously deposited bed and welds onto it, two beds will then appear to be one bed if the grainsizes were essentially the same. Scour surfaces are particularly common within the sandstone lithofacies throughout the whole field area.

Bedding was typically massive, although rapid normally graded bedding occurred. Mudstone deposits rarely exceeded 20% of the total thickness of any normally graded bed within this lithofacies. Carbonaceous material was often observed in moderate to high levels and several beds had concentrations of carbonaceous material above 60%.

Plant debris were observed in thick massive sandstones with long axes commonly preserved in the direction of flow.



Figure 2.7 – Massive sandstone lithofacies outcropping near the Waiau Ferry Bridge, dark lines diagonally cutting the sandstone body are thin to thickly bedded mudstone units, the bright green tree in the middle of the picture is ~10m tall.

Calcified fossils were observed in this lithofacies at two locations (figure 2.1). At one location they formed part of a shell rich siltstone bed (figure 2.8), and appeared to be similar to others observed within the interbedded lithofacies.

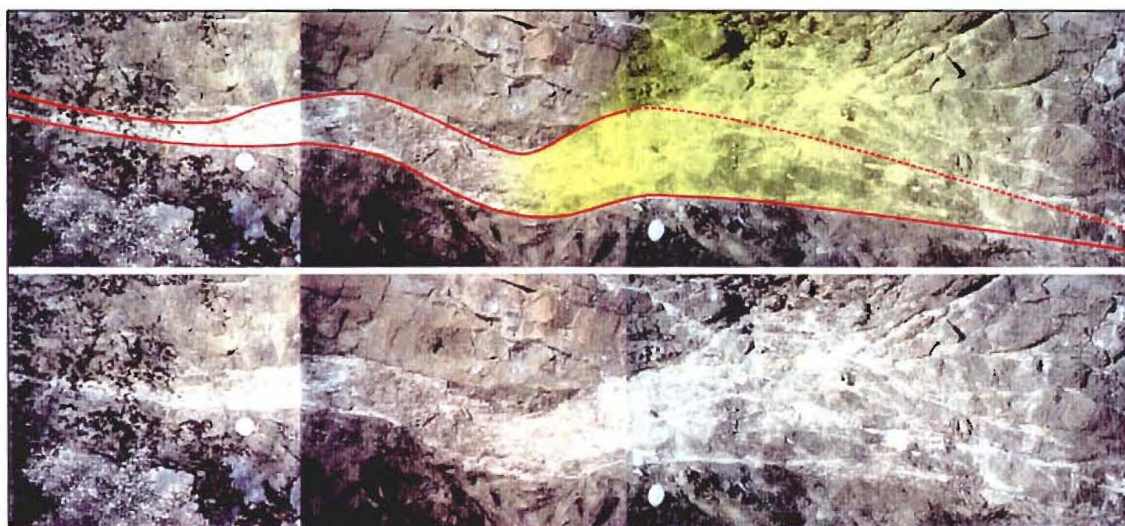


Photo 2.8 – A shell bed located to the west of Mt Saul, red lines indicate the limits of the bed, yellow shows the location and the intensity of the colour demonstrates influence of a shear zone trending perpendicular to the shell bed, 20cm coin for scale.

Sparse bedforms included parallel lamination, rare tool marks, and crossbedding. Intraclasts were commonly present and widely distributed, observed in dimensions up

to 100cm x 10cm, always composed of mudstone. Bioturbation was present at one locality in the form of circular feeding tracks (figure 2.9).

Lithologies other than sandstone also present within this lithofacies included uncommon pebbly sandstones, pebbly conglomerates and massive mudstone beds. Pebbly sandstones and conglomerates were typically thickly to very thickly bedded. They were either massively bedded or normally graded with sandstone beds. Both exhibited lensoidal geometries similar to the beds directly above and below. Massive mudstone beds were thinly to thickly bedded and can appear tabular. Texture and composition of these beds was very similar to those described in section 2.3.2.



Figure 2.9 – Bioturbation at the base of a normally graded thickly bedded sandstone at the top of Pahau River A section.

2.3.4 CONGLOMERATE LITHOFACIES

The conglomerate lithofacies was defined as having >80% of materials <-3 ϕ . Conglomerates outcropped as large lensoidal bodies over 1000m wide and up to 700m thick. Three conglomerate bodies make up the majority of the conglomerate lithofacies in the area, located at Mt Holmes, Mt Saul and a ridgeline to the east of Mt Saul. However, numerous thin <5m thick conglomerate beds were present throughout the field area, either located at the base of massive sandstone lithofacies or at the top of some coarsening and thickening upward sequences.

Bedding within the conglomerate lithofacies varied from thinly to very thickly bedded, commonly exceeding 100cm in thickness. Beds were typically moderately-sorted although poorly-sorted beds were common. Grading was often normal and less often reverse, although massive bedding was by far the most prevalent. Beds were well to very well-indurated.

Clast rounding within the conglomerate was also variable. Although typically sub-rounded to rounded, uncommon sub-angular grains were also observed. Rounding can be correlated with composition with sedimentary lithic clasts (excluding chert and intraclasts) being sub-rounded to well rounded. Igneous lithic clasts and chert were predominantly well rounded. The majority of clasts had a high sphericity although ~3% of clasts were oblate.

Intraclasts were widely distributed throughout the conglomerates, though often absent for large intervals of strata. Intraclasts were dominated by sandstone and mudstone compositions although normally graded granule and finely laminated sandstone intraclasts were also present. Pescini (1997) also observed a thinly-bedded, massive mudstone/sandstone intraclast. Intraclasts were predominantly angular though sub to well rounded intraclasts were observed.

Bedforms within conglomerate beds were limited to imbrication and cross-stratification. Imbrication was located at many sites, but cross stratification was rare and only seen twice (figure 2.10).



Figure 2.10

Cross stratification in a ~200cm thick pebbly conglomerate. Internal stratification supports a overall flow direction towards the east $\pm 30^\circ$ (left). Hammer present at the base of the crossbeds is 25cm long.

Large fragments of coal up to 20 x 20 x 20cm were found at many locations, usually exhibiting peripheral sulphur staining. Rootlets were also located within a massive sandstone interbed within the Mt Saul conglomerate. Percentage of plant fragments within sandstone beds was typically very high with numerous beds displaying fragment preferred orientation. Medium-bedded, very fine sandstones above the conglomerate at Mt Holmes had thick laminations with carbonaceous compositions frequently exceeding 60%.

Conglomerates were typically composed of a mixture of igneous and sedimentary lithics with rare bioclastic clasts. Igneous clasts included both extrusive and intrusive rocks, the composition of which were extensively studied in the past (Dean, 1993) and are presently being studied (Wandres, Unpubl. PhD Thesis). Intrusive clasts are predominantly monzogranites although granodiorites and syenogranites are also present. Volcanic clasts are principally composed of rhyolite with trachyte, trachydacite and dacite present (Dean, 1993). Sedimentary clasts are primarily sandstones with some mudstones and chert. The only bioclastic sediment present was in the form of large rare crinoidal limestone blocks (Pescini, 1997; Silberling *et al.*, 1988). Igneous clasts, vein quartz and chert often had a polished look to them.

Other lithologies commonly observed as lenses within the conglomerate lithofacies include massive mudstones, sandstones and normally graded sandstones. These lithologies outcropped together as horizons of laterally non-continuous lenses within conglomerates at Mt Saul. They also occurred as interbedded lithologies from adjacent lithofacies at Mt Saul, Mt Holmes and the ridgeline to the east of Mt Saul.

Unconformably bound, coarse sandstone to granule conglomerate occurred at the north-western base of the Mt Saul conglomerate (Pescini 1997). The thickness of these beds were poorly constrained though are at least 50cm thick. This was interpreted by Pescini (1997) to be a precursor to the deposition of the Mt Saul conglomerate. Coarse-grained sandstones were also observed at Mt Holmes beneath the conglomerate facies within the sandstone lithofacies.

Normally graded and massive sandstone channel forms within conglomerates, particular those at Mt Saul showed a variety of other bedforms (figure 2.11). Large

flame structures ejected from sandstone beds into the conglomerate were observed at Mt Saul. Ripples and cross stratification were uncommon but present. Load structures at the interface between fine grained beds and conglomerates were almost always present. Sandstones were often thinly to thickly laminated with massive mudstone.

Figure 2.11

Large flame structures to the left and the right of the hammer (scale 25cm), located on the western side of Mt Saul.



2.4 STRATIGRAPHIC COLUMNS

In total ten stratigraphic sections (figure 2.12) were logged covering all four lithofacies. Four reference sections were chosen as representative of each lithofacies, mudstone (Castle Hill), interbedded mudstone – sandstone (Pahau River A), sandstone (Pahau River C), conglomerate (Mount Saul B). Four sections (Mount Holmes, Pahau River B, Waiau River, and Shale Peak) were chosen as they cover a range of lithologies that record the transition between lithofacies. The remaining two sections (Mount Saul A & C) were chosen primarily because of features key to the interpretation of the depositional environment (e.g. *rootlets*, *macrofossils* etc.).

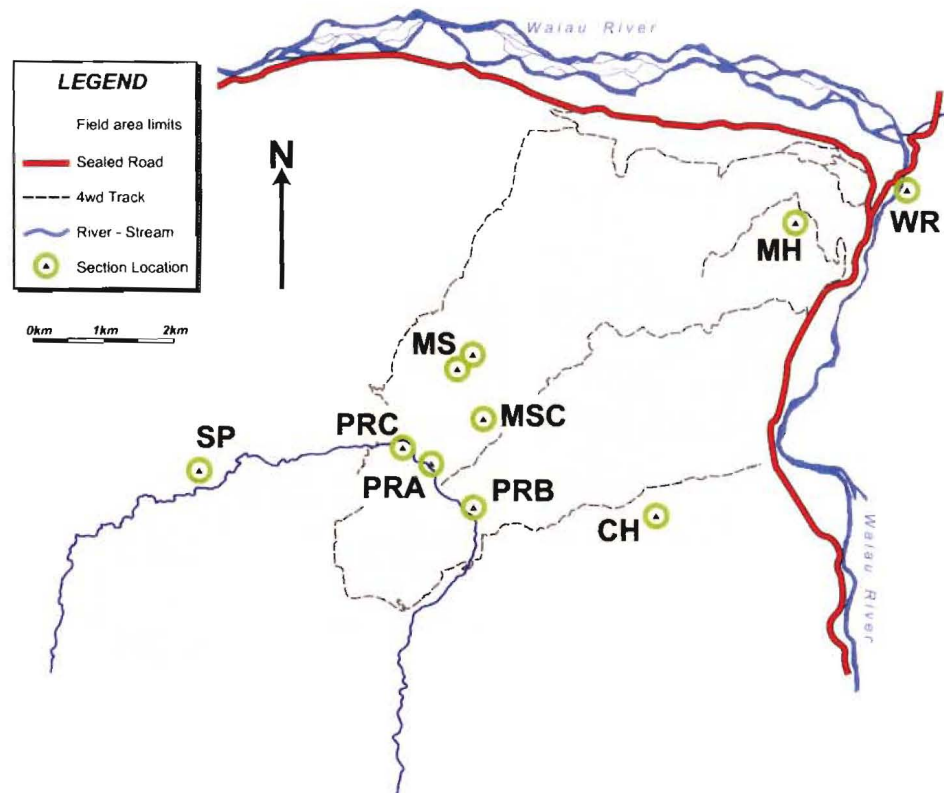


Figure 2.12 – The locations of the 10 stratigraphic sections logged in the Pahau River area, Pahau River A / B / C (PRA, PRB, PRC), Mount Saul A / B (MS), Mount Saul C (MSC), Shale Peak (SP), Castle Hill (CH), Mount Holmes (MH) and the Waiau River (WR) sections.

2.4.1 MT SAUL C

Mt Saul C (MSC; figure 2.12) was the smallest section logged measured at a 1cm scale. This section records just under 600cm of strata, no sequence of coarsening, fining, thinning or thickening beds was present (figure 2.13). It was chosen because of the unique combination of features in close proximity including macrofossils, rootlets, symmetrical and asymmetrical ripples, planar lamination, and flame structures.

Thin sandstone beds dominant within the section were characteristically 3-8cm thick, normally graded, and commonly rippled. Thick massive sandstone beds up to 40cm were present, often containing planar lamination. A macrofossil(s?) was present in one of these beds at 150cm (figure 2.6). Abundant *rootlets* were present in three thin normally graded beds separated by thin beds with flame structures in the upper 200cm of the section. Symmetrical ripples in close association with asymmetrical ripples

were observed in beds adjacent to rootlet bearing bedding. Palaeoflow indicators from ripples gave bi-directional flow indicators towards the northeast and southwest.

2.4.2 PAHAU RIVER A_{A-D}

Pahau River A (PRA) records a coarsening upwards sequence 175m thick measured at a 10cm scale (figure 2.12). The PRA section was dissected at 61m by three related faults with oblique normal displacements of 2m, 1m and an estimated offset of ~5m, stratigraphic continuity was maintained. Massive mudstones interspersed with sharp-based normally graded beds dominated the basal 100m of the section (figure 2.14).

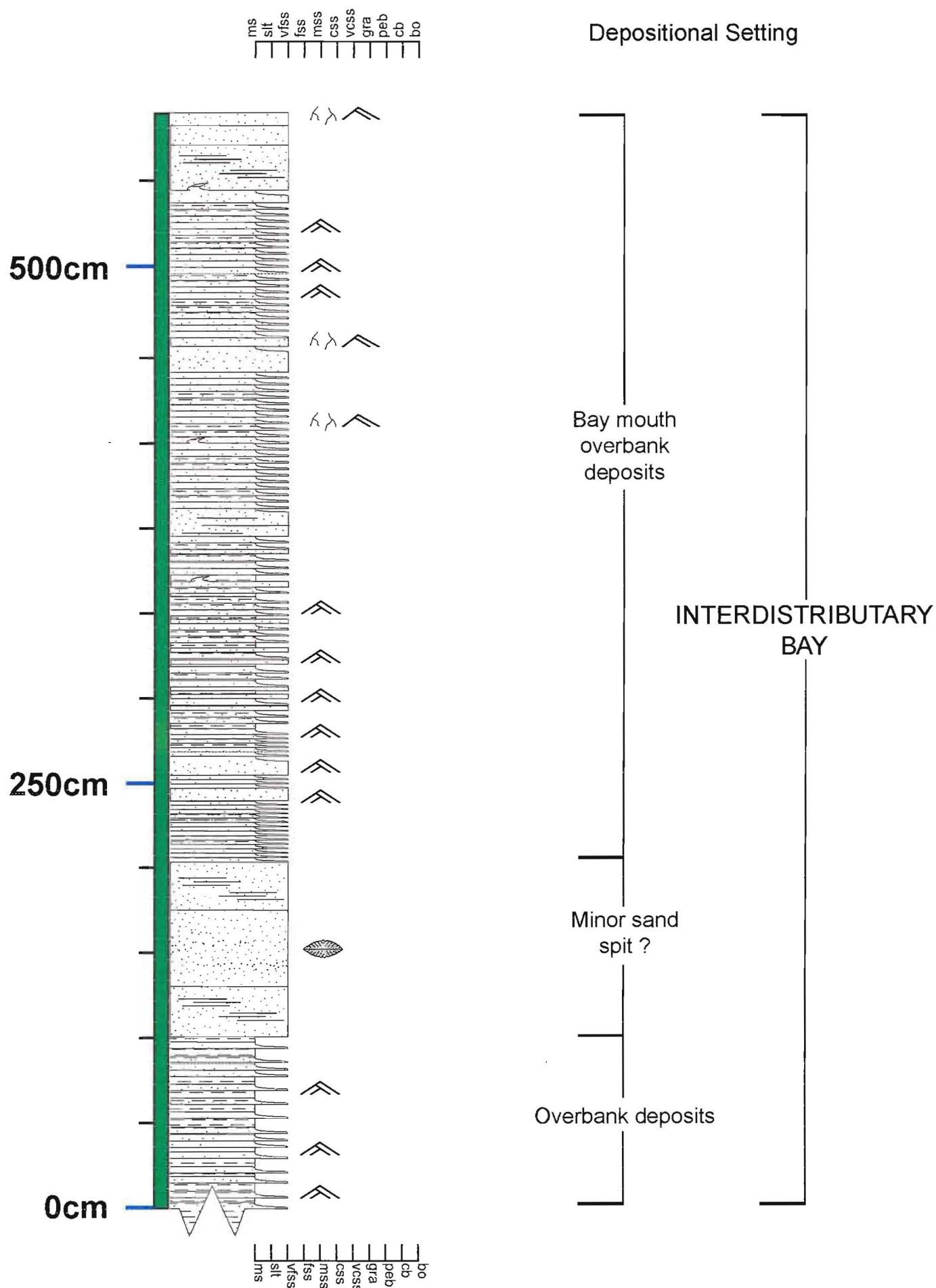
The thickness and frequency of graded bedding increased upward from ~10mm to 300-600mm. The frequency and thickness of massive mudstone decreased from the base in proportion to an increase in frequency and thickness of graded sandstone beds (many of the beds exhibit asymmetrical ripples and thin laminations).

The normally graded sandstones within the basal portion of the section had either sheet-like or broad lensoidal geometries. Sandstones deposits were usually in the very fine sandstone grainsize range and were typically well sorted. Although grain sizes in the fine to medium were often observed, granules and pebbles within these beds were rare and usually poorly sorted when present.

Interbedded sheet-like massive mudstones dominate the basal section especially in the lowermost 25m of the section. Soft sediment deformation structures were common within beds including flame structures, load casts and convolute lamination. Soft sediment deformation structures were locally present and dominate one portion of the section (figure 2.15 at 50m). Approximately 550cm of thinly to thickly bedded normally graded sandstone at this location exhibited signs of soft sediment deformation structures separated from undeformed but laterally equivalent beds by a curved concave upwards trace (figure 2.15).

Location - Mount Saul C

FIGURE 2.13



Lithology/structure	Deformation Levels	Miscellaneous
Mudstone	Deformation Level I	Macrofossil
Very Fine Sandstone	Deformation Level II	Symm. Ripple
Fine Sandstone	Deformation Level III	Asymm. Ripple
LEGEND	Deformation Level IV	Thin Mud Laminations
	Deformation Level V	Root Casts

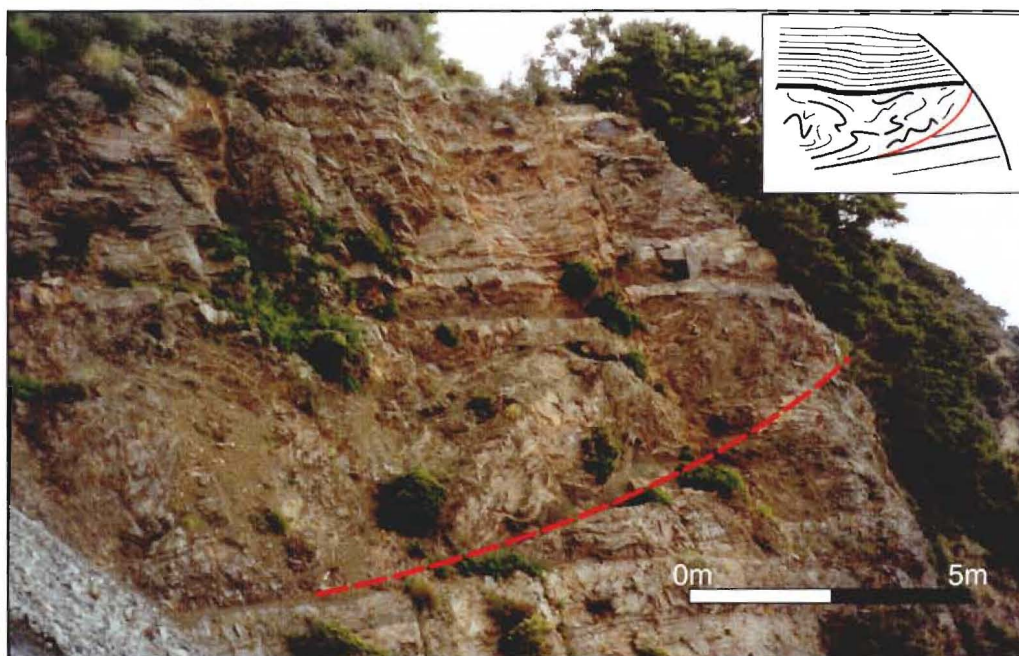


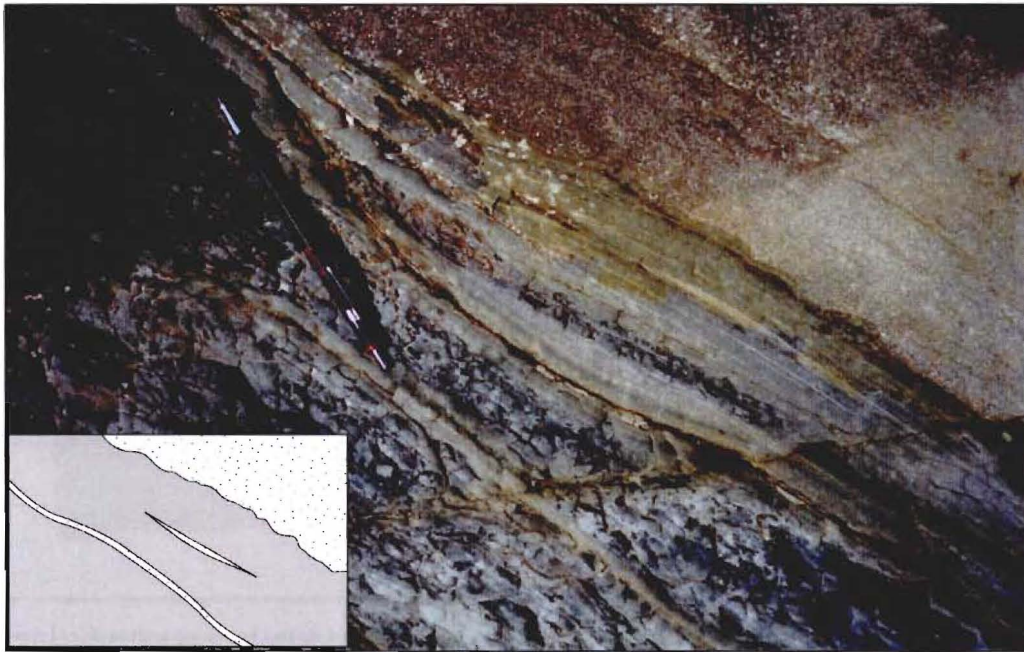
Figure 2.15 – Soft sediment deformation in the Pahau River.

Trough-like to lensoidal geometries in beds with erosional bases were observable in the basal portion of the section. These were typically filled with poorly to moderately sorted clasts up to a medium pebble grainsize and were always coarser than surrounding lithologies. Very small, less than 10mm x 150mm, U-shaped lenses were present in the lower part of the sequence (figure 2.16).

In the PRA mid-section (~100m) deposits change to regularly alternating beds of normally graded sandstone to mudstone in an overall coarsening and thickening upwards trend, larger scale crossbedding also increases in frequency. Carbonaceous laminations first appeared at 56m, rarely observed at first but then continually increasing in frequency throughout the section until in the upper 75m they appeared commonly within beds.

At 123m, beds contained the first observed rootlets in this section (figure 2.17). The rootlet bed was in erosional contact with the bed above it, a poorly sorted, normally graded, coarse-grained sandstone containing granules. Above this at 124m were two sequences in a fining upward relationship of thinly bedded, normally graded beds some of which contain asymmetrical ripples. This style of bedding was interrupted at 125m by another coarse-grained sandstone bed. Thin beds dominate directly above this at 126m where additional rootlets had been observed. Rootlets were not observed

again until 138m but the style of deposition remained unchanged, coarse-grained beds many with scour surfaces intermittently interrupting finer-grained deposition. Intraclasts and large scale cross stratification were commonly observed within coarse-grained deposits. Rootlets at 138m were observed in the same relationship as those at a lower level except that the average bedding thickness had marginally increased. No rootlets were observed above 139m.



Figures 2.16 – A sand lens encased in mudstone, also note the presence of load casts on the base of a sandstone bed a few centimetres above the sand lens. The pen in the photo is 14cm long.

Bedding style changed above 140m becoming poorly to moderately sorted and dramatically thicker and coarser. Carbonaceous laminations, crossbedding, intraclasts and scour surfaces were all relatively common up until 156m. Flat laminations of coarser grained grainsizes within sandstones were also commonly observed in this interval.

Bedding was obscured at 156m by scrub but reappeared at 163m, from this point bedding was dominated by massive mudstone to the very top of the section. Mudstone beds up to 300cm thick were interbedded with normally graded sandstone beds with a mudstone to sandstone ratio of ~ 4:1.

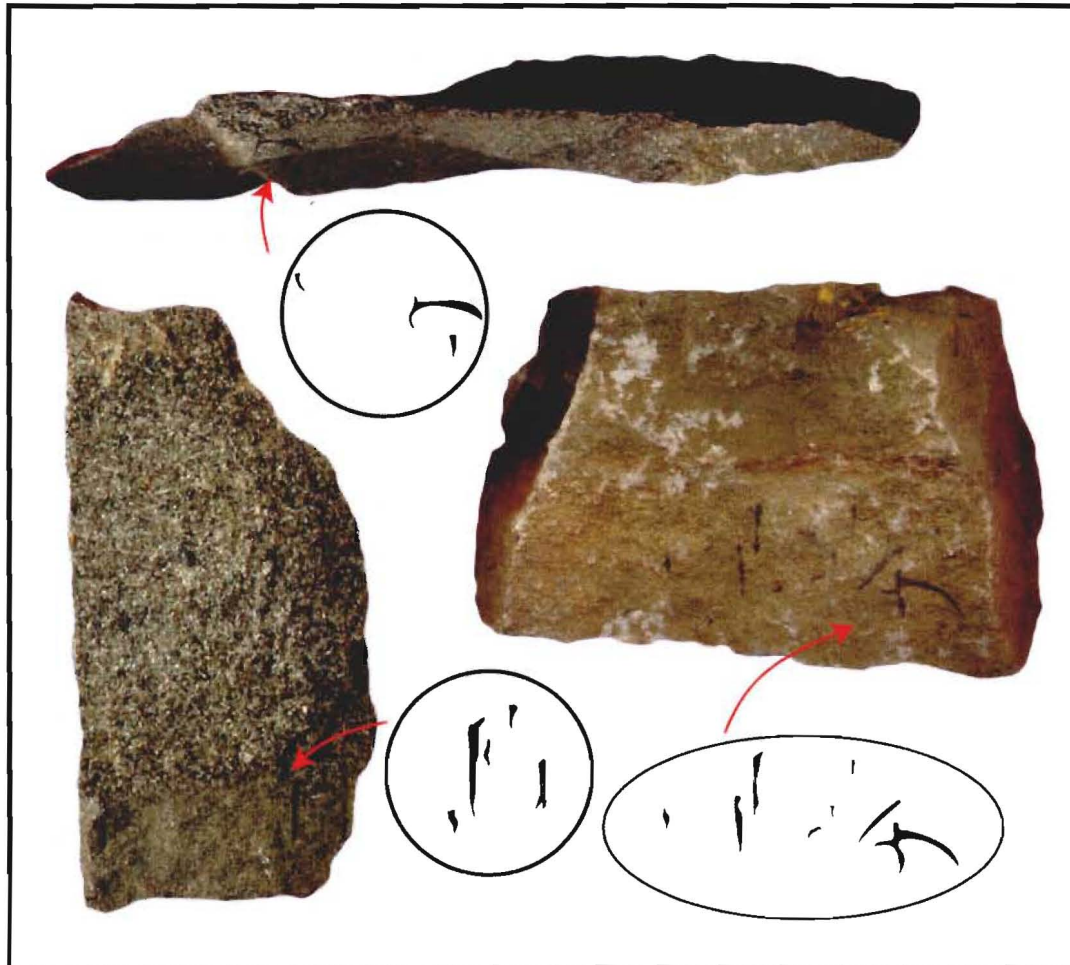


Figure 2.17 – Rootlets observed in various beds in the Pahau River area, rootlets were observed in PRA section (bottom left and top) as well as in a sandstone lens within the Mt Saul conglomerate (bottom right). All pictures shown are at the same scale, the very fine sandstone layer at the base of the bottom left picture is 16mm thick.

2.4.3 PAHAU RIVER B

Pahau River B (PRB) represents just over 75m of moderately to highly deformed sediment and was measured at a 10cm scale (figure 2.12). The basal 55m of this section were dominated by massive mudstone with a subordinate amount of thin to medium-bedded, normally graded sandstone beds. Unfortunately, as many of the sandstone beds were boudinaged, the thicknesses for most beds in the basal section were estimated. Although this section was highly deformed much information could still be extracted from it (figure 2.18).

The interbedded mudstone – sandstone lithofacies and the mudstone lithofacies were both present in the lower 55m of the section. High deformation levels within massive

mudstone in this section were ubiquitous. The basal 20m of the section was dominated by massive mudstone interrupted periodically by 10-30cm beds of massive very fine sandstone. Very thin sandstone beds present in the basal section were represented by non-continuous boudinaged blebs with the exception of a small assemblage of continuous beds (300 – 350cm thick) at 6m that were slightly less deformed. Sandstone to mudstone ratios ranged from 1:1 to 1:40 typical of mudstone dominated interbedded mudstone - sandstone or mudstone lithofacies. No sandstone or mudstone bed greater than 3cm or 40cm in thickness respectively was present below 20m, with the exception of bedding at 6m.

Above 20m, sandstone content increased to ~25%, sandstone and mudstone bedding were still typically massive with a few normally graded beds becoming apparent. At 28m all very fine sandstone beds became normally graded, thicker, and the sandstone to mudstone ratio dramatically increased. From ~33m bedding steadily became thinner once more, sandstone content decreased and grading was less commonly observed.

At 54m the section abruptly changed at an erosional contact from the interbedded mudstone – sandstone lithofacies to sandstone lithofacies (figure 2.18), carbonaceous material also steadily increased from this point. In the upper part of the section from 54m thick massive mudstone beds were rarely observed. Thick massive sandstone beds or normally graded sandstone beds with very thin mudstone tops between 200 and 500cm thick dominated bedding. Internal structures were largely absent from this or any part of the section although several unusual features were observed in the sandstones. Flute casts were observed in the lower portion of the section. At 64m a sandstone bed temporarily graded to mudstone then back to sandstone twice over the space of 60cm. In a bed above this at 69m an outsized clast (coarse pebble) was found 20cm from the base of a well-sorted, normally graded sandstone bed with carbonaceous laminations. A large mudstone intraclast was observed in a graded bed at 71m, approximately 60cm by 5cm.

2.4.4 PAHAU RIVER C

The Pahau River C (PRC) section (figure 2.12) was dominated by lightly deformed, very thick, massive sandstone beds, totalling ~150m measured at a 10cm scale (figure 2.19). The PRC section represents overturned strata in the eastern limb of a syncline probably plunging to the southeast. One fault cuts the sequence at 54m and was determined to have an offset in the order of 5-10m.

A few very thick beds dominated the lower 35m of the PRC section, the largest of which appeared to be 28.5m thick. No distinct internal bedding structures were observed in these beds and carbonaceous laminations/fragments were also conspicuously absent. Significant carbonaceous levels were observed between very thick beds in high concentrations at 2m, 64m and 112m. In the lower 2.5m of the section two 30cm thick beds contained up to 60% carbonaceous material in laminations typically 2mm thick. At 64m carbonaceous material was associated with an isolated shear zone approximately 50cm wide containing contorted carbonaceous laminations that reached concentrations exceeding 60%. At 112m a bed approximately 1m thick contained 3mm thick carbonaceous laminations containing up to 30% carbonaceous material.

An abrupt change to thinner sub-1m normally graded bedding at 34m was observed. Above 41.5m bedding thickened to and typically exceeded 2m with a ratio of massive to normal grading around 1:1. Thick normally graded beds up until 75m had poorly to moderately sorted bases generally containing significant percentages of medium sandstone to granule clasts in the basal 20 to 50cm.

Apart from two 20cm massive mudstone beds at 78m and 79m massive very fine sandstone dominates deposition. Scour surfaces were quite frequently observed from 79m to the top of the section. Very minor carbonaceous content observed from 80m was not observed above the scour surface terminating the bed at 97m.

Upwards from ~113m beds slowly became thinner and mudstone content increased. Carbonaceous material and intraclasts became the dominant internal bedding features from this point on. A change obscured by vegetation, from sandstone lithofacies to interbedded mudstone – sandstone lithofacies occurred at ~127m. Bedding above this point altered to normally graded, thin beds generally around 5cm thick with a sandstone to mudstone ratio of 1:3. Thin beds were periodically interrupted at 1-2m intervals by 10-40cm normally graded sandstone beds with the inverse ratio of sandstone to mudstone. A small channel body ~100cm x 50cm with an erosional base interrupted this section at 140m, compositionally and sedimentologically indistinguishable from poorly sorted channel beds described in the basal PRA section 2.4.2.

2.4.5 WAIAU RIVER

The WR section (figure 2.20) can be viewed directly opposite to Skippers Canyon beside the Waiau River Ferry Bridge (figure 2.12). The Waiau River (WR) section (figure 2.20) was ~115m thick and composed of steadily coarsening and thickening upwards beds, logged at a 10cm scale. The WR section covered a transition from interbedded mudstone - sandstone to the sandstone lithofacies in a fault block separated from all other sections. The WR section was well exposed and was only slightly deformed.

Normally graded fine sandstone to siltstone beds typically with subordinate massive mudstone dominated the basal 50m of the section. A fault with no determined offset dissected the section at 12.5m. No lithofacies or significant sedimentological changes were observed in direct contact across this fault trace, bedding below this point was therefore considered representative of an actual continuous stratigraphic section.

The mudstone content within normally graded beds decreased between 6m and 20m. Directly above and below this interval were sequences of normally graded, thinly bedded sandstones. Typically throughout the Pahau River area as normally graded sandstone beds thicken the finer grained mudstone tops of these beds decrease proportionally. Mudstone content in bedding conversely increased in proportion to sandstone thickness as bedding thickens from 21m to 46m.

Mudstone content dramatically decreased and was infrequently more than 20% of any normally graded sandstone bed above a scour surface at 46m. Crossbedding and asymmetrical ripples were the only internal bedding structures commonly observed. Mudstone lenses within normally graded sandstones, uncommon intraclasts and sparse carbonaceous laminations were also found in the basal section.

Sandstone beds above 46m dramatically increased in thickness (often >3m) and marginally increased in grain size to dominantly very fine sandstone with minor inclusions of fine sandstone. Carbonaceous material, largely absent below 46m appeared sparingly at first increased towards the top of the section when laterally continuous thick laminations up to 3mm were observed. A thickening upward sequence can be clearly demonstrated above 46m as normally graded sandstones graded to very thick massive sandstones up to 16m thick at the top of the section. This thickening upward sequence was interrupted twice by thinner bedding, once at 62m by regularly alternating layers of massive very fine sandstone and mudstone 5 to 10cm thick and again at 85m by several thin normally graded beds <40cm thick. Scour surfaces were abundant within the upper, sandstone dominated, portion of this section.

A second fault cut the section at ~65m with a determined offset of ~4m, stratigraphic continuity was retained. A thin (~5cm thick) volcanic dyke crosscut the section from 45m to 46m (figure 2.21). Several thin volcanic dykes up to 100cm thick were observed during the course of fieldwork and were almost always extremely weathered. Dyke emplacement in the WR section was post lithification.



Figure 2.21 – A volcanic dyke crosscuts the WR section at 45.5m, 50cm ruler for scale in the middle of the picture.

2.4.6 MT HOLMES

The Mount Holmes (MH) Section (figure 2.12) was the thickest of all the stratigraphic logs, totalling just over 192m measured at a 25cm scale. The MH section represented a slowly thickening and coarsening sequence of deposits periodically interrupted by large conglomeratic beds (figure 2.22).

The basal 75m of this section were dominated by alternating massive mudstones (up to 8m thick) and thinly bedded, very fine to fine, normally graded sandstones. Moderately high deformation probably masks any internal bedding structures in most of the section as relatively few were observed. Several coarsening and fining upwards sequences were observable in the basal section. Fossil casts were located in two beds at 13m and 25m, these appeared to be shell macrofossils possibly bivalves or brachiopods, no formal identification or moulds were possible.

Normally graded beds became thicker above an 8m thick massive mudstone bed at 60m. Sandstone beds were observed at 65m consistently pinching out towards the top of the outcrop and thickening towards a common source at the base of the outcrop.

Dominantly poorly-sorted thin to medium beds at 70m graded up into moderately to well-sorted, thick to very thick, massive sandstone deposits with subordinate poorly sorted deposits above 80m. Poorly sorted deposits typically included clast supported, well-rounded, conglomerates (<80cm thick) or matrix supported pebbly mudstones and sandstones (<4m thick). A bed at 88m had an imprint of a log (in the middle of which was a 20cm² block of coal; figure 2.23) within poorly sorted sandstone contained fine pebble and granule clasts and exhibiting a trough-like geometry. This sequence was truncated by an erosional contact at ~99m, interestingly overlain by a very thick massive mudstone deposit 8m thick. The presence of very fine-grained material over an erosional contact may represent an unconformity of significant lateral extent. Vegetation and deformation unfortunately hampered the examination of this.

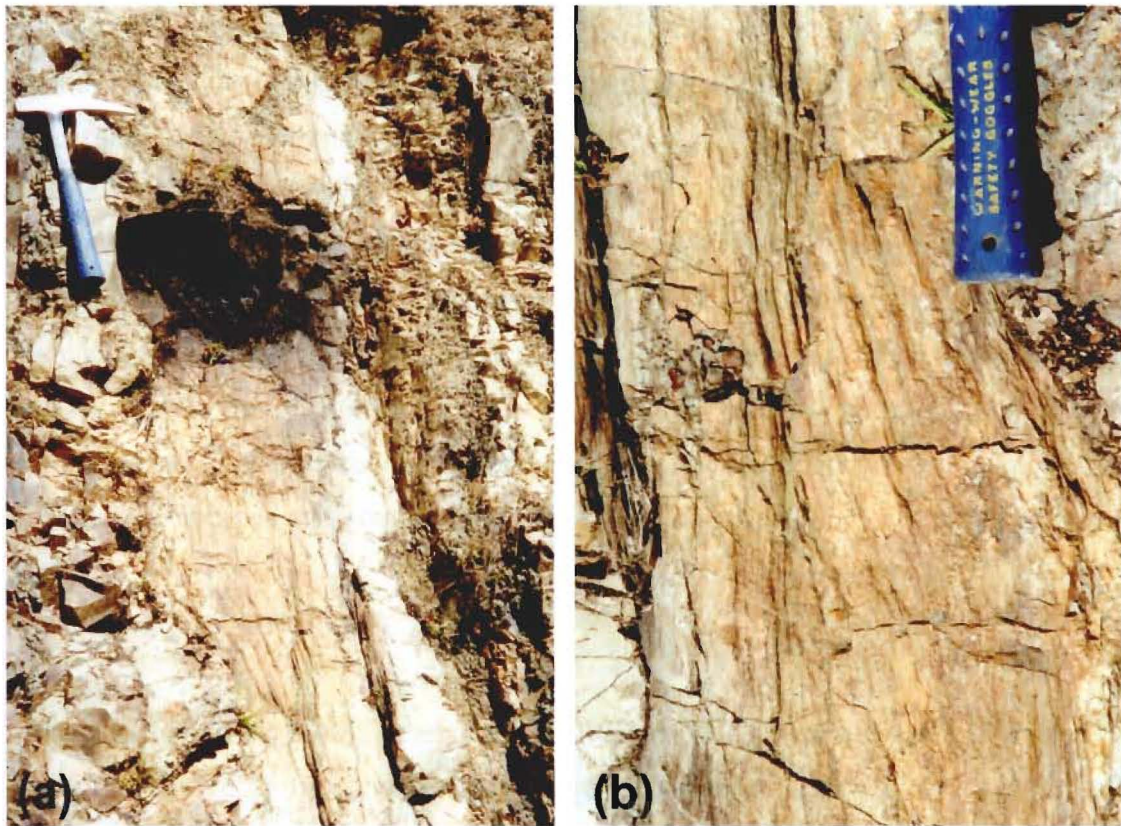


Figure 2.23 – A log imprint within a lensoidal pebbly sandstone channel form, the coal block by the hammer in photo (a) is located within the core of the lens, the point of the hammer denote younging direction. Notice the texture of the log print in the close up photo (b). The hammer is 25cm long and the width of the handle is 3.5cm.

Overlying the mudstone was a thin coarsening upward, well-sorted, thinly bedded, normally graded sandstone sequence. An erosional contact at the base of an overlying matrix-supported conglomerate truncated this sequence at 107m. The nature of the conglomerate changed abruptly at 109m where at least two clast supported conglomerate beds were located. An erosional contact separated the upper and lower clast-supported conglomerates from each other, which were moderately and well sorted respectively. Vegetation obscured the outcrop part way through the well-sorted bed, when the outcrop reappeared thin to medium, normally graded sandstone beds dominated the section.

Normally graded beds above the conglomerate slowly thickened upward towards another assemblage of conglomerate beds at ~160m. This sequence was periodically interrupted by 30-100cm thick, massive to normally graded, poorly sorted, coarse sandstone beds commonly including granule to fine pebble clasts. A very high level of carbonaceous material (up to 60% carbon) in several massive mudstone beds was

present as laminations up to 5mm thick. Directly above the uppermost carbonaceous bed (~160m), bedding transformed into regular thinly interbedded sandstone and mudstone several metres thick.

A lithofacies change was clearly apparent at 164m from the interbedded sandstone – mudstone lithofacies to the conglomerate lithofacies. The conglomerate lithofacies were dominated here by clast support, massive, poor sorting, sub to well rounding, and grainsizes ranging from granules to coarse pebbles with a sandy matrix. Conglomerates disappeared at 186m when the interbedded mudstone – sandstone lithofacies remerged and continued to the top of the section.

2.4.7 MOUNT SAUL A - B

The Mt Saul A & B (MS) conglomeratic (figure 2.12) sections were comprised of small correlative fault segments each up to ~25m thick (figure 2.24). Seven faults dissect all of the MS conglomerate sections, all offsets were determined to be less than 5m except for a single fault separating the Mt Saul A section from Mt Saul B section. Faulting in this instance was ~5° off of bedding parallel and no offset could be determined, though it is suggested that the offset was consistent with other faults. The MS section was particularly important for depositional environment interpretation as it contained one of the few localities where rootlets were observed.

MS section conglomerate clasts were often polished and typically sub to well-rounded. Bedding was principally massive though normal and inverse grading was common. Bedding contacts were gradational, sharp, or erosional though gradational contacts were easily the most common. Erosional and sharp contacts were essentially only seen in association with sandstone interbeds. Imbrication and clast preferred orientation were the only internal bedding structure present within conglomerate beds measured section at Mt Saul, usually in beds with low matrix percentages.

Conglomerate beds typically ranged from 30cm to 150cm thick although beds up to ~7m thick were logged. Bedding was *primarily* composed of *clast supported* pebble conglomerates, matrix support was observed only once. Matrix support was not observed at a large scale anywhere within the conglomerate lithofacies in the Pahau River area.

Clast grainsizes up to boulder (30x25cm) were observed within the section, although grainsizes typically ranged from fine to coarse pebble. Beds in which boulders were present often had very large sandstone or mudstone intraclasts present, up to 2m x 1.5m.

No consistent coarsening or fining upward sequence was observed in the Mt Saul section, other features were graphed to see if any trends could be established at the locality. Clast sorting and matrix type were plotted next to an abbreviated stratigraphic column (figure 2.25). Matrix was dominantly sandstone with mud and mud-sand mixtures locally pervasive, percentages of matrix range from 10% to 40%. Poorly sorted beds form ~34% of the conglomerates at the MS section.

On average conglomerate beds were moderately sorted with zones of increased and decreased sorting scattered throughout. Three evenly spaced portions of the section at 10m, 40m and 60m can be identified with decreased sorting. Zones of decreased sorting typically included the increased presence of sub- to angular intraclasts often larger than the maximum clast size, slightly higher matrix percentages (>20%) with clasts ranging from granule to cobble. A single zone of increased sorting at 70m has finer clasts in the medium pebble range, low matrix percentages (<20%) and relatively minor intraclast inclusions typically smaller than the average clast size.

Interbedded with the conglomerates in the MS section were lensoidal bodies of massive or normally graded, very fine to fine sandstone. The lateral continuity of these sandstone beds at Mt Saul very rarely exceeded 100m, singular beds were particular rare. Sandstone interbeds were typically 5-30cm thick and grouped in clusters of four or more beds in direct contact with each other. One example of clustered sandstone beds at 45m showed several beds separated by fingers of conglomerate other locations showed no interbedded conglomerates.

One bed contained downward branching *rootlets* in a single massive sandstone bed at 5m. Plant fragments were frequently present within sandstone interbeds often preferentially aligned roughly east – west. Internal bedding structures were largely absent from interbeds although one large flame structure (figure 2.11) was observed at 43.5m.

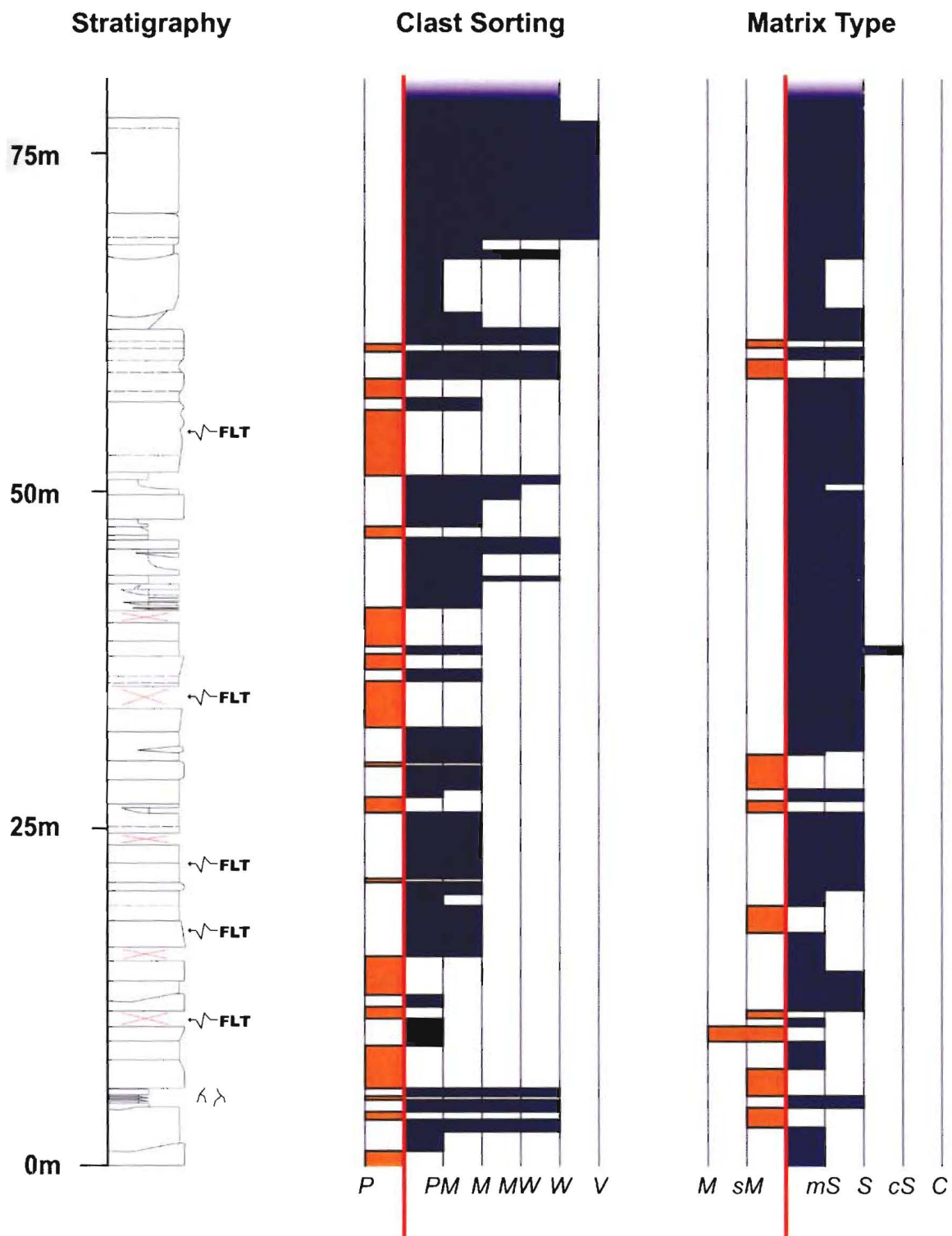


Figure 2.25 – Matrix type and clast sorting comparison with lithology. Orange colour denotes poorly sorted and mudstone dominated matrix as opposed to blue which represents moderate to very well sorted and sandstone dominated matrix.



Figure 2.26 – Blocks of coal within the conglomerate deposits in the Pahau River area are a common occurrence easily observed as sulphur and iron staining often occur around them. The length of pen visible in the picture is 12cm.

2.4.8 SHALE PEAK

The section logged near Shale Peak (SP; figure 2.12) on one of the Pahau Rivers tributaries comprised a little over 35m of strata (figure 2.28). The assemblage was fairly simple although moderately deformed.

The SP section represents a single rapid fining upward then thickening and coarsening upward sequence. The basal 30m of the section were dominated by normally graded, thinly bedded sandstone and siltstones with equal amounts of thick massive mudstone beds. Normally graded siltstone and sandstone beds fine into massive mudstone at 6m then thicken and coarsen at 21m. Normally graded beds attain a maximum thickness of 15cm before being cut at 30m by an erosive contact. A 3m thick sandstone body rests above the contact at 30m (figure 2.28) then rapidly coarsens into a well-sorted, well-rounded, clast-supported conglomerate. No environmental indicators were present at this section, although what was interpreted to be a crinoid stem was found in a conglomerate block at the base of the section.

2.4.9 CASTLE HILL

Very little deformation was observed in the Castle Hill section (CH; figure 2.12), thus in a rare opportunity 50m of the mudstone lithofacies can be observed in great detail (figure 5.29).

For the most part, this section was composed of massive mudstone interbedded at surprisingly regular intervals (14 – 16cm) with normally graded, very fine sandstone beds typically not thicker than 60mm (figure 2.27). Background deposition was punctuated every 300cm to 600cm by a thicker massive or normally graded sandstone bed.

Thicker sandstone beds show internal bedding structures such as parallel laminations, flames structures ripple, cross lamination and intraclasts. Flute casts were present at the base of one massive sandstone bed.

No cycles or sequences were discernable in this section.

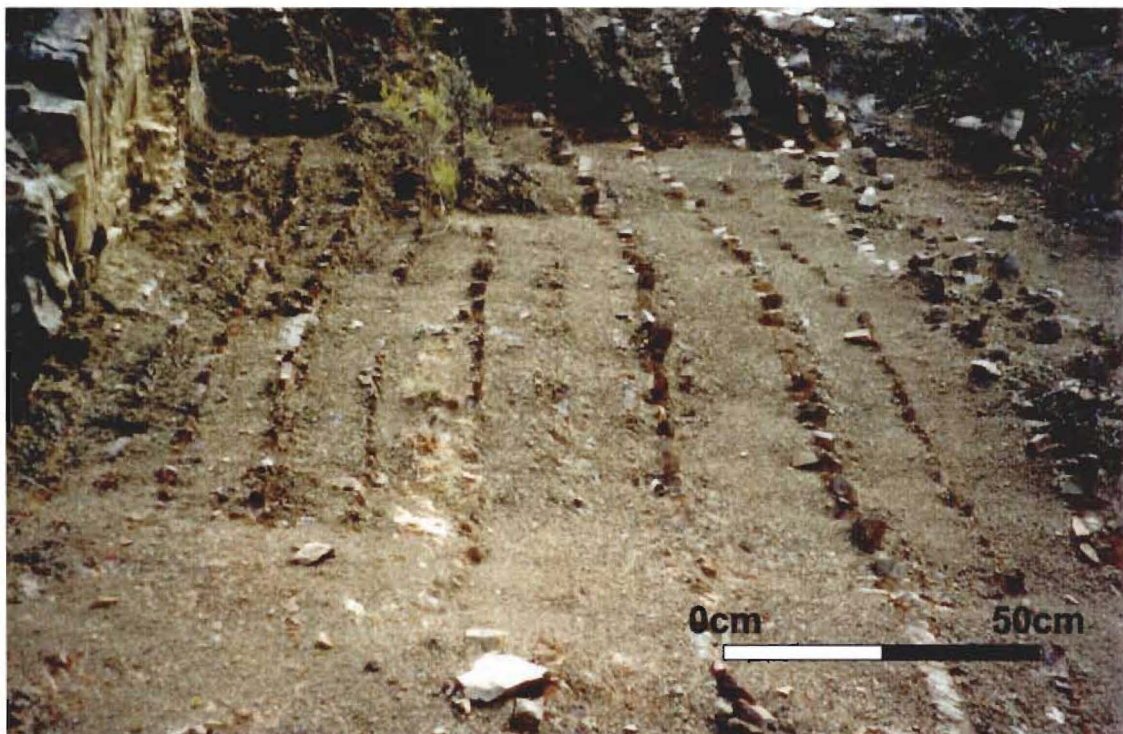
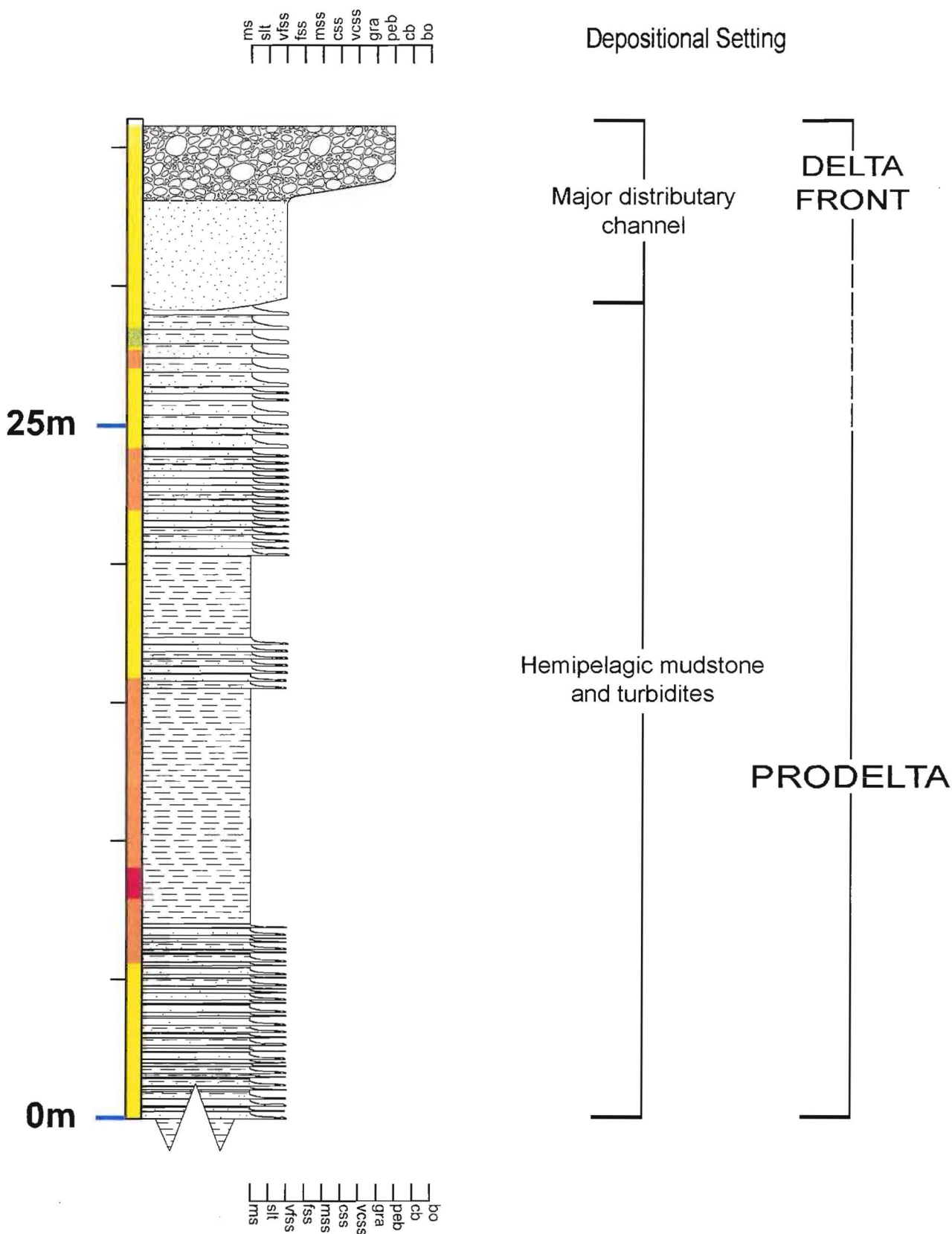


Figure 2.27 – Massive mudstone interbedded at very regular intervals with very thin normally graded sandstone beds.

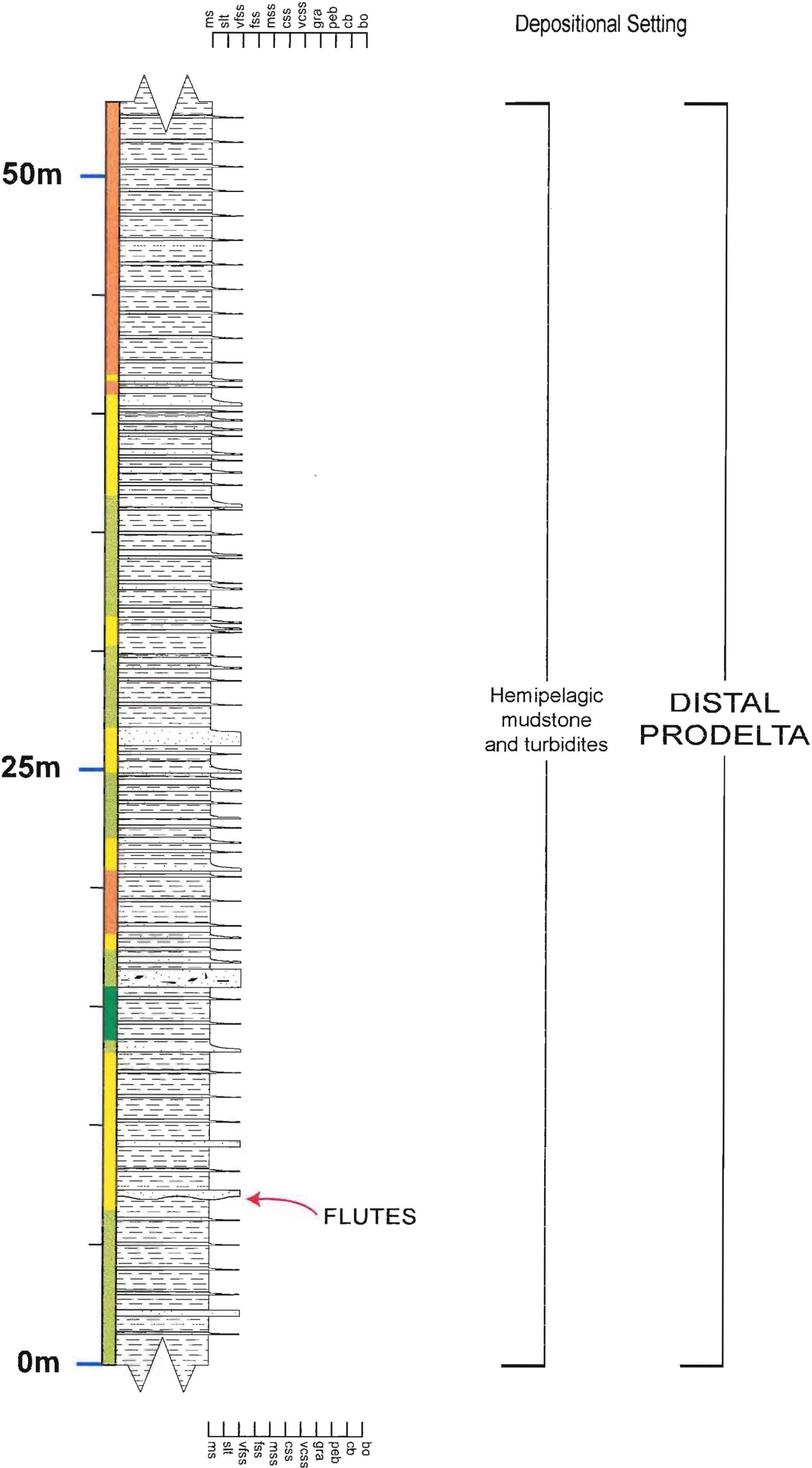
Location - Shale Peak

FIGURE 2.28



Location - Castle Hill

FIGURE 2.29



Lithology/structure

Mudstone

Fine Sandstone

LEGEND

Deformation Levels

Deformation Level I

Deformation Level II

Deformation Level III

Deformation Level IV

Deformation Level V

2.5 DISCUSSION

Deposits in the Pahau River area can be categorised into four distinct lithofacies distinguished by grainsize percentage and bedding structures. Lithofacies were observed in sequences slowly grading into each other (e.g. PRA, WR, MH) or in large, relatively monotonous bodies (e.g. MS, CH). Each lithofacies can be identified (figure 2.1) to interfinger with other lithofacies of relatively similar characteristics (e.g. the conglomerate and sandstone lithofacies or the mudstone and interbedded lithofacies). Boundaries around individual lithofacies were relatively easy to define as each lithofacies has characteristic weathering geomorphologies in the field. The conglomerate lithofacies appears as relatively rounded mountains while the sandstone lithofacies can be observed forming elongated strike ridges. The mudstone lithofacies is typically observed forming wide valley floors. The interbedded facies tends to form smaller elongate ridges within valley floors or topography with lower relief adjacent to sandstone strike ridges.

Geometries became increasingly lensoidal as grainsize increased through the lithofacies, though bedding with sheet-like geometries at least at the outcrop scale dominated.

Conglomerates were almost always clast supported except in the finer lithofacies where they were a relatively even mixture of both matrix and clast supported. Conglomerates in the mudstone and interbedded lithofacies can be traced back to and taper away from large conglomerate bodies, such as those at Mt Holmes or Mt Saul indicating these were the channel axis.

A variety of bedforms were present within all of the lithofacies, often indicating a lack of dewatering between depositional events (e.g. flame structures and load casts). Other bedforms such as parallel lamination, asymmetrical and symmetrical ripple cross stratification indicate deposition from a variety of flow regimes and flow types.

Stratigraphic logs clearly support the descriptions of each lithofacies. Each of the stratigraphic logs can be analysed and have been shown to support lithofacies

descriptions. In addition to supporting the proposal of four lithofacies several stratigraphic logs document the transition from one lithofacies to another.

PROPOSED STRATIGRAPHIC NOMENCLATURE

CHAPTER THREE

3.1 INTRODUCTION

Descriptions and definitions of the Torlesse (Series, Formation, Group, Supergroup, Terrane and Superterrane) sediments are notoriously scattered and vague. Currently there are no formal sedimentological definitions developed from stratigraphic sections for any of the Torlesse Subterrane. This is quite appalling as Julius Von Haast, who was the first to refer to the Torlesse, did so in the late 19th Century. What is even more embarrassing is that the Torlesse forms approximately 60% of the New Zealand landmass (Campbell and Grant-Mackie, 2000).

One of the main purposes of this thesis is to officially describe and name the deposits of the unofficial type locality. The proposal of Group and Formation names for sediments in the Pahau River area herein can be viewed as the first step towards defining part of the largest geological body in the New Zealand continent.

3.2 DESCRIPTIVE HISTORY

3.2.1 THE TORLESSE SEDIMENTS

The Torlesse was first referred to by Julius von Haast who described all the "undifferentiated" sediments of the Southern Alps and the Canterbury foothills as the *Mount Torlesse Series* and later as a *Formation* (Haast, 1879; Haast, 1885). Other prominent geologists debated the age range and subdivision of the Mount Torlesse Formation vigorously at the time (Hector, 1885). Hector (1885), supported by significant fossil evidence suggested that the Mount Torlesse Formation had too large an age range for it to be simply one formation. Even in the face of this evidence Haast (1885) remained adamant that the Southern Alps simply represented one formation.

The Torlesse name was used again in 1890 describing sediments in the Mount Cook area as *Torlesse slates* (Gordon, 1890).

The Torlesse name was abandoned in the early 20th Century in preference for *Undifferentiated Jurassic-Triassic-Permian rocks* as mapped on the 1:1 031 760 New Zealand Geological Survey (NZGS) map 1947 (Willet, 1948). This was later changed to *Undifferentiated Greywackes* by the bulletin accompanying the 1:2 000 000 NZGS map (Grindley *et al.*, 1959).

Torlesse was relisted as a stratigraphic name in the 1950s, although not intended to be used in the all encompassing manner as used by Haast (1885) or Hector (1885). It was used to describe a localised series of beds termed the *Mount Torlesse Annelid Beds*, comprised of the annelid Terebillina formally known as Torlessia (Adkin, 1954).

The status of the Torlesse was reinstated once more during the 1960s when Suggate (1961) published his account of the ‘Rock Stratigraphic Names for South Island’. Suggate (1961) promoted the unit to the *Torlesse Group* grouping all previously mentioned names with undifferentiated Permian – Jurassic South Island sediments. This revision of nomenclature was based upon the assertion that future formations within the Torlesse Group were imminent and previously described ones were readily confirmable.

The first mention of the *Torlesse Supergroup* in the literature was in a single line written by Campbell and Coombs (1966) while ironically defining the Murihiku Supergroup. This increased the significance of the Torlesse and was formalised by the Sheet 17 NZGS 1:250 000 Hokitika map (Warren, 1967). This was later challenged by Maxwell Gage who did not accept that the Torlesse was a useful assemblage of units of Group magnitude (Gage, *I will find out*). The Supergroup status of the Torlesse remained despite Gage’s objections throughout most of the 1970s (Bradshaw, 1971; Fordyce, 1976; Raine, 1977).

The sedimentological nomenclature was widely abandoned during the early 1980s in favour of a tectonostratigraphic nomenclature (Bishop *et al.*, 1985; Bradshaw and Andrews, 1980; MacKinnon, 1983). The new terminology introduced an order of

units ranging from superterranes to terranes to subterranes. The fundamental unit of tectonostratigraphic nomenclature is a terrane, defined as a significant assemblage of strata that is completely fault bounded and exhibits no genetic relationship to rocks immediately adjacent to the fault block. Superterranes and subterranes are groups of related terranes and subdivisions of individual terranes respectively.

The *Torlesse Terrane* was first proposed by in 1976 by both Andrews et al. (1976) and Speden (1976). The Torlesse Terrane was widely adopted and more fully described as a terrane by Bradshaw *et al.* (1980) who proposed its subsequent three-fold subdivision. The three Subterranes are still known as the Rakaia, Esk Head and Pahau Subterranes.

The Torlesse Subterranes are described in detail in the ‘Origin of the Torlesse terrane and coeval rocks, South Island, New Zealand’ by MacKinnon (1983). Sedimentological descriptions of these units were quite generalised, as the primary subject of the paper was the provenance and age of the sediments. The terrane status of the Torlesse is still currently in use although many authors now refer to the Torlesse as a Superterrane (Campbell and Grant-Mackie, 2000; Wandres, Unpubl. PhD Thesis). These same authors promote the Rakaia, Esk Head and Pahau to Terrane status.

3.2.2 THE PAHAU SEDIMENTS

The deposits in the catchment of the Pahau River were first mapped in 1964 by the New Zealand Geological Survey (Gregg, 1964). These were assigned an age of Herangi to Oteka Series or Mid-Late Jurassic. They were described as ‘moderately indurated, mostly graded, greywacke and argillite, with beds of basic volcanics with associated sediments; minor limestone and conglomerate; sparse cannonball and tabular concretions’ (Gregg, 1964). They also noted that to the west it graded into an older, more strongly indurated version of itself with a higher metamorphic rank. These sediments were estimated to be around 40,000 ft thick.

In the 1970s the Pahau River catchment was part of palynological studies by the geological division of Department of Scientific and Industrial Research (DSIR) designed to date Cretaceous sediments. An age range of Late Early Cretaceous (late

Neocomian to early Aptian) was recorded based upon spores, pollens and rare dinoflagellates (Raine, 1977). As part of the DSIR research Peter Andrews mapped the area and described in great detail depositional setting (Ian Raine pers. comm. 2001). Unfortunately, the completed maps and the manuscript produced by Peter Andrews were never published and the originals lost. Remnants of this research still remain in a small six-page section in a field trip excursion program (Bradshaw and Andrews, 1980) and various discussions remembered by his staff and colleagues. Peter Andrews came to the conclusion that the sediments in Pahau River area to the east of the Pahau Pass fault are of an alluvial-deltaic association. The rocks to the west of the fault were interpreted as being deposited as an older, Valanginian – Early Albian, flysch-type depositional environment.

The depositional setting has been addressed once since 1980 by Hamish Pescini who mapped and described the area as part of his BSc Honours project (Pescini, 1997). Pescini (1997) concluded that the area was not of an alluvial-deltaic association but rather the result of channelised mass-flow deposits. He interpreted these as deposited in a submarine canyon or major submarine channel such as would be seen in an upper portion of a very large submarine fan.

The age of the sediments in the Pahau River is being readdressed currently as part of the time scale project designed to define Cretaceous deposits in New Zealand (Ian Raine pers. comm. 2001). Samples collected in the late 1970s have been re-examined and new samples have been collected along the Pahau River. This new analysis of spores, pollens and sparse dinoflagellates has yielded an age of approximately Early Aptian to Early Albian, with the possibility of being as old as very Late Barremian. Figure 3.1 illustrates the poor age control present within the Cretaceous, no New Zealand stages have been differentiated for the Taitai Series except for the Korangan Stage between 116 and 113Ma.

The ‘1980 New Zealand Geological Society Conference Field Trip Guide’ is also the earliest and perhaps only time at which the Pahau River is cited as the reference area for the Pahau Subterrane. Since 1980 the sediments at the Pahau River have remained informally known as the Pahau Subterrane or Terrane (Adams and Graham, 1996;

Bradshaw, 1989; Campbell and Grant-Mackie, 2000; MacKinnon, 1983; Mortimer, 1995; Wandres, Unpubl. PhD Thesis).

Age (Ma)	International		New Zealand		
70	Late	Maastrichtian	Mata	Haumurian	Mh
		80			
Santonian		Raukumara	Piripauan	Mp	
90			Coniacian	Teratan	Rt
Turonian			Mangaotanean	Rm	
Cenomanian			Arowhanan	Ra	
100	Early	Albian	Clarence	Ngaterian	Cn
Moluan				Cm	
Urutawan				Cu	
110		Aptian	Taitai	?	
Korangan				Uk	
Undifferentiated Taitai Series					
		120			Barremian
		130			Hauterivian
		Valanginian			
140		Berriasian			

Figure 3.1 – The provisional Cretaceous time scale as of 1995 (Crampton *et al.*, 1995)

3.3 PROPOSED STRATIGRAPHIC NAMES

I believe it is necessary to formalise the type locality for the vast volume of sediment represented by the Pahau Terrane. To achieve this, deposits in Pahau River catchment need to be described sedimentologically and formally named. I propose a name change for these sediments from the standing undifferentiated Torlesse Supergroup to one new group name and two new formation names. I propose the adoption of the Mt Saul Formation for the conglomerate lithofacies and the Ship Spur Formation for the fine-grained lithofacies encompassed by the Pahau River Group in the Torlesse Supergroup.

3.3.1 THE MT SAUL FORMATION

The Mt Saul Formation is proposed to encompass all rocks in the Pahau River area that fall within the conglomerate lithofacies described in section 2.3.4. The type section for this Formation is located at NZMS 260 M32 861 444. This location was logged and described as Mt Saul A and B (Appendix I, section 2.4.7). Mt Saul Formation outcrops en masse throughout the area with the relationships to other lithologies, geometries and boundary characteristics of these sediments as described in section 2.3.4. A detailed description of the sediments within the type section is described in section 2.4.7.

These sediments were assigned an age of Aptian to Albian by IGNS during their currently ongoing palynological studies in the Pahau River area (Ian Raine, *in prep*).

Correlations of individual Mt Saul Formation bodies are difficult, sometimes impossible as there are faults separating many of their locations with as yet unknown displacements on them. The delineation and measurement of displacements along these faults could be a topic for future research in the area.

3.3.2 THE SHIP SPUR FORMATION

The Ship Spur Formation is proposed to include all the fine-grained lithofacies in the area. This includes all rocks located within the sandstone, interbedded sandstone-mudstone, and mudstone lithofacies. The distribution, geometries and characteristics of these sediments are described in detail in section 2.3.1, 2.3.2, and 2.3.3. The type section for the formation is the Pahau River A section located at NZMS 260 M32 856 432. The Pahau River A is described in extensive detail in section 2.4.2. The age of these sediment is the same as for the Mount Saul Formation.

3.3.3 THE PAHAU RIVER GROUP

The Pahau River Group is the name proposed to at least embrace all sediments in the Pahau River region. This includes both the Mt Saul Formation and the Ship Spur Formation. The lateral extent of the rock units fitting the description of Pahau River Group deposits is unknown but it is interpreted to be regionally extensive. Pahau River Group deposits are probably present in the Clarence River 20km to the north across the Hope Fault. Clarence River deposits share similar characteristics with sediments observed in the Pahau River area.

It is hoped that the Pahau River Group through the use of the Mount Saul and Ship Spur Formations will be able to be applied to very large area. This will require further detailed mapping and sedimentological studies in other locations.

3.4 STRATIGRAPHIC CODES AND REQUIREMENTS

The unit names proposed in this chapter have followed guidelines set by the North American Stratigraphic Code 1982 (NASC). The NASC can be found in (Boggs, 1987) and is itself based upon the International Stratigraphic Guide published by the International Subcommittee on Stratigraphic Classification. Further input into the NASC came from both the International Union of Geological Sciences (IUGS) and UNESCO (Boggs, 1987).

The original publication of this code can be found in the American Association of Petroleum Geologists Bulletin, vol 67, no. 5 (May 1983) pp 841-875.

3.5 DISCUSSION

There is a need in New Zealand for the largest sedimentary body to be formally defined sedimentologically. It has been nearly 130 years since the Torlesse was first described but no type section yet exists for it or any of its major constituents.

The proposal of group and formation names for the currently “unofficial Pahau Terrane reference locality” goes some way in making the unofficial the official. The ultimate goal is to allow geologists, wherever they are in the Pahau Terrane, to compare and contrast their sediments to *one* reference description.

DEPOSITIONAL PROCESSES IN MARGINAL MARINE ENVIRONMENTS

CHAPTER FOUR

4.1 INTRODUCTION

The Pahau River area deposits in the past have been described as either marginal marine representing an alluvial-deltiac setting (Bradshaw and Andrews, 1980) or a submarine canyon to fan (Pescini, 1997). One of the main purposes of this research was to verify one of the existing depositional models or to propose a new model that more adequately described the sedimentology of the Pahau River area.

Stratigraphic logs were compiled for over 900m of section at a high resolution (mostly 10cm scale). Unfortunately the sections are essentially non-correlative as the Pahau River area is composed of several fault blocks. Perhaps the question of marginal marine versus fully marine can finally be laid to rest through the interpretation of these stratigraphic logs.

This chapter will address the definitions of depositional processes and what kind of deposits can be formed from them. Firmly indicating the types and relative ratios of processes present in the field area can restrict the possible deposition environments. For example, the dominance of paired sand-mud couplets may suggest bi-directional deposition in the tidal zone rather than in a deep marine environment dominated by debris flows.

Definitions within the literature of widely occurring depositional processes often vary considerably, the finest example of this is turbidity currents (Sanders 1965; Middleton

and Hampton 1973; Lowe 1982; Middleton 1993; Shanmugam 1997). A lack of agreement on fundamental processes makes it necessary to clearly define depositional processes before interpreting the depositional environment.

The conglomerates in the Pahau River area have been cited several times in the past 130 years. Early reconnaissance geologists were the first to discover the conglomerates around the Hanmer basin (Haast 1871; McKay 1885; Fyfe 1931, 1935). Since 1931 relatively few accounts of the conglomerates in the Pahau River area have been published (Bradshaw and Andrews, 1980; Freund, 1971) or unpublished (Dean, 1993; Pescini, 1997; Wandres, Unpubl. PhD Thesis). Unfortunately none of these papers interpret depositional setting in sufficient detail or describe the provenance of these sediments.

The NZMS 1:250 000 regional geological map does not differentiate Torlesse sediments in the Pahau River area. Two unpublished maps differentiate sediments in the Pahau River, separating lithological assemblages into associations (lithofacies). The first was a map was prepared at a high resolution by Peter Andrews who worked for the geological division of the DSIR in the 1970s, now known as IGNS. This map was published in a short summary although at a medium resolution (*précis* map), in the 1980 Geological Society conference field book (Bradshaw and Andrews 1980). A map composed at a significantly higher detail and an indepth manuscript outling the depositional environment of the area has since been lost from the archive at IGNS (Mark Rattenbury, pers. comm. 2000). Hamish Pescini (1997) constructed the second map for his BSc. Honours project, on the structure and depositional setting of the Pahau Subterrane in the Pahau River/Mount Saul area.

The area was assigned two depositional facies by Andrews and Bradshaw (1980), a flysch facies denoting a submarine origin separated from a marginal marine alluvial-deltaic facies by the Pahau Pass Fault. The flysch facies is associated with relatively highly deformed, alternating sandstone and mudstone beds including occasional thick massive sandstone beds to the west of the Pahau Pass fault. The marginal marine alluvial-deltaic facies is associated with thick conglomeratic bodies with coarsening and thickening upward fine-grained deposits observed in the east of the field area. A

marginal to fully marine depositional setting was chosen because of the following reasons:

- the identification of coarsening upwards sequences in the area.
- the presence of thick conglomerate bodies
- abundance of plant material (stems, leaves etc) in all lithologies.

Pescini (1997), however, disagreed with this interpretation suggesting that deposition within a submarine fan was a simpler explanation. Pescini postulated that the conglomeratic bodies were the result of channelised mass flow deposits based upon the shape of the Mt Saul conglomerate body. Proposed evidence against Andrews and Bradshaw (1980) deltaic interpretation includes:

- numerous normally graded deposits (some with parallel or convolute lamination) all interpreted as Bouma (1962)’s T_{a-e} divisions in a deep water environment.
- the absence of shallow water deltaic deposits as interpreted by Pescini (1997).
- the interfingering of conglomerates with thinly normally graded sandstones alternating with mudstones.
- the great thickness coupled with uniform character of the conglomerates was interpreted as consistent with a major marine depositional basin.

Pescini (1997) proposed that the conglomerate at Mt Saul, Mt Holmes and other locations were the result of channelised mass flow deposits confined in a large canyon or channel.

Two palynological studies, the first in the late 1970s (Raine, 1977) another currently ongoing (Raine *et al.* In Prep) have examined palynology. Both of these studies show an abundance of *spores and pollens* as well as *sparse dinoflagellates* in mudstone and very fine sandstone deposits in the Pahau River directly below Mt Saul. This suggests that both terrestrial and marine environments influenced the area. It was also implied that the levels of dinoflagellates observed was particularly low for the Torlesse Superterrane, while the level of spores and pollens was above average (Ian Raine pers. comm., 2001).

Numerous environmental indicators were observed during the course of this research that endorses the interpretation of a marginal marine depositional model. The most significant discovery found was the identification of *rootlets* in several beds at three widely separated locations (figure 2.11; PRA, PRC, MS). The discovery of rootlets indicates that at least part of the area was subaerial. This finding refutes the submarine canyon model put forward by Pescini (1997).

Subaerial to shallow marine deposition is supported by an abundance of carbonaceous laminations and rare low-grade coal seams (typically less than 30cm thick) that can be found in the sandstone and conglomerate facies. The presence of carbonaceous material in any one lamination can reach as high as 60%. These were probably formed from vegetation that has experienced rapid burial, or minor transportation.

Several *macrofossil* sites were located in close proximity to as well as at some distance from the rootlets. The macrofossils have not been able to be formally identified due to fragmentation probably during deposition or post-depositional alteration. The macrofossils are most likely bivalves or brachiopods inferring the presence of some marine influence. This is also supported by previous palynological studies (Raine, 1977; Raine *et al.* in prep, 2001).

4.2 FLUVIAL PROCESSES

Interpreting the presence and type of sedimentary processes that form deposits in the terrestrial environment is very important in defining the overall depositional environment. Bedload and suspension are the primary methods of transport in the

fluvial environment, these are produced by excess current flow and fludial turbulence. In high sediment flow conditions clasts may become supported to a limited extent by other processes such as grain dispersive pressure.

4.2.1 CURRENT FLOW BEDLOAD TRANSPORT

Bedload transport is the result of a process that causes grains to roll, slide or bounce across a substrate. Transport is initiated by increasing shear stresses imposed on unlithified sediments by the medium in which they exist, air or water. For grains to be transported they need to (a) be dilated above underlying grains and (b) have enough kinetic energy transferred to them from the overlying flow to move (Leeder, 1999).

Several factors affect the rate at which grains are eroded, transported and deposited (figure 4.1). Factors include grainsize, grain sorting, grain rounding, grain shape, flow medium (air or water) and flow strength (Allen, 1997). Whether or not the flow is laminar or turbulent is irrelevant to the initiation and transportation of material (Leeder, 1999). Typically, fine sands with high degrees of rounding, sphericity, and sorting in flows with high velocity show the most rapid erosion and transport rates (Allen, 1997). Logic would dictate that the finer the grainsize the more likely grains will be eroded and transported, this is true to an extent depending on mineralogy. As grains become fine than silt sized particles, electrostatic forces on one grain may be enough to attract it to another grain bonding grains together; this process is called flocculation. Not all very fine particles are prone to flocculation (e.g. feldspars), as not all particles exhibit such strong electrostatic forces as clay minerals do.

The bouncing of grains across a substrate is called saltation. Saltation is not strictly bedload as it is intermediate between bedload and suspension but is most often included in the term "bedload" (Pye, 1994). References made to bedload within this thesis refer to the rolling, sliding and bouncing of grains. Saltation can occur either as small relatively local events or en masse over the substrate depending on the energy levels of the enveloping fluid (Leeder, 1999).

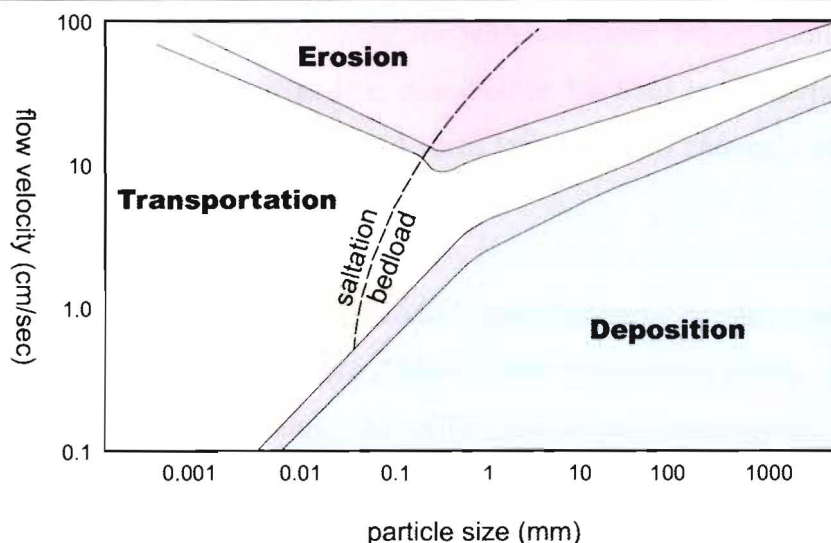


Figure 4.1 – A modified Hjulstrom diagram showing the relationships between erosion, transportation and deposition of sedimentary material. Note the marked increase in velocity needed to transport very fine material; this is due to electrostatic forces causing flocculation. Grey zones are transitional between the fields (Lewis and McConchie, 1994).

There are three major theories in how a grain launches itself into temporary suspension (Leeder, 1999; Pye, 1994).

- ▶ Fluid lift of individual grains into suspension can be induced by pressure differentials on the base and top of grains.
- ▶ In turbulent flow, vortices and eddies created by flow velocity and obstructions can become powerful forces, enough to lift clasts upwards into the flow for short periods.
- ▶ Grains transported by rolling or sliding across a substrate with irregularities (e.g. ripples, dunes etc.) can lose contact temporarily causing saltation.

As grains descend and impact on the substrate, the energy transfer at impact is often enough to other launch grain(s) into the overlying fluid.

Bedload deposits vary markedly depending on regional conditions such as sediment type, sediment load, flow velocity, and location (e.g. channel verses floodplain). Coarse-grained bedload deposits often show imbrication indicative of high flow conditions and crossbedding at the downstream end of bars. Deposits indicative of fluctuating flow conditions result in alternating layers of massive conglomerates and

tabular sets of crossbedded conglomerates with sandstone lenses (Collinson, 1996). Coarse-grained sediment such as that observed at Mt Saul in subaerial channelised bedload dominated environment would form large braided channels separated by a variety of bars (Collinson, 1996).

Fine-grained bedload deposits either produce meandering or braided channel systems, again dependant regional conditions (Allen, 1997; Collinson, 1996). Braided fine-grained systems tend to produce lensoidal geometries representing bar deposits dominated by ripples, dunes, and cross-stratification. Scour surfaces are common within these deposits and should show broad concave upward traces. All varieties of grading are present within braided systems, with clast coarsening indicating increasing flow energy, fining indicating a waning flow. Fine-grained deposits exhibiting meandering patterns show similar bedforms and grading patterns although bedding geometries are different. In deposits representing meander bends asymmetrical geometries thickening towards the apex of the bend should be observed, regularly bedded normally graded deposits adjacent to these represent levee deposits. These were not observed in the Pahau River area.

Bedload is mainly confined to locations that have a high percentage of coarse sediments, predominantly within the conglomerate lithofacies. Bedload sediments in the Mt Saul Formation often display poor to well developed imbrication. Bedding exhibiting stratification and moderate sorting or better is interpreted to indicate deposition from bedload transport. Tabular and lensoidal conglomerate bodies with bedload characteristics probably represent the bar deposits in an alluvial environment. Thin narrow bodies of sandstone within conglomerates were probably deposited by bedload and are likely to be the result of deposition in transverse bars during waning flow.

Bedload current flow with inferred high sediment densities are referred to in the interpretations as hyperconcentrated flow deposits, whereas lower density deposits are referred to as streamflow deposits. Hyperconcentrated flow deposits are typically less sorted with higher degrees of matrix compared to streamflow deposits.

4.2.2 CURRENT FLOW SUSPENSION

Suspension is a process by which sediment is continuously elevated above the substrate (Collinson, 1996; Leeder, 1999). Sediment is transported by fluidal turbulence in both low and high sediment concentrations. Sediment is typically entrained into suspension when flow reaches velocities sufficient to continually support saltating bedload. Flow velocities may be sufficient to transport sediment but not to erode it (c.f. very fine grainsizes – figure 4.1). However suspension can still be observed in these flow conditions as sediment can become blown into the river by winds (Collinson, 1996). Coarse sediment (e.g. coarse pebbles), typically unable to be suspended except in very high flow conditions, may also be rafted downstream on vegetation in lower than expected flow.

Deposition from suspension in current systems is typically only preserved when suspended sediments enter standing bodies of water such as river pools, lakes, lagoons or the ocean (Leeder, 1999; Pye, 1994). Suspended sediments are also deposited in transverse channels in braided river systems during waning flood flows. When suspended sediment enters these locations, normally graded deposits composed of very fine sandstone to mudstone are typically produced (Collinson, 1996). Suspension deposits tend to be destroyed as they settle through saltation and then to bedload in flowing channels, thus they not often observed in the main channel system but rather in zones of quiet depositions (Collinson, 1996).

Alluvial and coastal marine current flow suspension is most likely the primary process that causes thin massive mudstone beds within very large outcrops of conglomerate lithofacies, especially at Mt Saul. It may also be a dominant process in the formation of extensive thin mudstone layers in thick sequences of the sandstone lithofacies. These are likely to be deposited in areas of quiet flow (e.g. as overbank deposits or the settling of jets and plumes ejected into standing bodies of water as hypopycnal flow).

4.3 SHORELINE PROCESSES

The occurrence and distribution of sedimentary structures produced by shoreline processes defines the coastal environment in ancient deposits. A myriad of structures can be produced from processes causing wave reworking, tidal currents and density interactions.

4.3.1 DENSITY INTERACTIONS

The interaction between fresh and saline water at the coastal interface can lead to a variety of interesting phenomenon. River waters can be equally, more, or less dense than saline water depending on river temperatures and sediment load. Density differences lead to underflow, overflow and thorough mixing, which are also known as hyperpynical, hypopynical and homopynical flow respectively (Reading and Collinson, 1996).

Hyperpynical flows typically occur in cold-water rivers with heavy suspended loads entering warm bodies of water or in coarse-grained deltas building out into deep water. In deltaic environments, sediment typically bypasses the shoreline tending to deposit itself on the lower delta slope or prodelta. Deposition outside of the delta front thus inhibits delta progradation (Reading and Collinson, 1996). Hyperpynical flow can produce low-density turbidity currents that are particularly high in mud and silt (Leeder, 1999).

Hypopynical flows also inhibit delta progradation in that material is ejected from the delta front as a plume or jet that can travel for considerable distances. Sediment separation occurs commonly in deltas, denser material (bedload) is deposited and buoyant material is carried out above denser saline water (Reading and Collinson, 1996). Hypopynical flows produce extensive hemipelagic deposits composed of mud or siltstone.

Homopynical flow characteristically creates less widespread and thicker deposits (Reading and Collinson, 1996). This is due to the rapid loss of velocity, which

accompanies the three dimensional mixing that takes effect as fresh water enters saline. Homopynical flow encourages delta growth and normal grading. It is the primary flow type observed in coarse-grained river mouths, although it is seen more often in fresh – fresh water interactions.

Hyperpynical, hypopynical and homopynical more than likely all occurred during the formation of the marginal marine deposits in the Pahau River area. The abundance of extensive mudstone deposits suggests hypopynical flow was common. Hyperpynical flow may have initiated many of the turbidite or debris flow deposits observed in the finer grained lithofacies. Homopynical flow may caused large deposits in areas although none were identified specifically.

4.3.2 WAVE REWORKING AND TIDAL CURRENTS

The action of waves and tides serves to erode, transport, deposit and shape grains. Tides manipulate the coastline by raising and lowering the level of the ocean. This has several effects, it creates a zone in which a specific species live, it changes the height at which waves affect the coastline and if confined, creates currents which can redistribute/rework sediment (Leeder, 1999). The most common product of tides is a sand-mud couplet or a paired mud drape forming parts of ripples. Sands are deposited during higher energy floods and ebbs of the tidal cycle with mud being deposited in the relatively lower energy still stand between the flood and ebbs (Reading and Collinson, 1996).

Depending on the relative strength of the ebb or the flood tides, different lithologies can be deposited within laminations. For example, if the ebb tide was strong while the flood time was particularly weak a couplet of alternate sand-mud laminae would form (sand representing the ebb tide and mud representing the flood tide). As high tide is observed once every 12hr 26min (Reading and Collinson, 1996), a pair of sand-mud couplets would form in approximately a day. Stacked couplet pairs in regularly cyclical sequences are known as *rhythmites* and are often observed in gentle ripples (Reading and Collinson, 1996). Ripples are either symmetrical if the ebb and flood tides are of equivalent strength or asymmetrical if they differ in strength (e.g. the North Sea where landmasses confining tidal currents; Leeder, 1999). Regularly

bedded laminations were observed rarely in study area, in the mudstone lithofacies, although never in close association with a bed(s) that was highly carboniferous or contained rootlets.

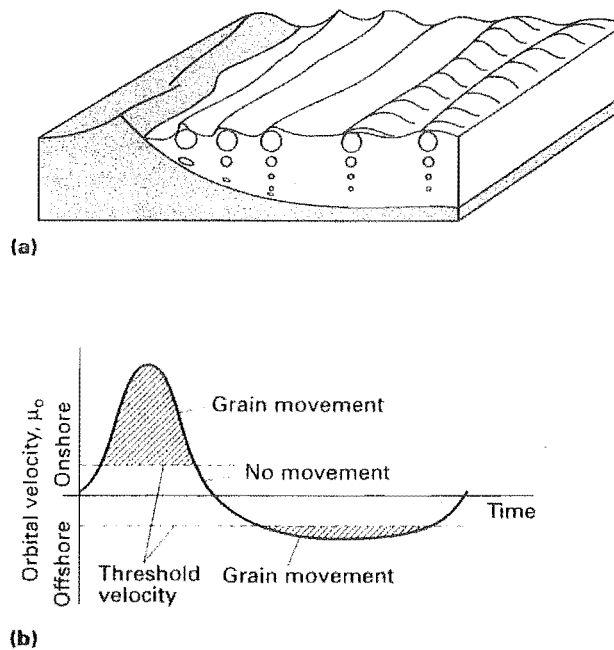
Waves create bars, beaches, barriers and a high-energy zone in which more resistant species can live (Allen, 1997; Leeder, 1999). Waves are produced by either localised wind or nearby storms. Waves are composed of water particles that oscillate in a circular orbit with a diameter equal to the wave height measured from an intervening trough (figure 4.2; Reading 1996). Wave energy is transferred down through the water column in a series of diminishing orbits, affecting an area half the length of the wave (Reading and Collinson, 1996). Waves gain height and grains are moved as the depth of the water column decreases below that of the vertical area affected by the wave orbits (Allen, 1997). Sediment is moved forwards and backwards as waves move over them, this action correlates to the front and back of the orbits as they move forward (figure 4.2). The most common bedform produced by this is a symmetrical ripple (Reading and Collinson, 1996). Waves begin to oversteepen and eventually break as the water becomes shallow, creating a breaker zone along the shoreline. Breaker zones create deposits that become steeper with increasing grainsize, with planar lamination within sediments in this zone particularly common (Reading and Collinson, 1996). Figure 4.2 (b) shows how during fair-weather there is a net accumulation of sediment along a shoreface, this is reversed during storm weather when there is net erosion of sediment from the shoreface. Material migrating out from the shoreface during storms creates a series of bars up to a few hundred metres out from the coastline. Abundant shelly material can be caught with this and may concentrate within these deposits to form storm bed assemblages (Leeder, 1999).

Many geologists believe that specific environments have little or no effect on the overall shape of the grain with individual rock characteristics predetermining grain shapes (Lewis and McConchie, 1994). That aside, specific grain shapes have been documented to be more likely to found in one environment rather than another. One example is oblate clasts on beach and rollers and blades in fluvial environments (Folk *et al.*, 1970; Luttig, 1962).

Deposits indicating wave reworking are present within the Pahau River area, these include bedforms such as planar lamination and ripples, a bed full of broken shelly fragments and oblate clasts in the Mt Saul Formation.

The dominance of prolate spheroid clasts with minor oblate clasts within the Mt Saul conglomerate may suggest that pebbles were formed in an alluvial environment (Lewis and McConchie, 1994). The minor presence of oblate clasts may indicate a beach environment source as oblate clasts are commonly seen on present day coarse-grained beaches (e.g. Kaikoura, NZ).

Figure 4.2 – The morphology of a wave (a) as it approaches a beach, circular to oval, this is a result of the wave circles interaction with the ocean floor. The sediment transport effects of shoaling wave (b) create a net landward movement of sediment through time thus leading to an accumulation of sediment along the beach front during periods of fair-weather, during periods of storm weather there is a net migration of sediment seaward (Reading and Collinson, 1996).



The action wave and tidal processes on the sediments in the Pahau River at the time of deposition was probably minor. Symmetrical ripples are typically very common in both tidal and wave influenced environments but are uncommon within the Pahau River area. It may be possible to explain the relative abundance of asymmetrical ripples by invoking the dominance of flood or ebb flow in the case of tidal processes but it is somewhat more difficult to explain in a beach environment. The noticeable lack of paired mud drapes or mud-sand couplet ripples also does not encourage speculation about tidal dominance. Only at one location (Mt Saul Section C) is wave activity suggested by the presence of symmetrical ripples (refer to section 2.4.1 for full description).

4.4 OFFSHORE DEPOSITIONAL PROCESSES

Sediment gravity flow can be defined as “A process where sediment is driven downslope by gravitational forces exceeding frictional forces, in which particles move independently within that mass” (Adapted from Lewis and McConchie 1994). This can be initiated in a variety of ways (e.g. river flood, slope overloading, earthquake etc.). Sediment gravity flows include turbidity currents, cohesive debris flows, non-cohesive debris flows, fluidised flows and liquefied flows.

4.4.1 BOTTOM CURRENT REWORKING

Bottom current reworking has been proposed to be a process by which ripples may form on the ocean floor (Shanmugam, 1997; Shanmugam, 2000). Ocean floor current velocities can exceed 100cm per sec in confined topography; sufficient to rework, erode, transport and deposit sediment. The most common bedform of ocean bottom currents is a contourite, a rippled layer that bears superficial resemblance to a turbidite (Stow *et al.*, 1996).

Ocean bottom currents probably have not had an impact on sediments in the Pahau River area. The depositional environment for these sediments was probably too shallow and proximal to the coastline. The most distal mudstone lithofacies (Appendix I – Castle Hill section) does not show evidence supporting the formation of contourites.

4.4.2 HEMIPELAGIC – PELAGIC FALLOUT

Hemipelagic and pelagic fallout are the deposition of grains from prolonged suspension (Leeder, 1999; Stow *et al.*, 1996). Grainsize is typically clay to silt, although large individual isolated clasts have been found in these types of deposits. Floating logs and icebergs can carry and drop large individual clasts far out into the ocean before they become water laden and sink or melt (Miller, 1996). Hemipelagic deposits are composed of at least 25% terrigenous material, thus the presence of

terrigenous deposits infers, to some extent, the proximity of a major landmass. Hemipelagic deposits derive their sediment from windblown silts and clays, pyroclastic eruptions or river input. Pelagic deposits are composed primarily of biological material (typically calcareous or siliceous) containing less than 25% terrigenous material.

Massive mudstone that could potentially be attributed to either hemipelagic or pelagic fallout deposits in the Pahau River area does not exhibit high levels of siliceous or calcareous material. Calcareous veins are common throughout the field area, it is a possibility that much of the calcareous material has been dissolved out of the mudstone beds. If this were the case most of the material within massive mudstone beds would be composed of calcite veins, which they are not. Massive mudstone is dominantly present within the mudstone, interbedded mudstone – sandstone, and sandstone lithofacies, these are interpreted to be deposited from hemipelagic fallout.

4.4.3 FLUIDISED – LIQUIFIED FLOW

Fluidised and liquefied flows occur as a result of the rapid repacking of loosely bound grains in a medium such as air or water. Fluidisation and liquefaction are processes in which masses may be changed insitu into a fluid-like state (Leeder 1999).

Liquefaction results from temporary breakdown of grain-to-grain cohesion due to an increase in pore fluid pressure (Leeder, 1999; Pye, 1994). This often occurs in unlithified sediments as a product of shock forces (e.g. earthquakes, repeated shock from storm waves, rapid emplacement of an overlying unit etc.). As grain-to-grain cohesion breaks down, the mass of water and sediment acts as one continuous phase. If this occurs on a slope, then the mass will flow downslope causing a liquefied flow. Slow dewatering takes place as the flow moves, leading to tighter packing of sediments, resulting in the deposition of sediment from the base up. Liquefaction in slope environments tends to destroy internal bedding structures when grains are repacked leaving little trace of the process. Liquefaction does occur in non-slope and/or subsurface environments, in these cases easily identifiable traces are left behind. Two of the most common internal bedding structures, flame structures (figure 2.11) and load casts (figure 2.16), in the Pahau River area were interpreted as being

caused by liquefaction induced by the rapid deposition of sandstone units over mudstone beds that had not yet dewatered. Other examples of structure produced by liquefaction and observed in the study area included convolute lamination and a sandstone dyke (Stow *et al.*, 1996).

Fluidisation is the upward displacement of pore fluid commonly causing the overlying sediment to be held in suspension (Leeder, 1999; Lewis and McConchie, 1994). A variety of water escape structures can form ubiquitously (particulate) or locally (aggregative). Aggregative structures include pipe-like or concave morphologies whereas particulate fluidisation is marked by an uniform grainsize distribution (figure 4.3). The upward displacement of water that initiates fluidisation is often due to the dewatering of flows such as liquefied flows, turbidity currents and debris flows. If fluidisation occurs on a slope, flow is likely to occur.

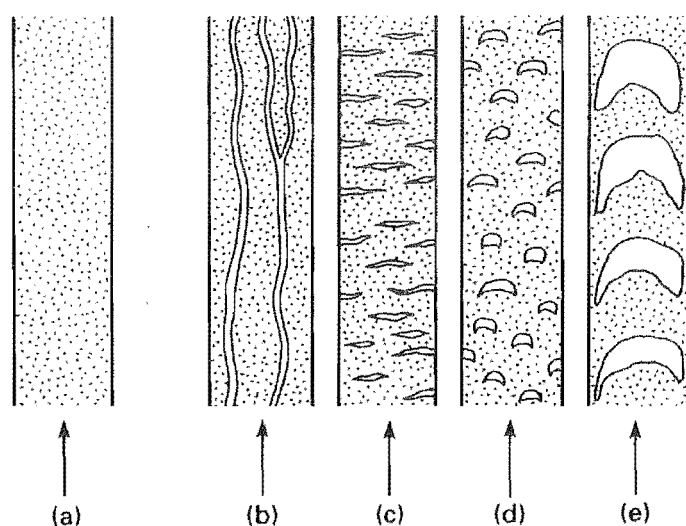


Figure 4.3 – Structures formed as a result of fluidisation, (a) particulate fluidisation, (b-e) aggregative fluidisation, (b) channelling, (c) parvoids, (d) bubbling, (e) slugging. Aggregative fluidisation is more commonly seen when the supporting fluid is gaseous and particulate fluidisation is commonly seen at the toes of levees (Pye 1994).

Liquefaction and fluidisation of sediments and their resulting flows do not contribute significantly as long distance flow support mechanisms. Bedding structures within these flows are typically absent, destroyed by the dewatering structures that replace them. These processes can assume important roles as components of flows that travel long distances. The liquefaction of turbidites produces features such as flame structures, convolute lamination, and sedimentary dykes. Observations about these features can allow interpretations pertaining to palaeoflow, rate of deposition and process.

Liquefied and fluidised flows make up a very small percentage of the sediments in the Pahau area. Convolute lamination was observed twice only, although flame structures and sedimentary dykes are relatively common.

4.4.4 DEBRIS FLOWS

Debris flows are non-newtonian flows in which sediment and water are thoroughly mixed, supported by internal matrix strength or by dispersive grain pressure. There are two varieties of debris flow, cohesive and cohesionless, that can be treated as end members of a continuum across which flow support mechanisms and clast characteristics grade. Debris flows have a moderate to high viscosity and are plastic in their rheology due to their high sediment to interstitial fluid ratio. Flows that have a plastic or pseudo-plastic rheology typically flow in a laminar state.

Cohesive debris flows are predominantly supported by the internal cohesive strength of its matrix as well as the overall buoyancy of the flow (Stow *et al.*, 1996). Other support mechanisms that often exist to lesser degrees within cohesive debris flows include excess pore pressure, escaping pore fluids, and turbulence. Debris flows are non-newtonian fluids having a plastic rheology, thus they have internal yield strength which must be exceeded in order to initiate flow. If shear stress is applied but the yield strength is not exceeded then any deformation imposed is recoverable.

The morphology of a cohesive debris flow is defined by a rigid internal plug of non-mixing sediment bounded by a zone of mixing (Major, 1998; Stow *et al.*, 1996). In the boundary layers shear stresses may not be large enough to overcome the internal shear strength of the flow leading to local deposition. Boundary layer shear stresses as well as flow velocity increases toward the central plug (figure 4.4).

Flow is maintained until shear stresses applied upon the flow fail to overcome the internal shear strength of the flow (Stow *et al.*, 1996). Internal shear strength typically increases as the flow dewateres, eventually exceeding the external shear stress and leading to deposition. Debris flow deposition occurs instantaneously over the whole flow *en masse*; the reason being that internal shear strength exceeds the external shear stresses over the whole at once (Leeder, 1999). The front of the flow,

or snout, is often very steep at the time of deposition because of en masse freezing, this can lead to secondary slumping and sliding at the front of the flow (Allen, 1997).

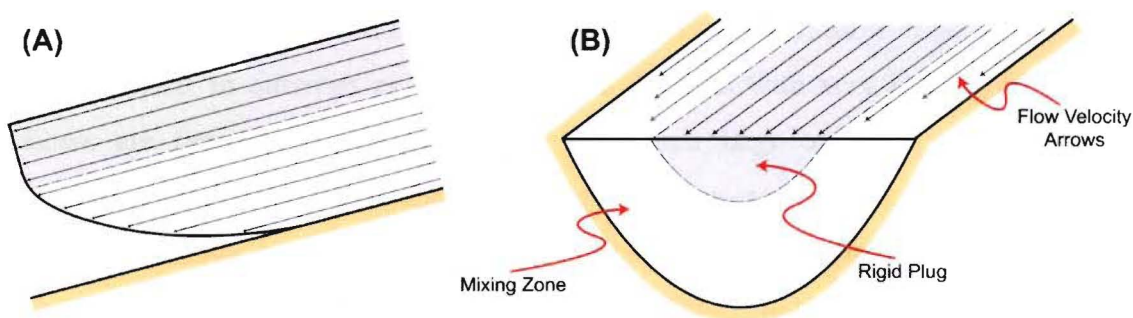


Figure 4.4 – The simplified morphology of a debris flow. (A) a length profile shows a cross section through the centre of (B). The lengths of the flow velocity arrows are relative to their individual speeds (after Stow et al., 1996).

Due to en masse freezing of the flow, clasts are preserved in the same position they were in while being transported. Cohesive debris flows are typically poorly sorted, massive deposits that lack internal structure. Poor to moderate grading can occur as other flow mechanisms such as turbulence (*normal grading*) and dispersive grain pressure (*inverse grading*) increase in intensity within the flow (Allen, 1997; Leeder, 1999).

Cohesive debris flows deposits in the Pahau River area include many mudstones, sandstones, conglomerates, and all pebbly mudstones/sandstones. These flows are most commonly observed in the mudstone and conglomerate lithofacies and, to a lesser extent, within the other lithofacies. Grading is typically absent, although when present grading is either vaguely normal or inverse. Grainsize sorting within the debris flows deposits is typically poor to moderate. Several debris flow deposits have well developed bi-modal clast size distributions with each mode typically moderately to well sorted. Pebbly mudstones within the mudstone lithofacies appear to be in a lateral or basal relationship to major conglomeratic bodies (e.g. Mt Saul, Mt Holmes and the large conglomerate body to the east of Mt Saul).

Non-cohesive or cohesionless debris flows differ from cohesive flows primarily by flow support mechanism. Non-cohesive debris flows are supported predominantly by dispersive pressure created by intergranular collisions. Pure non-cohesive flows most commonly occur within well-sorted sands and gravels. Pure end member

cohesionless debris flows are known as *grain flows*, in which sediment is transported downslope by the avalanching of grains. Grain flows in their pure form occur on steep slopes in well-sorted sediments where the slope angle exceeds the angle of repose for the average clast size (Leeder, 1999; Lowe, 1982; Stow *et al.*, 1996). Grain flows appear in outcrops as clast-supported deposits with very little matrix. Grain flows are typically not a mechanism by which large amounts of sediment are remobilised at the heads of submarine canyons (Stow *et al.*, 1996). There is no reason why grain flows could not be a common occurrence as a minor sediment transport mechanism within a coarse-grained delta where slopes are typically high.

Gradations between end member cohesive (*mudflows*) and end member non-cohesive (*grain flows*) were the most commonly observed debris flows, these can be termed *density modified grain flows*. Internal cohesive matrix strength is present to some degree in all density modified grain flows, absent only in grain flow transported purely by avalanching. Several beds containing well-sorted fine pebbles and very little matrix were observed in the Mt Saul conglomerate body these may have been formed by grain flow but were more likely formed by bedload or density modified grain flow. The abundance of debris flow deposits denotes the presence moderate to steep slopes within the depositional environment.

The terms matrix and clast supported can often be misconstrued to mean cohesive and non-cohesive debris flows respectively; this is incorrect. The terms clast and matrix supported has only been used within this research describing what the final deposits look like rather describing flow types. The term clast-supported was used to describe beds in which clasts were observed to frequently touch each other, matrix-supported was used when clasts were observed not to touch each other.

4.4.5 TURBIDITY CURRENTS

Turbidity currents and their deposits (turbidites) in the past have been described in a myriad of ways. Although there have been many attempts to accurately define what a turbidity current is, the broader geological community only agrees on a few key points (Kneller and Buckee, 2000; Lowe, 1982; Middleton and Hampton, 1973; Shanmugam, 2000). All agree that a turbidity current is a sediment gravity flow kept

in suspension by fluid turbulence. Sediment remains in suspension and flow is maintained by a feedback loop known as auto-suspension (Bagnold, 1962). If a cloud of sediment is sufficiently dense, upwelling intervening fluid becomes slightly turbulent and has the effect of slowing the settling process. Auto-suspension occurs when a sediment cloud is so dense that it begins to flow downslope; as it does, water and possibly unlithified sediment become entrained at the head of the flow increasing turbulence and adding to flow density, thus accelerating the flow. Turbulent flow is maintained until the loss of energy through friction of the flow with the substrate and grain settling exceeds the gain of energy through fluid and sediment entrainment (Leeder, 1999; Stow *et al.*, 1996).

The exact nature of the "turbidity current" is, however, still not fully understood some 70 years after their first discovery. Turbidity currents have been replicated in flume experiments since the early 1930s but to date no equipment has been deployed to actually observe the dynamics of the flow in the field (figure 4.5). The only real world data comes from inferences about submarine cable breakages and sediment discharge in fresh water dams and lakes (Leeder, 1999; Mulder *et al.*, 1997; Skinner and Porter, 1987).

Since the real world nature of turbidity currents has rarely been observed, our understanding is based upon flume experiments and field observations of ancient deposits. This has lead to the innumerable categorisation of turbidity currents ranging in increasing densities from low-density turbidity currents (sediment densities of ~1-3% vol.) to high-density turbidity current (sediment densities of 3 - 45% vol. in clay free flows), and even mega-turbidity current (>45% sediment densities?, mega-turbidity currents probably represent dilute debris flows). Most geologists agree upon the nature and flow mechanics involved in the generation, transportation and deposition of a low-density turbidity as well the deposits they create (Kneller and Buckee, 2000).

Low-density turbidity currents move as newtonian fluids capable of travelling large distances at high speeds on low slope angles (Stow *et al.*, 1996). They flow supported solely by fluidal turbulence, thus the deposits of low-density turbidity currents form progressively as energy is gradually lost from the flow. As the flow strength wanes,

the densest clasts fall out first, producing well to very well sorted, normally graded deposits. If the flow regime during deposition of low-density turbidity currents was sufficiently high velocity, bedforms, including a variety of ripple and lamination types, could be potentially formed. Normally graded beds with laminations and/or ripples are amongst the most commonly observed beds in the Pahau River area indicating significant deposition from turbidity currents.

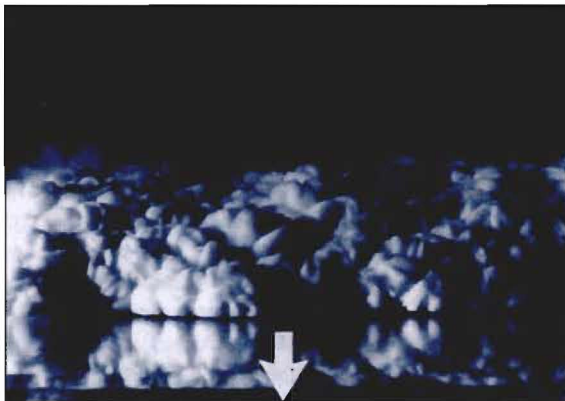
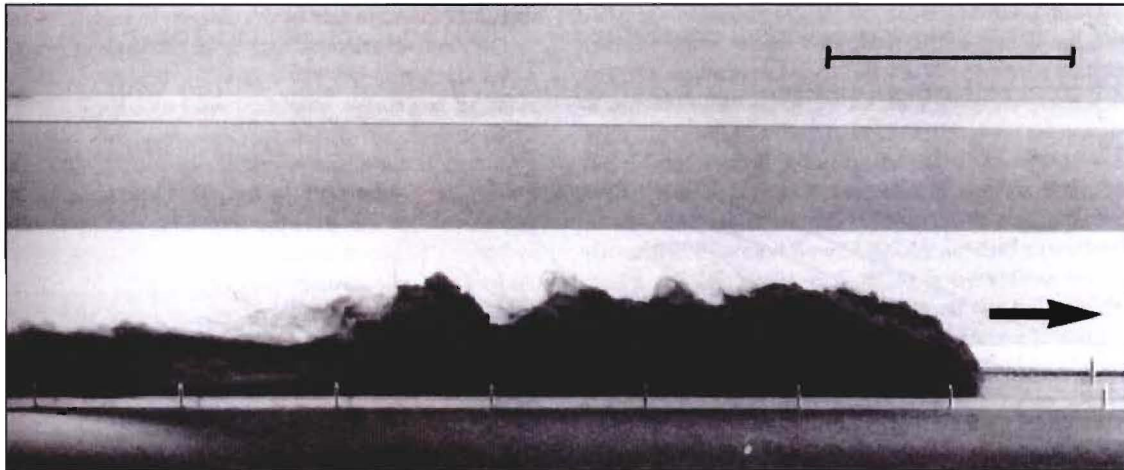


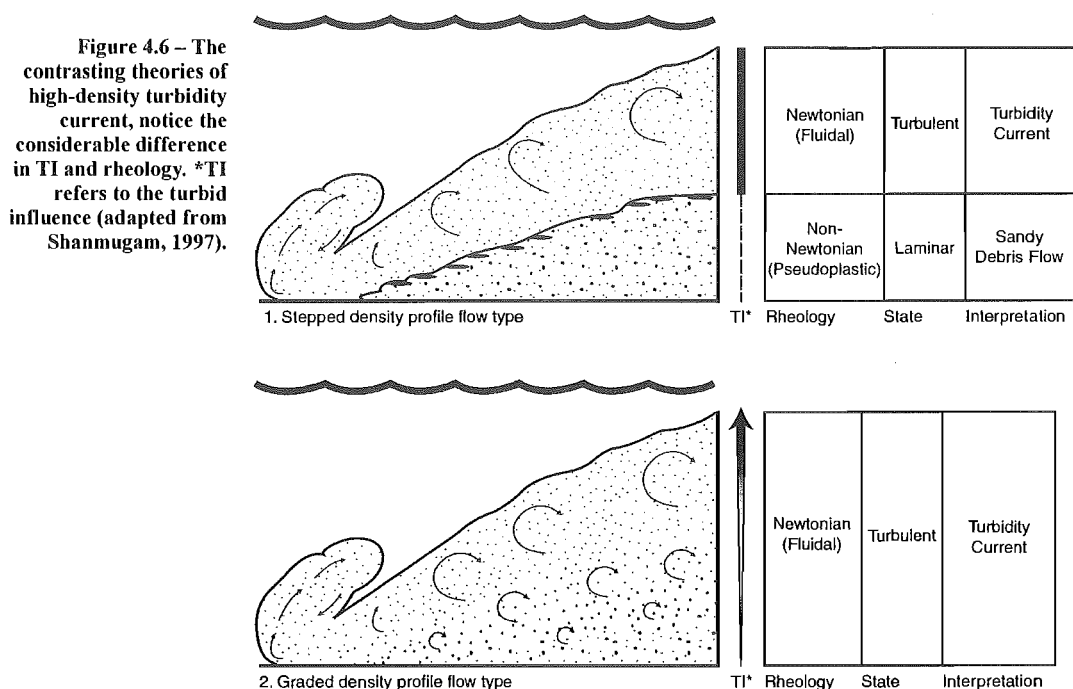
Figure 4.5 – Both photos show a low density turbidity current flume experiments, to the *left* is a flow head about 50cm in width between the reflected images of the head in the walls of the tank, the *above* image shows a side profile, scale is ~25cm (Pye, 1994).

Currently there is a raging debate on the definition of high-density turbidity currents. The debate centres around what occurs when the sediment load is raised and what effect this has on the rheology and deposition of the flow. There are currently two schools of thought on this (figure 4.6) –

- (a) Stepped Density Profiles (SDP) – This theory suggests that high-density turbidity currents are a misnomer and that deposits inferred to represent these flows are composed of one or two different flow types. Basal high-density flows are theorised to formed as non-newtonian fluids supported by matrix strength and grain-to-grain interactions rather than by turbulent flow

(essentially sandy debris flows), also believed to be deposited *en masse*. High-density flows may also have low-density turbidity currents riding on top of them at a different velocity; the top part of the flows would be deposited progressively and may extend much further than the basal flow. No interaction is inferred to occur across the flow boundaries (Mulder *et al.*, 1997; Postma *et al.*, 1988; Shanmugam, 1997; Shanmugam, 2000).

- (b) Graded Density Profiles (GDP) – Turbulence increases upwards through the flow profile; low levels of turbulence exist only in the lowest levels of the flow. Deposition in this theory occurs progressively as turbulence fails (Hiscott *et al.*, 1997).



There seems to be evidence in the rock record to support either view depending upon how you interpret that evidence. Shanmugam (1997) cites the abundance of poorly sorted beds, mud intraclasts, rafted outsized grains, inverse grading, planar and random clast fabric and plastic deformation structures as evidence that many of the previously interpreted turbidite deposits are in fact sandy debris flows. These criteria, which undermine many previously defined formations (Shanmugam and Moiola 1995), are rebutted by Hiscott *et al.* (1997) and Slatt *et al.* (1997) as they infer these features to be the result of late stage depositional effects.

The implication of accepting one model over another appears to be purely geometrical. The SDP model implies that the basal sandy debris flow layer would freeze en masse and a potential upper turbidity current would continue to flow. In this model thicker less extensive cores of poorly to moderately-sorted, massive sandstones overlain by more widely extensive, thinner, well-sorted, normally graded sandstone or siltstone beds would be expected. No interaction across the flow boundaries is implied in this model but it appears little consideration was given to the reworking of the sandy debris flow by the upper layer after deposition of the lower layer. Reworking of the lower deposit could either form scour surfaces or increase the gradation between the two units.

GDP high concentration turbidites would be expected to exhibit progressively increasing sorting upward throughout a deposit. Sorting would also be expected to increase as deposits become increasingly distal. The GDP theory supports the concept of traction-carpets travelling as coarse basal bedload in constant contact with the substrate.

Traction carpets in proposed high-density turbidity currents are also explained by the SDP model proposed by Shanmugam (1997). Stow et al. (1996) comments that turbidity currents can sustain a traction carpet of colliding grains close to the bed on low angle slopes. It was inferred that dispersive grain pressure is the dominant flow process, assisted considerably by the overlying turbulent flow in these circumstances. It should be noted that deposits like those interpreted to be traction carpets could be transported as bedload where grain dispersive pressure is not as important as a flow support mechanism. The flow nature of traction carpets should be apparent at the outcrop, grain flows are plastic in rheology therefore bedforms should be absent and grading may be inverse, deposition is en masse. Conversely, bedload is transported by rolling or bouncing (saltation) of grains; deposition is progressive so bedforms commonly exist.

Both theories SDP and GDP hold valid points and the use of either theory has important implications for interpreting depositional process and bedding geometry. Many of the larger beds in Pahau River have poorly to moderately sorted sandstone

bases which grade rapidly to mudstone in the top 10% of the bed (refer to Pahau River AD for examples, Appendix I). Assuming an interpretation is based on the SDP is it more accurate to define this as high density turbidity currents or dual process flows. I refer to SDP's as high density turbidity currents as these are the most likely natural progression from low-density turbidity currents through debris flows. Many normally graded beds were observed with moderately to poorly sorted bases that changed rapidly over a period of 5cm or less to a well-sorted top. It is my opinion that these beds were formed from high-density turbidity currents that had a SDP. Beds were observed to increase in grading upwards these might have been formed by graded density profile high density turbidity currents.

Turbidite deposits from low to high density dominate sandstone deposition in the mudstone – sandstone lithofacies everywhere in the field area. The same range of densities occur in the sandstone lithofacies although they do not dominate to the same degree. Only low density turbidite deposits are observed in the mudstone lithofacies, thin sandstone beds in this lithofacies were almost exclusively interpreted to be these. Turbidite deposits are not thought to be typically present within the conglomerate lithofacies.

The difficulties of interpreting well-sorted sandstones should also be mentioned at this point. If a bed is particularly well sorted, how is it possible to tell if the flow that formed it deposited grains progressively or en masse? Although confirmation can be made by examining the orientation of the a-axes (long axes) of individual grains to see if they were aligned in the direction of flow or randomly this is not practical in the field. Definitive clast orientation analysis of sandstones requires thin section analysis of bedding planes in more than one orientation. How then can one be completely confident that a massive sandstone bed is deposited by a turbidity current, or by a cohesive or non-cohesive debris flow?

4.5 INTRACLASTS

Intraclasts are developed from the incorporation of material scoured from the confining walls or from the substrate. Walls confining erosive flows can easily become basally scoured and unstable, often leading to localised collapse or slumping.

Intraclasts are also often incorporated into the base of a flow. Basal incorporation occurs when flows are erosive, possibly also occurring when underlying substrates are not fully dewatered by the upward injection sediment into the flow. Intraclasts in the Pahau River study area were dominantly composed of massive mudstone encased in sandstone, although within the Mt Saul Formation intraclasts composed of lithologies ranging from mudstone to granule was observed.

Intraclasts are commonly observed within all lithofacies except the mudstone lithofacies in the Pahau River area. Intraclasts in the Pahau River area often exhibit curved faces and angular faces together on the same clast and have been observed partially broken apart (figure 4.7). It is inferred that most, if not all, intraclasts represent partially lithified sediment.

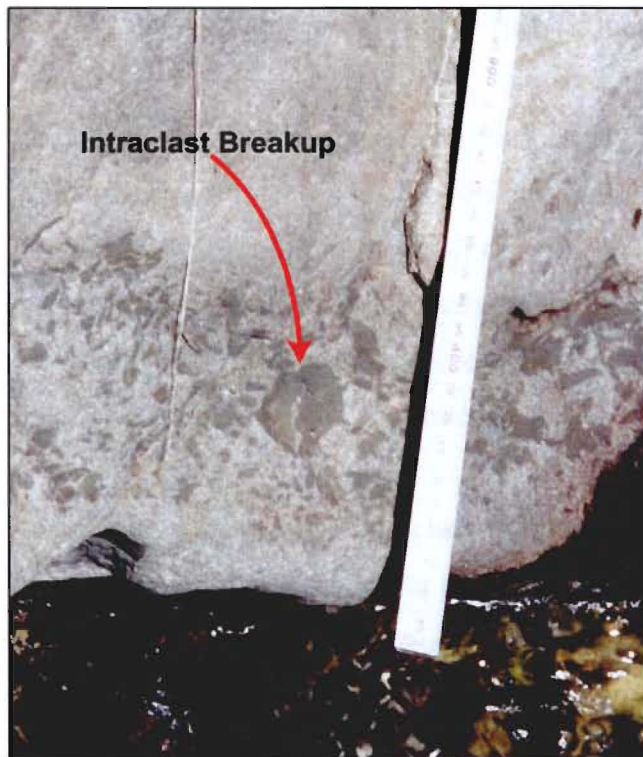


Figure 4.7 – Mudstone intraclasts within a sandstone bed in the PRA section. Notice the thin crenulated sliver of the sandstone separating two parts of a previously whole intraclast.

Literature on the incorporation, transportation and final emplacement of intraclasts is particularly sparse. The terms ‘intraclasts’ or ‘intraclast’ or ‘rip-up clasts’ collectively returned 80 positive hits in GEOREF in March 2001. All 80 of these referred to lithofacies descriptions of associated bedding or tectonically induced mega-breccias. As there are no published models or detailed accounts of the emplacement of intraclasts, one of the most common features observed in bedding within my field

area, I felt it necessary to attempt a paradigm. Intraclasts in the Pahau River area contain the following characteristics --

- Finer grainsizes than encasing lithologies.
- Increased frequency within thicker beds.
- Increasing angularity proportional to increasing intraclast size
- Rounding and size of intraclasts within a single bed is generally uniform.
- Consistently composed of mudstone except in the Mt Saul Formation where intraclasts of up to granule grainsizes were observed.
- Intraclasts within moderately to poorly sorted beds were not observed in consistent distributions.
- Intraclasts within well-sorted beds were usually located along distinct horizons although never in the upper parts of the bed.

It can be inferred that since intraclast lithologies are always finer than encasing beds that either (a) intraclasts inside a unit of the same lithology are not readily apparent or are unobservable due to the uniform grainsize, or (b) that energy levels have to be sufficiently great to entrain partially lithified sediment. The inference that flows entraining intraclasts need specific erosive strength or flow velocities is supported by the increased frequencies of intraclasts observed in thicker and coarser beds.

Increasing angularity of intraclasts proportional to size suggests that the angularities of clasts are directly related to transport distance. Transport distances are suggested here to be relatively short in all cases except when intraclasts were located within beds exhibiting characteristics indicative of a plastic flow rheology.

Uniform rounding and size within individual beds implies that the intraclasts were introduced into the flow at the same time. Some beds show bimodal or trimodal rounding and size distributions, probably reflecting two or three bank fall collapse events and/or equivalent periods of basal erosion. Beds that have no coherent size or rounding distributions most likely the result of inclusions of intraclasts at numerous periods throughout the flow.

Implications drawn from the distribution of intraclasts within a bed are based on flow rheologies described from debris flows (Leeder, 1999; Shanmugam, 1997; Stow *et al.*, 1996) and turbidity currents (Allen, 1997; Lewis and McConchie, 1994; Shanmugam, 2000; Stow *et al.*, 1996) discussed in section 4.2.1 and 4.2.2. Three distributions of intraclasts were observed, 1) in the basal portion of the bed, 2) in the upper cover portion of the bed, and 3) throughout the bed excluding the base or cover. *Basal intraclasts* are inferred to be the result of settling of the intraclasts through flows or inclusion of intraclasts at the base of the flow. The presence of *cover intraclasts* is suggested to be caused by a several methods; the rafting of clasts on a plastic debris flow, late inclusion of intraclasts after substantial aggradation in a turbidity current, or ascending through the flow from the base aided by density differences and grain dispersive pressure. *Internal intraclasts* (i.e. not within the basal or cover 10cm) are either caused by inclusion at or near depositional level from a wall confining the flow or as a partial evolution of a basal to cover or cover to basal intraclast.

It is also plausible that fluvial processes could create intraclasts at least near channel banks where collapse can take place. This can be interpreted for some deposits in which very large intraclasts were observed in the Mount Saul conglomerate body (Appendix I, MSB at 33m).

Several interpretations can be made about distributions of intraclasts in well-sorted versus moderately to poorly sorted beds with differing grading styles (figure 4.8).

In turbidity currents, intraclasts are expected to exist along either well-defined horizons and/or as a chaotic assemblage at the base of flow (lower 10cm). Well-defined horizons are interpreted to represent bank collapse inclusion of intraclasts during the progressive aggradation of turbidity currents. Chaotic basal assemblages in beds interpreted as turbidites are suggested to represent basal inclusion through erosion of the substrate. Scattered distributions of intraclasts are suggested to be indicative of debris flows.

Grading	Sorting	Distribution	Interpretation
Normal	Moderately to poorly sorted	Basal	Basal entrainment, settling (<i>debris flow, high-density turbidity current</i>)
		Cover	Buoyant lift, rafting (<i>debris flow, high-density turbidity current?</i>)
		Throughout	Settling, basal entrainment, rafting, buoyant lift, channel wall entrainment, early to late stage aggradation inclusion (<i>debris flow, high turbidity current?</i>)
Normal	Well to very well sorted	Basal	Basal entrainment (<i>turbidity current</i>)
		Cover	Not observed
		Throughout	Basal entrainment, inclusion during aggradation of turbidity current (<i>as long as along equal horizons</i>)
Massive	Moderately to poorly sorted	Basal	Basal entrainment or settling (<i>debris flow</i>)
		Cover	Rafting or buoyant lift (<i>debris flow</i>)
		Throughout	Channel wall or basal entrainment, settling, rafting, buoyant lift (<i>debris flow</i>)
Massive	Well to very well sorted	Basal	Basal entrainment or settling (<i>turbidity current, debris flow, grain flow?</i>)
		Cover	Rafting, buoyant lift, very late stage inclusion (<i>debris flow, turbidity current, grain flow?</i>)
		Throughout	Settling, basal entrainment, rafting, buoyant lift, channel wall entrainment, early to late stage aggradation inclusion (<i>high or low density turbidity current, debris flow, grain flow?</i>)

Figure 4.8 – Interpretative chart for the recognition of intraclasts in sedimentary beds, distributions in red were the most common observed distributions in the field (Pahau River Area).

The composition of intraclasts reflects the composition of the substrate or confining walls of the flow. Assuming the distance between inclusion and deposition in turbidity currents is short and intraclasts are basally incorporated, intraclasts should be of the same composition as the underlying bed. If intraclasts are not composed of the lithology of the bed directly beneath it, it can be inferred that the intraclast was probably sourced from a confining wall or from a source a significant distance away. Debris flows can transport intraclasts for large distances without breakup. Thus it is not reasonable to expect the basal bed to always be of the same composition as the intraclasts because of plug flow.

Problems arise with unknown rheological models such as high-density turbidity currents. The stepped density profile theory suggests a two tiered flow process. The lower debris flow dominated regime, based on observations here, would have intraclasts evenly distributed throughout. The upper turbidity current flow however, would probably only have intraclasts along well-defined horizons or near the interface of the two flows. Intraclast distribution within the graded density profile turbidity currents could be expected to represent a slow transition from scattered to discrete horizons as turbulence increases upwards. Unfortunately neither of those two intraclast distributions was observed in the field.

(It is interesting that no one has thought to test their theory by this method!!)

4.6 DISCUSSION

The inferred depositional environment of the Pahau River area has been suggested to be marginal marine including both terrestrial and fully marine deposits. It is possible to identify gradations between deposits which are dominated by offshore processes and grading into deposits controlled by coastal processes into deposits that are dominantly terrestrial (e.g. the PRA section 2.4.2).

The Pahau River area is interpreted as dominated by hemipelagic deposits, turbidites, current flow bedload, and suspension. Although deposits caused by other processes are interpreted to be present they are thought to be relatively minor (e.g. fluidisation, tidal currents etc.).

Intraclasts can be used as an aid in the interpretation of these deposits, especially their flow histories. The most likely reason for the absence or low levels of intraclasts in massive mudstones and conglomerate bodies is their extreme energy levels. Erosion is not observed in hemipelagic fallout and current flow bedload transport would probably break intraclasts up extremely rapidly.

DEPOSITIONAL SETTING

CHAPTER FIVE

5.1 INTRODUCTION

Previous theories considering the Pahau River area have proposed depositional environments ranging from deltaic to a submarine canyon (Bradshaw and Andrews, 1980; Pescini, 1997). Both depositional environments produce similar facies architecture but yet occur in radically different settings with different paleogeographic implications.

To validate a submarine canyon model, canyon walls need to be identified. These were proposed by Pescini (1997) however upon examination of these I find I do not come to the same conclusion. Pescini (1997) interprets the canyon wall or possibly a syndepositional Cretaceous fault at grid reference 260-M32 871 445. Upon close inspection of this location beds were found to grade laterally from clast-supported conglomerate to matrix-supported conglomerate to sandstone. An interpretation of canyon walls requires that some erosional contact in one form or another should be observed on at least two sides of the conglomerate. While there is an erosional contact at the base of the conglomerate this was not observed on either side. A basal erosional contact is not unusual for any coarse-grained sedimentary body. The conglomerate at Mt Saul is conformable to the southwest and northeast, but fault bounded in the northwest and southeast.

Stratigraphic sections logs supported by previous palynological studies (Raine, 1977; Raine *et al.* in prep. 2001) clearly indicate the presence of a marginal marine depositional environment, endorsing a deltaic model. Several other key features in the area support the presence of a marginal marine environment. Carbonaceous content almost universally increases with grain size in the finer grained sections. Fragments of coal in a variety of sizes (with faces up to 20cm²) are relatively

common, located both within finer grained sections (e.g. MH – log imprint core) and in the conglomerate deposits. Coarsening upwards sequences are indicative of increasing energy levels associated with most prograding environments, including coastlines. Conglomeratic bodies with abundant bedload deposits, are commonly imbricated indicative of terrestrial streamflow deposits. However, most importantly is the discovery of *rootlets* strongly indicating the presence of a terrestrial environment in close proximity to *dinoflagellates* and *macrofossils* indicating a marine environment.

5.2 DEPOSITIONAL SETTING

Establishing a marginal marine environment significantly reduces the amount of possible depositional settings. Regional depositional settings could include deltas, beaches, barrier islands, tidal flats and inlets, and estuaries. A depositional setting dominated by beach lines or barrier islands can be dismissed due to the lack of bi-directional wave structures, well sorted conglomerates, hummocky and large scale low angle cross-stratification. Tidal flats, tidal inlets, and estuaries all fail to provide adequately for high energy levels needed to support thick poorly to moderately sorted debris flow deposits commonly observed within the conglomerates throughout the area. The only possible marginal marine depositional environment left is *deltaic*, which does provide for all the features observed in the study area. Due to the large scale of the conglomerates in the area deposition is most likely to be predominantly deposited in a *fan-delta depositional environment*.

Deltas have three major deposition components, the delta plain, the delta front - slope and the prodelta. Deposition in the Pahau River area can be categorised into one of the three aforementioned depositional components.

5.2.1 THE PRODELTA

Prodelta environments are the lowermost portions of a deltaic sequence, permanently unaffected by wave or tidal processes. Conceptually they are dominated by hemipelagic mudstone periodically interrupted by sharp-based normally graded beds

produced by flood generated hyperpycnal flow (Reading and Collinson, 1996). Cohesive to cohesionless debris flow deposits are often common features in prodeltas and may dominate the environment (Reading and Collinson, 1996).

The prodelta is roughly equivalent to the mudstone lithofacies and the mud dominated interbedded mudstone – sandstone lithofacies in the Pahau River area. It is interpreted to be present within most of the stratigraphic sections with the exception of Mount Saul sections (A, B and C).

The conceptual model of the prodelta is best investigated at the base of the PRA section. Very thick, poorly sorted, pebbly mudstones interpreted as debris flows 20m *below* the base of the PRA section are suggested as being derived from the delta front. One of these debris flow deposits can be traced back along strike towards the Mt Saul conglomerate into which it eventually grades. At the base of the PRA massive mudstone interpreted as being deposited by hemipelagic fallout dominates bedding. This is regularly interrupted by thick laminations or very thin beds of normally graded sandstones interpreted to represent distal turbidite deposits (c.f. PRA figure 2.14 from 0m to 10m). This style of deposition is also observed at the top of the PRC section (c.f. figure 2.19 above 138m) and probably exists in the lower WR, PRB, and SP sections though moderate to high levels of deformation mask a clearer interpretation. At all of these locations very thin turbidites eventually thicken and coarsen upwards, massive mudstone also generally decreases upwards throughout each section.

Small channelised debris flows can be observed in the bases of the PRA and MH sections, observed as 1-2m wide, <1m thick, bodies with trough-like geometries. Other highly concentrated flow deposits are present, including debris flows (c.f. PRA figure 2.14 at 17m) and high concentration turbidity currents with stepped density profiles (Appendix I – PR_{AB09} at 56.5m).

Slumping can often be a common feature within a prodeltaic environment. A body of strata showing signs of soft sediment deformation within the PRA section at 50m is interpreted to represent a slump on a rotational slide surface.

Processes controlling distal deposition in the prodelta are interpreted as being dominated by hemipelagic fallout and turbidity current, with relatively subordinate debris flow influence. Delta progradation is observed by the increasing frequency, thickness and coarseness of deposits by turbidity currents. Turbidites are observed in two geometries, sheet-like geometries interpreted to characterise nonchannelised flows and lensoidal geometries inferred to represent channelised flows. Sheet-like geometries dominate in the distal prodelta, whereas the presence of channelised flows signifies gradually increasing proximal deposition. Debris flows are observed in both the proximal and distal prodelta, although these are *typically* channelised in the proximal prodelta and nonchannelised in the distal prodelta.

5.2.2 THE DELTA FRONT – SLOPE

The delta front – slope environments are characterised in the Pahau River area by large thickening and coarsening upwards sequences that can be clearly seen in the Pahau River A, Waiau River and Mt Holmes sections.

A general model for delta front processes and facies is outlined in (Reading and Collinson, 1996). Essentially this is the zone where fresh water charged with sediment enters interfaces with an array of processes and environments controlled by the body of water it enters into. The bulk of the deposition occurs at the delta front, this typically includes the construction of distributary channels, distributary mouth bars, subaerial and subaqueous levees, lagoons, interdistributary bays, crevasse splays, tidal channels and barrier beaches. Depositional features such as these are represented in varying degrees depending on the relative influence of wave, tidal and fluvial processes. Deposition on the delta slope depending on the dominant depositional process can be either confined within broad shallow channels or almost totally unconfined.

Deposits on the delta slope record the transition between proximal prodeltaic deposits and the delta front, these essentially appear as coarser and thicker equivalents of the prodelta. Depositional processes between the two environments are essentially the same, thus the relative ratios of those processes differentiate these environments.

General models for mouth bar sequences suggest a coarsening and thickening sequence with upper parts of the sequence often eroded by prograding distributary channels (Leeder, 1999; Reading and Collinson, 1996). Feeding the mouth bar are large distributary channels represented in the rock record by thick massive sandstone or conglomerate deposits. To the sides of distributary channels levees are often observed. Levees represent the raised edges of both subaerial and subaqueous meandering channels commonly observed as regularly bedded alternating sandstone and mudstone beds.

Interdistributary bays are zones of low energy between distributary channels at the terrestrial – marine interface, often greatly influenced by tidal currents or wave reworking (Leeder, 1999; Reading and Collinson, 1996).

Unconfined flow on the delta slope, subaerial and subaqueous distributary channels, mouth bars, interdistributary bays, crevasse splays, subaerial and subaqueous levees were all commonly represented in coarsening upwards sequences in the Pahau River area. Lagoons, tidal channels and barrier beaches were not identified, suggesting that the wave and tidal influence on this delta was minimal.

The transition to the delta front is manifested in the delta slope by comparatively thinner and less frequent deposits of hemipelagic mudstones with thicker, coarser, and more frequent turbidites (c.f. PRA figure 2.14 at 10m and 100m). Two types of flow can dominate on the delta slope, unconfined and confined flow in the Pahau River area. Most of the turbidite deposits in delta front are interpreted as unconfined flows. Confined flows often occur together in small clusters of beds are interpreted to represent subaqueous channels (c.f. PRA figure 2.14 at 91m).

A mouth bar sequence is interpreted at the PRA section from 140m (figure 2.14) where bedding generally increases in thickness, grain size, and carbon content until 160m when the sequence is lost in vegetation. The appearance of flame structures at 153m indicates rapid deposition and suggests that the depositional environment may have been subaqueous. Internal bedding structures present include crossbedding, ripple lamination, and planar lamination these are consistent with a fluvially

dominated model. No erosional trace is observed before the sequence is lost in vegetation.

Very thick massive or normally graded sandstones (>2m) are intercalated with thin beds (<20cm) of massive mudstone are often observed in the upper parts of very large coarsening and thickening upward sequences. These are interpreted as channel fill deposits located within major distributary channels (c.f. WR figure 2.20 at 70 – 100m; PRB figure 2.18 at 60m). Deposits up to 26m thick were observed without any internal bedding structures (c.f. PRC figure 2.19 at 10m). Extremely thick deposits such as these not interpreted to be produced by one depositional event but rather by several events through a process called amalgamation (c.f. section 2.3.3). The lack of internal bedding structures suggests many of these beds may have been deposited *en masse* by debris flows or deposition was extremely fast. High concentrations of carbonaceous material are repeatedly observed within thick sandstone bodies (often increasing in percentage upwards) supporting distributary channel interpretations (c.f. WR figure 2.20 from 86m to 115m).

A solitary coarse pebble clast was observed in a graded bed with numerous basal intraclasts interpreted to be in a distributary channel (PRB at 69m). It is possible this clast was transported within a high density turbidity current exhibiting a stepped density profile. If this were the case, the clast could have been transported on the top of the basal plastic layer sliding along the plastic-turbulent flow interface (Postma *et al.*, 1988). An equally plausible alternative is that a tree stump carrying sediment dropped the clast into an unlithified deposit with the above characteristics (Leeder, 1999), this is supported by the identification of a log surface imprint in the MH section. The imprint is fixed on the bedding surface of a poorly sorted coarse sandstone channel, 2m wide x .4m thick (c.f. MH figure 2.22 at 88.5m). At the core of the imprint is a large block (250 x 200mm) of coal indicating part of the log was lithified.

Distributary channels within the delta front – slope composed of conglomerate beds can also be observed in the area. In the MH section a large distributary channel is interpreted to rest on an erosional contact overlying levee deposits (c.f. MH figure

2.22 at 107m). The MH distributary channel is interpreted to be at least 9m thick. An increasing energy level is interpreted here as deposits grade up through a matrix supported pebble conglomerate to a moderately sorted, clast supported conglomerate and finally to a well sorted, clast supported conglomerate.

Levees are frequently observed in the Pahau River area, especially in close proximity to deposits interpreted as distributary channels (c.f. WR figure 2.20 at 64.5m). Subaerial levees in tidally submerged to terrestrial environments tend to have high levels of carbonaceous matter as they are often covered with vegetation. Levees which most likely had high levels of vegetation become beds containing carbonaceous laminations (c.f. WR figure 2.20 at 85m), rootlets (c.f. PRA figure 2.14) or ubiquitously high organic content (c.f. MH figure 2.22).

Interdistributary bay deposits have been interpreted within the PRA, PRC, MSC and MH sections. With the exception of the MSC section all interdistributary bay deposits are located at the top of or between sequences interpreted as distributary channels (c.f. PRA figure 2.14; c.f. MH figure 2.22; PRC figure 2.19). Interdistributary bay sequences observed in the Pahau River area are typically dominated by overbank flooding (c.f. PRA figure 2.14), including frequent crevasse splays (e.g. PRA figure 2.14) and moderately high levels of carbonaceous matter. The lower portions of beds representing crevasse splays are almost always absent, indicating erosion during maximum flow. The dominance of crevasse splays within the interdistributary bay deposits supports the previous assertion that wave reworking and tidal currents were negligible.

One exception to the dominance of fluvial processes was logged as the MSC section. An almost uniformly thin-bedded sequence with a variety of bedforms at this location indicates bi-directional current flow in a very shallow low energy setting (c.f. section 2.4.1). Although these could have potentially been formed by wind blowing on water, this is not considered likely as several beds with the same symmetrical ripples provided similar palaeoflow current directions. Bedforms at MSC are more suggestive of either a wave or tidally influenced environment. The presence of a

macrofossil and rootlets within 3m of strata at this location suggests the water was very shallow to terrestrial.

A wide range of processes forming deposits is interpreted in the delta front including bedload (c.f. MH figure 2.22), suspension (c.f. PRA figure 2.14), hyperconcentrated streamflow (c.f. PRA figure 2.14), and debris flows (c.f. MH figure 2.22). Bedload traction related processes were the most common observed, interpreted to cause most of the deposition in distributary channels, and mouth bars. Equal amounts of suspended load and bedload are observed in the distributary bay and levee depositional environments.

5.2.3 THE DELTA PLAIN

Delta plains are almost completely subaerial with fluvial processes dominating deposition. This is recorded within the MS section and to a limited extent at top of the MH section. A subaerial depositional environment is interpreted for two reasons, the pervasiveness of carbonaceous material (rootlets, laminations, blocks and seams of low to moderate rank coal etc.) and because bedload deposition dominates suggesting fluvial processes.

Sorting and matrix type have been graphed in addition to stratigraphic logs at Mt Saul. Figure 2.25 shows a dominance of moderately to well-sorted deposits with a matrix composed generally dominated by sandstone. Imbrication is often present within moderately to well-sorted beds within the Mt Saul sections as well as at other conglomerate localities indicating traction-related bedload processes. Submarine currents are generally too weak to transport conglomerates by these processes therefore deposition was most likely in a fluvial environment.

An assortment of debris flow and fluvial current flow deposits are observed within the Pahau River delta plain deposits. A few rare deposits represent matrix supported cohesive debris flows possibly suggesting the nearby presence of subaerial relief (c.f. MSA figure 2.24). Most clast-supported deposits with a modest amount of matrix are interpreted as being situated toward the cohesionless debris flow end of the debris

flow continuum (c.f. MH figure 2.22). Clast-supported beds with lower and very low matrix percentages are interpreted as hyperconcentrated flow deposits and streamflow deposits respectively (c.f. MSB figure 2.24).

Laterally extensive sheet-like geometries are common within the Pahau River delta plain environment suggesting major unconfined flooding events occurred over a wide area. Conversely typically, confined lensoidal bodies of normally graded and massive sandstone periodically interrupt conglomerate deposits. Sandstone deposits are interpreted to be minor channels recording deposition in the distal delta plain (c.f. MS figure 2.24) and the infilling of channels following avulsion of a larger channel (c.f. MH figure 2.22 at 189m). Some sandstone deposits that are regularly bedded are interpreted to be subaerial levee deposits. Levee deposits often contain rootlets and/or carbonaceous laminations (c.f. MS figure 2.24). Deposition of sandstone and mudstone probably occurred during waning flow to normal streamflow conditions.

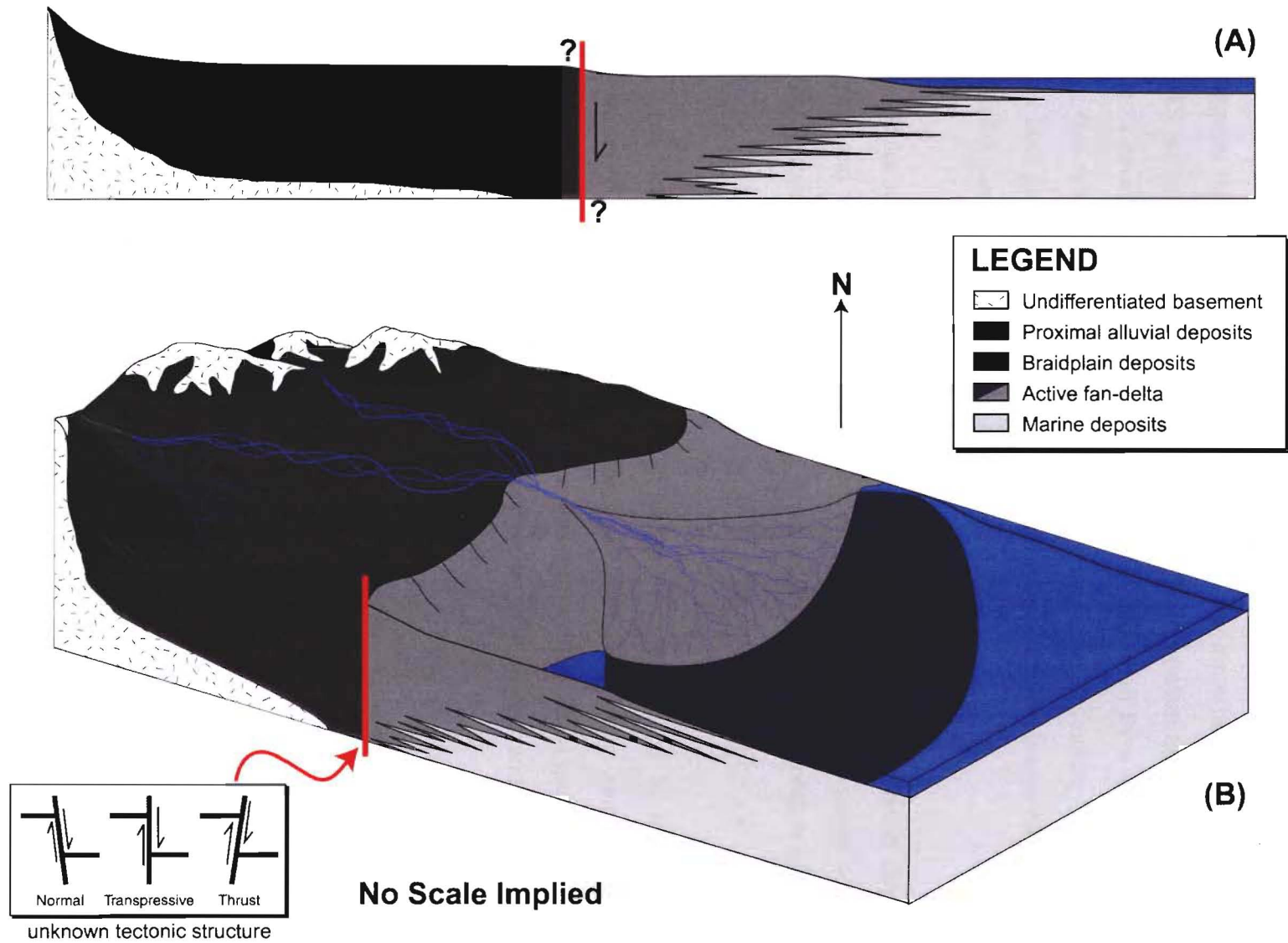
Flame structures within the Mount Saul conglomerate (c.f. MSB figure 2.24 at 43m) suggest that rapid deposition took place within the delta plain and dewatering did not always occur before successive events.

The abundance of hyperconcentrated flow deposits suggests considerably high energy levels in the delta plain (Appendix I, MSB). This may suggest the hinterland is proximal to the delta, some other relief was nearby, or the delta was prone to relatively high fluctuations in discharge.

5.3 FAN DELTA MODEL

A deltaic depositional model can be justified by the identification of delta plain, delta front – slope, and prodelta deposits. Coarse deposits in the area (c.f. MSA, MSB, upper MH) are interpreted to represent delta plain to delta front deposits whereas finer deposits (PRA, PRB, PRC, WR, CH, SP) are interpreted as delta front to prodelta deposits.

Figure 5.1 – The interpreted depositional Pahau River Fan-Delta depositional model. Note that no scale is implicated from this diagram nor is any lateral direction inferred in suggesting a transpressive fault regime. Undifferentiated basement covers the entire rock assemblage for the conglomerate bodies in the area.



The abundance and variety of depositional processes in the coarser deposits in the area suggests there was some appreciable relief in the hinterland. This is inferred from MS section A at 5.5m where sandstone beds containing rootlets directly underlies a poorly sorted conglomerate most likely deposited by a debris flow. The cause of this relief is interpreted as probable syndepositional faulting, which would allow for both on and offshore relief and the high subsidence levels needed to produce the 700m Mt Saul conglomerate deposits (figure 5.1).

A fan – delta model is interpreted as it provides for very thick coarse deposits, coarsening and thickening upward sequences, and the significant subaerial relief required to produce debris flow deposits observed directly above rootlets in section MSA.

Three main types of coarse-grained fan deltas are summarised in Reading and Collinson (1996) based upon various papers published in (Colella and Prior, 1990; Nemec and Steel, 1988a). The three main coarse-grained fan delta types are known as Gilbert-type fan deltas, Slope-type (or deep water) fan deltas, and Shelf-type (or shallow water) fan deltas.

A Gilbert-type fan delta is characterised by a tripartite system (figure 5.2); sub-horizontal topsets, steeply dipping foresets and gently dipping bottomsets (Nemec, 1990). Gilbert fan deltas are usually dominated by hyperpycnal flow (underflow) and thus are usually seen in lakes, as the sediment laden water is typically denser than the lake water it enters. This does not tend to happen at the marine interface as salt water is often denser than fresh water with suspended sediment. This typically results in a jet or a plume with sediment being deposited by fallout, this is also one method by which fine sediment (<sand) can be winnowed from coarse-grained deposits (Leeder, 1999). No tripartite or large scale crossbedding system was observed at Mt Saul, Mt Holmes or any other conglomerate body in the Pahau River area. It is unlikely that any of these conglomerates represent Gilbert-type fan deltas.

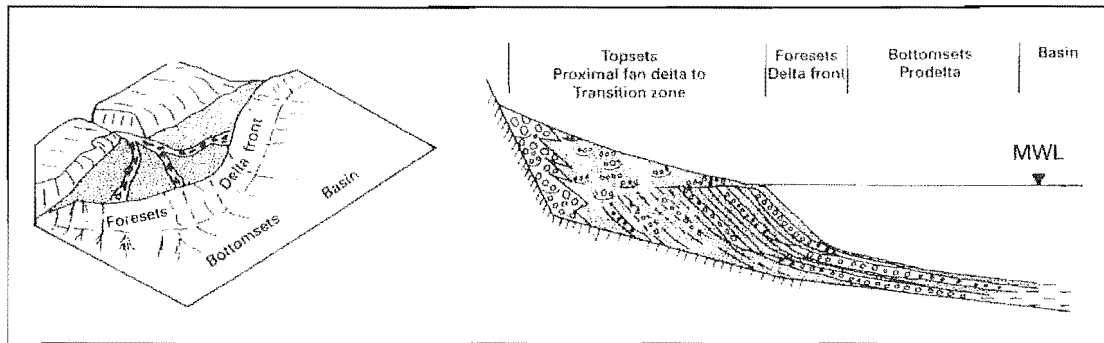


Figure 5.2 – A Gilbert-type fan delta, plan view and cross section, notice the tripartite structure in the cross section (Reading and Collinson, 1996).

Slope-type fan deltas have a slope separating the prodelta from a poorly developed delta front (figure 5.3; Reading and Collinson, 1996). This may be due to an intrinsic constructional component such as the delta slopes created by progradation into a fjord or a tectonic feature such as faulting. These fan delta systems may be dominated by coarse-grained, mass flow deposits and lack most of the shallow water, delta front features of the other two delta types. Many shallow water features in the Pahau River area were observed and although mass flow deposits are common in the area they rarely dominate.

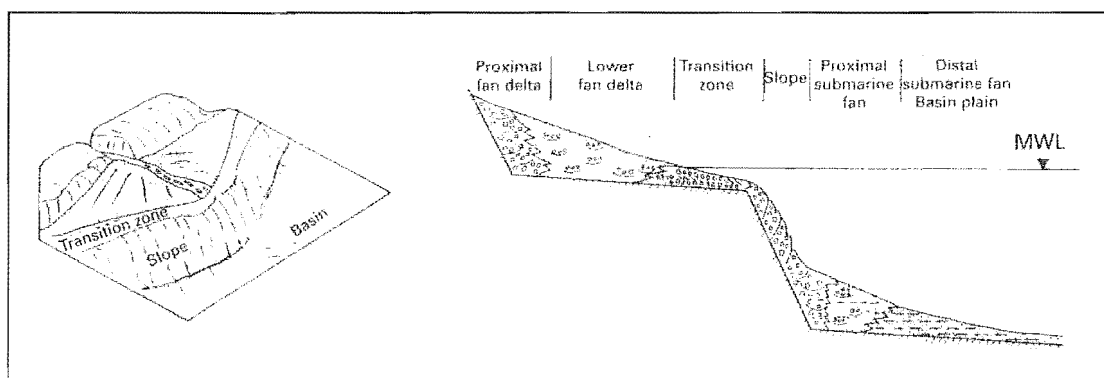


Figure 5.3 – Slope-type fan delta, plan view and cross section (Reading and Collinson, 1996).

Shelf-type fan deltas are identified by the abundance of shallow water features and have well developed delta plains, fronts, and prodeltas (figure 5.4; Reading and Collinson, 1996). These may or may not be influenced to a great degree by waves and/or tidal currents if environmental or local conditions are right. They characteristically diminish gradually in grainsize from source giving well-developed, coarsening-upwards deltaic sequences. Finer grained distal parts of the sequences are often crossbedded to rippled. The geometries and distribution of lithofacies in the Pahau River area tend to support the shelf-type depositional model best. The

proximal fan delta and mid-fan deltas of figure 5.4 can be seen to correlate with the conglomerate and sandstone lithofacies. The sandstone and interbedded lithofacies can be viewed as being located dominantly within the distal fan-delta to the transition zone with the mudstone lithofacies occupying the prodelta.

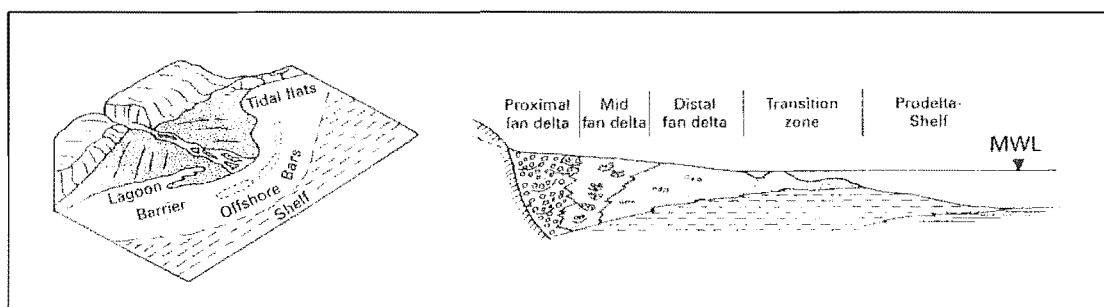


Figure 5.4 – Shelf-type fan delta, plan view and cross section, the Pahau River sediments probably resemble this model more than the previous two (Reading and Collinson, 1996).

The Pahau River sediments are most likely shelf-type fan deltas but this end-member model does not account for the relative abundance of massflow deposits. In reality the Pahau River sediments are probably somewhere between a shelf and slope-type fan delta possibly closer to the shelf-type model. The marine basin was probably quite shallow probably with some additional relief granted by tectonically imposed structure just behind the apex of the delta plain (figure 5.1).

5.4 ANCIENT AND MODERN ANALOGUES

5.4.1 COLOSO - LOMBRIZ FORMATIONS CHILE

The Coloso - Lombriz Formations in Northern Chile provide an excellent example of an ancient analogue for the Pahau River sediments (Flint and Turner, 1988). The Coloso – Lombriz Formations were formed in a forearc extensional setting during the Cretaceous (Flint and Turner, 1988).

The Coloso Formation (~1500m) represents an alluvial fan complex, which is overlain by the Lombriz Formation (~130m) representing a fan delta (Flint and Turner, 1988). The Coloso Formation is split into a lower and upper conglomerate body with an intervening sandstone wedge. Depositional processes include bedload, channelised debris flows, and unconfined hyperconcentrated flood flows (sheetflows;

Flint and Turner, 1988). Bedding is predominately pebble conglomerate characteristically medium to very thickly bedded (25 – 200cm) and poorly to moderately sorted (often depending on whether grading was present or not). Interbedded with conglomerates are thin massive sandstone units interpreted as being deposited between flood events (Flint and Turner, 1988).

The Lombriz Formation deposits are interpreted to represent a fan-delta depositional environment influenced by marine processes (Flint and Turner, 1988). The Lombriz Formation is composed of extensive fine-grained deposits exhibiting coarsening upward sequences interpreted as progradation of the delta-front (Flint and Turner, 1988).

Bedding geometries between the two Chilean Formations and the deposits in the Pahau River correlate quite well. In particular the hyperconcentrated flows exhibiting sheet-like geometries appear equivalent to many deposits within the Mount Saul Formation.

Conglomerate deposits in the Pahau River are finer grained and exhibit a higher degree of sorting compared with those described for the Coloso Formation. This may simply represent a difference of relief promoting debris flow or hyperconcentrated flow deposition in the Coloso Formation over bedload deposition in the Mt Saul and other conglomerate deposits.

5.4.2 KOSI FAN, INDIA

The Kosi Fan located in northern Indian is a fluvial fan 160km long and 120km wide (Collinson, 1996). Braided rivers dominantly composed of sandy gravel control proximal deposition in the Kosi Fan. Downstream the Kosi Fan changes to a braided system dominated by sand further transforming in the lower reaches to a meandering system (Collinson, 1996; Wells and Dorr, 1987). The Kosi Fan is unusual in that the apex of the fan is not at the foothills of the hinterland. Tectonically induced relief in the middle of a braidplain has produced the Kosi Fan at a considerable distance in front of its catchment that includes Mt Everest (Collinson, 1996; Nemec and Steel,

1988b; Wells and Dott, 1987). The Kosi Fan illustrates an important fact, alluvial fans need not be small high gradient depositional environments fed by relatively minor source areas.

Kosi Fan is not truly analogous of the Pahau River deposits but they both share several features in common. The deposits observed within the Kosi Fan contain, proximal sandy gravels through to deposits dominated by sands. Unfortunately the Kosi Fan lacks a subaqueous component preventing a comparison of submarine deltaic deposits, although deposits produced by the delta plain and fluvial fan depositional environments are essentially the same. The scale of the Kosi Fan is obviously much larger than the deposits at Mt Saul but the principles controlling its development are suggested to be the same. Consider how large a Kosi Delta would be if the coastline were only few kilometres in front of the fan apex.

It is quite likely that the drainage basin of the Pahau River sediments was quite large. Dean (1993) indirectly substantiates a large catchment by suggesting igneous clasts in the Mt Saul conglomerate are from three geochemically different cogenetic suites. It is possible that the drainage basin was small and all three suites simply intersected there. This is considered unlikely, as geochemical contamination of at least one of the igneous suites would have probably occurred during their emplacement if their proximity were so confined.

Significant relief is required to produce the deposits interpreted within the delta plain deposits. If this relief were produced by a nearby hinterland then a significant portion of the rocks (>5%) within Pahau River conglomerates would probably be sub-angular or angular. The angularity of clasts is largely dependant on composition and transportation distance. Clasts within the conglomerates in the Pahau River are mainly composed of very well indurated sandstones, igneous clasts (intrusive and extrusive), with subordinate granitoids and mudstones. All of these clasts are dominantly sub-rounded to well-rounded with relatively high sphericities indicating significant fluvial transport. The nature of the clasts in these conglomerates does not support an adjacent hinterland. Therefore it is possible that, like the Kosi Fan, the deposits in the Pahau River were controlled by some feature (probably

syndepositional tectonism) producing relief on a braidplain at some distance from source.

5.5 DISCUSSION AND CONCLUSIONS

Several minor problems were encountered during the interpretation of this research excluding section obscurity and deformation outlined in section 2.3.1.

In most coarsening upwards sequences described for fan-deltas conglomerate beds are observed at the top (Colella and Prior, 1990; Flint and Turner, 1988; Nemec and Steel, 1988a). Pahau River conglomerate beds were not present in the coarsest portions of coarsening upwards sequences (PRA, PRB, and WR) but were at other locations (MH). One suggestion is that conglomerates may have been eroded or bypassed these locations in favour of higher energy, centrally located channels. Alternatively, very few of these coarsening upwards sequences may have actually been exposed subaerially and are simply lower expressions of the delta (i.e. delta front – delta slope – prodelta). This alternative interpretation is supported by numerous pebbly mudstones (cohesive debris flows) that are often located in the finest sediments between sequences. This alternative suggests that only beautiful stratigraphic sections representing a full deltaic assemblage (delta plain to prodelta) are published.

A northeast – southwest coastline perpendicular to the dominant SE palaeoflow direction is interpreted for the Pahau River deposits (refer to section 6.3.2 for a discussion of methodology). Wave direction could have been roughly perpendicular to the coastline if wave reworking source is accepted for westerly palaeoflow indicators. Additional palaeoflow indicators need to be logged to be sure of dominant wave direction as this is based on *one* location.

Contrasting palaeoflow directions were observed at one location (MSC section) in several beds with asymmetrical 3D ripples. Palaeoflows periodically reversed themselves upward throughout the column suggesting the reworking of tidal currents or waves influenced these deposits. Alternatively these ripples may have formed in

very shallow calm water by alternating wind currents blowing on the waters surface, conceivably by onshore and offshore breezes.

Additionally, relatively few journal articles in the last 10yrs have been published describing and interpreting marine fan-delta models without gilbert-type geometries. The description of and interpretation of fan-delta models is dealt with in detail in two volumes of articles written in 1988 and 1990 (Colella and Prior, 1990; Nemec and Steel, 1988a). Recent sedimentological textbooks written for advanced undergraduates and post-graduates refer to papers exclusively in these volumes when describing fan-deltas without Gilbert-type geometries (Allen, 1997; Leeder, 1999; Reading, 1996).

The Pahau River rock assemblage most likely represents a slope-type delta based primarily on lithofacies geometry, lithofacies distribution, and the dominance of fluvial bedload deposits in delta plain deposits. Well-developed delta-plains, delta fronts and prodeltas are all present in the Pahau River. The prodelta to delta front in particular show excellent examples of coarsening and thickening upward sequences typical of shelf-type deltas. Shallow water structures are also present within the Pahau River area suggestive of shelf-type deltas. Several large sheets of debris flows interfingering the mudstone lithofacies from large conglomerate bodies suggesting that relief was present in the subaqueous component of the fan-delta.

Relief interpreted in the subaerial component of the Pahau River fan delta is inferred to be the result of processes similar to that controlling the alluvial Kosi Fan. The Kosi Fan analogue raises some interesting possibilities in that the Pahau River fan-delta is not required to be directly adjacent to a hinterland. This fits especially well as angular to sub-angular clasts that would be expected to be common if the hinterland were close are essentially absent from all conglomerates in the Pahau River area.

The Pahau River fan delta will be an interesting addition to the literature, as no modern fan-delta variant of the Kosi Fan exists. The interest value of this research is also increased by probably being the first account of ancient fan-delta proposed which uses this model.

PROVENANCE

CHAPTER SIX

6.1 INTRODUCTION

The provenance of Torlesse Superterrane sediments (Rakaia, Esk Head, Pahau, Waioeka Terranes) is one of the most hotly debated topics in New Zealand sedimentology. This primarily stems from a complete separation from and a lack of knowledge about the source. So far no source(s) are universally agreed upon that satisfy the petrographical, geochemical and age requirements for any of the Torlesse Terranes, although many proposals have been put forward. Potential candidates for the source of the Torlesse Superterrane sediments include; Victoria Land (Roser and Korsch, 2000), Marie Byrd Land (Andrews *et al.*, 1976), New England Fold Belt Northern Queensland (Adams, 1998; Campbell and Grant-Mackie, 2000), Western Province and Median Tectonic Zone (NZ) (Wandres, Unpubl. PhD Thesis), and SE China (Adams, 1998).

Zircons have been used to match the age of the Torlesse Superterrane source to a source area, as they yield consistent ages as well as being resistant to metamorphism weathering (Ireland, 1992; Kamp, 1999; Wandres, Unpubl. PhD Thesis). Some of the candidates above have been sampled geochemically (Adams, 1998) and can approximate the bulk composition for some of the Torlesse Superterrane sediments. Problems emerge when one or more requirements are not satisfied, often due to not containing zircons of the same age or lacking minor compositional components (Adams and Kelley, 1998; Campbell and Grant-Mackie, 2000; Wandres, Unpubl. PhD Thesis).

The Torlesse represents a huge amount of material that had to have been eroded from somewhere. Often many but not all of the requirements are met for being a possible source rock, and many theories have "almost qualify as the source". It is possible that the source of the Torlesse no longer exists at all or that only remnants remain and

several pieces of the puzzle were destroyed. Another possibility is that the Torlesse was formed by input from more than one of the above locations. Additionally it could be that the Torlesse Superterrane source rocks have not been sampled yet. There could be rocks in potential source areas that are covered by ice in Antarctica or by the ocean in the Tasman Sea.

6.2 THE HISTORY OF TORLESSE PROVENANCE ANALYSIS

Although there is no conclusive source for the whole of Pahau Terrane or the Torlesse Superterrane, there has been a significant amount of research towards deciphering what it is. Studies have so far examined the whole rock isotope geochemistry (Ar/Ar, Rb/Sr, Pb/U, Rare Earth Elements), igneous clast and sandstone petrology, detrital mineral geochronology (e.g. zircon, mica, apatite etc.), as well as sedimentary geochemistry of Torlesse sediments to determine the provenance (Barnes, 1990; Dean, 1993; Frost and Coombs, 1989; Mortimer, 1995; Roser *et al.*, 2000; Smale, 1997; Wandres, Unpubl. PhD Thesis).

MacKinnon (1983) identified five macrofossil and petrofacies zones in the South Island (figure 6.1). These show a generalised pattern of relative northeastward younging. Due to the structural complexity of the Torlesse Superterrane the younging direction of the fossil zones has so far presented the best indicator of overall palaeoflow. The inferred palaeoflow source of the Torlesse Superterrane would thus be located toward the southwest relative to the present position of the deposits.

6.2.1 PERMIAN TO TRIASSIC TERRANES – RAKAIA AND CAPLES

Several points are agreed upon by a vast number of geologists. It is unanimously agreed that in the Permian and Triassic the Rakaia Terrane sediments were being deposited adjacent to an undissected to transitional arc, along an active convergent continental margin. This is supported by Quartz – Feldspar – Lithic (QFL) counts from numerous thin section examinations within the Rakaia Terrane (Crampton and Landis, 1988; Barnes, 1990; MacKinnon, 1983; Mortimer, 1995). The Caples Terrane lies to the southwest of the Permian-Triassic Rakaia Terrane was likely coeval (MacKinnon, 1983).

The source of the Caples and the Rakaia were most likely active arcs, which is supported by QFL data (MacKinnon, 1983; Turnbull, 1979). Geochemistry and immobile trace element studies suggest that the source of the Caples was an evolved calc-alkaline arc with trace elements intermediated between a continental and oceanic arc systems (Roser and Cooper, 1990; Roser and Korsch, 2000). The Rakaia Terrane is thought to be composed solely of continental arc deposits (MacKinnon, 1983).

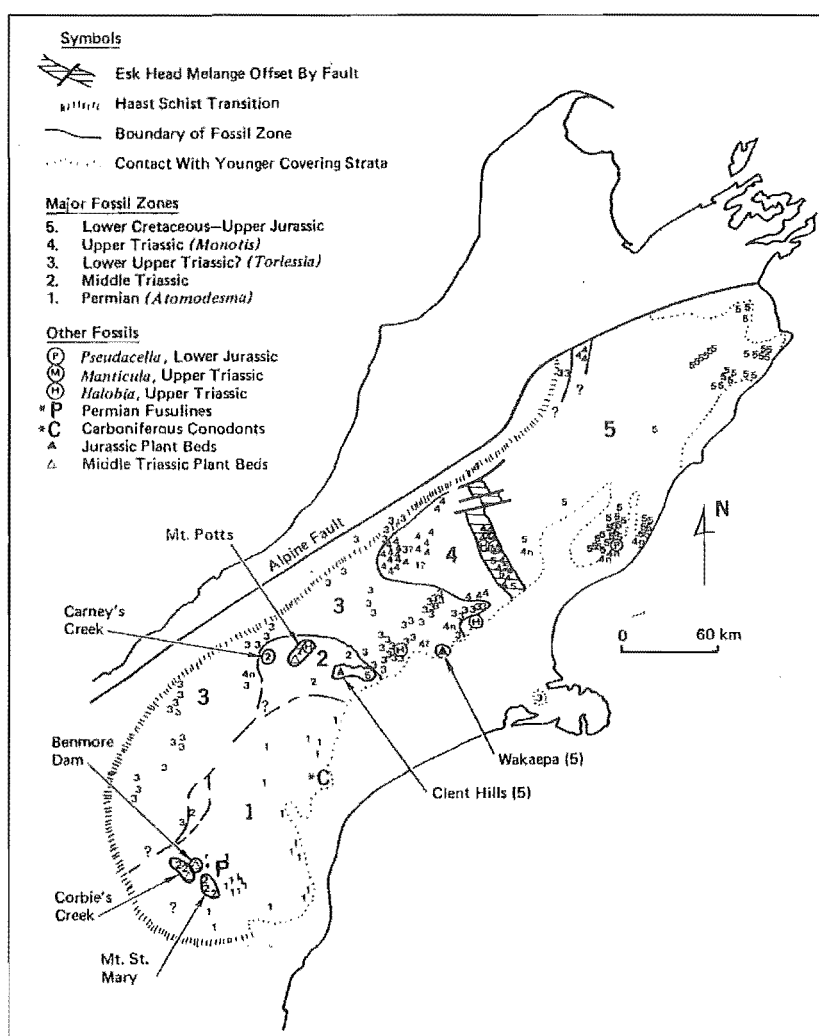


Figure 6.1 – The five fossil zones of the South Island Torlesse Superterrane, note that no published high detail recent versions of this map exist and subsequent revisions to the geometry of the Esk Head Melange mean that its geometry is not portrayed correctly. In a comparison with the latest Terrane map (figure 1.1) fossil zone five is to the Northeast of the Esk Head Melange, zone four is directly to the Southwest, both fossil zones also exist within the Esk Head Melange itself (MacKinnon, 1983).

The deposition of the Caples and Rakaia Terranes may be coeval, although petrographic, geochemical and isotope studies suggest that they have different provenances (MacKinnon, 1983). It is thought that the Caples Terrane was derived from an oceanic arc lacking or containing minor continental contamination (MacKinnon, 1983). Roser *et al.* (1993) suggests there are no provenance linkages

between the Caples, Maitai, Murihiku and the four Torlesse Terranes, based upon consistent geochemical differences. It is widely accepted that the Rakaia Terrane was not autochthonous relative to the Caples Terrane, rather allochthonous (Bradshaw *et al.*, 1993; Campbell and Grant-Mackie, 2000; Mortimer, 1995).

It is probable that the Torlesse was being deposited on a trench slope system controlled by the obliquely approaching Phoenix plate (Adams and Graham, 1996; Bradshaw, 1989; Campbell and Grant-Mackie, 2000). It is thought that the oblique convergence juxtaposed the Caples and Rakaia Terranes somewhere between 200Ma and 140Ma, resulting in the inception of the Haast Schist (Adams and Kelley, 1998; MacKinnon, 1983; Little and Mortimer, 1999). The Rakaia Terrane, deformed and metamorphosed by the collision with the Caples, was consolidated, tilted, and uplifted during most of the Jurassic and Early Cretaceous. This period of uplift is commonly referred to as the Rangitata I orogeny (Bradshaw *et al.*, 1980; Adams and Graham, 1996).

6.2.2 SOURCE AND EMPLACEMENT OF THE ESK HEAD TERRANE

Separating the Rakaia and Pahau Terranes is the Esk Head Terrane, commonly referred to as the Esk Head Melange. It is a chaotic assemblage composed of blocks of Pahau and Rakaia Terrane sediments, limestone, chert, and volcanics (Bradshaw *et al.*, 1980; MacKinnon, 1983; Silberling *et al.*, 1988) with a Pahau Terrane based mudstone matrix (Campbell and Grant-Mackie, 2000). Laterally extensive bedding planes are largely absent from Esk Head Terrane and any rarely preserved bedding extends for no more than a few metres due to the severity of mixing and deformation (Silberling *et al.*, 1988). All the contacts observed in the Esk Head Melange between clastic terrigenous sediment and limestone or chert were fault related (Silberling *et al.*, 1988). The only known depositional contacts of limestone and siliceous sediments in the Esk Head are with basalt.

Limestone blocks present within the Esk Head have yielded Late Triassic and Jurassic ages, interpreted as deposited on a seamount or seafloor (Silberling *et al.*, 1988). Incorporation of material from the seamount (volcanics, carbonates, volcaniclastics etc.) was probably scraped off the obliquely approaching Phoenix Plate during its

subduction beneath the Gondwana Plate during the Jurassic to Early Cretaceous (Silberling *et al.*, 1988).

It has been suggested that the emplacement of the Esk Head Terrane occurred sometime post 100Ma (Adams and Graham, 1996) although the methods of emplacement are not widely agreed upon. Hypotheses regarding emplacement range from olistostromal diapirism, faulting, or a combination of the two in the form of high-pressure injection along fault planes (Bradshaw, 1973; Bradshaw, 1989; Silberling *et al.*, 1988; Underwood and Moore, 1996). Hypotheses are to some extent suggested with a specific tectonic regime in mind. For example, the change of tectonic regime from compression to extension leading to trench roll-back may have helped to provide a mechanism for diapir emplacement (Wandres, pers. comm. 2001). Alternatively high pressure injection and fault emplacement also seems more likely in a compressional regime.

The incorporation of the Pahau Terrane matrix as a component of the Esk Head Melange is implied to have not occurred prior to subduction. This is based on the complete lack of Pahau Terrane sediments being located (so far) in depositional contact with marine Esk Head material. The formation of the Esk Head Melange matrix probably occurred during the subduction of seamount(s) and/or an ocean floor assemblage. Incorporation of the matrix principally during subduction could explain why there is no observable signature of the Rakaia Terrane in the matrix of the Esk Head, as the seamount assemblage would have not travelled past Rakaia Terrane sediments. Alternatively the Rakaia Terrane may have been too indurated due to lithification and subsequent metamorphism related to the collision of the Rakaia to the Caples Terrane to be significantly incorporated.

6.2.3 THE ORIGINS OF THE PAHAU TERRANE

During the latter half of the Rangitata I orogeny ~150Ma, the slightly more volcanoclastic Pahau Terrane began to form (Adams and Graham, 1996; MacKinnon, 1983). The Pahau Terrane is mostly in fault contact at the present day with the Rakaia but in some localities lies unconformably over the Rakaia (Bradshaw *et al.*, 1980). When present, the Esk Head Melange is always in fault contact with the Pahau

Terrane. Based primarily on faunal data ~50 million years of deposition is not recorded in the Torlesse Superterrane between the youngest strata in the Rakaia to the oldest in the Pahau (Adams and Graham, 1996; Bradshaw, 1989; Kamp, 1999).

Comparatively, the Pahau Terrane is under explored and interpreted with respect to the Rakaia. The current theory is that the Pahau represents an allochthonous juxtaposed accretionary wedge (Adams and Kelley, 1998; Campbell and Grant-Mackie, 2000; Kamp, 1999). Why and where it formed is speculative, but considering the time of inception was roughly coeval to the Rangitata I orogeny, perhaps this had something to do with it.

Sedimentologically the Rakaia and the Pahau are almost identical, differing slightly in the ratios of sandstone to mudstone (MacKinnon, 1983). Petrographically the two Terranes are very similar, differing only subtly. The Pahau Terrane appears to have a higher lithic content than the Rakaia Terrane. Most geologists account for this by suggesting that the Rakaia was the dominant sediment source for the Pahau with additional material supplied by an active arc (MacKinnon, 1983; Kamp, 1999; Mortimer, 1995; Wandres, Unpubl. PhD Thesis).

Adams and Graham (1996) dismiss the dominance of Rakaia sediment in the Pahau. They reason that the initial $^{87}\text{Sr}/^{86}\text{Sr}$ ratios at the initiation of metamorphism in the Pahau are incompatible with having a source dominated by the Rakaia. This is contradicted by Wandres (Unpubl. PhD Thesis) who is currently preparing his PhD thesis on the "Provenance of the Torlesse". Wandres (Unpubl. PhD Thesis) has shown that the sandstone clasts within conglomerates scattered throughout the Pahau are virtually indistinguishable from Rakaia in composition. In addition to he has shown that igneous activity is contemporaneous with depositional ages based on shrimp-data from igneous clasts and detrital zircons.

Recent studies suggest that a Caples Terrane signature can be observed in the Pahau Terrane (Wandres, Unpubl. PhD Thesis). This is based on conglomerate clasts that appear to have geochemical signatures similar to Caples Terrane, although this is not supported by petrography.

6.3 PROVENANCE IN THE PAHAU RIVER AREA

The provenance of the Pahau River deposits has in the past been addressed several times using various methods. The first published contribution to provenance studies was by Silberling *et al.* (1988) who examined two cobbles of crinoid-brachiopod limestone and two pebbles of radiolarian chert in the Mount Saul conglomerate. Silberling *et al.* (1988) came to the tentative conclusion that these gave a Late Triassic to Jurassic age, much older than the sediments dated by Peter Andrews. Silberling *et al.* (1988) noted the limestone had a similar composition, age, and sedimentological character to the blocks of limestone in the Esk Head Melange. Silberling (1988) used these features to suggest that the limestone and other blocks were probably derived from the Esk Head Melange.

The conglomerate at Mt Saul was examined by Dean (1993) who researched igneous clasts as part of a comparative study between several conglomeratic bodies in the Torlesse. Dean (1993) concluded that the source for the Mount Saul conglomerate was dominated by calc-alkaline to alkaline volcanics. The volcanic source province contained a wide assemblage of silicic rocks including rhyolitic domes and/or lava flows, ignimbrites, and pyroclastic deposits. Dean (1993) suggested that these were most likely formed in response to subduction along an active continental margin. Intrusive igneous rocks were also thin sectioned and geochemically examined. Dean (1993) identified the presence of peraluminous I-type granites, S-type granites, and weak to moderately peralkaline A-type granites in the examined samples. A single cogenetic suite is not implied as geochemical data suggests many of the granites are unrelated. Dean (1993) implied that the volcanic clasts could indicate rifting and an extensional tectonic regime prior to or during the Early Cretaceous.

Pescini (1997) studied the Pahau River area as part of a BSc Honours project designed to interpret the depositional setting of the area. Pescini (1997) also examined the QFL ratios of sandstone intraclasts within the Mt Saul conglomerate with those in adjacent sandstone bodies. He found that the QFL ratios within the conglomerate and outside the conglomerate were virtually identical. He concluded as a result that the intraclasts were locally derived, probably from canyon wall collapse or bank failure, and only

travelled a short distance. The QFL values for these are indicated in figure 6.4 and correspond to the transitional arc region of the QFL ternary diagram.

The Mt Saul conglomerate is currently part of a PhD provenance study by Wandres (Unpubl. PhD Thesis). Wandres is examining sandstone clasts within the conglomerate, comparing and contrasting QFL values of these with those of the Rakaia Terrane. Through geochemical, petrological and geochronological methods he has been able to demonstrate recycling of Rakaia sediment into the Pahau Terrane. One aspect of his petrological study included analysing QFL values of sandstone clasts within Pahau Terrane conglomerates, he found that these were virtually indistinguishable from those found in sandstone beds in Rakaia Terrane. He also found that the analysed clasts in the Mt Saul and Mt Ethelton conglomerates were subrounded and well indurated whereas cannibalistic clasts tend to be less indurated and sub-angular. This may suggest a longer transportation distance than is normally observed for cannibalistic clasts.

6.3.1 AGE CONTROL

Peters Andrews sampled Pahau River deposits in the late 1970s. These the palynology of these samples was subsequently studied at the Department of Scientific and Industrial Research yielding ages of Aptian to Albian (Raine, 1977).

Recently, the some of the original 1977 samples have been reanalysed and new samples have been collected (Raine *et al.*, in prep). IGNS has taken 22 new palynological samples predominantly from a 2km section along the Pahau River from NZMS 260-M32 846 433 to 856 432, (Raine *et al.* in prep). Generally only mudstone samples were retrieved, although several very fine sandstones were sampled, mudstone matrix was also retrieved from the Mt Saul conglomerate. Preliminary results submitted by Raine *et al.* (in prep) indicate an age range of approximately Upper Barremian – Lower Albian (Ian Raine, pers. comm. 2001)

6.3.2 PALAEOFLOW INDICATORS

Previous studies by Bradshaw and Andrews (1980) on the palaeoflow of 24 imbrication readings in the Mt Saul conglomerate suggest a unimodal palaeoflow direction towards the southeast. It is noted within (Bradshaw and Andrews, 1980) that this is "opposite to palaeocurrent directions for the Triassic Torlesse" which is interpreted to be towards the northeast based on fossil zones (MacKinnon, 1983).

Palaeoflow indicators in this study were primarily observed in ripple cross stratification, three dimensional exposures of asymmetric and symmetric ripples, flute casts, imbrication, large scale cross stratification, and tool marks. Common inaccurate palaeoflow indicators include preferential orientation of plant fragments, flame structures, and two dimensional exposures of asymmetrical and symmetrical ripples.

Palaeoflow indicators observed on beds within macroscopic folds were unfolded to regional strike of ~40° NE and rotated back to a 0° dip. A total of 14 beds gave accurate palaeoflow indicators, which were plotted on a rose diagram (figure 6.2). Since the deposition of these beds during 110-120Ma the Pacific Plate on which they are now situated has rotated anticlockwise ~55° (John Bradshaw pers. comm., 2001), this rotation can be easily removed to observe the syn-depositional palaeoflow direction (figure 6.2).

Prior to the removal of plate rotation, the generalised palaeoflow direction (i.e. derived from flame structures, ripple cross stratification, and imbrication) point towards the northeastern quadrant (figure 6.2 - a) or roughly parallel to current day strike. A northeast directed palaeoflow is also interpreted for higher definition indicators such as flute casts and tool marks. Once these are rotated clockwise 55° (figure 6.2 - b) palaeoflow is inferred to be derived from the west to northwest in agreement with interpretations made by Bradshaw and Andrews (1980).

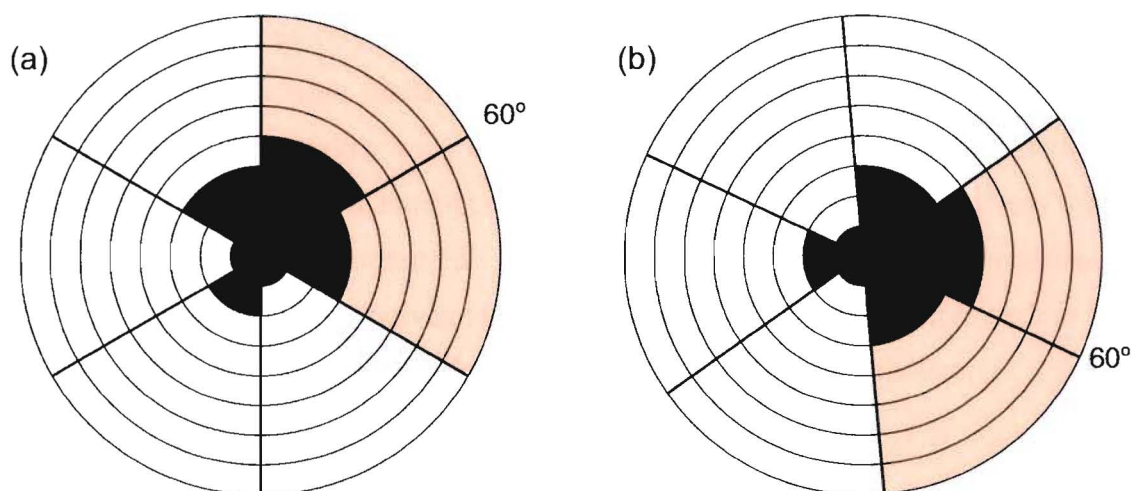


Figure 6.2 – Palaeoflow directions, present day unfolded palaeoflow directions (a) can be rotated back to the original cretaceous configuration with the addition of 55° of clockwise rotation (b). Refer to APPENDIX III for raw data.

6.4 QFL PROVENANCE METHODOLOGY

Superficially at the outcrop scale Torlesse Superterrane sedimentology appears ubiquitously uniform. QFL analysis has thus been used as primary means of Terrane identification in the past and present (Crampton and Landis, 1988; MacKinnon, 1983; Mortimer, 1995; Pescini, 1997; Wandres, Unpubl. PhD Thesis). The main purpose of QFL analysis in this study was to show that the Pahau River sediments were petrographically distinct from Rakaia Terrane sediments and comparative to other known Pahau Terrane sediments. Sample collection, preparation and examination followed a predetermined routine in order to accurately correlate samples.

6.4.1 SAMPLE COLLECTION

Samples of sandstone throughout the field area were collected for thin section analysis. In all 50 samples were collected (figure 6.3), 22 of which were for thin section analysis.

Prerequisites for collecting samples, in order from highest to lowest priority, include very low degree of weathering, medium sandstone grainsize, and location. Preference was given to well-sorted, well-indurated fine to medium sand sized samples so the results could be compared with previous studies that used the same

parameters (MacKinnon, 1983; Mortimer, 1995). It was difficult to source rocks of these requirements as very fine sand and finer deposits dominate the field area, thus some compromises were made (e.g. finer grainsizes, poorer sorting, low-moderate weathering etc.). Samples were collected in a line $\sim 45^\circ$ clockwise from strike to analyse the largest possible amount of non-correlative stratigraphy to see if any trends or relationships could be observed. No samples were collected from the southeast of the field area as weight was given to the above analysis, additional factors such as fine grainsizes and deformation also played a role in the exclusion of this area.

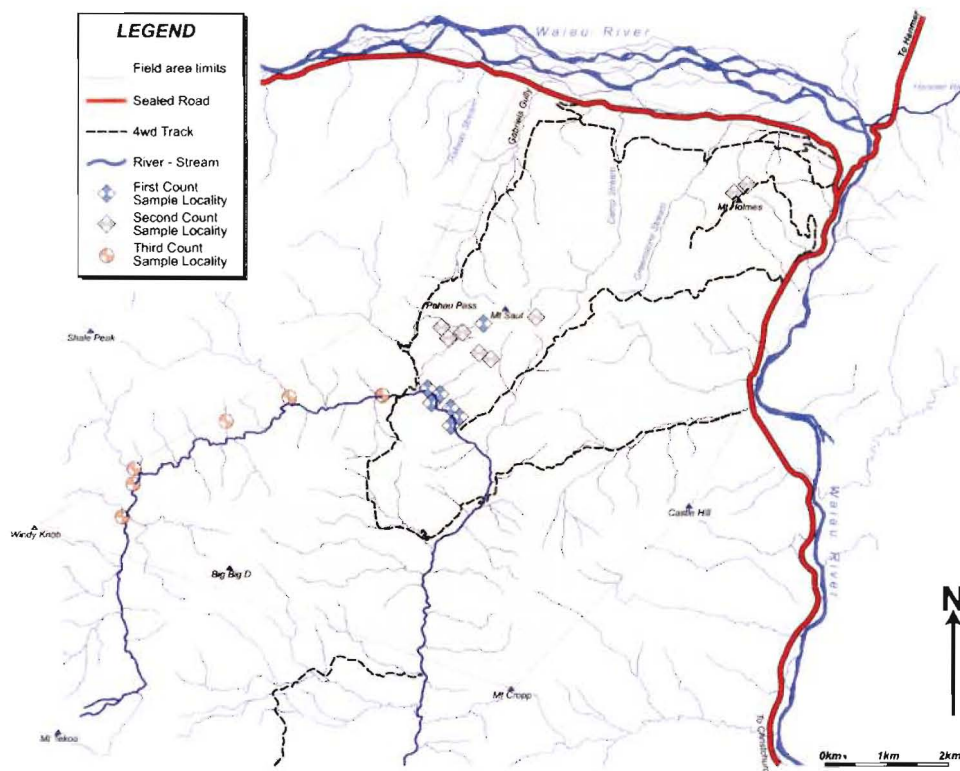


Figure 6.3 – Sample Location map, showing the locations of the various counts.

6.4.2 FELDSPAR STAINING

Samples were thin sectioned and then stained for both plagioclase and alkali feldspar. Three sets of thin sections were made totalling 22 samples, nine in the first set, eight in the second, and five in the third.

Staining techniques differed slightly between the first group and the second and third groups. In the first staining, thin sections were etched with hydrofluoric acid, washed, dried, and then both stains were applied shortly one after another. The second

staining employed almost exactly the same method but was left to fully dry after it was stained for plagioclase before adding the alkali feldspar stain. The second staining method produced significantly clearer stains allowing for a speedier interpretation. Parts of the slides were left unstained for reference in case the matrix clays took up the stain and obscured the grains.

6.4.3 GAZZI – DICKINSON POINT COUNTING TECHNIQUE

At least 500 detrital grains greater than 5ϕ (0.03mm, thin section thickness) were identified using a Swift point counting machine. The point counter was calibrated to step across each slide with increments roughly equal to the mean grain diameter. Counting was from left to right using an automated Swift point counter, once the far right of the slide was reached it was moved three times the mean diameter down the thin section and reset to the far left.

The point counting procedure followed the Gazzi-Dickinson method outlined in Ingersoll *et al.* (1984). This method classes all monomineralic minerals larger than 4ϕ (0.06mm, very fine sand) irrespective of the nature of the grain to the category of a single crystal. For example, a quartz phenocryst larger than 4ϕ within a volcanic clast greater would be classed as quartz rather than as a volcanic rock fragment. This methodology compensates for variations associated with modal grainsizes (i.e. lack of lithics in fine grain rocks).

The possibility of the introduction of human error in estimating the size of grains exists. It is quite conceivable that one could count grains slightly smaller than 5ϕ or monomineralic minerals smaller than 4ϕ as quartz, feldspar or something else. The errors induced by these are thought to be negligible considering the amount of grains counted. There is also the possibility that any count (even if the section is moved by mechanical means) is not a representative sample of the rock it was retrieved from. Given that 500 grains were counted an error of 4% would be expected on each of the percentages (Blatt, 1982).

Each thin section was counted primarily for quartz, feldspar, lithics, carbonaceous material and matrix (APPENDIX II). All other minerals were grouped into a broad miscellaneous category, with composition listed. No differentiation was made between volcanic lithics (Lv), sedimentary lithics (Ls), or metamorphic lithics (Lm) as staining for both feldspars made Lv and Ls appear essentially the same.

6.5 QFL PROVENANCE RESULTS

Raw values of the QFL ratios predominately correspond to the transitional arc zone (Dickinson, 1985) of the QFL ternary plot (figure 6.4), although some values fall in within the dissected arc province of the diagram. After counting the thin sections and re-examining their respective hand specimens, it was decided that two specimens would be discarded due to their very fine sandstone/silt grainsize (these were plotted as discard data – figure 6.4).

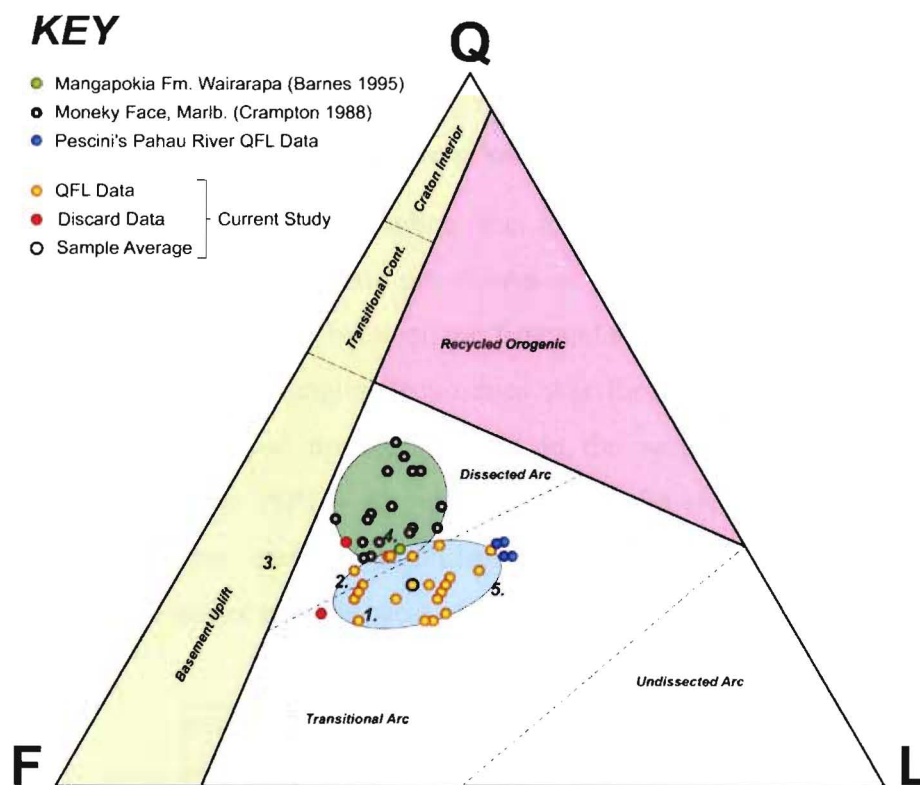


Figure 6.4 – QFL ternary plot for sandstone provenance (after Lewis, 1994). Numbers 1 – 5 correspond with mean QFL values for each of the five fossil zones, (1) Permian, (2) Mid – Triassic, (3) Lower Upper Triassic, (4) Upper Triassic, (5) Upper Jurassic – Lower Cretaceous (MacKinnon, 1983).

The sample average of the QFL results plots within the 95% confidence limits of the South Island Pahau (figure 6.5) given by Mortimer (1995) supporting the previous

Pahau Terrane designation. All of the samples, including those that were discarded, plotted within the two standard deviations from the mean (figure 6.5) given by Mortimer (1995).

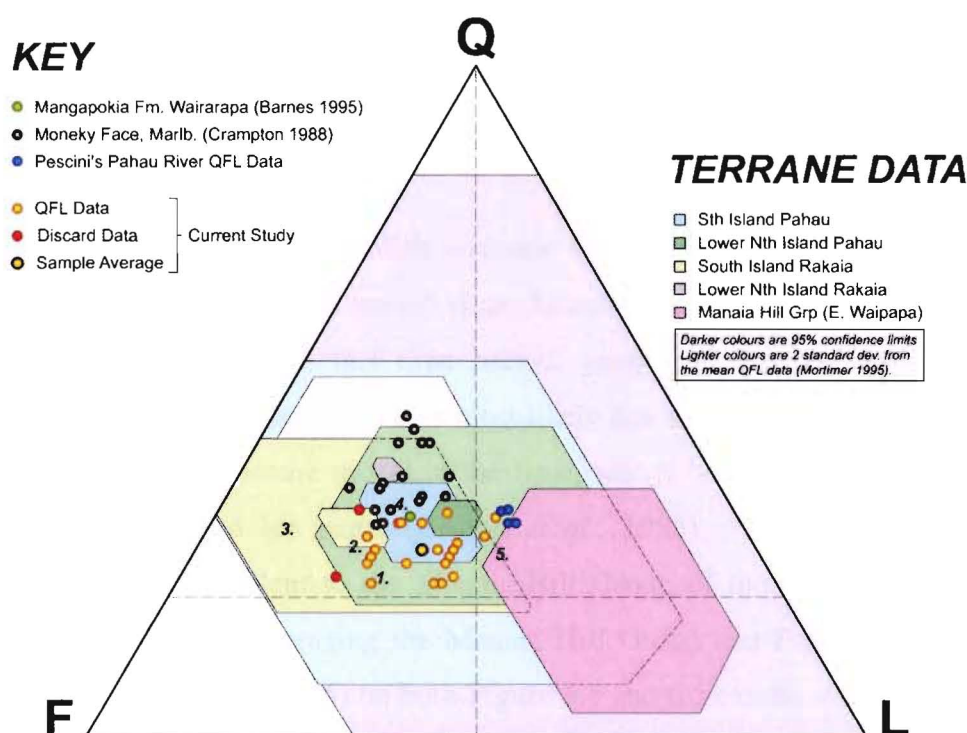


Figure 6.5 – QFL comparison between MacKinnon (1983) and present study.

Abbreviated statistical values including the mean, standard deviation, and 95% confidence levels for the QFL data are shown in figure 6.6. There is a negligible difference in mean QFL values between the first and second staining techniques. The only benefit therefore in changing techniques was the speed of the point counting procedure, which was sped up considerably in the second technique. With the exception of one sample (SP1 – Appendix II) all of the samples in the third count were depleted in lithics, enriched in feldspar, with marginally more quartz. All of these samples were gathered to the west of the Pahau Pass Fault.

Mineral Type	Quartz	Feldspar	Lithics
95% confidence	1.46%	2.42%	2.18%
Average %	28.18%	42.71%	29.12%
Std deviation	3.32%	5.52%	4.98%
3 rd count aver.	29.20%	46.40%	24.40%
2 nd count aver.	28.90%	41.20%	29.90%
1 st count aver.	27.80%	41.50%	30.70%

Figure 6.6 – Abbreviated statistical values for Pahau River QFL analysis, refer to Appendix II for full information

6.6 DISCUSSION

The QFL values describe in this study are similar to results gathered for the Pahau Terrane by other geologists describing a transitional to dissected arc provenance (Crampton and Landis, 1988; MacKinnon, 1983; Mortimer, 1995).

MacKinnon (1983) did not publish any raw QFL Pahau Terrane data but instead publishing QFL data for fossil zone 5 (Late Jurassic – Early Cretaceous). QFL values appear to be averaged for this time period, geographically corresponding to the Waioeka and Pahau Terranes. This is most likely due to the underdevelopment of the tectonostratigraphic Terrane model at the time, which later gained momentum after MacKinnon published his paper (Bishop *et al.*, 1985). The Waioeka Terrane is petrographically equivalent to the Manaia Hill Group of the Waipapa Superterrane (Mortimer, 1995). In averaging the Manaia Hill Group and Pahau Terrane a value roughly equivalent to point (5) on both Figure 6.4 and 6.5 can be attained. This is the reason why Pahau River sediments do not plot around this point.

The QFL analysis used by MacKinnon (1983) and Mortimer (1995) differed from the techniques used here. The biggest difference being that the aforementioned authors exclusively used samples that had a medium sandstone grainsize. This study used samples that ranged in grainsize from very fine to medium sandstone due to the unavailability of medium-grained clasts. Lithic clasts break down into their monomineralic constituents as they become smaller. This means that coarser samples tend to give results that are skewed towards the lithics corner of the QFL ternary plot. MacKinnon (1983) and Mortimer (1995) followed the Gazzi-Dickinson point counting method with one exception, rather than counting phenocrysts within rare aphanitic rocks as the mineral itself they counted these as rock fragments, increasing the skew towards the lithic corner. Both MacKinnon (1983) and Mortimer (1995) stained for plagioclase and K-feldspar in line with this study. Considering the similarities and differences in technique and sample collection the results in this study correlate remarkably well with those in previous studies indicating a well defined QFL petrofacies for Pahau Terrane rocks.

Crampton and Landis (1988) studied Cretaceous sediments in the Monkey Face region including Pahau Terrane sediments. The Monkey Face area is located immediately south of the Hope Fault, approximately 20km west of Kaikoura, roughly 70km Northeast of the Pahau River field area (figure 1.1). Sample grainsizes (very fine to medium sandstones) as well as counting procedures (Gazzi-Dickonson) are comparable between Crampton and Landis (1988) and this study. The raw QFL data from Crampton and Landis (1988) are plotted along side Pahau River results from this study in figure 6.4. The location of the two areas provides an interesting opportunity to compare and contrast older versus younger Pahau sediments. QFL data from Monkey Face plots wholly within the dissected arc field of the QFL ternary plot whereas Pahau River data suggests the provenance was in the partially dissected transitional arc field. From this it can be inferred that over time the arc from which the Pahau Terrane was derived slowly became progressively more dissected. Assuming a northeastward younging direction, the Monkey Face sediments are likely to be significantly younger than the approx. 120 – 110 My old Pahau River sediments. The tectonic regime is thought to have changed during 110 – 80Ma from subduction-related compression to extensional rifting of the Gondwana Plate (Bradshaw, 1989; Kamp, 1999; Luyendyk, 1995). The shutdown of subduction would have effectively halted arc formation causing any existing arc(s) to become dissected with continued erosion. Thus it is unknown just how many very fine-grained rocks were used in the Crampton and Landis (1988) study. It is possible that the skew away from the lithics corner is the result of sampling relatively finer grained rocks. If this were the case it would be expected they would plot closer to the "discard data" points from this study, which does not appear to be the case.

Palaeoflow in the Pahau River area appears consistent with the younging directions inferred through fossil zones interpreted in Mackinnon (1983). Some evidence of bi-directional current flow in the Pahau River area also evidence probably relating to marginal marine reworking processes.

CONCLUSIONS

CHAPTER SEVEN

7.1 LITHOFACIES SUMMARY

The deposits in the Pahau River can be subdivided into four different lithofacies; these include mudstone, interbedded mudstone-sandstone, sandstone and conglomerate lithofacies.

Thick massive mudstone beds regularly interrupted by thin beds of massive or normally graded sandstone dominate the mudstone lithofacies. Internal bedding was essentially confined to the thin intervening sandstone beds, typically showing ripples and crossbedding. Scour structures were locally present as flute casts or erosional traces. Dewatering structures are present at the tops of massive mudstone beds including both load casts and flame structures suggesting depositional rates were rapid. This lithofacies outcrops in dominantly sheet-like geometries suggesting that the depositional environment was dominated by nonchannelised deposition. Rare beds interpreted as channels were present within this lithofacies, and were typically composed of sandstone and exhibit lensoidal geometries.

The interbedded sandstone – mudstone lithofacies was the most widely distributed lithofacies in the study area. It is typically present as coarsening and thicken upwards sequences between the mudstone and sandstone lithofacies. This lithofacies was also observed as interbedded with the mudstone and sandstone lithofacies. Numerous bedforms were present, dominated by ripples, laminations, cross-stratification often the result of current deposition or reworking. Bedding geometries are consistent with channelised and unchannelised flows dominated by processes from turbidity currents to bedload. Coarsening up sequences are associated with both terrestrial and marine markers such as root casts and macrofossils.

The sandstone lithofacies is observed best as elongate strike ridges up to several hundred metres thick. Carbonaceous material can be present in this lithofacies up to very high levels indicating close proximity to a terrigenous sediment supply. Bedding is typically massive and can attain thicknesses up to 26m with very few internal bedding structures indicating rapid deposition possibly dominated by debris flows. Crossbedding and scour surfaces are relatively common within this facies.

The conglomerate lithofacies is observed in three groups of large lensoidal bodies. This lithofacies is typically observed in erosional or gradational contact with the sandstone and interbedded lithofacies. Conglomerates are typically clast-supported, moderately sorted, sub-rounded to well rounded, well indurated, with pebble grainsizes. Conglomerate deposits are dominated by features suggestive of deposition by either bedload, hyperconcentrated streamflow, or debris flows. Other than imbrication, relatively few internal bedding structures are present within the conglomerate beds. Large scale crossbedding was observed but only once, large flames and load casts were present when in association with sandstone lenses.

Several subordinate lithologies were present throughout the area in all lithofacies. These typically included muddy sandstones, sandy mudstones, pebbly mudstones, pebbly sandstones. Many of these beds could be traced along strike grading into or interfingering with large conglomeratic bodies

7.2 STRATIGRAPHIC NOMENCLATURE

Three new names describing lithostratigraphic assemblages have been proposed, two formations and one group. The Mt Saul Formation is predominantly composed of conglomerates with minor sandstone lenses. These deposits are predominately formed by mass flows (cohesive debris flows or density modified grain flows) or traction transport in a current flow, current flow suspension deposits may be present to a very limited extent.

The second proposed formation, known as the Ship Spur Formation, is composed of thickly to thinly bedded, normally graded sandstones, massive sandstone, and massive mudstones. The deposits within this formation are interpreted as dominantly being

turbidites and hemipelagites. Debris flow deposits occur identified as pebbly mudstones, sandy mudstones or poorly sorted massive sandstones. Beds having the appearance of stepped density profile high-density turbidity currents are were also observed in this formation.

The Pahau River Group has been proposed to encompass the previously mentioned formations. The stratigraphic limits of this Group are as yet unknown but are thought to extend regionally in the Pahau Terrane. Stratigraphic unit names are necessary to allow other geologists to compare and contrast other locations to a well-documented lithostratigraphic unit.

7.3 DEPOSITIONAL SETTING

A fan-delta model is proposed for the Pahau River deposits based primarily on –

- ▶ large coarsening and thickening upwards sequences (PRA, WR, MH)
- ▶ mixed terrestrial - marine depositional setting indicators (e.g. rootlets and dinoflagellates)
- ▶ large conglomeratic bodies with deposits indicative of both bedload and debris flows (MS).

A deltaic model is justified by the identification of delta plain, delta front – slope, and prodelta deposits. The PRA section, for example, illustrates the transition from deep marine turbidites in the prodelta environment to bedload deposits in fluvially dominated delta front environment. Soft sediment slumping and common debris flows at the base of the section as opposed to rootlets in levee deposits associated with crevasse splays at the top of the section support this conclusion. Interdistributary bay deposits were also identified in the PRA section above thick sandstone beds interpreted to represent a large distributary channel.

Four classic coarsening upwards sequences have been logged indicative of transitions from the prodelta to the delta front; Pahau River A & B, Waiau River, and Mt Holmes. All coarsening upwards sequences have significant carbonaceous content that increases in proportion to grainsize. Bidirectional palaeoflow indicators were

observed at only one location suggesting that most deposition was fluvially dominated. Tidal and wave processes were probably minor, although notable level of oblate clasts (<5%) in the conglomerates suggests accumulation in a coastal environment (Lewis and McConchie, 1994). Extensive sequences of beds in the area interpreted to be turbidites suggest much of the area was submarine. Coarsening upwards sequences in the Pahau River are punctuated by substantial volumes (20 - 200m) of mudstone facies. These periods of finer grained material probably relate to episodes of channel avulsion. Large cohesive debris flow deposits can also be observed in these. The origins of these are interpreted to be from the upper delta slope or delta front as the deposits can be traced laterally towards conglomerate channel bodies.

Delta plain deposits are illustrated in the MS section where channelised and nonchannelised, bedload and debris flow deposits have been described. Rootlets were also found in a sandstone lens interbedded with these deposits supporting a subaerial depositional environment.

A fan-delta depositional environment is chosen over a coarse-grained delta as relief in the delta plain can be high enough to produce debris flows in the delta plain. The location of the rootlets in the Mt Saul A section directly underlies a cohesive debris flow indicating debris flows were present in a subaerial environment. It is inferred that the flow that caused this deposit probably was not initiated immediately adjacent to the shoreline, as the shear stress threshold would be too high due to low relief. A source in the fan apex would appear to be the best option.

It is unlikely there was a hinterland near to the Pahau River fan-delta. Sub to well rounded igneous clasts in the conglomerate at Mt Saul suggest derivation from three separate cogenetic suites suggesting that the catchment for the conglomerate was significantly large. This is probably not what would be expected from an alluvial fan protruding from a directly adjacent mountain range. The most likely interpretation therefore is that much of the morphology of the fan-delta was controlled by an unknown tectonic structure landward of the coastal interface, probably on a braidplain.

Linkages with lithofacies and depositional environment are variable, especially within the interbedded mudstone-sandstone, sandstone and conglomerate lithofacies. Loose generalisations can be made between grain size and depositional environment. Coarse deposits in the area can generally be interpreted as representing proximal deposition, finer deposits representing a deeper offshore environment. These environments can be identified with the Mt Saul Formation (proximal) and the Ship Spur Formation (distal).

7.4 TECTONIC SETTING AND PROVENANCE

The location of the Pahau River sediments is interpreted to be in front of an active continental margin, most likely a continental arc (MacKinnon, 1983).

Deformation in the eastern Pahau River is relatively low compared with that to the west across the Pahau Pass fault. It is probable then that the Pahau River sediments were being deposited in a relatively undeformed forearc or on top of the accretionary prism.

It is unknown whether the tectonic regime at the time of deposition was extensional or compressional, although there is tentative evidence for coeval volcanism suggesting compression was still ongoing (Anekant Wandres pers. comm. 2001). It is thought that the tectonic regime changed from compression to extension at $\sim 105 \pm 5$ Ma (Bradshaw, 1989). The depositional time frame for sediments in the Pahau River is Latest Barremian? to Early Albian (~ 122 Ma – 110Ma; Ian Raine et al, In prep). Thus the Pahau River deposits could record the change in tectonic regime or be the final deposits of an earlier regime.

An average QFL of Q28 F43 L29 was counted for Pahau River sandstones. A transitional arc bordering on dissected arc provenance is suggested based on these QFL results. This implies that the arc source was becoming eroded to the point where plutonic bodies in the lower parts of the volcanic complex were exposed.

Two tentative relationships have been proposed between sediments in the Pahau River and at Monkey Face, 20km west of Kaikoura. One hypothesis is that sediments can

be inferred to decrease in lithic content in that direction. An alternative to this hypothesis is that lithic content is greater in environments where the sediment has travelled a shorter distance. The second hypothesis is supported by feldspar-enriched QFL data retrieved from the flysch-association on the west side of the Pahau Pass fault (Bradshaw and Andrews, 1980). If the first hypothesis is correct, then lower lithic percentages at Monkey Creek directly relate to increasing dissection of the arc province.

The interpretation made in this thesis contends that there was a tectonic feature landward of the coastal interface providing relief for the creation of the fan-delta deposit. The nature of this fault largely depends on which tectonic regime was active at the time of deposition. It is completely possible that this feature was either a thrust, normal or transpressional strike-slip fault. The data from this research is inconclusive but does suggest some sort of tectonic activity.

7.5 IMPLICATIONS

Several major implications can be inferred from the interpretations in this thesis. The largest implication is that the Pahau Terrane was not deposited in a fully marine depositional environment. It has previously been thought that the Pahau Terrane was deposited offshore allochthonous to the Rakaia Subterrane (James Crampton, pers. comm. 2000). This is now very difficult to accept as terrestrial deposits have been found. Several other localities within the Pahau Terrane also appear to have shallow water deposits (Malcolm Laird, pers. comm. 2001), suggesting the Pahau deposits may not be the only terrestrial deposits in the Pahau Terrane.

The various terranes of the Torlesse Superterrane have been described as accreted subduction prisms or accretionary complexes (Campbell and Grant-Mackie, 2000; MacKinnon, 1983; Mortimer, 1995), perhaps this should be questioned. The deformation within the Pahau River sediments is largely post-depositional and low relative to the majority of the Torlesse Superterrane. It has been suggested here that deposition could have either occurred in some part of the distal forearc basin or proximal subduction prism. Whichever hypothesis is accepted it is implied that

deposition was rapid relative to subsidence and that a net progradational regime existed for some time.

A significant portion of the Pahau Terrane has been derived from Rakaia Terrane sediments (Wandres, Unpubl. PhD Thesis). Terrestrial Pahau deposits suggest that much of the Rakaia was exposed subaerially in the Early to Mid Cretaceous. Subaerial erosion of the Rakaia Terrane is the most likely answer in response to the ~50Ma of missing between the Rakaia and Pahau ages.

It is also implied that limestone blocks in the Mt Saul conglomerate were not derived from the same source as the Esk Head Melange, even though they have the same fauna and sedimentological characteristics (Silberling *et al.*, 1988). The limestone in the Esk Head was interpreted to have formed around a seamount, which subsequently became subducted and incorporated into a melange. Adams and Graham (1996) state that the Esk Head was emplaced at sometime post 100Ma. The depositional age of the Mt Saul conglomerate is interpreted to be the same as interfingering deposits in the Pahau River dated at 120 – 110 Ma. If these blocks of limestone really do come from the Esk Head Melange then the Melange *must* have been exposed in the catchment of the Mt Saul deposits at least 120Ma. If Adams and Graham (1996) are to be believed, then the most likely explanation is that a different limestone deposit of similar sedimentological nature was deposited somewhere in what was to become the catchment of Mt Saul conglomerate during the Jurassic.

REFERENCES

- Adams, C.J., 1998. A provenance in northeast Australia and South China for New Zealand Paleozoic terrane sediments. *Journal of African Earth Sciences*, **27**, pp 218-219.
- Adams, C.J. and Graham, I.J., 1996. Metamorphic and tectonic geochronology of the Torlesse Terrane, Wellington, New Zealand. *New Zealand Journal of Geology and Geophysics*, **39**, pp 157-180.
- Adams, C.J. and Kelley, S., 1998. Provenance of Permian-Triassic and Ordovician metagreywacke terranes in New Zealand: Evidence from $^{40}\text{Ar}/^{39}\text{Ar}$ dating of detrital micas. *Geological Society of America, Bulletin*, **110**, pp 422-432.
- Adkin, G.L., 1954. Bibliographic Index of New Zealand Stratigraphic Names. *New Zealand Geological Survey Memoirs*, **9**.
- Allen, P.A., 1997. *Earth Surface Processes*, Blackwell Science, Cambridge, 404 pp.
- Andrews, P.B., Speden, I.G. and Bradshaw, J.D., 1976. Lithological and paleontological content of Carboniferous to Jurassic Canterbury Suite, South Island, New Zealand. *New Zealand Journal of Geology and Geophysics*, **19**, pp 791-819.
- Bagnold, R.A., 1962. Auto-suspension of transported sediment; turbidity currents. *Royal Society of London Proceedings, Series A*, **265**, pp 315-319.
- Barnes, P.M., 1988. Submarine fan sedimentation at a convergent margin: the Cretaceous Mangapokia Formation, New Zealand. *Sedimentary Geology*, **59**, pp 155-178.
- Barnes, P.M., 1990. Provenance of Cretaceous accretionary wedge sediments: the Mangapokia Formation, Wairarapa, New Zealand. *New Zealand Journal of Geology and Geophysics*, **33**, pp 125-135.
- Barnes, P.M. and Korsch, R.J., 1991. Melange and related structures in Torlesse accretionary wedge, Wairarapa, New Zealand. *New Zealand Journal of Geology and Geophysics*, **34**, pp 517-532.
- Bishop, D.G., Bradshaw, J.D. and Landis, C.A., 1985. Provisional terrane map of South Island, New Zealand. In: Howell, D.G. (Ed), *Tectonostratigraphic Terranes of the Circum-Pacific Region*. Circum Pacific Council for Minerals and Energy, Houston, Texas, pp 515-521.
- Black, P., 1996. Omahuta, Bay of Island and Manaia Hill Terranes: Waipapa Composite Terrane, North Island, New Zealand. *Geological Society of New Zealand Miscellaneous Publication*, **91A**, pp 29.
- Blatt, H., 1982. *Sedimentary Petrology*, W H Freeman & Co, San Francisco, 564 pp.
- Boggs, S., 1987. *Principals of Sedimentology and Stratigraphy*, Merrill Publishing Company, Columbus, 784 pp.
- Bouma, A.H., 1962. *Sedimentology of some Flysch Deposits: A Graphic Approach to Facies Interpretation*, Elsevier, Amsterdam, 168 pp.
-

- Bradshaw, J.D., 1971. Stratigraphy and structure of the Torlesse Supergroup (Triassic - Jurassic) in the foothills of the Southern Alps near Hawarden (S60-61), Canterbury. *New Zealand Journal of Geology and Geophysics*, **15**, pp 71-87.
- Bradshaw, J.D., 1973. Allocthonous Mesozoic fossil localities in melange within the Torlesse rocks of North Canterbury. *Royal Society of New Zealand Journal*, **3**, pp 161-167.
- Bradshaw, J.D., 1989. Cretaceous geotectonic patterns in the New Zealand Reigon. *Tectonics*, **8**, pp 803-830.
- Bradshaw, J.D. and Andrews, P.B. (Eds), 1980. *Torlesse Terrane Excursion*. In: Series, Geological Society of New Zealand Conference 1980, Field Trip Guides. Geol. Soc., N.Z., New Zealand, Christchurch, C1-C12 pp
- Bradshaw, J.D., Andrews, P.B. and Adams, C.J., 1980. Carboniferous to Cretaceous on the Pacific margin of Gondwana: The Rangitata Phase of New Zealand. *Fifth International Gondwana Symposium*, pp 11-16. Wellington, New Zealand.
- Bradshaw, J.D., Dean, A.A., Ireland, T.R., Muir, J. and Weaver, S.D., 1993. Fingerprinting the sources of allochthonous sedimentary terranes - An example from the Torlesse terrane of New Zealand. *Circum-Pacific and Circum-Atlantic terrane conference*.
- Busby, C.J. and Ingersoll, R.V. (Eds), 1995. *Tectonics of Sedimentary Basins*. In: Series, Blackwell Science 579 pp
- Campbell, H.J. and Grant-Mackie, J.A., 2000. The Marine Triassic of Australasian and its interregional correlation. In: Yin, H., Dickins, J.M., Shi, G.R. and Tong, J. (Eds), *Permian-Triassic Evolution of Tethys and Western Circum-Pacific*. Elsevier Science Publishers B.V., Amsterdam, pp 235-255.
- Campbell, J.S. and Coombs, D.S., 1966. Murihiku Supergroup (Triassic-Jurassic) of Southland and South Otago. *New Zealand Journal of Geology and Geophysics*, **9**, pp 393-398.
- Colella, A. and Prior, D.B. (Eds), 1990. *Coarse-Grained Deltas*. In: Series, Blackwell Science Publications, Oxford,
- Collinson, J.D., 1996. Alluvial sediments. In: Reading, H.G. (Ed), *Sedimentary Environments: Processes, Facies and Stratigraphy*. Blackwell Science Ltd, Oxford, pp 37-82.
- Cooper, R.A., 1989. Early Paleozoic Terranes of New Zealand. *Journal of the Royal Society of New Zealand*, **19**, pp 73-112.
- Crampton, J.S., Bru, A.G., Campbell, H.J., Cooper, R.A., Morgans, H.E.G., Raine, I.J., Scott, G.H., Stevens, G.R., Strong, C.P. and Wilson, G.J., 1995. IGNS New Zealand Geological Time Scale Report 95/9, Institute of Geological and Nuclear Sciences, Lower Hutt.
- Crampton, J.S. and Landis, C.A., 1988. Petrography of Jurassic-Cretaceous sedimentary rocks of the Monkey Face area, Southern Marlborough. *New Zealand Geological Survey Record*, **35**, pp 77-85.
- Dean, A.A., 1993. Analysis and Correlation of Igneous Clast Geochemistry and Petrography from four Mesozoic Conglomerates. Masters Thesis, University of Canterbury.
- Dickinson, W.R., 1985. Interpreting provenance relations from detrital modes of sandstones. In: Zuffa, G.G. (Ed), *Provenance of Arenites*. *NATO ASI series. Series C, Mathematical and physical sciences*. Reidel Publishing Company, Hingham, USA, pp 333-361.

- Flint, S. and Turner, P., 1988. Alluvial fan and fan-delta sedimentation in a forearc extensional setting: the Cretaceous Coloso Basin of northern Chile. In: Nemec, W. and Steel, R.J. (Eds), *Fan Deltas: Sedimentology and Tectonic Setting*. Blackie, London, pp 387-399.
- Folk, R.L., Andrews, P.B. and Lewis, D.W., 1970. Detrital sedimentary rock classification and nomenclature for use in New Zealand. *New Zealand Journal of Geology and Geophysics*, **13**, pp 937-968.
- Fordyce, R.E., 1976. Zoophycos from the Torlesse Supergroup, North Canterbury, New Zealand. *New Zealand Journal of Geology and Geophysics*, **19**, pp 289-291.
- Freund, R., 1971. The Hope Fault - A strike-slip fault in New Zealand. *New Zealand Geological Survey, Bulletin*, **86**.
- Frost, C.D. and Coombs, D.S., 1989. Nd Isotope character of New Zealand: Implications for terrane concepts and crustal evolution. *American Journal of Science*, **289**, pp 744-770.
- Fyfe, H.E., 1931. *Amuri Subdivision*. New Zealand Geological Survey, Annual Report No. 25 pp 5-6
- Fyfe, H.E. and Healy, J., 1935. *Amuri Subdivision*. New Zealand Geological Survey, Annual Report No 29 pp 4-5
- Gage, M., 1971. Torlesse: "Group" or "Supergroup". *Geological Society of New Zealand Miscellaneous Publication*, **30**, pp 9-10.
- George, A.D., 1992. Deposition and deformation of an Early Cretaceous trench-slope basin deposit, Torlesse terrane, New Zealand. *Geological Society of America, Bulletin*, **104**, pp 570-580.
- Gordon, H.A., 1890. Explorations, South Westland. *Appendix J. House of Representatives, New Zealand*, pp 96-97.
- Gregg, D.R., 1964. Sheet 18, Hurunui, (1st Edition) "Geological Map of New Zealand 1:250 000", Department of Scientific and Industrial Research, Wellington, NZ.
- Grindley, G.W., Harrington, H.J. and Wood, B.L., 1959. The Geological Map of New Zealand., New Zealand Geological Survey Bulletin, n.s. 66.
- Haast, J., 1871. *On the geology of the Amuri District, in the Provinces of Nelson and Marlborough*. Reports of Geological Exploration for 1870-71 pp 26-46
- Haast, J., 1879. *Geology of the Provinces of Canterbury and Westland, New Zealand*. Times Office, Christchurch,
- Haast, J., 1885. On the Geological Structure of the Southern Alps of New Zealand, in the Provincial Districts of Canterbury and Westland. *Transactions and proceedings of the New Zealand Institute*, **17**, pp 332-337.
- Hector, J., 1885. Note on the Geology of the Canterbury Mountains. *Transactions and proceedings of the New Zealand Institute*, **17**, pp 337-340.
- Hiscott, R.N., Pickering, K.T., Bouma, A.H., Hand, B.M., Kneller, B.C., Postma, G. and Soh, W., 1997. Basin-Floor Fans in the North Sea: Sequence Stratigraphic Models vs Sedimentary Facies: Discussion. *American Association of Petroleum Geology*, **81**, pp 662-665.
- Ingersoll, R.V., Bullard, T.F., Ford, R.I., Grimm, J.P., Pickle, J.D. and Sares, S.W., 1984. The effect of grain size on detrital modes: a test of the Gazzi-Dickinson point counting method. *Journal of Sedimentary Petrology*, **54**, pp 103-116.

- Ireland, T.R., 1992. Crustal evolution of New Zealand: Evidence from age distributions of detrital zircons in Western Province paragneisses and Torlesse grewacke. *Geochemica et Cosmochimica Acta*, **56**, pp 911-920.
- Kamp, P.J.J., 1999. Tracking crustal processes by FT thermochronology in a forearc high (Hikurangi margin, New Zealand) involving Cretaceous subduction termination and mid-Cenozoic subduction initiation. *Tectonophysics*, **307**, pp 313-343.
- Kneller, B.C. and Buckee, C., 2000. The structure and fluid mechanics of turbidity currents: a review of some recent studies and their geological implications. *Sedimentology*, **47**, pp 62-94.
- Landis, C.A., Campbell, H.J., Aslund, T., Cawood, P.A., Douglas, A., Kimbrough, D.L., Pillai, D.D.L., Raine, I.J. and Willsman, A., 1999. Permian-Jurassic Strata at Productus Creek, Southland, New Zealand: Implications for Terrane Dynamics of the Eastern Gondwanaland Margin. *New Zealand Journal of Geology and Geophysics*, **42**, pp 255-278.
- Leeder, M., 1999. *Sedimentology and Sedimentary Basins: From Turbulence to Tectonics*, Blackwell Science, Cornwall, 592 pp.
- Lewis, D.W. and McConchie, D., 1994a. *Analytical Sedimentology*, Chapman & Hall, New York, 197 pp.
- Lewis, D.W. and McConchie, D., 1994b. *Practical Sedimentology*, Chapman & Hall, New York, 213 pp.
- Little, T.A., Mortimer, N. and McWilliams, M., 1999. An Episodic Cretaceous Cooling Model for the Otago-Marlborough Schist, New Zealand, Based on Ar-40/Ar-39 White Mica Ages. *New Zealand Journal of Geology and Geophysics*, **42**, pp 305-325.
- Lowe, D.R., 1976. Grain Flow and Grain Flow Deposits. *Journal of Sedimentary Petrology*, **46**, pp 188-199.
- Lowe, D.R., 1982. Sediment gravity flows: II - depositional models with special reference to the depositions of high-density turbidity currents. *Journal of Sedimentary Petrology*, **52**, pp 279-297.
- Luttig, G., 1962. The shape of pebbles in the continental, fluvatile, and marine facies. *International Association of Scientific Hydrology Publication* 59, pp 253-258.
- Luyendyk, B.P., 1995. Hypothesis for Cretaceous rifting of east Gondwana caused by subducted slab capture. *Geology*, **23**, pp 373-376.
- MacKinnon, T.C., 1983. Origin of the Torlesse terrane and coeval rocks, South Island, New Zealand. *Geological Society of America, Bulletin*, **94**, pp 967-985.
- Major, J.J., 1998. Pebble orientation on large, experimental debris-flow deposits. *Sedimentary Geology*, **117**, pp 151-164.
- McKay, A., 1885. *On the Geology of the East Part of Marlborough Province*. Reports of Geological Exploration 17 pp 22-136
- Miall, A.D., 2000. *Principals of Sedimentary Basin Analysis*, Spinger, New York, 616 pp.
- Middleton, G.V. and Hampton, M.A., 1973. Sediment gravity flows: mechanics of flow and deposition. *Proceedings of Pacific Section Society of Economic Paleontologists and Mineralogists, Los Angeles*, pp 1-38.
- Miller, J.M.G., 1996. Glacial Sediments. In: Reading, H.G. (Ed), *Sedimentary Environments: Processes, Facies and Stratigraphy*. Blackwell Science Ltd, Oxford, pp 454-484.

- Mortimer, N., 1995. Origin of the Torlesse Terrane and Coeval Rocks, North Island, New Zealand. *International Geology Review*, **36**, pp 891-910.
- Mulder, T., Savoye, B. and Syvitski, J.P.M., 1997. Numerical modelling of a mid-sized gravity flow: the 1979 Nice turbidity current (dynamics, processes, sediment budget and seafloor impact). *Sedimentology*, **44**, pp 305-326.
- Nemec, W., 1990. Aspects of sediment movement on steep delta slopes. In: Colella, A. and Prior, D.B. (Eds), *Coarse-Grained Deltas*. Blackwell Science Publications, Oxford, pp 29-73.
- Nemec, W. and Steel, R.J. (Eds), 1988a. *Fan Deltas Sedimentology and Tectonic Setting*. In: Series, Blackie and Son Ltd, London, 444 pp
- Nemec, W. and Steel, R.J., 1988b. What is a fan delta and how do we recognize it? In: Nemec, W. and Steel, R.J. (Eds), *Fan Deltas: Sedimentology and Tectonic Settings*. Blackie, London, pp 3-13.
- Pescini, H.S., 1997. Structure and Depositional setting of the Pahau Subterranean rocks, Pahau River / Mount Saul area. Honours Project Thesis, Canterbury University, 87 pp.
- Postma, G., 1986. Classification for sediment gravity-flow deposits based on flow conditions during sedimentation. *Geology*, **14**, pp 291-294.
- Postma, G., Nemec, W. and Kleinspehn, K.L., 1988. Large floating clasts in turbidites: a mechanism for their emplacement. *Sedimentary Geology*, **58**, pp 47-61.
- Pye, K. (Ed) 1994. *Sediment Transport and Depositional Processes*. In: Series, Blackwell Science Publications, Oxford, 397 pp
- Raine, I.J., 1977. *Palynology of the Early Cretaceous Torlesse Supergroup in the Pahau River and upper Clarence River valleys, North Canterbury, open file report*. New Zealand Geological Survey
- Ramos, A., Sopena, A. and Perez-Arduena, M., 1986. Evolution of Buntsandstein fluvial sedimentation in the northwest Iberian ranges (central Spain). *Journal of Sedimentary Petrology*, **56**, pp 862-875.
- Reading, H.G. (Ed) 1996. *Sedimentary Environments: Processes, Facies and Stratigraphy*. In: Series, Blackwell Science Ltd, Oxford, 688 pp
- Reading, H.G. and Collinson, J.D., 1996. Clastic coasts. In: Reading, H.G. (Ed), *Sedimentary Environments: Processes, Facies and Stratigraphy*, 3. Blackwell Science Ltd, Oxford, pp 154-231.
- Reading, H.G. and Richards, M., 1994. Turbidite Systems in Deep-Water Basin Margins Classified by Grain Size and Feeder System. *American Association of Petroleum Geology*, **78**, pp 792-822.
- Reineck, H.E. and Singh, I.B., 1980. *Depositional Sedimentary Environments*, Springer-Verlag, New York, 549 pp.
- Retallack, G.J. and Ryburn, R.J., 1982. Middle Triassic deltaic deposits in Long Gully, near Otematata, North Otago, Zealand. *Journal of the Royal Society of New Zealand*, **12**, pp 207-227.
- Roser, B.P., Coombs, D.S., Korsch, R.J., Campbell, H.J., Mortimer, N. and Grapes, R.H., 2000. *Whole-Rock Analyses of Sandstones, siltstones, and Tuffs from the Murihiku Terrane, New Zealand. Research Report 7*. Victoria University of Wellington, School of Earth Sciences, Wellington, pp 26


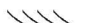


- Roser, B.P. and Cooper, A.F., 1990. Geochemistry and Terrane Affiliation of Haast Scist from the Western Southern Alps, New Zealand. *New Zealand Journal of Geology and Geophysics*, **33**, pp 1-10.
- Roser, B.P. and Korsch, R.J., 1999. Geochemical Characterization, Evolution and Source of a Mesozoic Accretionary Wedge; the Torlesse Terrane. *New Zealand Geological Magazine*, **136**, pp 496-512.
- Roser, B.P., Mortimer, N., Turnbull, I.M. and Landis, C.A., 1993. Geology and Geochemistry of the Caples Terrane, Otago, New Zealand: Compositional Variations near a Permo-Triassic Arc Margin. In: Ballance, P.F. (Ed), *South Pacific Sedimentary Basins: Sedimentary Basins of the World*. Elsevier Science Publishers B.V., Amsterdam, pp 3-19.
- Sanders, J.E., 1965. Primary sedimentary structures formed by turbidity currents and related resedimentation mechanisms. In: Middleton, G.V. (Ed), *Primary sedimentary structures and their hydrodynamic interpretation*. Society of Economic Palaeontologists and Mineralogists Special Publication, pp 192-219.
- Shanmugam, G., 1997. The Bouma Sequence and the turbidite mind set. *Earth-Science Review*, **42**, pp 201-229.
- Shanmugam, G., 2000. 50 years of the turbidite paradigm (1950s - 1990s): deep-water processes and facies models - a critical perspective. *Marine and Petroleum Geology*, **17**, pp 285-342.
- Shanmugam, G., Bloch, R.B., Damuth, J.E. and Hodgkinson, R.J., 1997. Basin-Floor Fans in the North Sea: Sequence Stratigraphic Models vs Sedimentary Facies: Reply. *American Association of Petroleum Geology*, **81**, pp 666-672.
- Silberling, N.J., Nicholas, K.M., Bradshaw, J.D. and Blome, C.D., 1988. Limestone and chert in tectonic blocks from the Esk Head subterrane, South Island, New Zealand. *Geological Society of America, Bulletin*, **100**, pp 1213-1223.
- Skinner, B.J. and Porter, S.C., 1987. *Physical Geology*, John Wiley & Sons, New York.
- Smale, D., 1997. Heavy minerals in the Torlesse Terrane of the Wellington area, New Zealand. *New Zealand Journal of Geology and Geophysics*, **40**, pp 499-506.
- Speden, I.G., 1976. Fossil Localities in Torlesse rocks of the North Island, New Zealand. *Journal of the Royal Society of New Zealand*, **6**, pp 73-91.
- Stow, D.A.V., Reading, H.G. and Collinson, J.D., 1996. Deep seas. In: Reading, H.G. (Ed), *Sedimentary Environments: Processes, Facies and Stratigraphy*. Blackwell Science Ltd, Oxford, pp 395-453.
- Suggate, R.P., 1961. Rock stratigraphic names for the South Island schists and undifferentiated sediments of the New Zealand geosyncline. *New Zealand Journal of Geology and Geophysics*, **4**, pp 392-399.
- Turnbull, I.M., 1979. Petrography of the Caples Terrane of the Thomson Mountains, Northern Southland, New Zealand. *New Zealand Journal of Geology and Geophysics*, **22**, pp 709-727.
- Underwood, M.B. and Moore, G.F., 1996. Trenches and Trench-Slope Basins. In: Busby, C.J. and Ingersoll, R.V. (Eds), *Tectonics of Sedimentary Basins*. Blackwell Science Inc., Oxford, pp 179-220.
- Walker, R.G. and James, N.P. (Eds), 1992. *Facies models: response to sea level change*. In: Series, GEOtext, Geological Association of Canada, St John's, 454 pp
- Wandres, A., Unpubl. PhD Thesis. The Provenance of the Torlesse Terrane, Canterbury University.

-
- Warren, G., 1967. Sheet 17, Hokitika (1st Edition) "Geological Map of New Zealand 1:250 000", Department of Scientific and Industrial Research, Wellington.
- Wells, N.A. and Dorr, J.A., 1987. A reconnaissance of sedimentation on the Kosi alluvial fan of India. *Third International Fluvial Sedimentology Conference*, pp 51-61.
- Willet, R.W., 1948. Undifferentiated Jurassic-Triassic-Permian, *The Outline of the Geology of New Zealand*. New Zealand Geological Survey, Wellington.
- Wood, R.A., Pettinga, J.R., Bannister, S., Lamarche, L. and McMorran, T.J., 1994. Structure of the Hammer strike-slip basin, Hope fault, New Zealand. *Geological Society of America, Bulletin*, **106**, pp 1459-1473.
-




APPENDIX I

LEGEND





Bedforms

-  Planar lamination
-  Cross stratification
-  Asymmetrical ripples
-  Symmetrical ripples






Soft sediment deformation - Liquefaction structures

-  Flame structures
-  Load casts
-  Soft sediment deformation

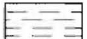



Miscellaneous

-  Flute casts
-  Weathered section
-  Macrofossil(s)
-  Rootlets

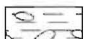
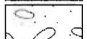
Deformation Levels

-  Deformation Level I
-  Deformation Level II
-  Deformation Level III
-  Deformation Level IV
-  Deformation Level V


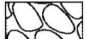

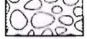


Lithology

-  Mudstone
-  Fine sandstone
-  Medium sandstone
-  Coarse sandstone

Matrix Supported Conglomerates

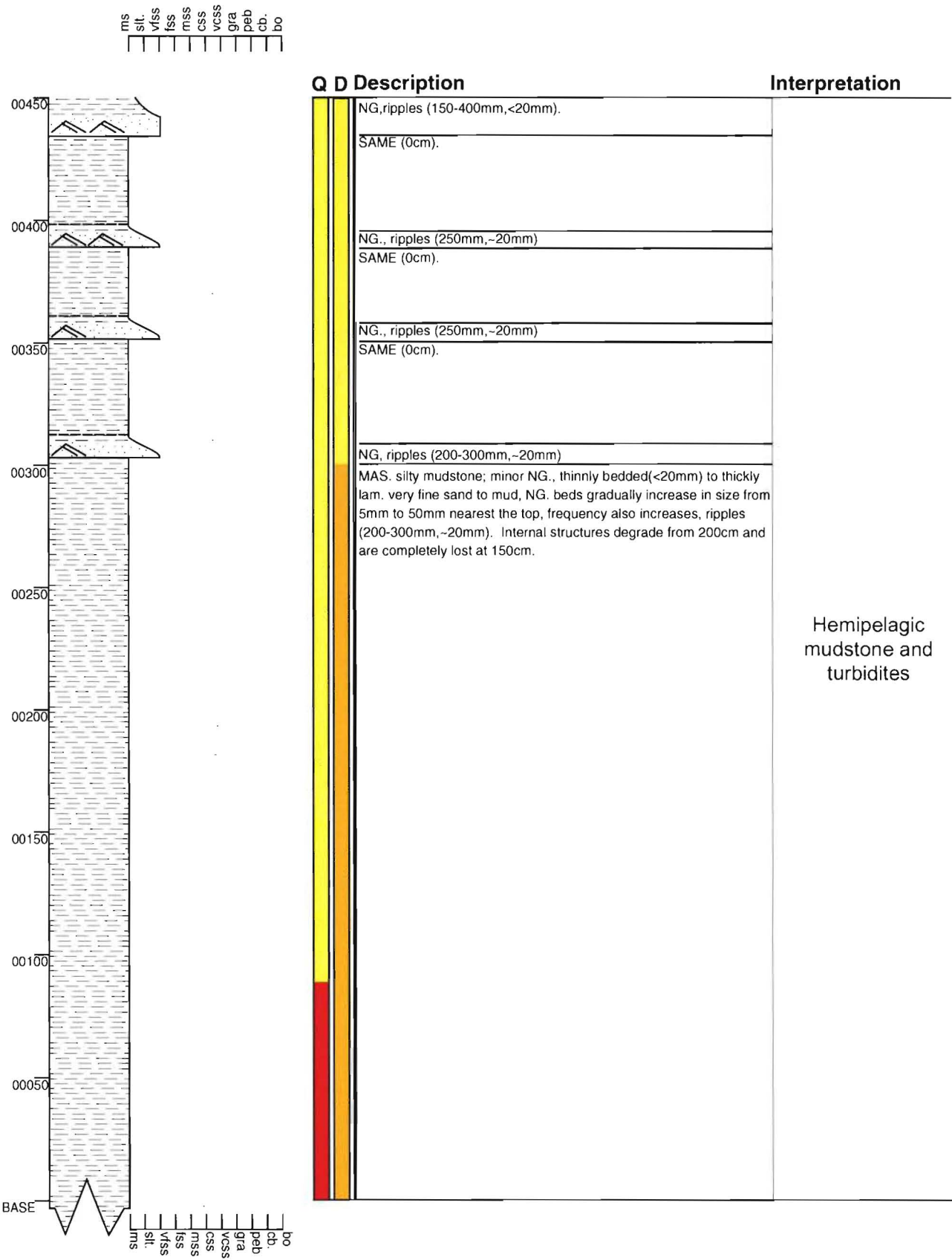
-  Muddy Pebble conglomerate
-  Sandy Pebble conglomerate

Clast Supported Conglomerates

-  Well sorted fine pebble
-  Well sorted coarse pebble
-  Moderately sorted pebble
-  Poorly sorted granule to pebble
-  Poorly sorted coarse sandstone to pebble
-  Poorly sorted fine to coarse pebble

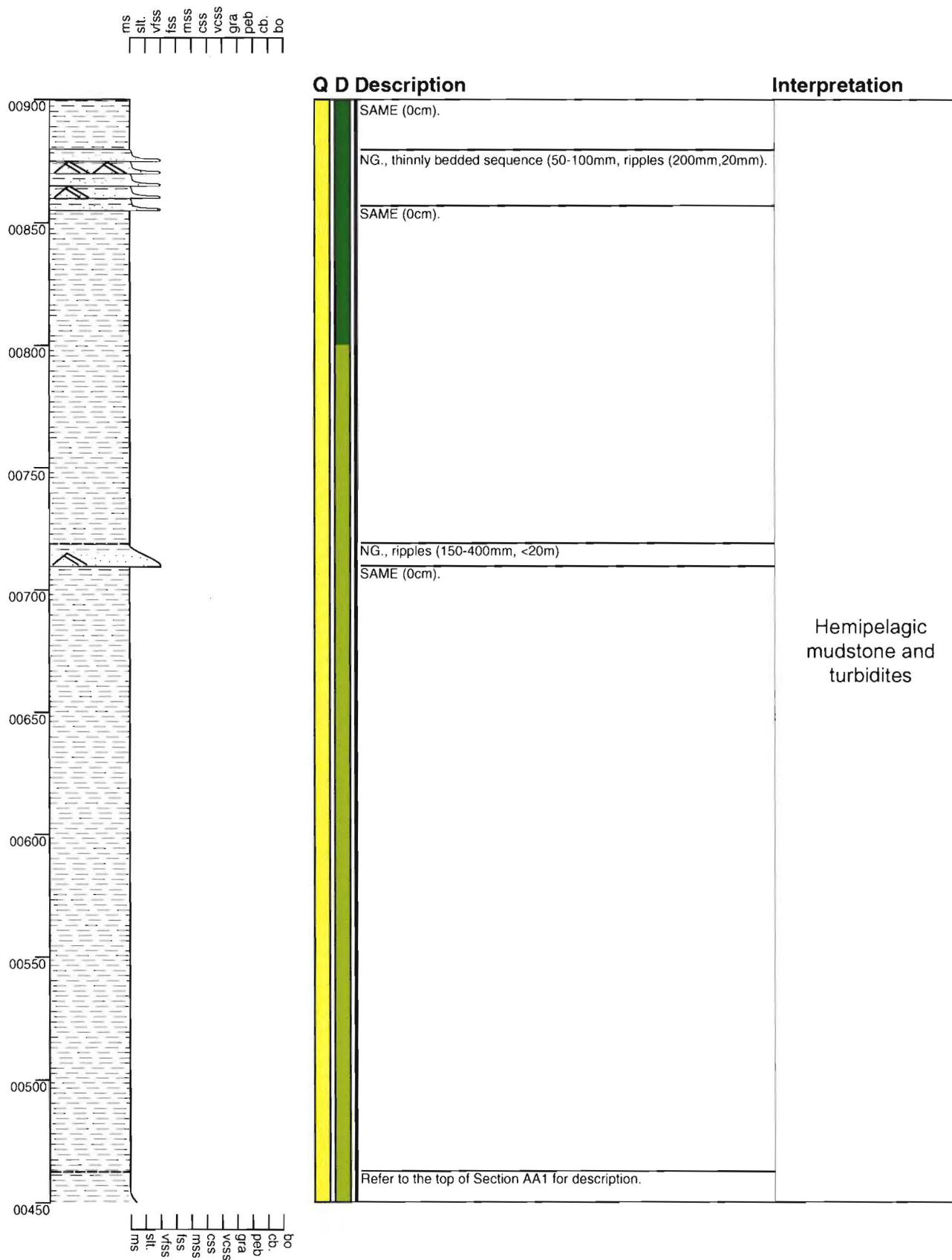
Section - Pahau River AA01

Grid Reference M32 856 432



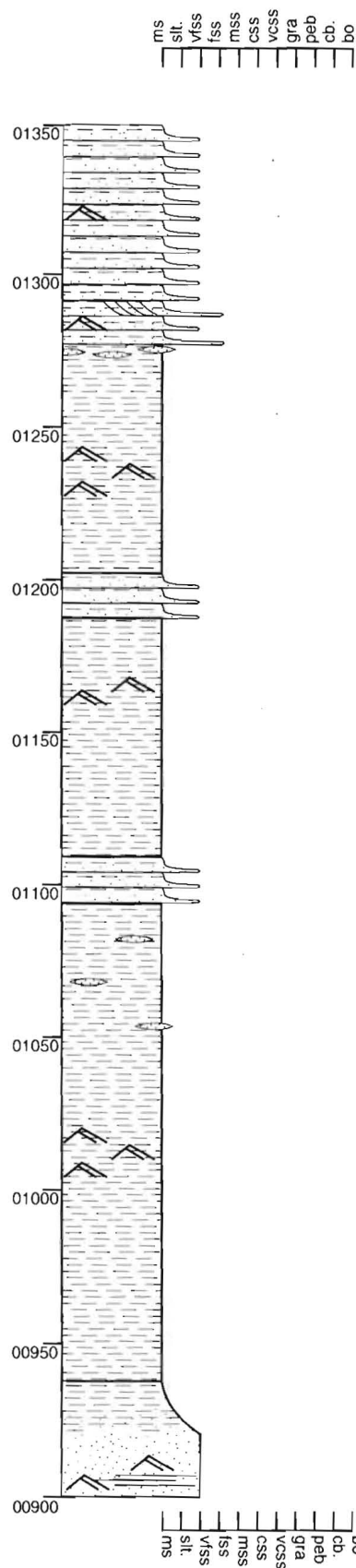
Section - Pahau River AA02

Grid Reference M32 856 432



Section - Pahau River AA03

Grid Reference M32 856 432



Q D Description

Interpretation

NG., thinly bedded sequence (10-50mm), basal 10cm fs lenses, crossbedding, ripples(300mm,15mm).

SAME (940cm).

SAME (1100cm).

MAS., ripples (no full ripples observed).

NG., thinly bedded sequence (5-30mm), ripples(250mm,<10mm).

MAS., abundant vfs/fs lenses above 1050cm, silty and NG vfs lams throughout, lam. frequency increases upwards, ripples(250-300mm, <10mm).

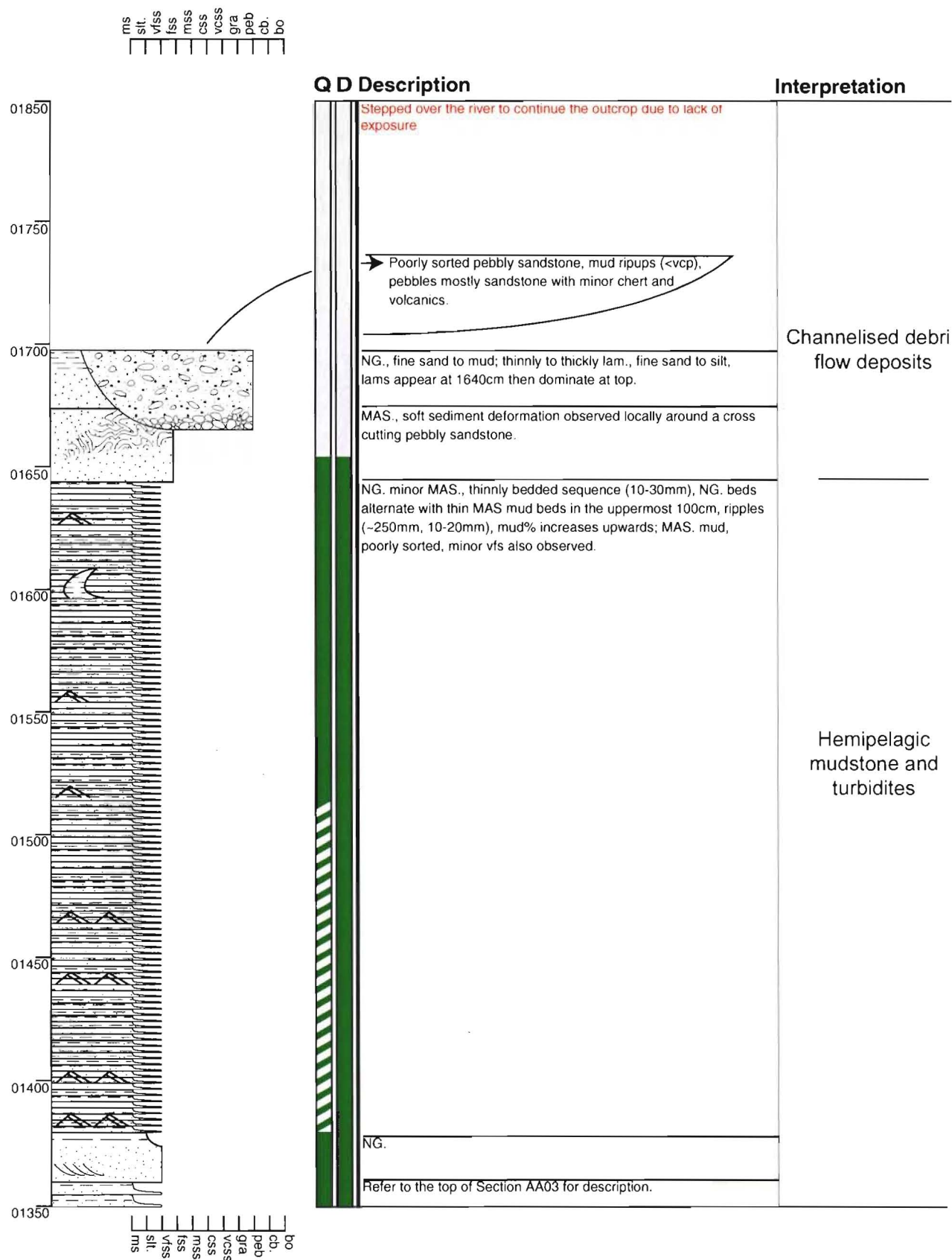
Extreme weathering from 950cm to 1000cm has left little to interpret, no fragments coarser than mud were observe. I assume this interval is massive mudstone.

NG, silty lams in basal 15cm, ripples (150-200mm, ~10mm).

Hemipelagic
mudstone and
turbidites

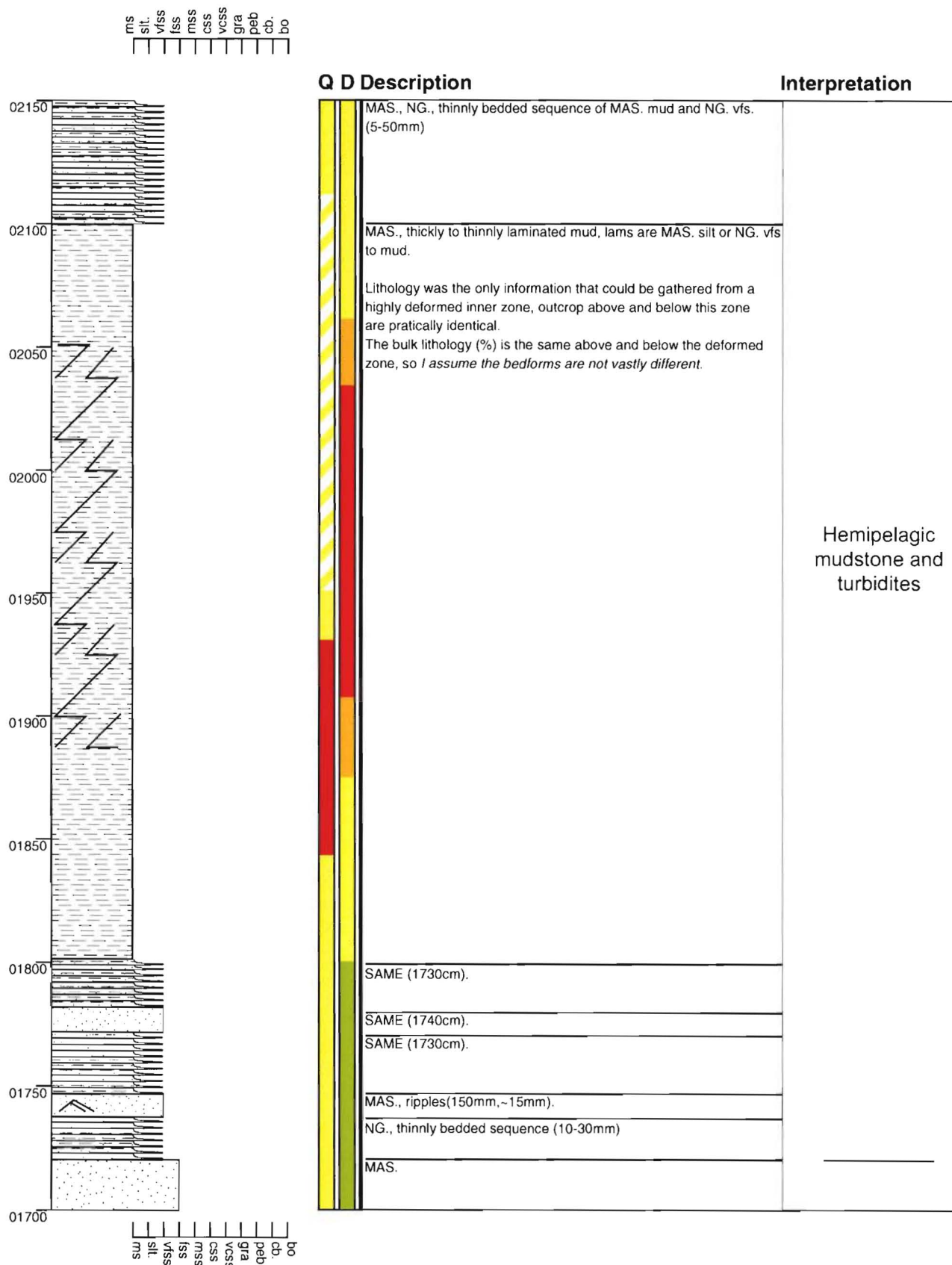
Section - Pahau River AA04

Grid Reference M32 856 432



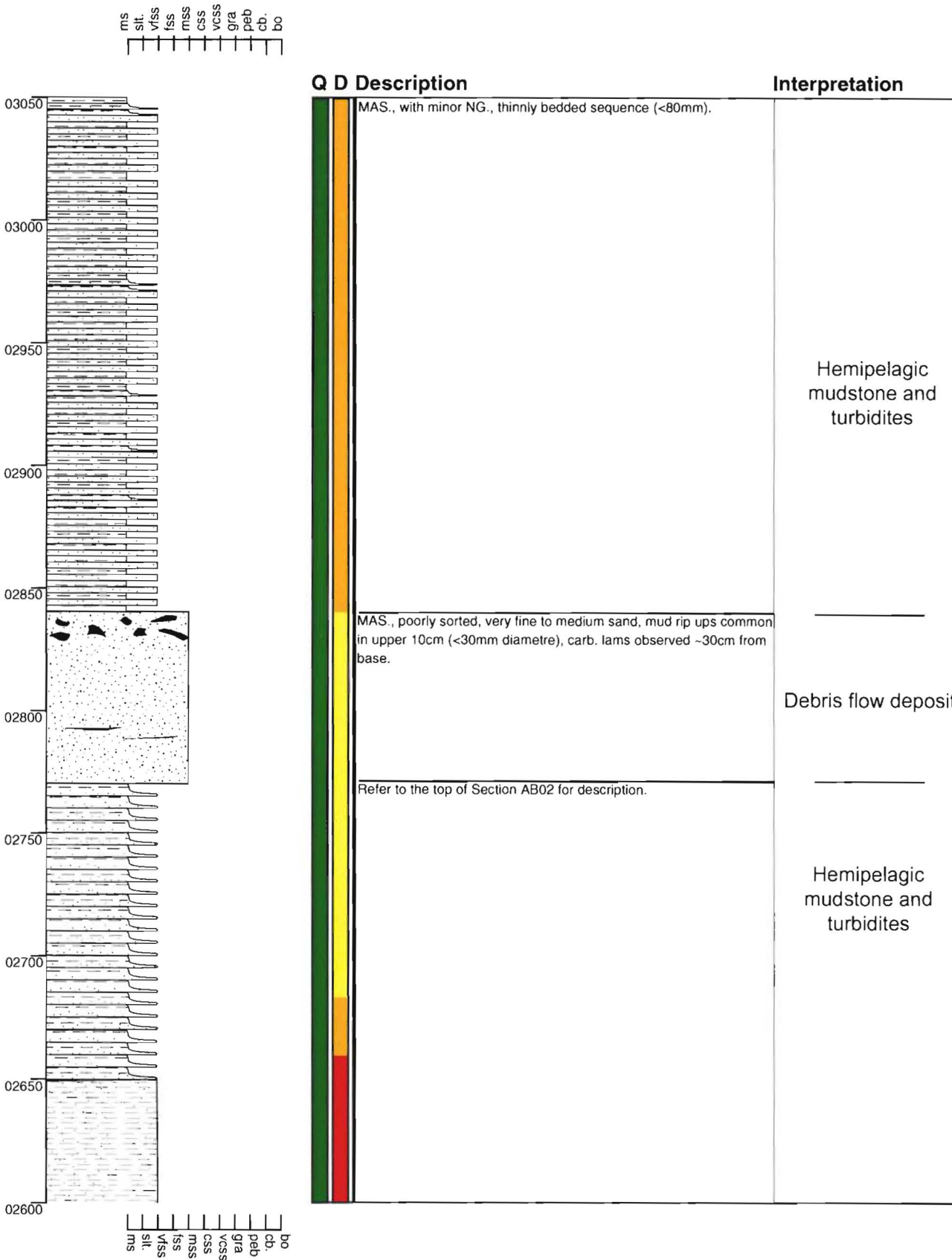
Section - Pahau River AB01

Grid Reference M32 856 432



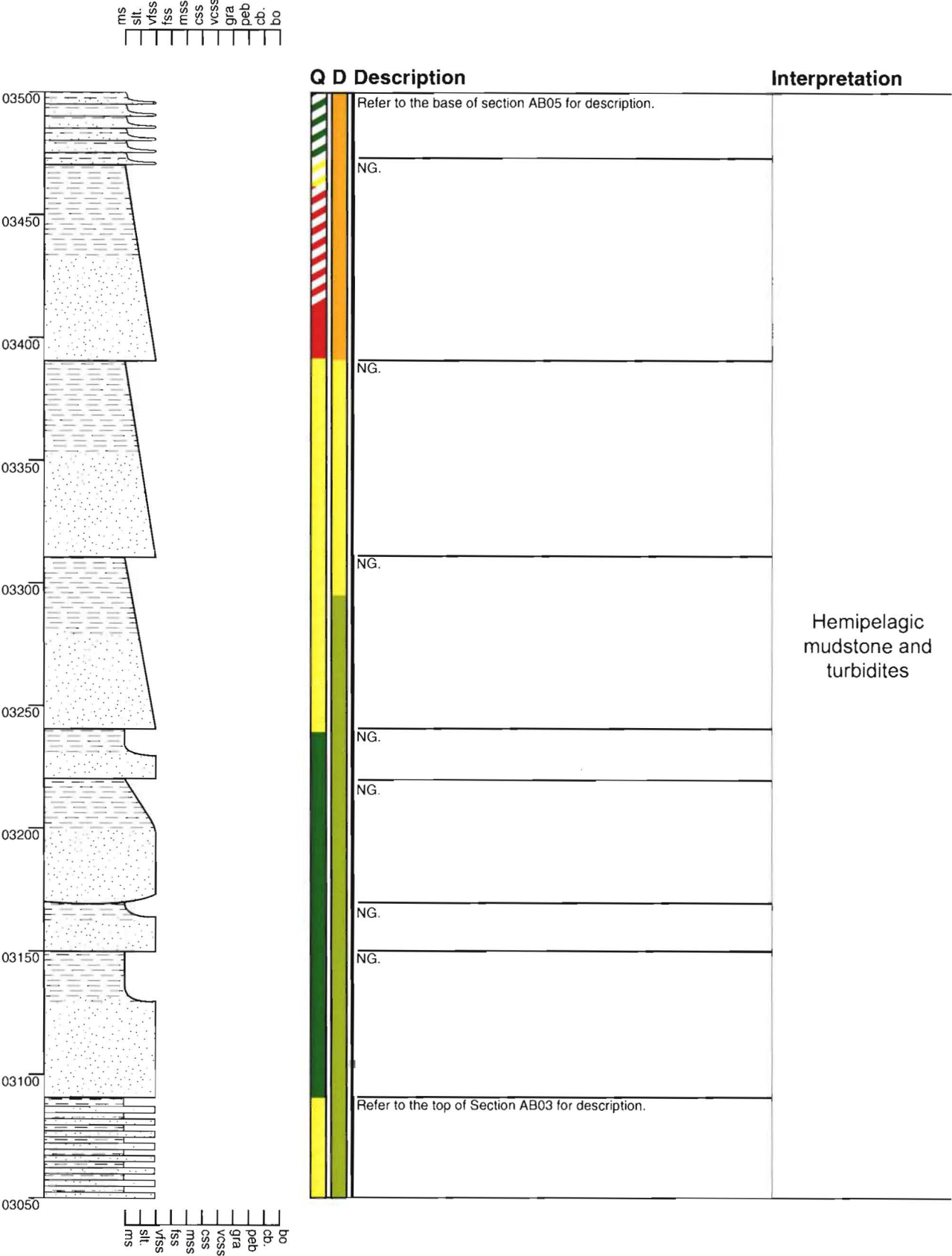
Section - Pahau River AB03

Grid Reference M32 856 432



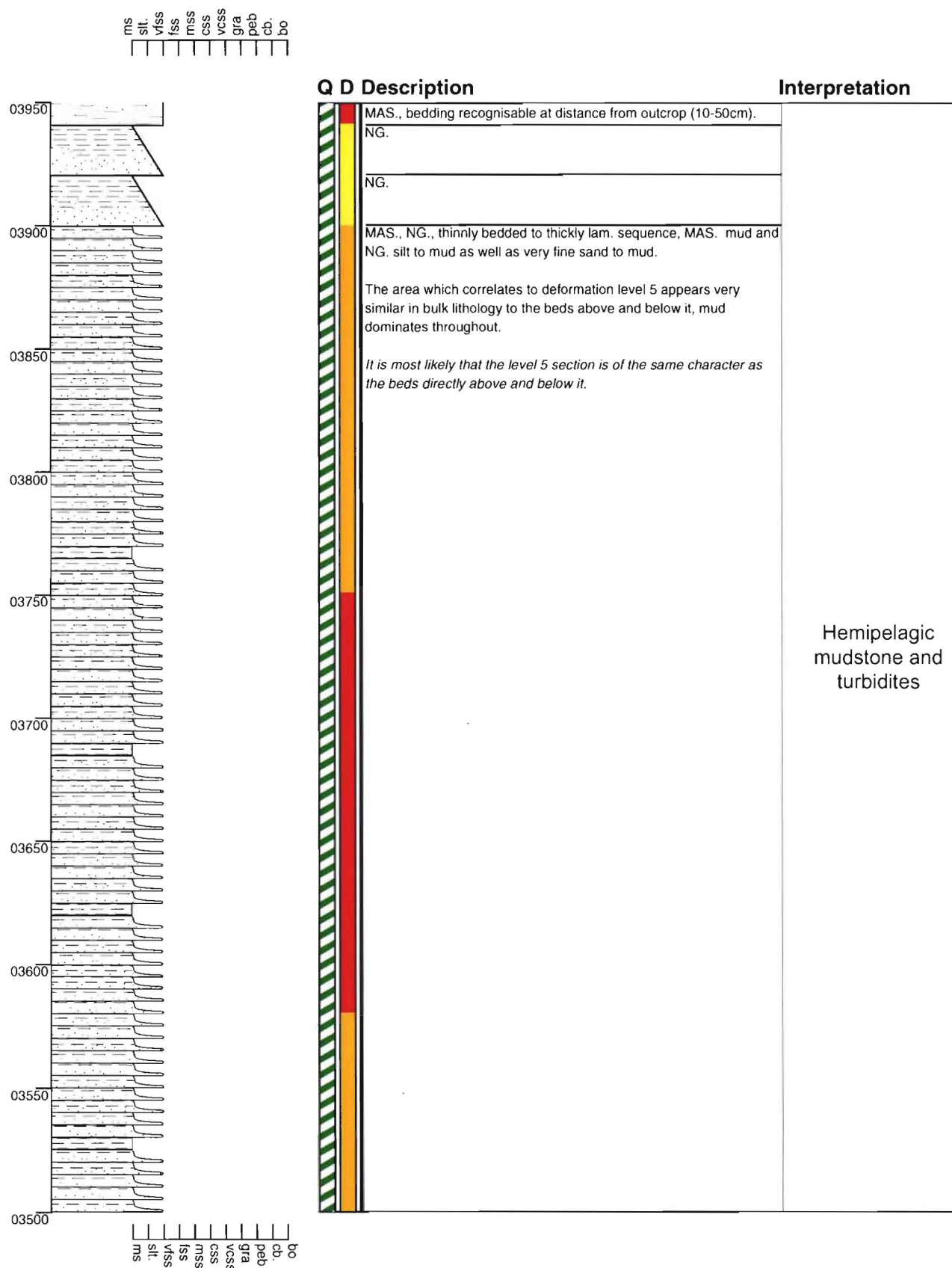
Section - Pahau River AB04

Grid Reference M32 856 432



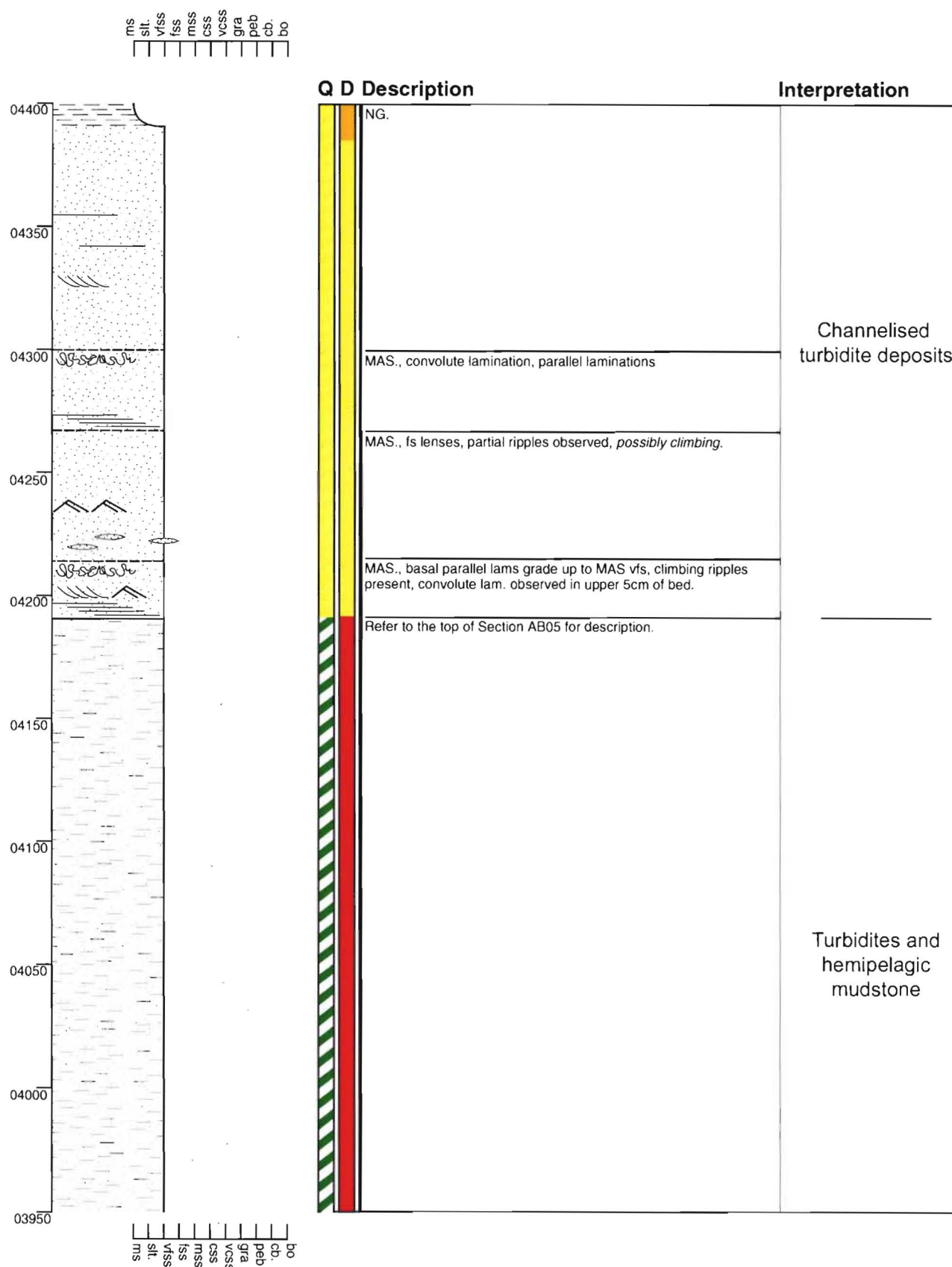
Section - Pahau River AB05

Grid Reference M32 856 432



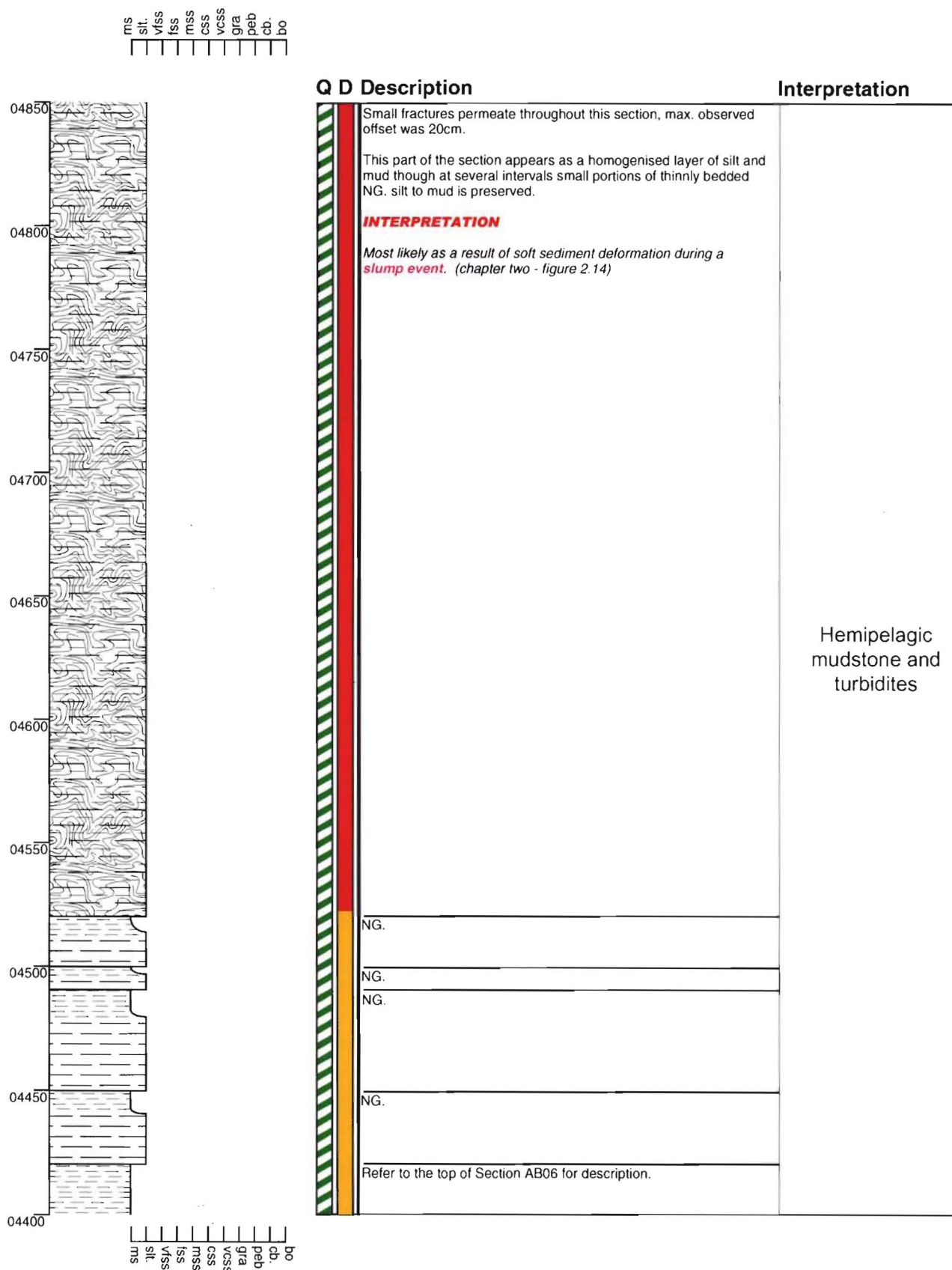
Section - Pahau River AB06

Grid Reference M32 856 432



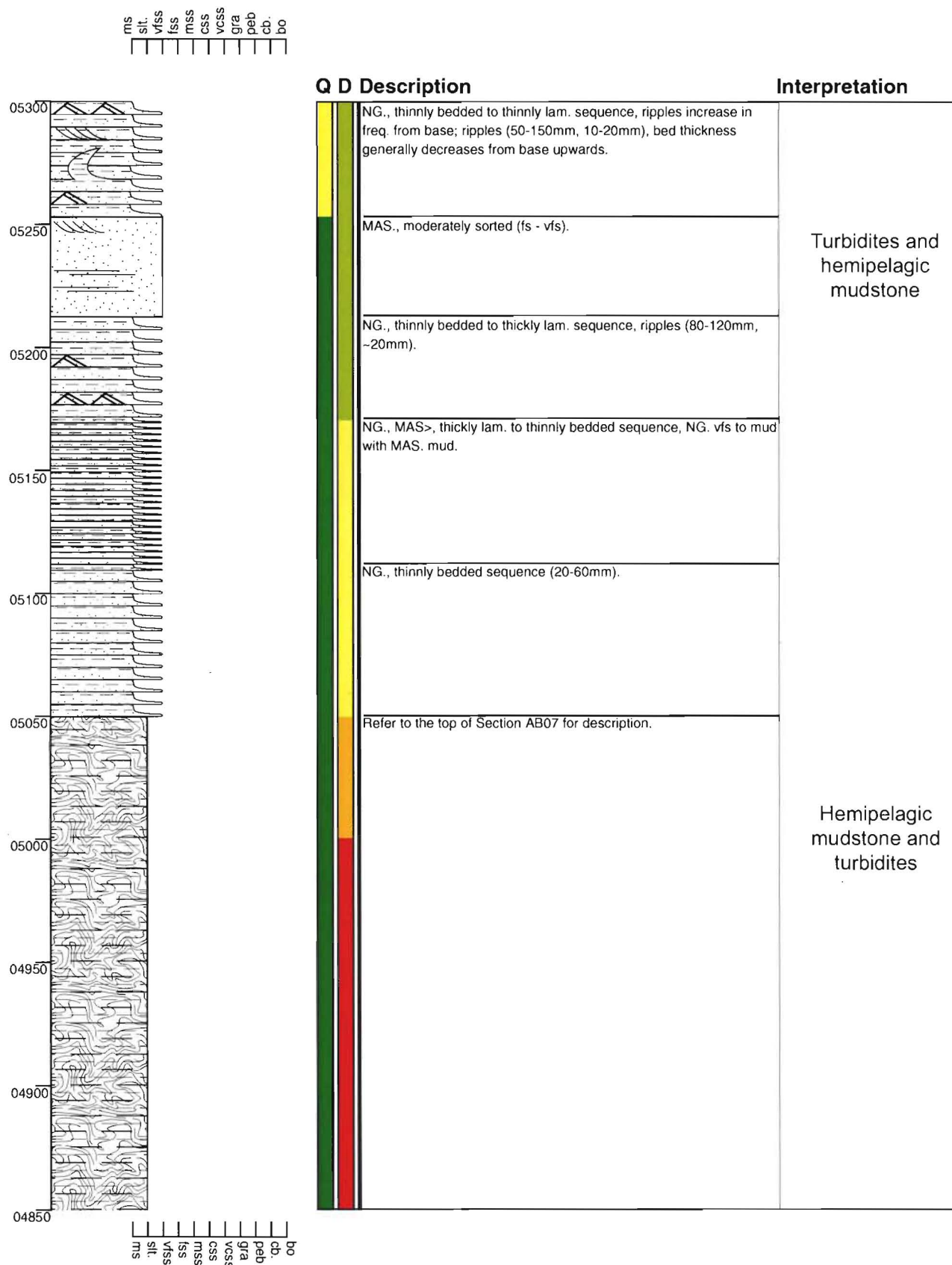
Section - Pahau River AB07

Grid Reference M32 856 432



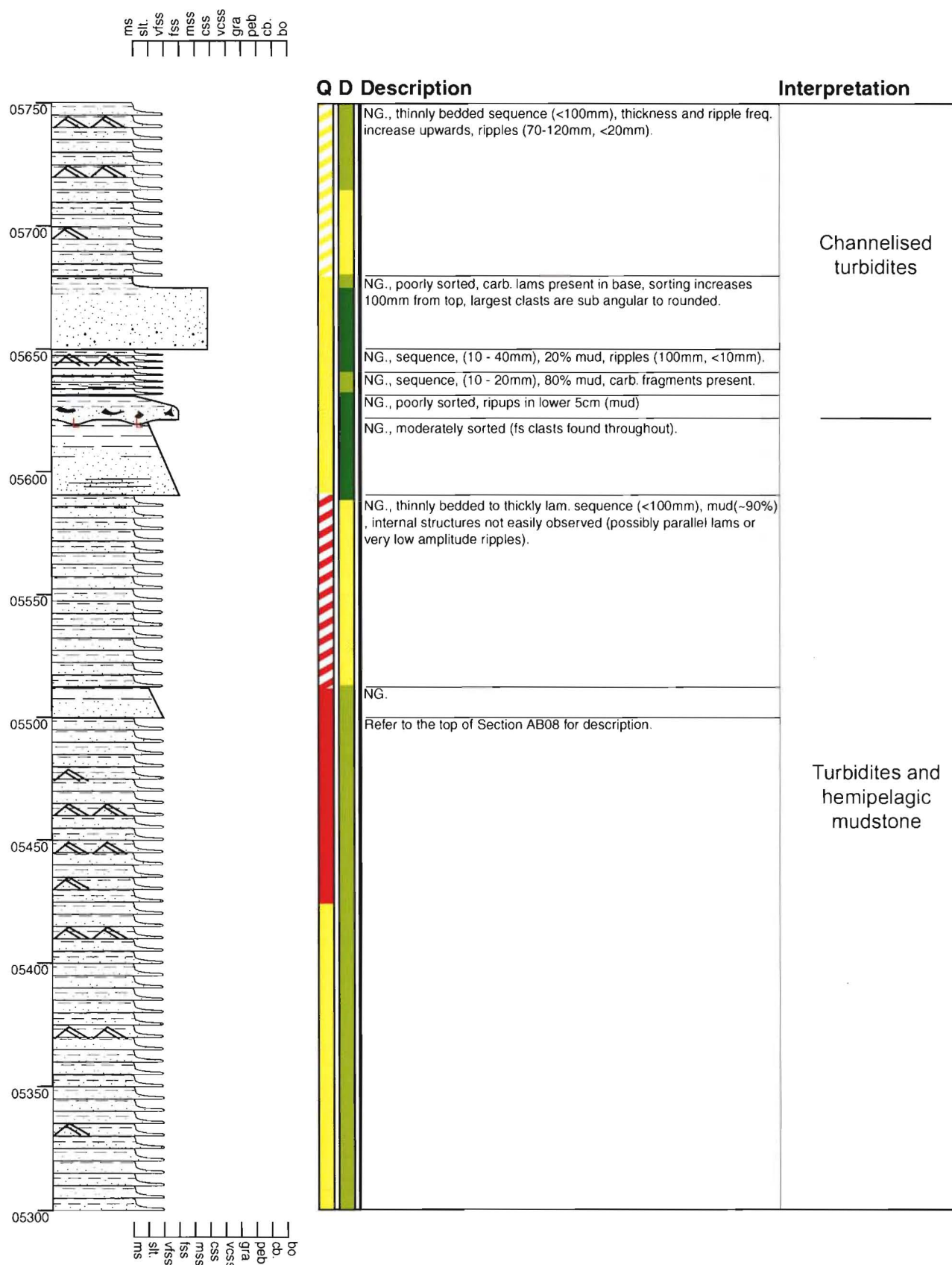
Section - Pahau River AB08

Grid Reference M32 856 432



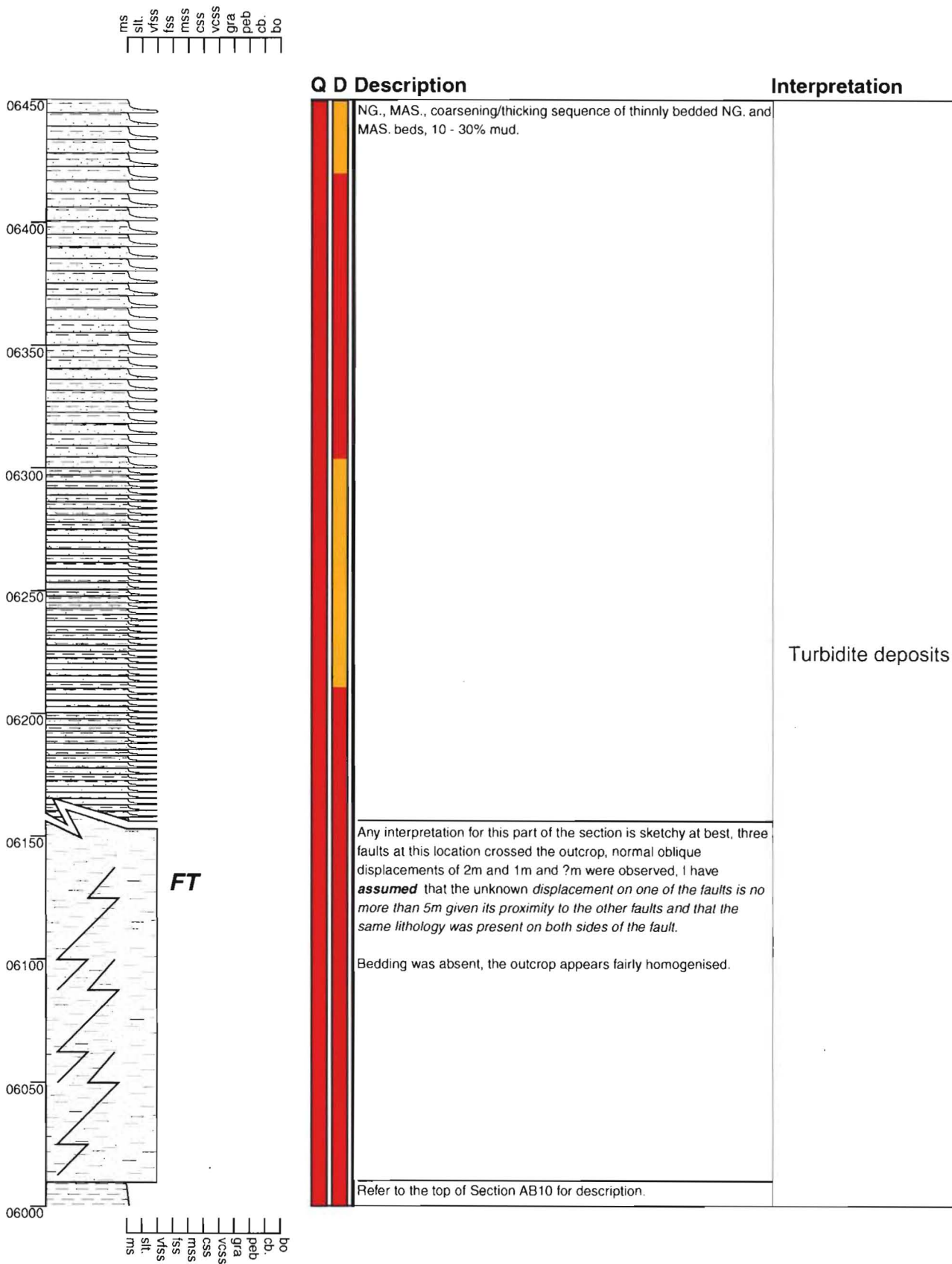
Section - Pahau River AB09

Grid Reference M32 856 432



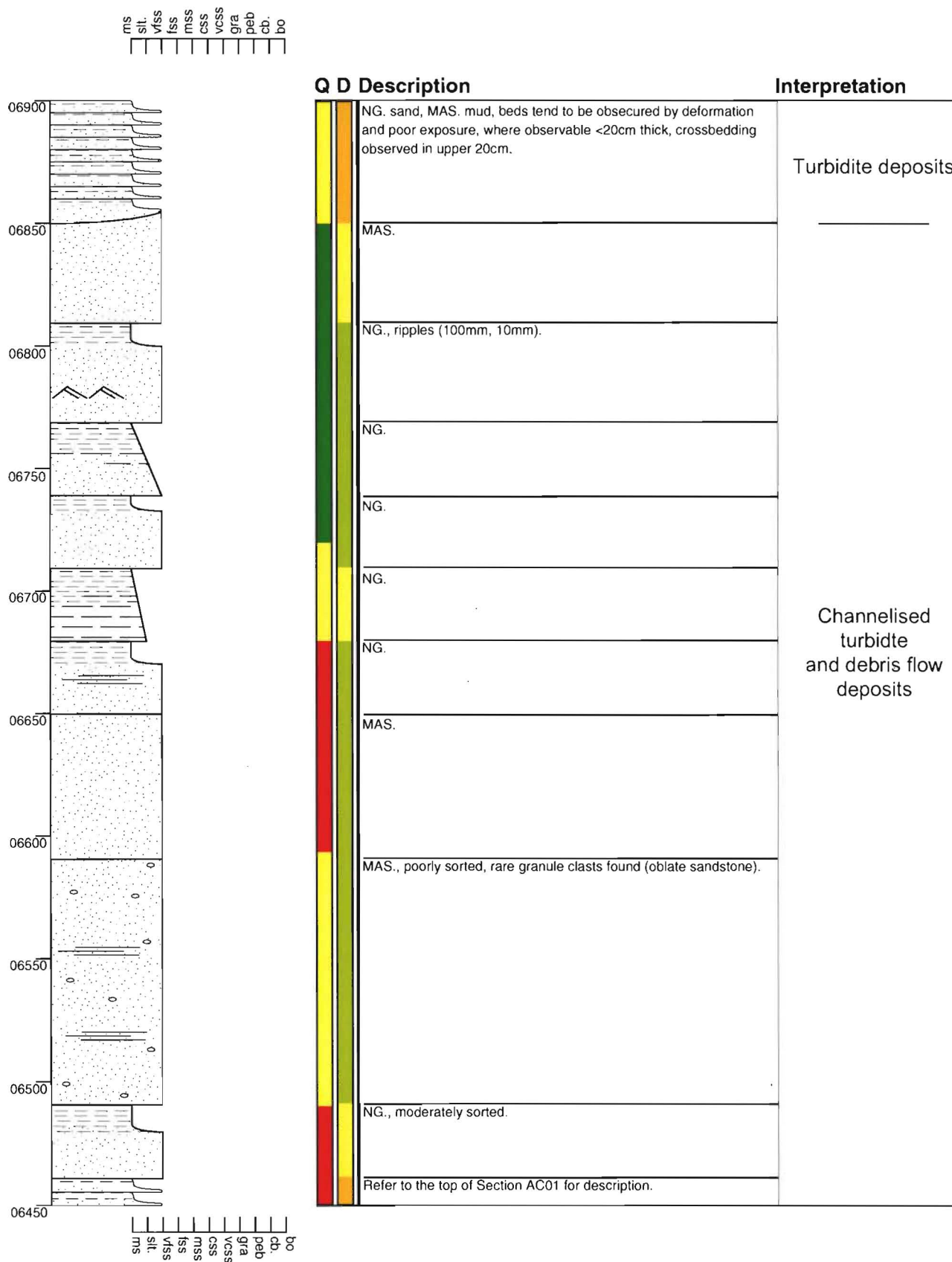
Section - Pahau River AC01

Grid Reference M32 857 432



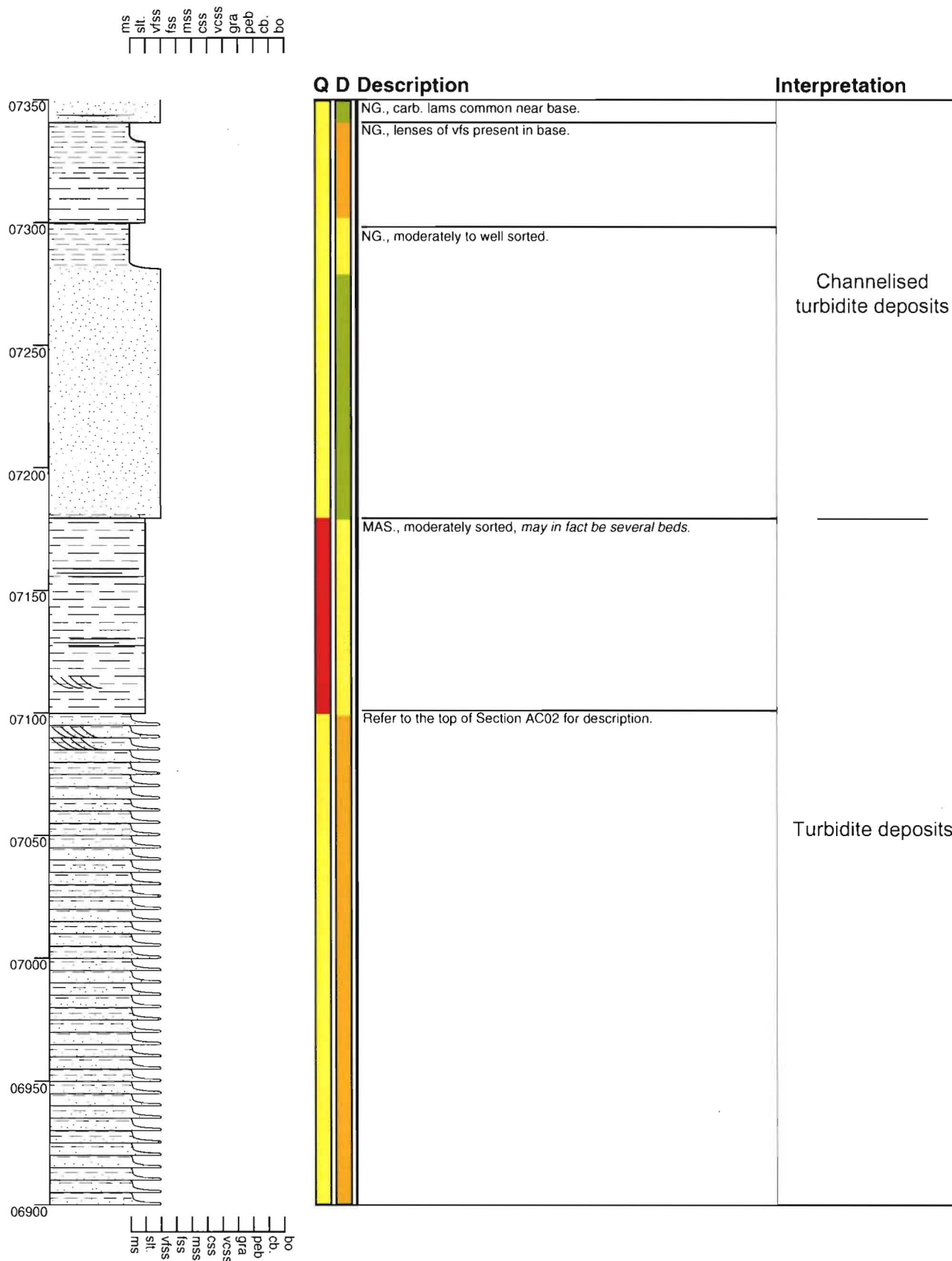
Section - Pahau River AC02

Grid Reference M32 857 432



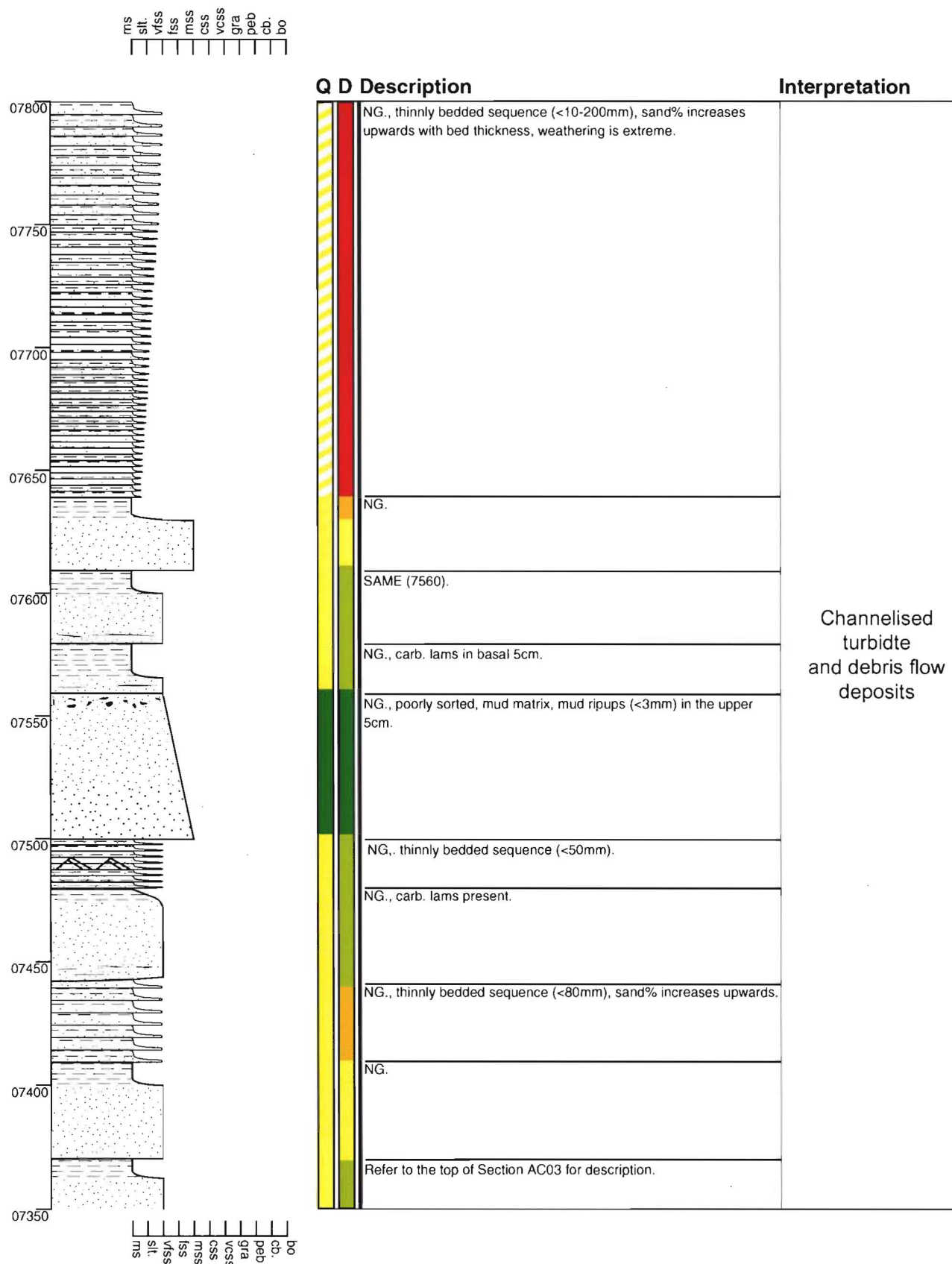
Section - Pahau River AC03

Grid Reference M32 857 432



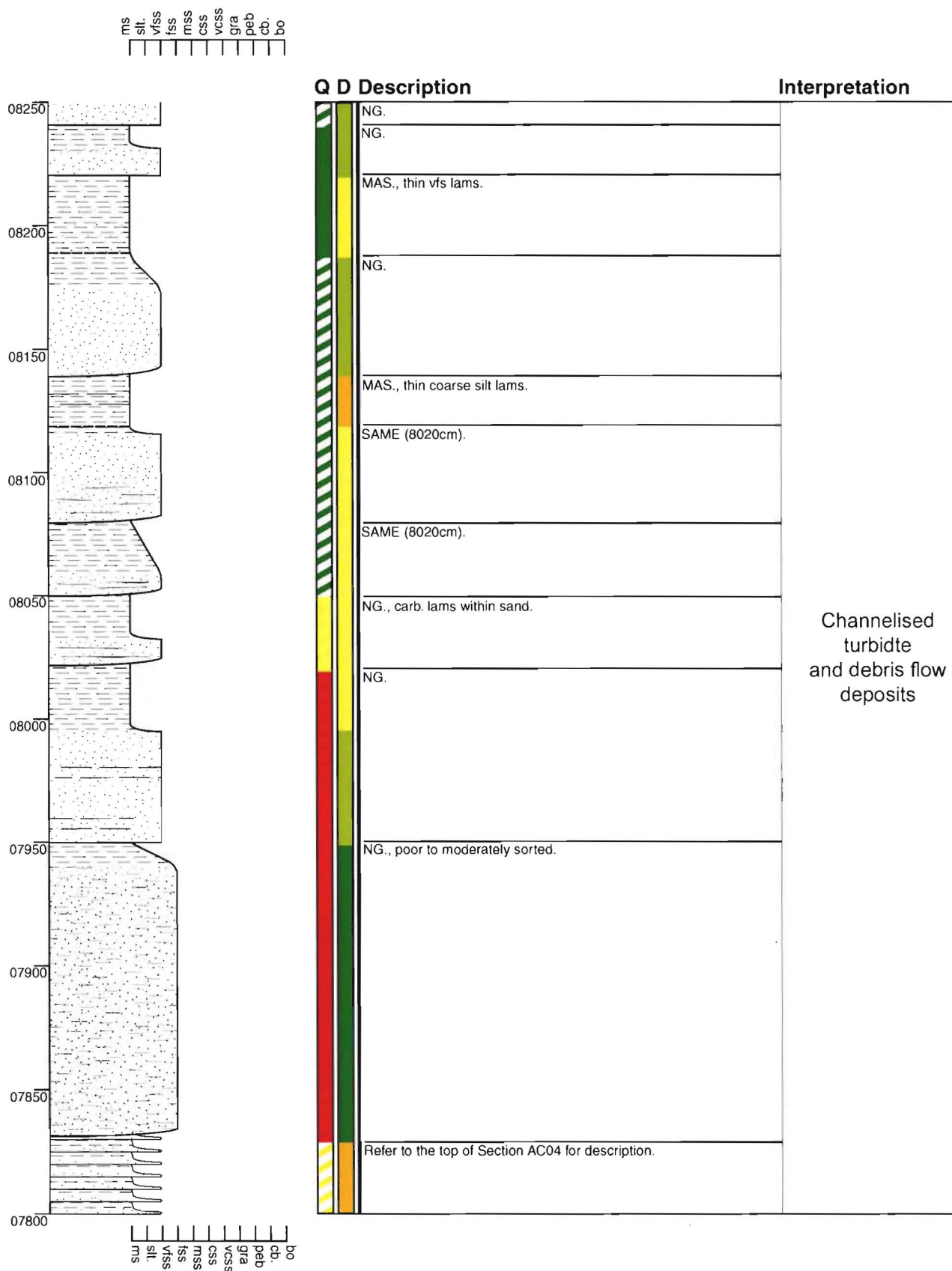
Section - Pahau River AC04

Grid Reference M32 857 432



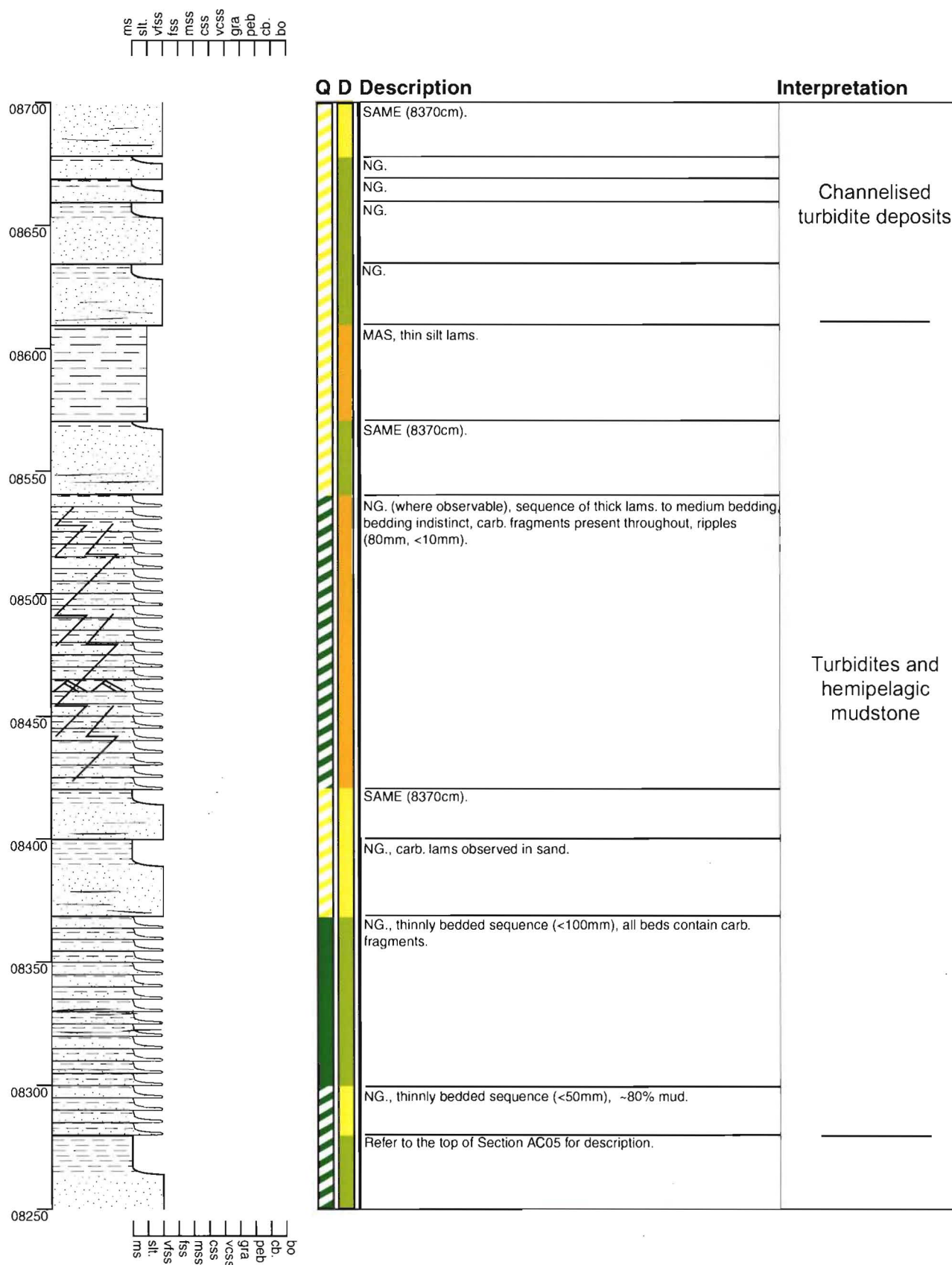
Section - Pahau River AC05

Grid Reference M32 857 432



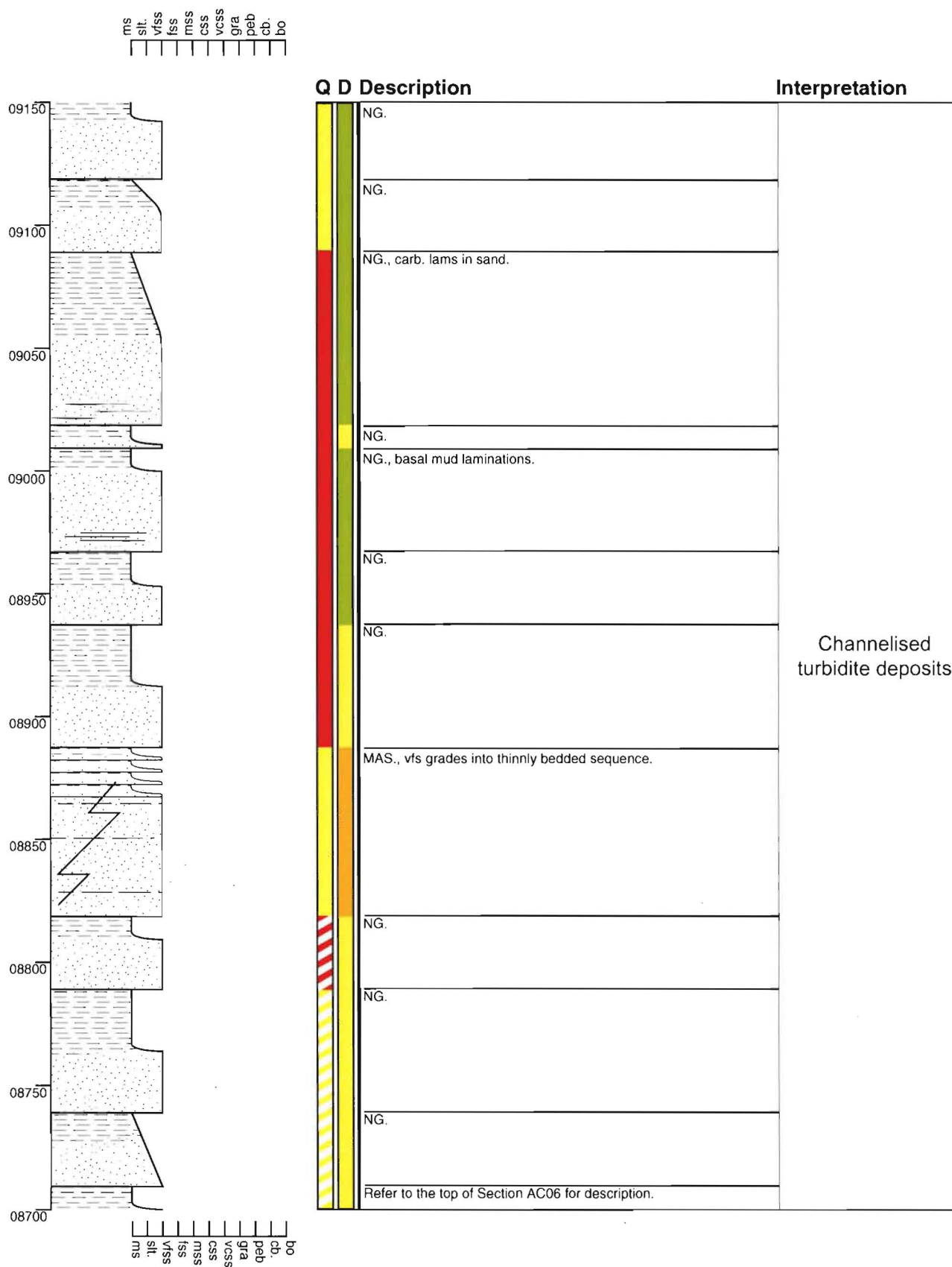
Section - Pahau River AC06

Grid Reference M32 857 432



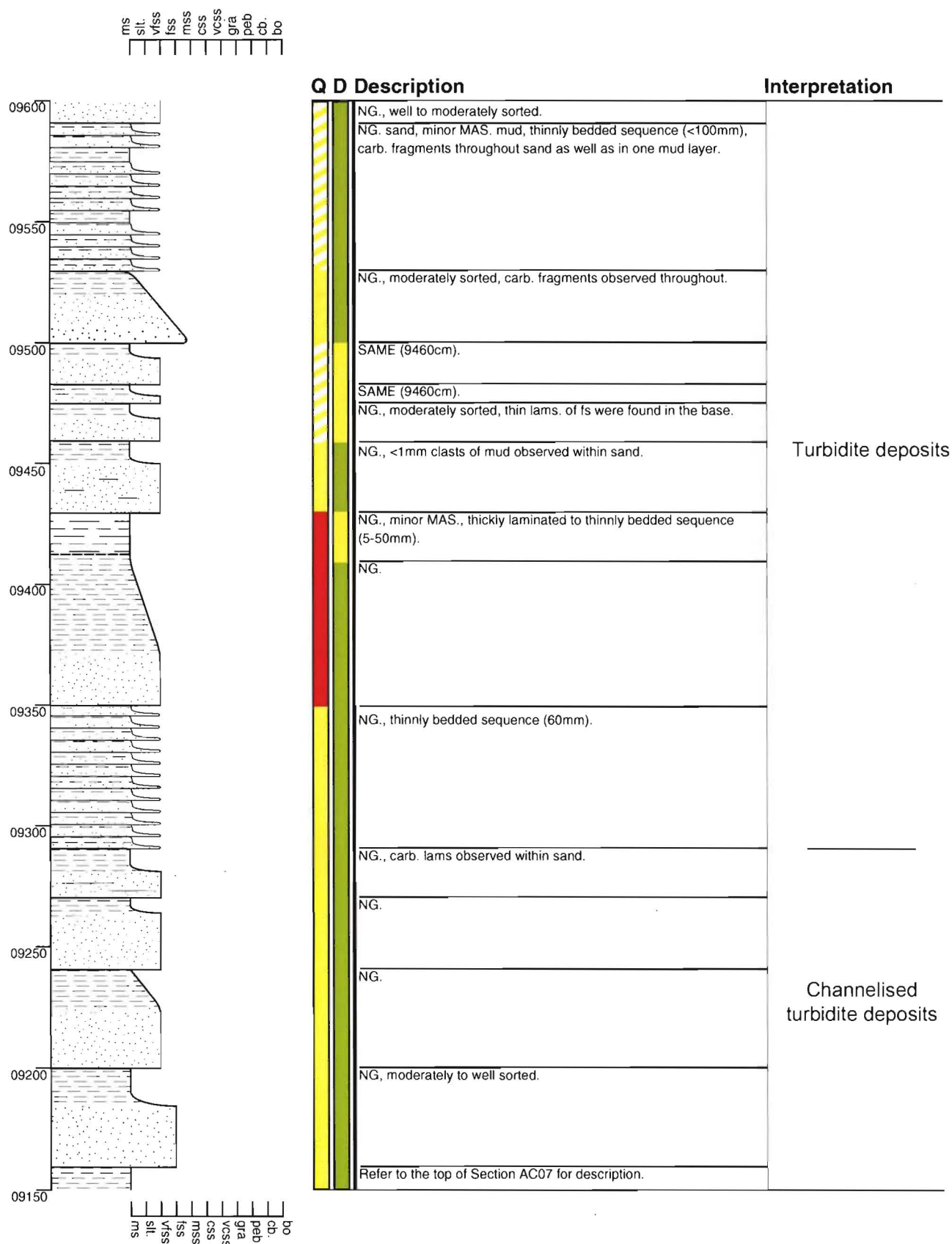
Section - Pahau River AC07

Grid Reference M32 857 432



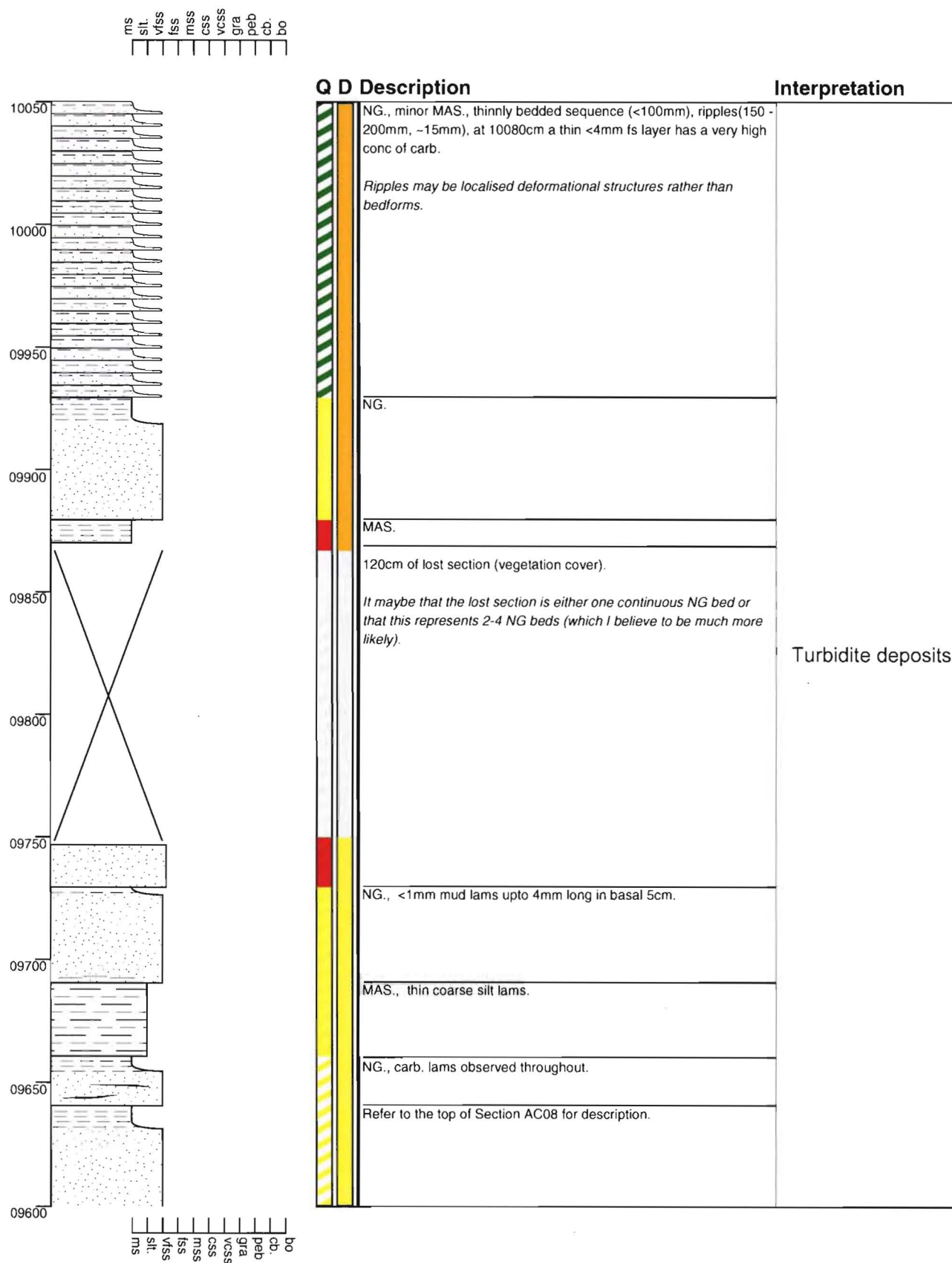
Section - Pahau River AC08

Grid Reference M32 857 432



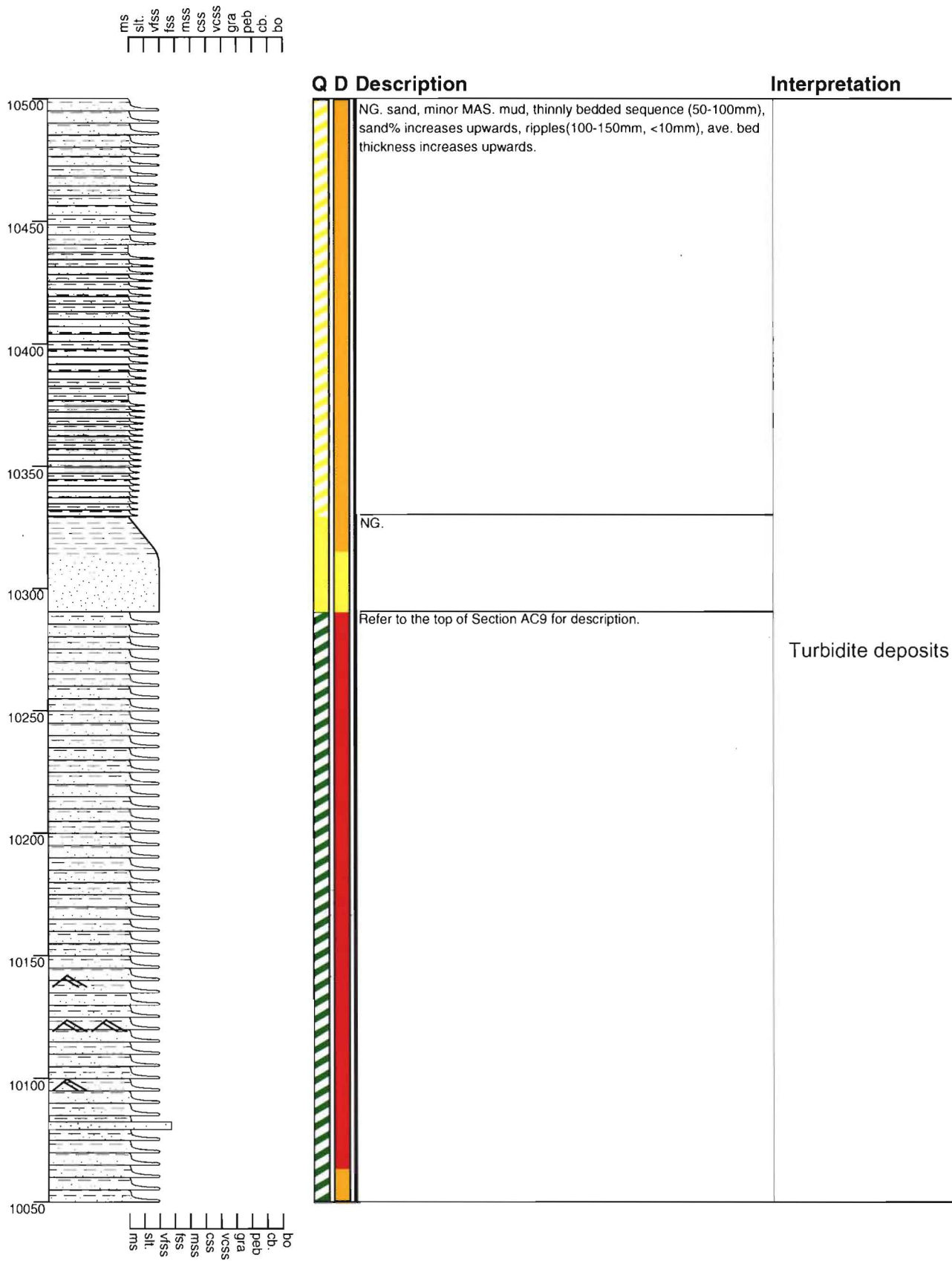
Section - Pahau River AC09

Grid Reference M32 857 432



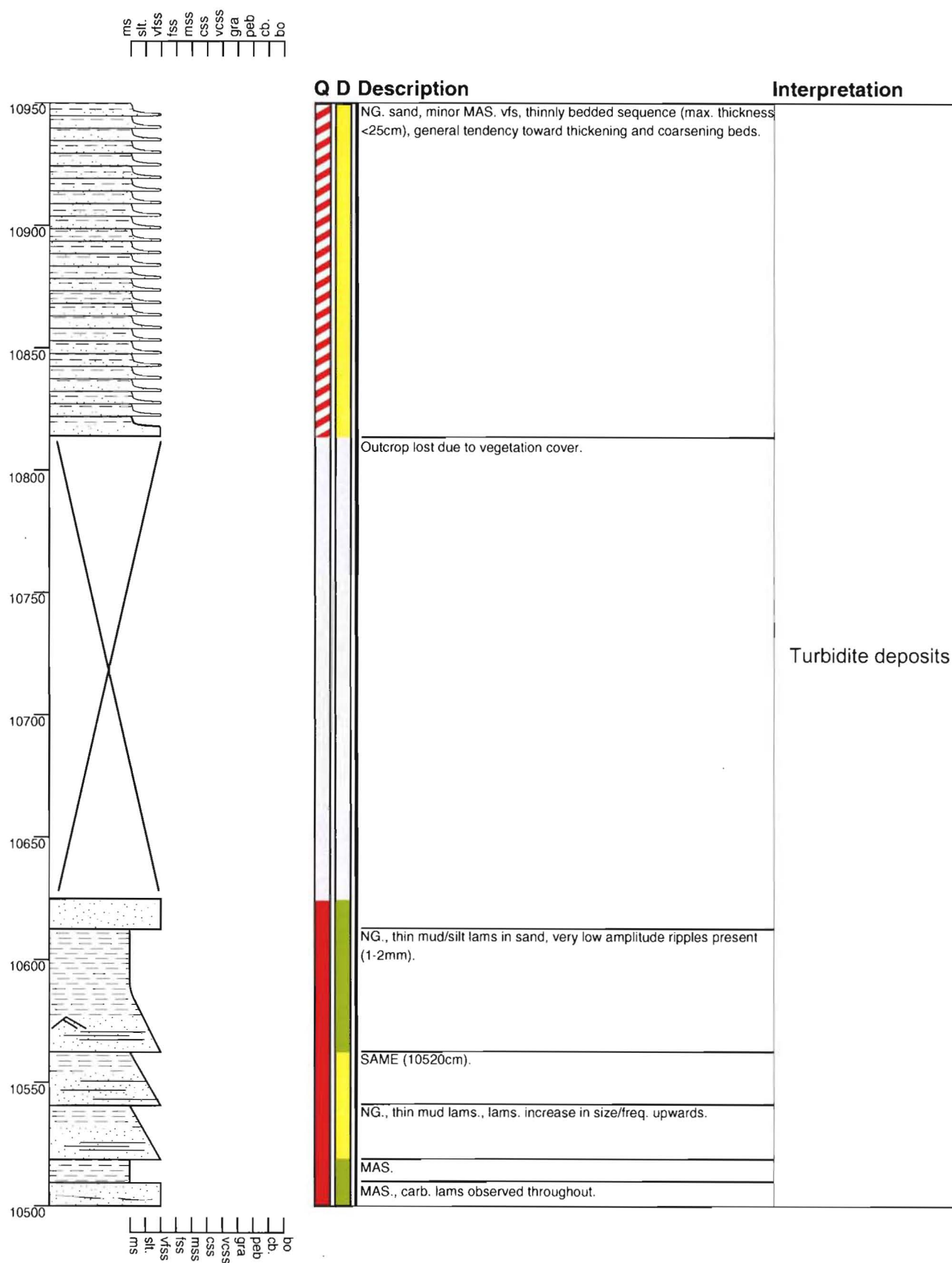
Section - Pahau River AC10

Grid Reference M32 857 432



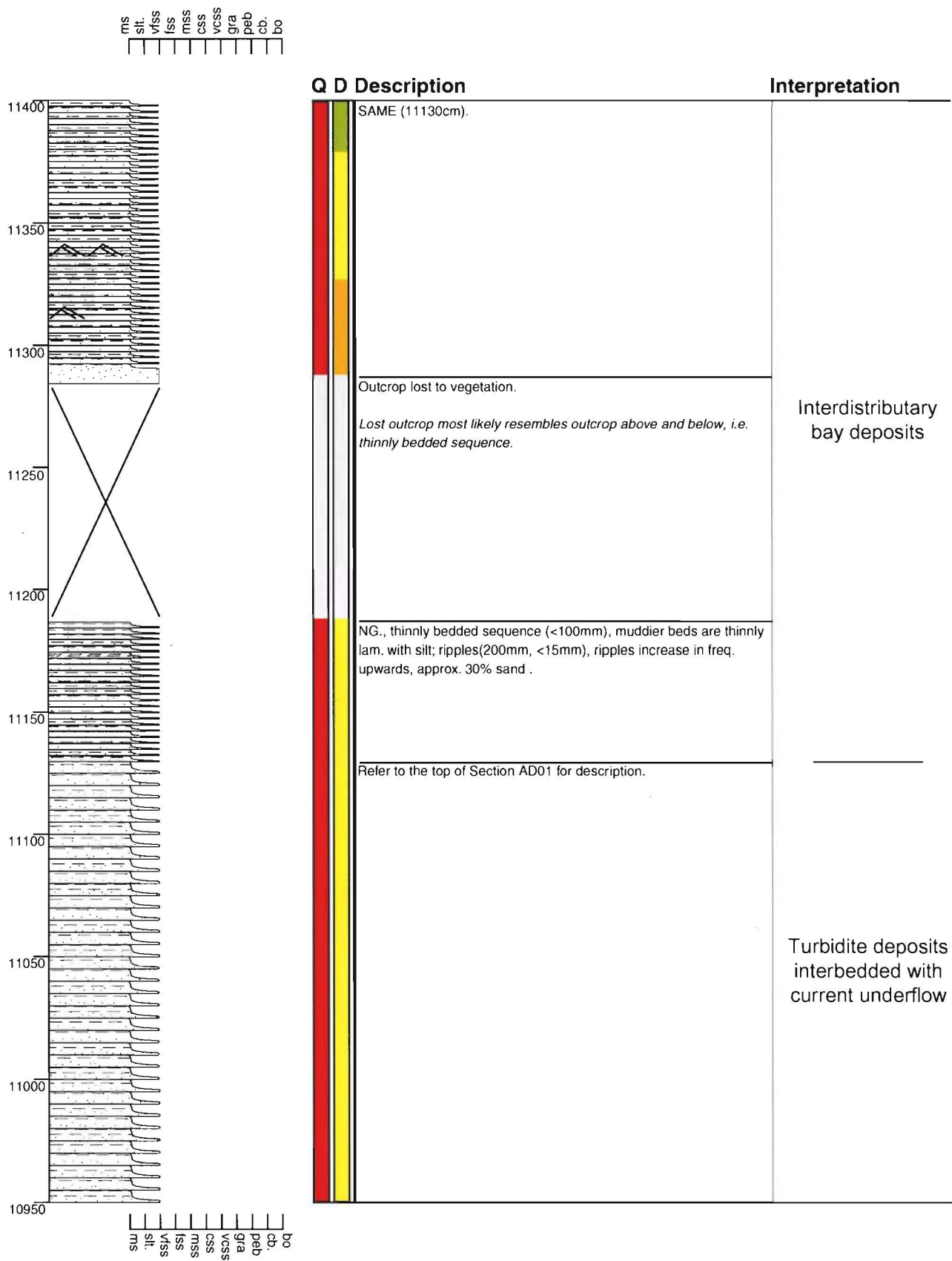
Section - Pahau River AD01

Grid Reference M32 857 431



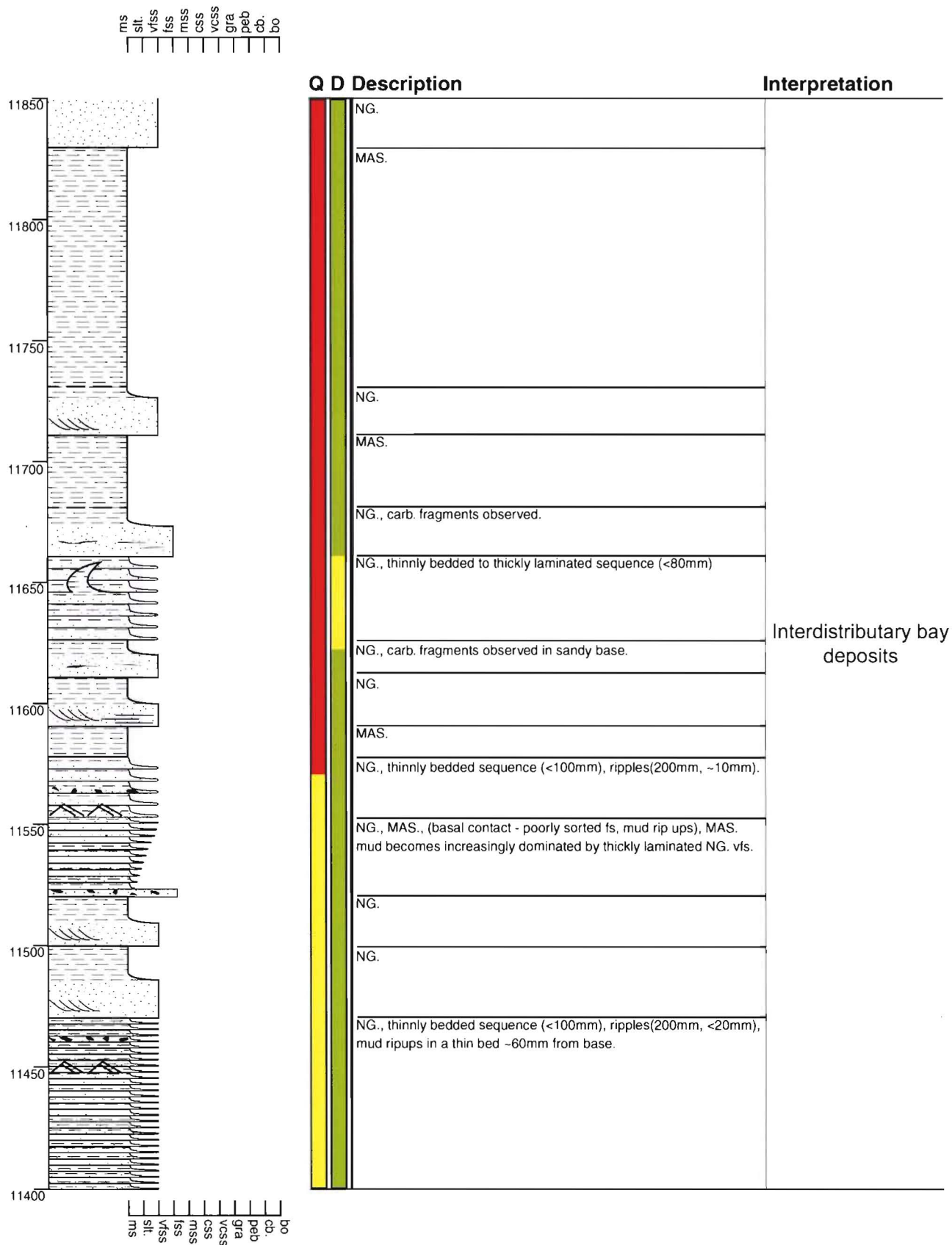
Section - Pahau River AD02

Grid Reference M32 857 431



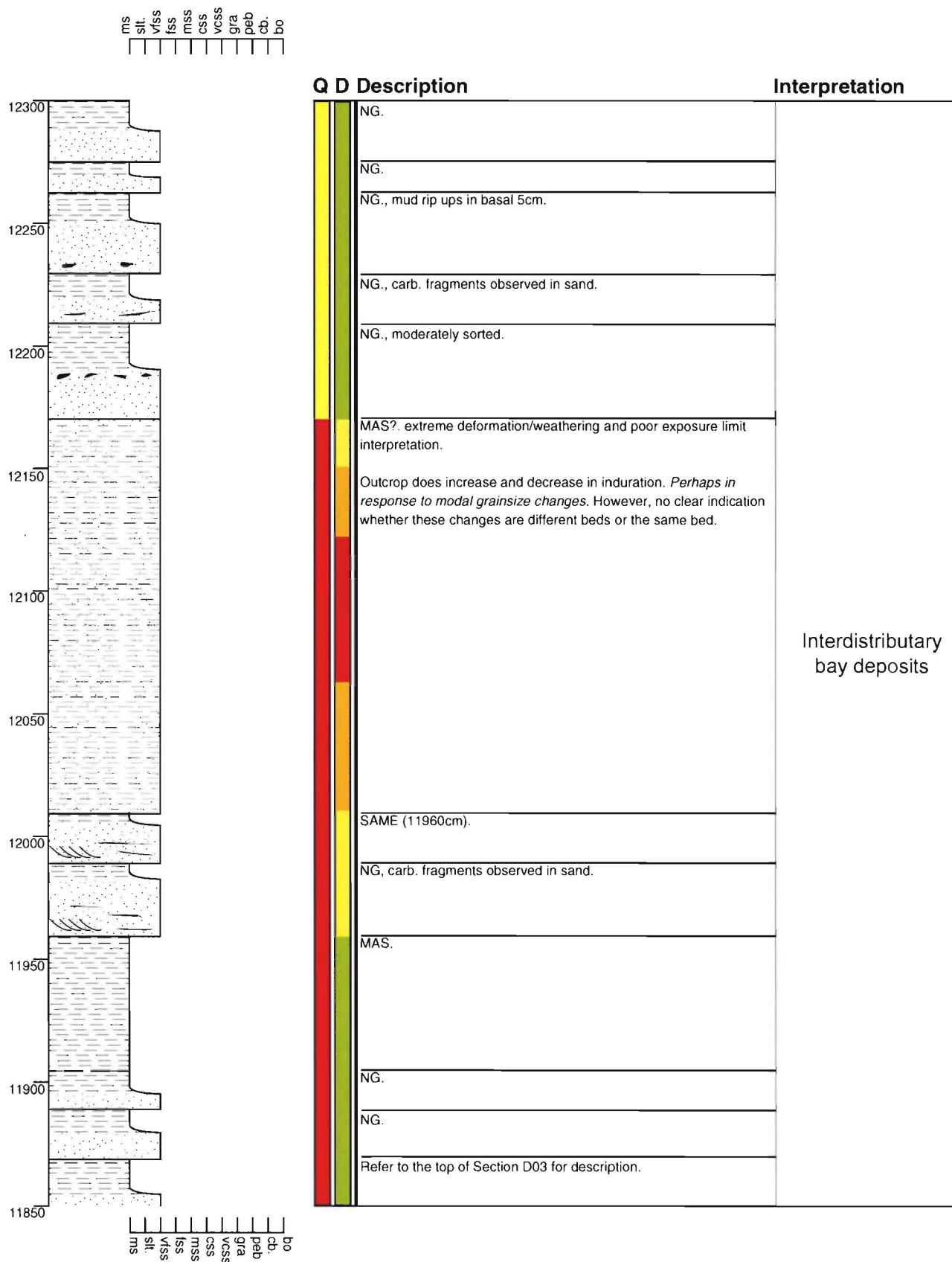
Section - Pahau River AD03

Grid Reference M32 857 431



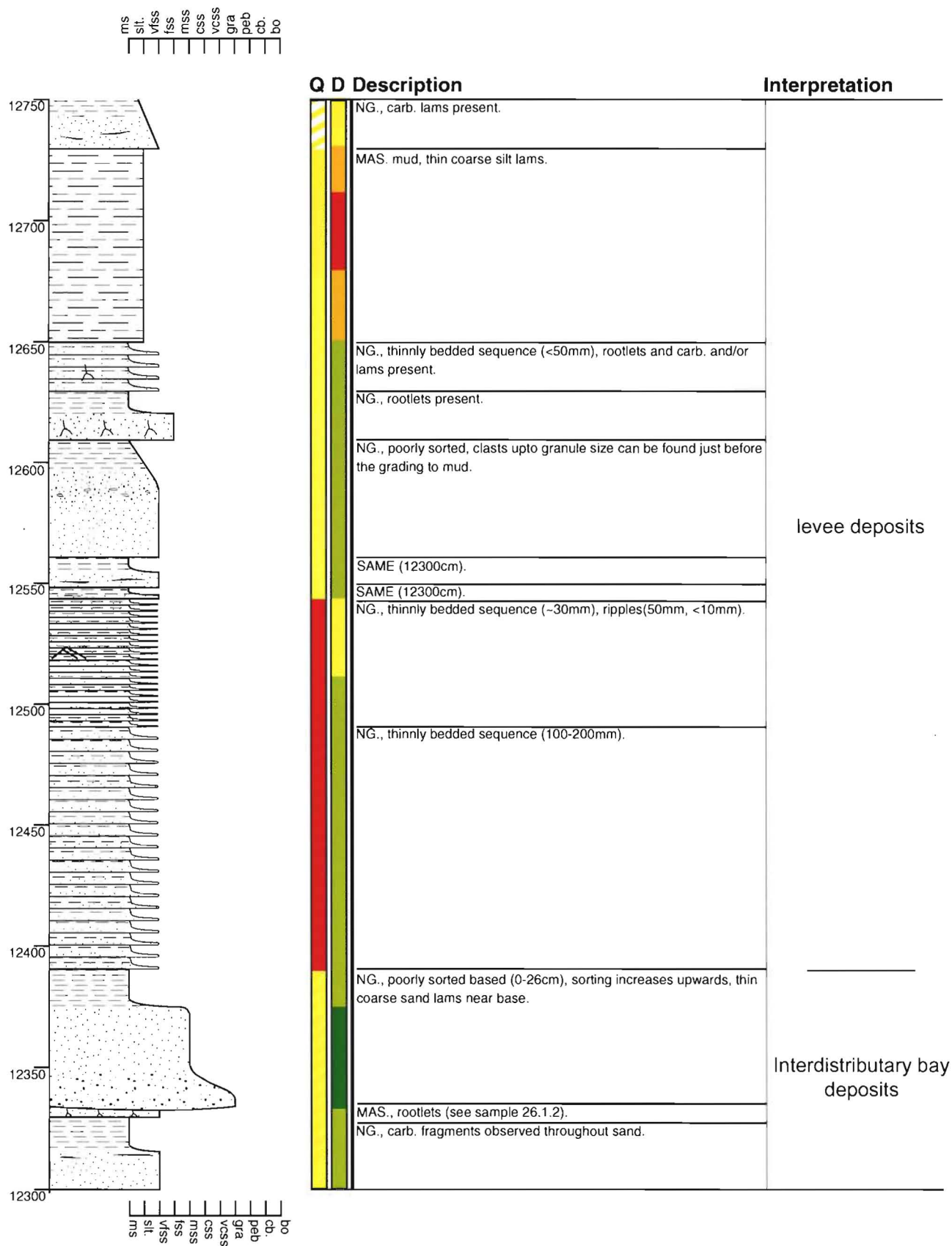
Section - Pahau River AD04

Grid Reference M32 857 431

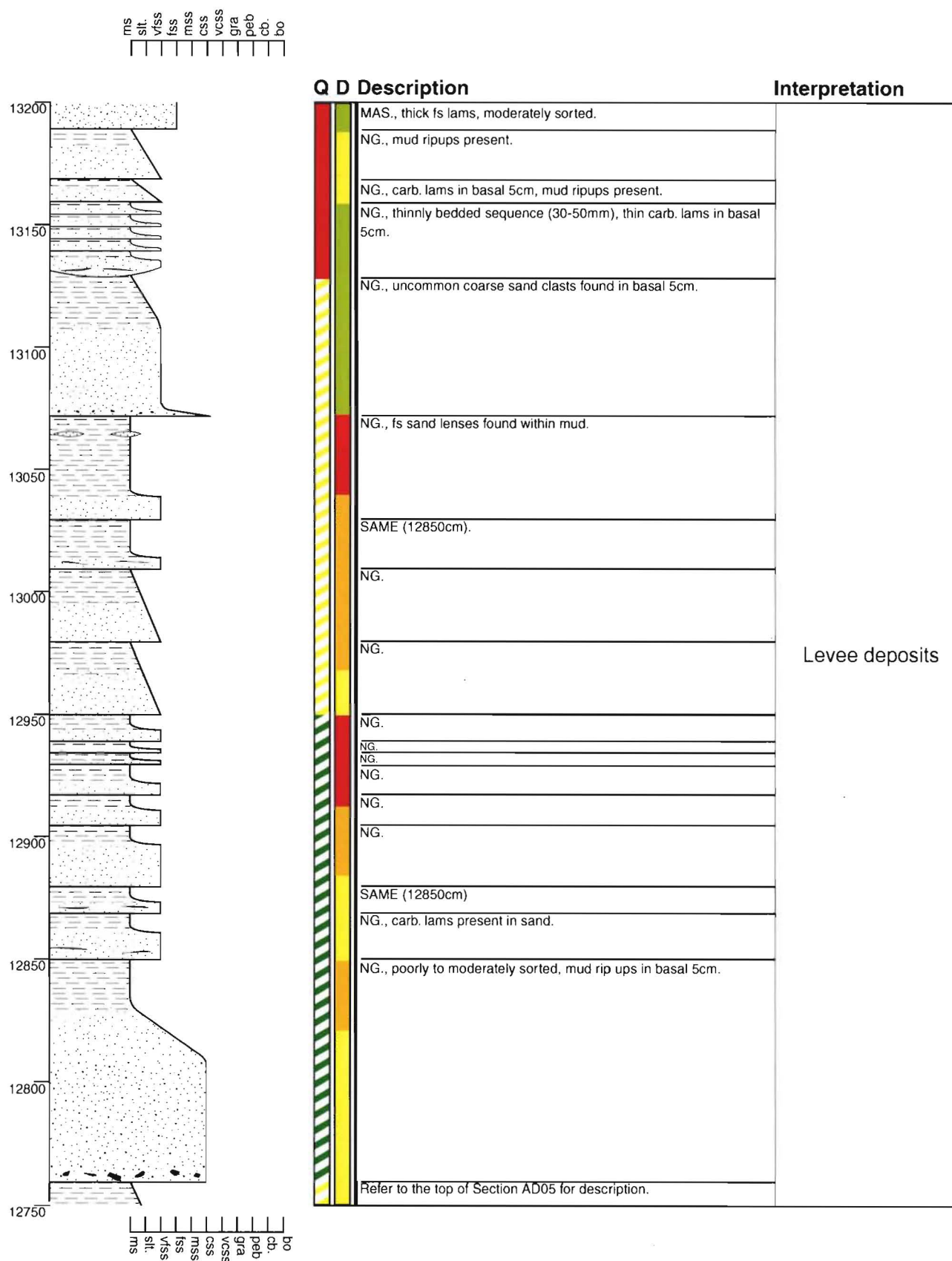


Section - Pahau River AD05

Grid Reference M32 857 431

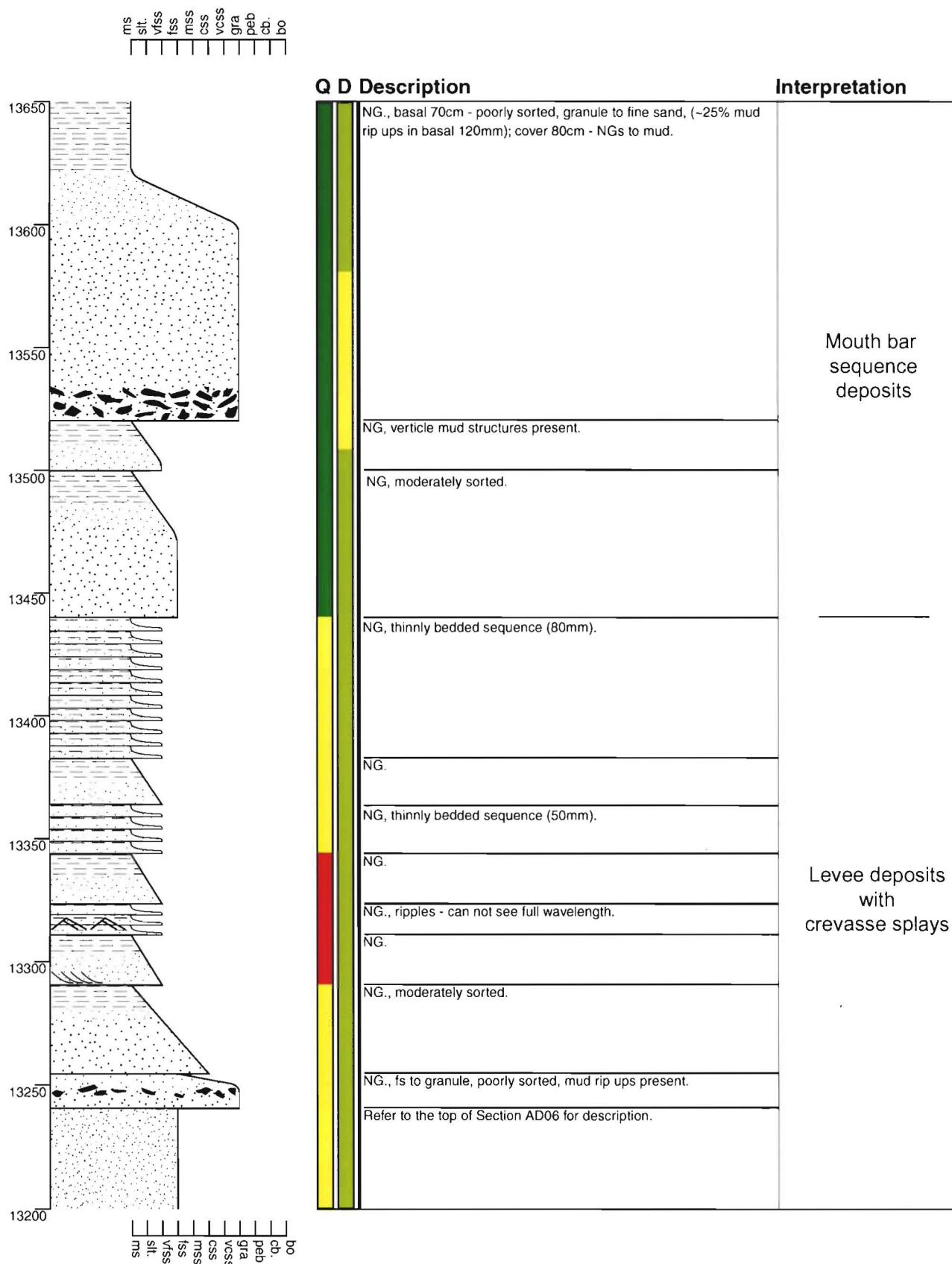


Grid Reference M32 857 431



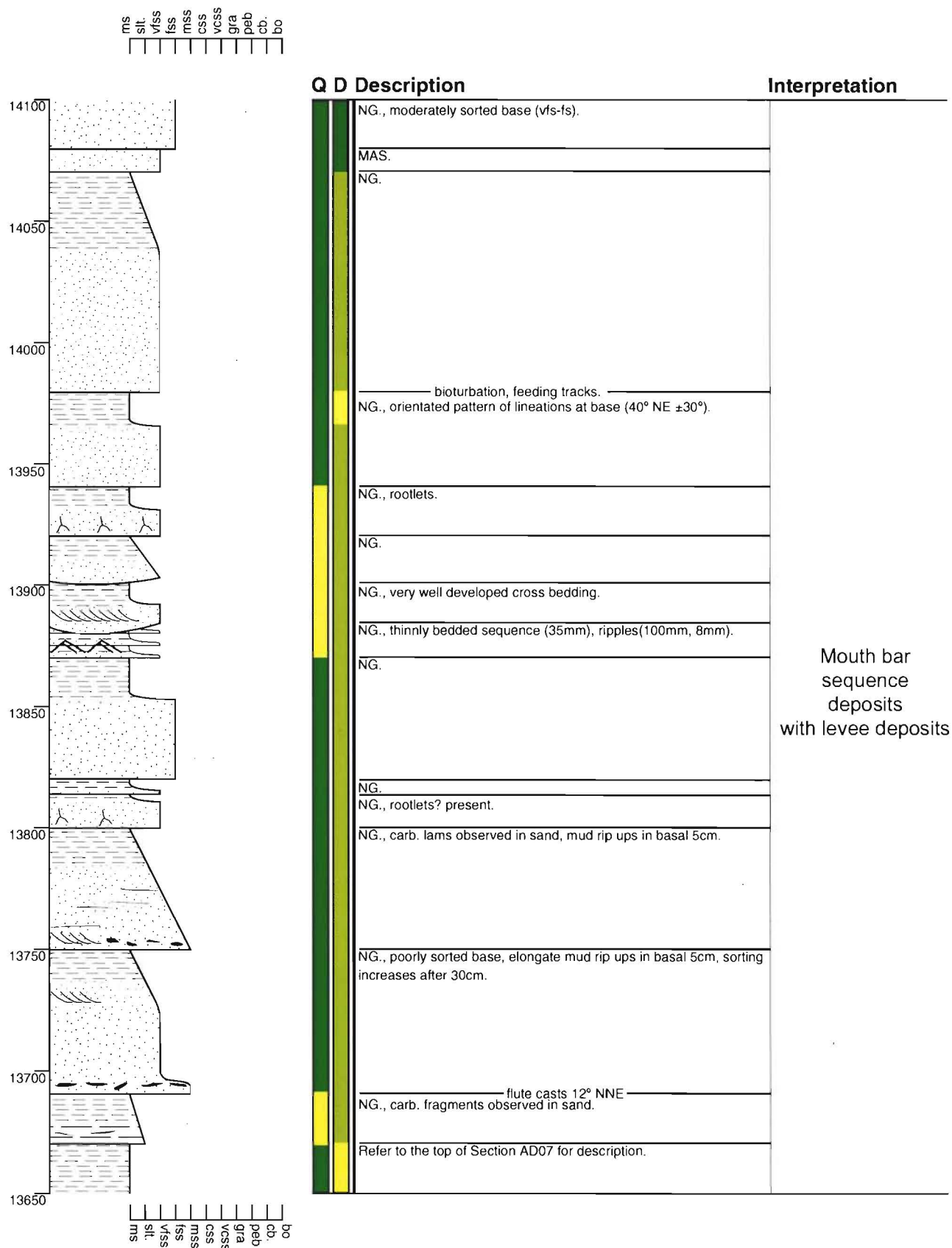
Section - Pahau River AD07

Grid Reference M32 857 431



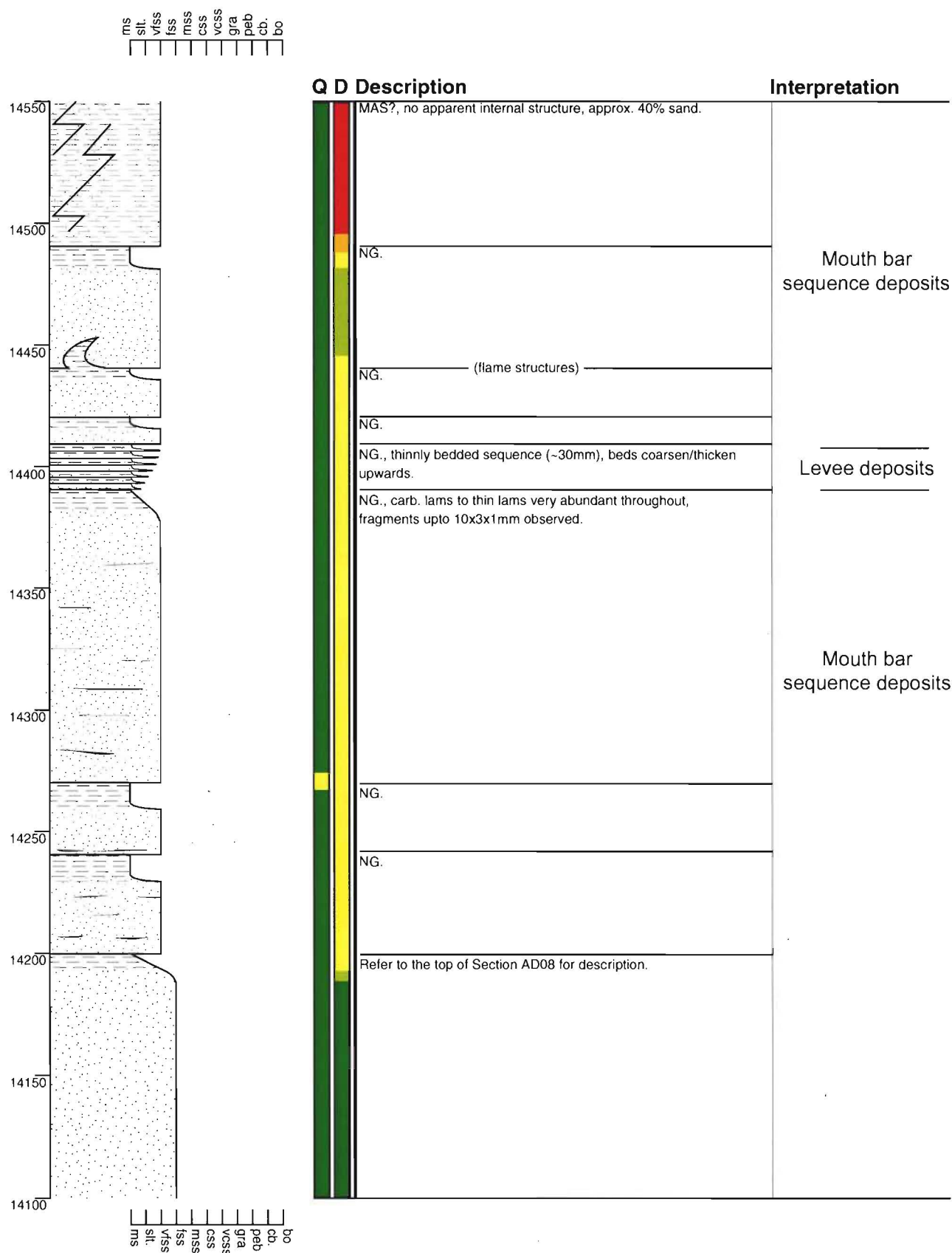
Section - Pahau River AD08

Grid Reference M32 857 431



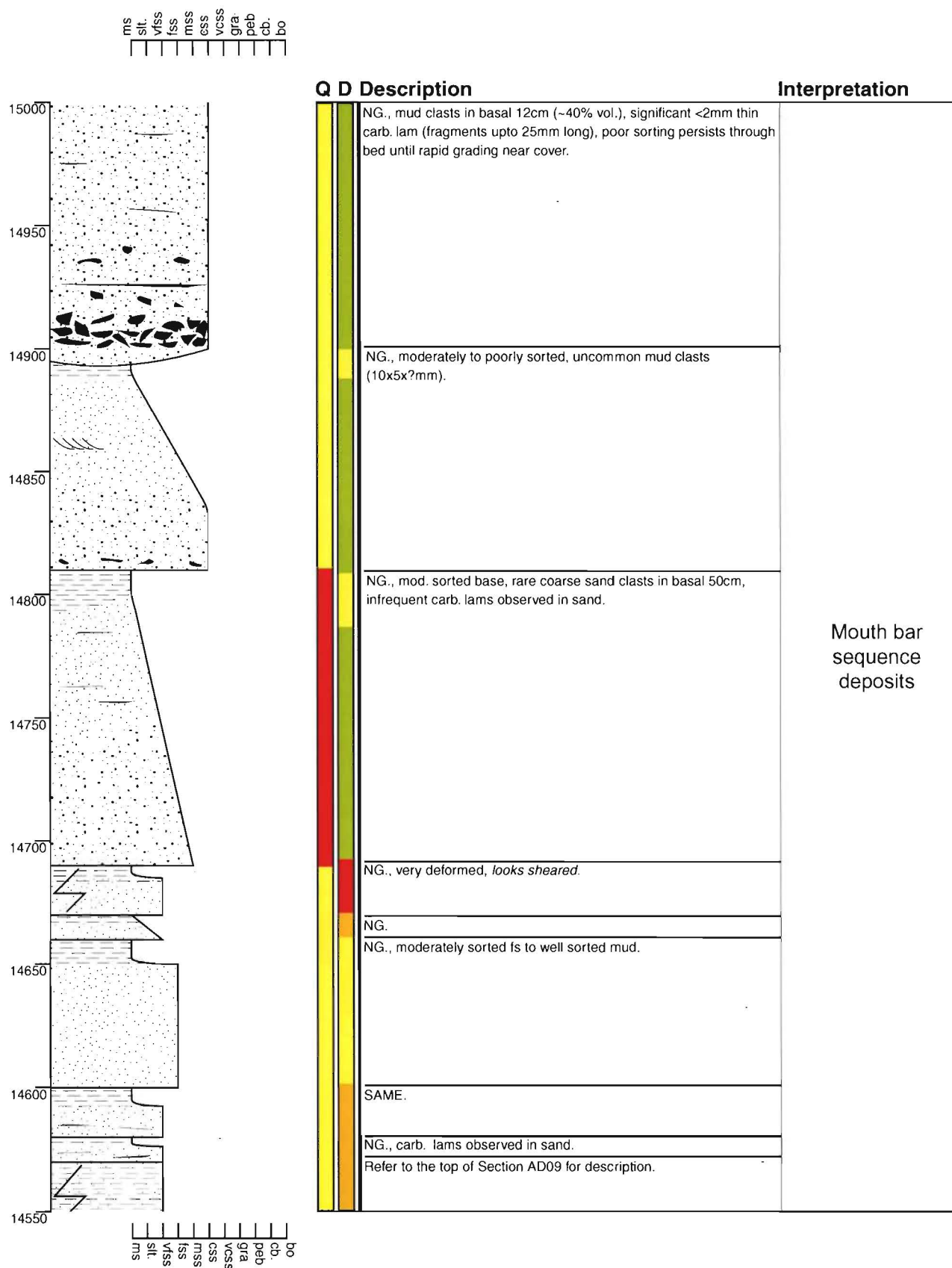
Section - Pahau River AD09

Grid Reference M32 857 431



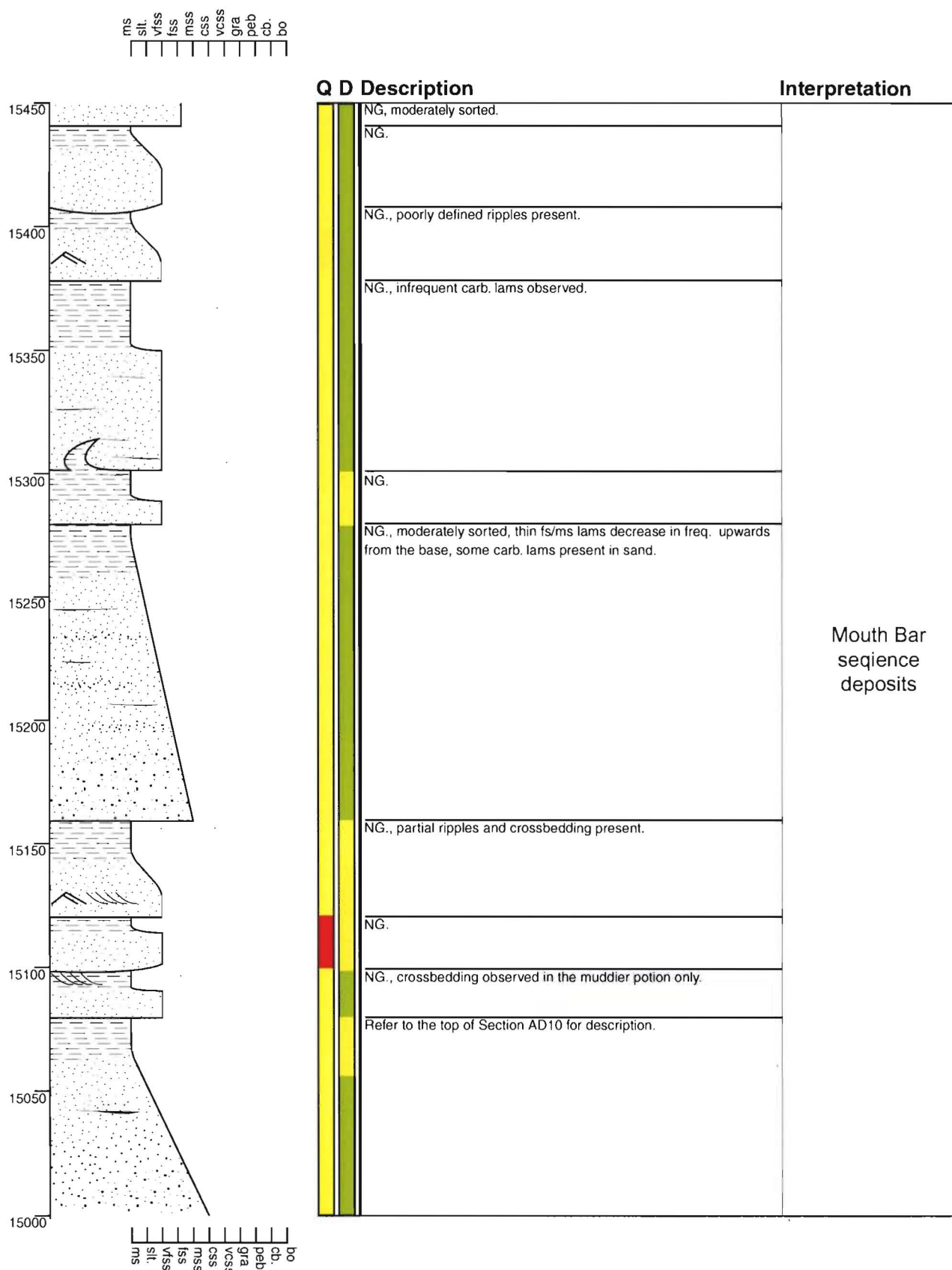
Section - Pahau River AD10

Grid Reference M32 857 431



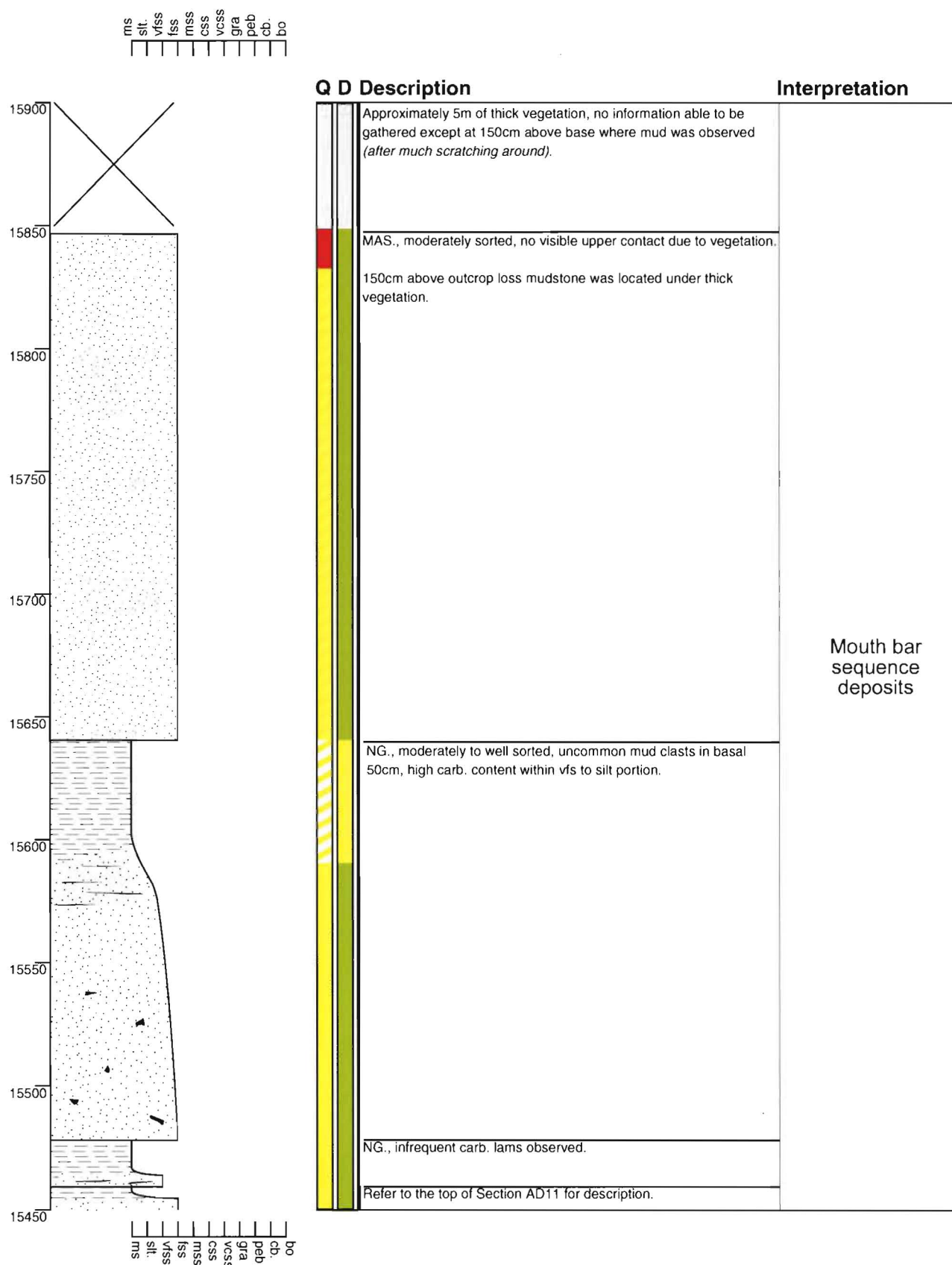
Section - Pahau River AD11

Grid Reference M32 857 431



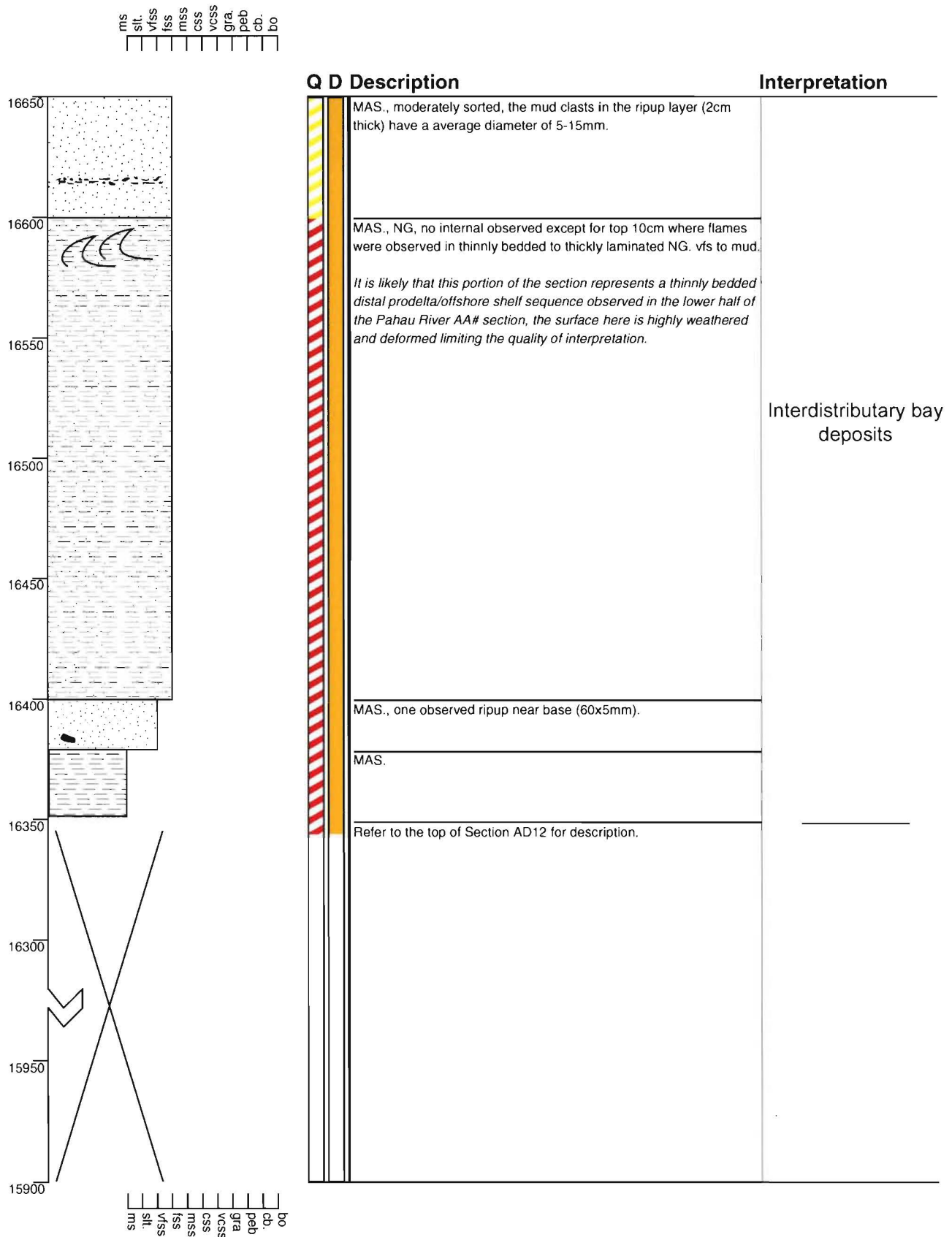
Section - Pahau River AD12

Grid Reference M32 857 431



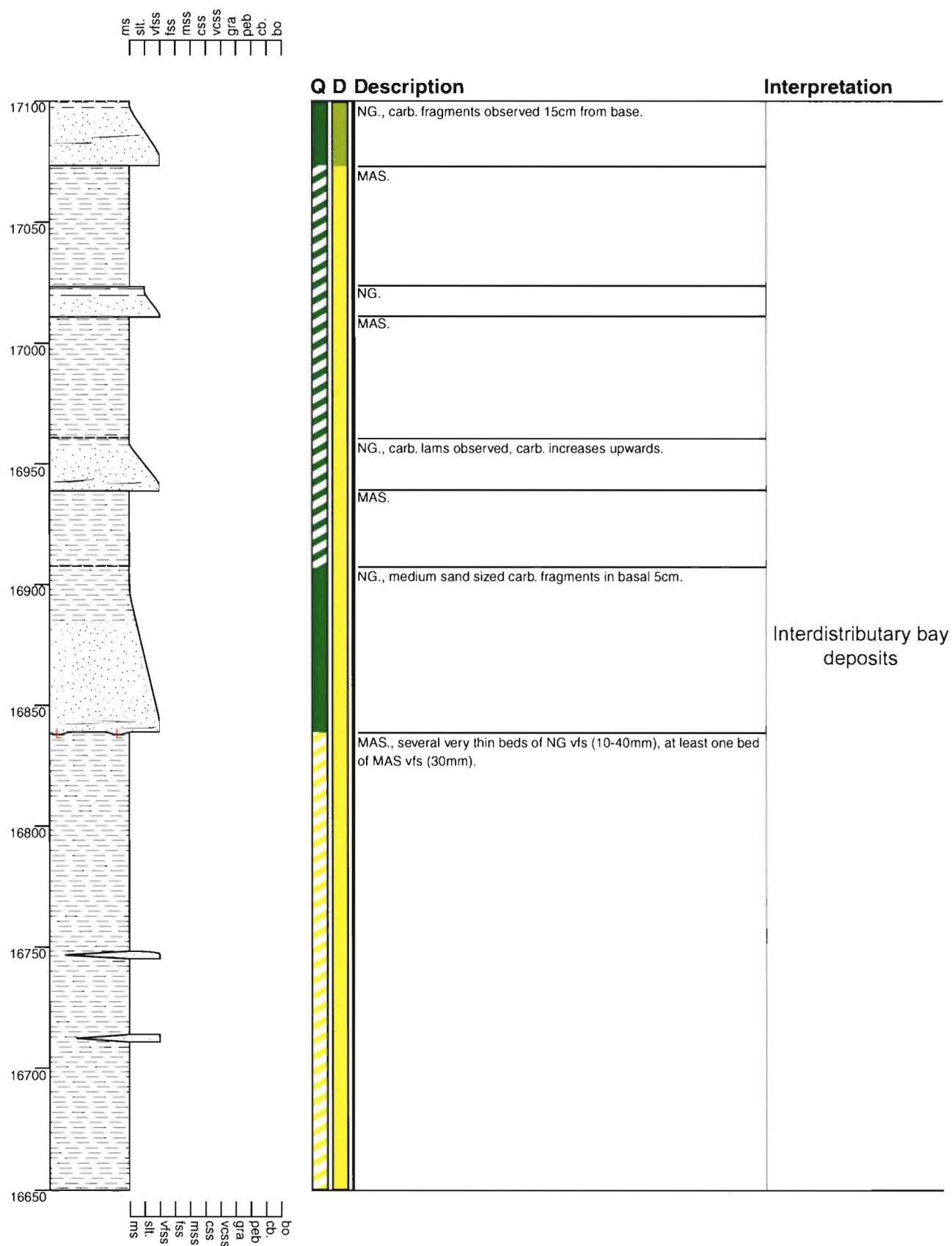
Section - Pahau River AD13

Grid Reference M32 857 431



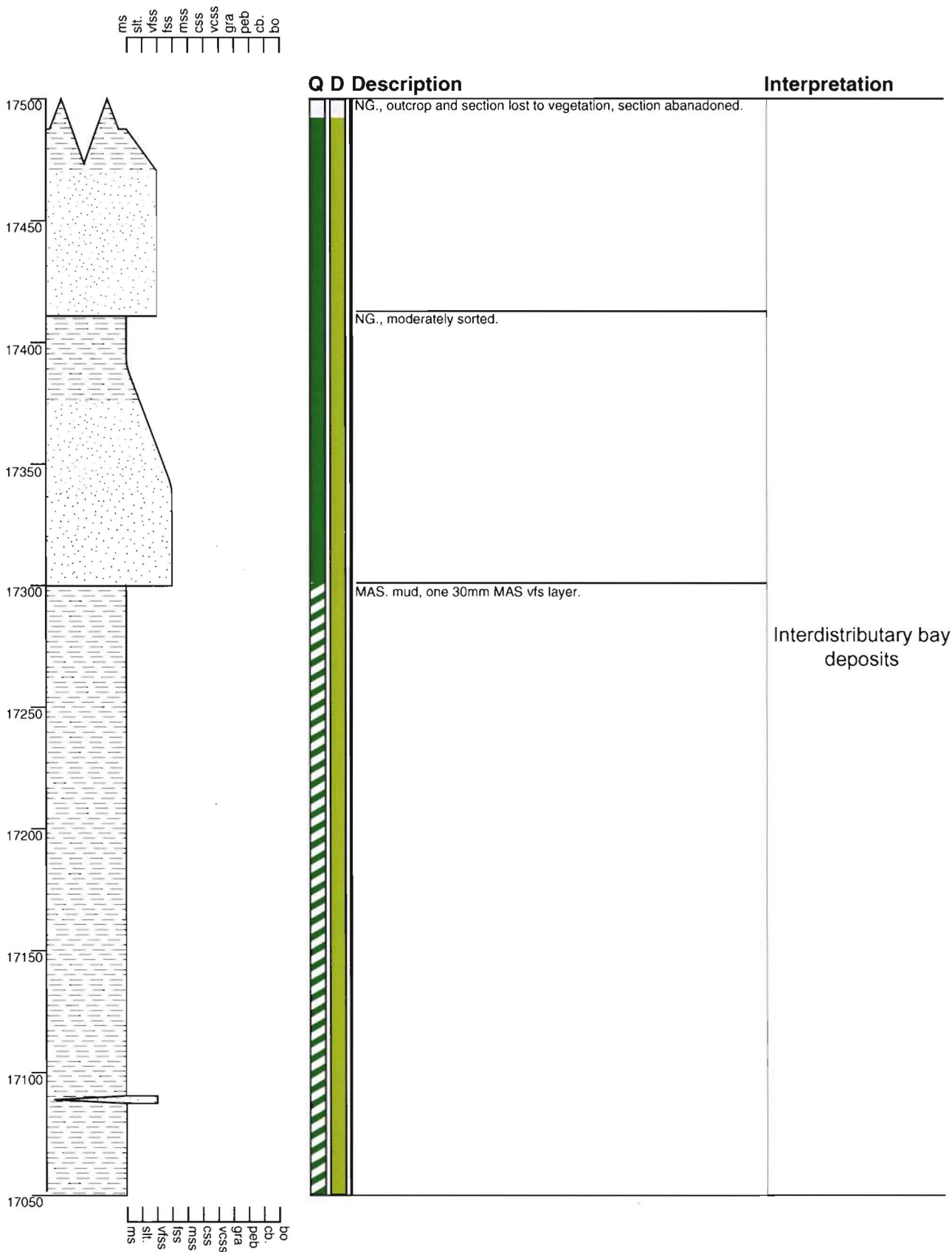
Section - Pahau River AD14

Grid Reference M32 857 431



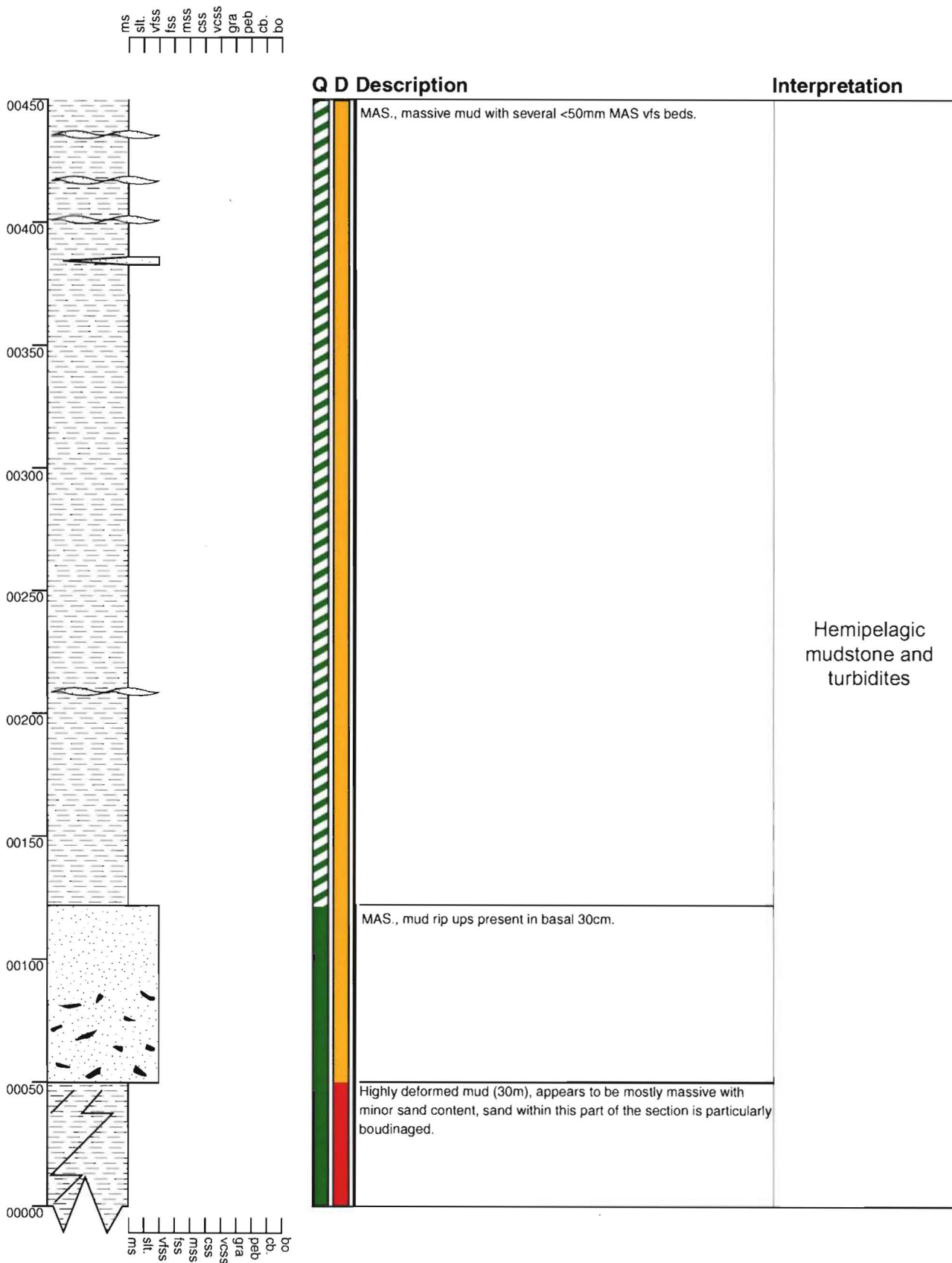
Section - Pahau River AD15

Grid Reference M32 857 431



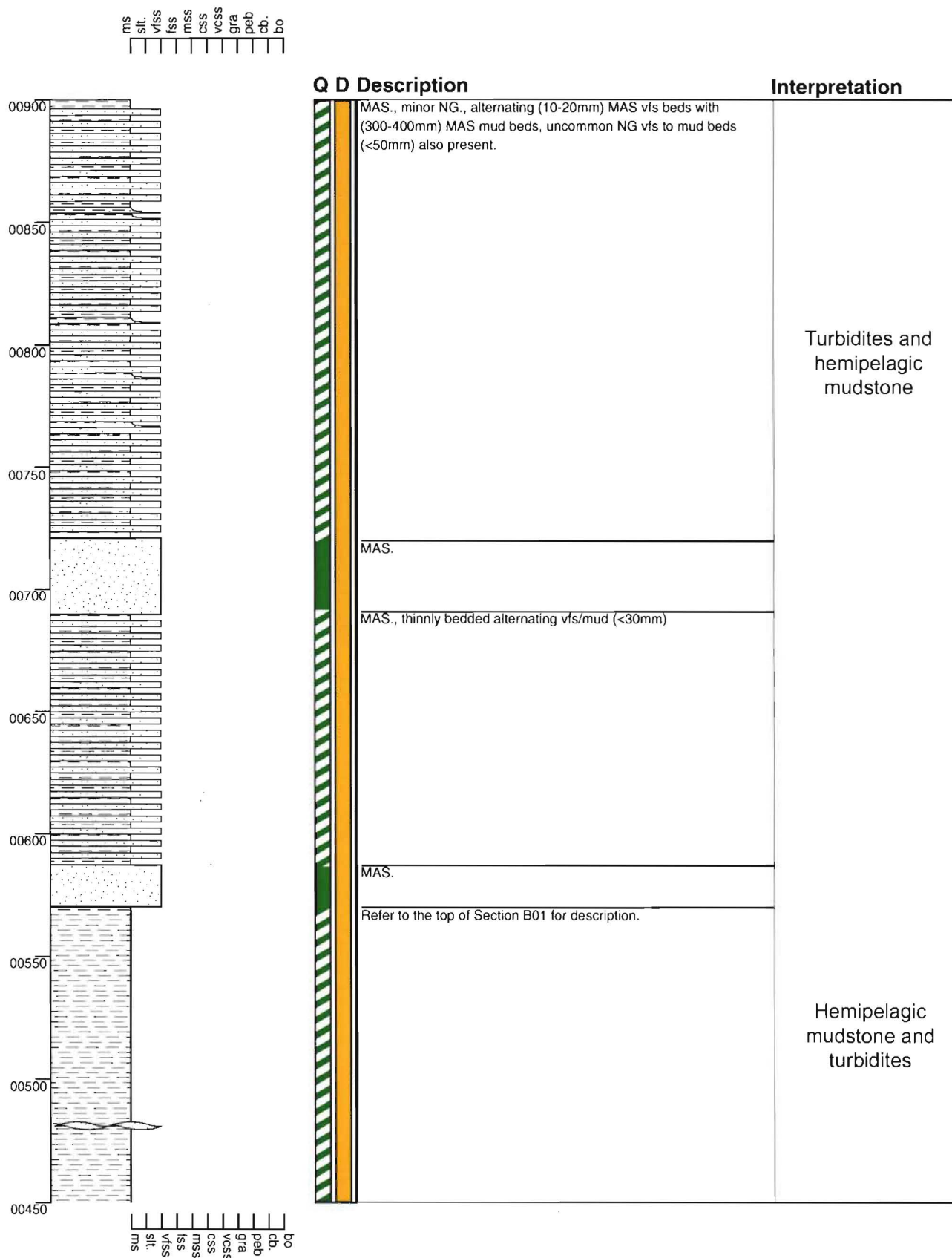
Section - Pahau River B01

Grid Reference M32 861 425



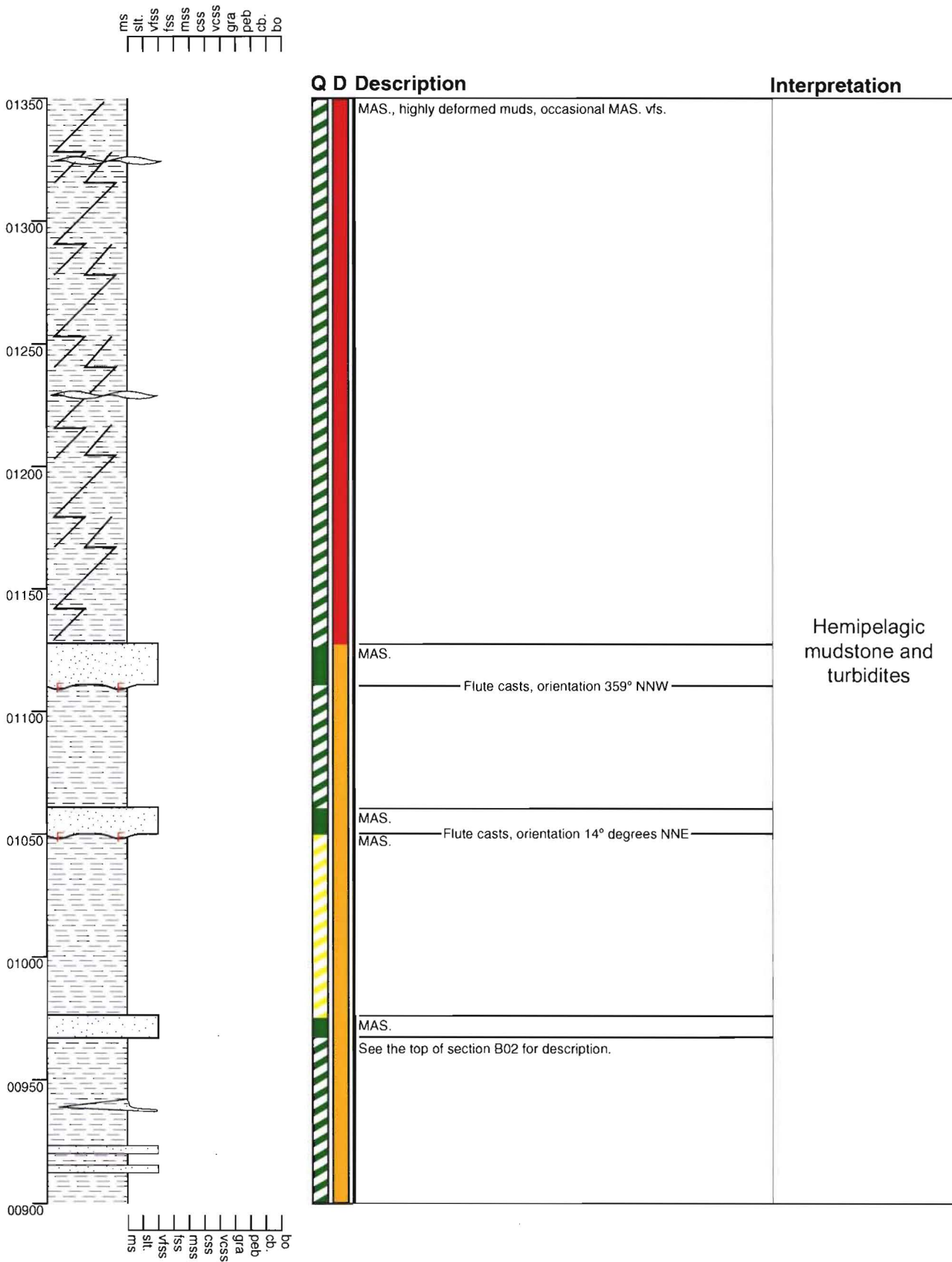
Section - Pahau River B02

Grid Reference M32 861 425



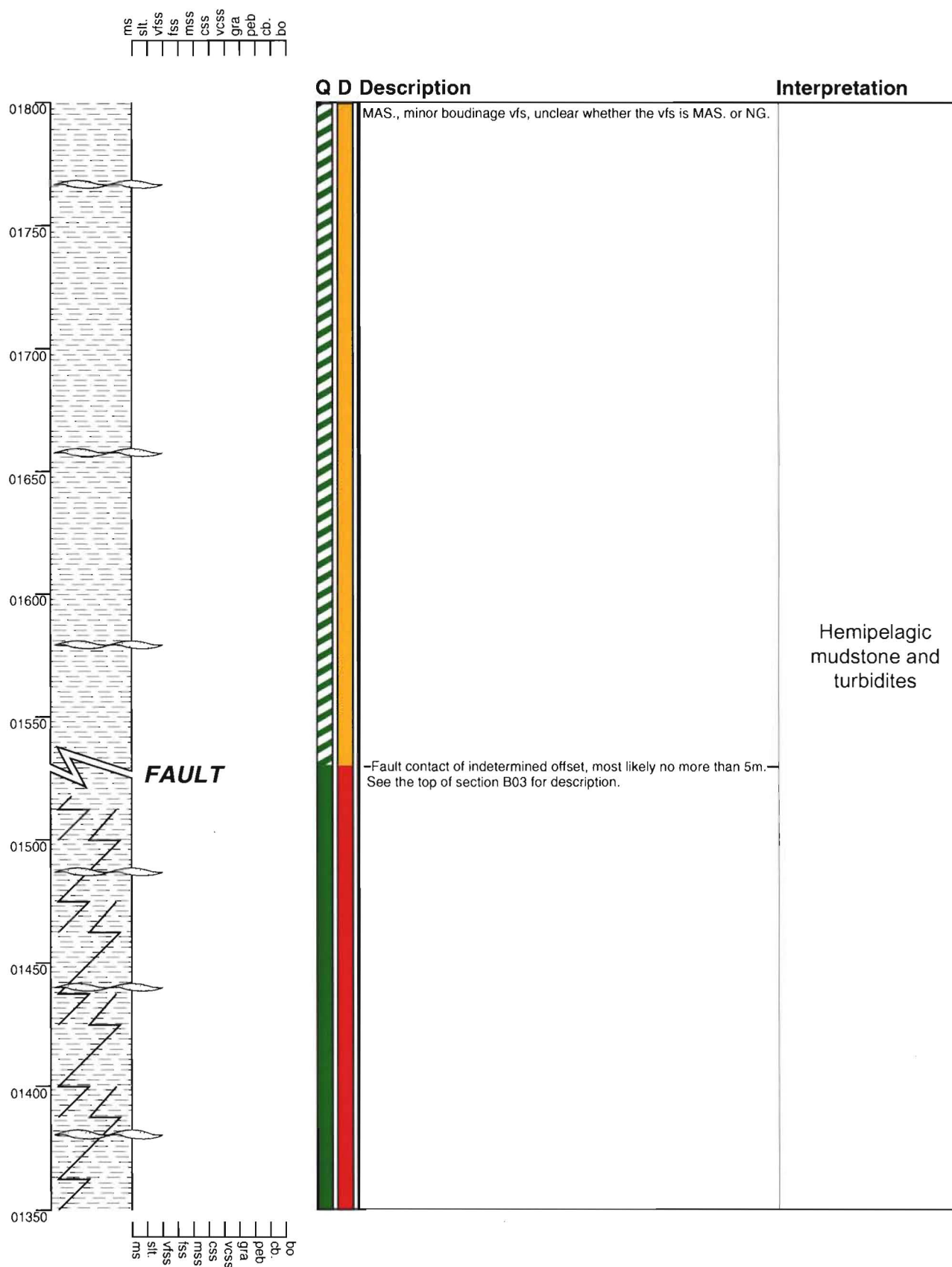
Section - Pahau River B03

Grid Reference M32 861 425



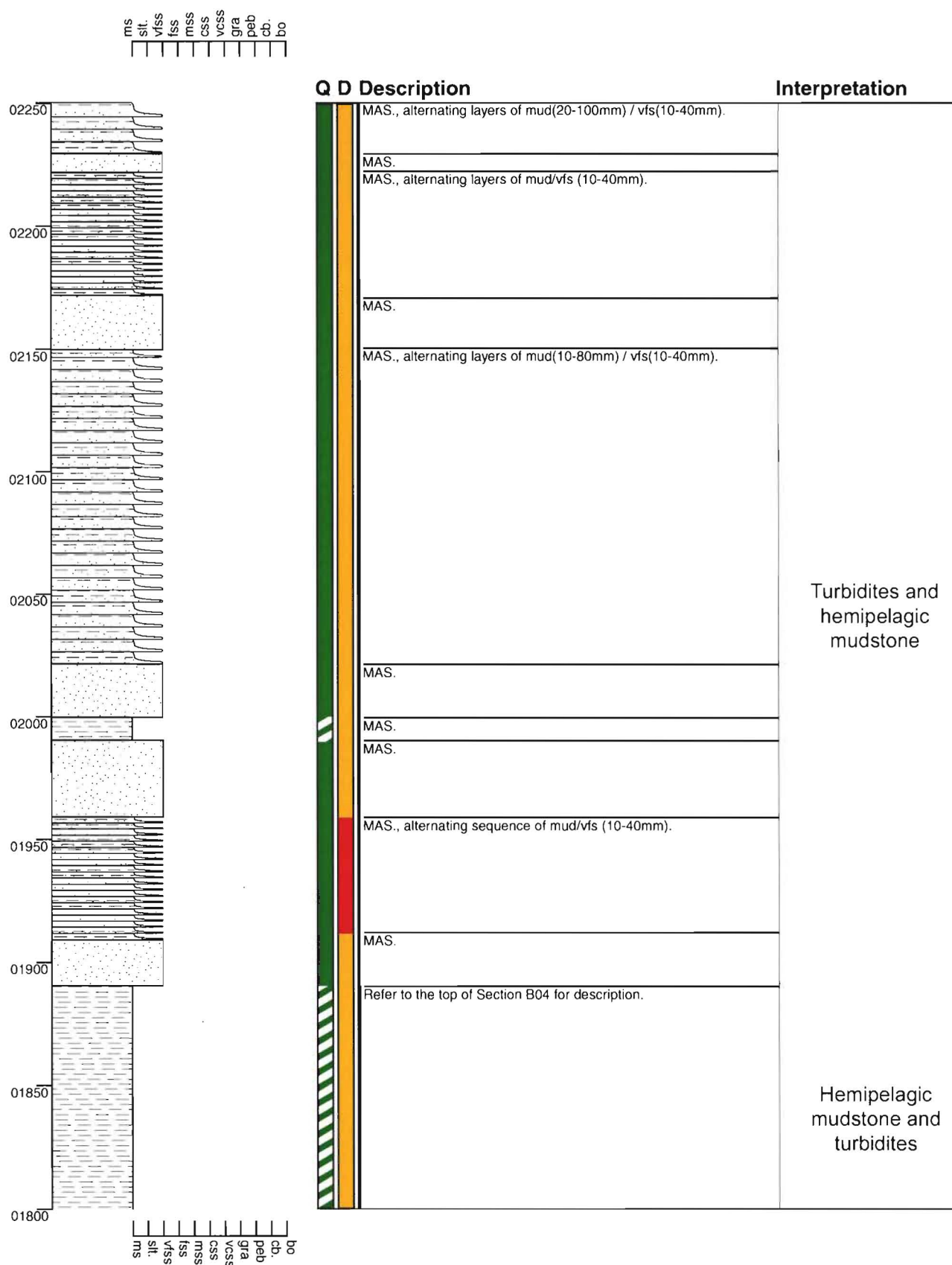
Section - Pahau River B04

Grid Reference M32 861 425



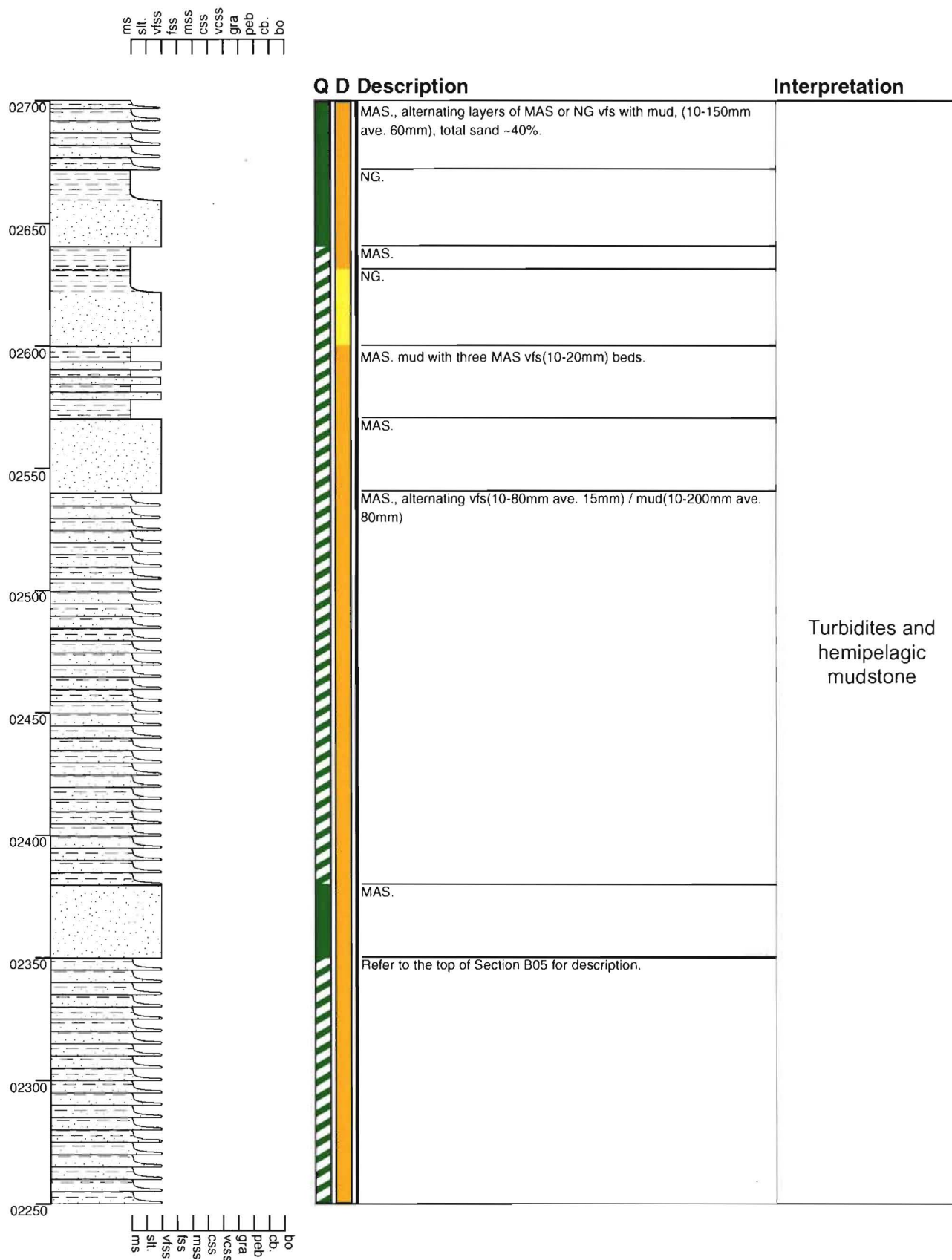
Section - Pahau River B05

Grid Reference M32 861 425



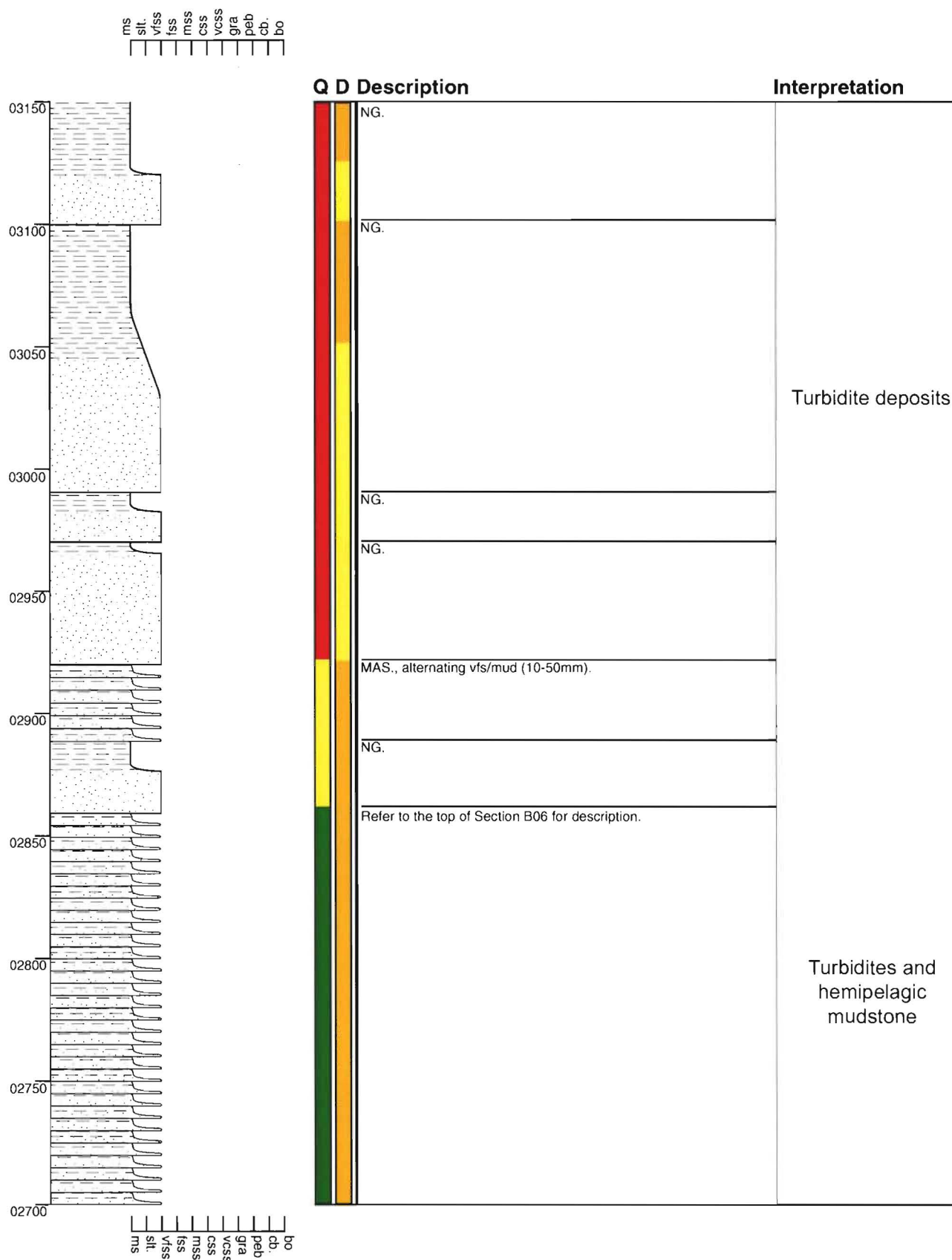
Section - Pahau River B06

Grid Reference M32 861 425



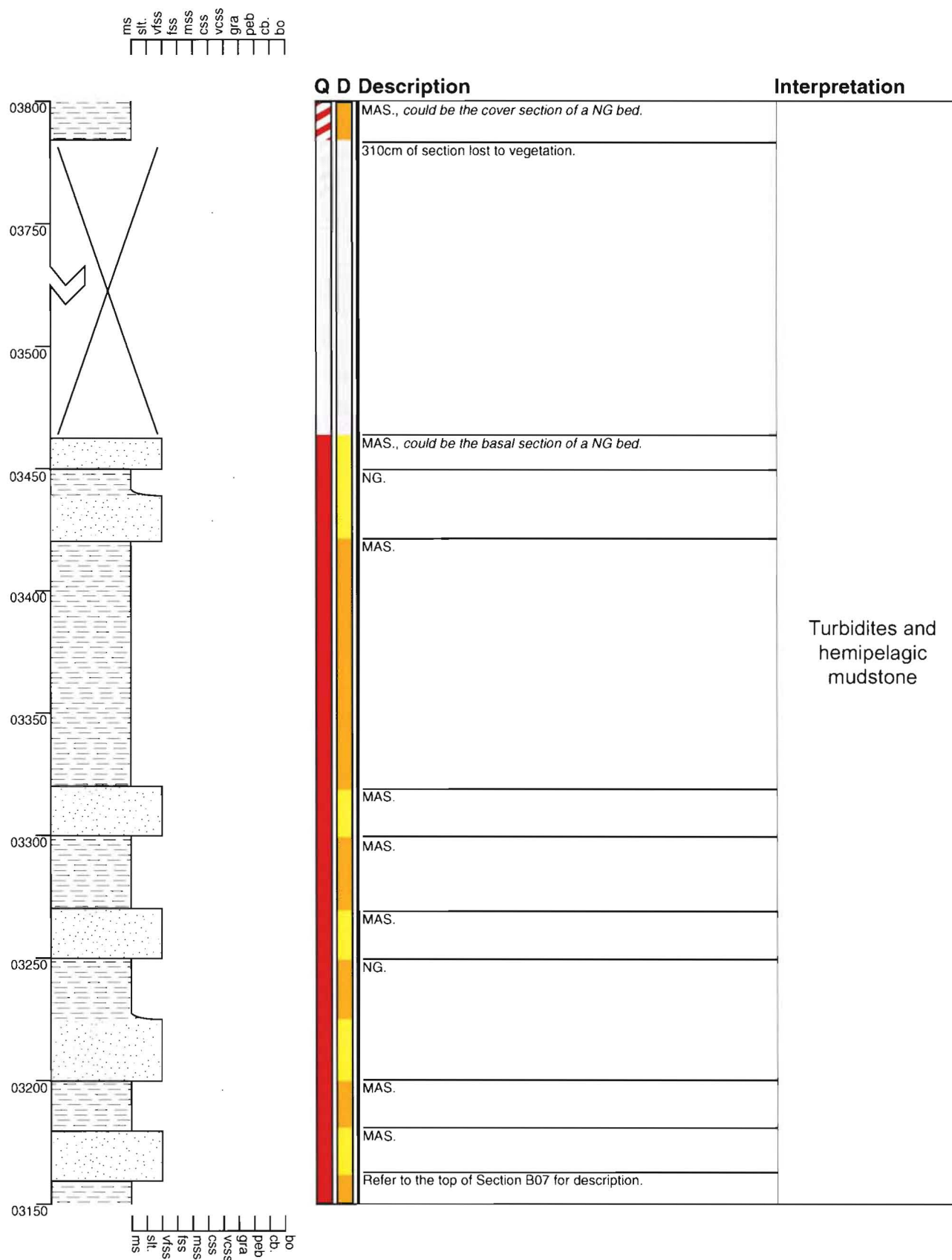
Section - Pahau River B07

Grid Reference M32 861 425



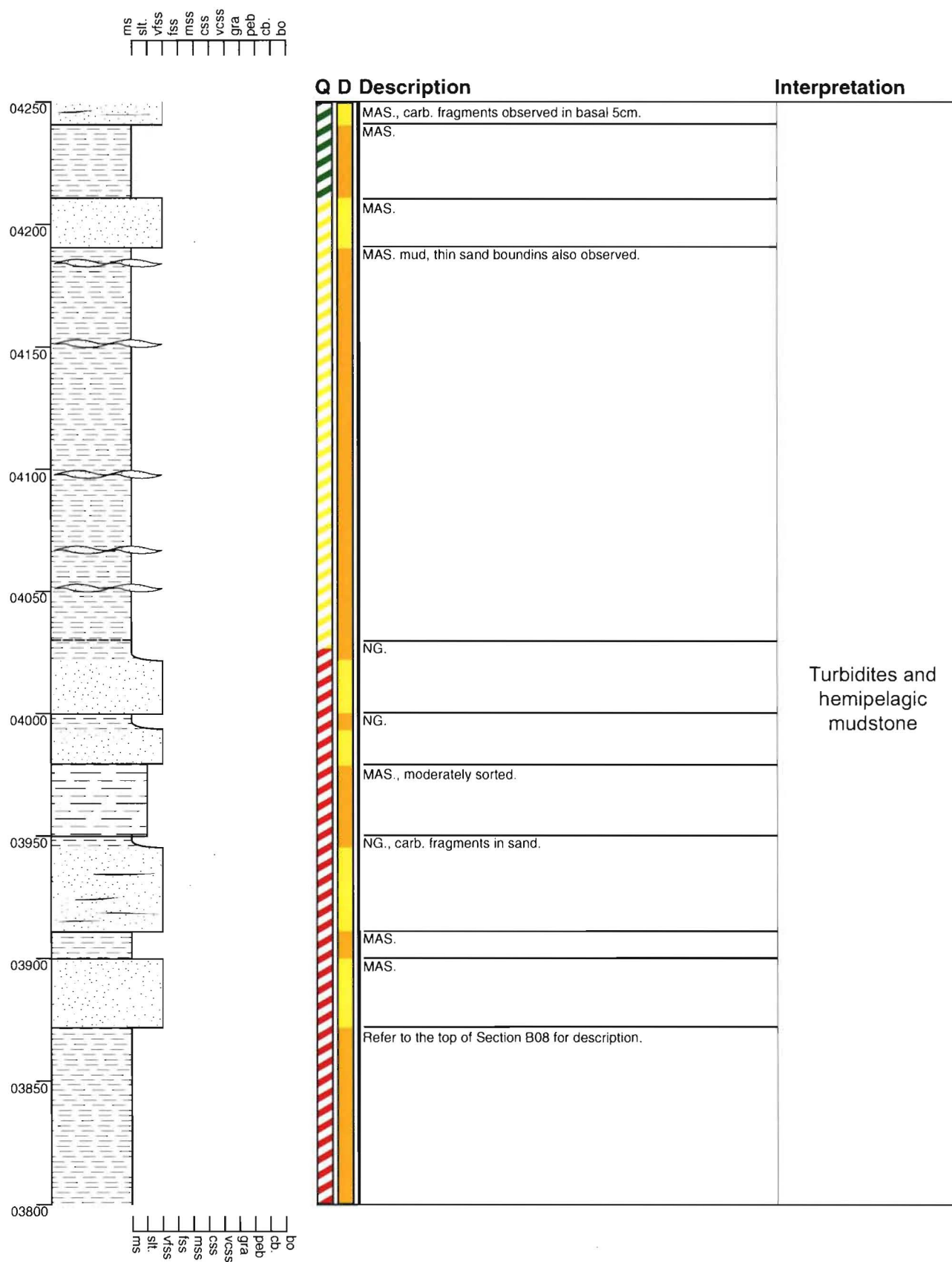
Section - Pahau River B08

Grid Reference M32 861 425



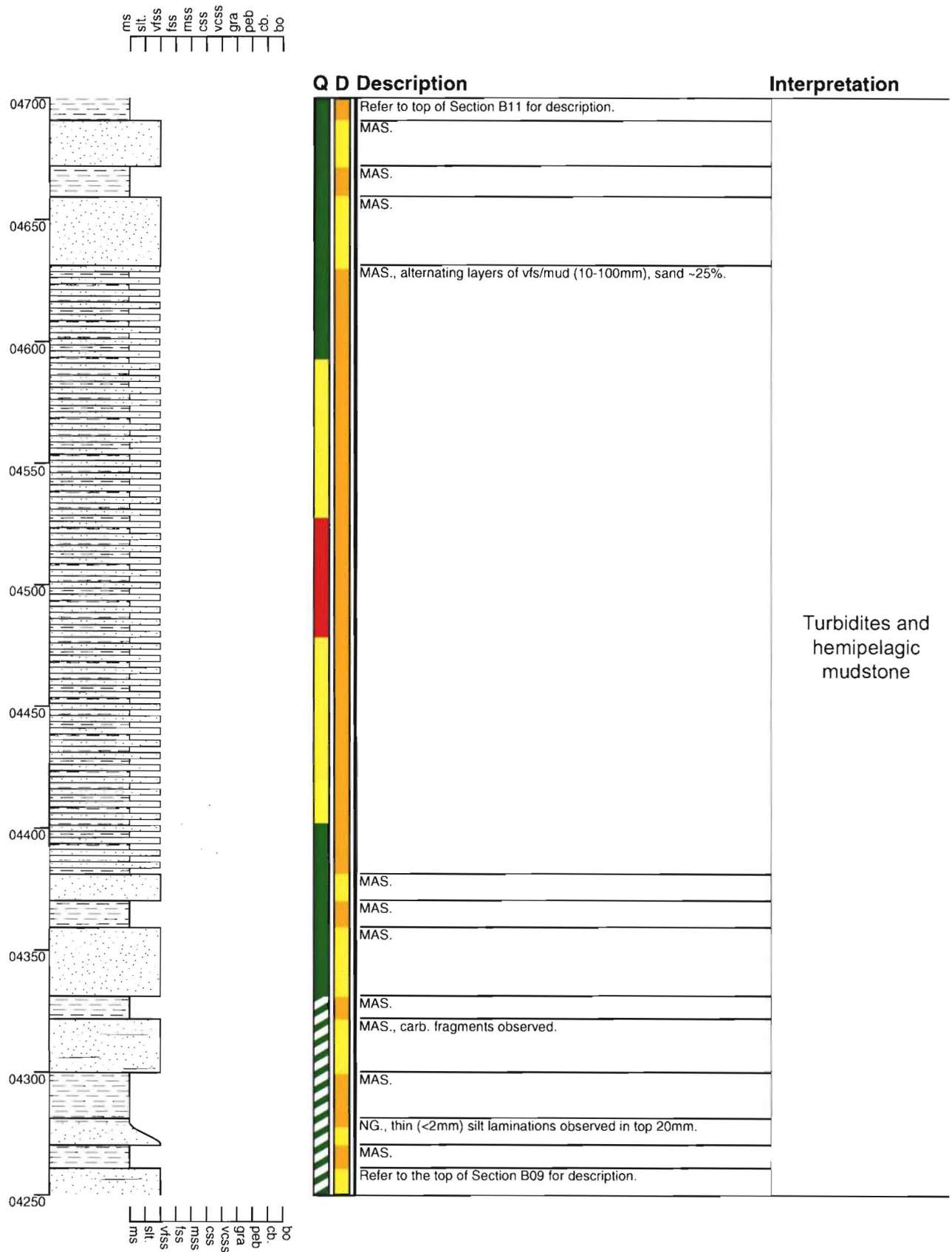
Section - Pahau River B09

Grid Reference M32 861 425



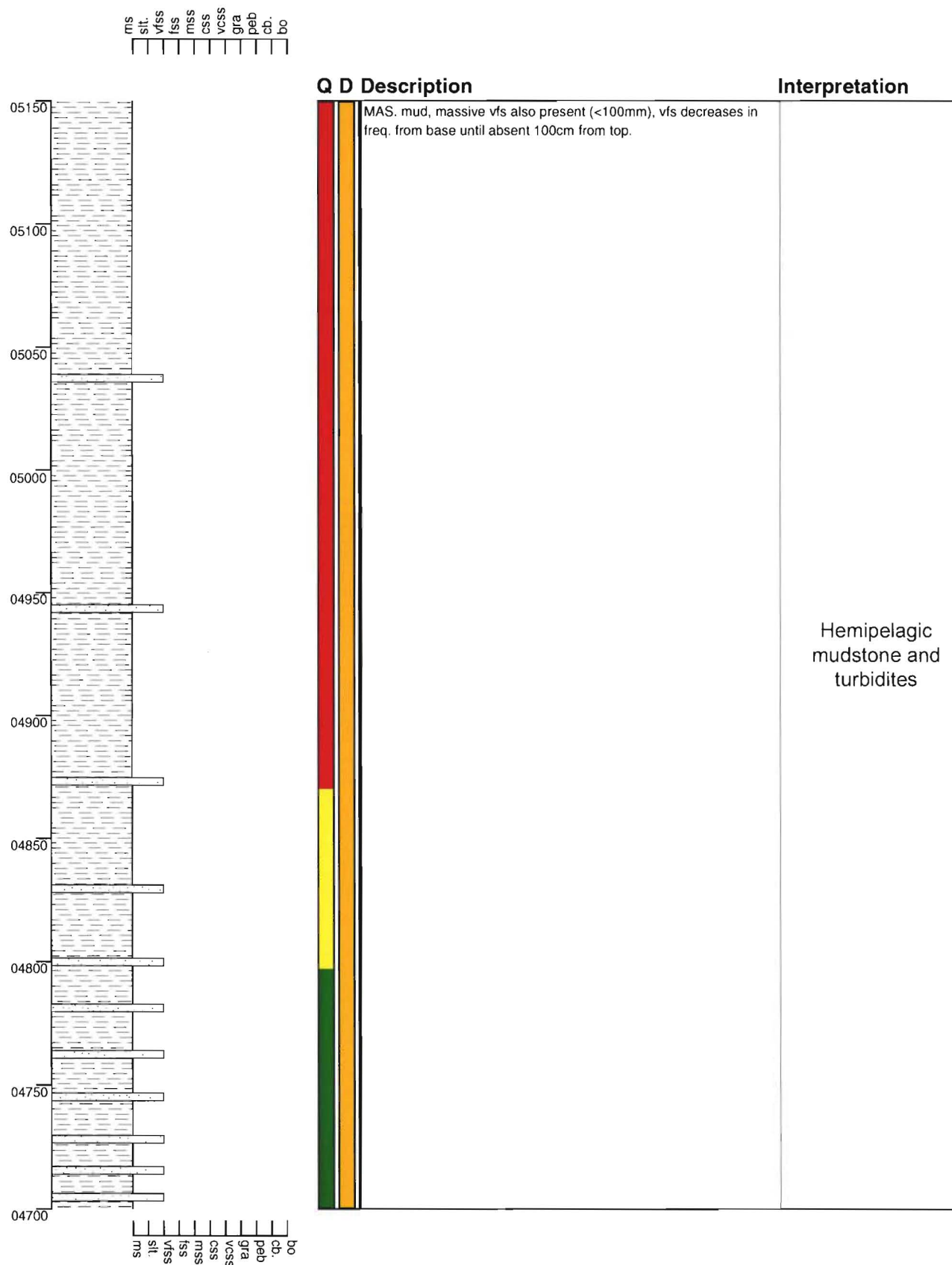
Section - Pahau River B10

Grid Reference M32 861 425



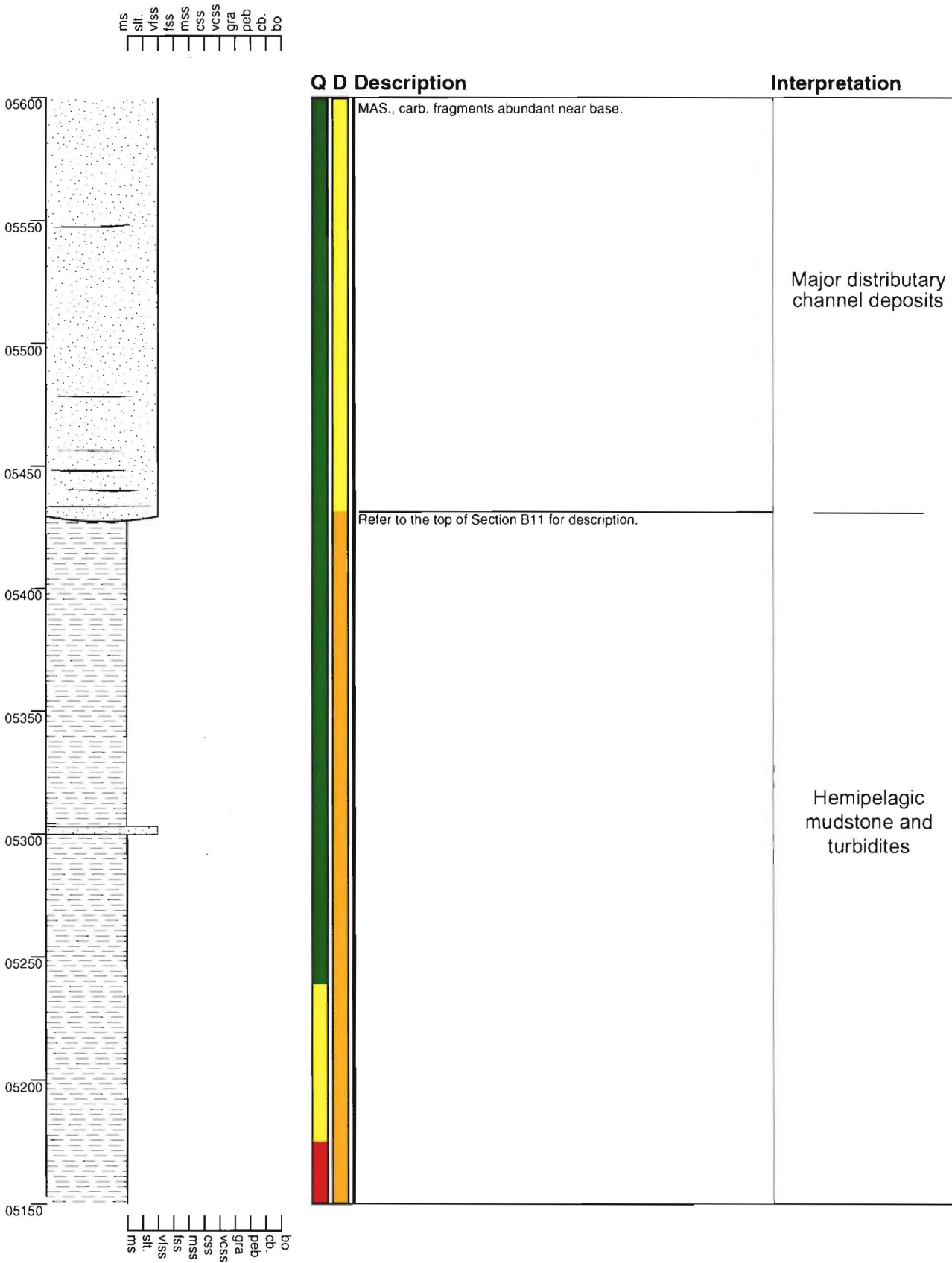
Section - Pahau River B11

Grid Reference M32 861 425



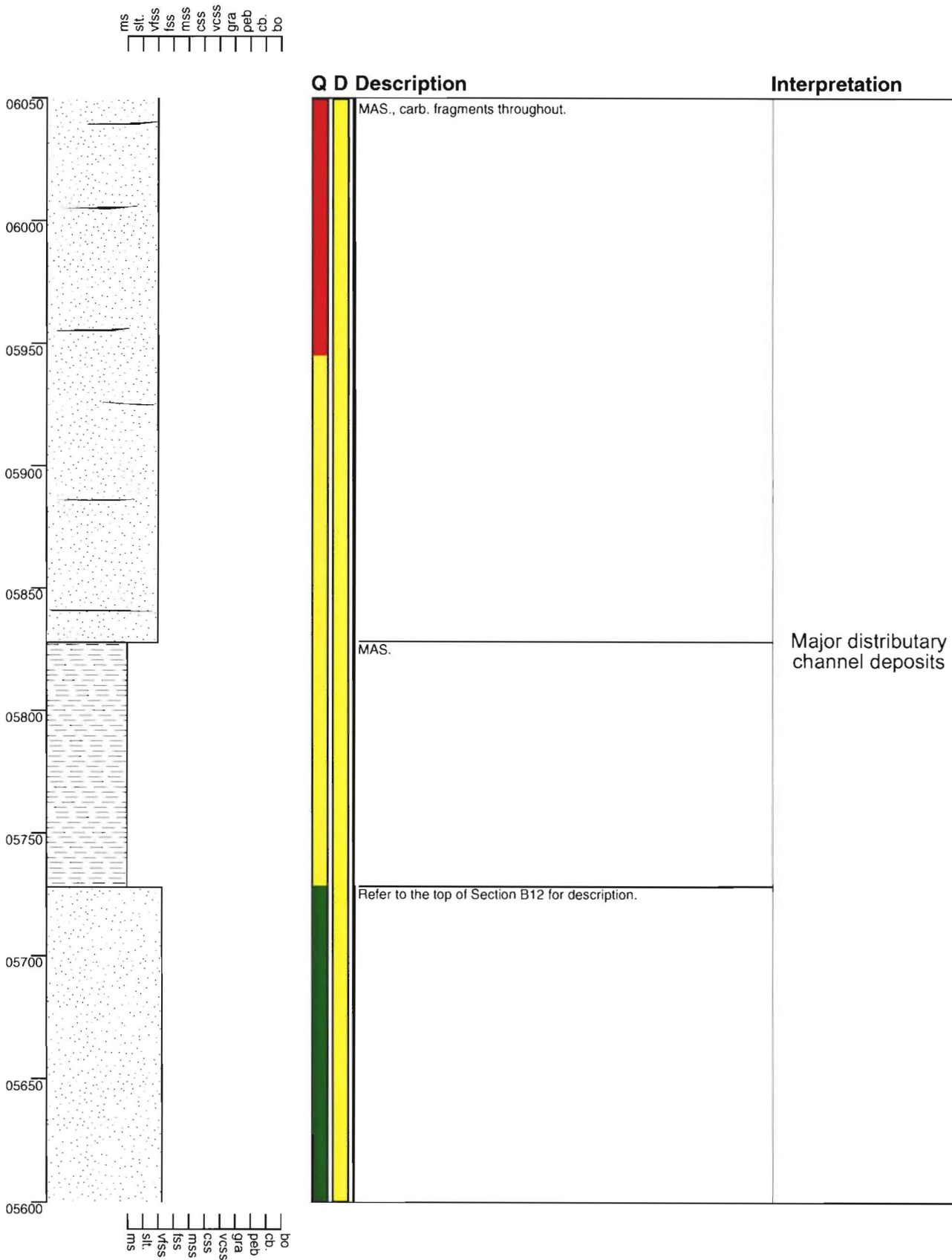
Section - Pahau River B12

Grid Reference M32 861 425



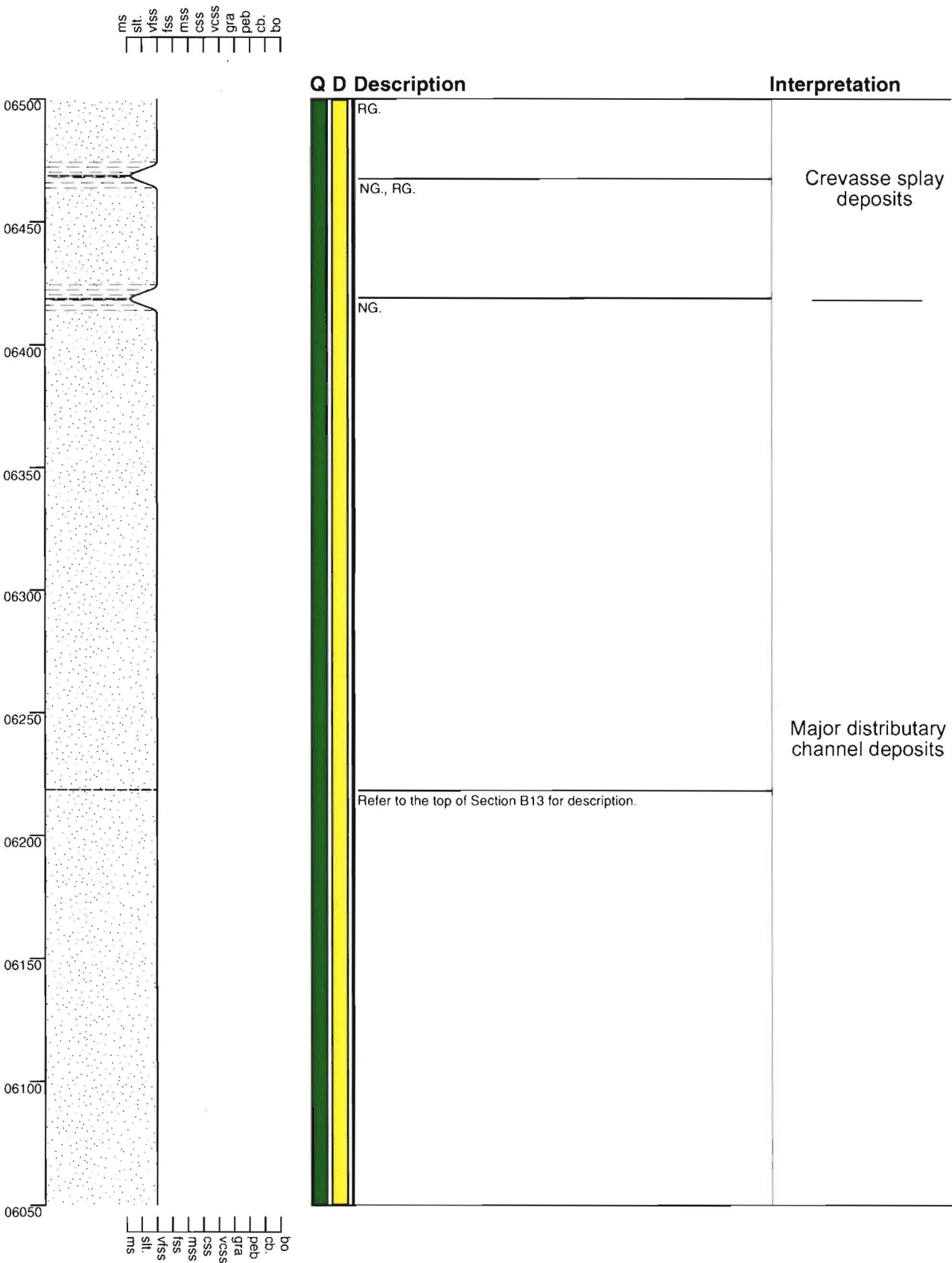
Section - Pahau River B13

Grid Reference M32 861 425

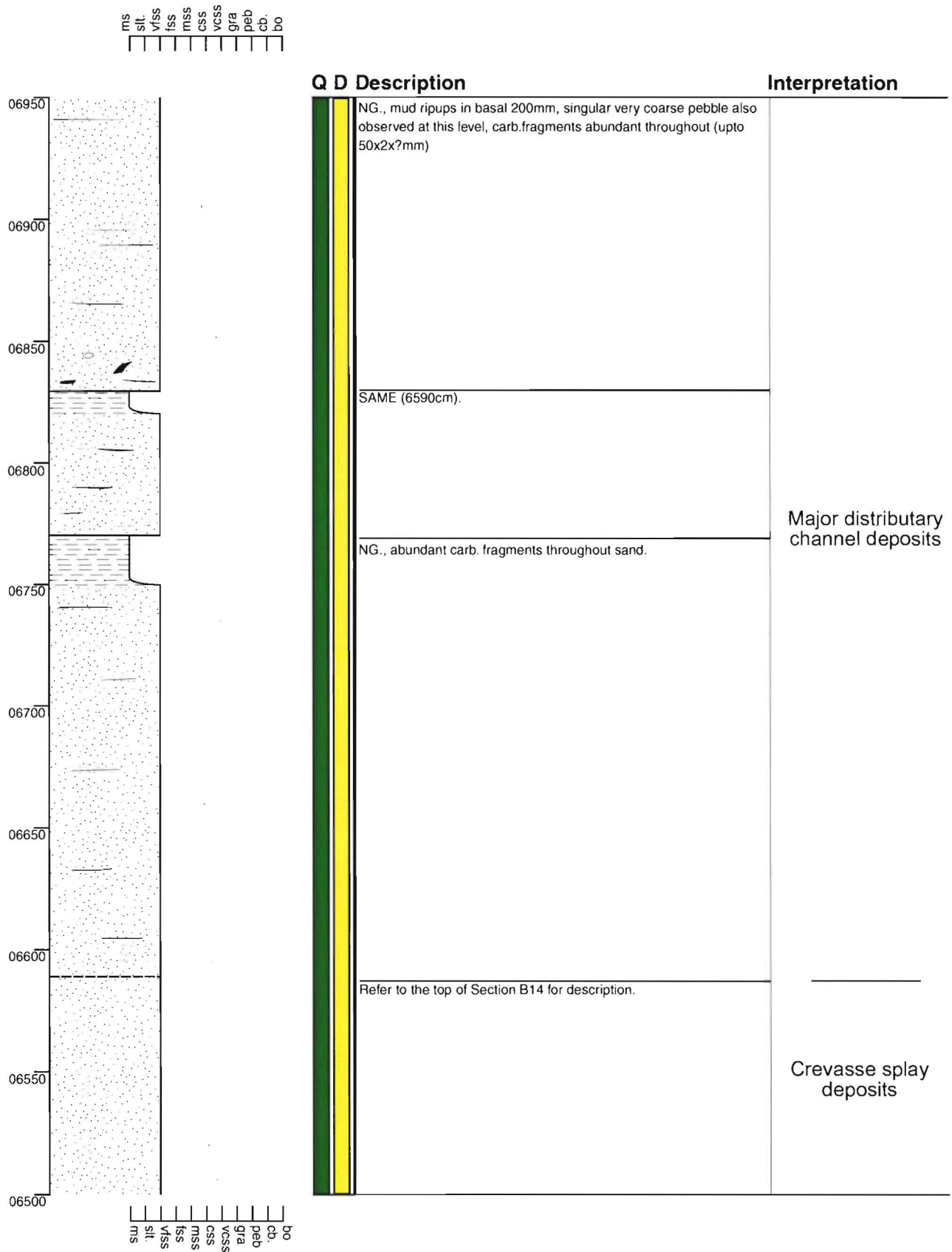


Section - Pahau River B14

Grid Reference M32 861 425

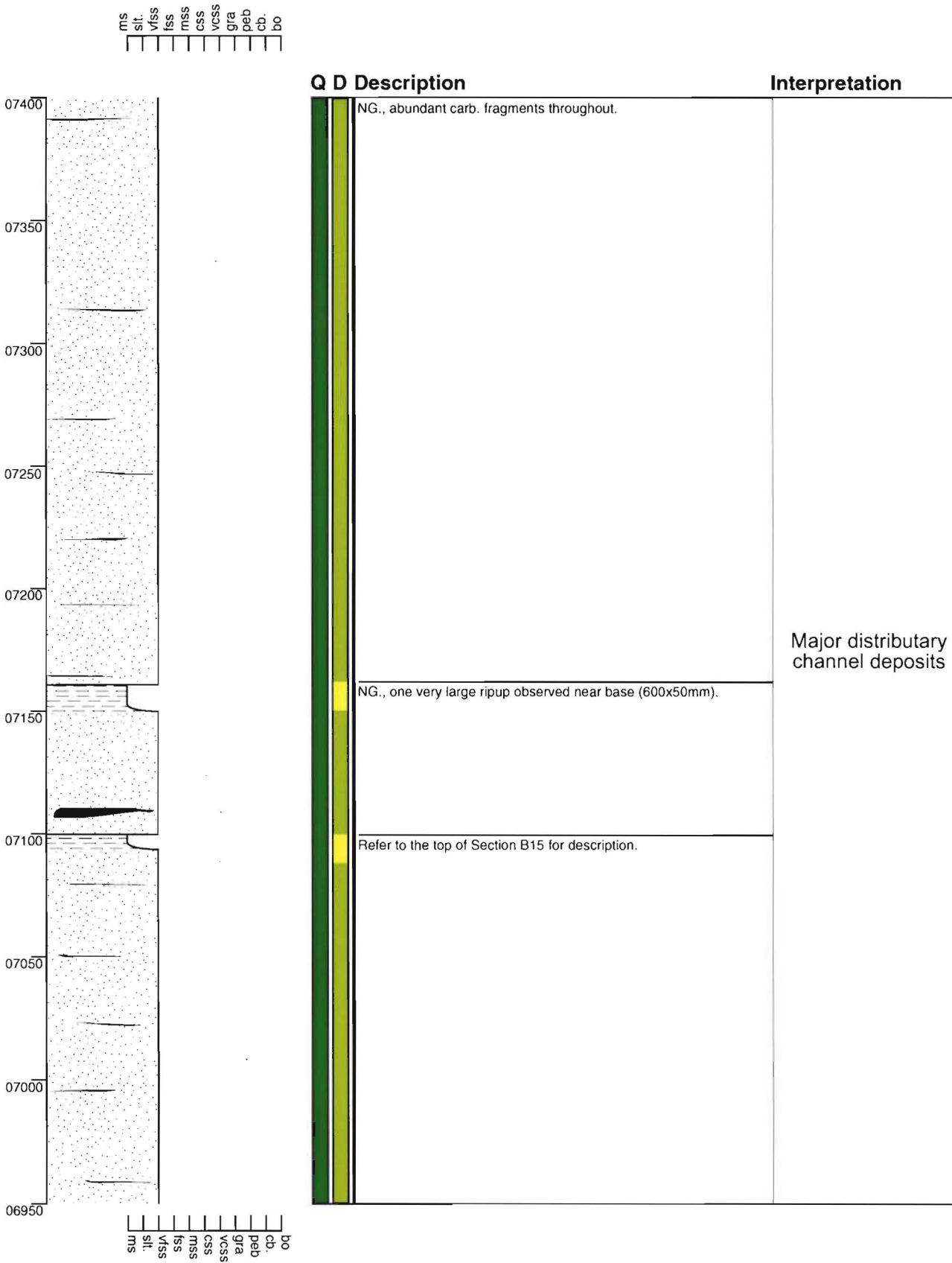


Grid Reference M32 861 425



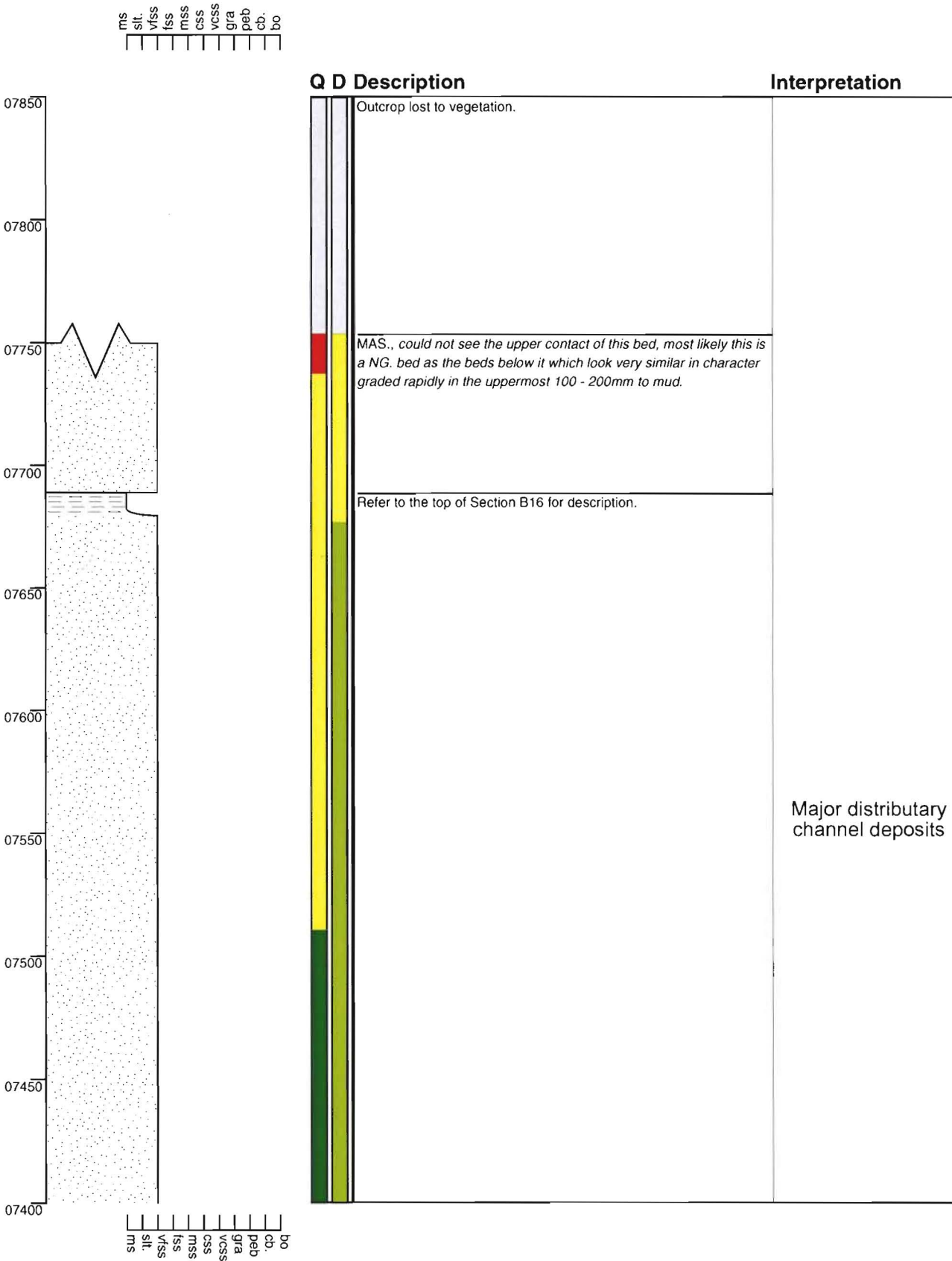
Section - Pahau River B16

Grid Reference M32 861 425



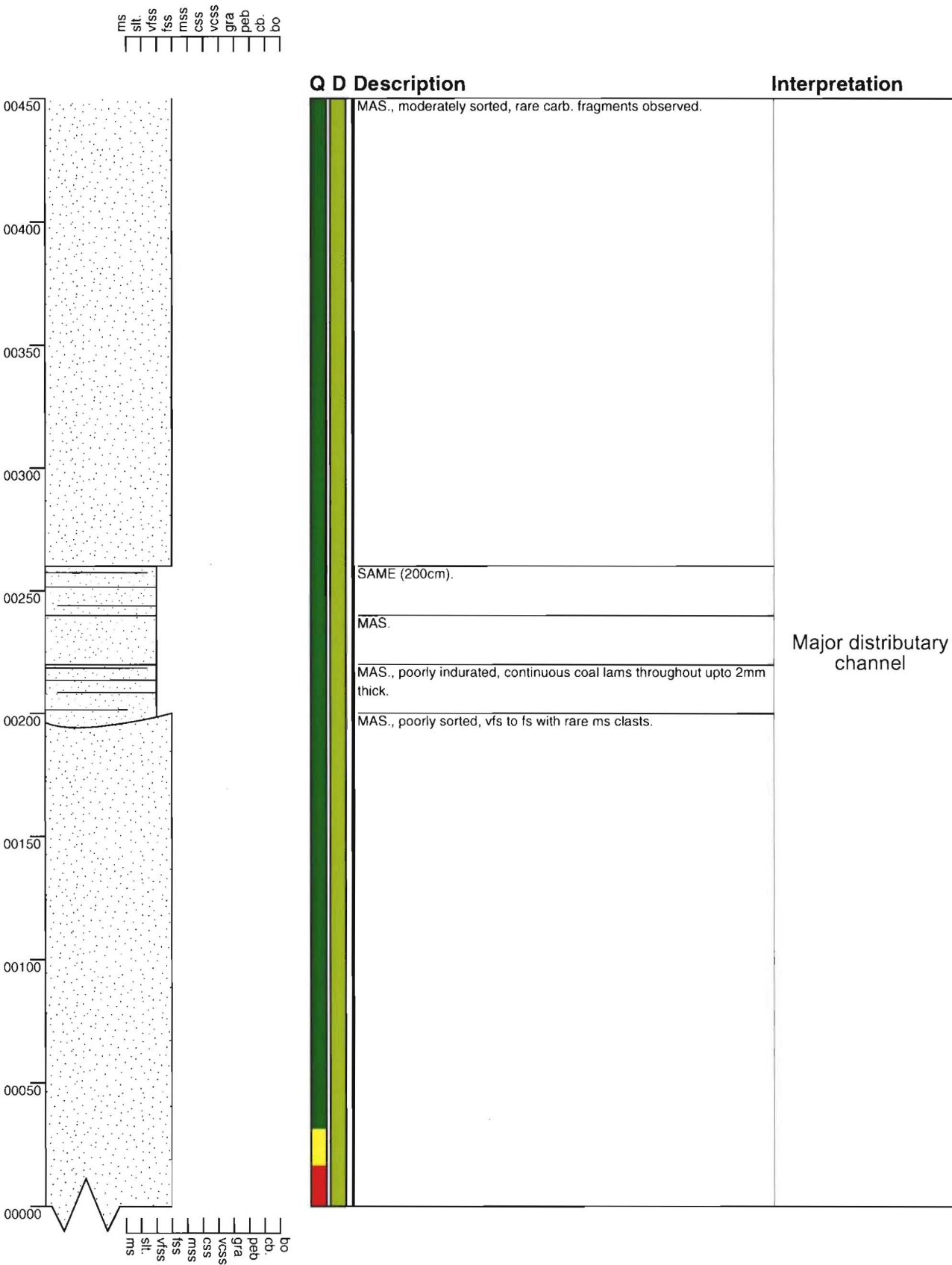
Section - Pahau River B17

Grid Reference M32 861 425



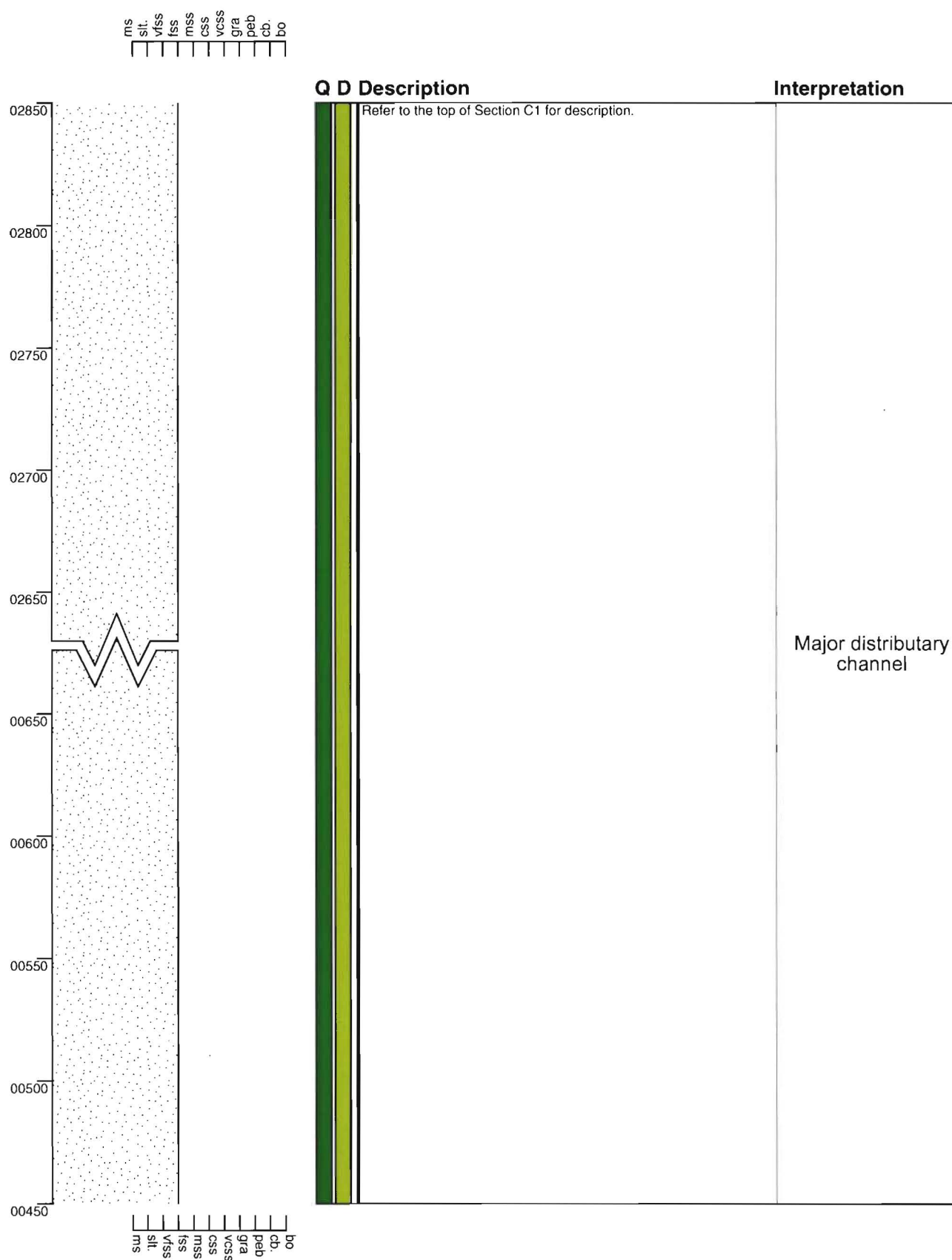
Section - Pahau River C01

Grid Reference M32 853 433



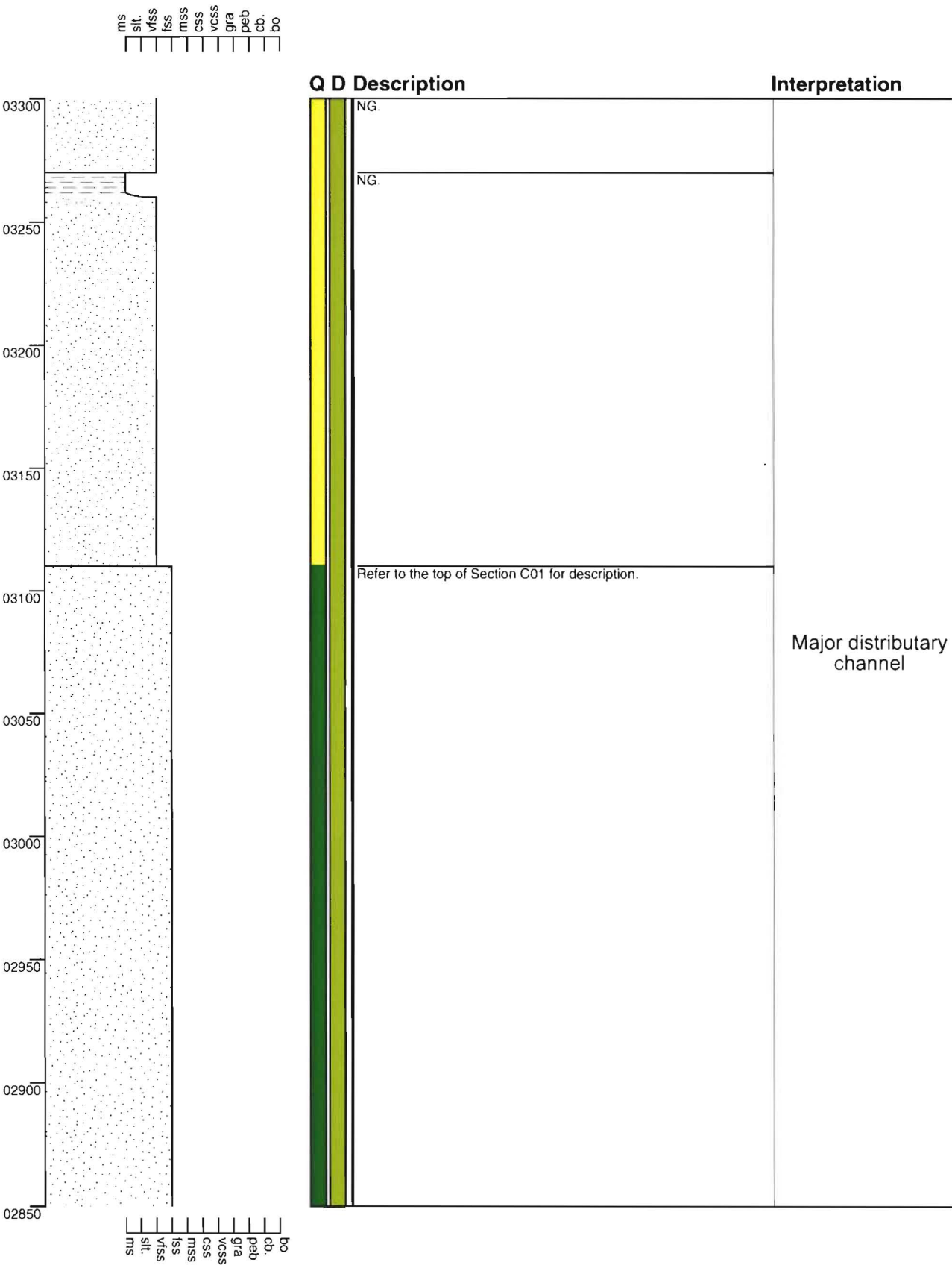
Section - Pahau River C02

Grid Reference M32 853 433

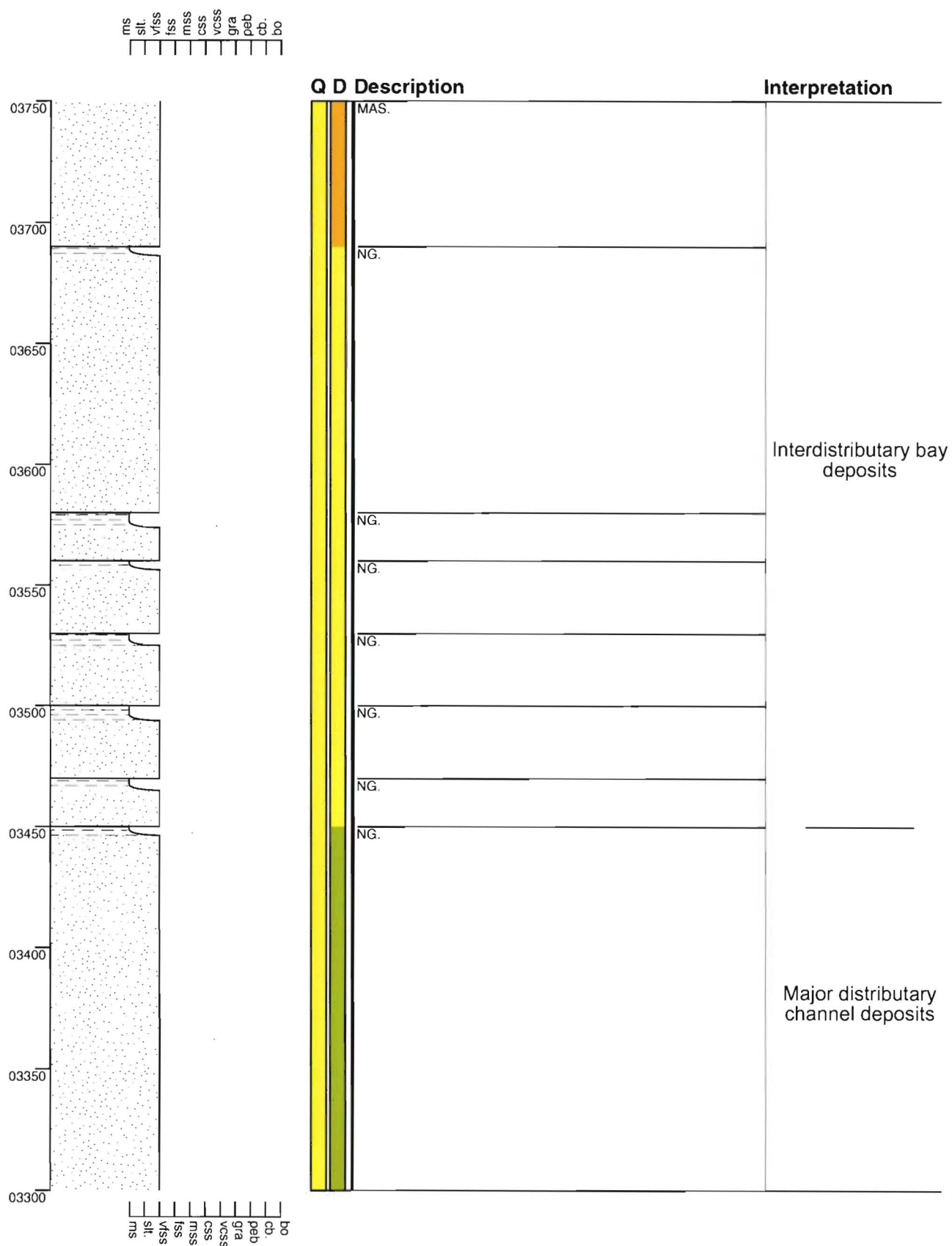


Section - Pahau River C03

Grid Reference M32 853 433

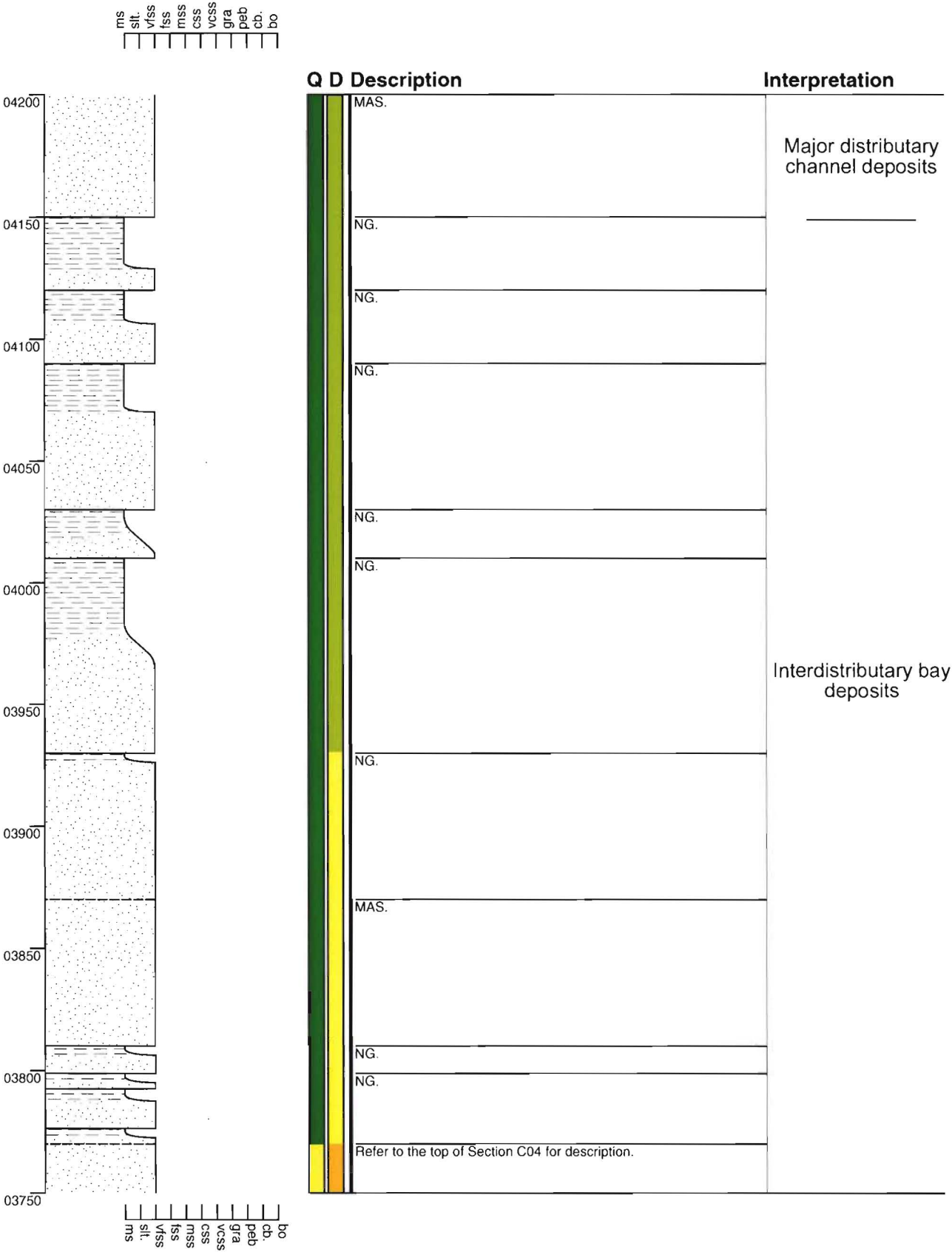


Grid Reference M32 853 433



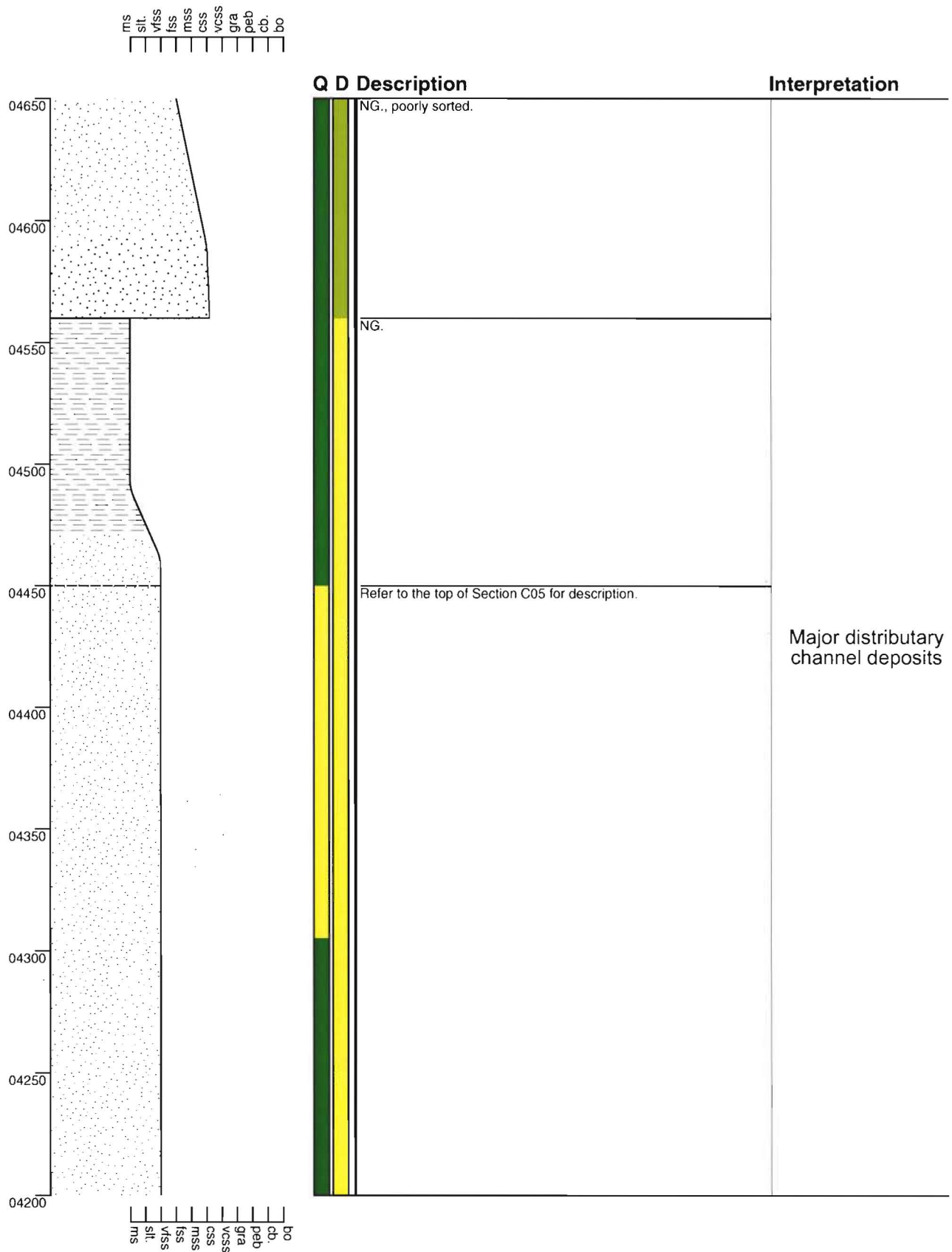
Section - Pahau River C05

Grid Reference M32 853 433



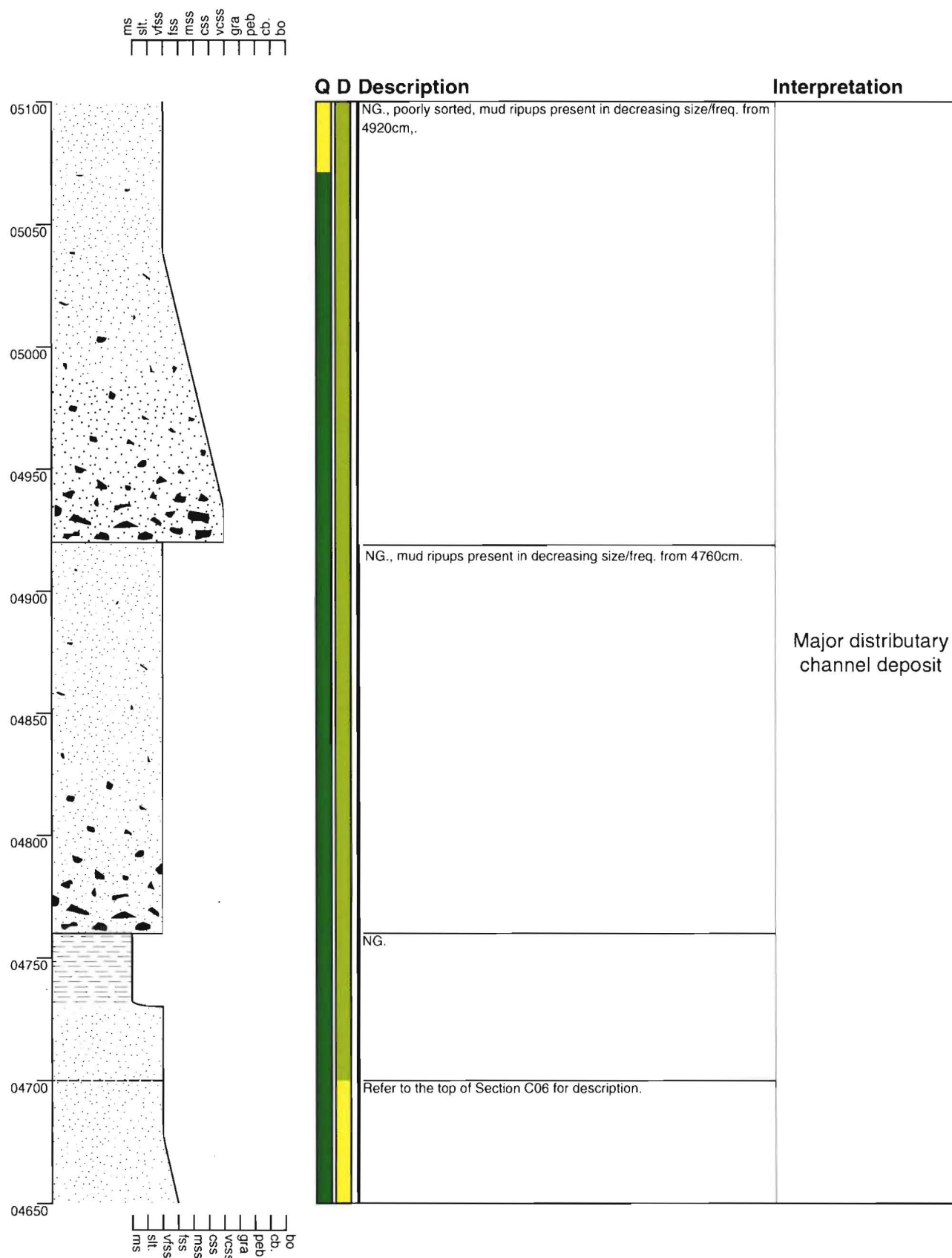
Section - Pahau River C06

Grid Reference M32 853 433

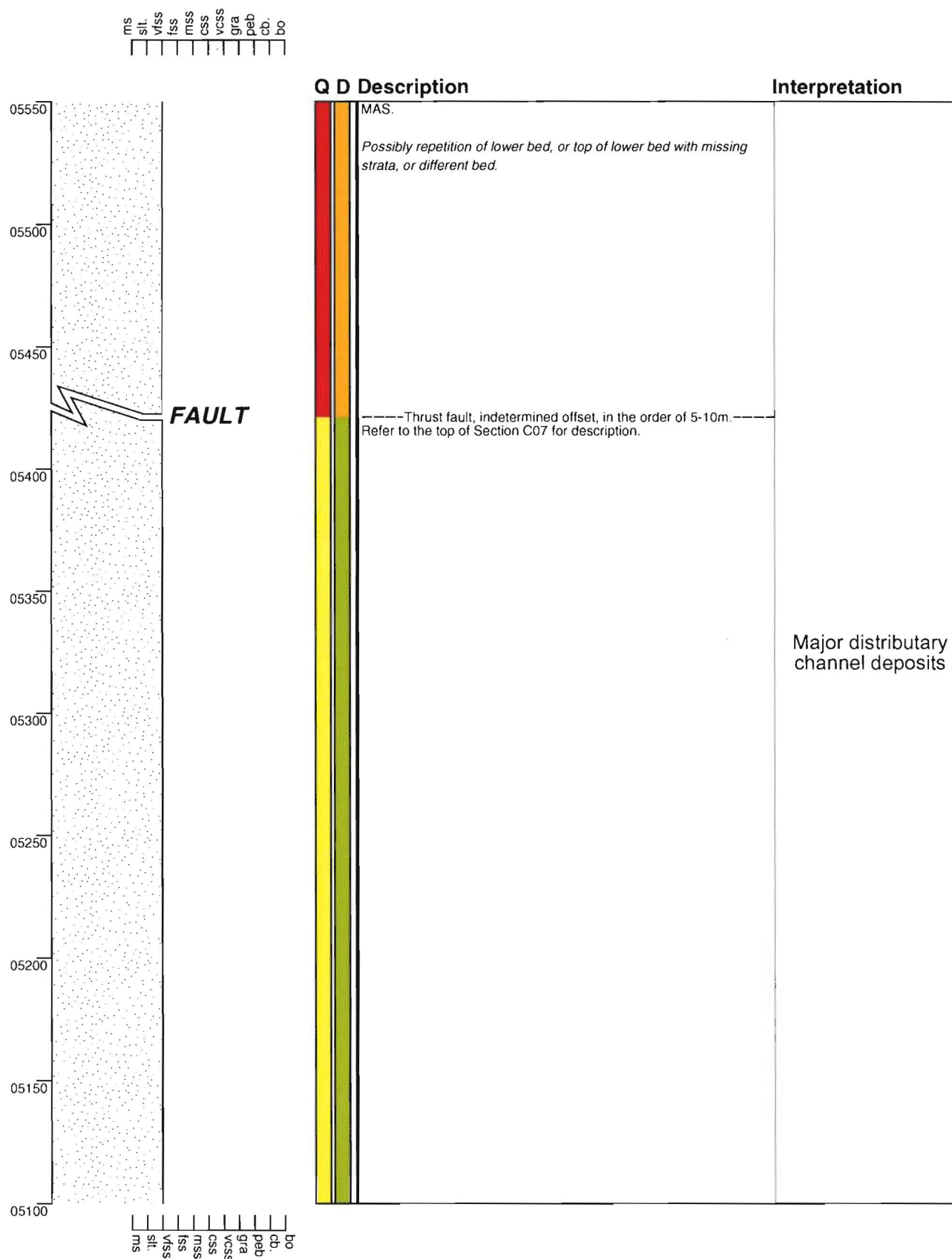


Section - Pahau River C07

Grid Reference M32 853 433

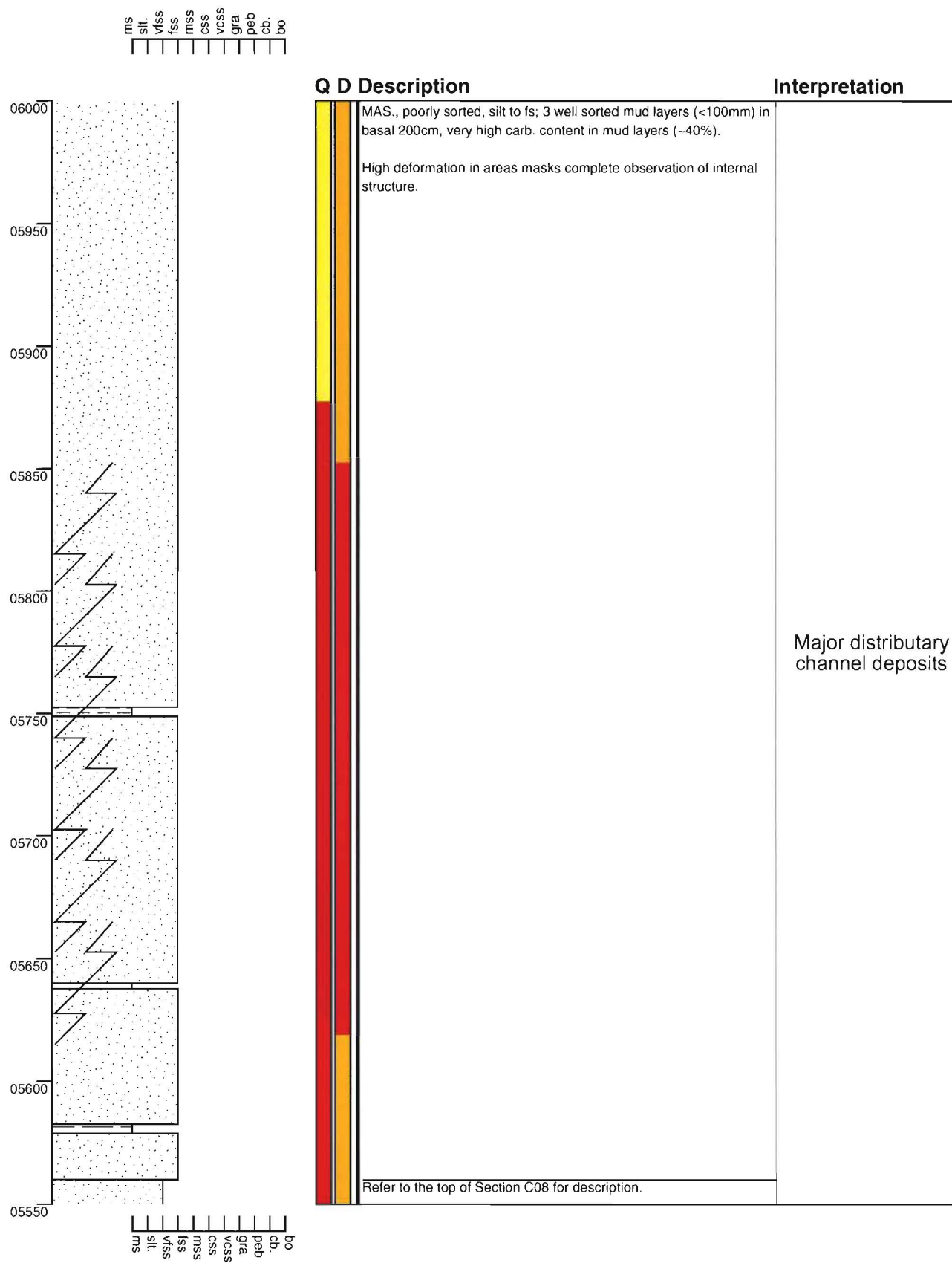


Grid Reference M32 853 433



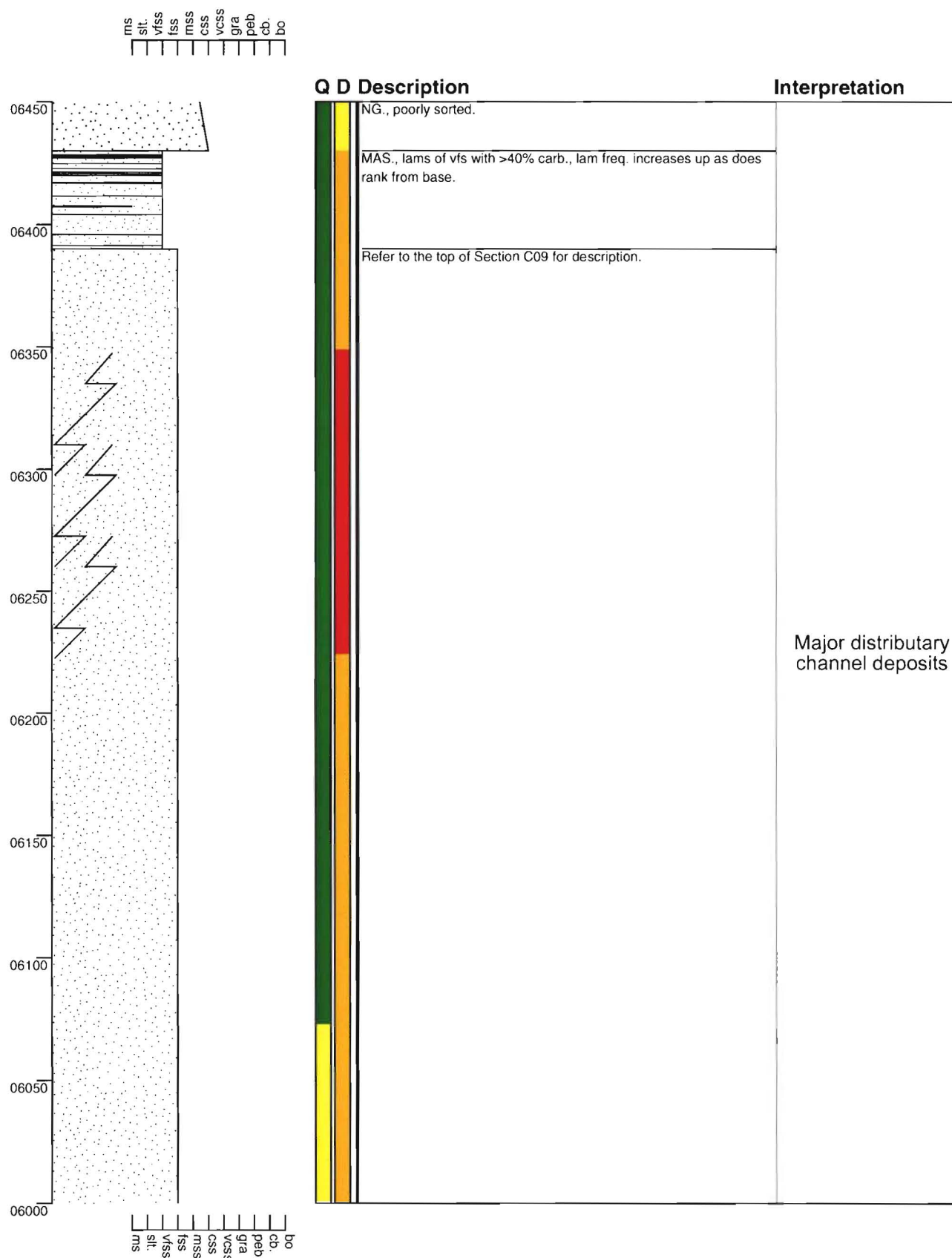
Section - Pahau River C09

Grid Reference M32 853 433



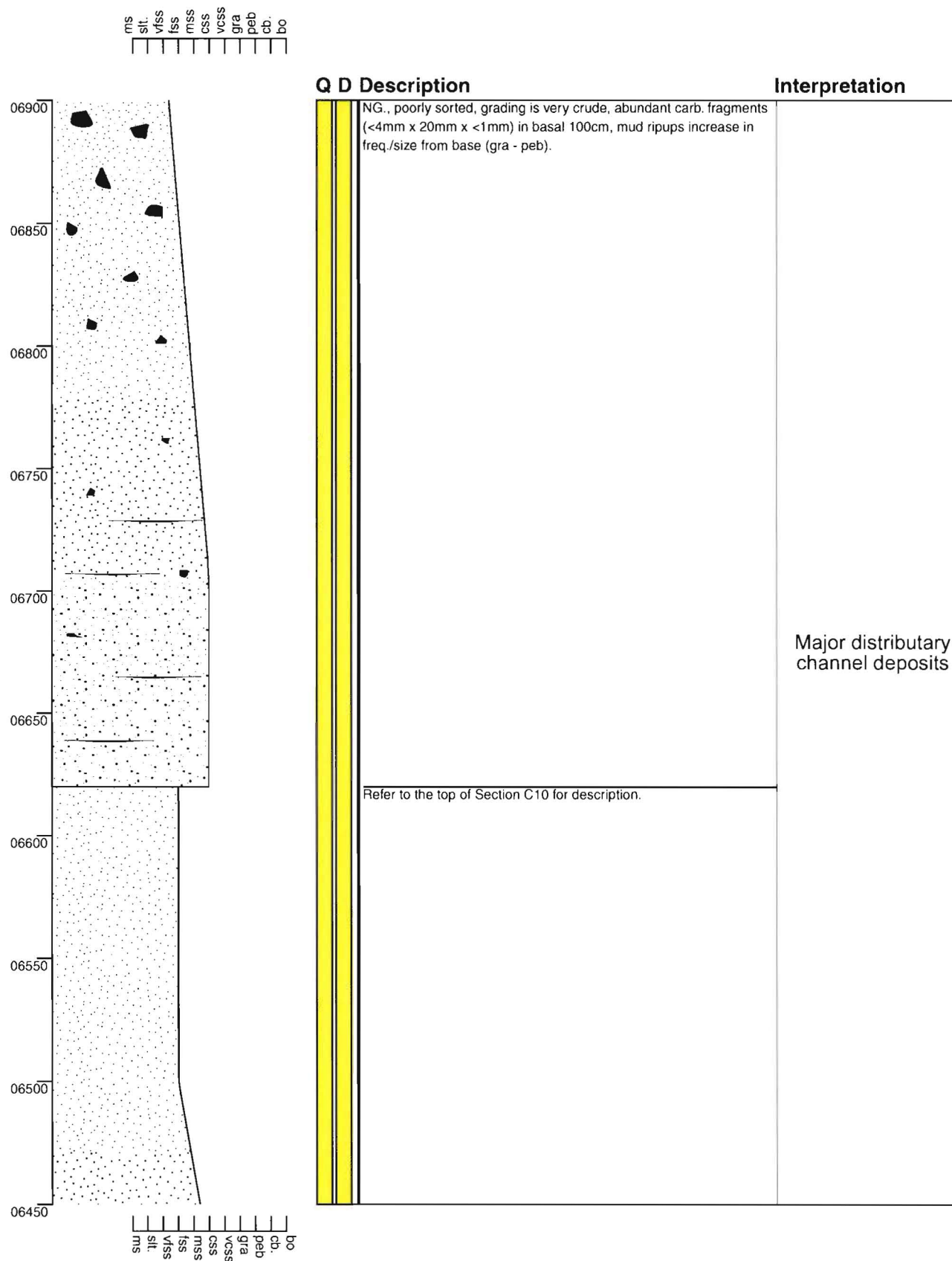
Section - Pahau River C10

Grid Reference M32 853 433



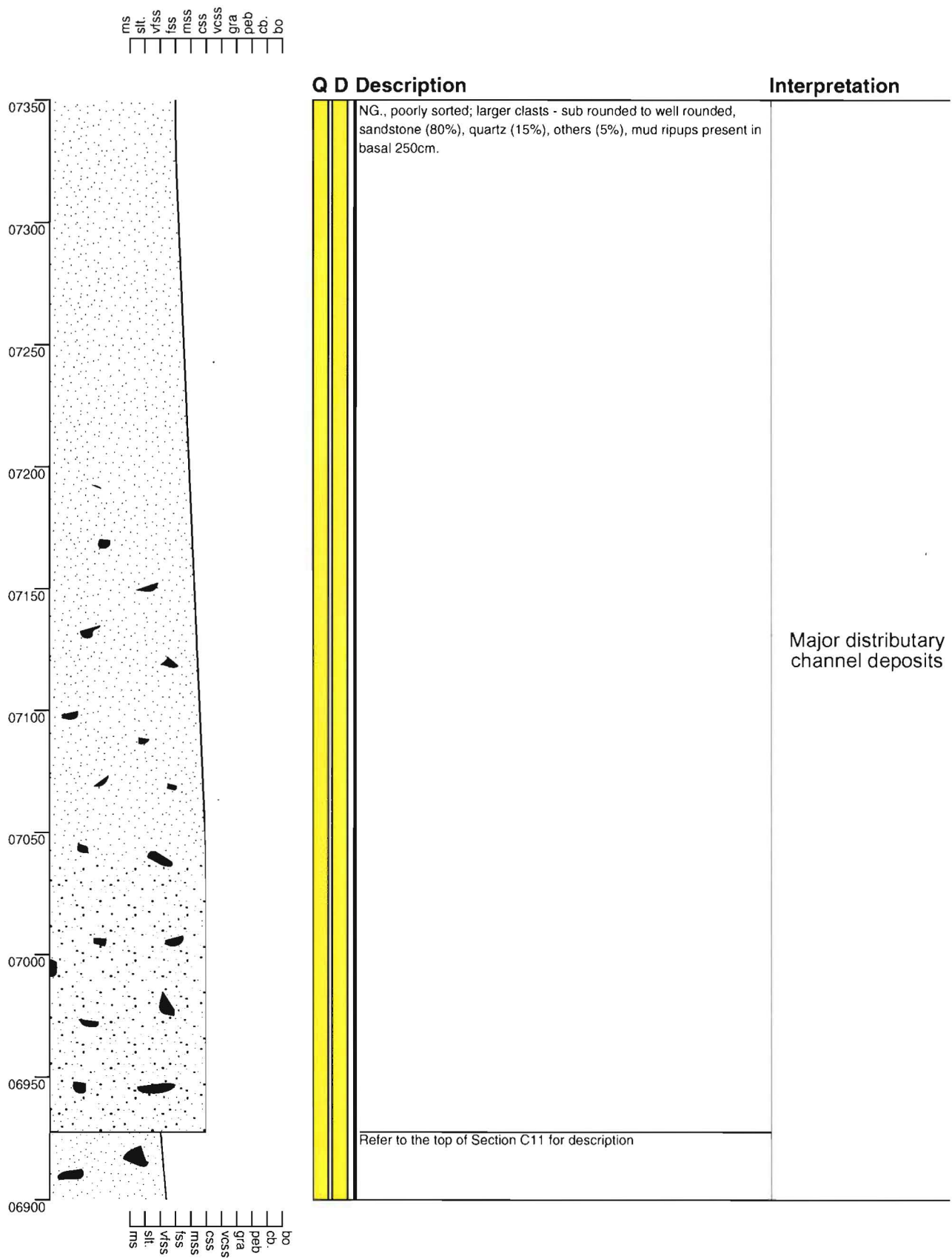
Section - Pahau River C11

Grid Reference M32 853 433



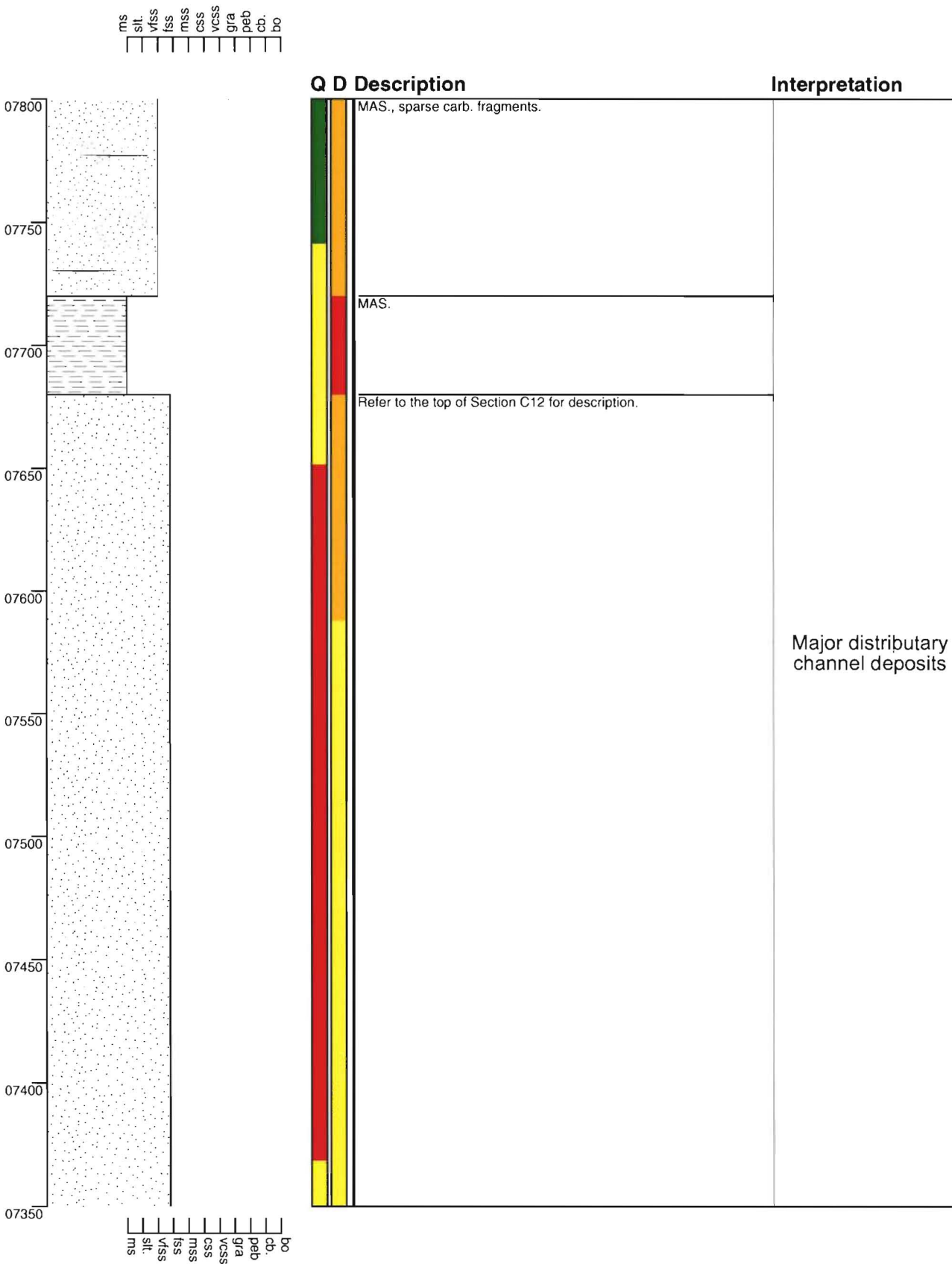
Section - Pahau River C12

Grid Reference M32 853 433



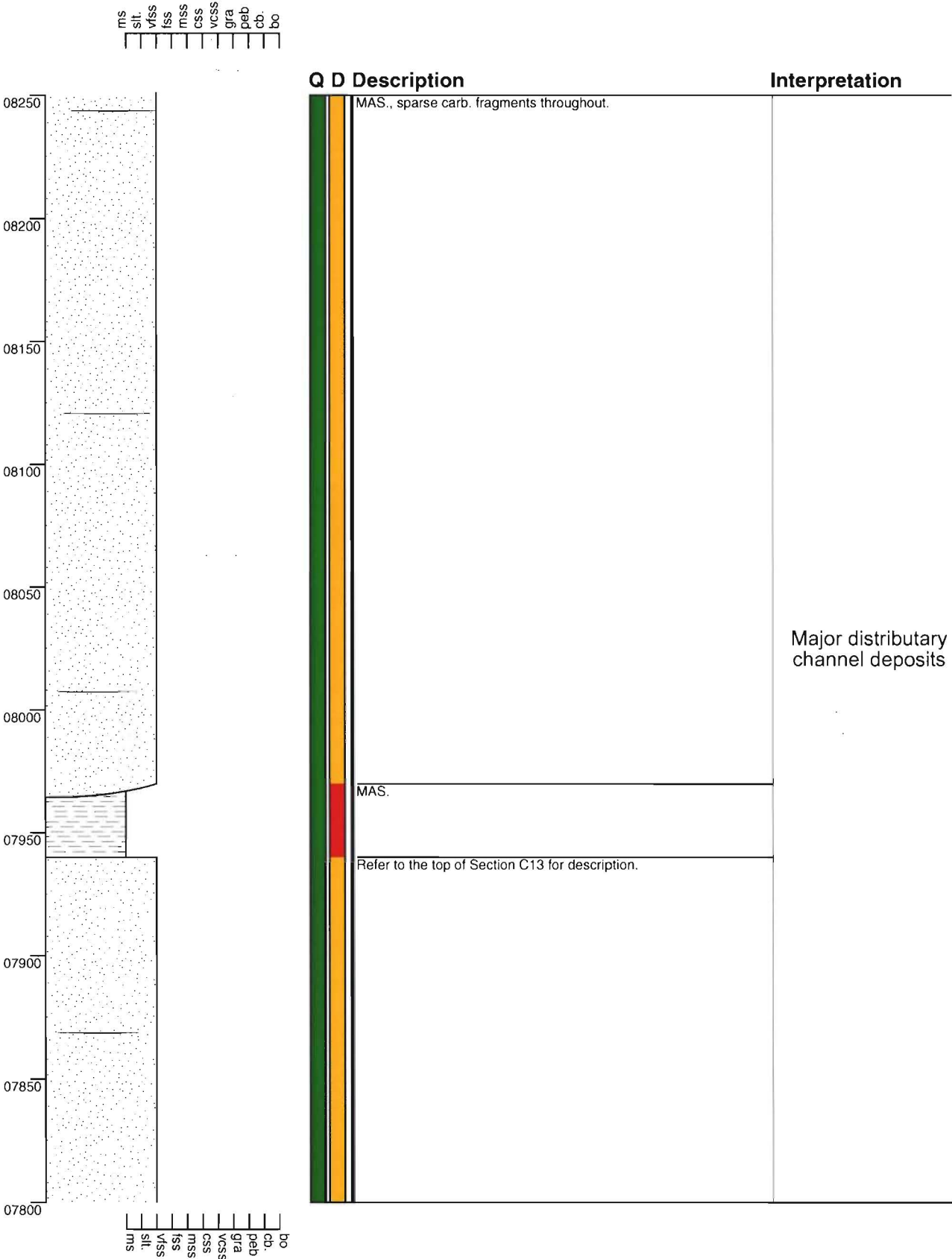
Section - Pahau River C13

Grid Reference M32 853 433



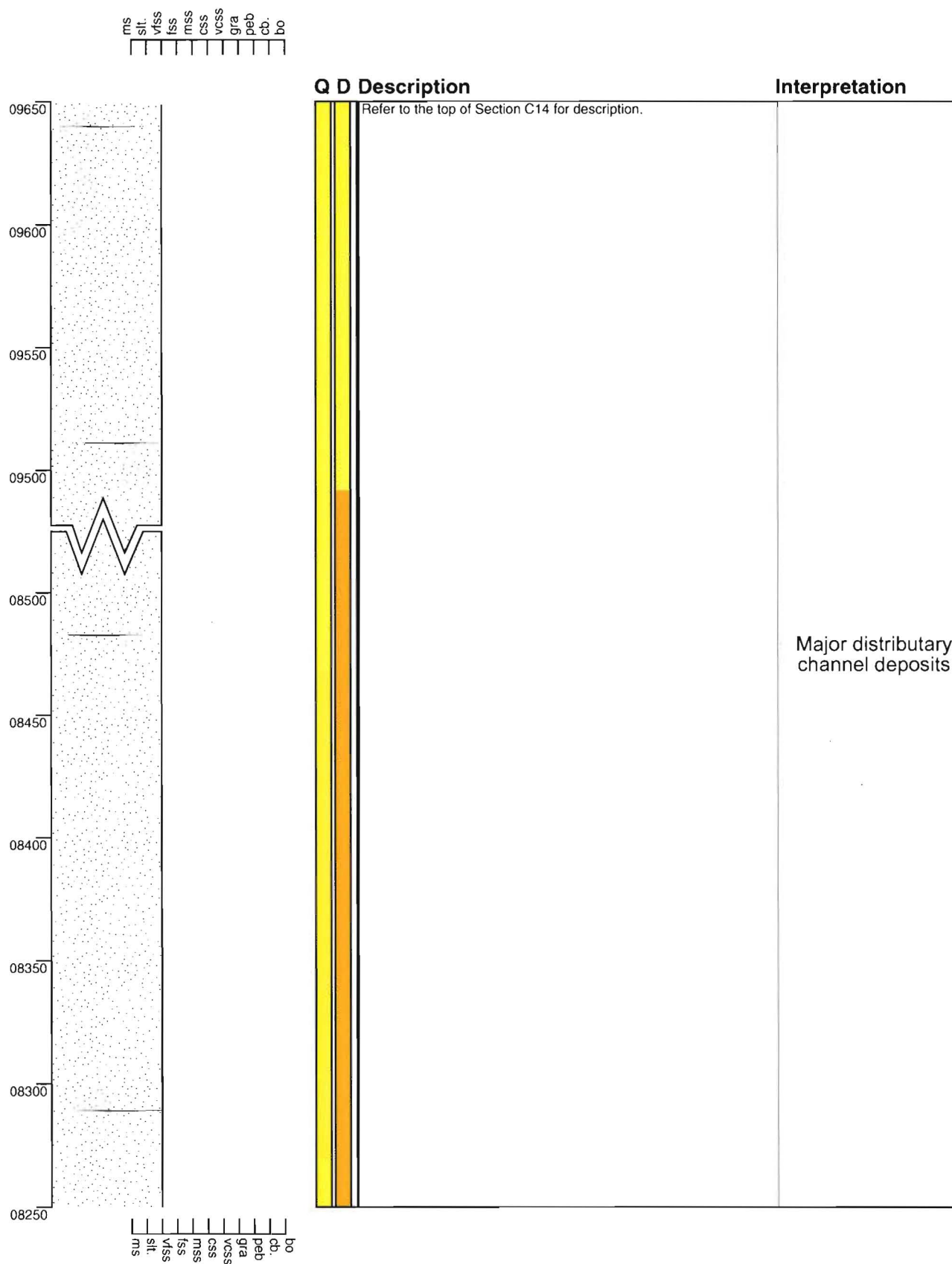
Section - Pahau River C14

Grid Reference M32 853 433



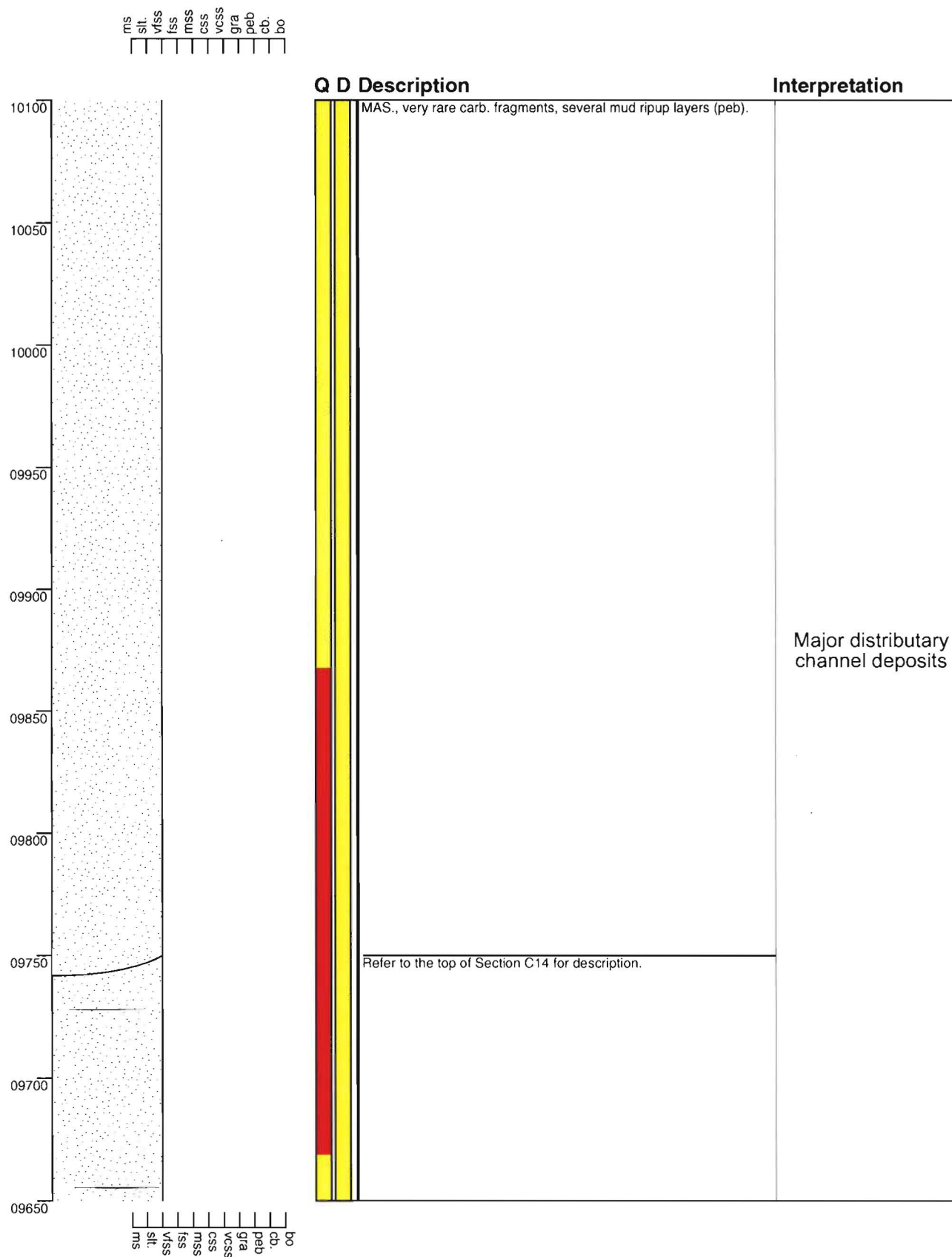
Section - Pahau River C15

Grid Reference M32 853 433



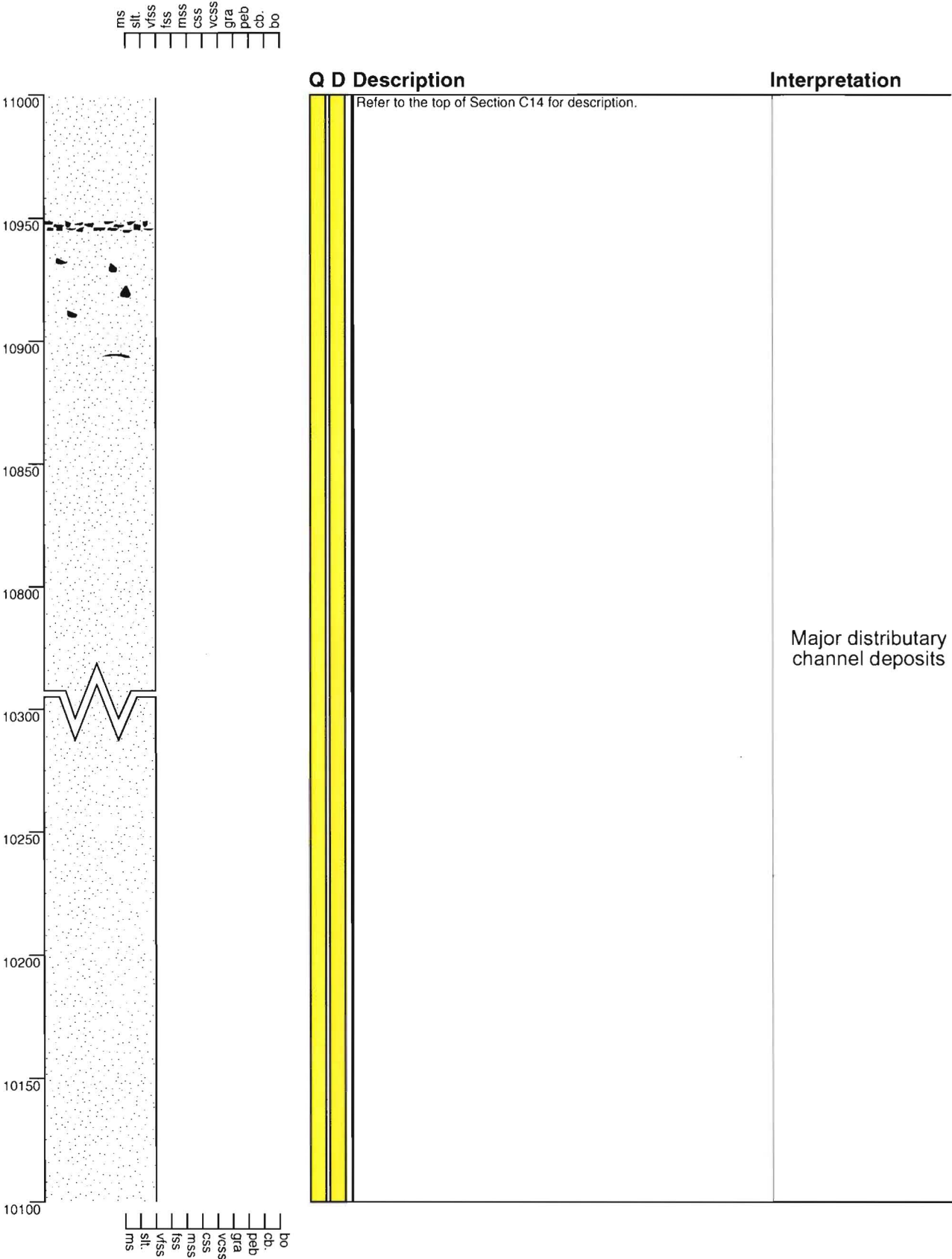
Section - Pahau River C16

Grid Reference M32 853 433



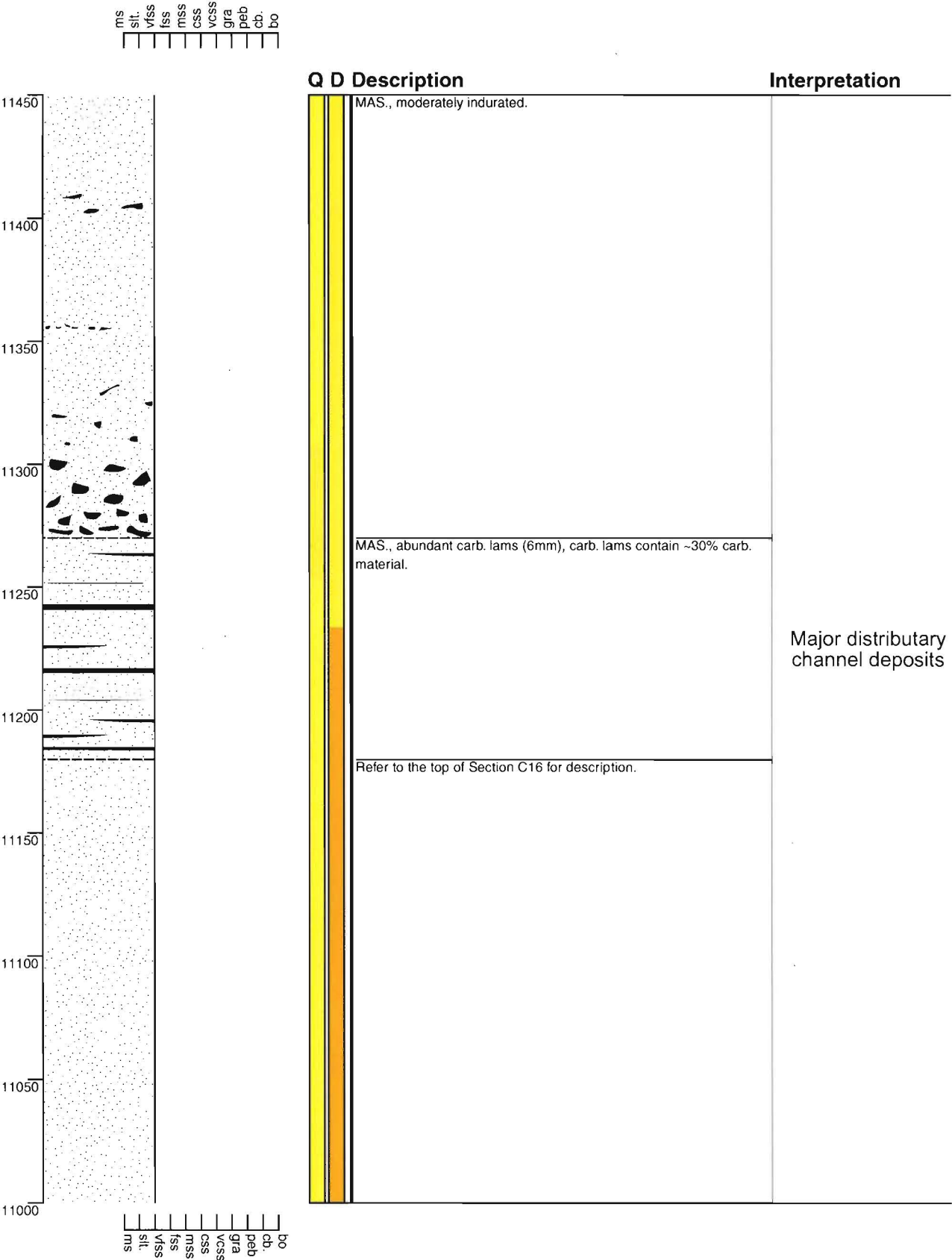
Section - Pahau River C17

Grid Reference M32 853 433



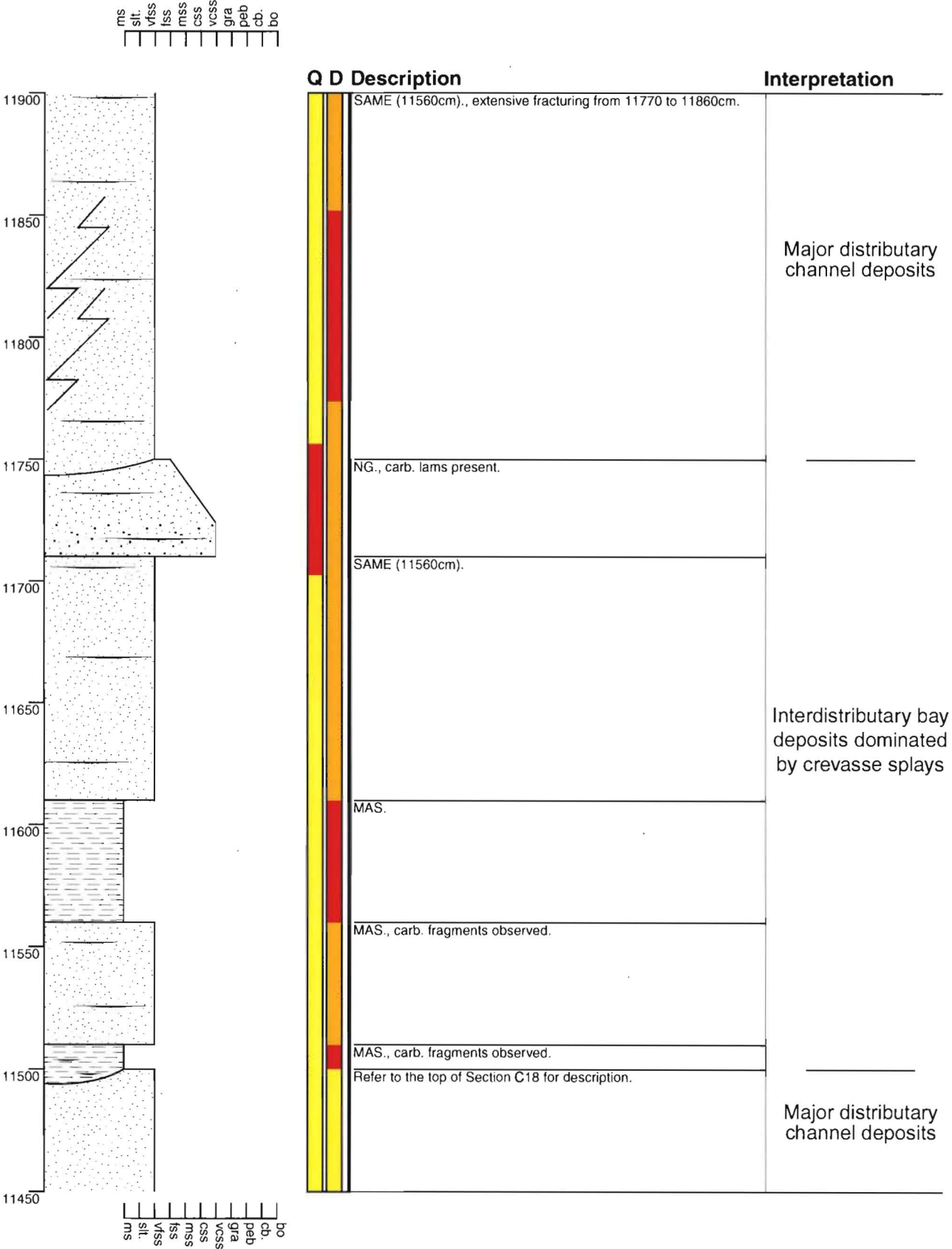
Section - Pahau River C18

Grid Reference M32 853 433



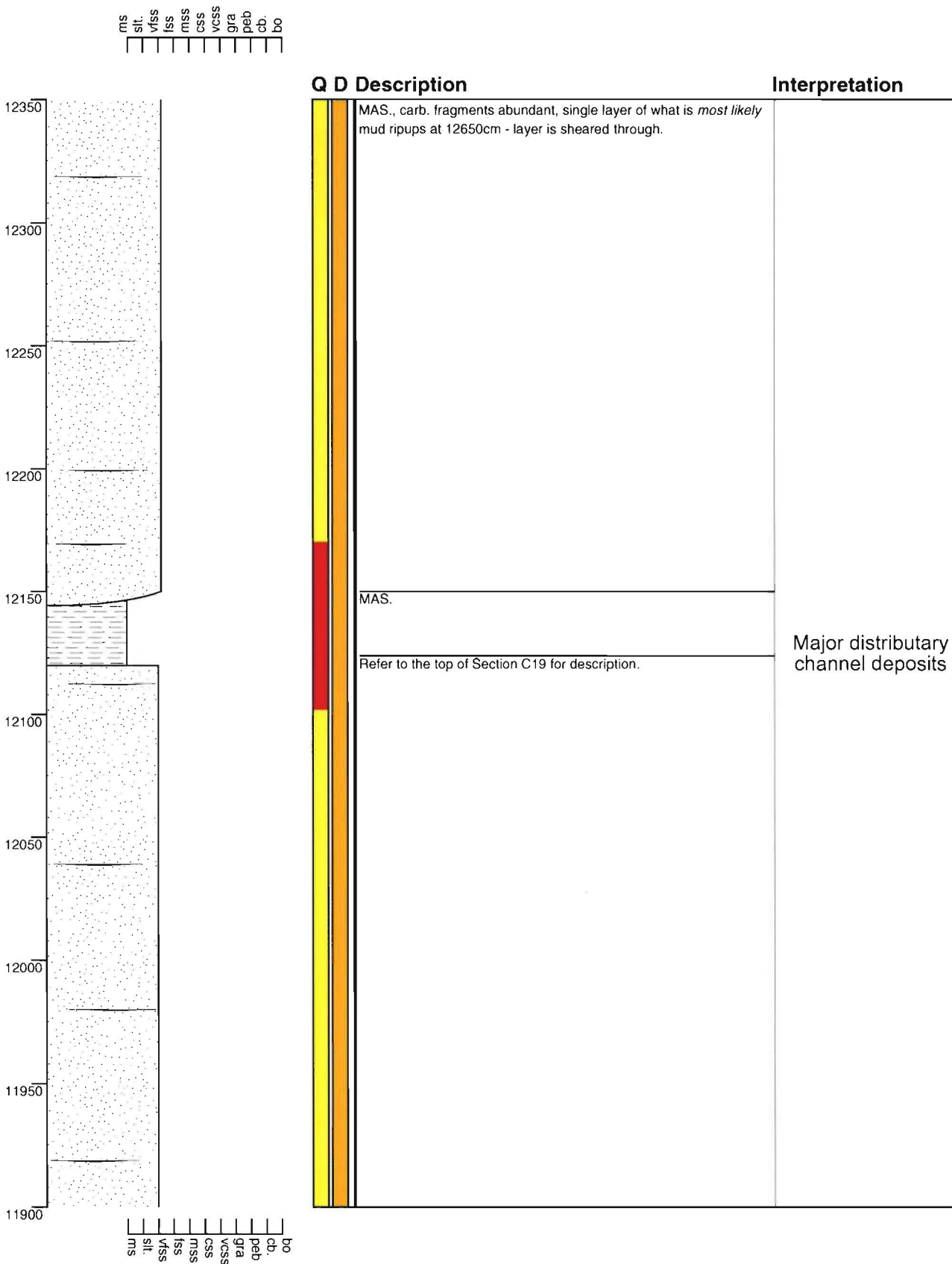
Section - Pahau River C19

Grid Reference M32 853 433

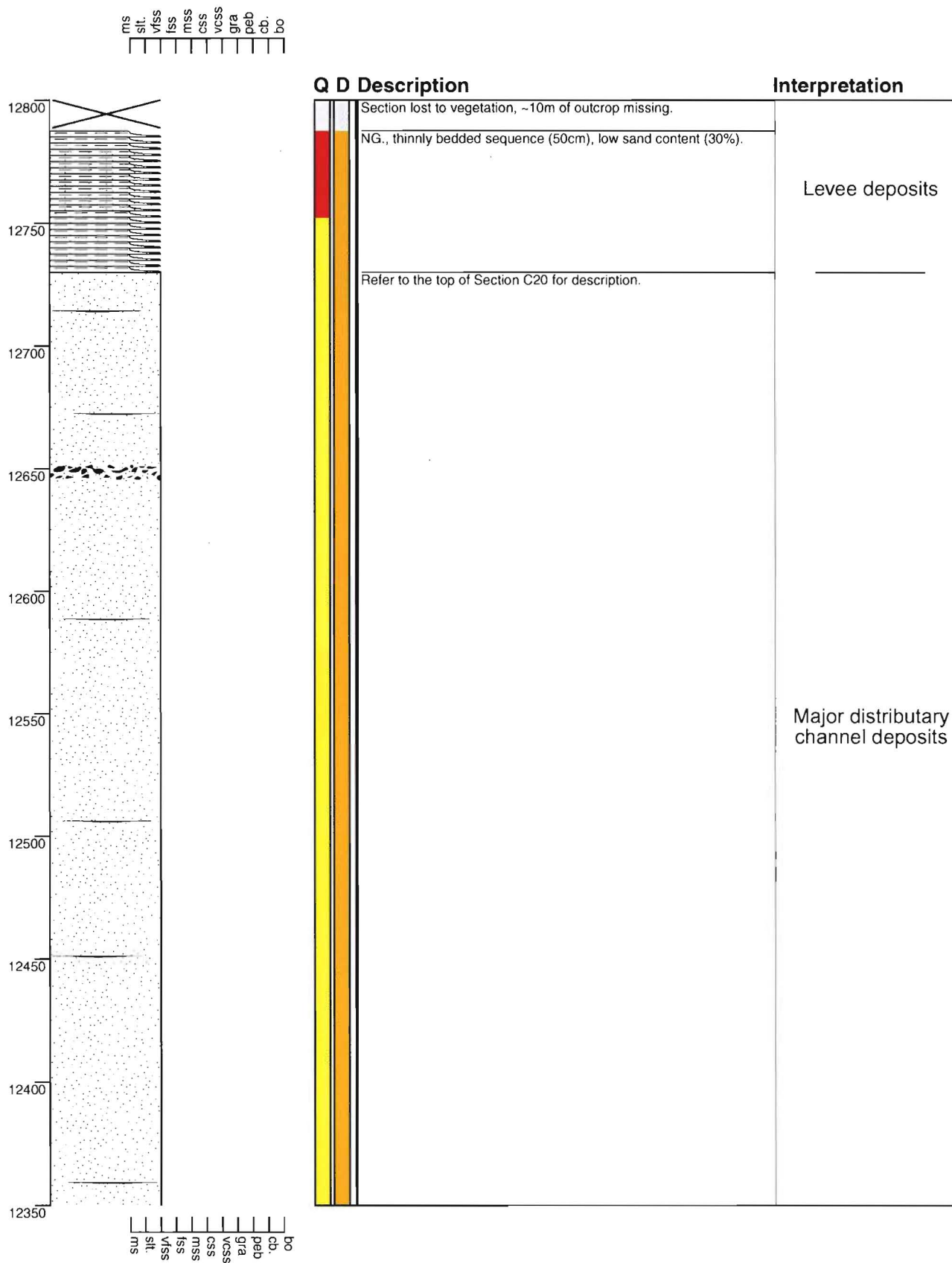


Section - Pahau River C20

Grid Reference M32 853 433

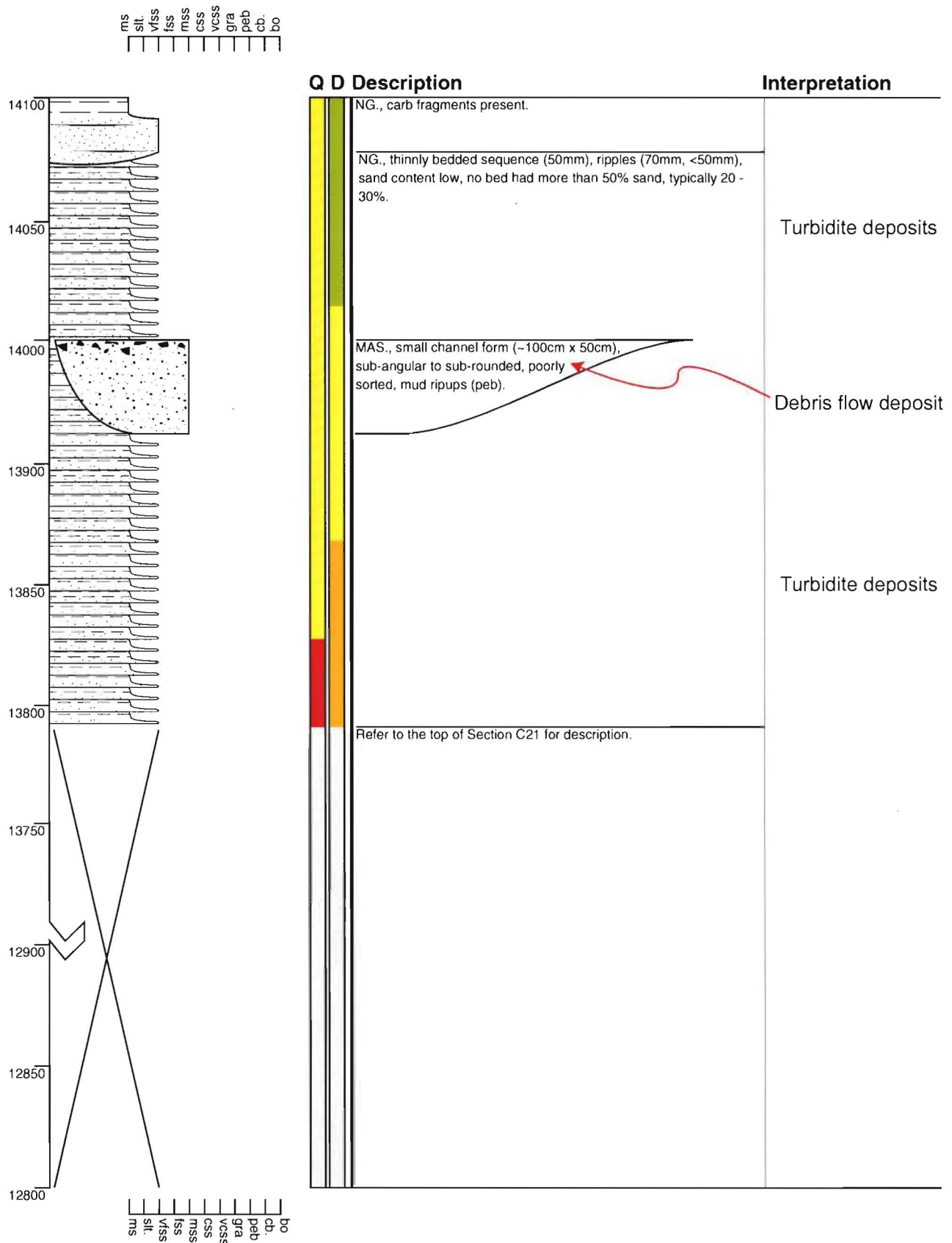


Grid Reference M32 853 433



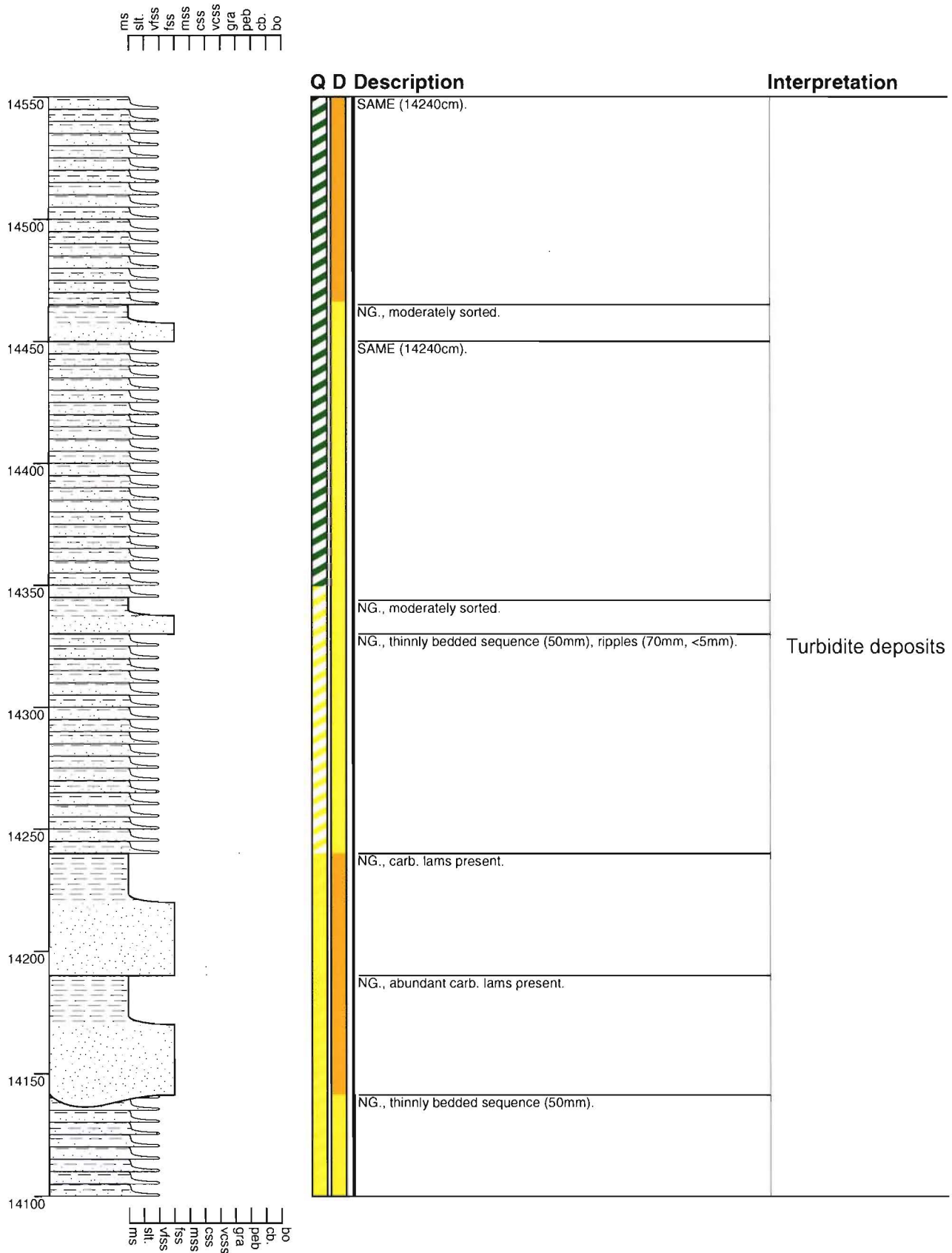
Section - Pahau River C22

Grid Reference M32 853 433



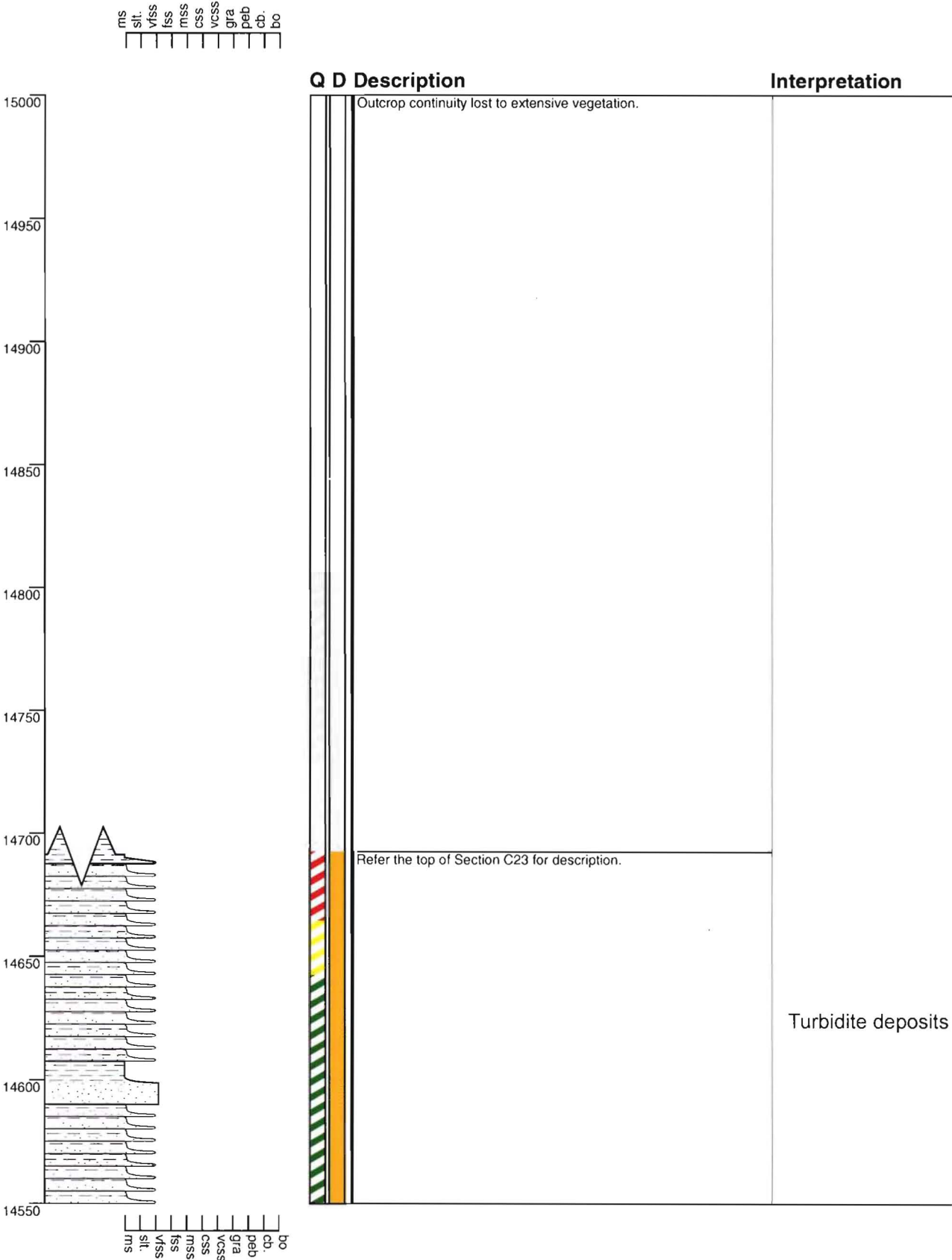
Section - Pahau River C23

Grid Reference M32 853 433



Section - Pahau River C24

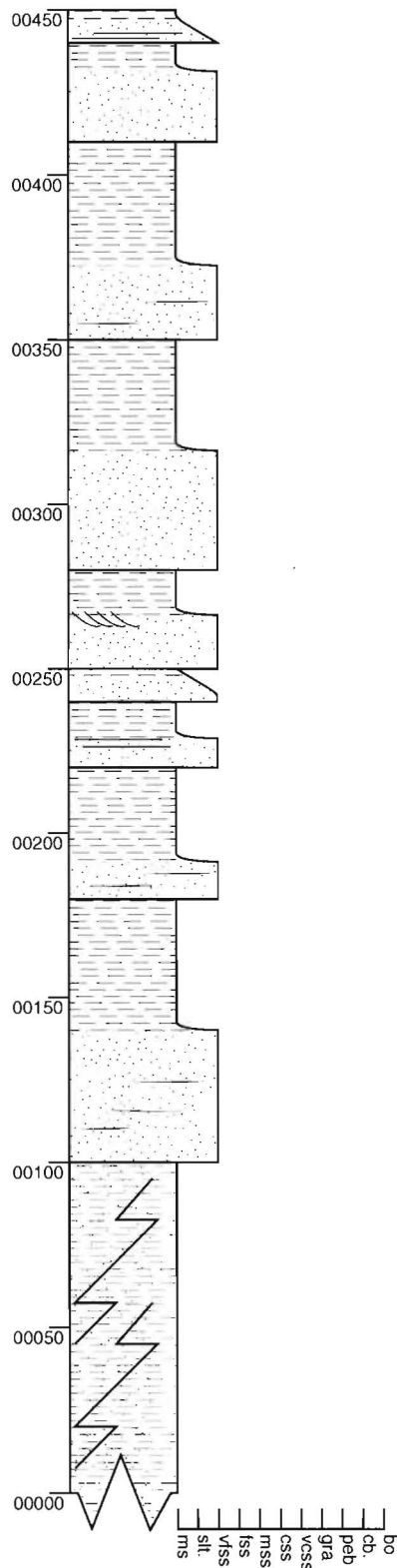
Grid Reference M32 853 433



Section - Waiau River WR01

Grid Reference N32 923 469

ms
silt.
vss
fss
mss
css
vcss
gra
peb
cb.
bo



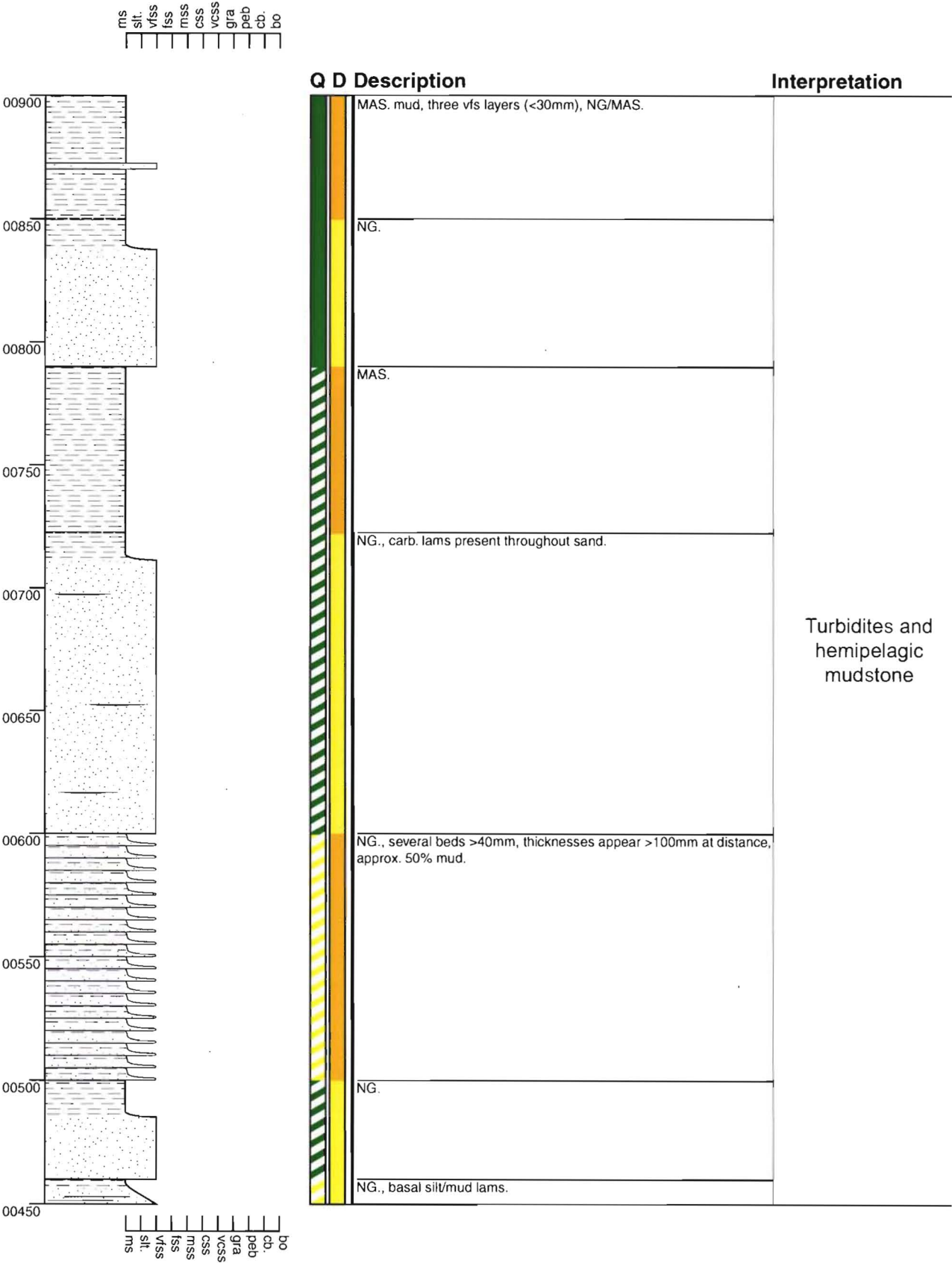
Q D Description

Interpretation

NG., basal mud lams.	Turbidites and hemipelagic mudstone
NG.	
SAME (100cm).	
NG.	
NG., crossbedding observed at transition to mud.	
NG.	
NG., thin silt/mud lams at rapid transition to mud.	
SAME (100cm).	
NG., carb. fragments observed in sand.	
High deformation, bedding indistinct, approx. 80% mud.	
Could be either —	
MAS. mud with thin <50mm beds of vss perhaps NG or it could be NG thinly bedded sequence (<100mm) with a very high mud content. Probably more likely to be the former.	

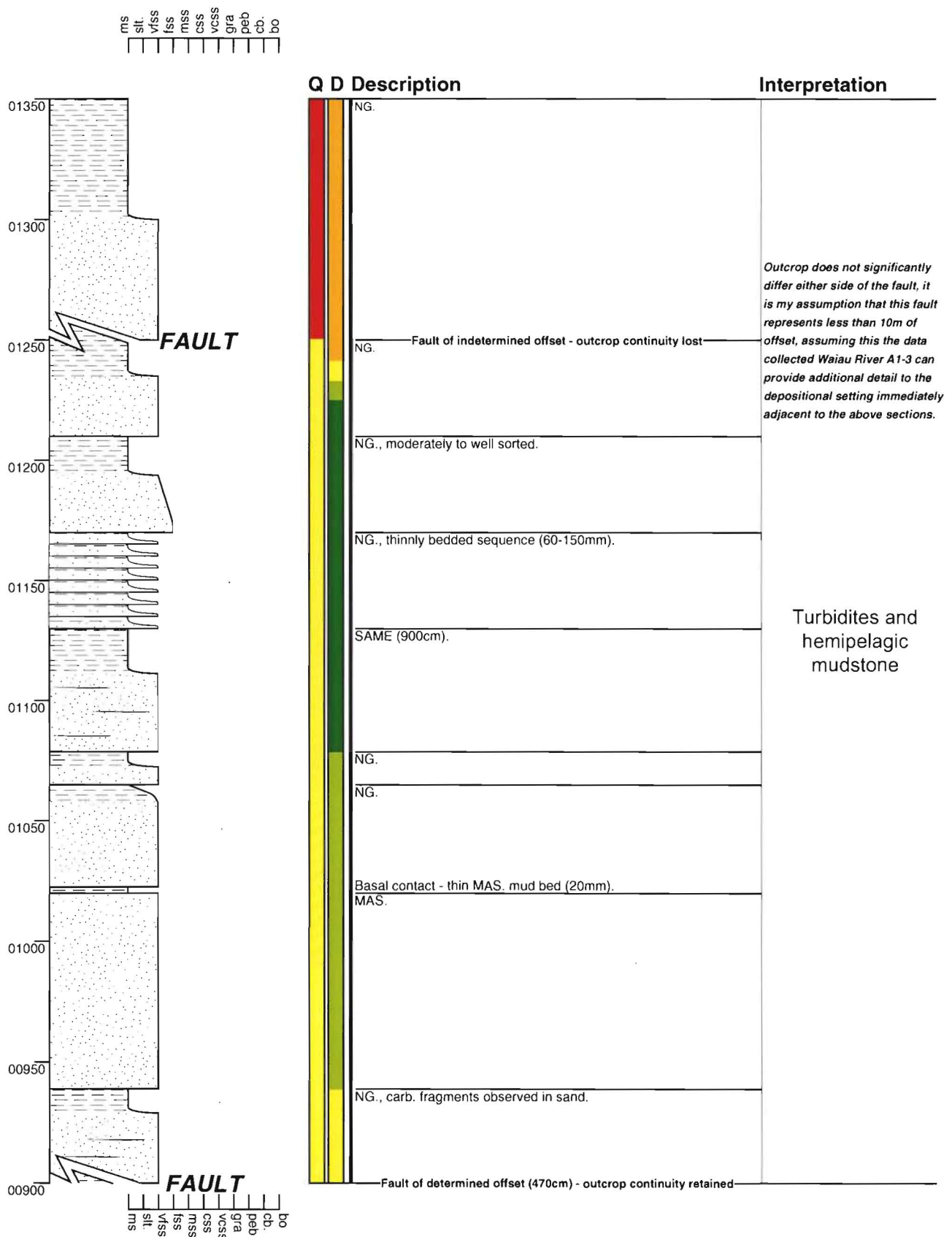
Section - Waiau River WR02

Grid Reference N32 923 469



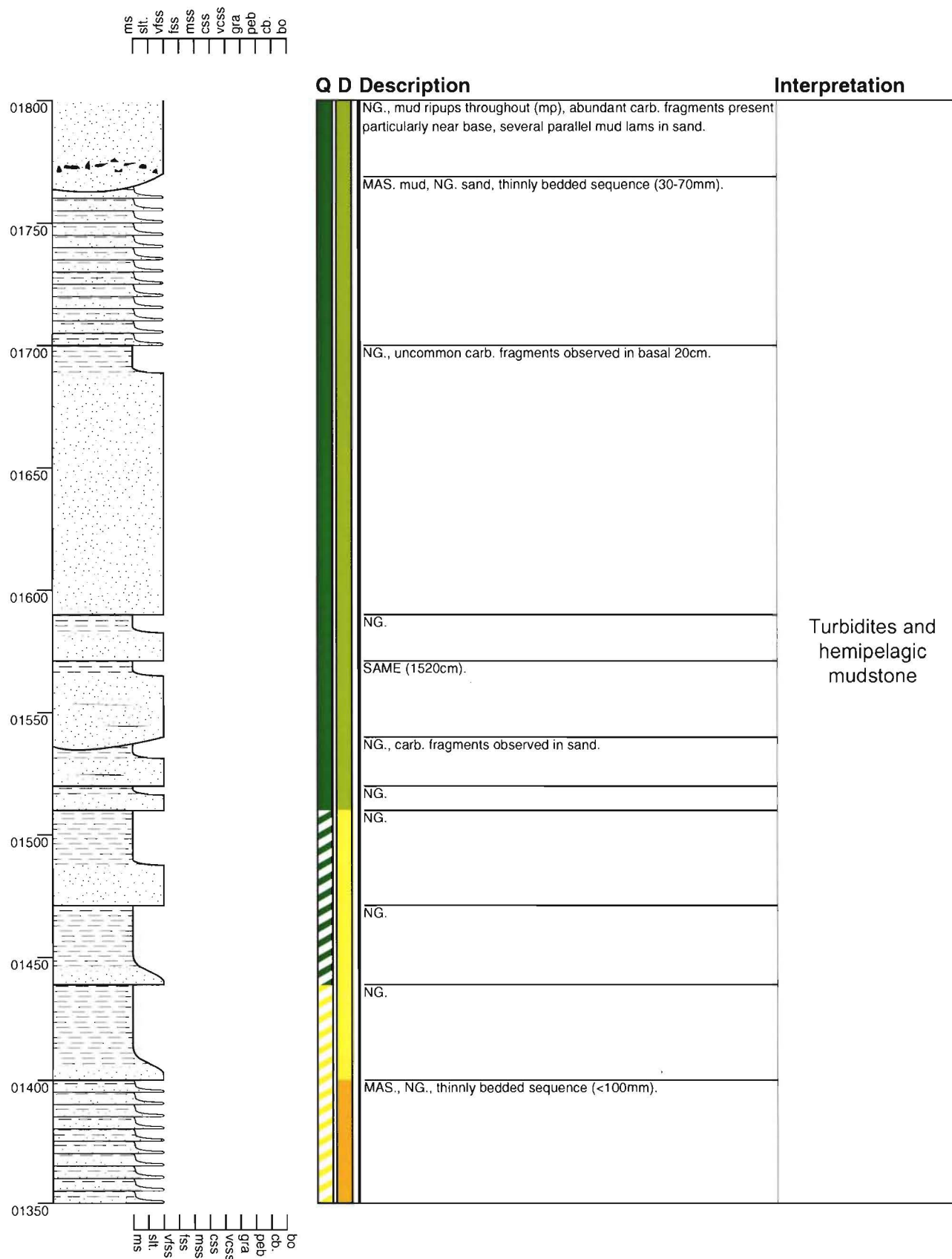
Section - Waiau River WR03

Grid Reference N32 923 469



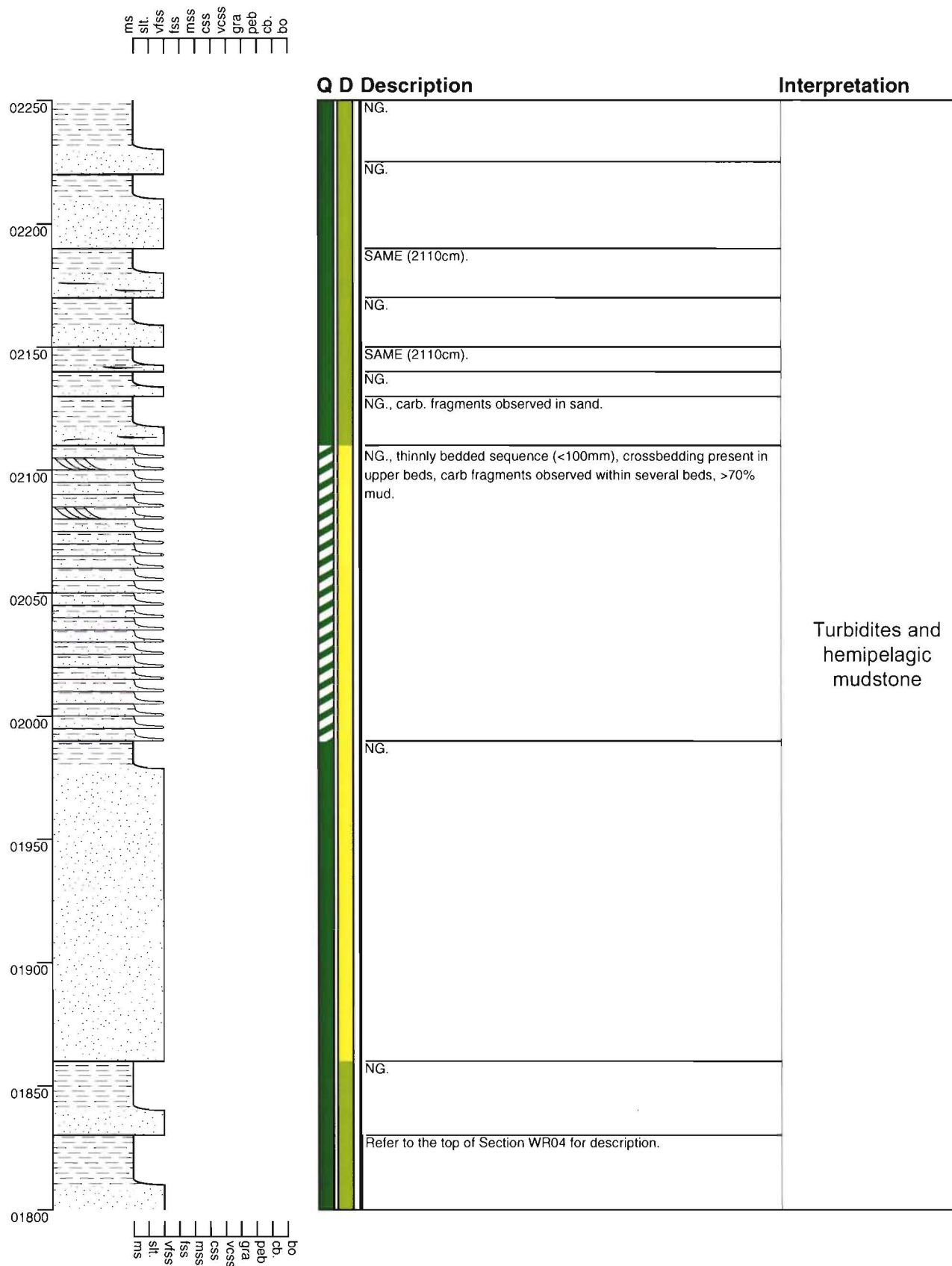
Section - Waiau River WR04

Grid Reference N32 923 469



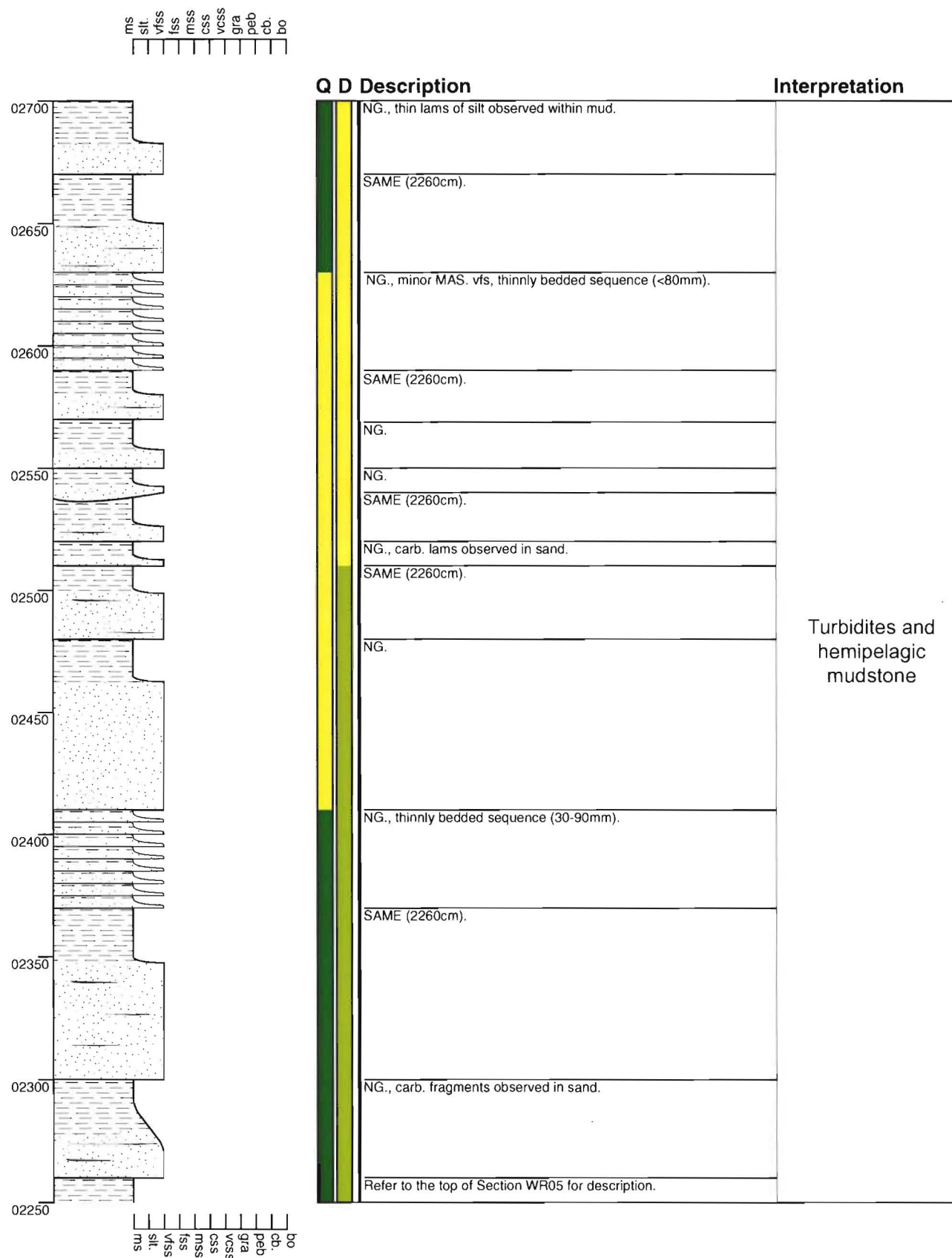
Section - Waiau River WR05

Grid Reference N32 923 469



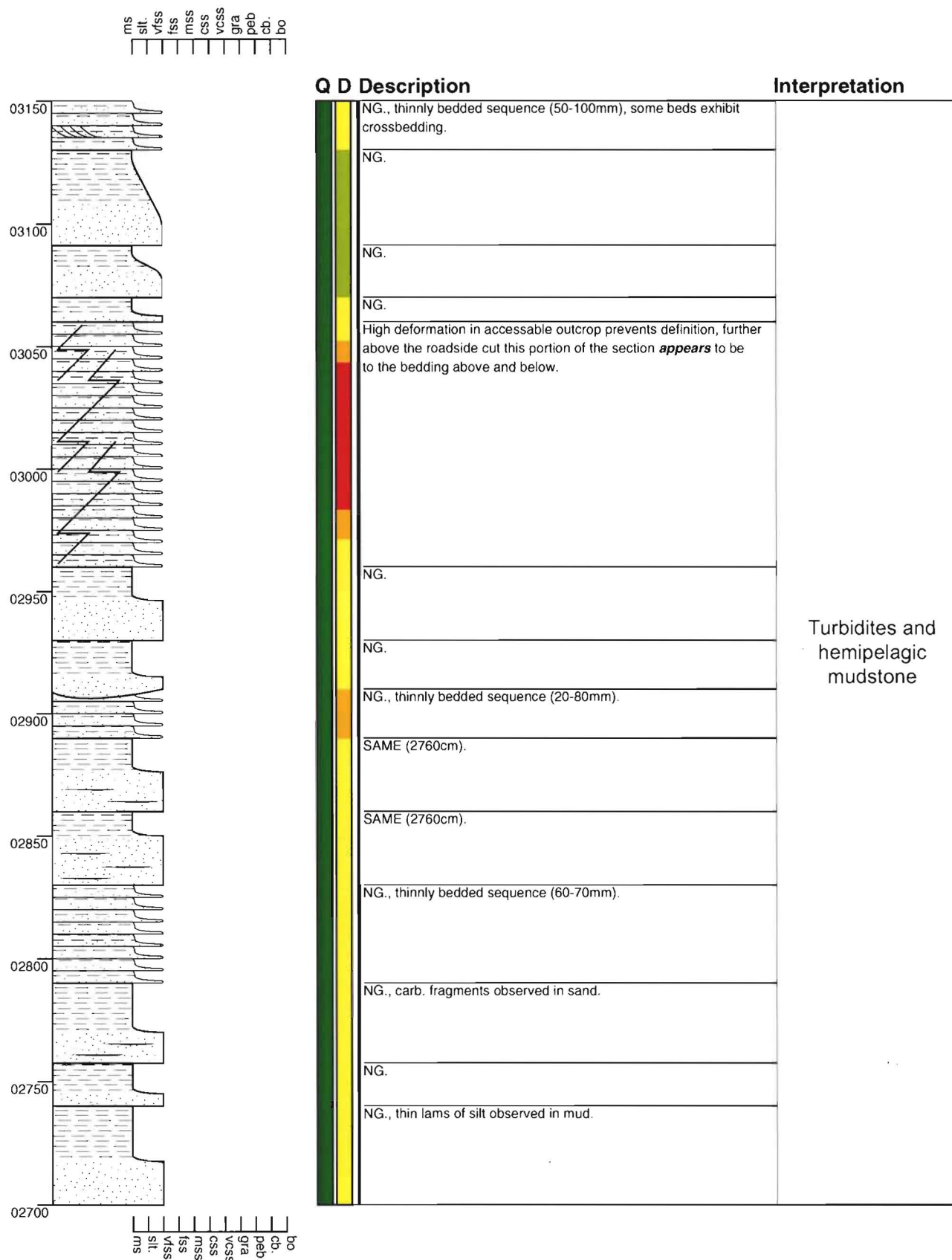
Section - Waiau River WR06

Grid Reference N32 923 469



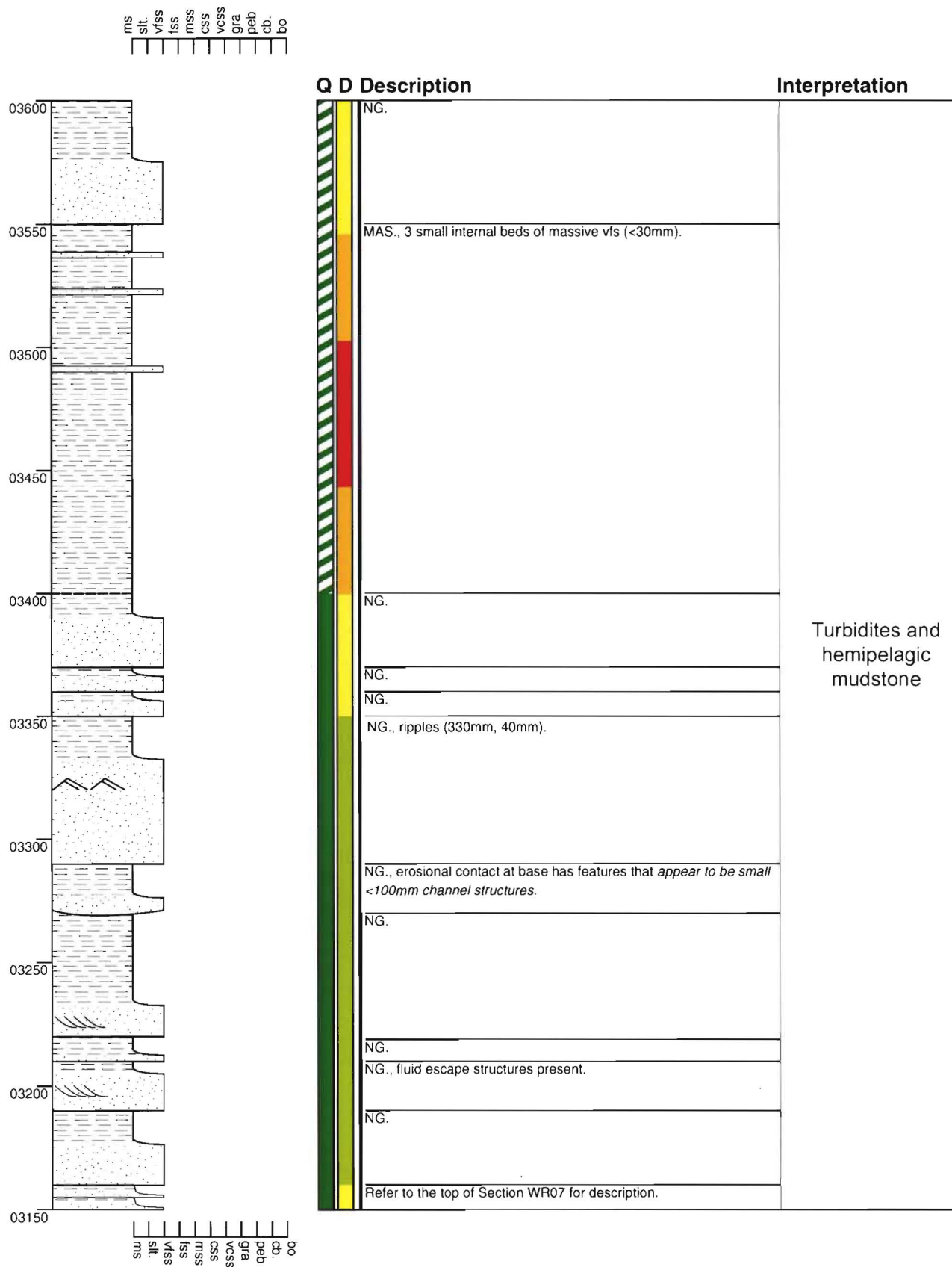
Section - Waiau River WR07

Grid Reference N32 923 469



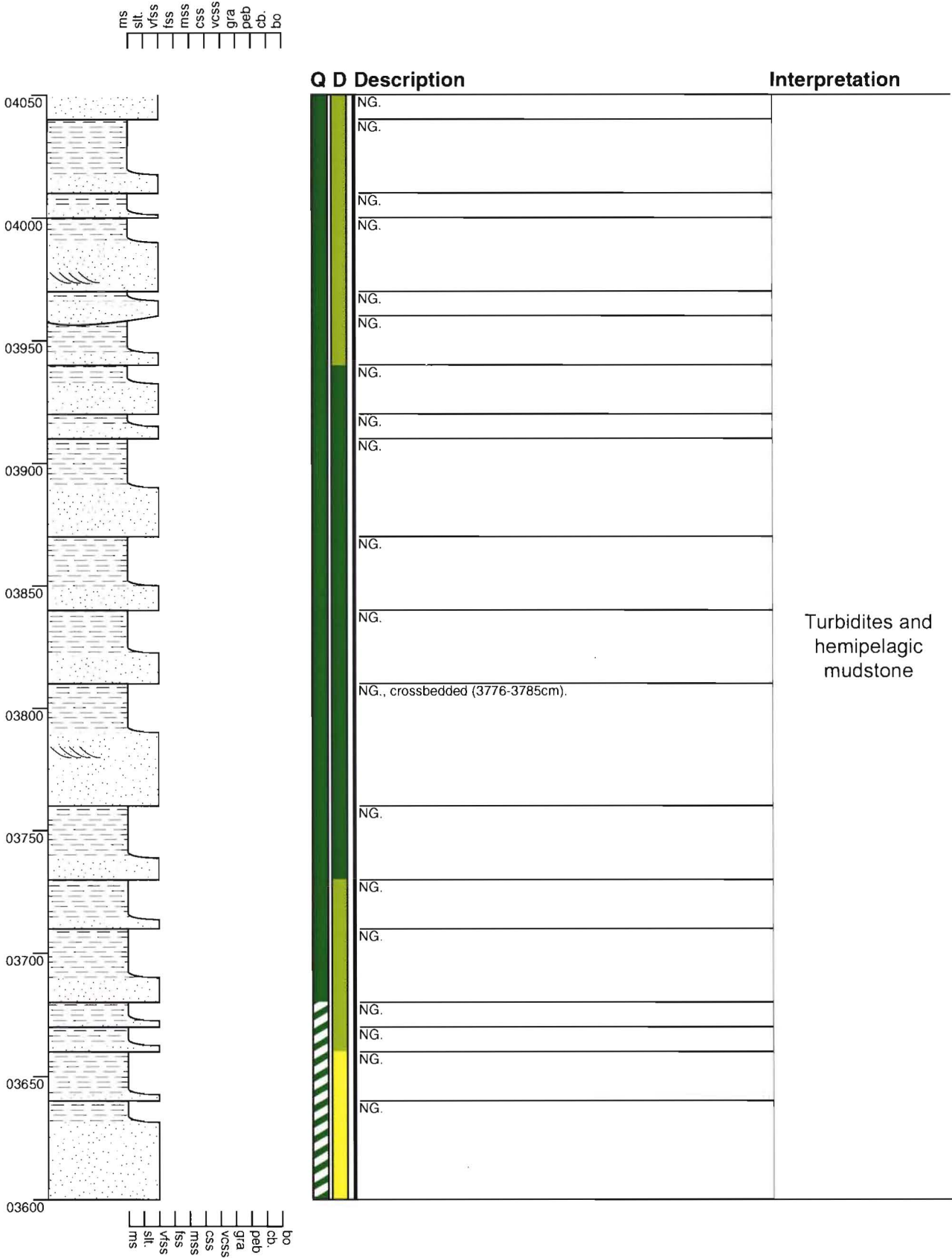
Section - Waiau River WR08

Grid Reference N32 923 469



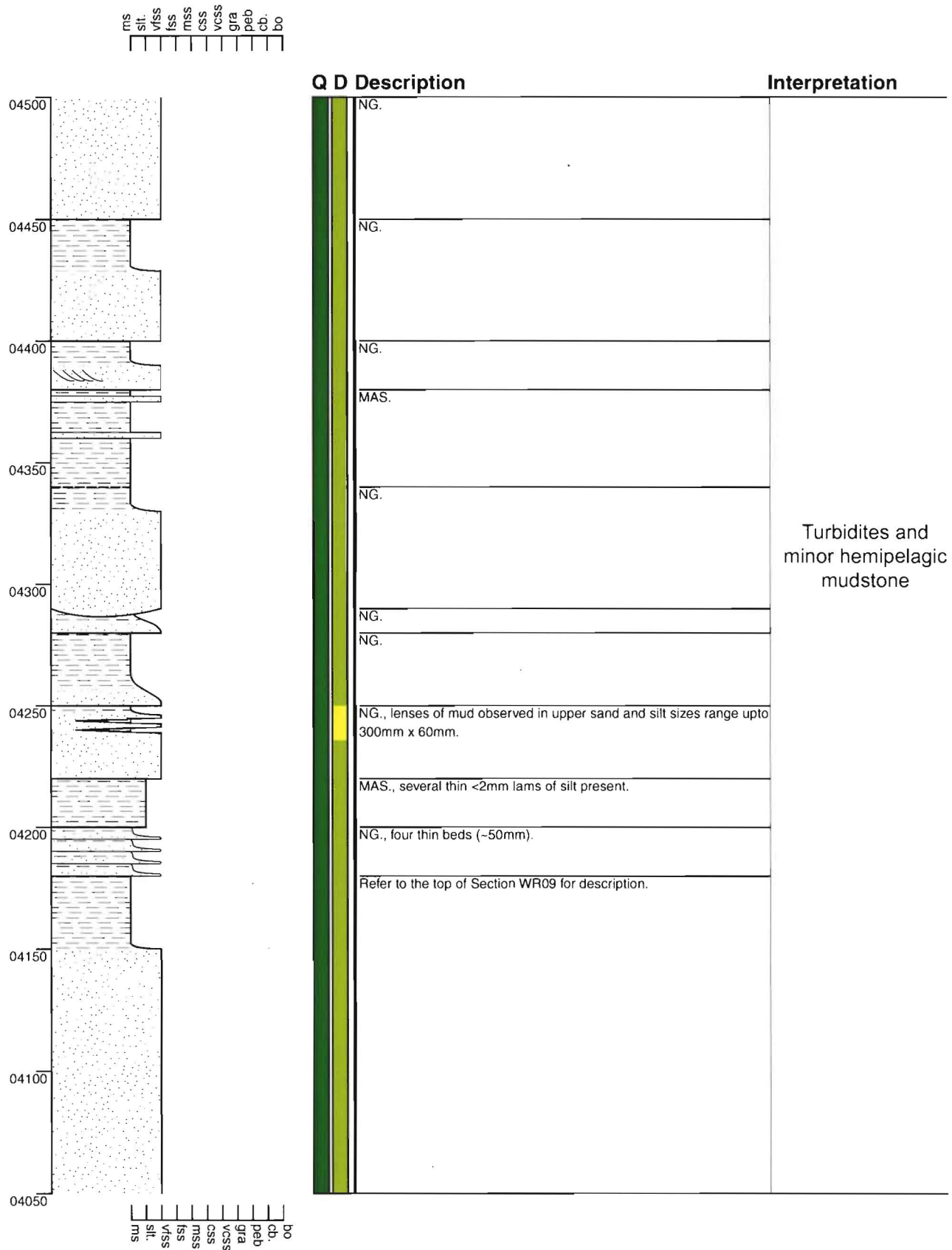
Section - Waiau River WR09

Grid Reference N32 923 469



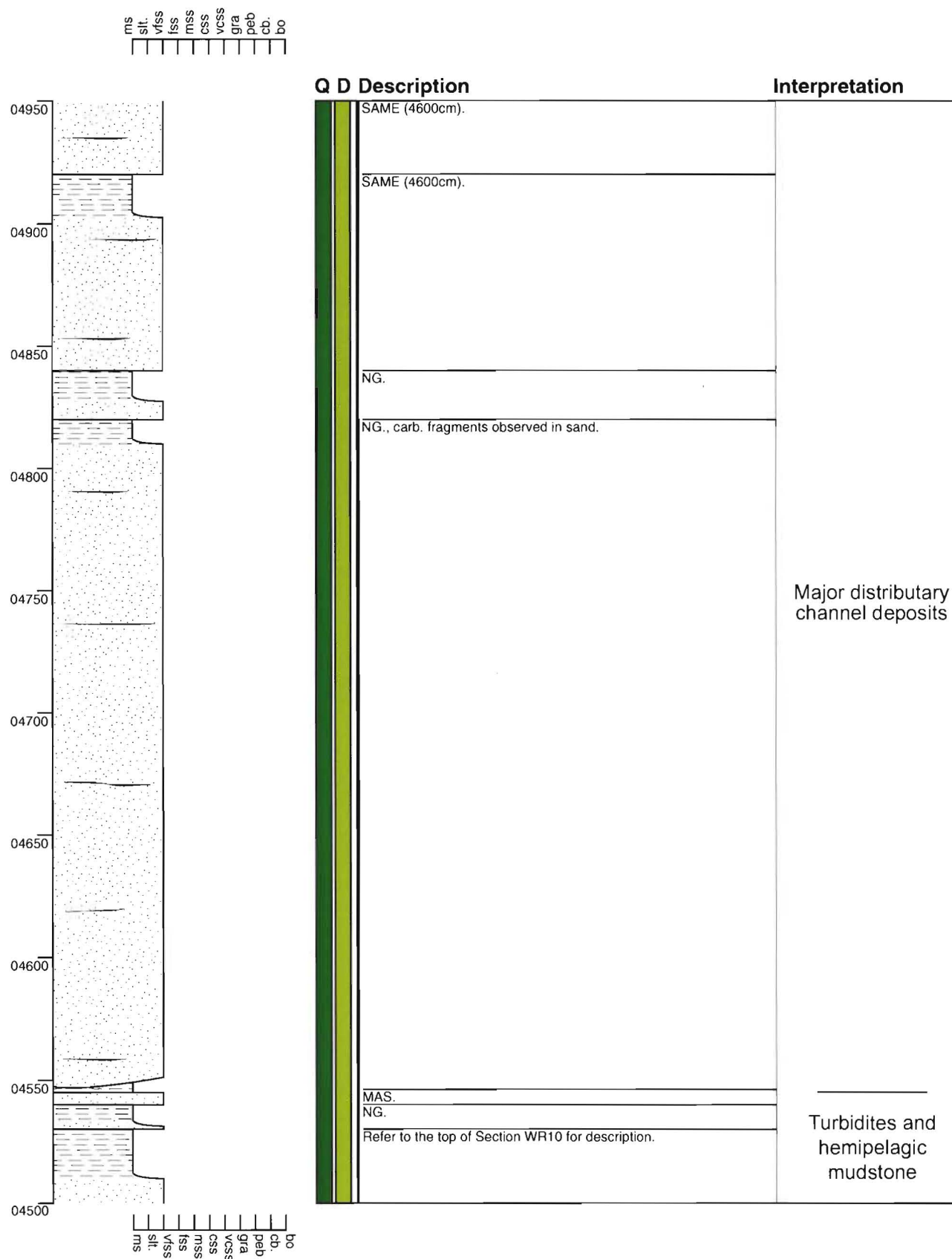
Section - Waiau River WR10

Grid Reference N32 923 469



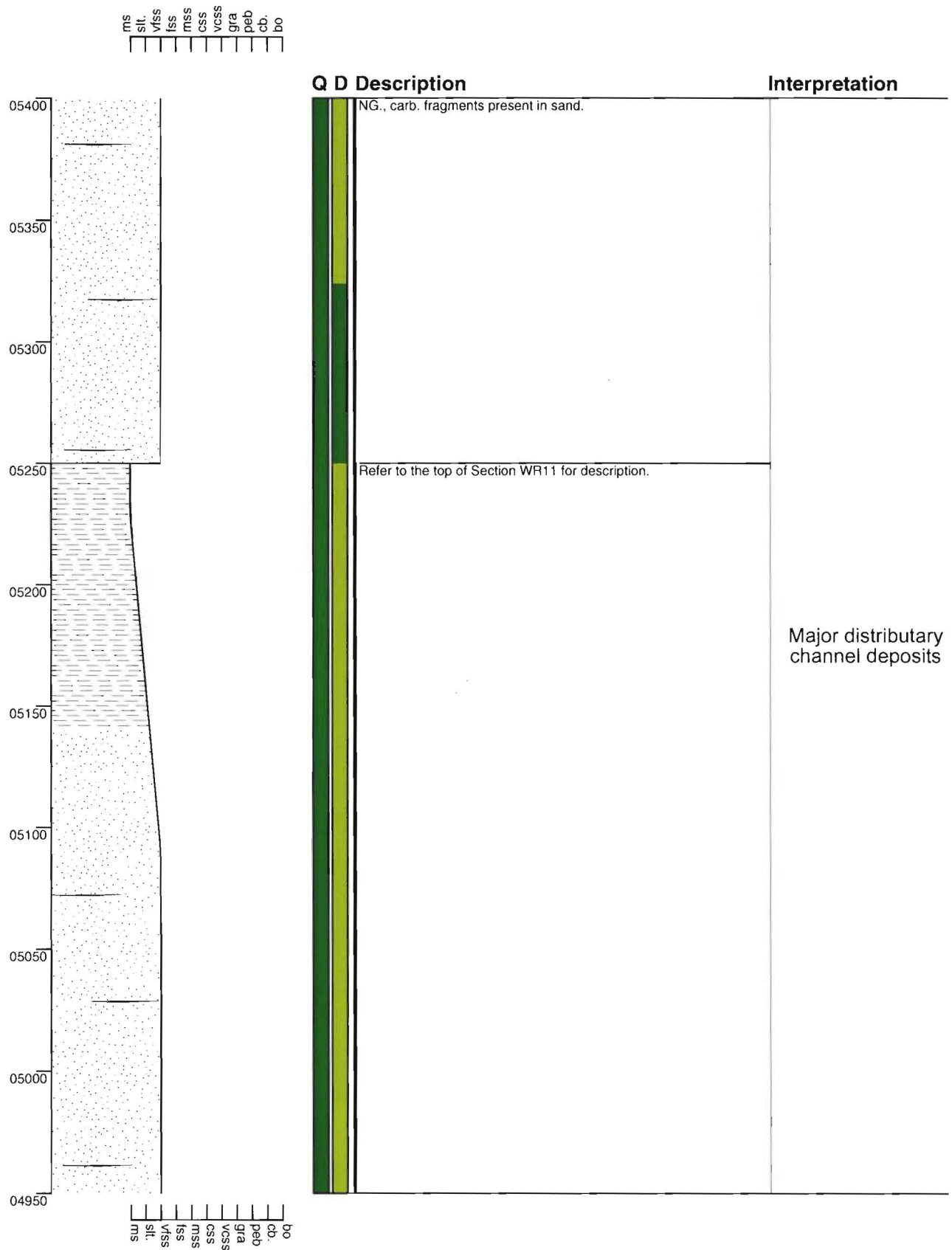
Section - Waiau River WR11

Grid Reference N32 923 469



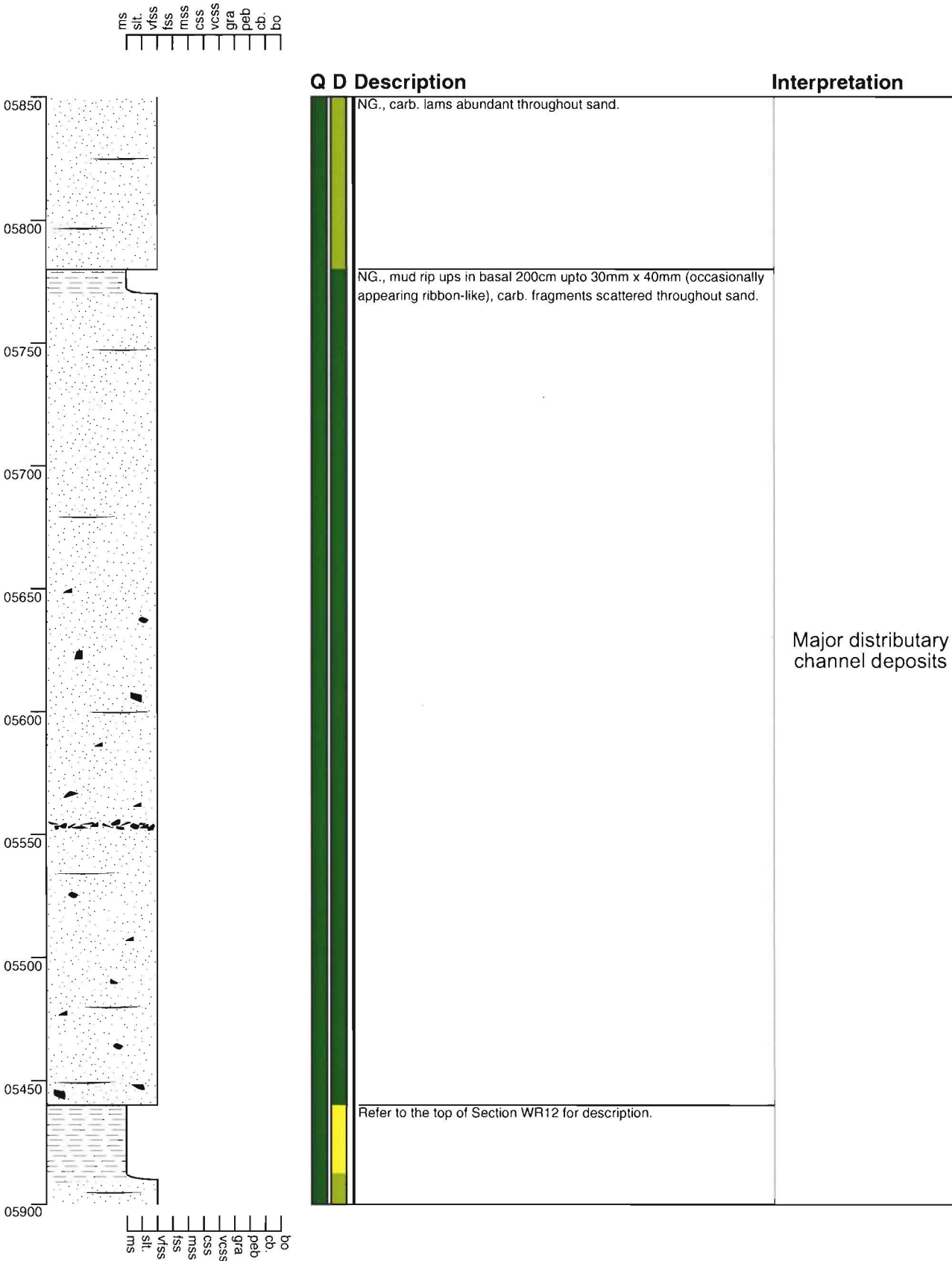
Section - Waiau River WR12

Grid Reference N32 923 469



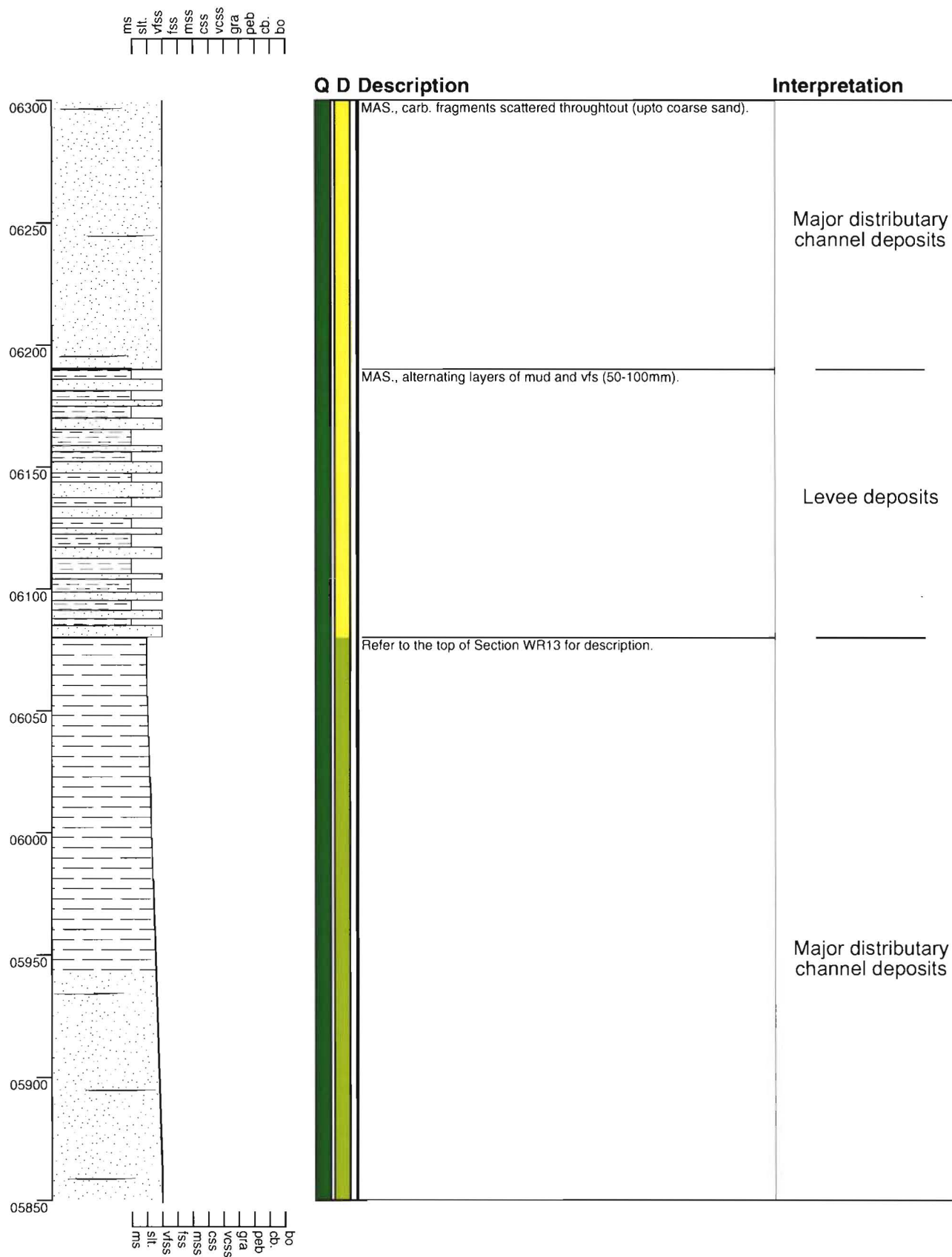
Section - Waiau River WR13

Grid Reference N32 923 469



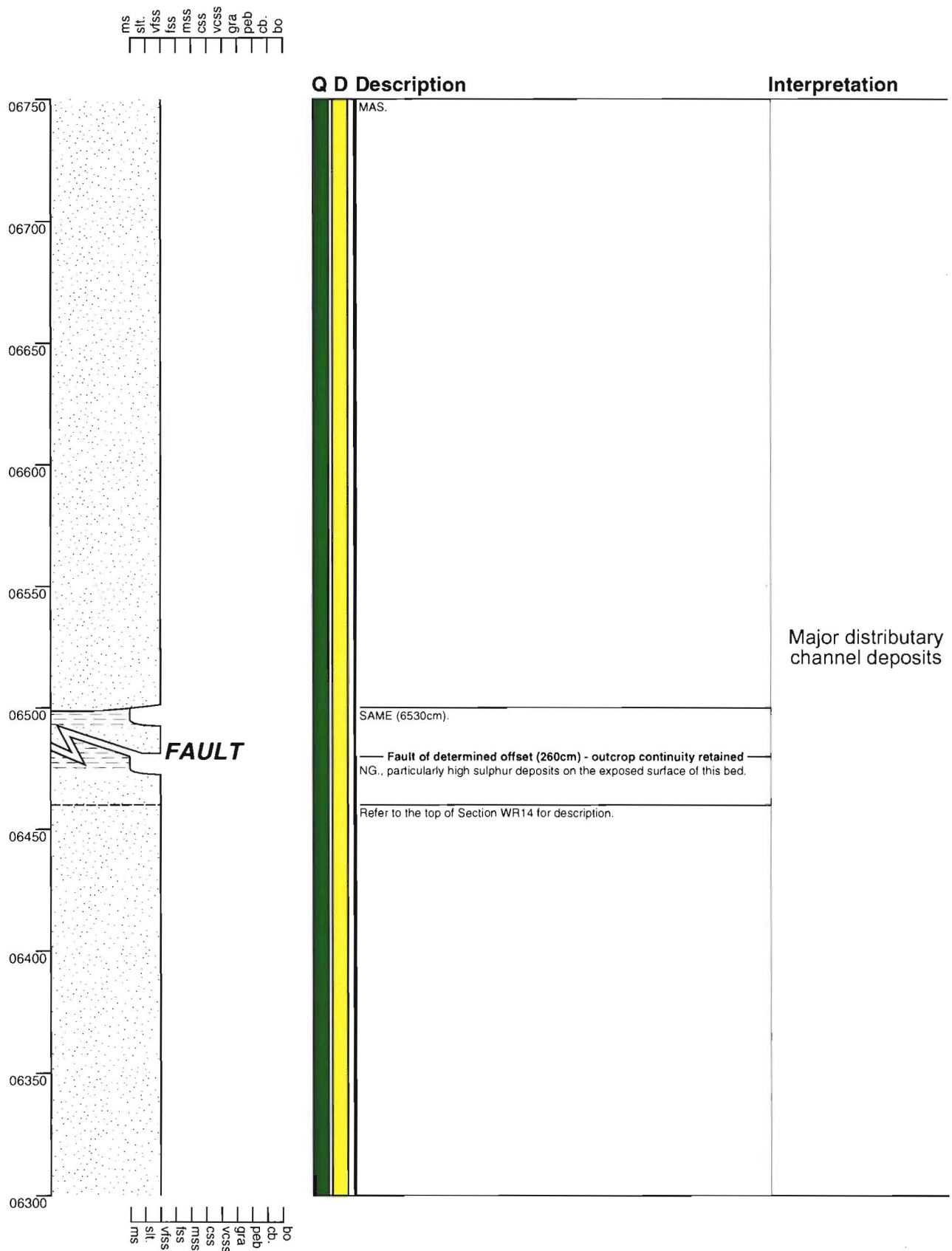
Section - Waiau River WR14

Grid Reference N32 923 469



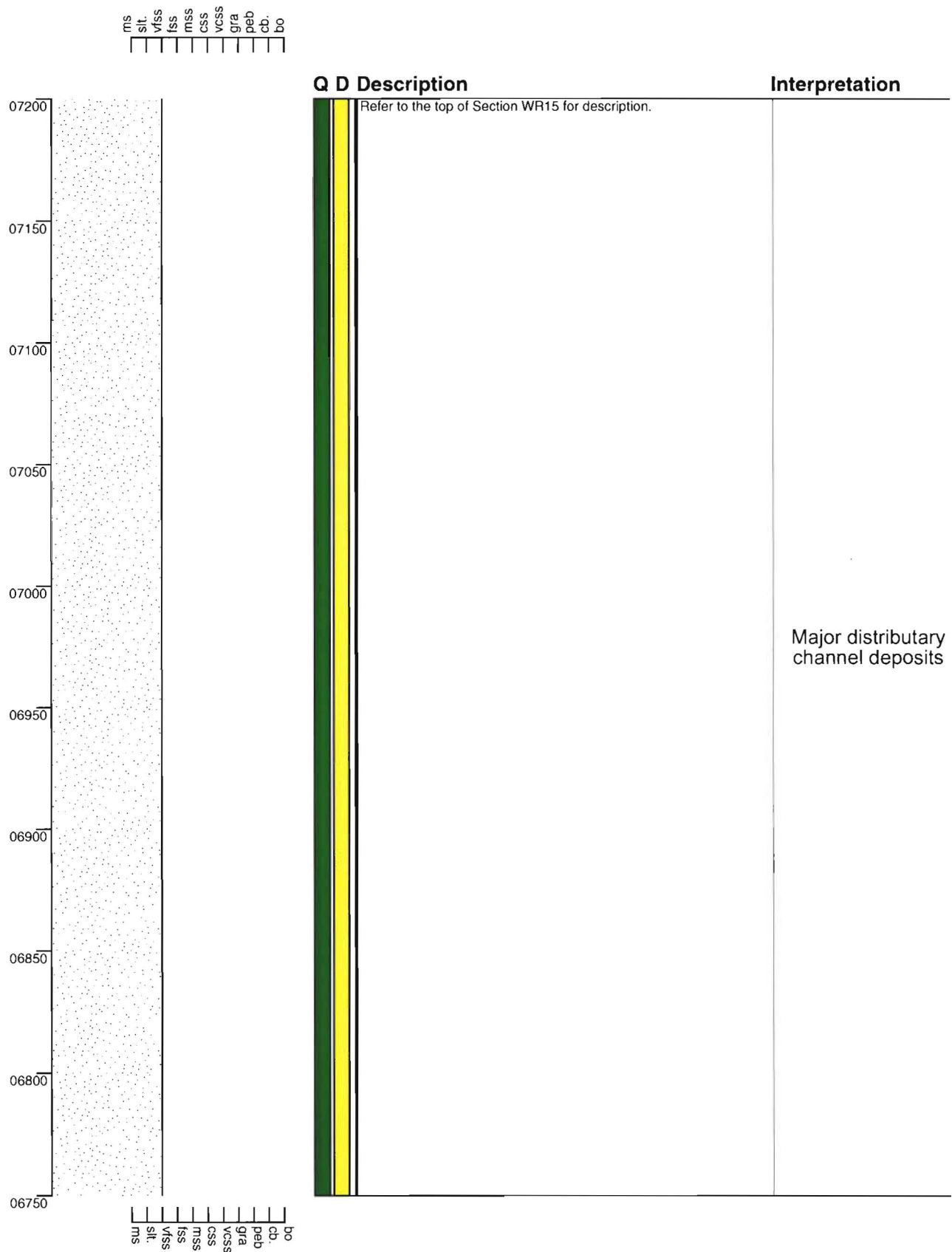
Section - Waiau River WR15

Grid Reference N32 923 469



Section - Waiau River WR16

Grid Reference N32 923 469



Section - Waiau River WR17

Grid Reference N32 923 469

ms
silt
vss
fss
mss
css
vcss
gra
peb
cb.
bo

07650
07600
07550
07500
07450
07400
07350
07300
07250
07200

bo
cb.
peb
gra
vcss
css
mss
fss
vss
silt
ms

Q D Description

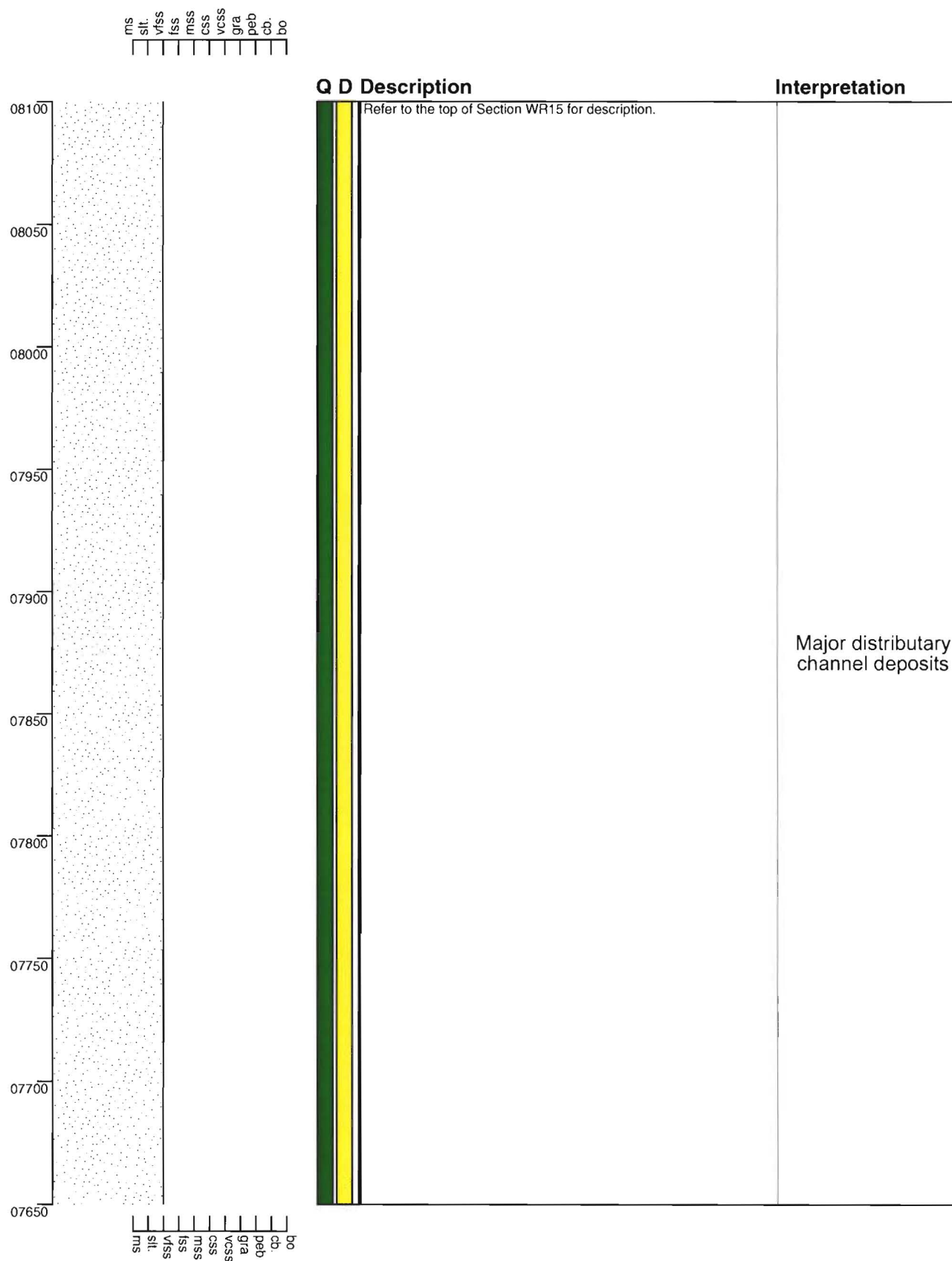
Refer to the top of Section WR15 for description.

Interpretation

Major distributary
channel deposits

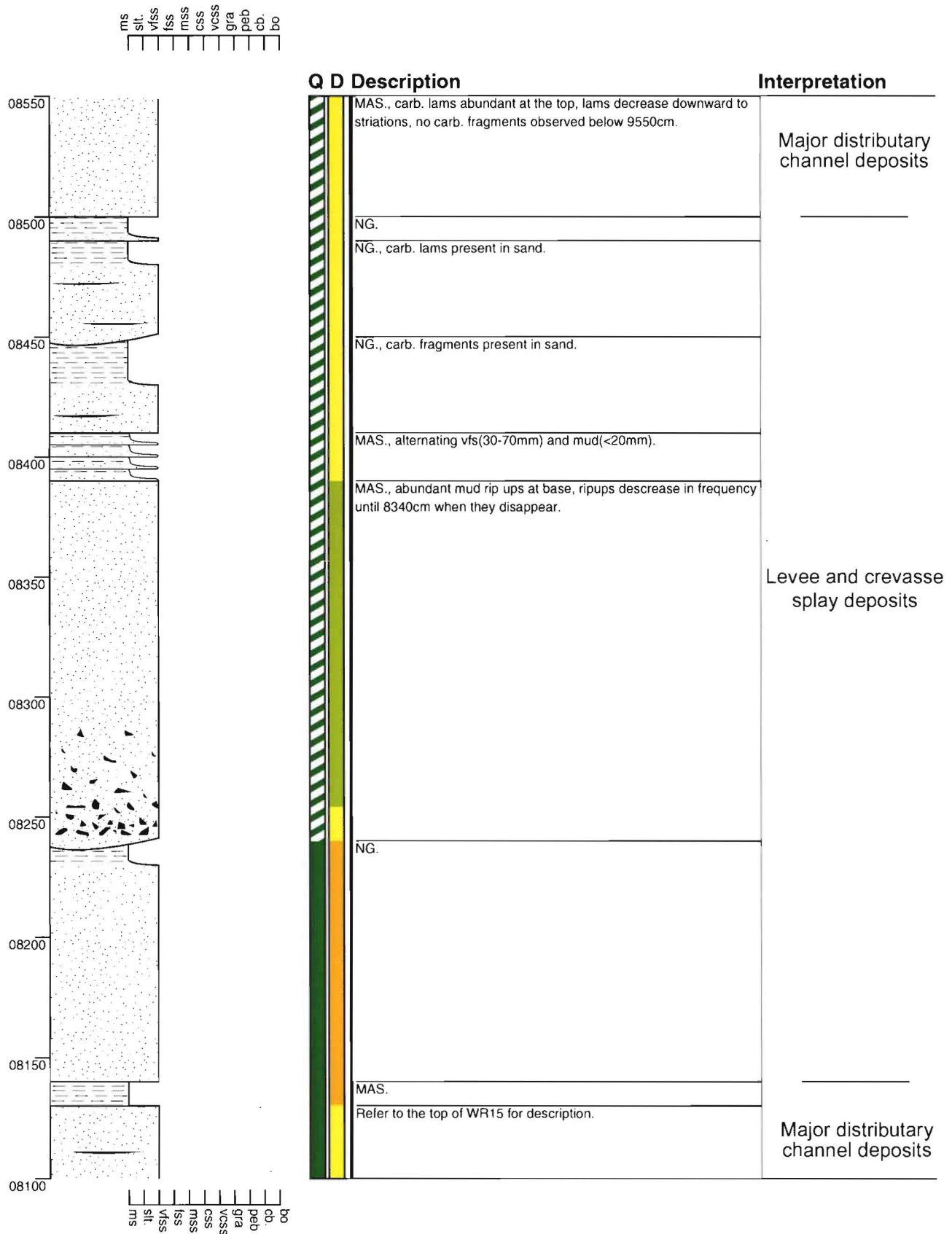
Section - Waiau River WR18

Grid Reference N32 923 469



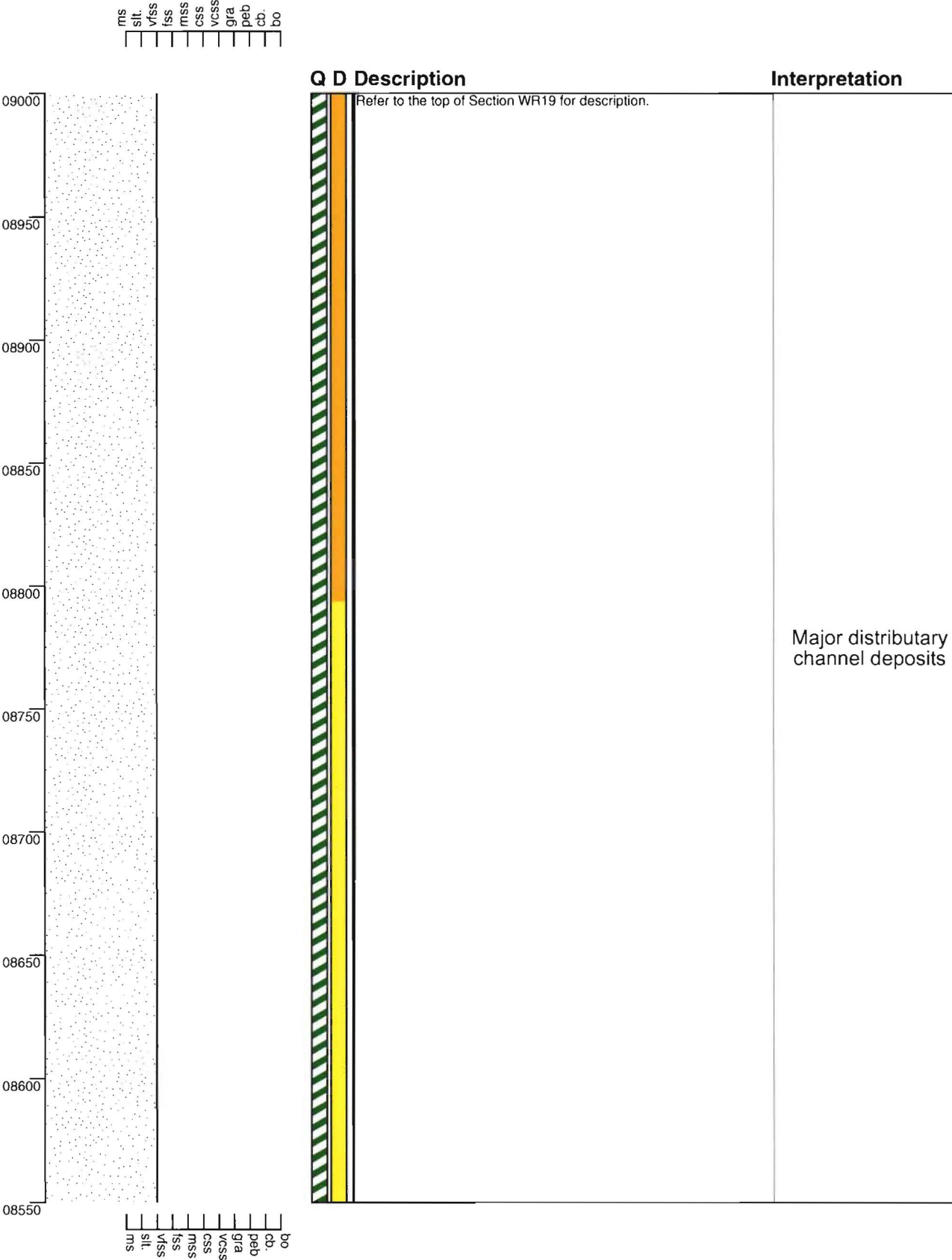
Section - Waiau River WR19

Grid Reference N32 923 469



Section - Waiau River WR20

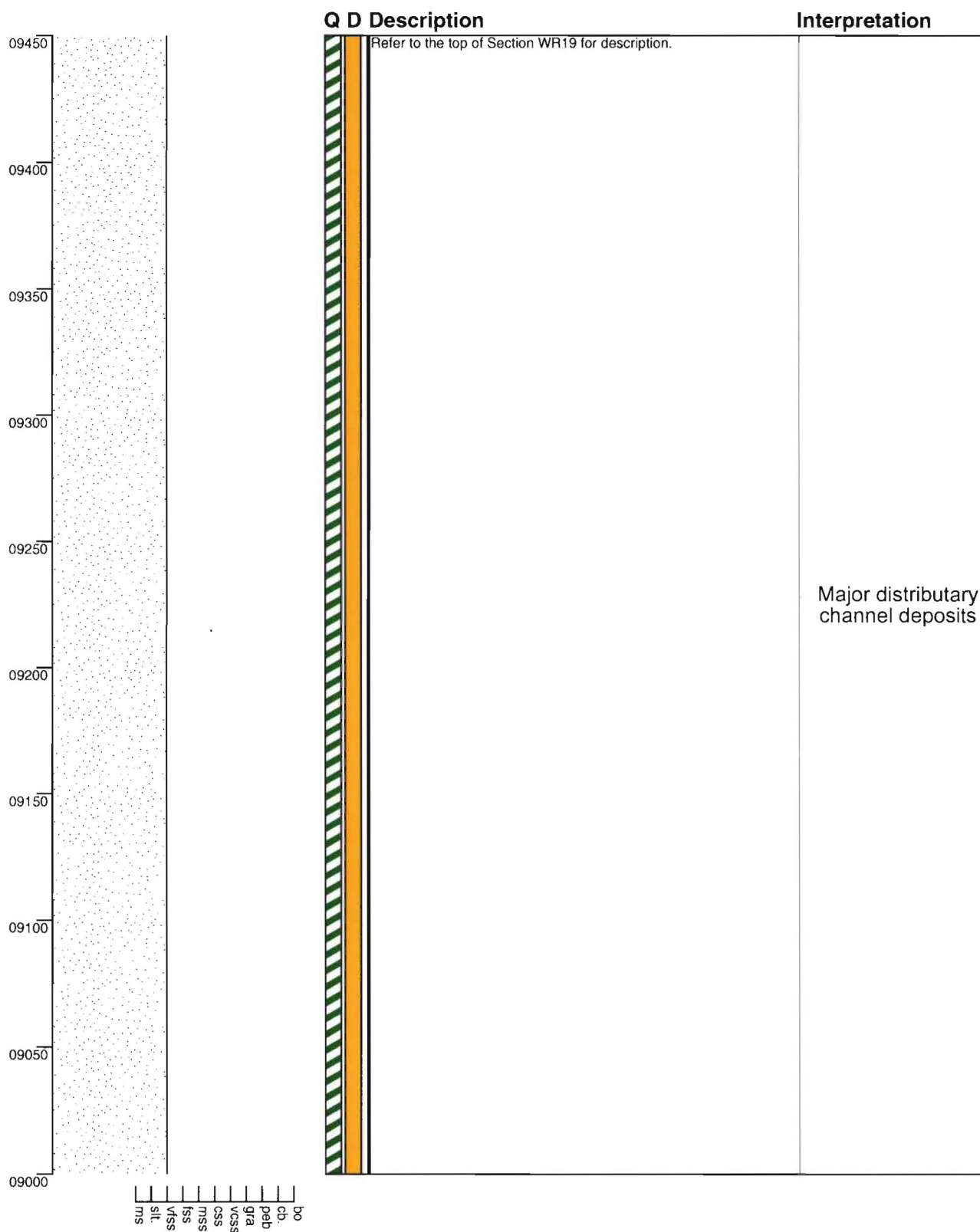
Grid Reference N32 923 469



Section - Waiau River WR21

Grid Reference N32 923 469

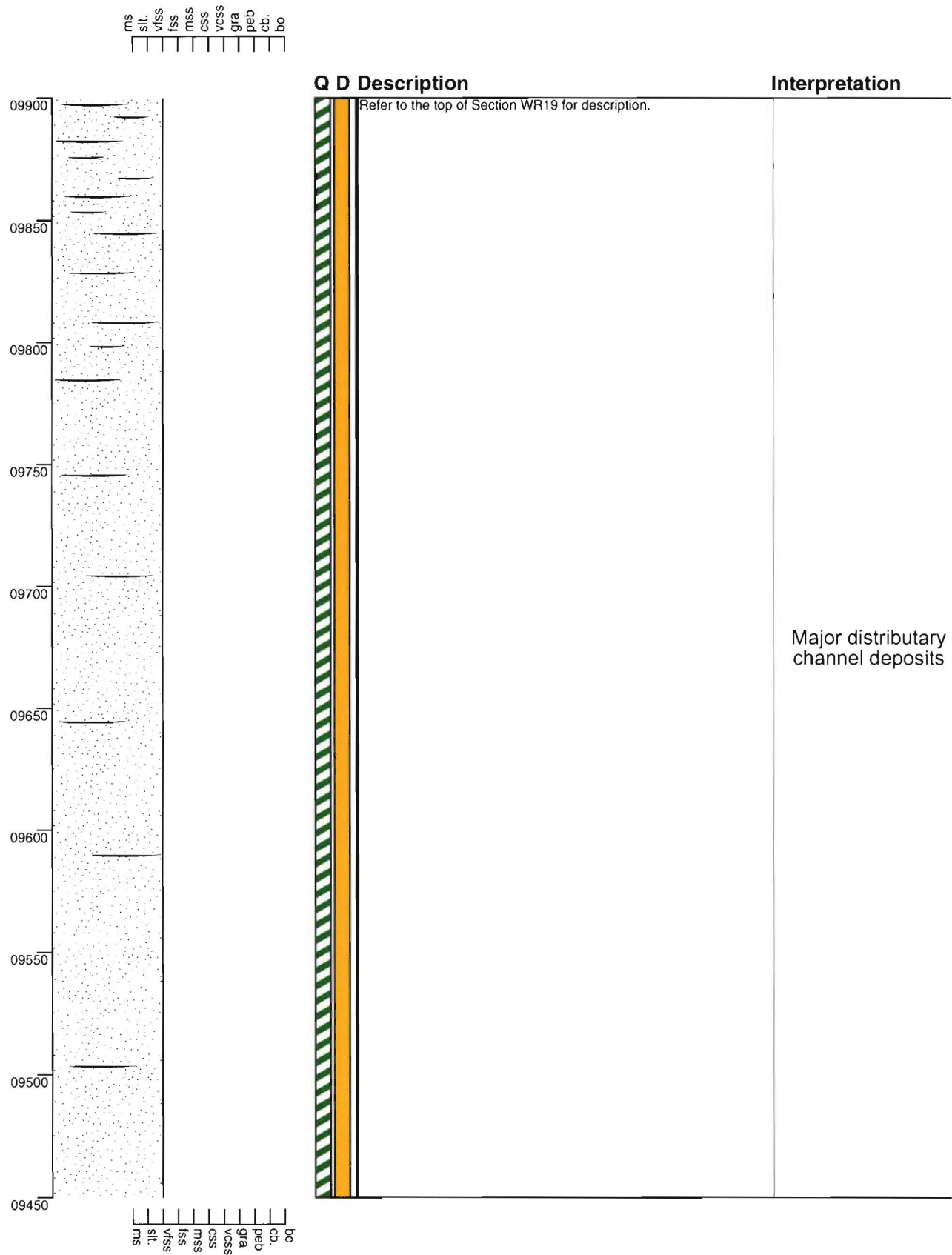
ms
silt
vss
fss
mss
css
vcss
gra
peb
cb
bo



Major distributary
channel deposits

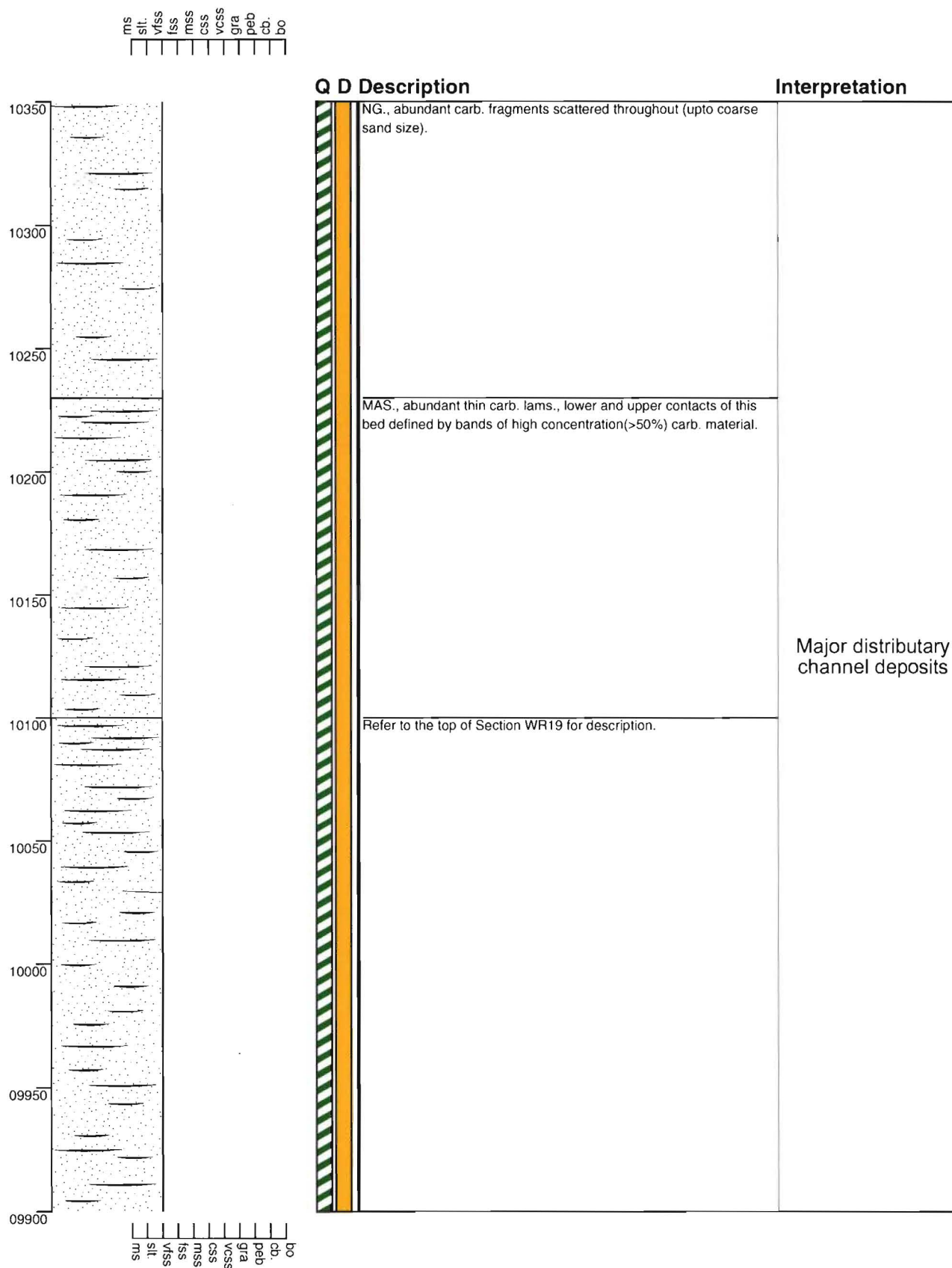
Section - Waiau River WR22

Grid Reference N32 923 469



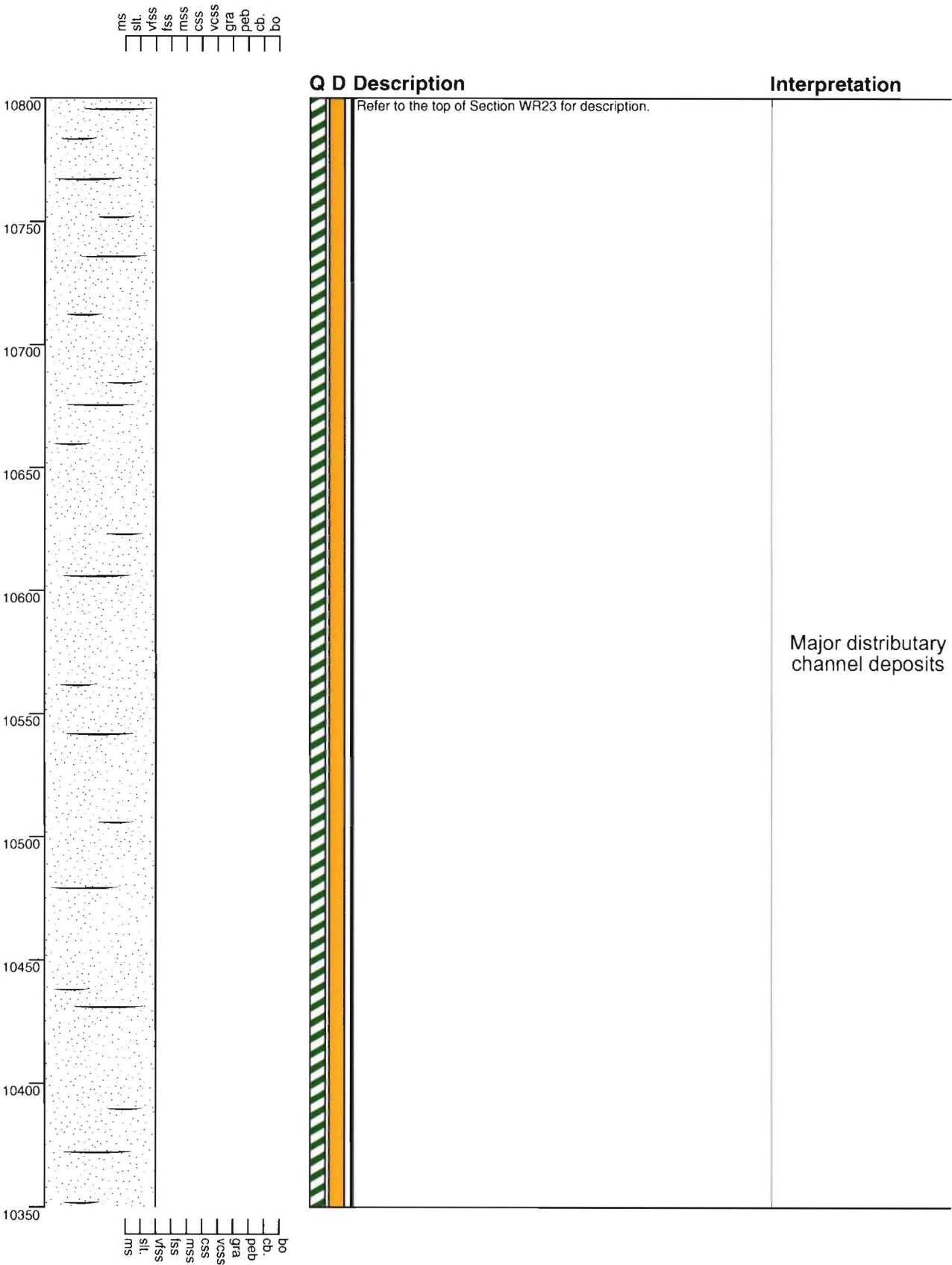
Section - Waiau River WR23

Grid Reference N32 923 469



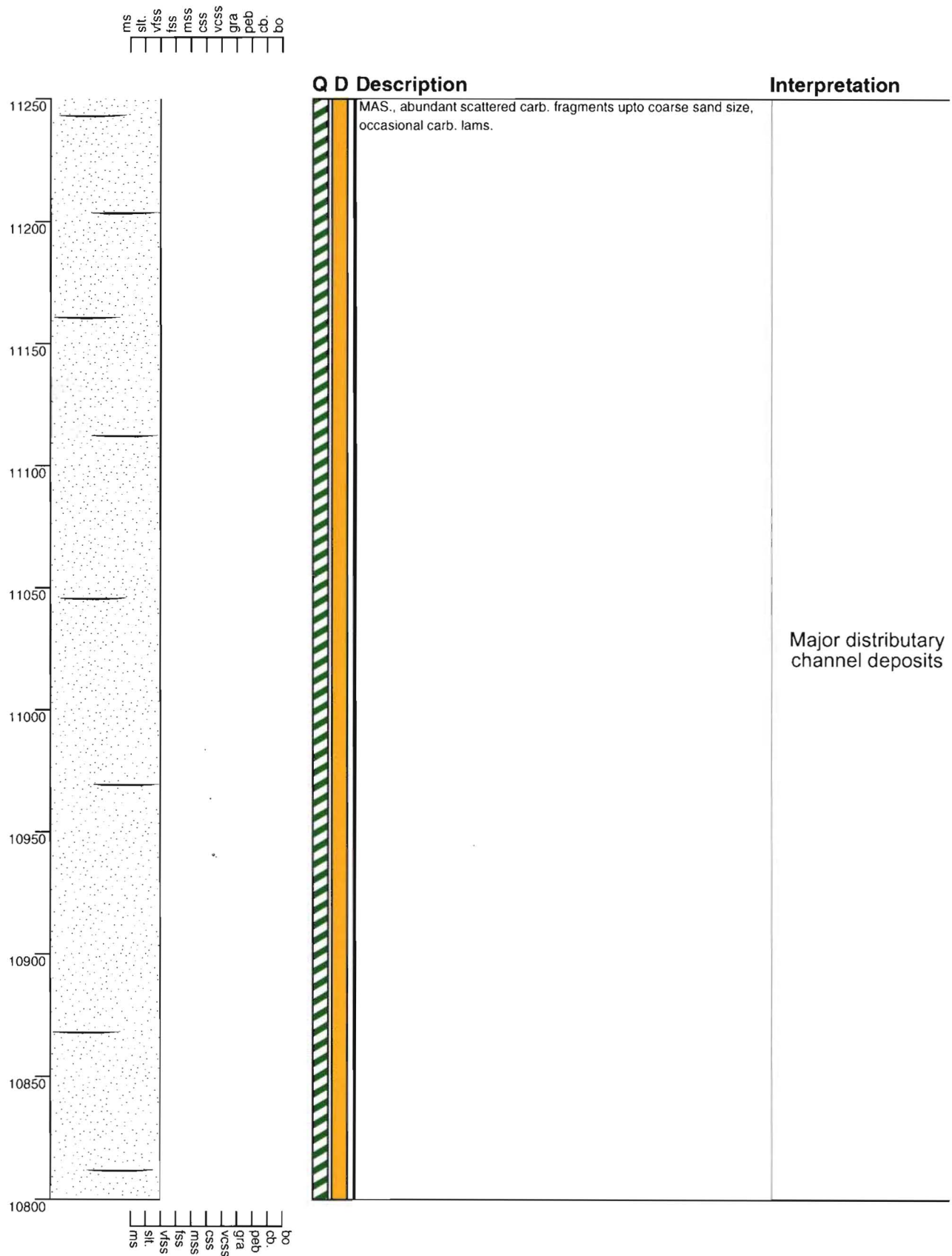
Section - Waiau River WR24

Grid Reference N32 923 469



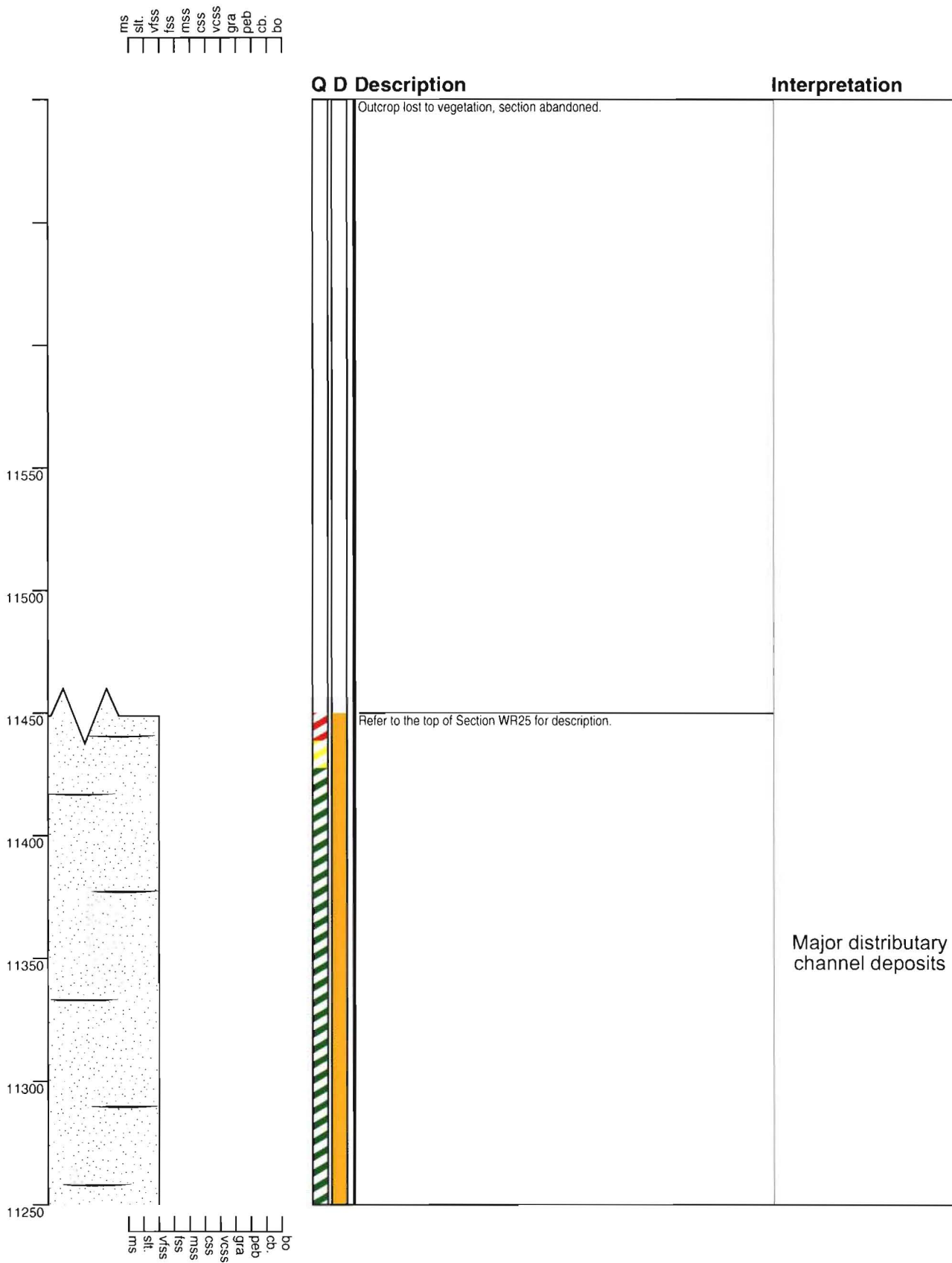
Section - Waiau River WR25

Grid Reference N32 923 469



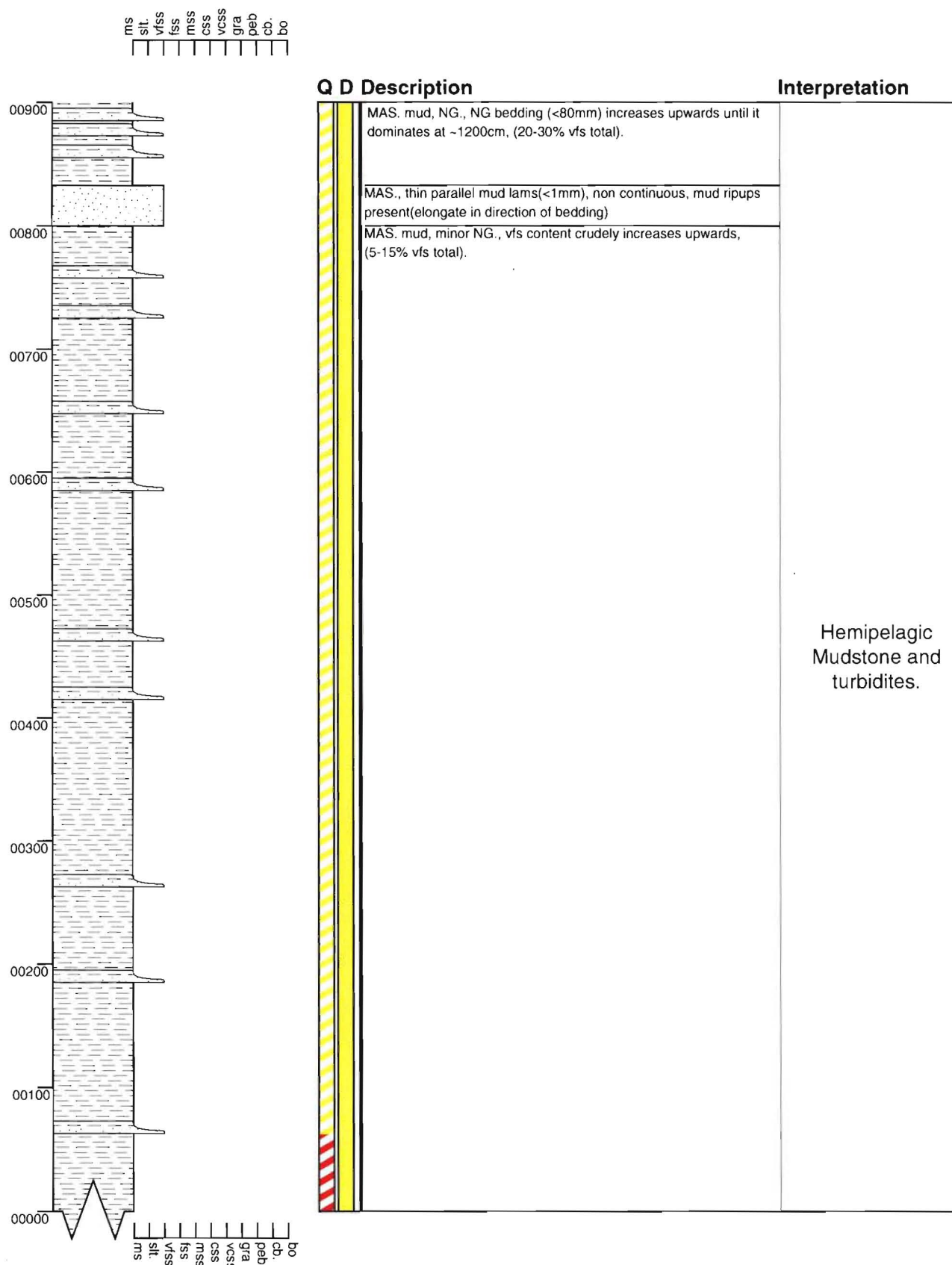
Section - Waiau River WR26

Grid Reference N32 923 469



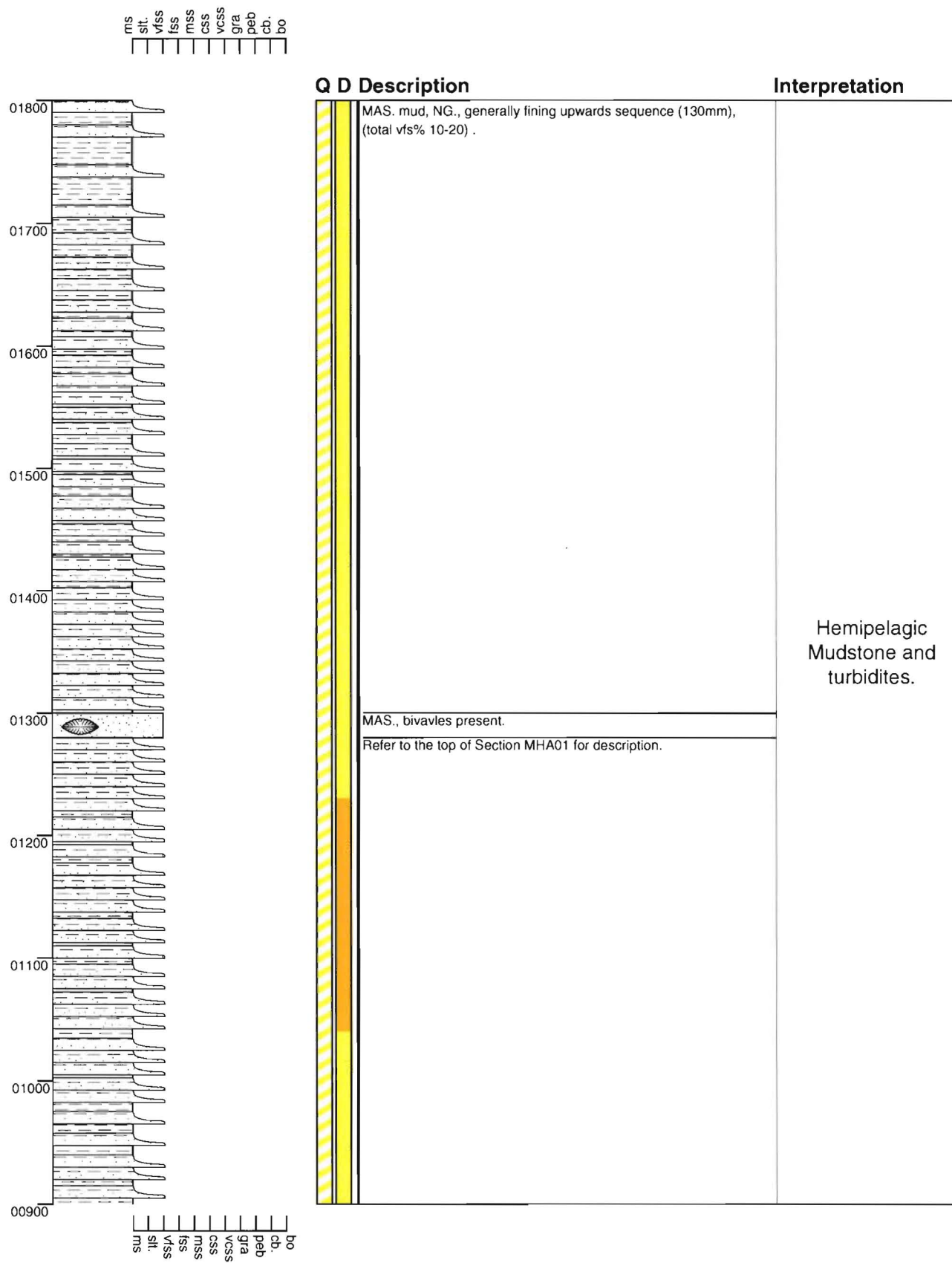
Section - Mt Holmes MH01

Grid Reference N32 907 465



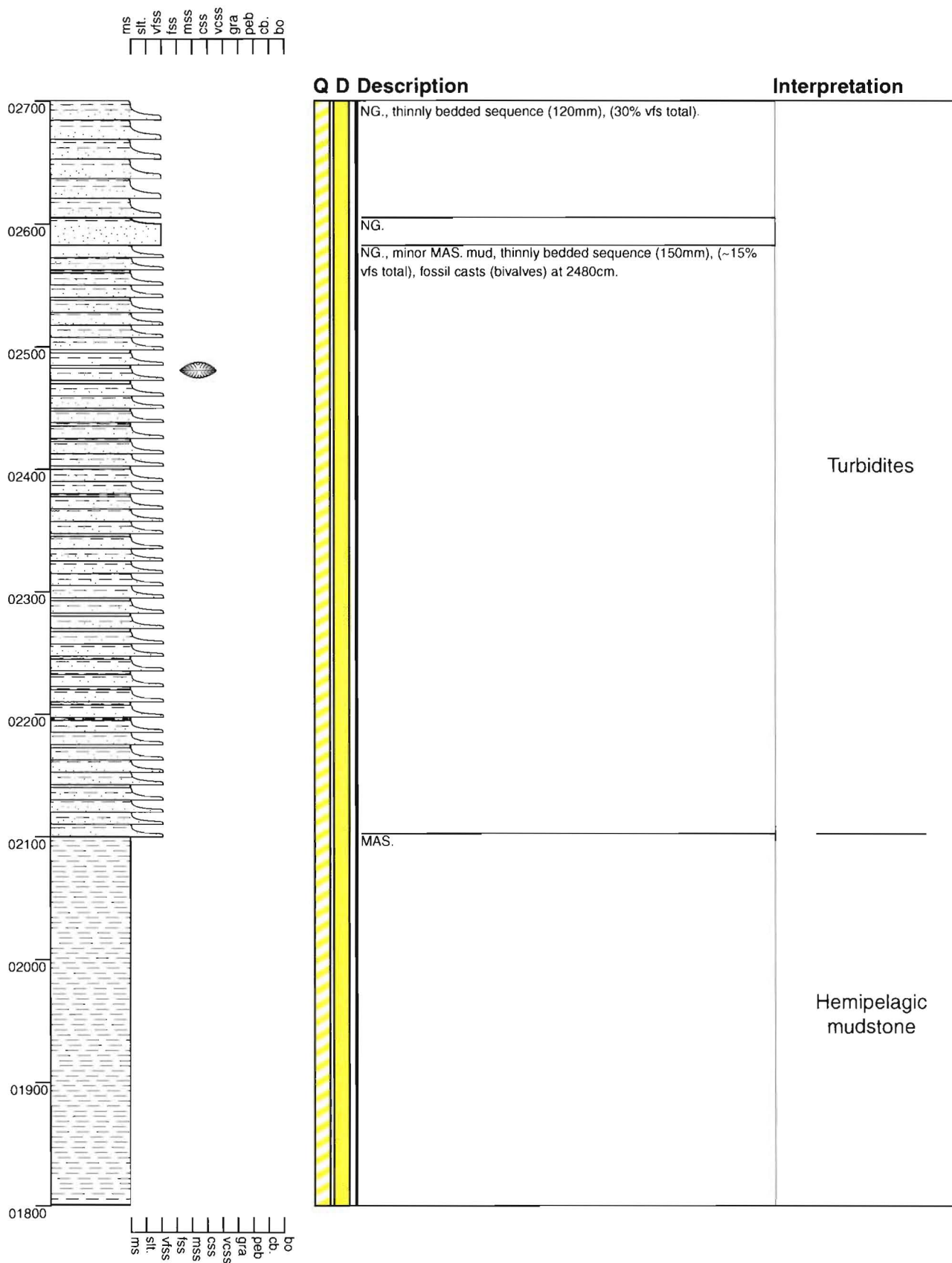
Section - Mt Holmes MH02

Grid Reference N32 907 465



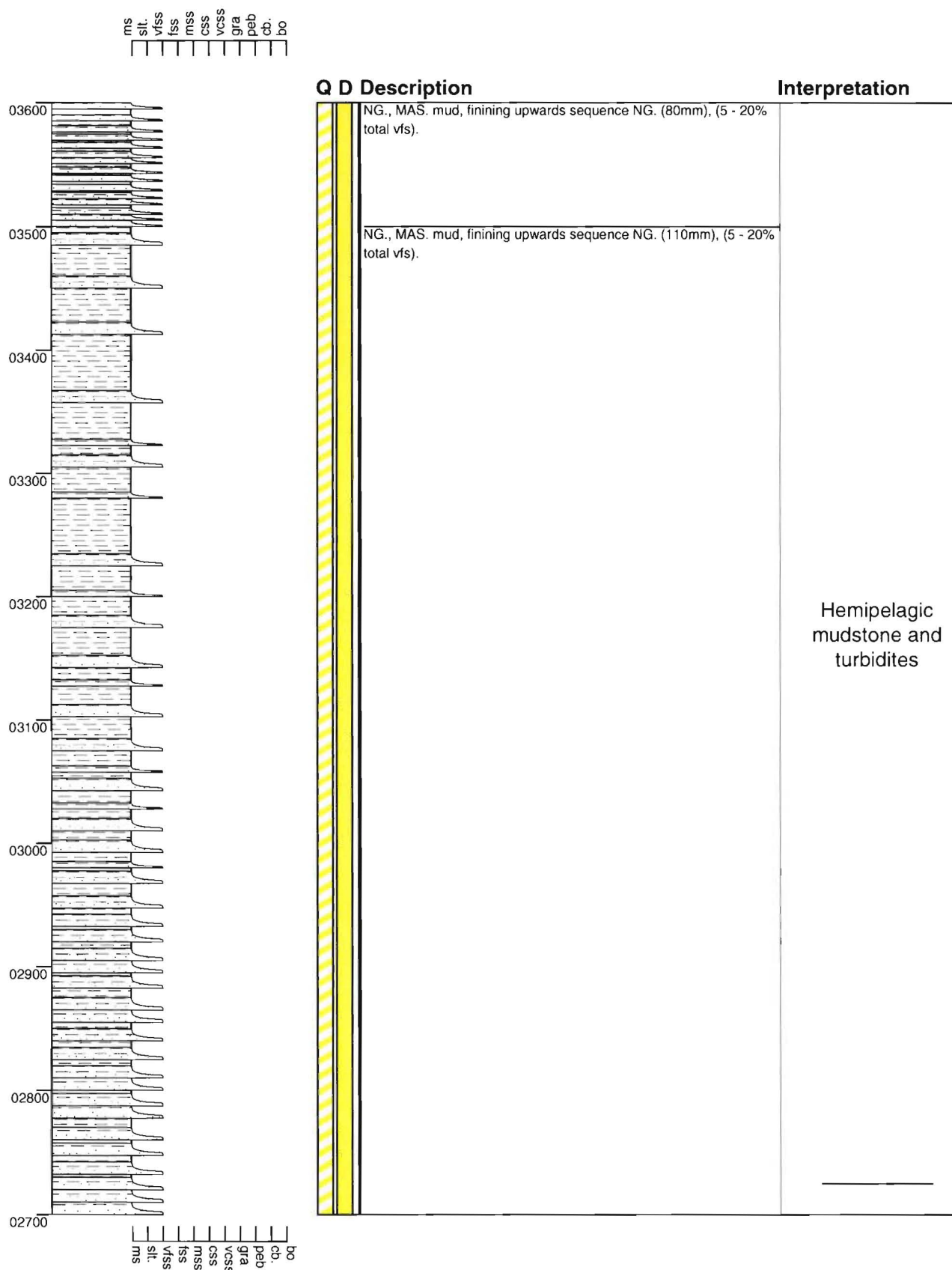
Section - Mt Holmes MH03

Grid Reference N32 907 465



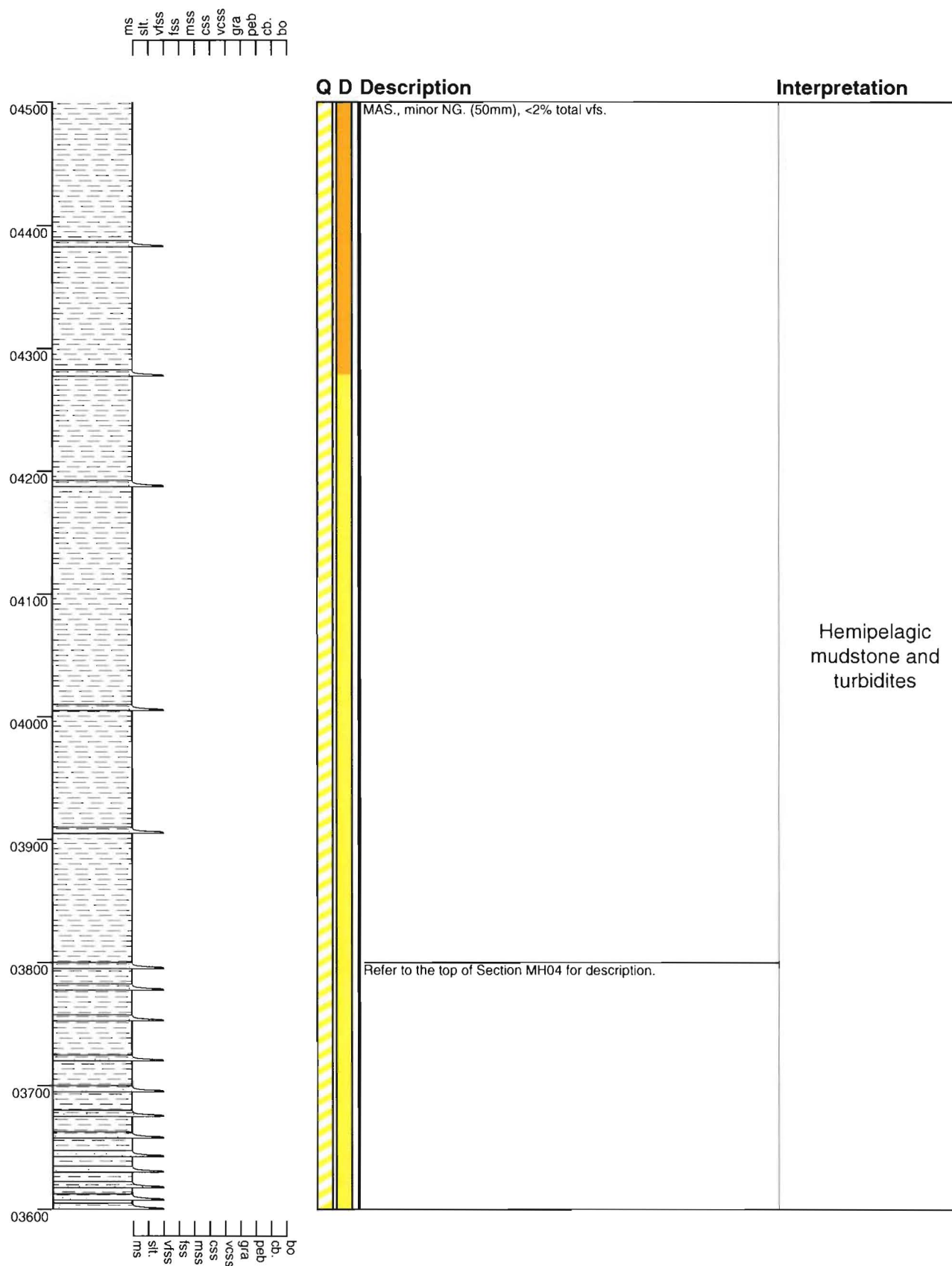
Section - Mt Holmes MH04

Grid Reference N32 907 465



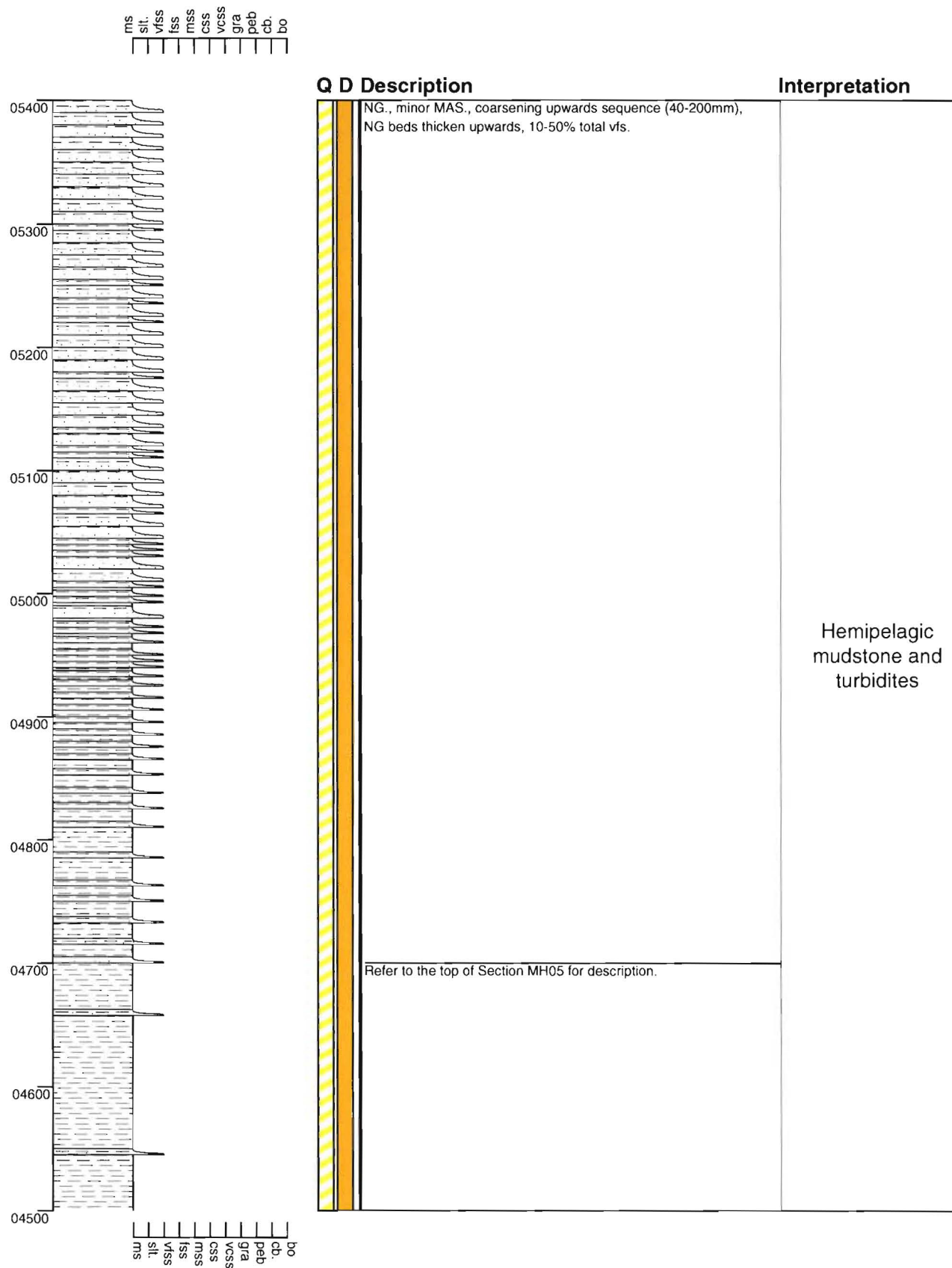
Section - Mt Holmes MH05

Grid Reference N32 907 465



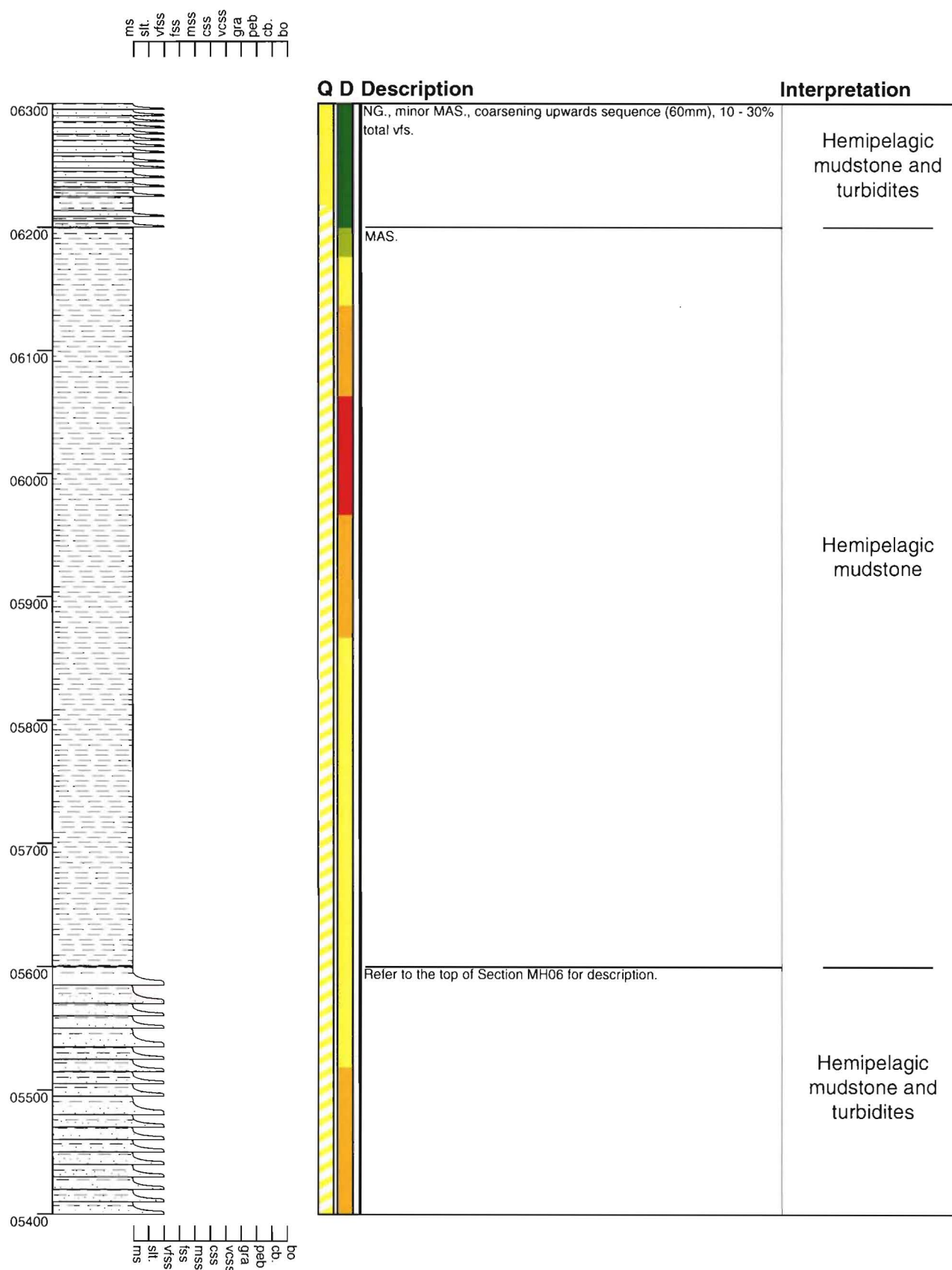
Section - Mt Holmes MH06

Grid Reference N32 907 465



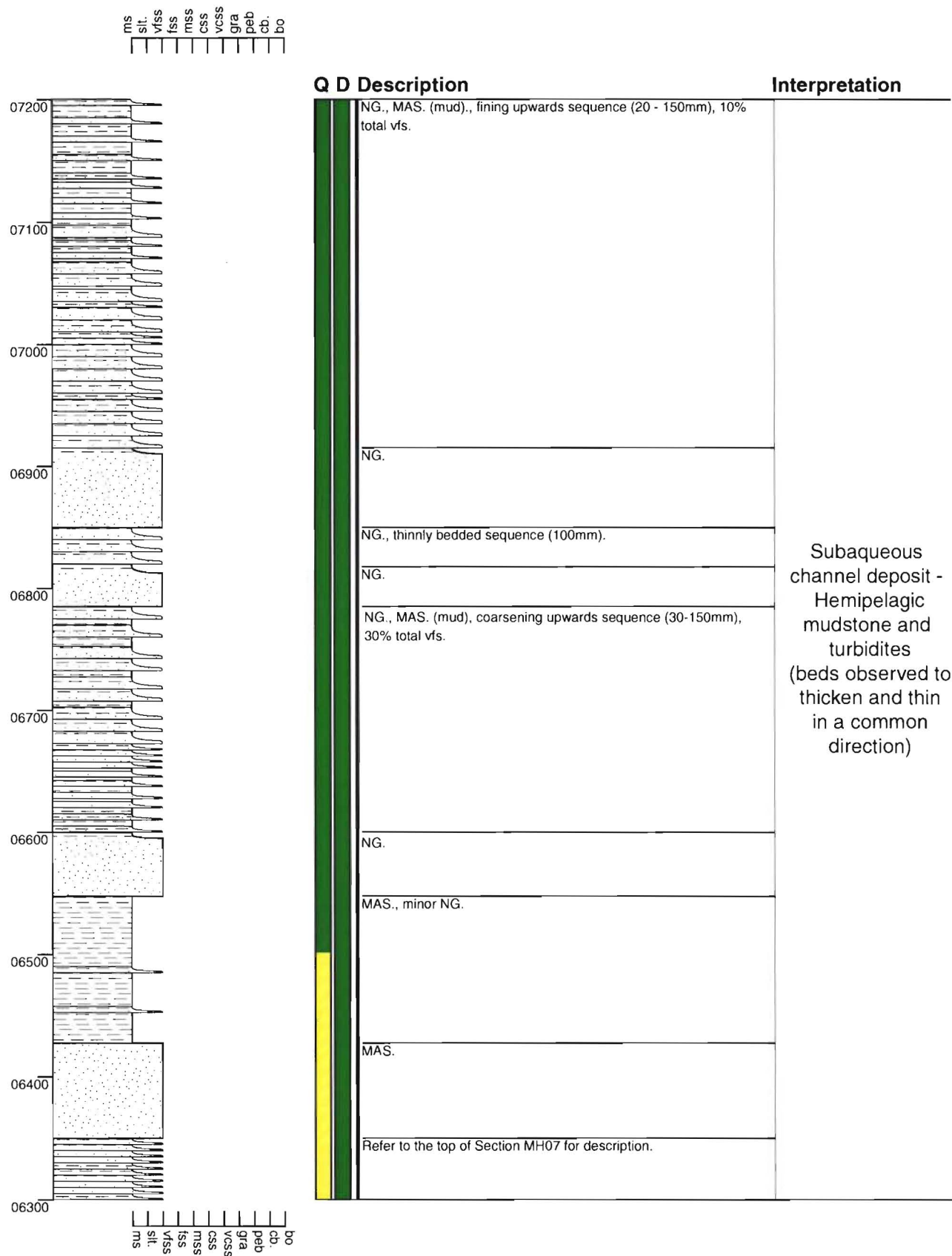
Section - Mt Holmes MH07

Grid Reference N32 907 465



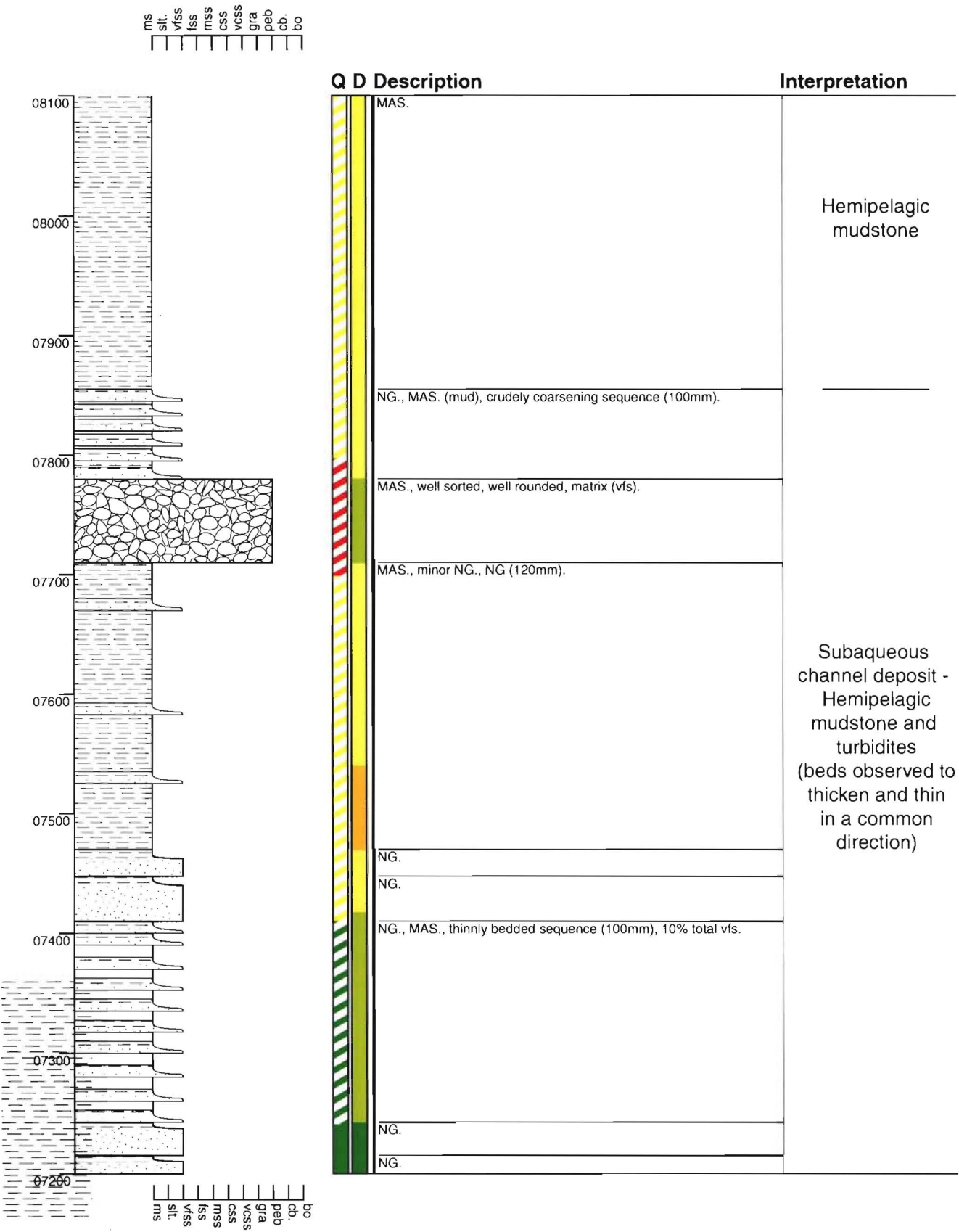
Section - Mt Holmes MH08

Grid Reference N32 907 465



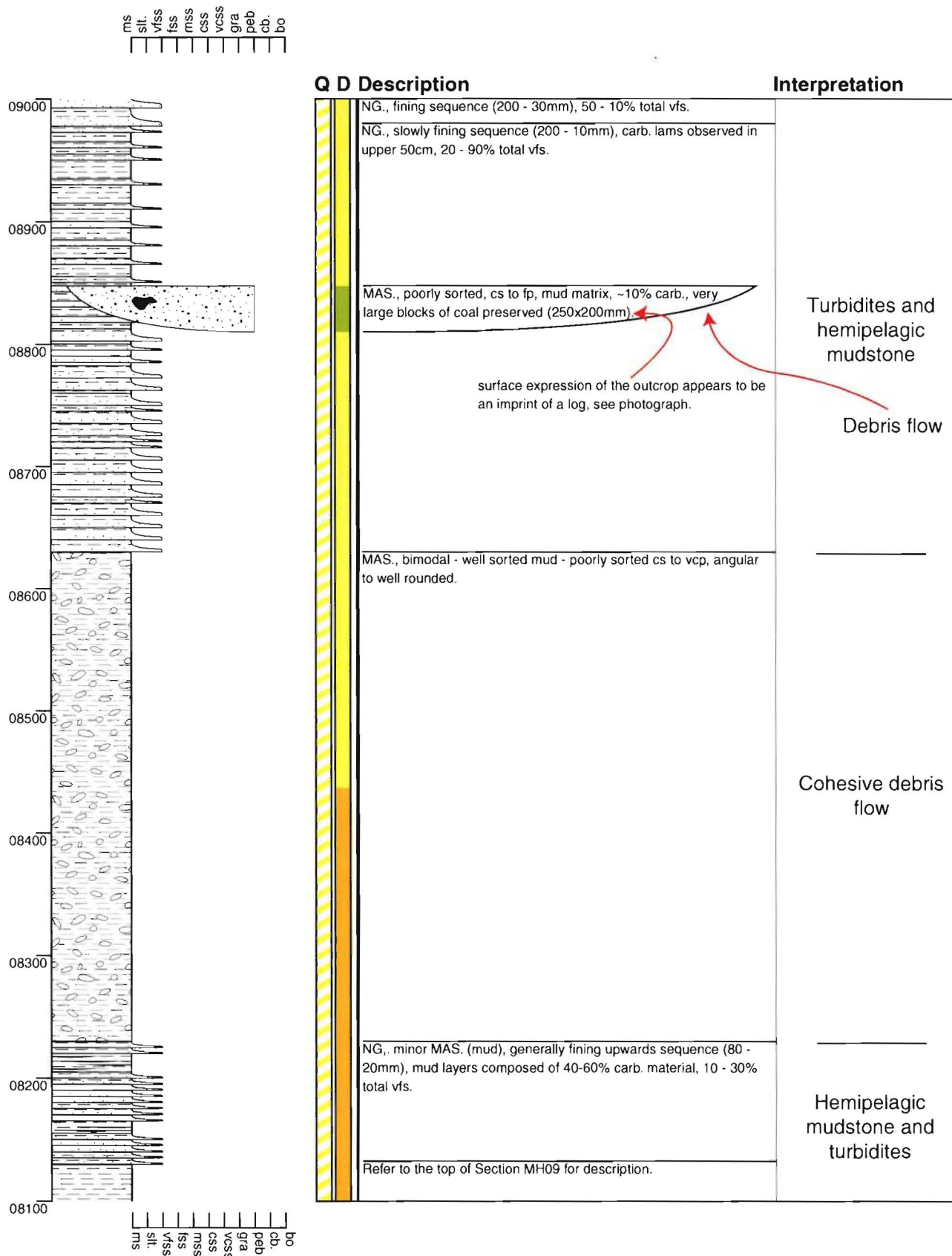
Section - Mt Holmes MH09

Grid Reference N32 907 465



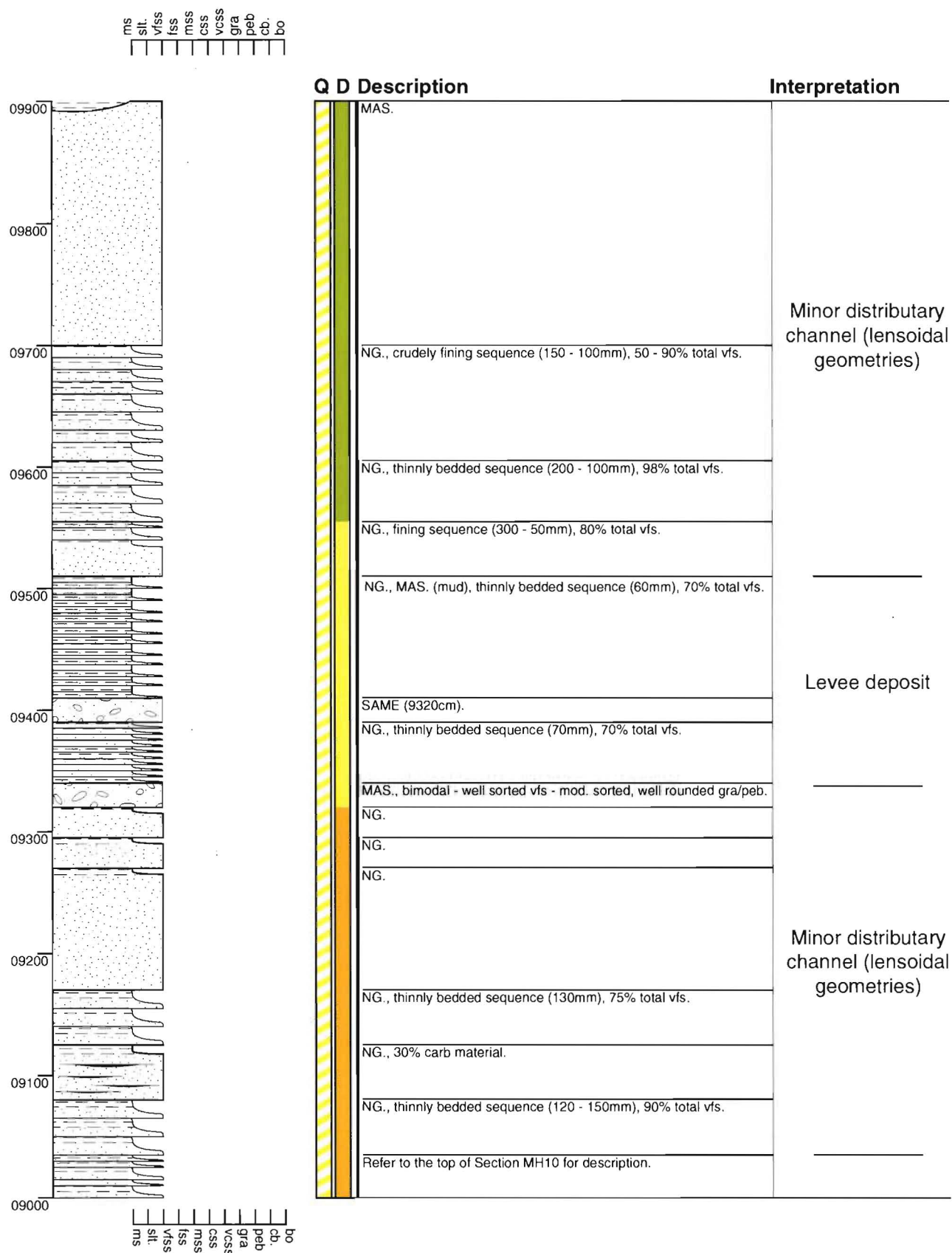
Section - Mt Holmes MH10

Grid Reference N32 907 465



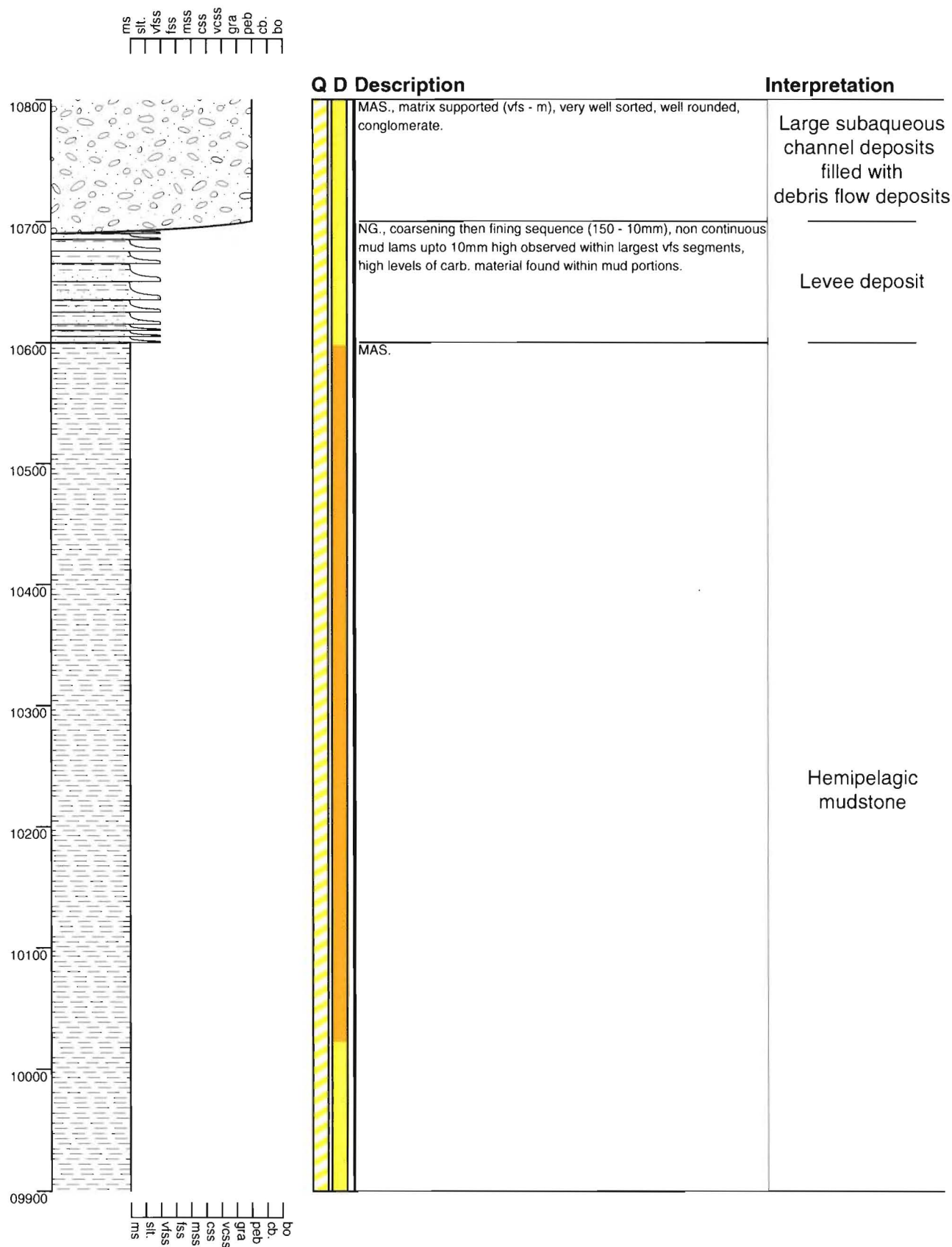
Section - Mt Holmes MH11

Grid Reference N32 907 465

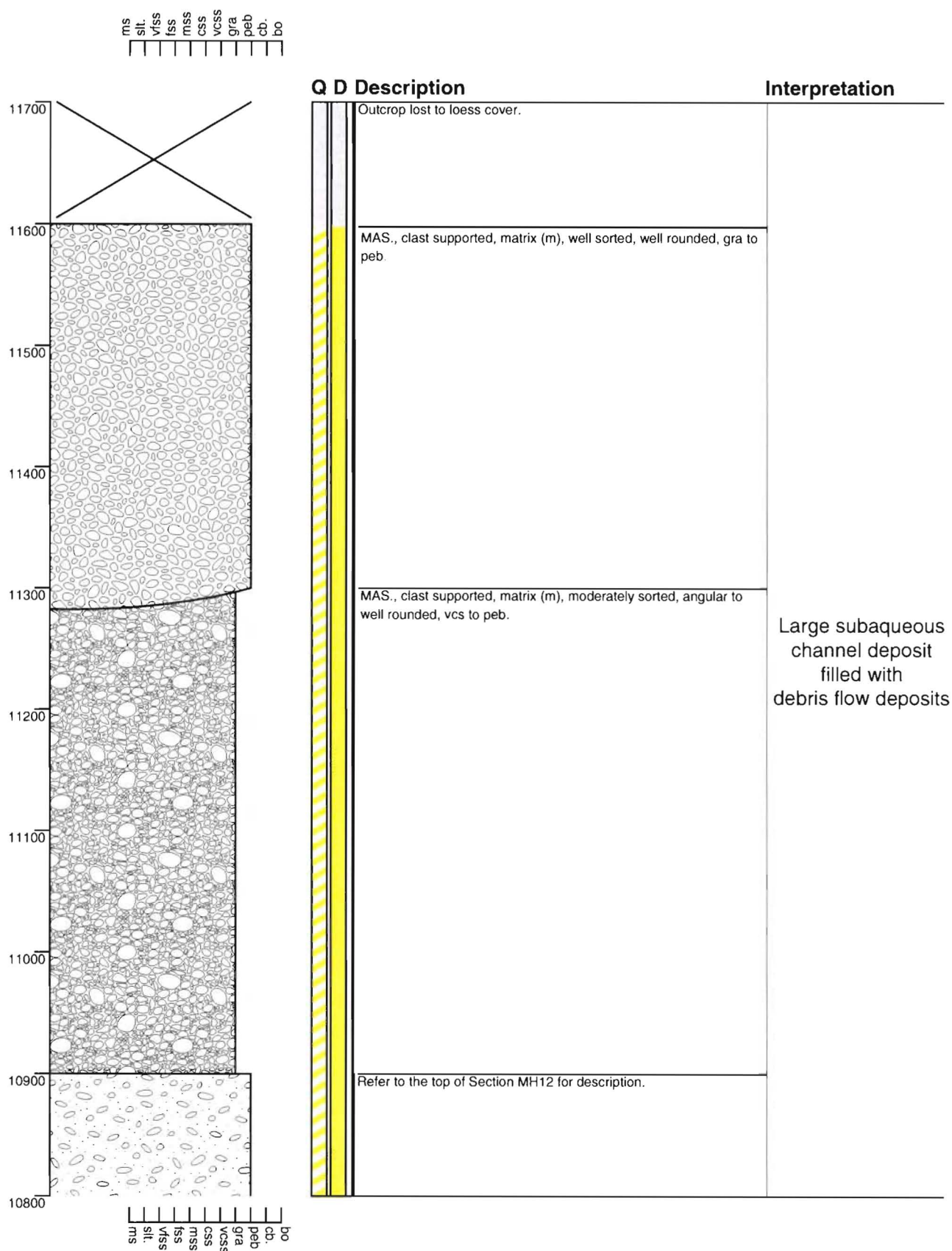


Section - Mt Holmes MH12

Grid Reference N32 907 465

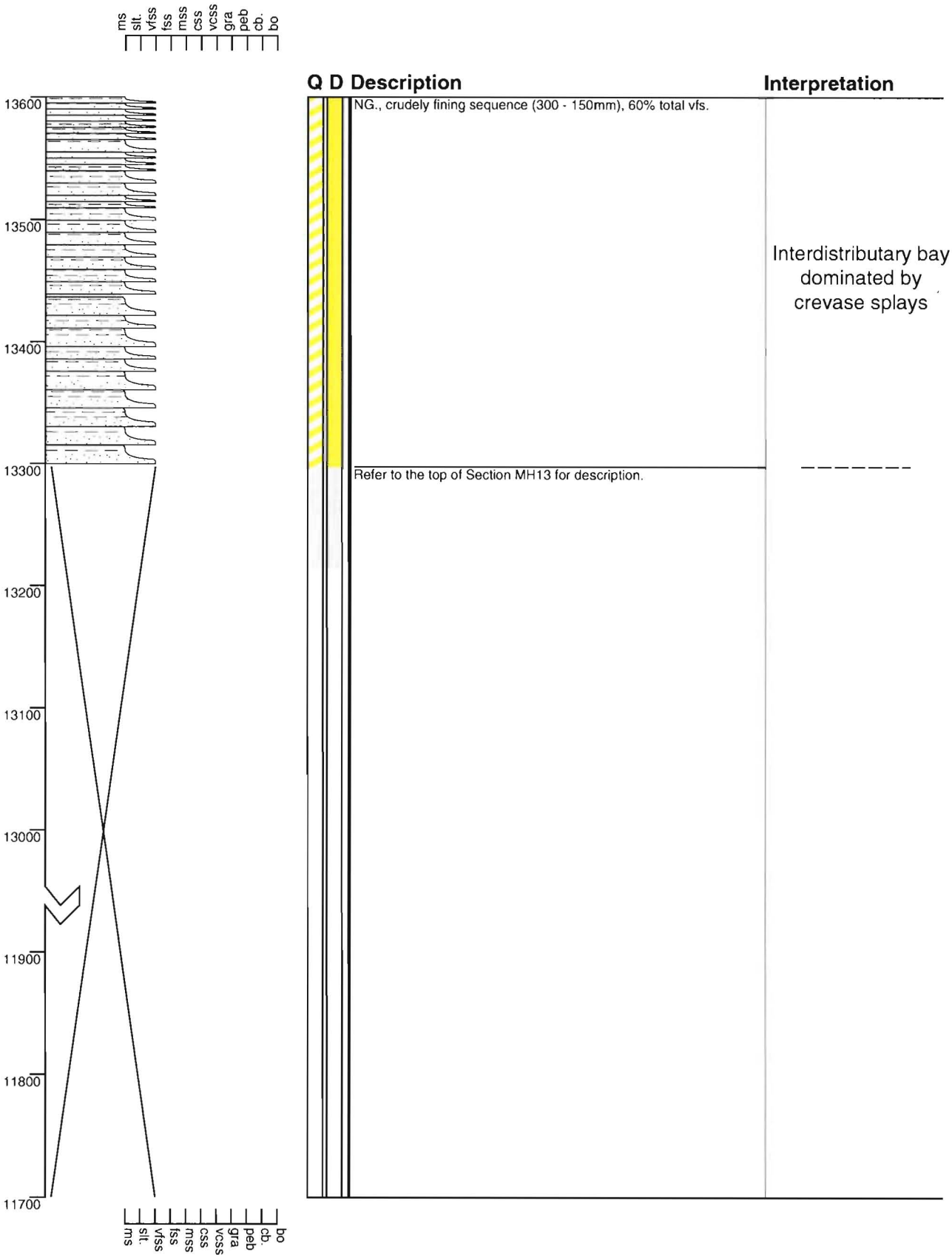


Grid Reference N32 907 465



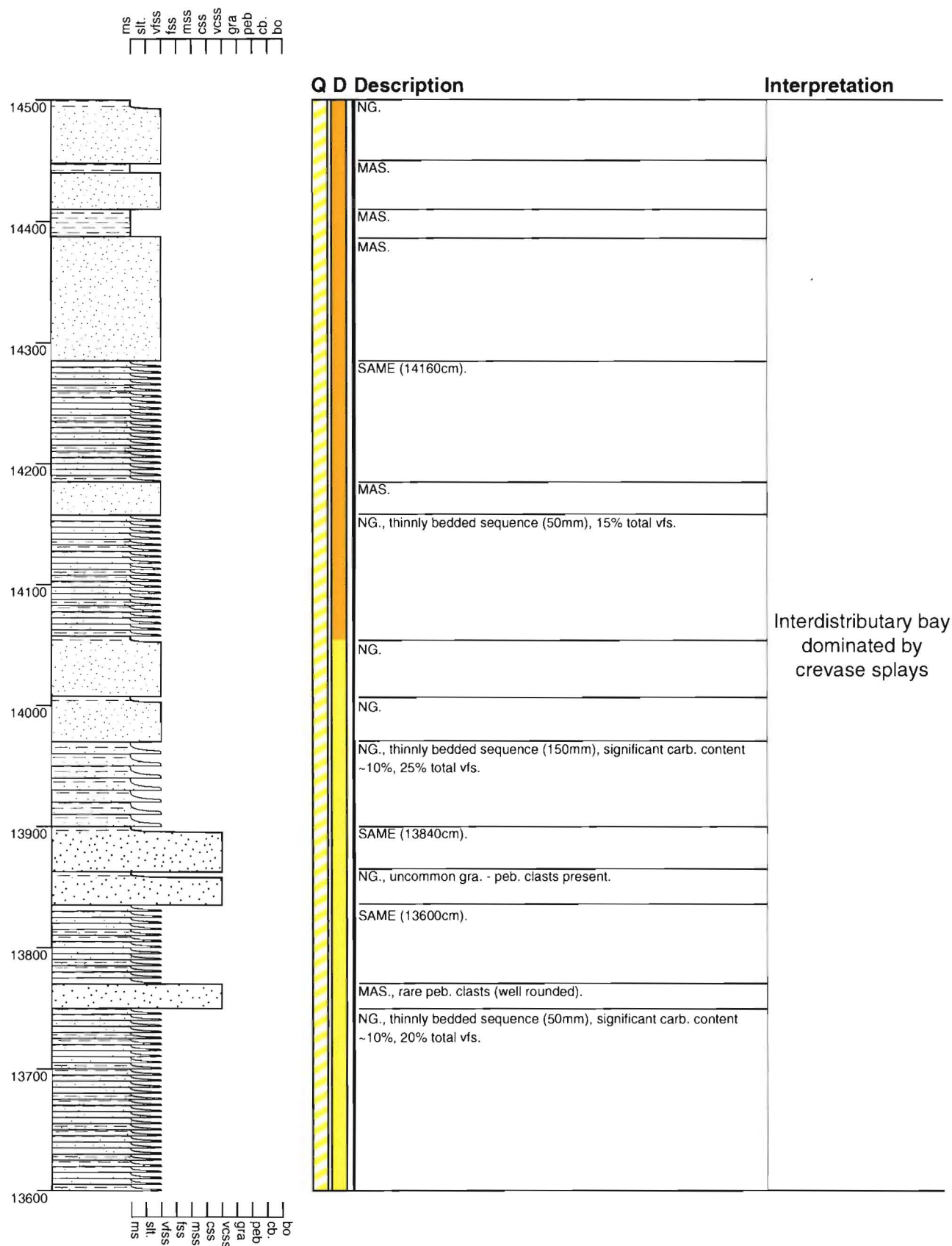
Section - Mt Holmes MH14

Grid Reference N32 907 465



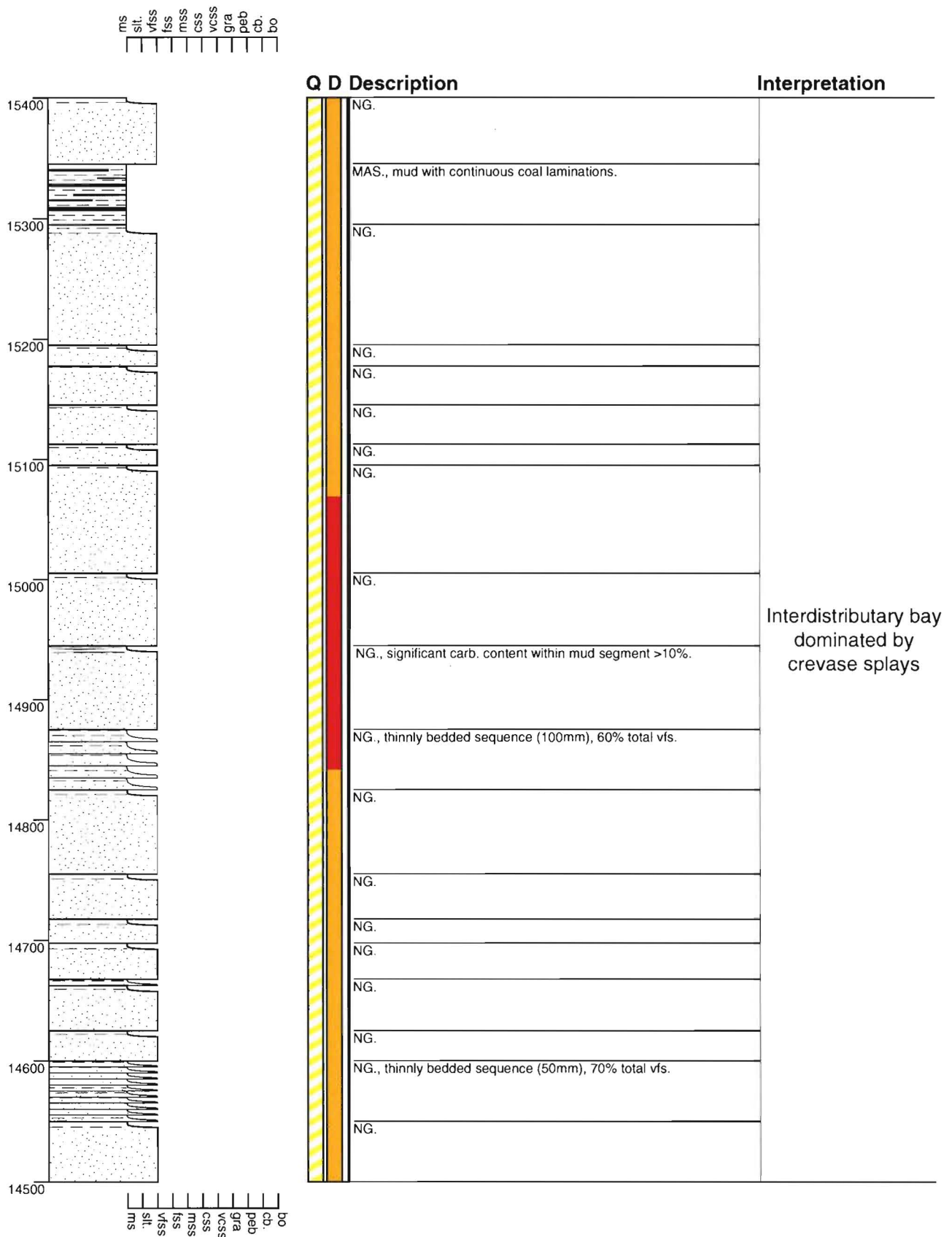
Section - Mt Holmes MH15

Grid Reference N32 907 465



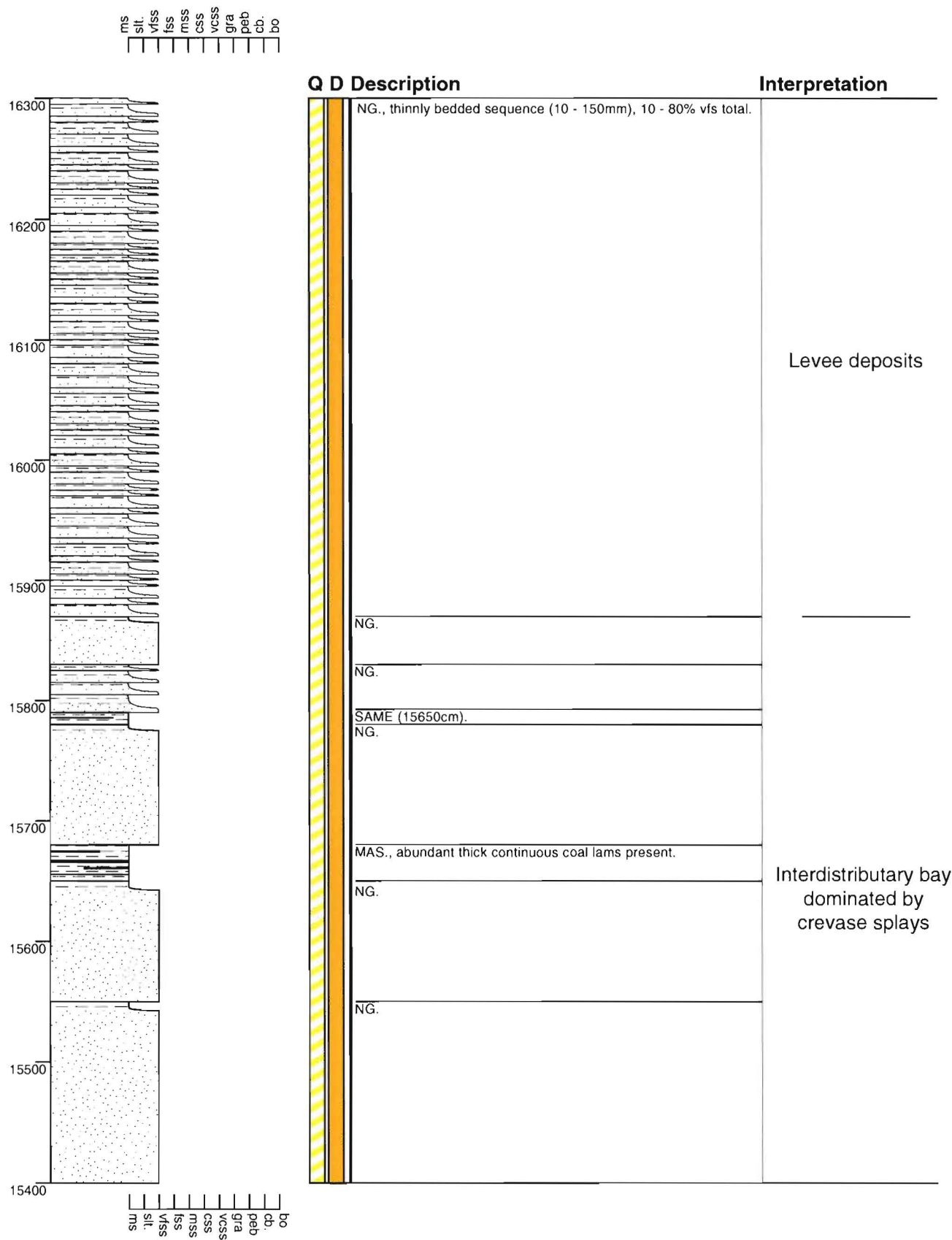
Section - Mt Holmes MH16

Grid Reference N32 907 465



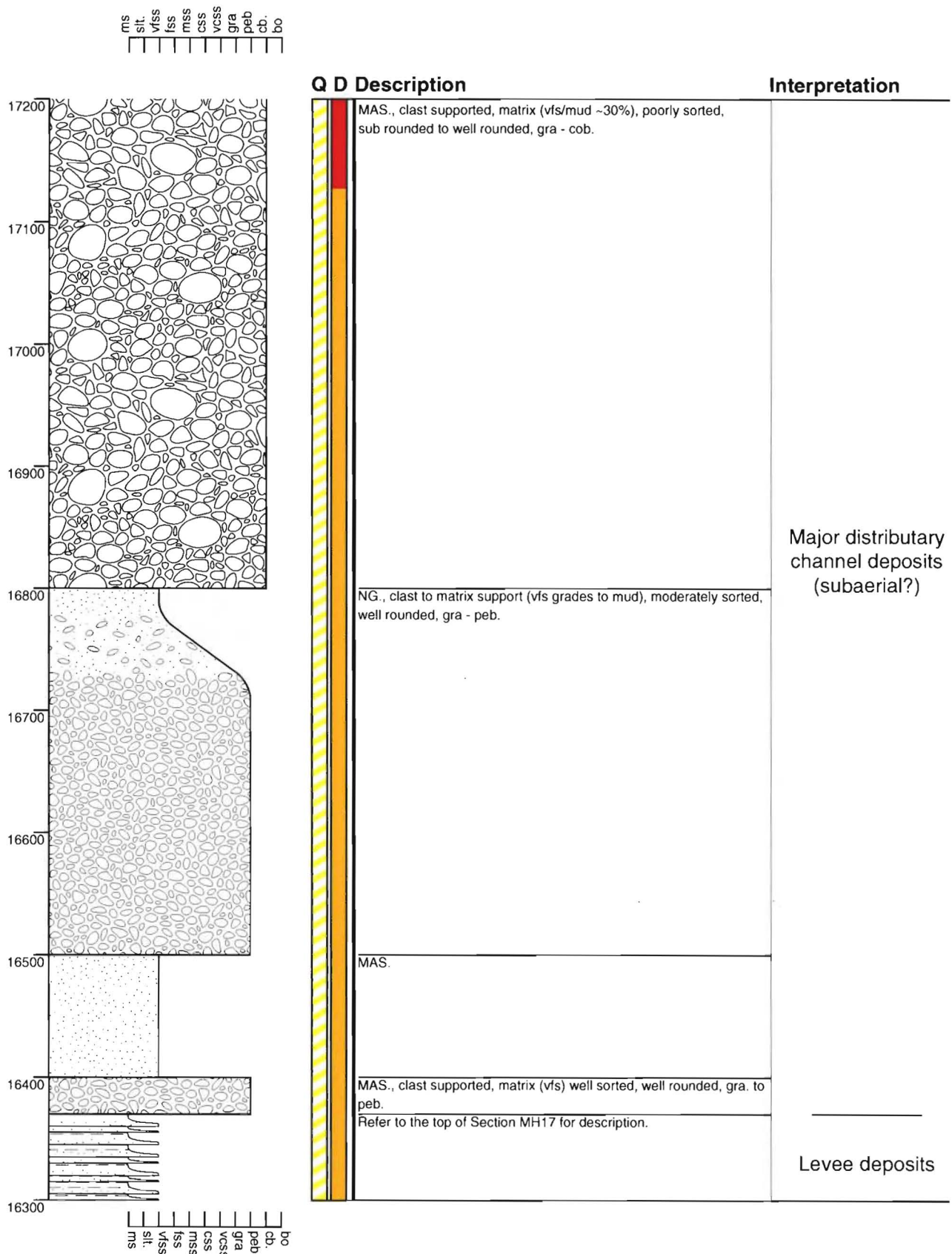
Section - Mt Holmes MH17

Grid Reference N32 907 465



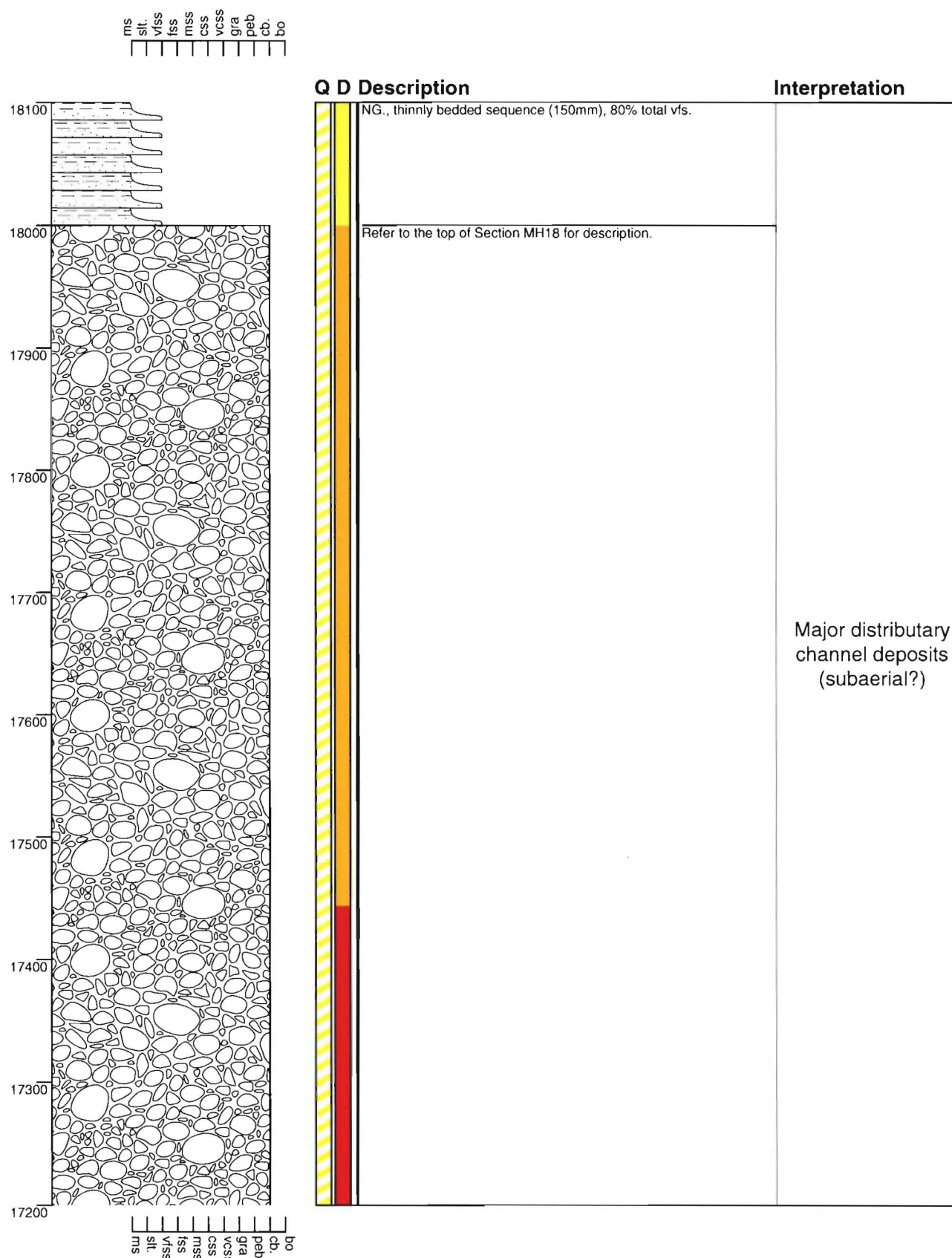
Section - Mt Holmes MH18

Grid Reference N32 907 465



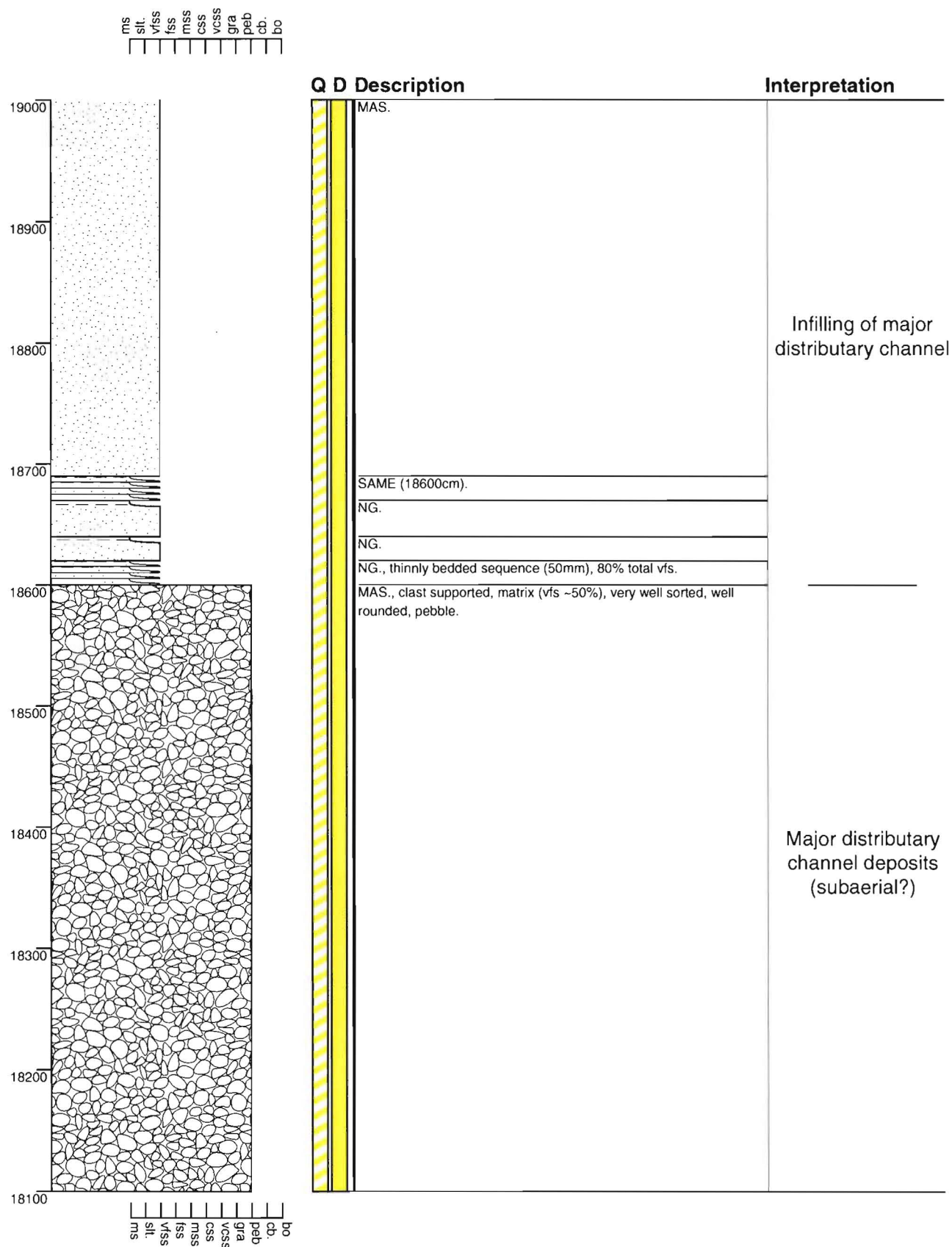
Section - Mt Holmes MH19

Grid Reference N32 907 465



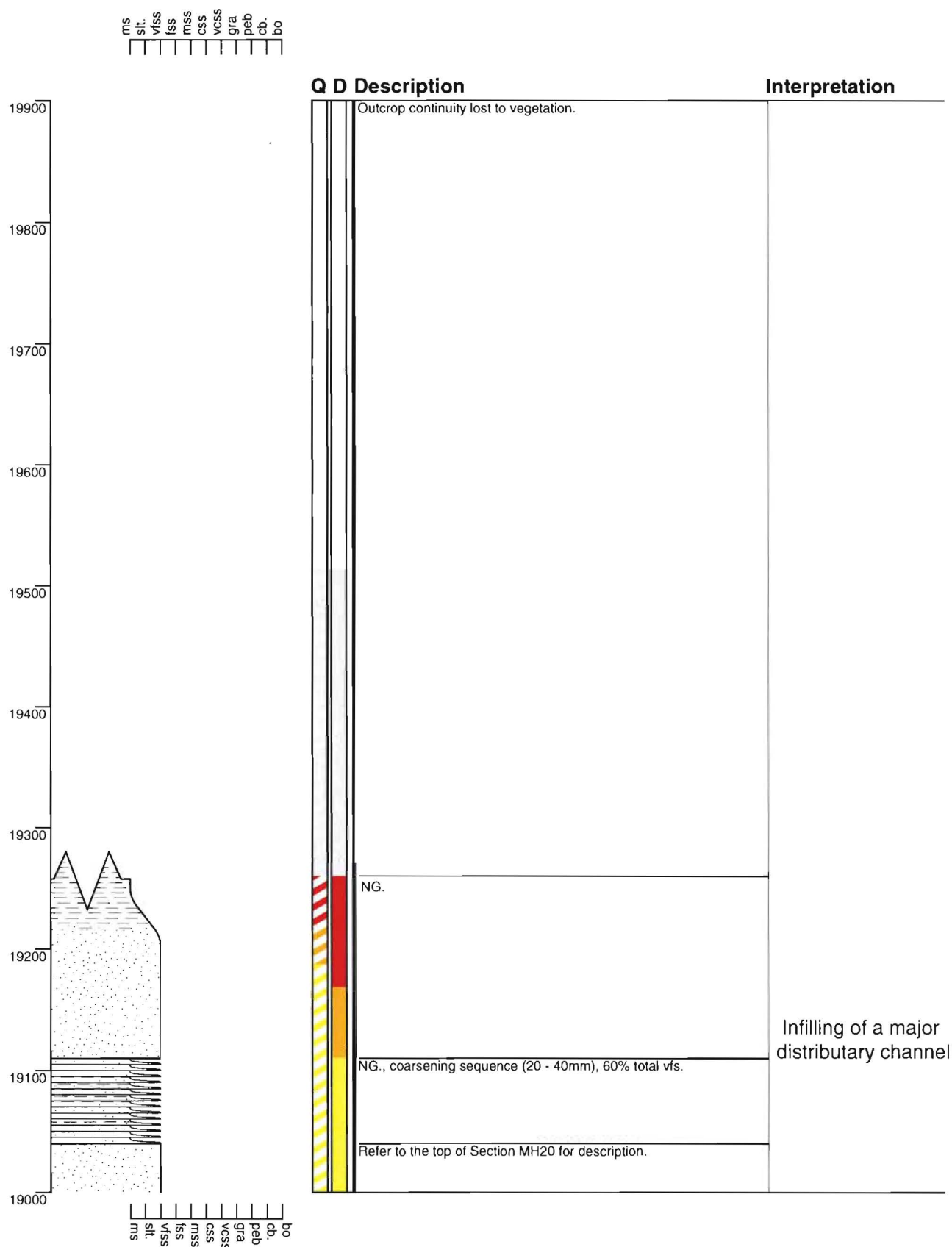
Section - Mt Holmes MH20

Grid Reference N32 907 465



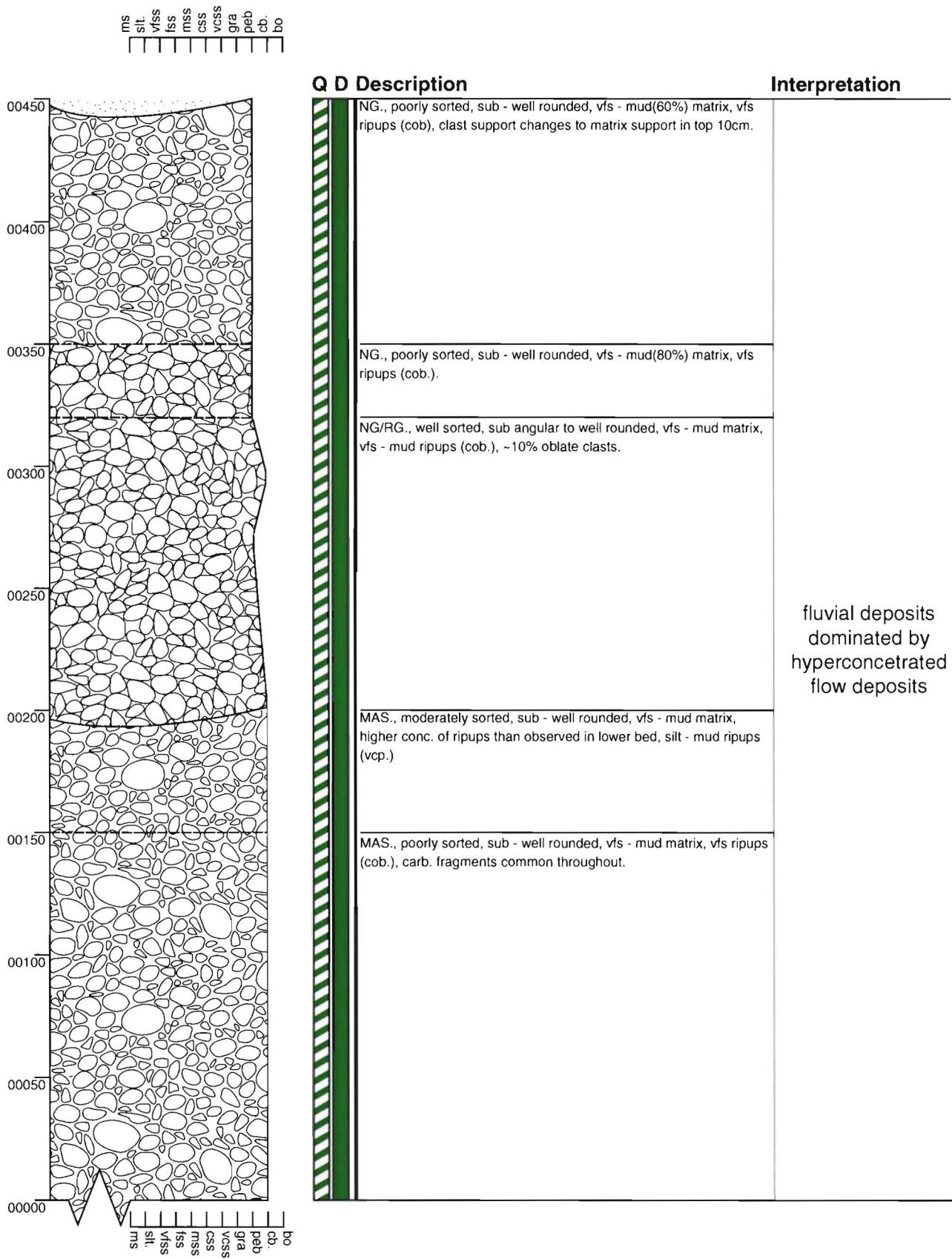
Section - Mt Holmes MH21

Grid Reference N32 907 465



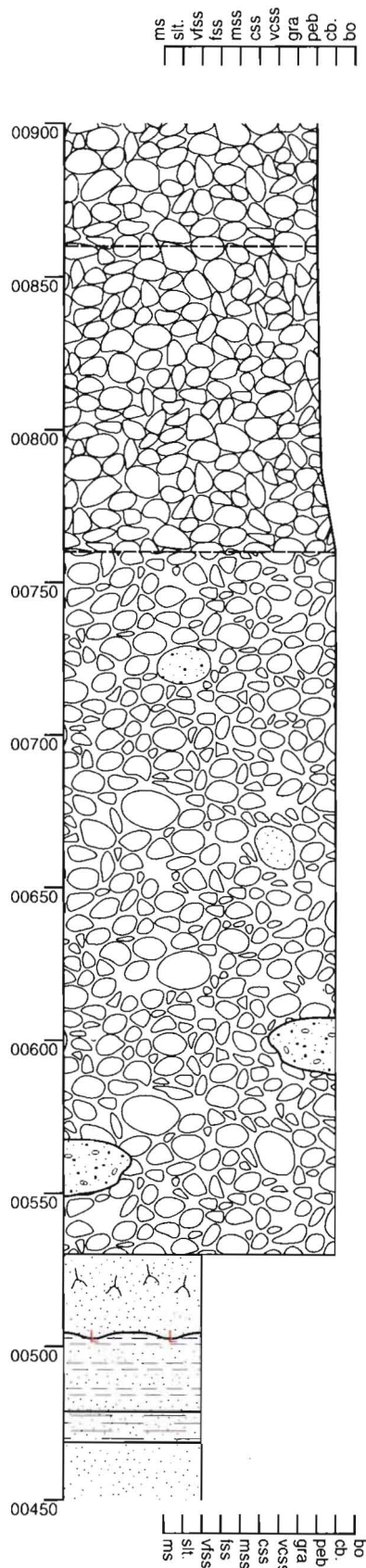
Section - Mt Saul A01

Grid Reference M32 861 444



Section - Mt Saul A02

Grid Reference M32 861 444



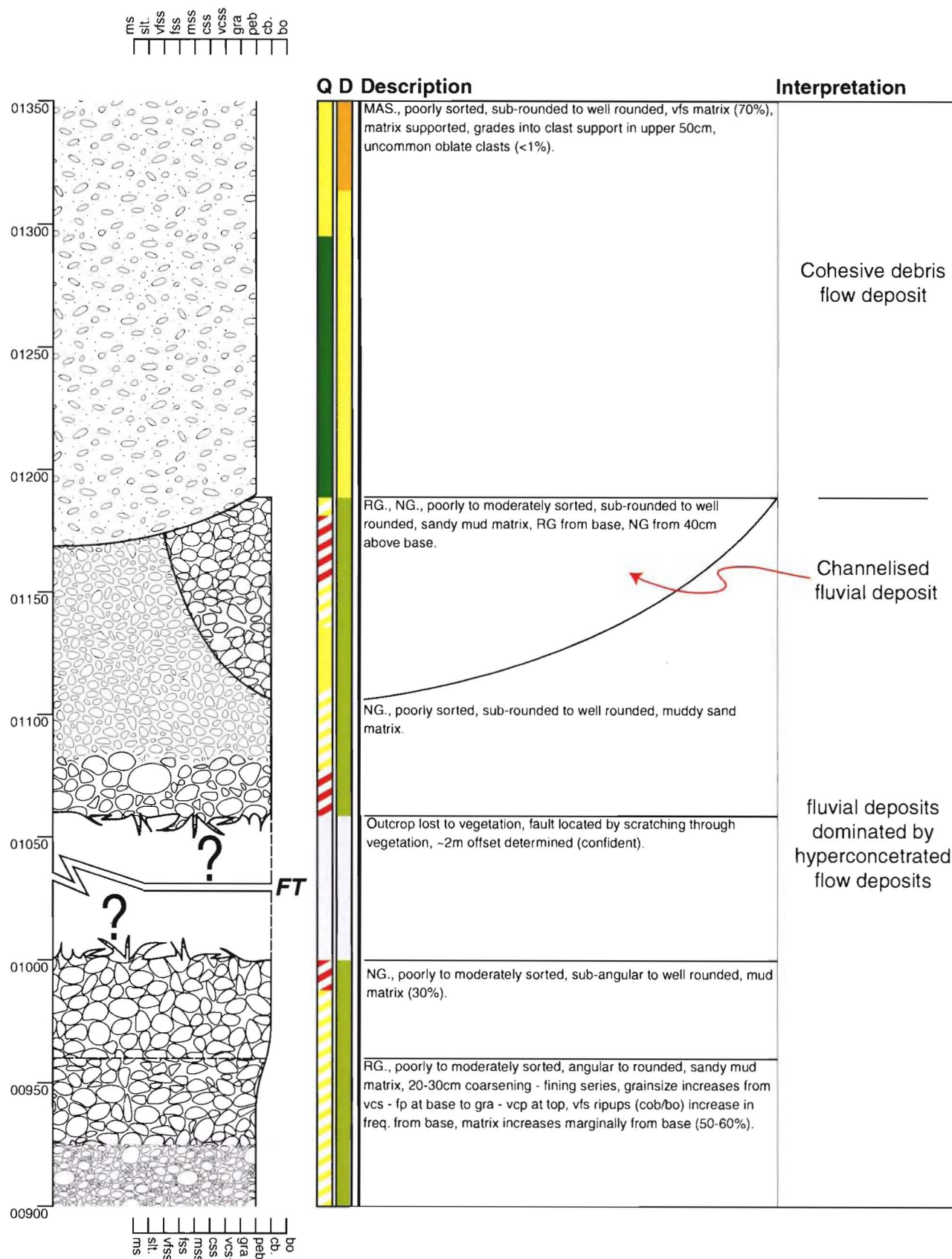
Q D Description

Interpretation

MAS., poorly sorted, vfs - mud matrix, angular to sub rounded, mud - vfs ripups (cob).	fluvial deposits dominated by hyperconcentrated flow deposits
NG., poorly sorted, vfs - mud matrix, angular to well rounded, mud - vfs ripups (cob).	
MAS., poorly sorted, silty mud matrix, sub - well rounded, mud - fine peb. ripups (200x70cm), ripups decrease in freq. up.	Debris flow deposit
MAS., substantial quantity of branching rootlets.	
NG., thinly bedded sequence (<20mm), scattered mud ripups.	Levee deposits
MAS., poorly sorted (mud - vfs).	
MAS.	

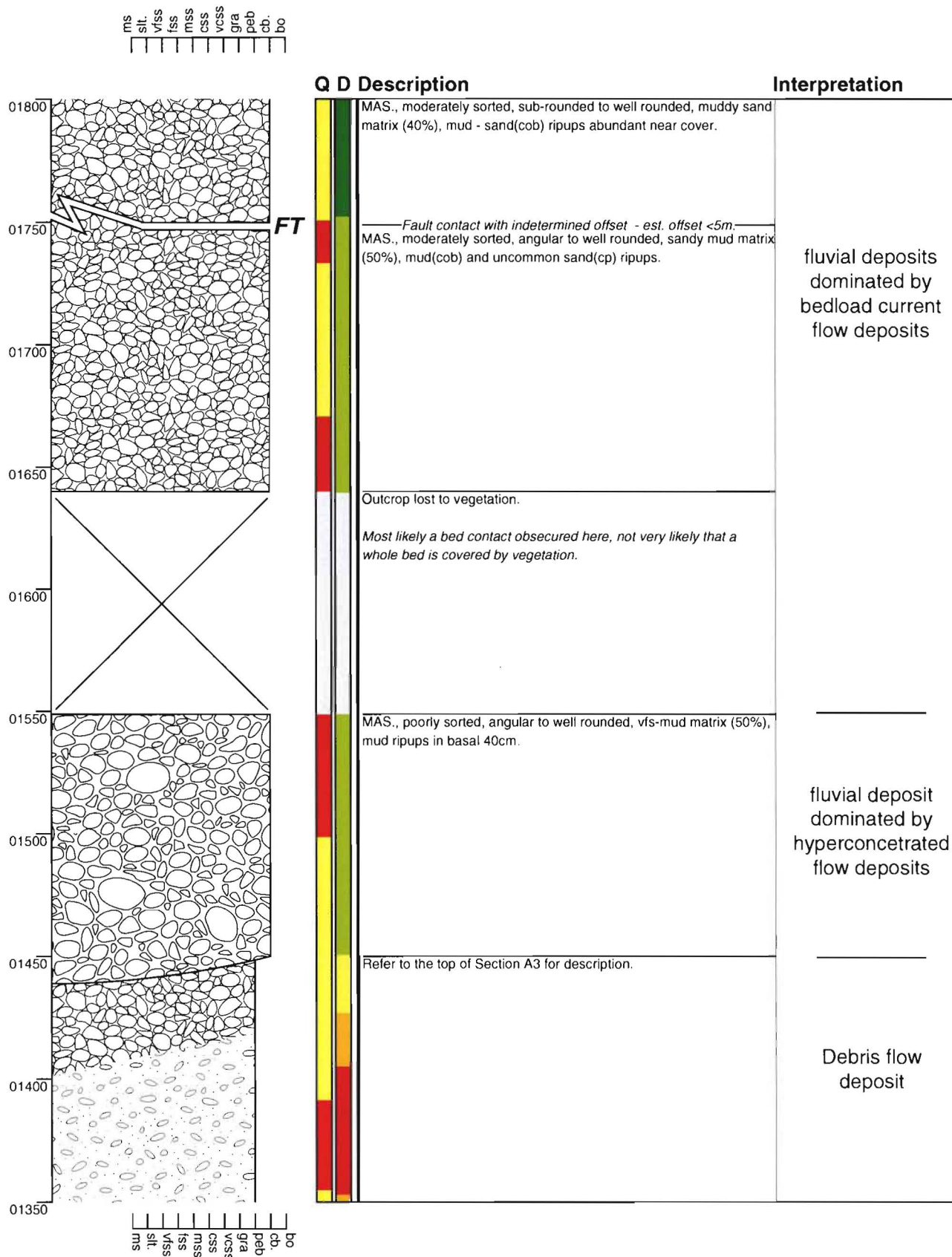
Section - Mt Saul A03

Grid Reference M32 861 444



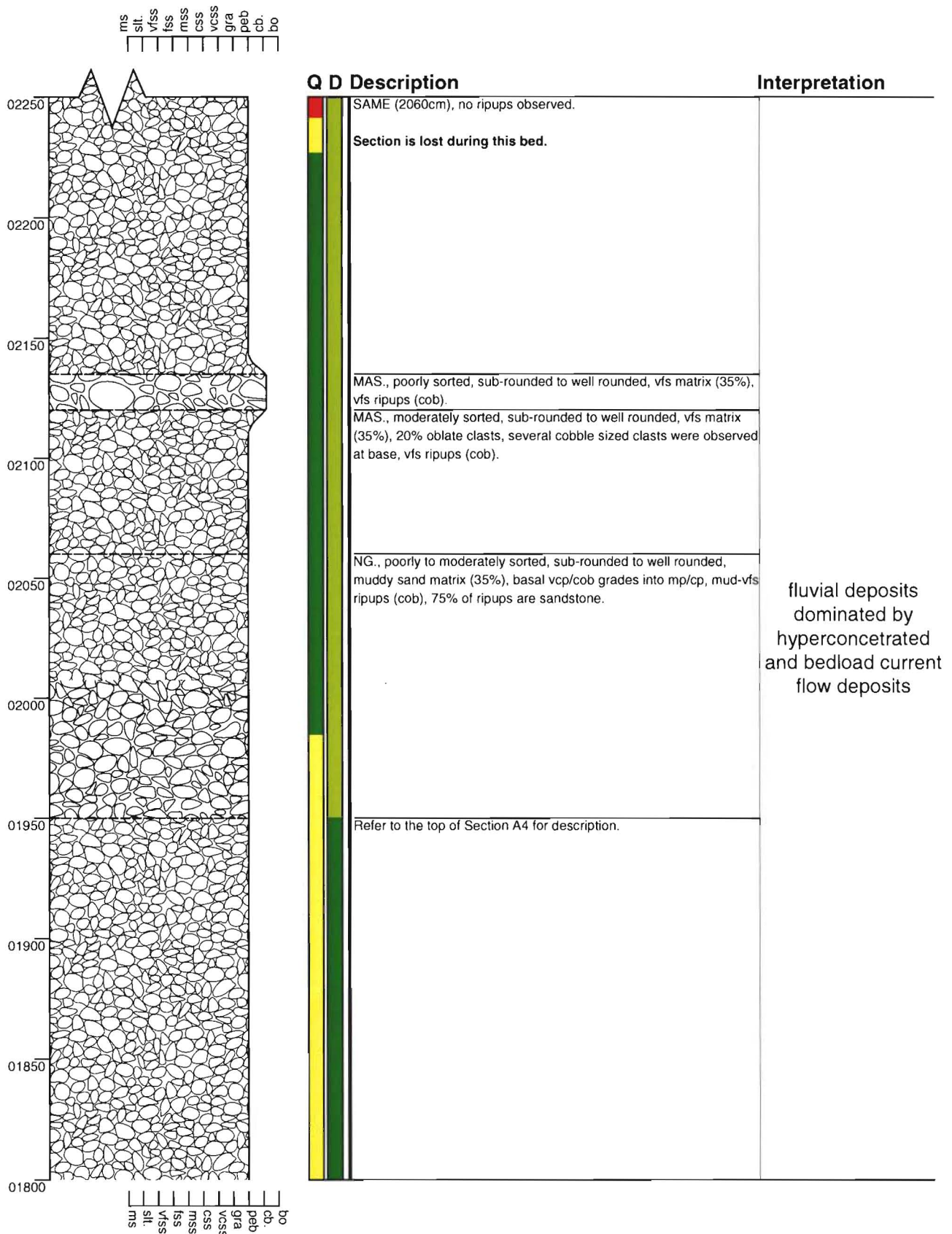
Section - Mt Saul A04

Grid Reference M32 861 444



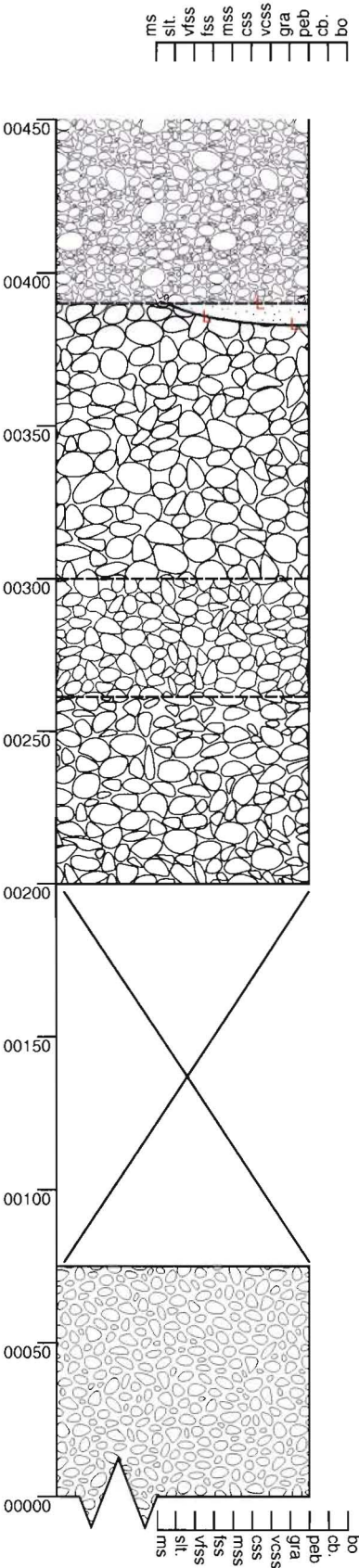
Section - Mt Saul A05

Grid Reference M32 861 444



Section - Mt Saul B01

Grid Reference M32 861 443

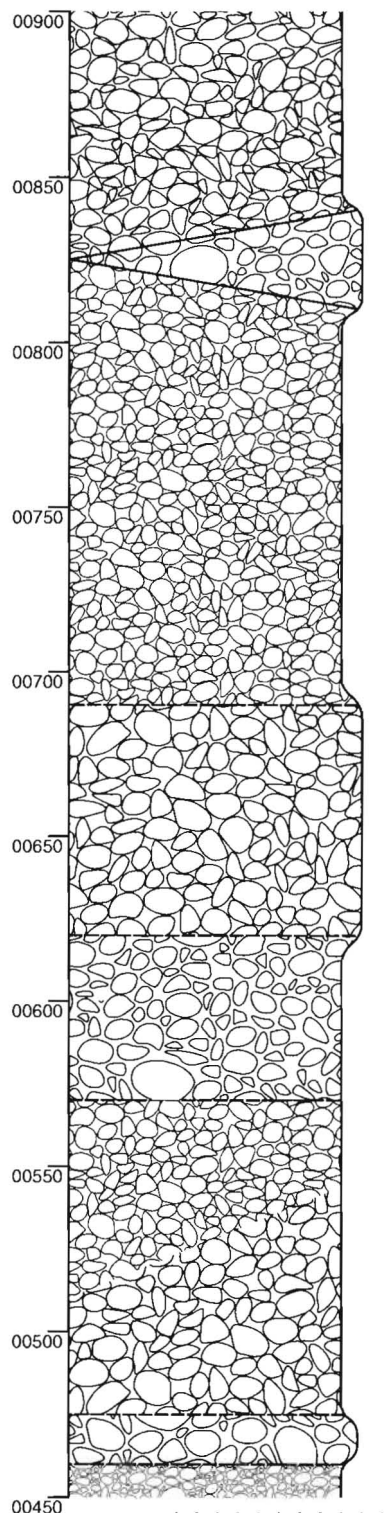


Q D Description	Interpretation
MAS., poorly sorted, sub - rounded to well rounded, mud - vfs matrix (40%), vfs ripups (cob).	fluvial deposits dominated by bedload current flow deposits
MAS. MAS., moderately sorted, sub - rounded to well rounded, vfs matrix (40%), oblate clasts (<20%), mud ripups (vcp), vfs ripups (cob).	
SAME (200cm), matrix (40%).	
MAS., moderately sorted, sub-rounded to well rounded, vfs matrix (60%), vfs - mud ripups (vcp), oblate clasts very common (~20%).	
Outcrop lost to vegetation.	
MAS., moderately sorted, sub - angular to well rounded, vfs matrix (60%).	

Section - Mt Saul B02

Grid Reference M32 861 443

ms
silt.
vss
fss
mss
css
vcss
gra
peb
cb.
bo



Q D Description

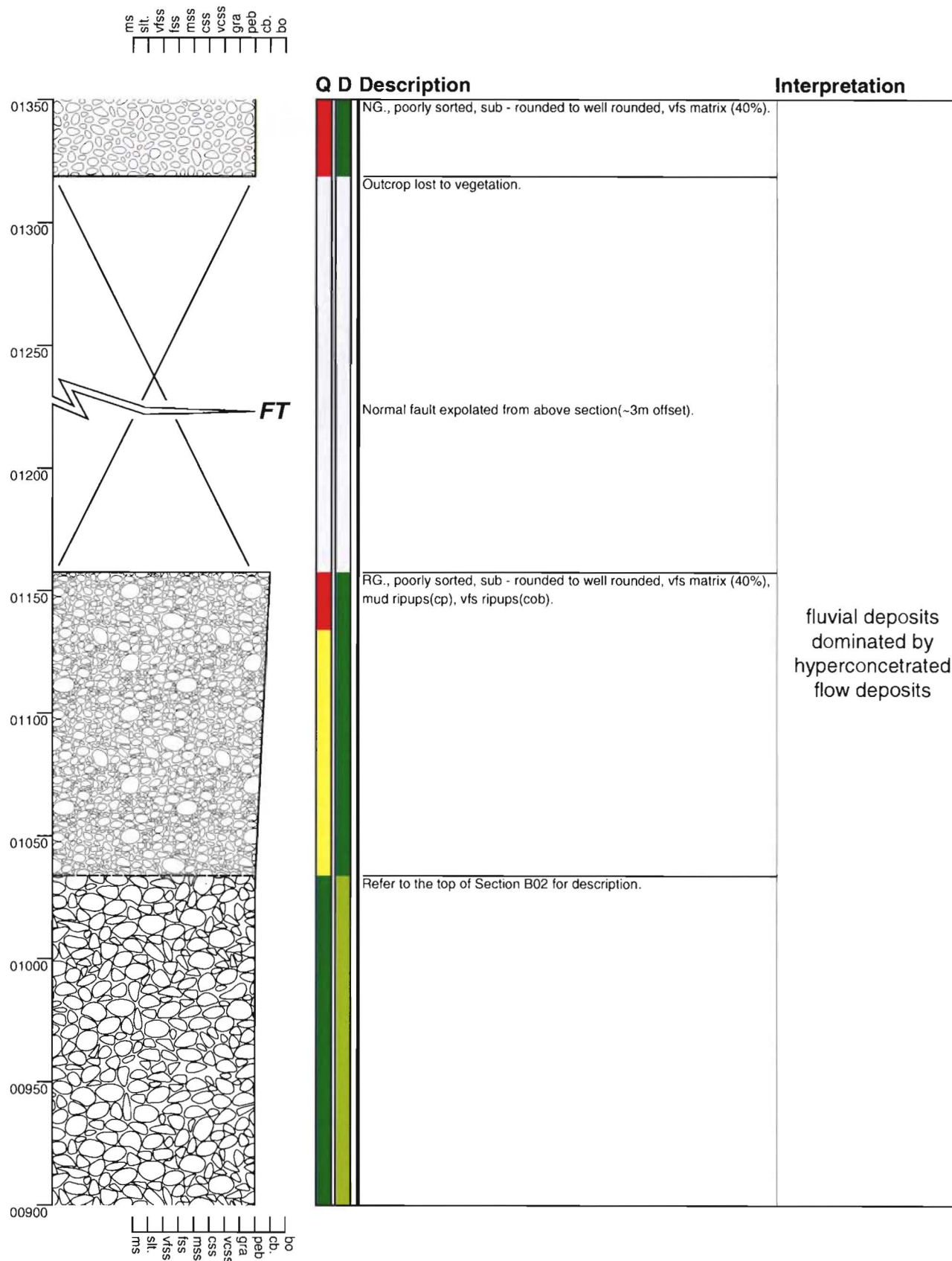
Interpretation

MAS., moderately sorted, sub - rounded to well rounded, vfs matrix (60%), vfs ripups(cob).	
MAS., poorly sorted, sub - rounded to well rounded, vfs - mud matrix, m/vfs ripups, s/s concretions.	
MAS., moderately sorted, sub - angular to well rounded, mud - vfs matrix (40%), mud - vfs ripups(cob), vfs ripups contain carb. material.	
MAS., moderately sorted, sub - rounded to well rounded, sandy mud matrix (40%), mud ripups(cp).	fluvial deposits dominated by hyperconcentrated and bedload current flow deposits
MAS., moderately sorted, sub - angular to well rounded, sandy mud matrix (40%), mud - vfs ripups(cob).	
NG., poorly to moderately sorted, sub - rounded to well rounded, vfs matrix (40%), mud - vfs ripups(cob).	
MAS., poorly sorted, sub - rounded to well rounded, vfs matrix (40%) vfs ripups (cob). Refer to the top of Section B01 for description.	

bo
cb.
peb
gra
vcss
css
mss
fss
vss
silt.
ms

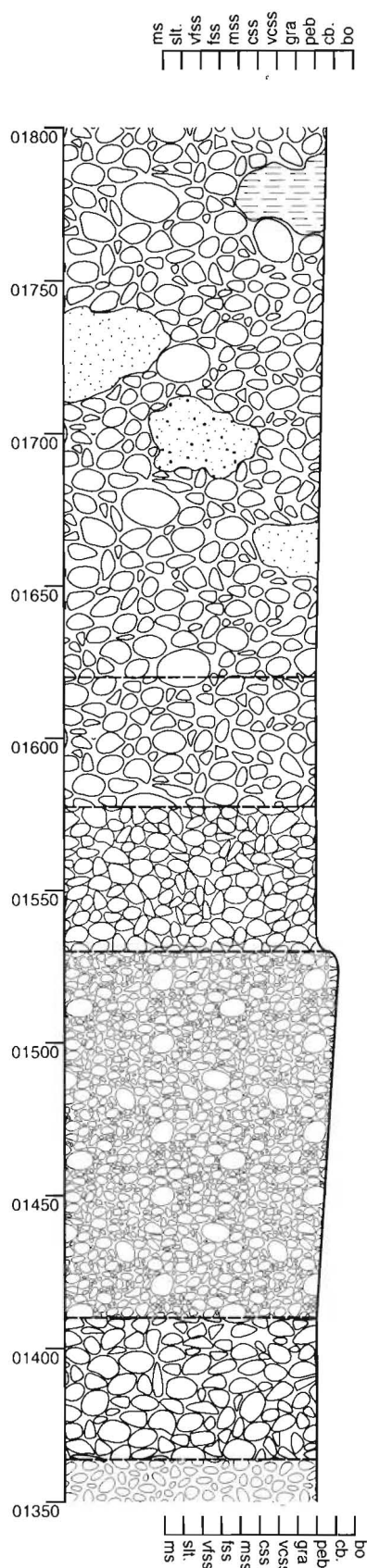
Section - Mt Saul B03

Grid Reference M32 861 443



Section - Mt Saul B04

Grid Reference M32 861 443



Q D Description

Interpretation

RG., poorly sorted, sub - angular to well rounded, vfs matrix, matrix decreases in % from 70% at base to 30 at cover, abundant large ripups mud - gra (max. 250x130x100cm).

MAS., poorly sorted, sub - rounded to well rounded, fs - vfs matrix (50%).

MAS., moderately sorted, sub - rounded to well rounded, vfs matrix (60%), mud ripups (vcp).

RG., poorly sorted, sub - rounded to well rounded, vfs matrix (40%), mud ripups (vcp).

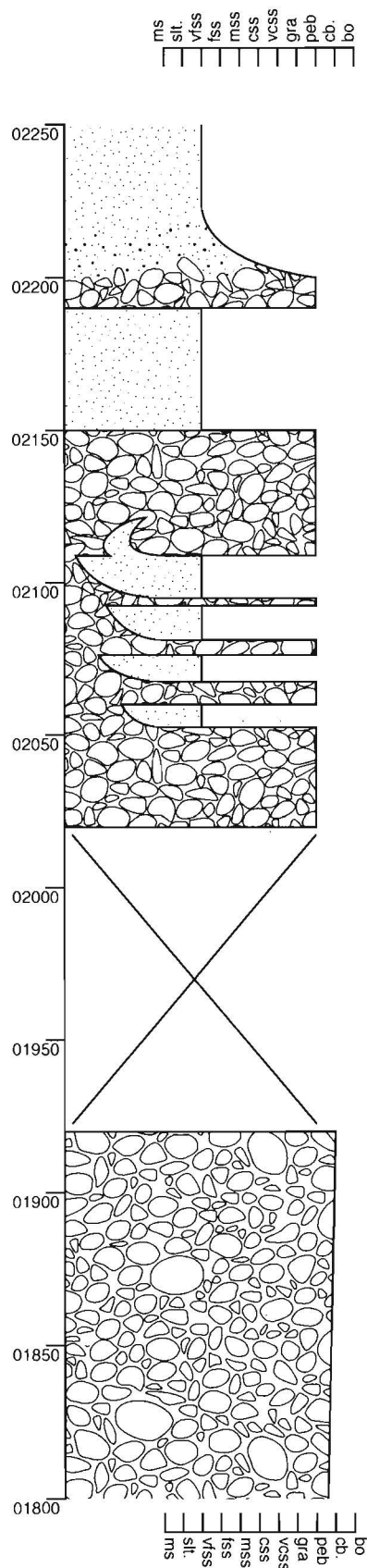
MAS., moderately sorted, sub - angular to well rounded, vfs matrix (40%), vfs ripups (cob - 20x12cm).

Refer to the top of Section B03 for description.

fluvial deposits
dominated by
debris flow and
hyperconcentrated
flow deposits

Section - Mt Saul B05

Grid Reference M32 861 443



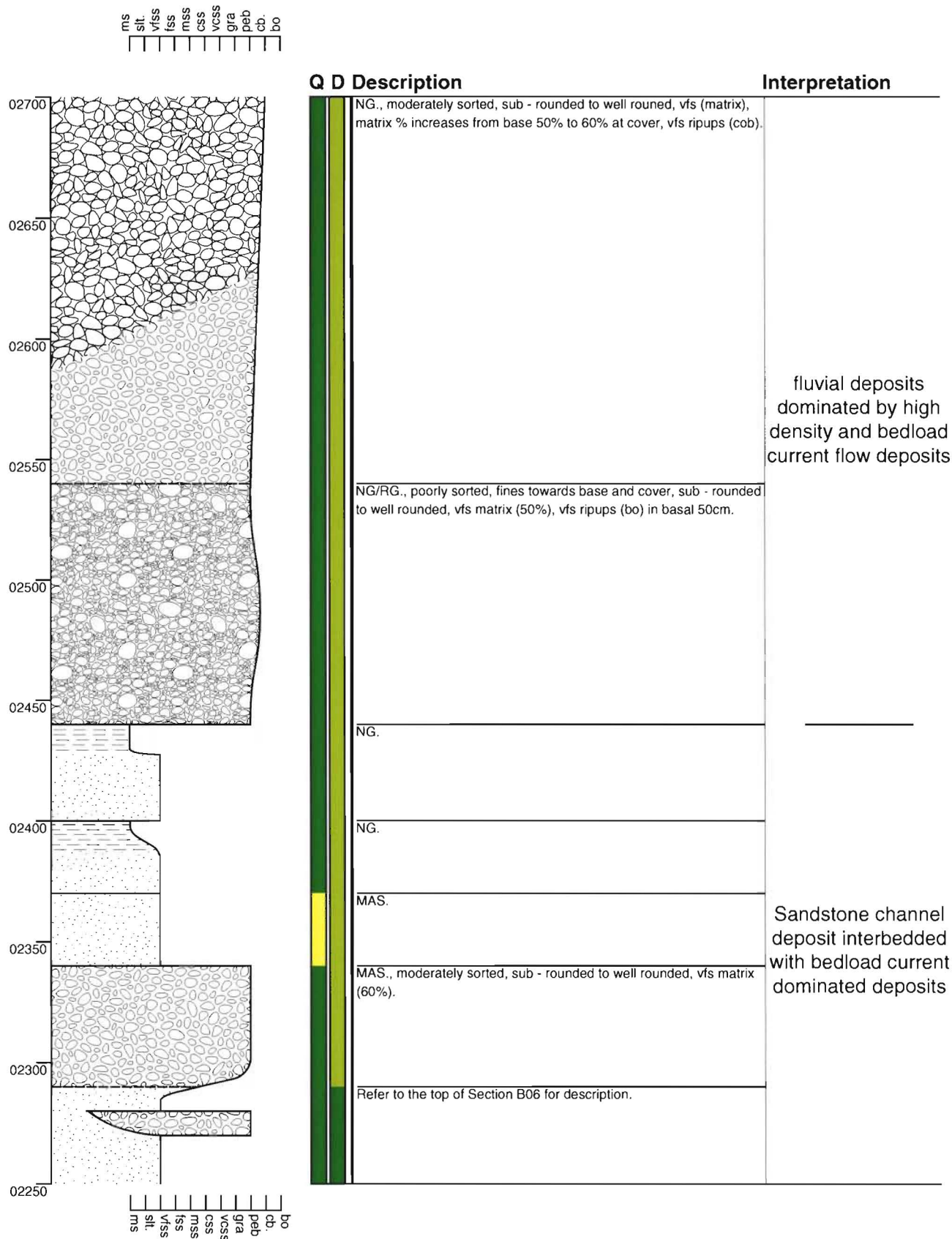
Q D Description

Interpretation

	NG., poorly to well sorted, sub - rounded to well rounded, a 10-15cm NG bed (fp - cp) interfingers vfs at 2270cm.	
	MAS.	
	MAS., moderately sorted, sub - rounded to well rounded, vfs matrix (60%); MAS., vfs beds interfingers quite visibly these can be traced to a very nicely formed vfs channel structure.	Sandstone channel deposit interbedded with bedload current dominated deposits
	Outcrop lost to vegetation. <i>A bed contact/additional beds may be obscured here.</i>	fluvial deposits dominated by high density flows
	Refer to the top of Section B04 for description.	

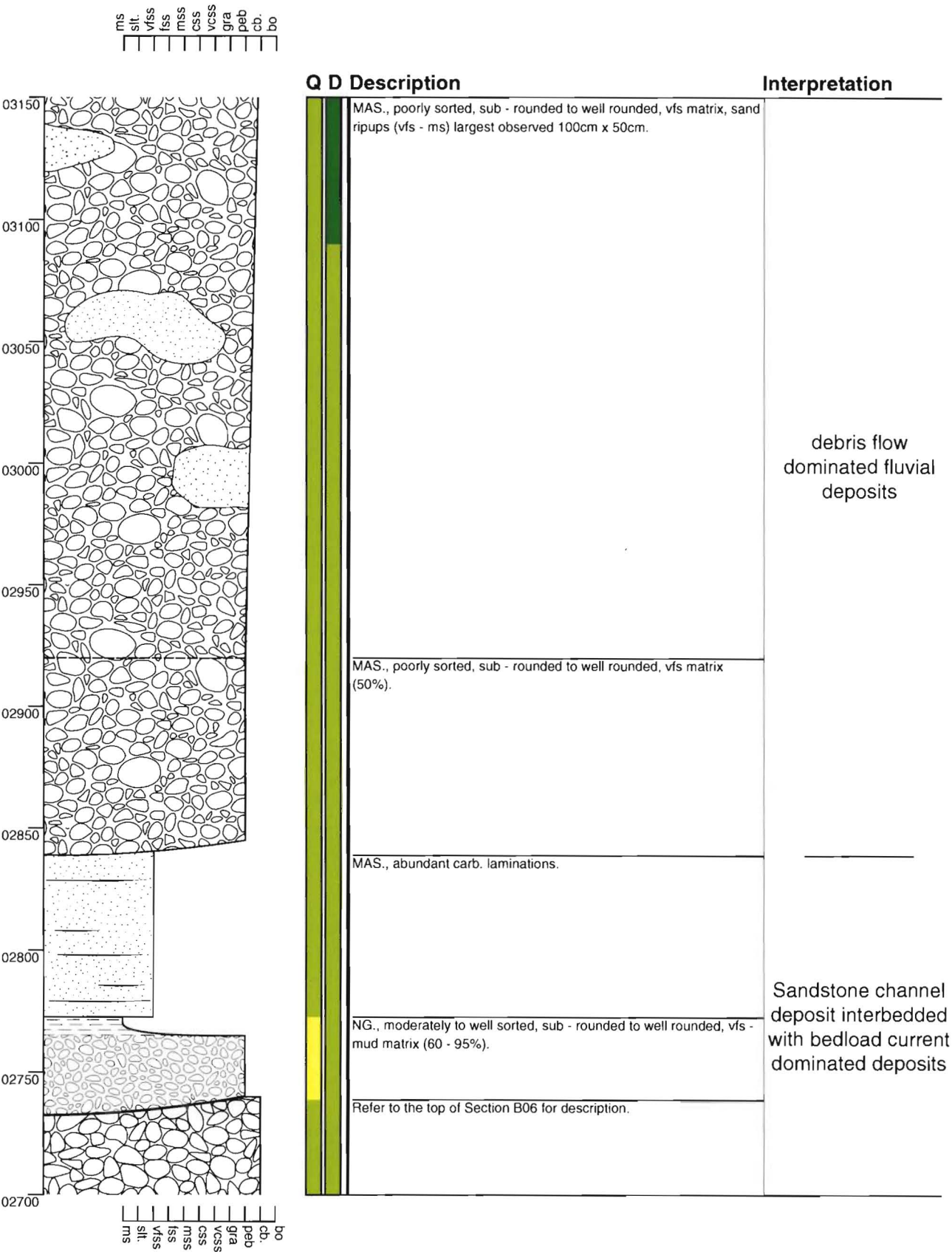
Section - Mt Saul B06

Grid Reference M32 861 443



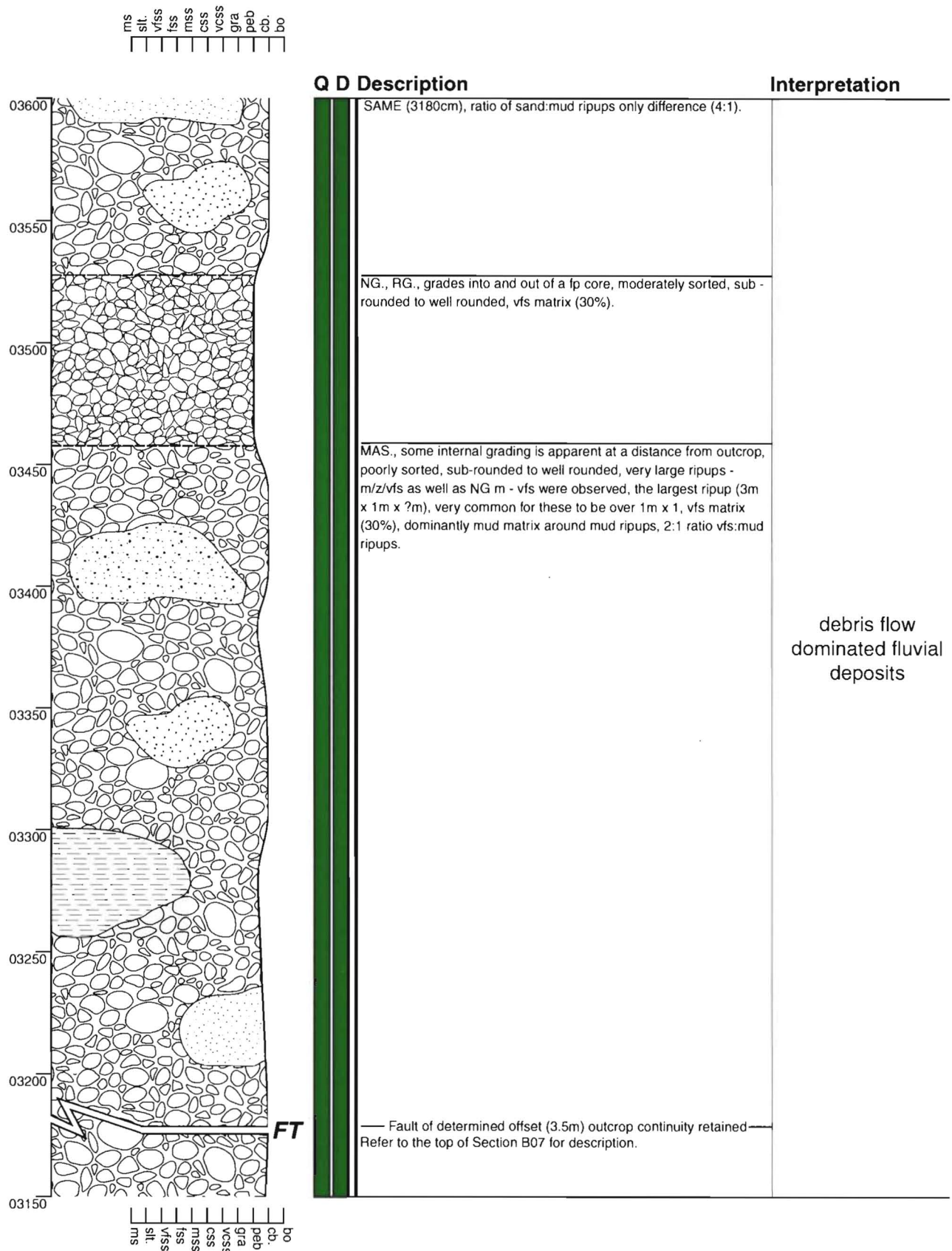
Section - Mt Saul B07

Grid Reference M32 861 443



Section - Mt Saul B08

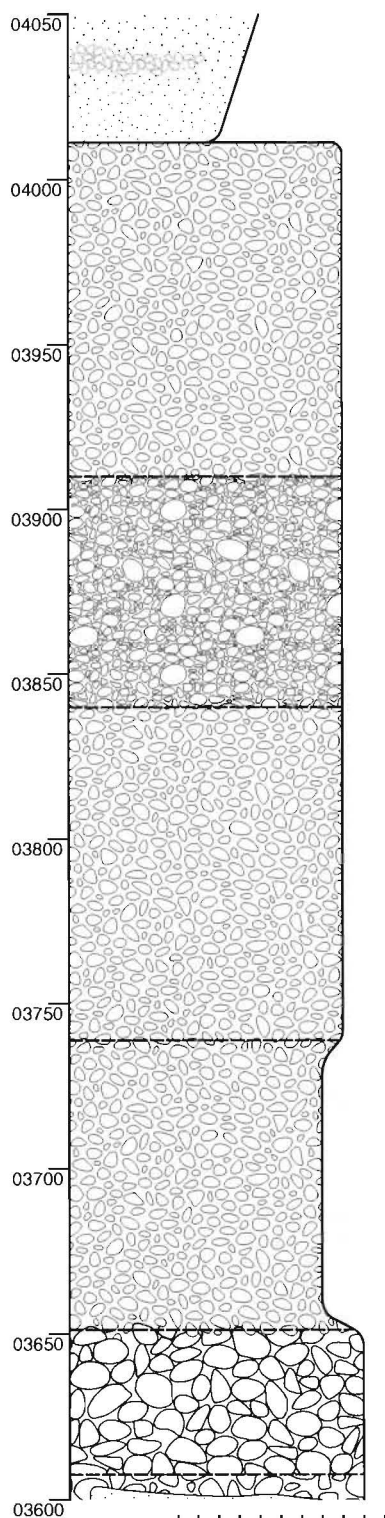
Grid Reference M32 861 443



Section - Mt Saul B09

Grid Reference M32 861 443

ms
sl.
vss
fss
mss
css
vcss
gra
peb
cb.
bo



bo
cb.
peb
gra
vcss
css
mss
fss
vss
sl.
ms

Q D Description

Interpretation

RG., interbeds of peb present, well to poorly sorted, ? - sub rounded, vfs - vcs.

MAS., moderately sorted, well rounded, vfs matrix, cob - bo sized mud/vfs ripups - some showing NG. in upper 20cm, gra - peb.

MAS., poorly sorted, well rounded, mud/vfs matrix, peb. sized vfs ripups, vcs - cob.

MAS., well sorted, sub rounded, vfs matrix (30-40%), several cp sized vfs ripups, gra - peb.

MAS., well sorted, well rounded, mud/vfs matrix, gra.

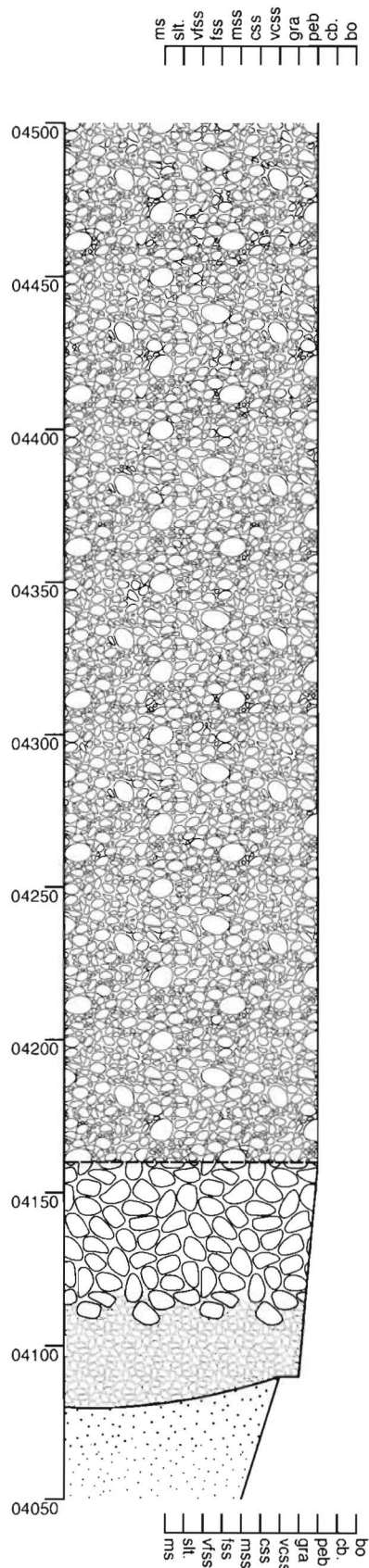
MAS., well sorted, well rounded, mud/vfs matrix, mud/vfs ripups present, peb - cob.

Refer to the top of Section MSB08 for description.

Below current flow
dominated fuvial
deposits

Section - Mt Saul B10

Grid Reference M32 861 443



Q D Description

Interpretation

MAS., moderately to poorly sorted, well rounded, vfs/mud matrix (40%), vcs - peb.

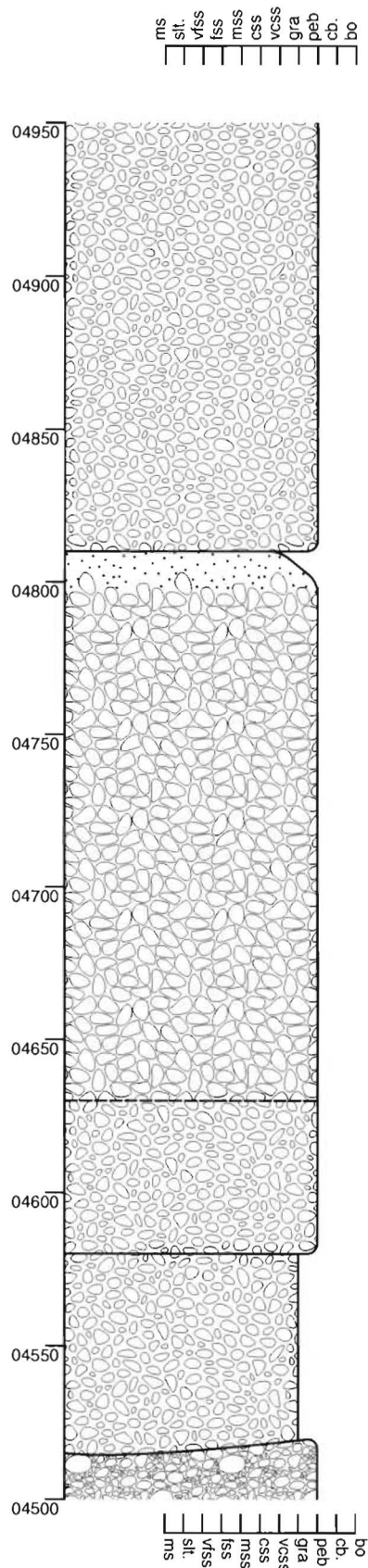
Below current flow
dominated fluvial
deposits

RG., moderately sorted, well rounded, vfs matrix (40-60%), clasts imbricated (~NE), gra - peb.

Refer to the top of Section MSB09 for description.

Section - Mt Saul B11

Grid Reference M32 861 443



Q D Description

Interpretation

MAS., very well sorted, well rounded, vfs matrix, uncommon vfs ripups observed near base, gra - peb, *grainsizes increase and decrease subtly throughout, it appears as though the depositional process was "pulsating", 7 coarsening then fining cycles were observed.*

NG., very well sorted, sub rounded to well rounded, vfs matrix (30%), imbricated (NE), peb - gra.

Below current flow dominated fluvial deposits

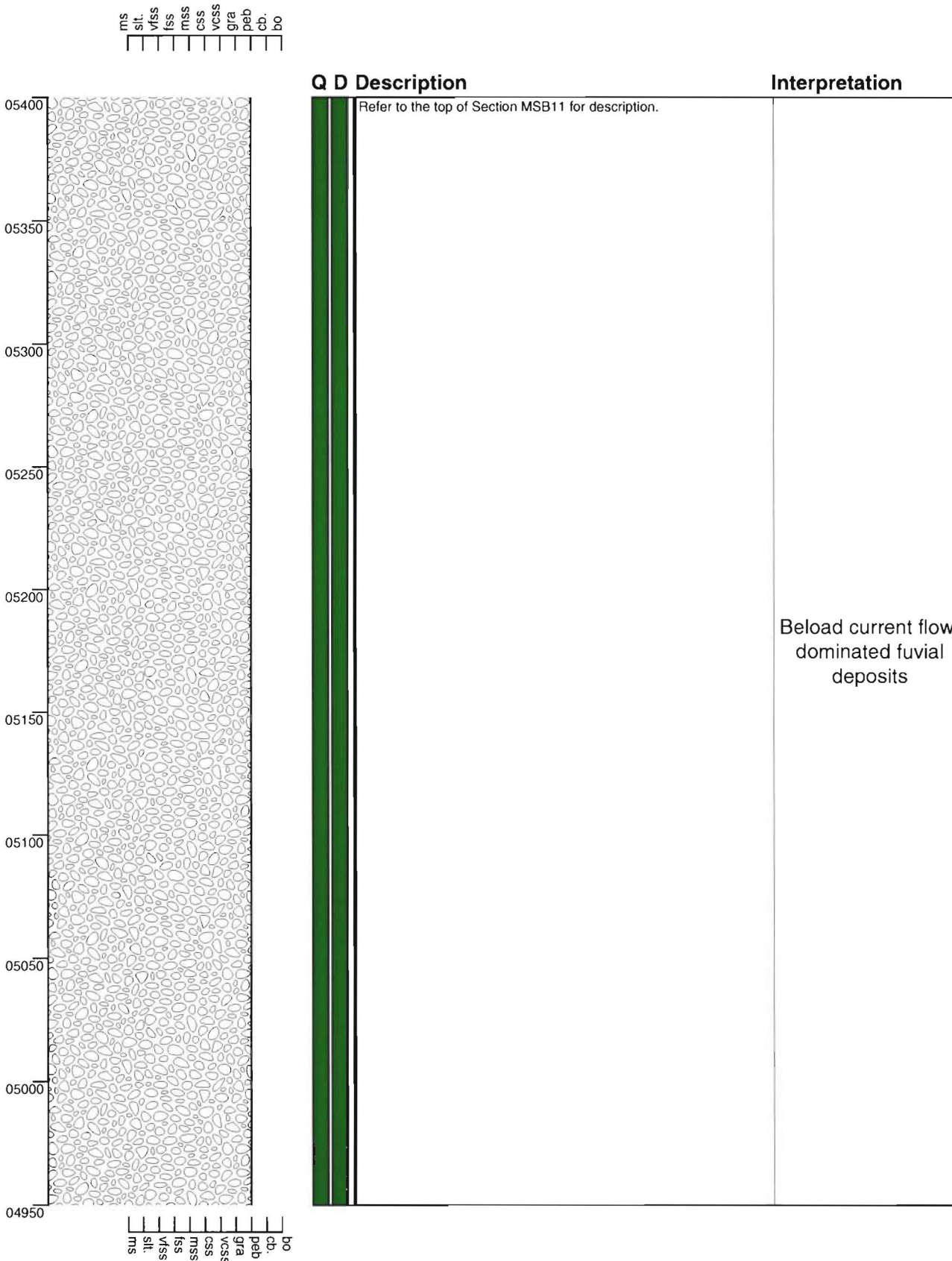
MAS., moderately sorted, sub rounded to well rounded, vfs matrix (40%), large cob. sized vfs ripups, gra - peb.

MAS., well sorted, sub angular to sub rounded, vfs matrix (50%), vcs - peb.

Refer to the top of Section MSB10 for description.

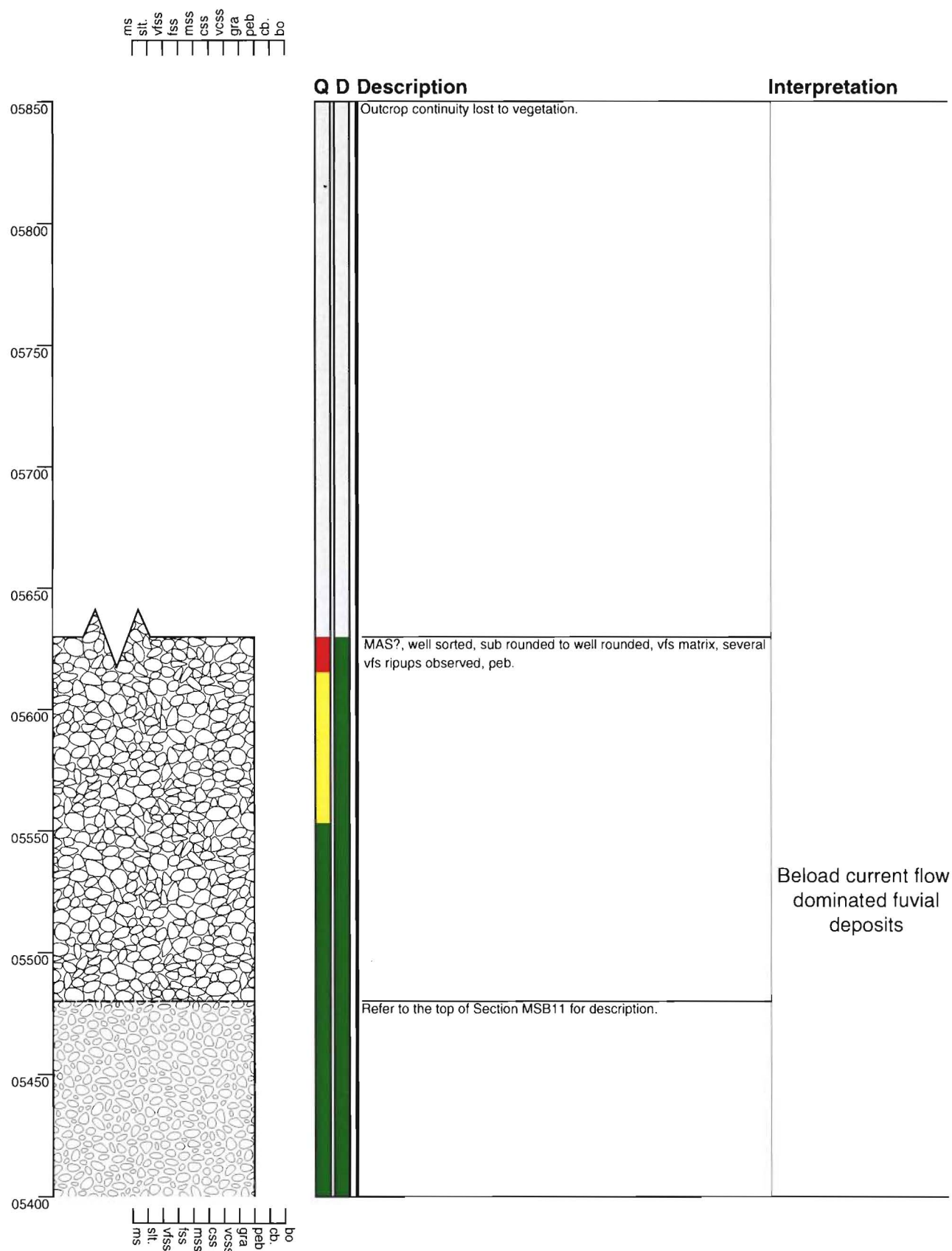
Section - Mt Saul B12

Grid Reference M32 861 443



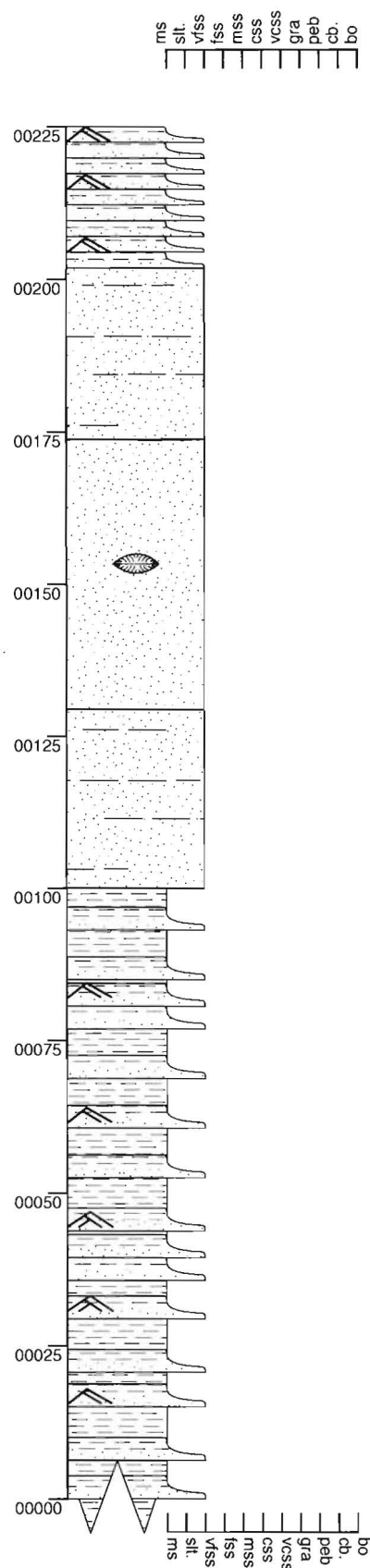
Section - Mt Saul B13

Grid Reference M32 861 443



Section - Mt Saul C01

Grid Reference M32 860 436



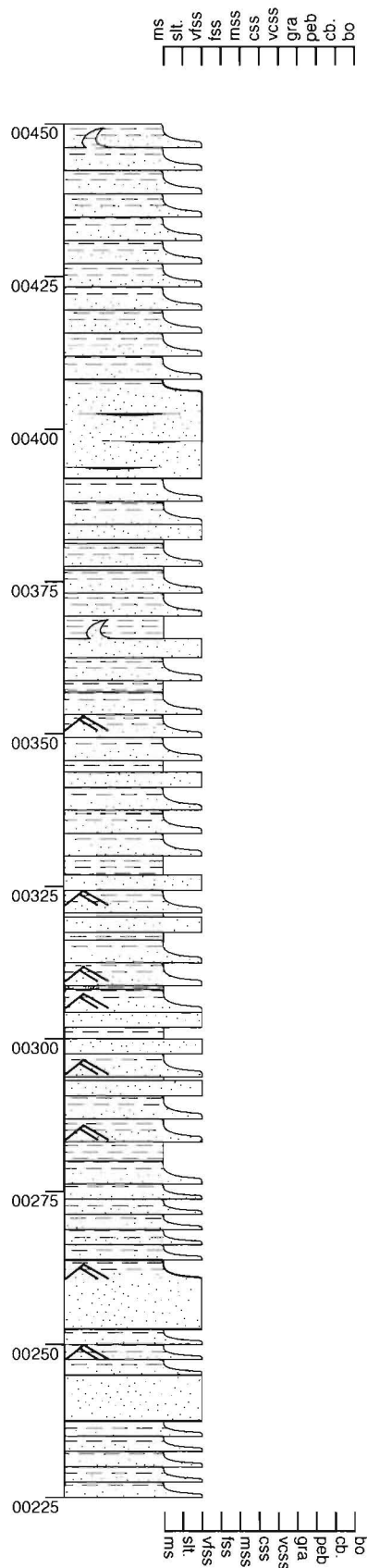
Q D Description

Interpretation

00225	NG., thinly bedded sequence (<50mm), ripples (100mm, 10mm).	Bay mouth interdistributary bay overbank deposits
00200	SAME (100cm).	
00175	MAS., a singular fossil was observed bivalve (see photo).	
00150		Minor sand spit ?
00125	MAS. vss, common very thin mud lams.	
00100	NG., MAS., thinly bedded sequence (<50mm), ripples (100mm, 10mm), paleoflow on ripples 165°SE ± 30°.	
00075		
00050		Interdistributary bay overbank deposits
00025		
00000		

Section - Mt Saul C02

Grid Reference M32 860 436



Q D Description

Interpretation

NG., thinly bedded sequence (<60mm).

NG., very thin carb. lams observed.

NG., MAS., thinly bedded sequence (<50mm), a singular 3D flame structure provided a paleoflow of 355°NW ±30°, ripples (100mm, 10 mm).

Bay mouth
interdistributary bay
overbank deposits

NG., ripples (100mm, 10mm).

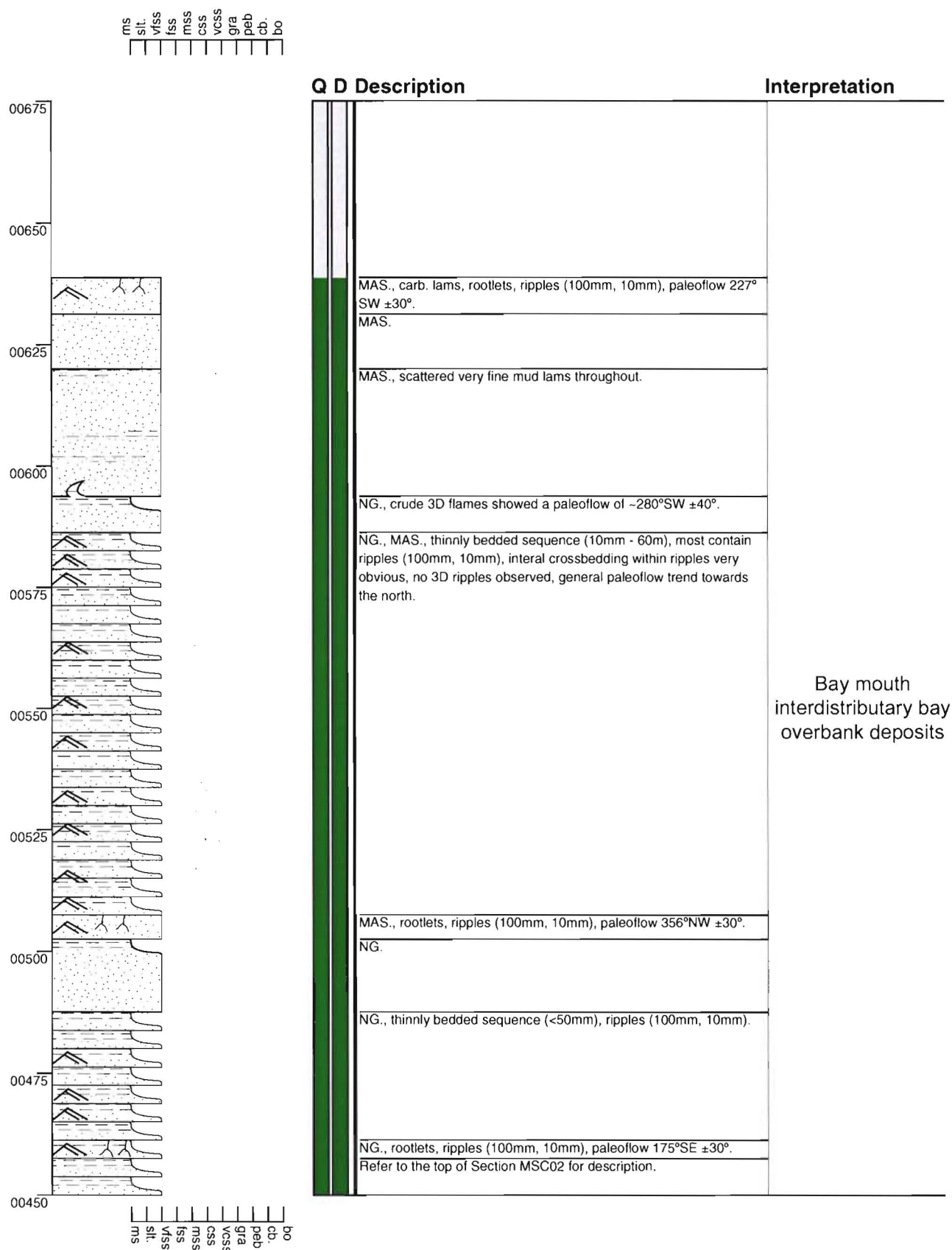
NG., thinly bedded sequence (<50mm), ripples (100mm, 10mm).

MAS., some very thin mud lams present.

Refer to the top of Section MSC01 for description.

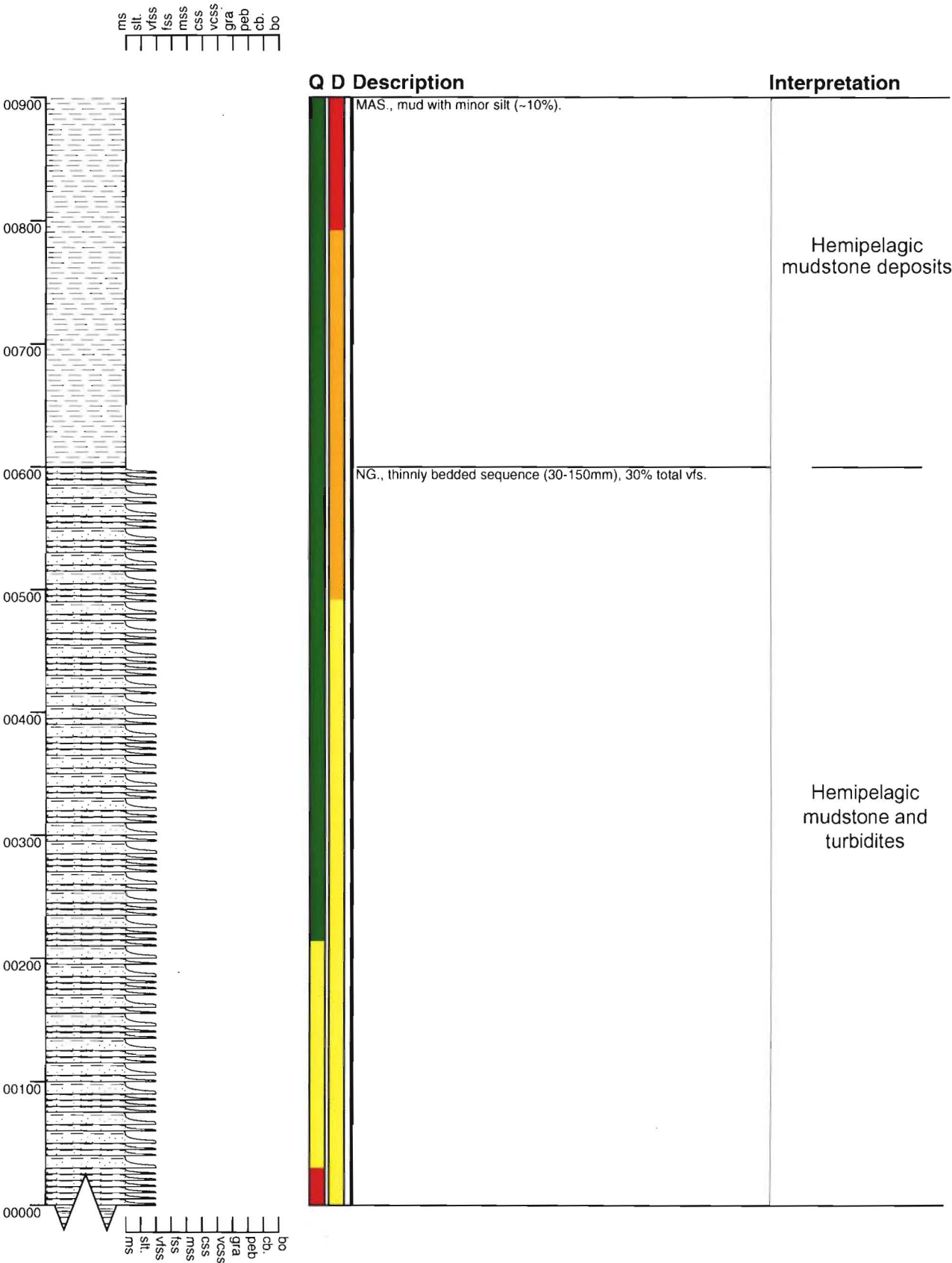
Section - Mt Saul C03

Grid Reference M32 860 436



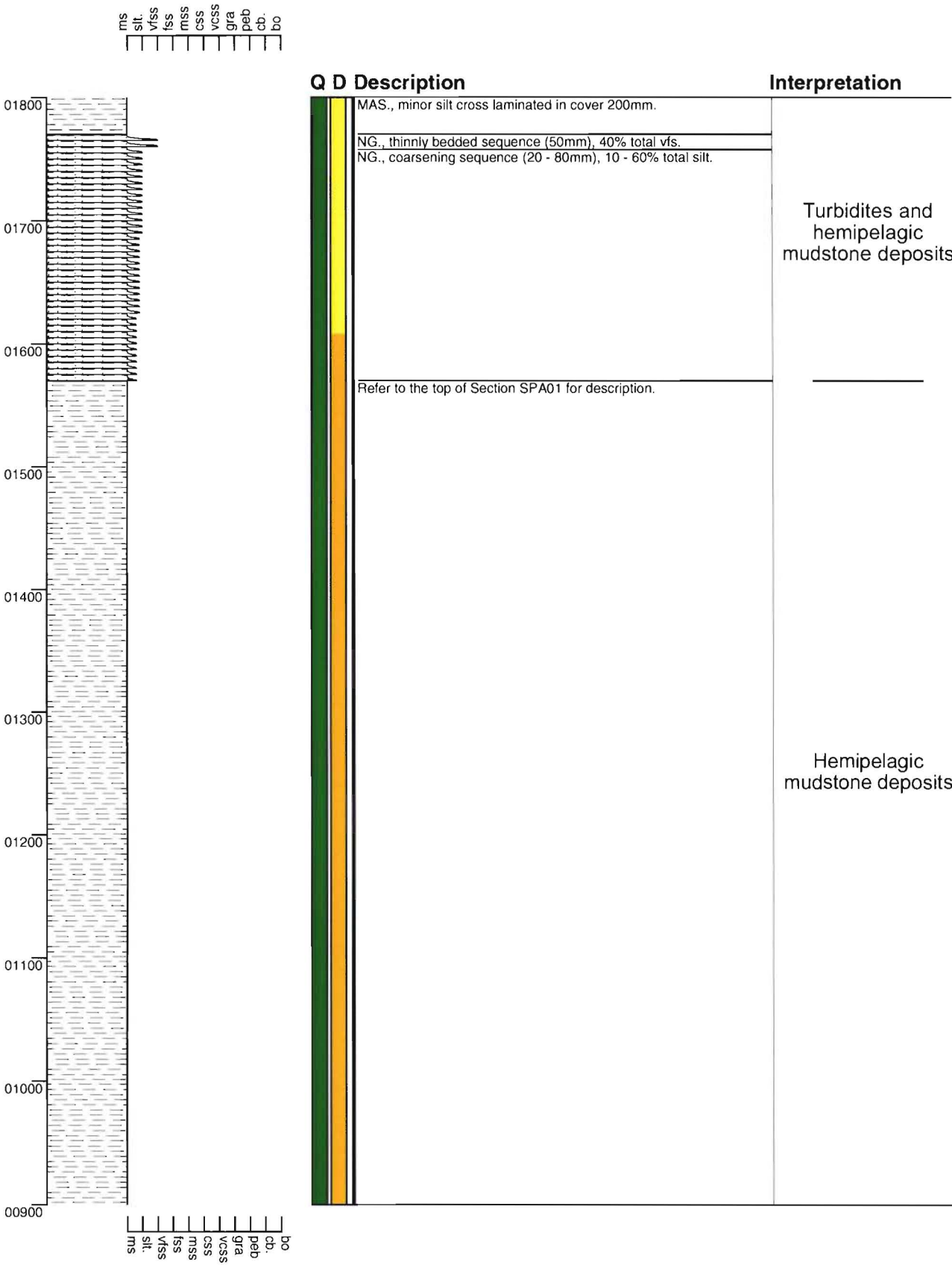
Section - Shale Peak SP01

Grid Reference M32 821 428



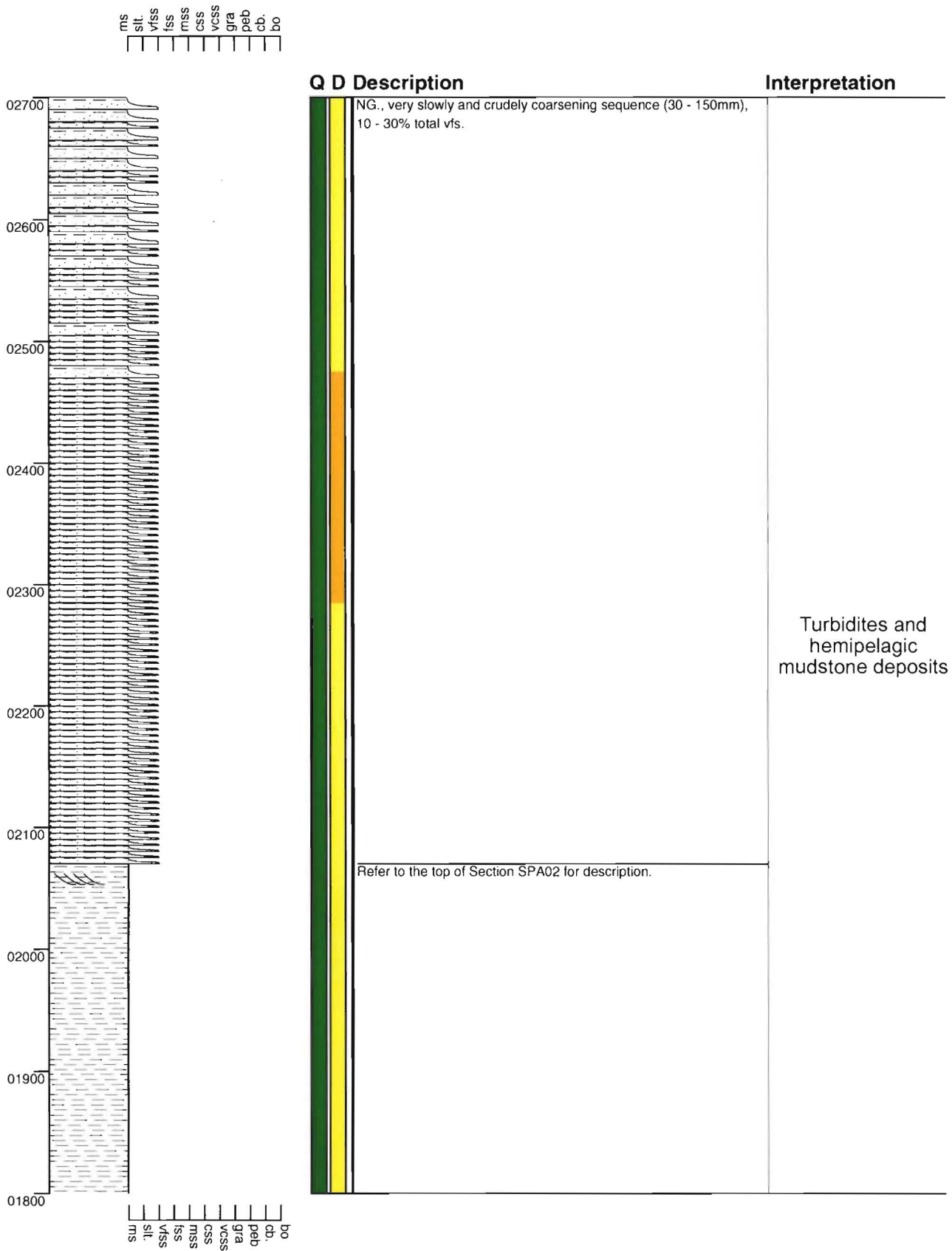
Section - Shale Peak SP02

Grid Reference M32 821 428



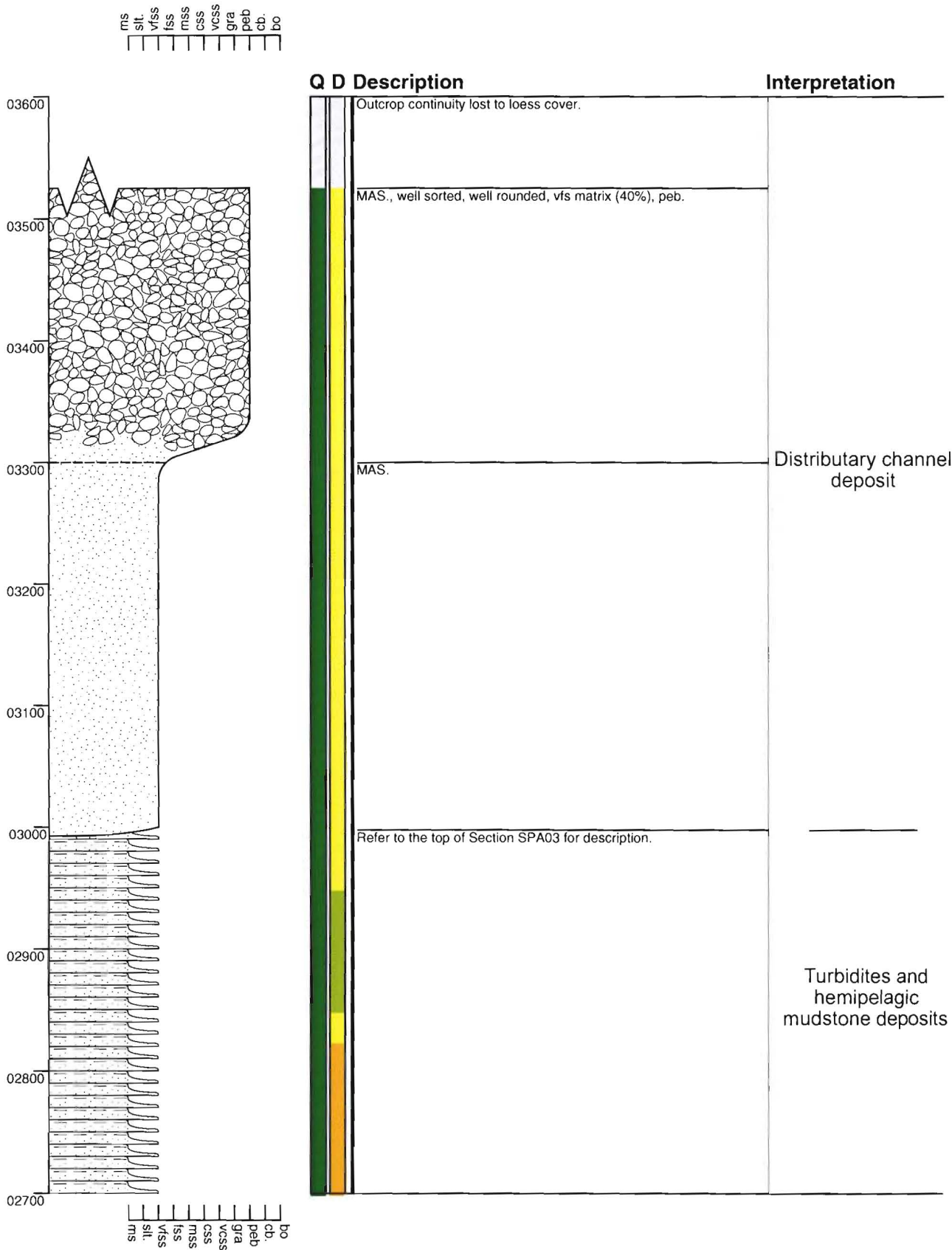
Section - Shale Peak SP03

Grid Reference M32 821 428



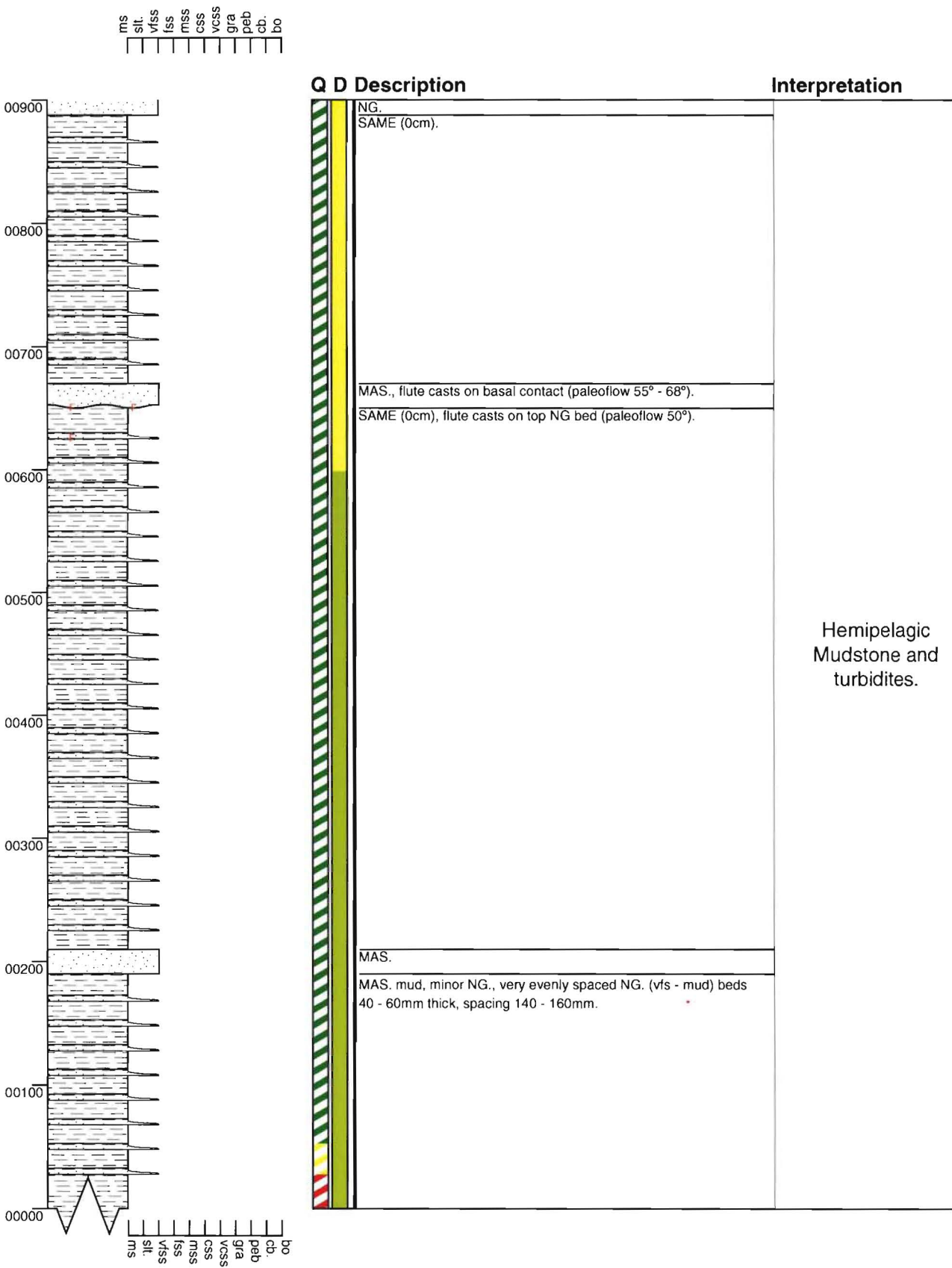
Section - Shale Peak SP04

Grid Reference M32 821 428



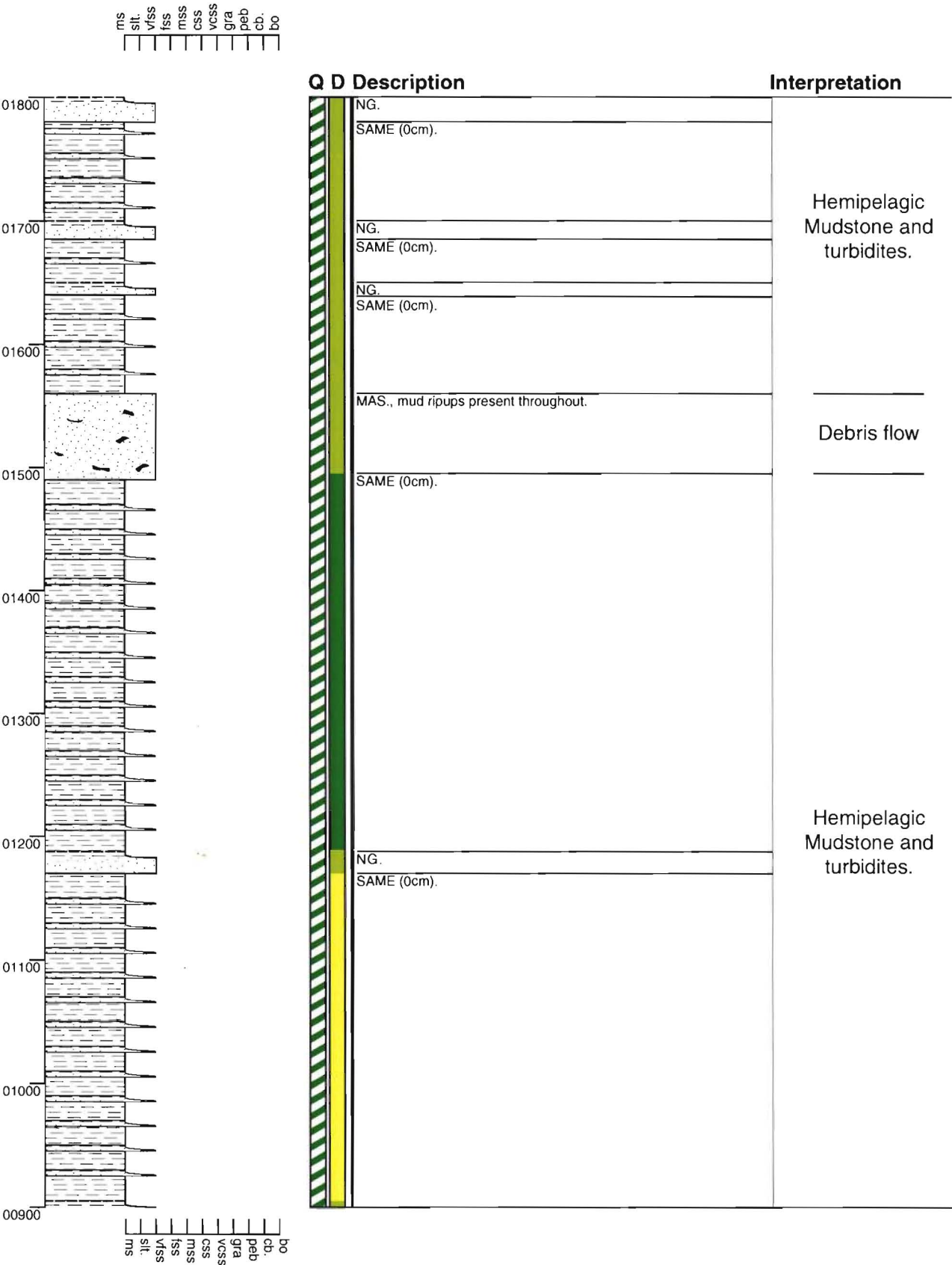
Section - Castle Hill CH01

Grid Reference M32 888 441



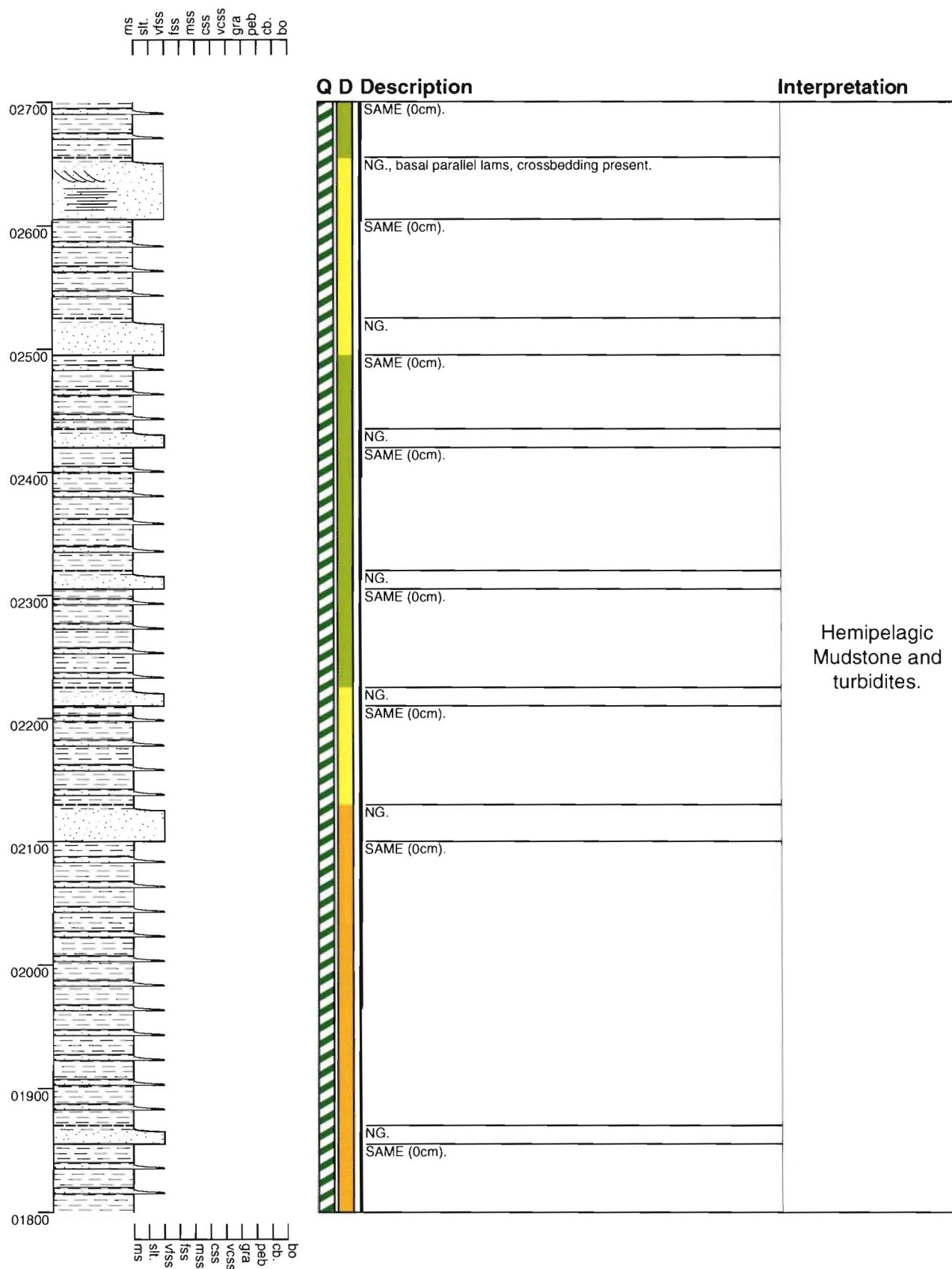
Section - Castle Hill CH02

Grid Reference M32 888 441



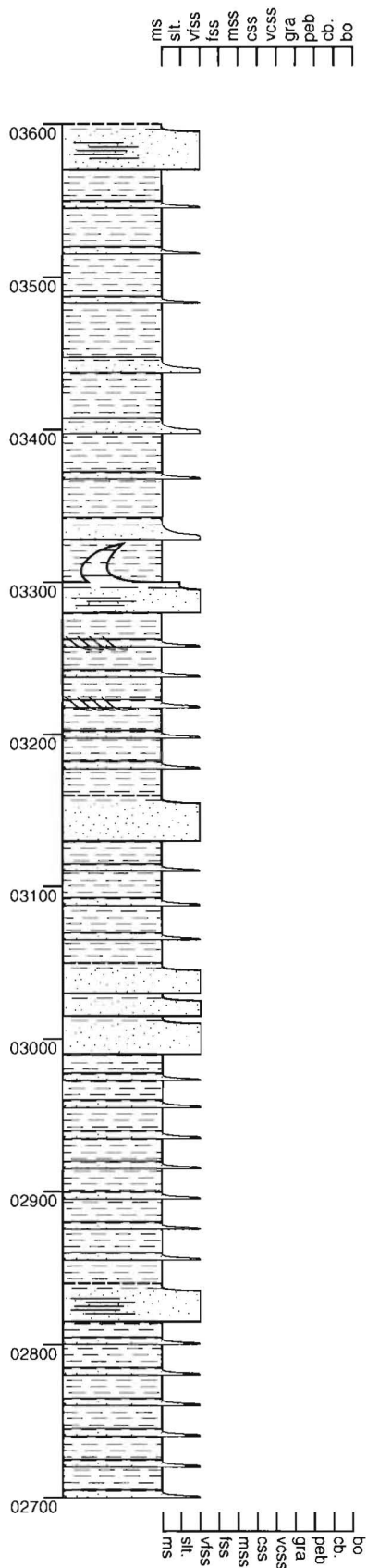
Section - Castle Hill CH03

Grid Reference M32 888 441



Section - Castle Hill CH04

Grid Reference M32 888 441



Q D Description

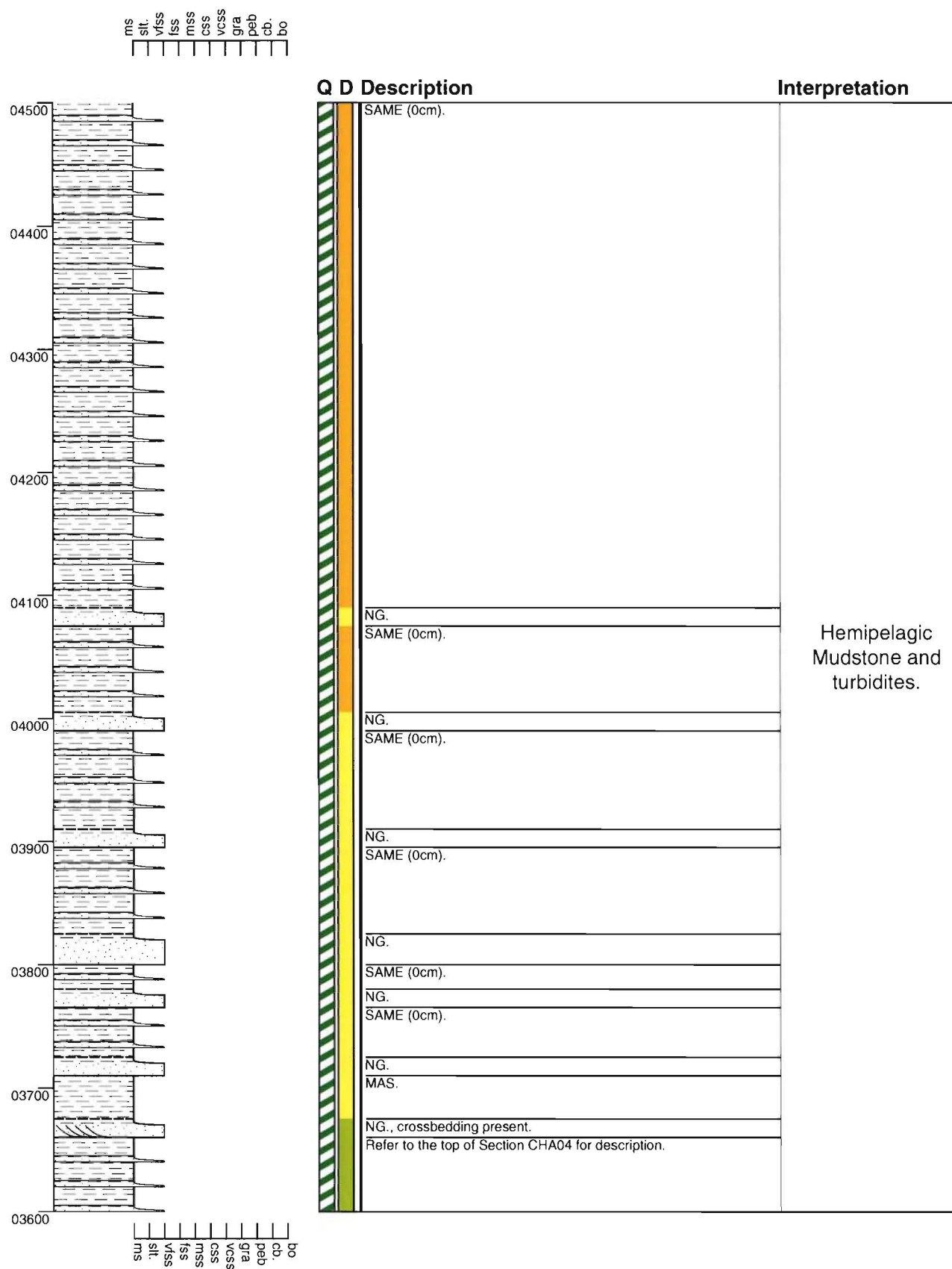
Interpretation

NG., parallel lams present.	
MAS., minor NG., NG crudely coarsens and thickens towards cover (100mm - 20mm).	
NG., parallel lams, flames present (appear to be trending - NE).	
SAME (0cm), crossbedding present in some of the NG beds.	
NG.	
SAME (0cm).	
NG.	
NG.	
NG.	
SAME (0cm).	
NG., parallel lams present.	
Refer to the top of Section CHA03 for description.	

Hemipelagic
Mudstone and
turbidites.

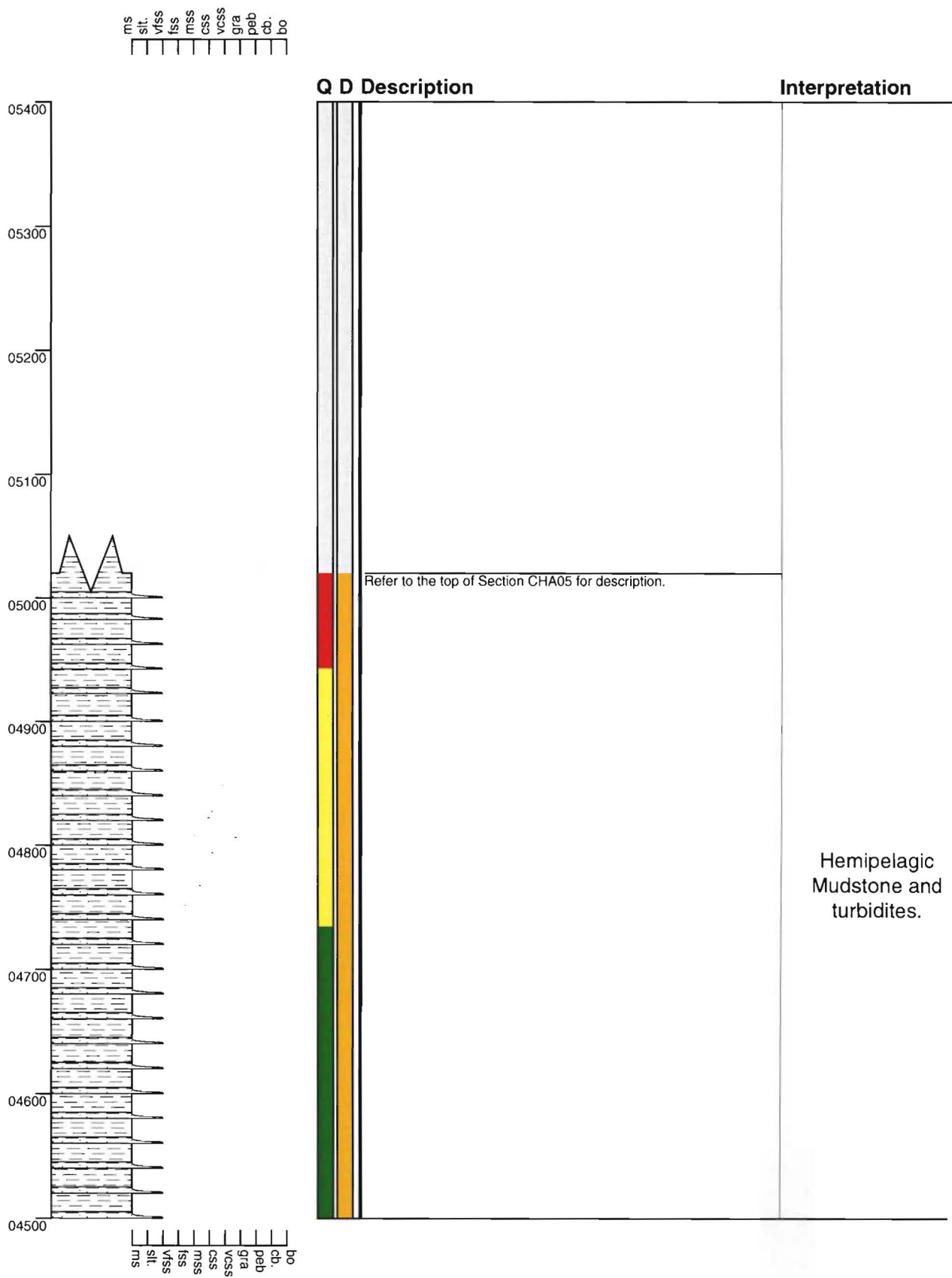
Section - Castle Hill CH05

Grid Reference M32 888 441



Section - Castle Hill CH06

Grid Reference M32 888 441



APPENDIX II

Thin Section Raw Data Analysis

Sample	Quartz	Akali/Kspar	Plag	Lithics	Carb.	Misc	Matrix
18.1/1	114	80	118	120	10	9	49
19.3/1	97	62	71	112	20	8	130
19.3/2	107	89	66	128	13	8	89
26.1/1	119	61	52	129	?	7	132
26.1/2	115	70	87	85	2	15	136
26.1/3	87	90	115	71	12	10	115
CRU	136	81	96	154	?	25	219
H1	113	53	79	140	2	18	95
H2	120	76	97	131	7	16	53
OS2	98	72	109	141	5	11	64
OS3	112	83	91	139	7	6	62
OS4	125	85	130	103	8	3	46
S2	133	62	108	112	13	8	64
S3	98	53	117	143	5	7	77
WS1	101	97	92	140	12	8	50
SP1	111	43	78	96	11	9	152
SP2	110	57	119	75	5	9	125
PR3	71	31	127	77	14	16	164
PR2	107	71	131	92	10	9	80
PR1	124	56	117	93	14	7	89
Total	2198	1372	2000	2281	170	209	1991

	<i>Initial staining technique and count</i>
	<i>Second staining technique and count</i>
	<i>Second staining technique and third Count</i>

Thin Section Statistical Analysis

Sample	Q	F	L	QFL TOTAL
18.1/1	11%	20%	69%	1000
19.3/1	10%	13%	77%	1000
19.3/2	11%	16%	74%	1000
26.1/1	12%	11%	77%	1000
26.1/2	11%	15%	73%	1020
ARB	26%	51%	23%	368
CRU	10%	12%	78%	1422
H1	11%	13%	76%	1000
H2	12%	17%	71%	1000
OS2	10%	18%	72%	1000
OS3	11%	17%	71%	1000
OS4	13%	22%	66%	1000
S2	13%	17%	70%	1000
S3	10%	17%	73%	1000
WS1	10%	19%	71%	1000
SP1	11%	12%	77%	1000
SP2	11%	18%	71%	1000
PR3	7%	16%	77%	1000
PR2	11%	20%	69%	1000
PR1	12%	17%	70%	1000

95 conf	1.60%	3.56%	5.05%
average	11.65%	18.08%	70.27%
std dev	3.65%	8.13%	11.52%
average	10.46%	16.60%	72.94%
average	12.9%	19.8%	67.3%
average	12.0%	18.6%	69.4%

	<i>Initial staining technique and count</i>
	<i>Second staining technique and count</i>
	<i>Second staining technique and third Count</i>

APPENDIX III

Palaeoflow Indicator	Palaeoflow direction
3D symmetrical ripple	120° SE – 300° NW
3D symmetrical ripple	130° SE – 310° NW
3D symmetrical ripple	130° SE – 310° NW
3D symmetrical ripple	131° SE – 311° NW
3D symmetrical ripple	55° NE – 235° SW
3D flame structure	182° SW
3D asymmetrical ripple	70° E
Flute cast	5° NE
Flute cast	10° NE
Flute cast	67° NE
Flute cast	290° SW
Tool marks	57° NE
Tool marks	340° NW
Imbrication	50° NE

** 2D asymmetrical ripples and flame structures suggest palaeoflow towards the northeast.